Quaiser Saquib
Mohammad Faisal
Abdulaziz A. Al-Khedhairy
Abdulrahman A. Alatar *Editors*

# Green Synthesis of Nanoparticles: Applications and Prospects

Springer

# Green Synthesis of Nanoparticles: Applications and Prospects

Quaiser Saquib • Mohammad Faisal •
Abdulaziz A. Al-Khedhairy •
Abdulrahman A. Alatar
Editors

# Green Synthesis of Nanoparticles: Applications and Prospects

Springer

*Editors*
Quaiser Saquib
Department of Zoology, College of Science
King Saud University
Riyadh, Saudi Arabia

Mohammad Faisal
Department of Botany & Microbiology, College of Science
King Saud University
Riyadh, Saudi Arabia

Abdulaziz A. Al-Khedhairy
Department of Zoology, College of Science
King Saud University
Riyadh, Saudi Arabia

Abdulrahman A. Alatar
Department of Botany & Microbiology, College of Science
King Saud University
Riyadh, Saudi Arabia

ISBN 978-981-15-5178-9 ISBN 978-981-15-5179-6 (eBook)
https://doi.org/10.1007/978-981-15-5179-6

© Springer Nature Singapore Pte Ltd. 2020
This work is subject to copyright. All rights are reserved by the Publisher, whether the whole or part of the material is concerned, specifically the rights of translation, reprinting, reuse of illustrations, recitation, broadcasting, reproduction on microfilms or in any other physical way, and transmission or information storage and retrieval, electronic adaptation, computer software, or by similar or dissimilar methodology now known or hereafter developed.
The use of general descriptive names, registered names, trademarks, service marks, etc. in this publication does not imply, even in the absence of a specific statement, that such names are exempt from the relevant protective laws and regulations and therefore free for general use.
The publisher, the authors, and the editors are safe to assume that the advice and information in this book are believed to be true and accurate at the date of publication. Neither the publisher nor the authors or the editors give a warranty, expressed or implied, with respect to the material contained herein or for any errors or omissions that may have been made. The publisher remains neutral with regard to jurisdictional claims in published maps and institutional affiliations.

This Springer imprint is published by the registered company Springer Nature Singapore Pte Ltd.
The registered company address is: 152 Beach Road, #21-01/04 Gateway East, Singapore 189721, Singapore

# Preface

It gives us immense pleasure to introduce the book entitled *Green Synthesis of Nanoparticles: Applications and Prospects*. This book is a blend of a number of ideas and perspectives for the synthesis of nanoparticles (NPs) employing biological materials. Our sincere thanks to all the contributors, who enthusiastically accepted our invitation and agreed to embellish chapters on the aforementioned topic. We also extend our exceptional thanks to the King Saud University for providing all support.

Research in NPs have gained enormous attention owing to their unique physicochemical properties. However, the use of toxic chemicals for NPs production via chemical methods have narrowed their wider applications. Consequently, the green method was developed for synthesizing NPs via the biological approach. In this context, the manipulation of nucleation and growth stages of NPs synthesis deserves special attention because it helped the nanotechnologists to produce varying types of NPs. Therefore, researchers tend to show enormous interest towards the synthesis of inorganic and organic NPs, enabling them to be used in a range of biomedical settings. Researchers have utilized varying types of biological materials for producing green NPs. The range of biological extracts prepared from plants, algae, bacteria, and viruses have shown the presence of bioactive molecules. These biomolecules reduce and cap the metal ions to produce green NPs, exhibiting less metal toxicity, and are more biocompatible. Apart from the low-cost productivity, the green NPs are ecofriendly too and do not need stabilizers. Surfaces of green NPs tend to adsorb biomolecules upon contact with cellular fluids, leading to the corona formation, which provide an additional advantage. The use of marine sources and medicinal plant extracts provide an excellent pharmacological property to the green NPs, which further raises their prospects to be used in biomedical and allied fields.

Hence, in this book, we have gathered up-to-date and state-of-the-art methods used for green synthesis of NPs and their potential applications in different fields. Special attention has also been given to explore the anticancer effects of green NPs. The book has been designed for scientists engaged in NPs research. Nonetheless, it should be of interest to a variety of scientific disciplines including marine biology,

environmental science, genetics, pharmacology, medicine, drug and food material sciences, and consumer products. Also, the compilations will be of interest to the environmental watchdogs, federal regulators, risk assessors, and policy makers.

Riyadh, Saudi Arabia — Quaiser Saquib
Riyadh, Saudi Arabia — Mohammad Faisal
Riyadh, Saudi Arabia — Abdulaziz A. Al-Khedhairy
Riyadh, Saudi Arabia — Abdulrahman A. Alatar

# Acknowledgments

The authors are grateful to the Deanship of Scientific Research, King Saud University for funding through Vice Deanship of Scientific Research Chairs.

# Contents

# Editors and Contributors

## About the Editors

**Quaiser Saquib** currently works as an Associate Professor of Molecular Toxicology and Coordinator of DNA Research, Department of Zoology, College of Science, King Saud University, Riyadh, Saudi Arabia. He has over 12 years of research experience in cellular and molecular toxicology. He has been conferred with SESR Bioscientist Award-2018, NESA-Scientist of the Year Award-2016, and EMSI-Young Scientist Award-2008. Dr. Saquib published 72 research articles, 4 books, and 4 book chapters and serves as an editor and reviewer of several international journals.

**Mohammad Faisal** has over 12 years of research experience in Plant Biotechnology and currently works as an Associate Professor in the Department of Botany and Microbiology at King Saud University, Riyadh, Saudi Arabia. He received the Plant Biotechnologist Award from the SESR, India (2017), the Scientist of the Year Award-2015 from NESA (2015), and several national and international fellowships. He is a member of several academic bodies/societies and Fellow of the SESR. He has published over 82 research articles, 7 book chapters, and 6 books and serves on the editorial board of several reputed journals.

**Abdulaziz A. Al-Khedhairy** is a Professor of Molecular Genetics and Genomics in Zoology Department, College of Sciences, King Saud University, Riyadh, Saudi Arabia. He also serves as Director of DNA Research Chair in King Saud University. He has published over 190 research articles in journals of international repute, 4 books, 9 book chapters, and one US patent. As a PI and CO-I, he has successfully supervised several projects funded by KACST, KSA.

**Abdulrahman A. Alatar** is a Professor in the Department of Botany and Microbiology at King Saud University, Riyadh, Saudi Arabia. He is a consultant for human resources and management at the Ministry of Higher Education, Saud Arabia. Prof. Alatar has published more than 101 scientific articles in international journals and 4 books.

## Contributors

**Yahaya Abdulrazaq** Department of Pure and Applied Chemistry, University of Fort Hare, Alice, South Africa
Department of Chemistry, Kogi State University, Anyigba, Nigeria

**Abdulrahman A. Alatar** Department of Botany & Microbiology, College of Science, King Saud University, Riyadh, Saudi Arabia

**Khursheed Ali** Department of Agricultural Microbiology, Faculty of Agricultural Sciences, Aligarh Muslim University, Aligarh, Uttar Pradesh, India

**Abdulaziz A. Al-Khedhairy** Department of Zoology, College of Science, King Saud University, Riyadh, Saudi Arabia

**Azzurra Apriceno** Institute for Bioengineering of Catalonia (IBEC), The Barcelona Institute of Science and Technology, Barcelona, Spain

**Moronkola Bridget** Department of Chemistry, Lagos State University, Ojo, Lagos State, Nigeria

**Mariafrancesca Cascione** Department of Mathematics and Physics "Ennio De Giorgi", University of Salento, Lecce, Italy

**Tijo Cherian** Department of Agricultural Microbiology, Faculty of Agricultural Sciences, Aligarh Muslim University, Aligarh, Uttar Pradesh, India

**Valeria De Matteis** Department of Mathematics and Physics "Ennio De Giorgi", University of Salento, Lecce, Italy

**Tiago Alves Jorge de Souza** Department of Civil Engineering, Adventist University of São Paulo—UNASP, Engenheiro Coelho, SP, Brazil
Department of Genetics, FMRP-USP, São Paulo University—USP, Ribeirão Preto, SP, Brazil

**Elias Emeka Elemike** Department of Chemistry, Federal University of Petroleum Resources Effurun, Effurun, Nigeria

**Mohammad Faisal** Department of Botany & Microbiology, College of Science, King Saud University, Riyadh, Saudi Arabia

**Saher Fatima** Department of Agricultural Microbiology, Faculty of Agricultural Sciences, Aligarh Muslim University, Aligarh, Uttar Pradesh, India

**Ayeni Gideon** Chemistry Department, Kogi State University, Anyigba, Nigeria

**Oladayo Amed Idris** Medicinal Plants and Economic Development (MPED) Research Centre, Department of Botany, University of Fort Hare, Alice, South Africa

**Wisdom Ivwurie** Department of Chemistry, Federal University of Petroleum Resources Effurun, Effurun, Nigeria

**Dianwen Ju** Department of Biological Medicine and Shanghai Engineering Research Center of Immunotherapeutics, School of Pharmacy, Fudan University, Shanghai, People's Republic of China

**Gun-Do Kim** Department of Microbiology, College of Natural Sciences, Pukyong National University, Busan, Republic of Korea

**Yubin Li** Department of Neurology, Xinqiao Hospital, Third Military Medical University (Army Medical University), Chongqing, People's Republic of China
Department of Dermatology, Perelman School of Medicine, University of Pennsylvania, Philadelphia, PA, USA
Corporal Michael J. Crescenz VA Medical Center, Philadelphia, PA, USA

**Eva Liatsi-Douvitsa** Department of Chemistry, University College London (UCL), London, UK

**Adriano Magesky** CHU de Québec-Université Laval, Québec-QC/Institut National de Santé Publique du Québec (INSPQ), Québec, QC, Canada

**R. V. Meenakshi** Department of Biotechnology, Bharathidasan Institute of Technology, Anna University, Tiruchirappalli, Tamil Nadu, India

**Javed Musarrat** Department of Agricultural Microbiology, Faculty of Agricultural Sciences, Aligarh Muslim University, Aligarh, Uttar Pradesh, India
School of Biosciences and Biotechnology, Baba Ghulam Shah Badshah University, Rajouri, India

**Chijioke Olisah** Department of Pure and Applied Chemistry, University of Fort Hare, Alice, South Africa

**Maheshkumar Prakash Patil** Research Institute for Basic Sciences, Pukyong National University, Busan, Republic of Korea

**Vandana B. Patravale** Department of Pharmaceutical Sciences and Technology, Institute of Chemical Technology, Mumbai, India

**Émilien Pelletier** Institut des sciences de la mer de Rimouski (ISMER), Université du Québec à Rimouski, Rimouski, QC, Canada

**Leonardo Franchi Pereira** Department of Genetics, FMRP-USP, São Paulo University—USP, Ribeirão Preto, SP, Brazil

**Bui Dai Phat** Faculty of Materials Science and Technology, University of Science, VNU-HCM, Ho Chi Minh City, Vietnam

**Sreeranjini Pulakkat** Department of Pharmaceutical Sciences and Technology, Institute of Chemical Technology, Mumbai, India

**K. Rajaram** Department of Biochemistry and Biotechnology, CSIR—Central Leather Research Institute, Chennai, Tamil Nadu, India

**K. Ravi Shankar** Department of Biotechnology, Bharathidasan Institute of Technology, Anna University, Tiruchirappalli, Tamil Nadu, India

**Rosaria Rinaldi** Department of Mathematics and Physics "Ennio De Giorgi", University of Salento, Lecce, Italy

**Loris Rizzello** Department of Chemistry, University College London (UCL), London, UK
Institute for Bioengineering of Catalonia (IBEC), The Barcelona Institute of Science and Technology, Barcelona, Spain

**Larayetan Rotimi** Department of Pure and Applied Chemistry, University of Fort Hare, Alice, South Africa
Department of Chemistry, Kogi State University, Anyigba, Nigeria

**Izabella Sant'Ana Storch** Department of Structures and Civil Construction, Federal University of São Carlos – UFSCar, São Carlos, SP, Brazil
Department of Civil Engineering, Adventist University of São Paulo-UNASP, Engenheiro Coelho, SP, Brazil

**Quaiser Saquib** Department of Zoology, College of Science, King Saud University, Riyadh, Saudi Arabia

**Lilian Rodrigues Rosa Souza** Department of Chemistry, FFCLRP-USP, University of São Paulo—USP, Ribeirão Preto, SP, Brazil

**P. Sureshkumar** Department of Biotechnology, Bharathidasan Institute of Technology, Anna University, Tiruchirappalli, Tamil Nadu, India

**V. Tamil Elakkiya** Department of Biotechnology, Bharathidasan Institute of Technology, Anna University, Tiruchirappalli, Tamil Nadu, India

**Cao Minh Thi** Ho Chi Minh City University of Technology (HUTECH), Ho Chi Minh City, Vietnam

**Pham Van Viet** Faculty of Materials Science and Technology, University of Science, VNU-HCM, Ho Chi Minh City, Vietnam

**Tran Hoang The Vinh** Faculty of Materials Science and Technology, University of Science, VNU-HCM, Ho Chi Minh City, Vietnam

**Shaofei Wang** Department of Cellular and Genetic Medicine, School of Basic Medical Sciences, Fudan University, Shanghai, People's Republic of China

**Chunlan Xu** The Key Laboratory for Space Bioscience and Biotechnology, School of Life Sciences, Northwestern Polytechnical University, Xi'an, Shaanxi, China

# Research Progression on Studies Related to Green Synthesis Nanoparticles: A Bibliometric Review

1

Rotimi Larayetan, Chijioke Olisah, and Oladayo Amed Idris

**Abstract**

The growing application of green synthesis nanoparticles (NPs) in medical and pharmaceutical sciences has made this area of research to be extensively explored by scientists. Here, we conducted a bibliometric investigation to evaluate the trend of research on green synthesis nanoparticle using articles retrieved from the WoS (Web of Science) from 2007 to 2018. A total of 710 articles (article, 699; review, 11) were retrieved from 243 journal sources. These articles were authored by 2473 authors with an article/author and author/article ratio of 0.287 and 3.48, respectively. A steady increase of article production in this area of research was noticed within the survey years with the high number of articles recorded in 2018 with 190 items. Asia countries dominated the top 20 countries on articles related to green synthesis nanoparticle research. India was ranked first with 308 articles, followed by Iran and Korea with 129 and 41 articles, respectively. A Lokta distribution based on a beta coefficient of 2.77 and goodness of fit of 0.92599 suggests that more articles are likely to be produced in this area of research in years to come. Sparse collaboration linkage was noticed between developed countries and developing countries in green synthesis-related research. To this end, more research should be encouraged to foster green synthesis research in

R. Larayetan (✉)
Department of Pure and Applied Chemistry, University of Fort Hare, Alice, South Africa

Department of Chemistry, Kogi State University, Anyigba, Nigeria

C. Olisah
Department of Pure and Applied Chemistry, University of Fort Hare, Alice, South Africa

O. A. Idris
Medicinal Plants and Economic Development (MPED) Research Centre, Department of Botany, University of Fort Hare, Alice, South Africa

Unit for Environmental Sciences and Management (UESM), Faculty of Natural and Agricultural Sciences, North West University, Potcheftroom, North West, South Africa

© Springer Nature Singapore Pte Ltd. 2020

Q. Saquib et al. (eds.), *Green Synthesis of Nanoparticles: Applications and Prospects*, https://doi.org/10.1007/978-981-15-5179-6_1

regions that depend on herbs as an alternative source of medicine, particularly in Africa.

**Keywords**

Green nanoparticles · Nanoparticles · Nanoresearch · Biogenic nanoparticles

## 1.1 Introduction

Plants used for traditional remedies contain a broad range of substances that can be used to treat chronic as well as contagious diseases. The plant empire is a virtual gold mine of prospective drug targets and other useful molecules waiting to be discovered. About 10–15% of the 750,000 known species of higher plants have been assessed for biologically active compounds [1]. Majority of consumers all over the globe still depend on therapeutic plants as a way out of the health problems militating against them [2]. Due to the astonishing growth in nanotechnology in recent years, researchers in this area have engaged themselves in the development of reliable routes to generate nanomaterials ranging from 1 to 100 nm, though the traditional technique employed since the time of Michael Faraday to produce metal NPs has still been used, which entails costly chemical and physical procedures involving toxic materials with probable dangers like toxicity to the environment and carcinogenicity [3]. The organic solvents used for the synthesis of these nanoparticles coupled with the stabilizers and reducing agents utilized are the sources of its toxicity, and this toxic factor prevents the application of such synthesized nanoparticles in biomedical and clinical execution; the reasons mentioned above can contestably be managed through biogenic synthetic route [4, 5]. Plant part/living organism-mediated synthesis of metal nanoparticles has been carried out by several natural product scientists as seen in published literature [6, 7] under the area of research tagged 'biogenic synthesis of nanoparticles'. This is usually done to check their antimicrobial, anti-plasmodium and anti-parasitic activities in animal and human cells. This fact and many others had made this area of research to be extensively studied. It is therefore paramount to carry out their bibliometric compilation. The bibliometric tool statistically analysed academic literature (journals, books, abstracts, symposiums and all kinds of documents) of a particular field of interest using various bibliometric indices. Such indices include 'most productive authors', 'top articles per citation', 'most productive country', 'total citation per country', 'most relevant sources' and 'most relevant keywords'. This tool also assists scientist to have a firm idea regarding which article to read and where to publish their findings/outcomes. A software with a bibliometric tool module is installed on computer support to retrieve information of a particular subject from a database based on the above-mentioned indices. To analyse the sequential growth in the field of 'green synthesis nanoparticles', data were retrieved from the databases of the Web of Science (WoS). The WoS database was employed due to the fact that it covers a large scope of scientific literature that spans through art and humanities, life and physical sciences, social sciences and management sciences. Besides, articles related to bibliometric survey have also

employed the use of WoS databases in the past [8, 9]. The main aim of this work is to employ bibliometry procedure to retrieve data on 'green synthesis nanoparticles' from publications covering a period of 2007–2015 in order to detect and evaluate the essential literature in this field and also to recognize international research productivity trend on this field through evaluation of articles published and important evolution over the years in this field of interest. To the best of our knowledge, there is paucity of information on the bibliometric data collection on biogenic synthesis of nanoparticles which if embarked upon will add to the cognitive, public and intellectual development of this field and also give researchers future direction in scientific work pertaining to this research area with particular emphasis on information provider to devise policies and strategies for the collection and acquisition of information resources.

## 1.2 Materials and Methods

Information on green synthesis nanoparticles was retrieved using a method described in Olisah et al. [9, 10]. Briefly, articles indexed on the WoS database were retrieved on September 27, 2019. The term 'green synthesis nanoparticles' was used as a search term for articles published from January 1, 2007, to December 31, 2018. Title-specific search (TSS) was chosen over topic search because in the former, errors related to sensitivity are minimized [8, 11]. Besides TSS has a high rate of recovery. Literature types such as proceeding paper, meeting abstract, correction, book chapters, editorial materials, letters, note, early access, correction addition and retracted publication were excluded from the search documents. Only article and review on green synthesis nanoparticle were used for the survey. These two document types were downloaded in BibTex format in two batches (500 documents in one batch and 210 documents in the second batch). The downloaded files were inputted into an RStudio (v.3.4.1 software) with installed bibliometric R-package. It is worth noting that only articles related to green synthesis nanoparticles were downloaded and articles were scrutinized before downloading by three principal investigators in the field of green synthesis. Command programmes for bibliometric indices were gotten from https://www.bibliometrix.org. Other statistical commands for Lokta and beta coefficient, Kolmogorov-Smirnov *p*-value, bipartite networks, co-citation network, keyword co-occurrence, most productive authors, top citation per article, international collaboration networks and author coupling were retrieved from https://cran.r-project.org/web/packages/bibliometrix/vignettes/bibliometrix-vignette.html.

## 1.3 Global Progression of Publications on Green Synthesis Nanoparticles

It has been established from a bibliometric analysis that the quantity of publications of a research field determines the overall output and efficiency yield of that field [12]. This current study revealed that a total of 710 publications was related to

**Table 1.1** Summary of statistics recovered on green synthesis nanoparticles from WoS (1994–2019)

| Representations | Counts |
|---|---|
| Period | 2007–2019 |
| Total number of articles | 699 |
| Number of research articles | 711 |
| Number of review articles | 11 |
| Source (journals, books, etc.) | 243 |
| Keyword plus (ID) | 1195 |
| Keywords used by author (DE) | 1753 |
| Average citations per documents | 29.11 |
| Authors | 2473 |
| Authors' participation | 3199 |
| Documents authored by single author | 12 |
| Documents authored by multiple author | 2461 |
| Documents per author | 0.287 |
| Authors per document | 3.48 |
| Co-authors per documents | 4.51 |
| Collaboration index | 3.53 |

studies on the biogenic synthesis of nanoparticles. The 710 articles were obtained from 243 sources from WoS during the investigation period (2007–2019) (Table 1.1). The various researches on this field were carried out by 2473 authors, and the analysis confirms that the article/author versus author/article ratio was 0.287 and 3.48 correspondingly. The record shows that 12 authors published singly during the period of investigation and were removed from the total number of authors. Thus this indicates that 2461 authors were engaged in multiple-authored publications. Our analysis showed a collaboration index of 3.53, thus showing high participation of co-authorship for every publication (Table 1.1) [13]. A careful observation of the annual scientific production of articles showed an increase in research publications in the area of green synthesis within a space of 12 years (2007–2019) (Table 1.1). Although some variations were recorded in article production within some years, factors such as standard working laboratory environment and the appearance of new researchers in the field of biogenic synthesis coupled with financial support and improved skills were believed to be responsible for the stable boost and improvement in publications associated with the green synthetic field [14]. The scientific productivity related to research on biogenic synthesis, as shown by Lokta's law, revealed a $\beta$ coefficient of 2.77 with a constant of 0.56 and the Kolmogorov-Smirnov $p$-value of 0.09 ($p < 0.05$) and goodness of fit of 0.92 (Fig. 1.1). The equation and R squared value of $y = 16.51x - 33.182$ and $R^2 = 0.880$ obtained from the linear regression plot of the number versus years of publication (2007–2018) confirmed that they were strongly correlated. An annual growth rate of 61.23% was recorded on research pertaining to the biogenic synthesis of nanoparticles. Compared to other research areas like organochlorine pesticides research with an annual growth rate of 5.13% [9] and *Plesiomonas*-related research with an annual growth rate of −0.8% [8] it is quite encouraging that research on biogenic synthesis is likely to keep

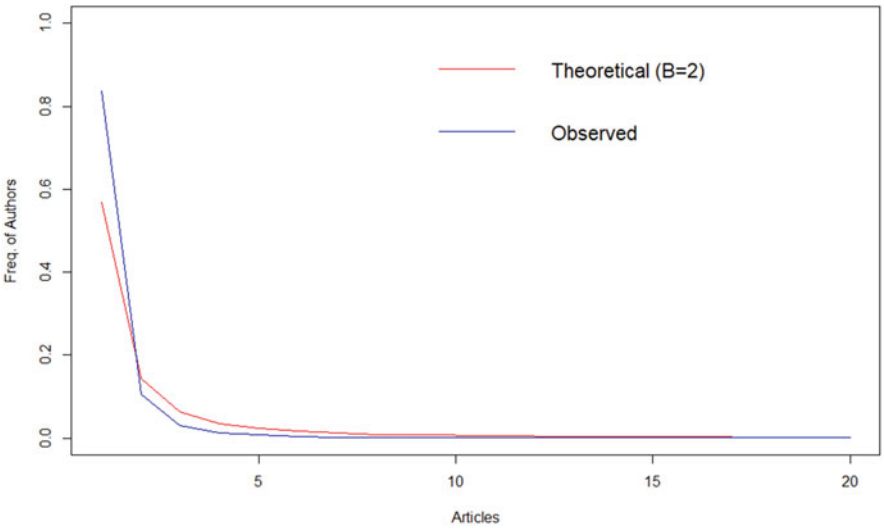


**Fig. 1.1** Scientific output of green synthesis research based on Lokta distribution

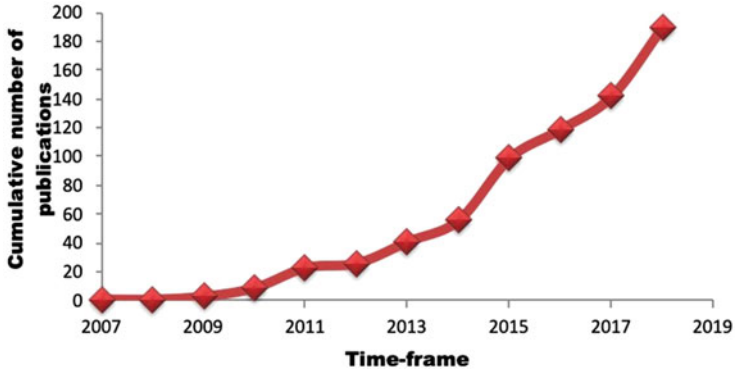


**Fig. 1.2** Global trend in green synthesis nanoparticles (1994–2019)

growing each year. The significant difference sandwiched between the theoretical and observed Lokta distributions also signifies that the number of publications on the research of biogenic synthesis is expected to rise in the nearest future [15].

The timeline in Fig. 1.2 was fractionated into a period of 1 year each. Only one article, each on green synthesis nanoparticle, was published between 2007 and 2008 as retrieved from WoS. An erratic trend was noticed concerning the nature of published articles on green synthesis between 2009 and 2010, and amplification of published articles was seen in the year 2009 where a total of 32 publications (amounting to 4.50% of the total publication of 710) were made. Still, sadly a downward trend was observed in the year 2010 where publication of articles plummeted from 32 in 2009 to 9 articles (about 1.26% of the total article of 710)

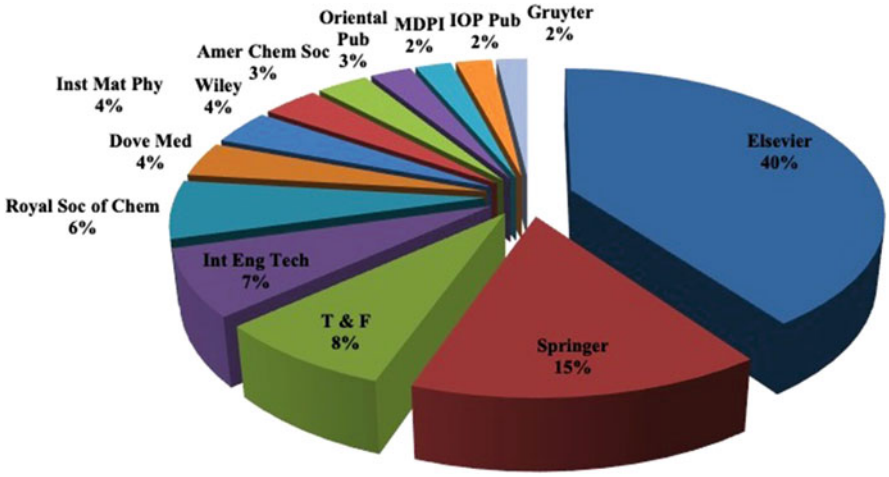


**Fig. 1.3** Percentage of distribution of the top 25 publishers on biogenic synthesis (1994–2019)

in 2010, and publications of articles improved again in the year 2011 with a total publication of 23 (3.23% of 710), and this kept increasing till 2018. The sudden upsurge in the number of articles published started in 2015 with a publication record of 99 (13.94% of 710), reaching its climax in 2018 with a published article of 190 (26.76% of 710). Research productivity is believed to continue to rise in as much as the enabling environment is maintained in various countries where research on biogenic synthesis is carried out yearly.

Some other bibliometric indices examined were the type and numbers of publisher engaged in the production of articles on researches carried out in the area of biogenic synthesis of nanoparticle. Forty per cent of the publications on this area of research were published by Elsevier with *Spectrochimica Acta Part A: Molecular and Biomolecular Spectroscopy* ($n = 29$) and *Materials Letters* ($n = 28$) occupying the first and second in the pecking order of the top 25 publishers with 29 and 28 articles, respectively (Fig. 1.3), while Springer with 15% ranked second in the order of publishers with *Journal of Cluster Science* ($n = 21$) and *Applied Nanoscience* ($n = 20$) topping the lead in Springer publisher category. The presence of Taylor and Francis was also noticed as shown in Fig. 1.3 with 8% of published articles of the top 25 publishers; taking the lead in this category is *Artificial Cells, Nanomedicine and Biotechnology* ($n = 18$) with a total of 18 publications. Some notable publishers in the top 25 categories are the International Engineering Technology (7%), Royal Society of Chemistry (6%), Wiley (4%), Dove Medical (4%) and Oriental publisher (3%) (Fig. 1.3).

## 1.4 Keywords Utilized in Biogenic Synthesis Research

Keywords used by authors in a publication symbolize the core information that the author is trying to articulate; in addition to this, they also capture, in summary, the idea expressed by the author. It is often a common practice for most journals to demand keywords ranging from three to eight depending on the journal type from authors before submission of their draft manuscripts can be considered for publications; this is usually required to facilitate online searches. In this report, the research trend of biogenic synthesis was carefully analysed using both keywords and keyword plus; the former predicts the progression trend of a precise subject matter obtained through WoS [16], while the latter is an effective and very useful means in capturing ideas and contents used in the investigation of this kind of green synthetic category [17].

Twenty most pertinent keywords comprising of both keyword plus and keywords obtained from the WoS database (journal list) on green synthesis nanoparticles are displayed in Table 1.2. Based on frequency of use it was established from Table 1.3 that keywords such as green synthesis silver nanoparticles nanoparticles and gold nanoparticles are often used by authors. These keywords were ranked first, second, third and fifth in author's keyword ($n$ = 286, 210, 93 and 68; 40.28%, 29.57%, 13.09% and 9.57%) respectively. These terms are usually employed when carrying out research on the biological synthesis of various metal nanoparticles while other terms like TEM (transmission electron microscopy), XRD (X-ray diffraction), FTIR (Fourier transform infrared) and SEM (scanning electron microscopy) ($n$ = 36, 35, 31 and 23; 5.07%, 4.92%, 4.36% and 3.23%) are characterization techniques used to ascertain the compositionstructure and morphology of the biogenic synthesized nanomaterials [7, 18, 19].

The keyword plus commonly used by authors are also displayed in Table 1.2. Keyword plus such as antioxidant, antibacterial and antibacterial activity ($n$ = 41, 50 and 51; 5.77%, 7.04% and 7.18%) are often used to depict the biological activities performed on the biosynthesized nanomaterials [7].

Both keywords and keyword plus have seven keywords in common. These are biosynthesis, AgNPs, AuNPs, antimicrobial, antioxidant, antibacterial and antibacterial activity ($n$ = 25, 45; 133, 210; 118, 68; 35, 35; 41, 25; 51, 33; 50, 90). Figure 1.4 presents the co-occurrence and interconnection of the highest 20 keywords used by authors in the area of biogenic synthesis of nanoparticles with every circled coloured node depicting a term; among the terms depicted by the coloured circle loop in Fig. 1.4 are biosynthesis, gold nanoparticles, metal nanoparticles, silver nanoparticles and leaf extract.

**Table 1.2** Twenty most relevant keywords used for biogenic synthesis retrieved from WoS 2007–2018

| Order | Keywords used by author | Publications (% of 710) | Order | Keyword plus | Publications (% of 714) |
|---|---|---|---|---|---|
| 1 | Green synthesis | 286 (40.28) | 1 | Biosynthesis | 258 (36.33) |
| 2 | Silver nanoparticles | 210 (29.57) | 2 | Leaf extract | 140 (19.71) |
| 3 | Nanoparticles | 93 (13.09) | 3 | Silver nanoparticles | 133 (18.73) |
| 4 | Antibacterial activity | 90 (12.67) | 4 | Gold nanoparticles | 118 (16.61) |
| 5 | Gold nanoparticles | 68 (9.57) | 5 | Metal nanoparticles | 81 (11.40) |
| 6 | Biosynthesis | 45 (6.33) | 6 | Extract | 63 (8.87) |
| 7 | TEM | 36 (5.07) | 7 | Reduction | 61 (8.59) |
| 8 | Antimicrobial activity | 35 (4.92) | 8 | Au | 60 (8.45) |
| 9 | XRD | 35 (4.92) | 9 | Gold | 60 (8.45) |
| 10 | Antibacterial | 33 (4.64) | 10 | Biological synthesis | 58 (8.16) |
| 11 | FTIR | 31 (4.36) | 11 | Particles | 55 (7.75) |
| 12 | X-ray diffraction | 30 (4.22) | 12 | Ag | 53 (7.46) |
| 13 | Silver | 28 (3.94) | 13 | Antibacterial | 51 (7.18) |
| 14 | Transmission electron microscopy | 26 (3.66) | 14 | Antibacterial activity | 50 (7.04) |
| 15 | Antioxidant | 25 (3.52) | 15 | Size | 46 (6.47) |
| 16 | SEM | 23 (3.23) | 16 | Antioxidant | 41 (5.77) |
| 17 | Electron microscopy | 22 (3.09) | 17 | Antimicrobial activity | 35 (4.92) |
| 18 | Green chemistry | 22 (3.09) | 18 | Degradation | 34 (4.78) |
| 19 | Antimicrobial | 20 (2.81) | 19 | Aqueous extract | 32 (4.50) |
| 20 | AgNPs | 19 (2.67) | 20 | Mediated synthesis | 32 (4.50) |

## 1.5 Progression of Publications on Biogenic Nanoparticle Synthesis by Countries

Research outputs that correlate to the number of publications are articulated in Table 1.3 for the 25 most productive countries on green synthesis retrieved from WoS (2007–2018). To study this variable in this present bibliometric analysis, countries were categorized according to the number of publications from 2007 to 2018. Republic of India ($n = 133$; 18.92%) in South Asia ranked first among the top 25 most productive countries of the world carrying out active research on green synthesis nanoparticles (Table 1.3) with a total number of 133 publications amounting to 18.62% of the overall publications within the investigation period. It

**Table 1.3** Twenty-five most productive countries on green synthesis retrieved from WoS (2007–2018)

| Most productive countries | | | | | | | | Summation of citations per country | | | |
|---|---|---|---|---|---|---|---|---|---|---|---|
| Order | Country | Publications | (% of 714) | Freq | SCP | MCP | MCP ratio | Order | Country | Total citations | Average publication citations |
| 1 | Indian | 133 | 18.62 | 0.187 | 125 | 8 | 0.06 | 1 | India | 1039 | 7.81 |
| 2 | Iran | 81 | 11.34 | 0.11 | 77 | 4 | 0.04 | 2 | Korea | 941 | 18.45 |
| 3 | Korea | 65 | 9.10 | 0.09 | 57 | 8 | 0.12 | 3 | Nigeria | 881 | 10.87 |
| 4 | China | 52 | 7.28 | 0.07 | 41 | 11 | 0.21 | 4 | Brazil | 710 | 10.92 |
| 5 | Pakistan | 51 | 7.14 | 0.07 | 41 | 10 | 0.19 | 5 | Japan | 668 | 26.72 |
| 6 | Saudi Arabia | 33 | 4.62 | 0.04 | 30 | 3 | 0.09 | 6 | Malaysia | 654 | 12.57 |
| 7 | Malaysia | 25 | 3.50 | 0.03 | 20 | 5 | 0.20 | 7 | China | 503 | 15.24 |
| 8 | South Africa | 25 | 3.50 | 0.03 | 22 | 3 | 0.12 | 8 | Taiwan | 455 | 32.50 |
| 9 | Egypt | 20 | 2.80 | 0.02 | 14 | 6 | 0.30 | 9 | Iran | 331 | 18.38 |
| 10 | Mexico | 18 | 2.52 | 0.02 | 18 | 0 | 0.00 | 10 | South Africa | 213 | 10.65 |
| 11 | Turkey | 14 | 1.96 | 0.01 | 13 | 1 | 0.07 | 11 | Italy | 193 | 19.30 |
| 12 | USA | 14 | 1.96 | 0.01 | 5 | 9 | 0.64 | 12 | USA | 172 | 34.40 |
| 13 | Brazil | 14 | 1.96 | 0.01 | 12 | 2 | 0.14 | 13 | Egypt | 162 | 13.50 |
| 14 | Nigeria | 12 | 1.68 | 0.01 | 7 | 5 | 0.41 | 14 | Thailand | 123 | 4.92 |
| 15 | Japan | 12 | 1.68 | 0.01 | 6 | 6 | 0.50 | 15 | Tunisia | 113 | 9.41 |
| 16 | Romania | 10 | 1.40 | 0.01 | 6 | 4 | 0.40 | 16 | Spain | 99 | 49.50 |
| 17 | Iraq | 9 | 1.26 | 0.01 | 7 | 2 | 0.22 | 17 | Hungary | 96 | 48.00 |
| 18 | Russia | 9 | 1.26 | 0.01 | 9 | 0 | 0.00 | 18 | Cameroon | 94 | 10.44 |
| 19 | Ecuador | 9 | 1.26 | 0.01 | 8 | 1 | 0.11 | 19 | Germany | 92 | 15.33 |
| 20 | Indonesia | 7 | 0.98 | 0.00 | 6 | 1 | 0.14 | 20 | Finland | 67 | 67.00 |
| 21 | Australia | 7 | 0.98 | 0.00 | 5 | 2 | 0.28 | 21 | Saudi Arabia | 67 | 4.78 |
| 22 | Czech Republic | 6 | 0.84 | 0.00 | 2 | 4 | 0.66 | 22 | Australia | 57 | 11.40 |

(continued)

**Table 1.3** (continued)

| Most productive countries | | | | | | | | Summation of citations per country | | | |
|---|---|---|---|---|---|---|---|---|---|---|---|
| Order | Country | Publications | (% of 714) | Freq | SCP | MCP | MCP ratio | Order | Country | Total citations | Average publication citations |
| 23 | Taiwan | 6 | 0.84 | 0.00 | 5 | 1 | 0.16 | 23 | Singapore | 54 | 54.00 |
| 24 | Thailand | 5 | 0.70 | 0.00 | 2 | 3 | 0.60 | 24 | New Zealand | 51 | 25.50 |
| 25 | Singapore | 5 | 0.70 | 0.00 | 3 | 2 | 0.40 | 25 | Czech Republic | 49 | 24.50 |

*SCP* single country publications, *MCP* multiple country publications

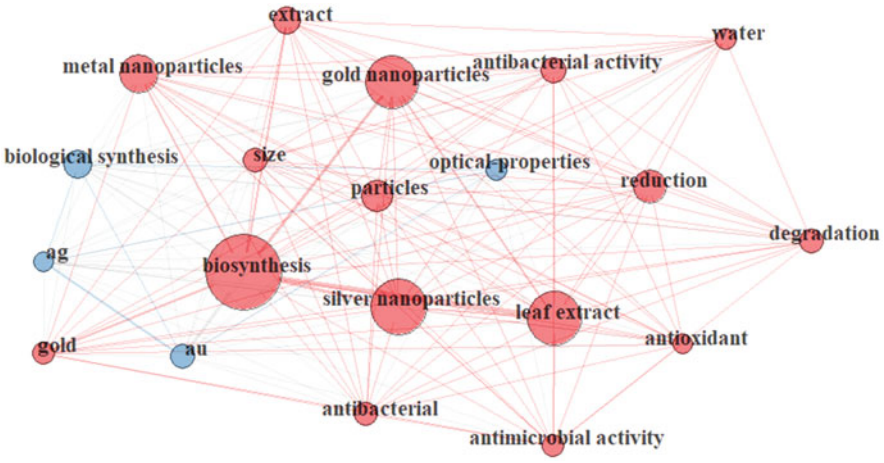


**Fig. 1.4** Co-occurrence network of the top 20 terms on biogenic synthesis research. The sphere of the terms depicts the frequency of occurrences in studies. The line thickness between terms shows the degree of cooperation

has been documented in the scientific impact of developing nations of the world by Gonzalez-Brambila et al. [20] that the most used tool to evaluate a nation's scientific feet is international comparison with peer countries [21–23]. The scientific input based on publications and citations of each country was compared to their relative impact; it was concluded that India which was among the other eight developing countries of the world is reducing her science gap with research and development (R&D) investment and the velocity of their scientific impact is rising at more than double the rate of the developed world [20], and this may be the reason why India a newly industrialized country (NIC) would have the largest number of publications than Australia ($n = 7$; 0.98%) which is among the developed nations of the world. Secondly, it could be that in the last few years, an increasing number of developing countries like India, China and South Africa ($n = 133$, 52, 25; 18.63%, 7.28%, 3.50%) ranking 1st, 4th and 8th position, respectively, have declared publicly their dedication to science and technology as a primary pillar to their economic development making them to rank as one of the top most prolific countries [20]. Nigeria ($n = 14$; 1.68%) ranked 14th position, while Brazil ($n = 13$; 1.96%) ranked 13th position among the top 25 most prolific countries in terms of biogenic research output obtained from the WoS (Table 1.3). The encouraging research output for Nigeria might be as a result of the recent input on the part of the Federal Ministry of Science and Technology with the 2012 inauguration of Science, Technology and Innovation (ST&I) revised policy which was centred at building a virile Science, Technology and Innovation competence and potentials necessary to generate a modern economy; a number of specific objectives were highlighted by this agency. These objectives include facts acquisition, sustaining the Nigeria institutions through adequate funding, innovation, sustaining the diffusion of local technology, improvement of ST&I database, producing and sustaining reliable mechanisms for funding

and commencing and strategizing on bilateral and multilateral collaboration in ST&I, among others. Also, the National Agency for Science and Engineering Infrastructure (NASENI) regarded nanotechnology as an essential upcoming area that the country is deficient and not making too much progress in expertise and skills. It was recommended by NASENI that the field of nanotechnology should be given more priority [24].

The stimulating research output by Brazil of 14 publications accounting for about 1.96% of the entire article published placed this country as number 13th in the area of biogenic nanoparticle synthesis. This outcome could be attributed to the fact that Brazil has declared her commitment to science and technology, knowing that it serves as a strong pillar to any country's economic growth [20].

Citation share is the number of cites that a given country received in comparison to the overall number of citations that were produced around the world in a given period [20]. The categorized order of these countries was slightly altered when productivity was calculated based on the number of citations per country. India still maintained itself in the list of top 25 prolific countries in terms of citations with a total citation of 1039 and an average publication citation of 7.81%, while Korea and Nigeria had 941 and 881 amounting to 18.45% and 10.87% of the total citation and were both 2nd and 3rd positions on the list of top 25 most productive countries based on the number of citations obtained per country. The efficient output of scientific research of a country is extensively based on the innovation in technology, population size, economic development and availability of fund for scientific research, existence of tranquil environment and excellent policies enacted by the government of that country, in addition to the existence of modern analytical instruments, and all these factors are exhibited by Korea [25].

The top 10 as regards average publication citations are India (7.81%), Korea (18.45%), Nigeria (10.87%), Brazil (10.92%), Japan (26.72%), Malaysia (12.57%), China (15.24%), Taiwan (32.50%), Iran (18.38%) and South Africa (10.65%), respectively. South Africa occupying the tenth position and number two position in Africa ranking behind Nigeria could be seen in their strong research and development initiatives in biology and agricultural sciences; they are at the same time bridging the gap with more research output in clinical medicine and biomedical research [20].

Figure 1.5 depicts the top countries' partnership network on green synthesis research. The bigger the coloured circle, the better the number of collaboration/teamwork among countries. In addition to this, a line having a thicker diameter in between two circles demonstrates the teamwork strength between the two countries. It is interesting to see that India, Iran, Saudi Arabia and Korea correspondingly exhibit the most collaborative partnership between 9 and 15 teamwork alliances with other countries. The generated cluster set-up discloses that India, Iran, Saudi Arabia and Korea top the list with a collaborative strength of 15, 10, 10 and 8, respectively, with the four countries going into partnership with each other and commonly entering into collaboration with Italy, Russia, South Africa, the USA and Taiwan as seen in Fig. 1.5. These four countries are the 1st, 2nd, 6th and 3rd on the list of most productive countries (Table 1.4), and their efficiency and productivity can be

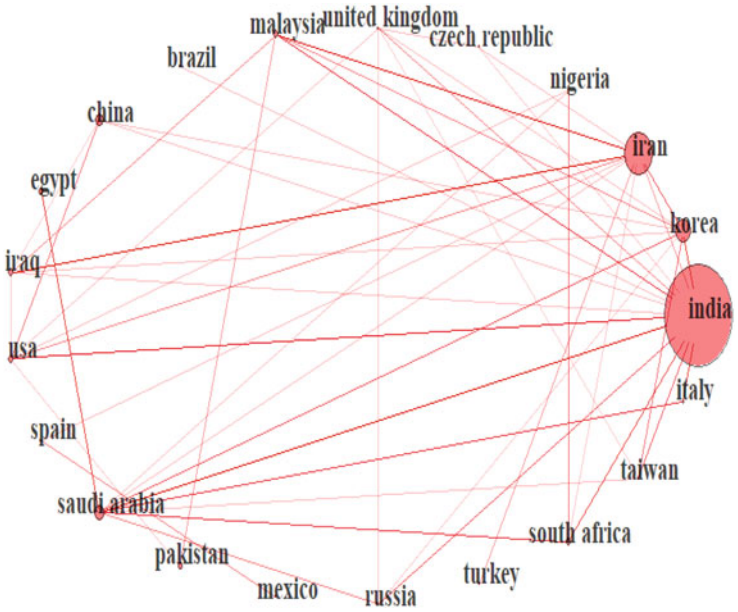


**Fig. 1.5** Country collaboration network on green synthesis research. Each sphere depicts a country. The line thickness between shows the collaboration strength between different countries

attributed to a high level of participation in international and probably multinational collaboration with other countries, which is capable of impacting research visibility and citation rate [26–28].

India and Iraq showed a greater teamwork alliance with Saudi Arabia, the USA, Iraq and Malaysia, as seen in the high degree of the coloured lines between these countries. Malaysia teamwork alliance with five countries of the world, viz. Pakistan, Iraq, India, Iran and Korea, is quite noticeable (Fig. 1.5). Although China is not top on the list of collaboration networks, their teamwork with about 4 countries from the top 20 nations might be due to some of their government policies like funding researchers and scientists to pursue career abroad and framework programme co-sponsored by China and European Union (https://www.enago.com). Nigeria collaborative linkage with three countries, viz. the USA, Saudi Arabia and South Africa, can be attributed to the good work of Tertiary Education Trust Fund (TETFund) which is intended to afford opportunity to lecturers in Nigeria University, Polytechnic and College of Educations to be trained abroad, thereby enabling them to interact with other researchers worldwide and benefit from such exposures and interaction to the advantage of research output in Nigeria educational system.

**Table 1.4** Bibliometric assessment on the 20 most prolific authors on green synthesis nanoparticles (1994–2019)

| Order | Author | Affiliation | Nation | Publications | *h*-index | *g*-index | TC |
|---|---|---|---|---|---|---|---|
| 1 | Nasrollahzadeh M | Department of Chemistry, Faculty of Science, University of Qom, Qom | Iran | 20 | 17 | 20 | 953 |
| 2 | Sajadi SM | Department of Petroleum Geoscience, Faculty of Science, Soran University, PO Box 624, Soran, Kurdistan Regional Government | Iraq | 14 | 12 | 14 | 712 |
| 3 | Veisi H | Department of Chemistry, Payame Noor University, Tehran | Iran | 12 | 9 | 12 | 368 |
| 4 | Bora U | Medicinal Chemistry Division, Regional Research Laboratory, Jorhat | India | 9 | 6 | 9 | 241 |
| 4 | Hemmati S | Department of Organic Chemistry, Faculty of Chemistry, Bu-Ali Sina University, Hamedan | Iran | 9 | 6 | 9 | 220 |
| 4 | Maaza M | School of Physics, University of Witwatersrand, Johannesburg, South Africa | South Africa | 9 | 6 | 9 | 433 |
| 4 | Rostami-Vartooni A | Department of Chemistry, Faculty of Science, University of Qom, Qom | Iran | 9 | 8 | 9 | 463 |
| 5 | Fardood ST | Department of Chemistry, University of Zanjan | Iran | 8 | 6 | 8 | 125 |
| 5 | Govindarajan M | Division of Phytochemistry and Vector Biology, Department of Zoology, Annamalai University, Annamalai Nagar | India | 8 | 7 | 8 | 239 |
| 5 | Khan M | King Abdullah Institute for Nanotechnology, King Saud University | Saudi Arabia | 8 | 4 | 8 | 134 |
| 5 | Ramazani A | Department of Chemistry, University of Zanjan | Iran | 8 | 6 | 8 | 125 |
| 5 | Shameli K | University Technology Malaysia (UTM) | Malaysia | 8 | 7 | 8 | 307 |
| 6 | Nagabhushana H | Department of Studies and Research in Physics, University of Tumkur | India | 7 | 6 | 7 | 225 |
| 7 | Benelli G | Department of Agriculture, Food and Environment, University of Pisa | Italy | 6 | 5 | 6 | 94 |
| 7 | Jafarizadeh-Malmiri H | Department of Chemical Engineering, Sahand University of Technology | Iran | 6 | 5 | 6 | 62 |
| 7 | Kim YJ | Department of Oriental Medicine Biotechnology, College of Life Sciences, Kyung Hee University, Yongin, Korea | Korea | 6 | 6 | 6 | 154 |

| | | | | | | | |
|---|---|---|---|---|---|---|---|
| 7 | Philip D | Department of Physics, Mar Ivanios College, Thiruvananthapuram | India | 6 | 6 | 6 | 697 |
| 7 | Singh P | Department of Oriental Medicine Biotechnology, College of Life Sciences, Kyung Hee University, Yongin | Korea | 6 | 6 | 6 | 278 |
| 7 | Suresh D | Department of Studies and Research in Chemistry, Tumkur University, Tumkur | India | 6 | 6 | 6 | 208 |
| 7 | Wang C | Department of Oriental Medicine Biotechnology, College of Life Sciences, Kyung Hee University, Yongin | Korea | 6 | 6 | 6 | 147 |

*TC* total citations

## 1.6 Most Prolific Authors Engaged in Green Synthesis Nanoparticle Research Retrieved from WoS (2007–2018)

Table 1.4 depicts the list of 20 most proactive authors on green synthesis nanoparticle research (2007–2018). These 20 most proactive authors contributed 171 research items of the total 710 publications, with an average of 8.55 articles per author. The total number of papers published by an author can be used to quantify his/her overall impact, although it may be overblown by an undersized number of a big hit that may not necessarily reflect the researcher's output if he or she is a co-author on a paper with many more authors. Seven of these authors published articles with a higher number than the group average (8.55). The authors are Nasrollahzadeh M (20 publications), Sajadi SM (14 publications), Veisi H (12 publications), Bora U (9 publications), Hemmati S (9 publications), Maaza M (9 publications) and Rostami-Vartooni A (9 publications) (Table 1.4). It is interesting to see that five out of these seven authors are from Iran; this could be as a result of the unwavering economy of Iran, which ranks second in the world on natural gas reserve and fourth in crude oil reserve. It has been opined that the economy potency of a country has an effect on the research productivity of that country [26, 28–30]. In addition, citation analysis (a procedure that measures the quality of an article by quantifying the number of times other researchers cited it in their published work) was obtained from WoS (2007–2018) and used for this bibliometric investigation. Citation per paper enables a comparison of researches irrespective of age. As regards citation, these 20 top prolific authors have an overall cumulative citation of 6185 as depicted by Table 1.3, and the 7 authors mentioned above have a citation of 953, 713, 368, 241, 220, 443 and 463, respectively (Table 1.4). The *h*-index summation of the top 20 proactive researchers was computed to be 140, with an average *h*-index value of 7. *h*-index is usually employed to compute the scientific research productivity of researchers [31]. Only three authors, as seen in Table 1.3, exhibited higher *h*-index value than the group average. These are Nasrollahzadeh M with *h*-index of 17, Sajadi SM with an *h*-index of 12 and Veisi H with an *h*-index of 9; other authors fell below the average group *h*-index.

## 1.7 Most Cited Journal on Green Synthesis Nanoparticle Research

The 710 articles considered under this bibliometric investigation were published in 243 journals from different scientific fields. The most cited journal in terms of green synthesis research during this survey period (2007–2018) is *Green Chemistry* published by Royal Society of Chemistry with total citations of 1715 of the overall citation of the 25 most cited articles gotten from WoS. The number of citations recorded for *Green Chemistry* above exceeds the average citations (232) of the most referenced publication, followed by *Colloids and Surfaces A: Physicochemical and Engineering Aspects* published by Elsevier Science BV with an overall citations of 763; this also surpasses the average citations 232 of the most cited article, while the

third on the list is *Colloids and Surfaces B: Biointerfaces* also published by Elsevier with an entire citations of 398. It has been documented by Mo et al. [32] that citation is not an ideal index to assess author's impact on a particular field. An article with the title Green Synthesis of Metal NPs using plants authored by Iravani [33] and published by Royal Society of Chemistry under the journal *Green Chemistry* was the most cited with a total citation of 910 with a total citation per year of 113.8. In this research work, the author discussed eco-friendly ways in the production of green synthesis nanoparticles using plant parts; he enumerated that nanoparticles synthesized via green route are more stable and faster and concluded by saying the various advantages of this route had spurred researchers into exploring the mechanisms of metal ion uptake and bioreduction brought about by plant extract [33]. Different researchers carried out their research on the green method of synthesizing nanoparticles and encouraged going the greener pathway as it has a lot of advantages over the chemical method of synthesis (Table 1.5).

## 1.8 Future Prospect

Future prospect in the area of green synthesis is to revamp this flourishing technology from laboratory scale to commercial mass production; there should also be a thorough evaluation of the biological effects of biogenic synthesis with the conventional and physical synthetic pathway. Efforts should be geared by natural product researchers towards the recognition of bioactive components of plants responsible for the reduction, growth, nucleation and stabilization of metal oxide NPs.

## 1.9 Challenges Posed by Green Nanotechnology

Regardless of the promising prospect of green nanotechnology, there is this heightened apprehension that some particular NPs unintentionally may create serious unfavourable health challenges and environmental pollution; this reason has catalysed the emergence of nanotoxicology field in examining the effect and possible risks that biogenic NPs might pose to man and his immediate environment. Zhang et al. [34] highlighted some of the possible environmental risks linked with nanotechnology:

- Distribution of harmful persistent nanomaterials bringing about environmental trauma
- Unpredictable effect on the life cycle phases in our immediate environment.
- Penetration of toxic/harmful nanomaterials into human body through inhalation and pricking the skin nodes and through blood circulation

In the same vein, another challenge experienced in this field is the unambiguous blueprint for scientist and researchers in the embryonic stage of green nanotechnology; additionally, most nanotechnologies are carried out on a laboratory scale, and

**Table 1.5** Twenty-five most referenced publications retrieved from WoS 2007–2019

| Order | Reference | Topic | Journals | TC | TC/ year |
|---|---|---|---|---|---|
| 1 | Iravani et al. (2011) | Green synthesis of metal NPs using plants | *Green Chemistry* | 910 | 113.8 |
| 2 | Li et al. (2007) | Green synthesis of AgNPs using *Capsicum annuum* L. extract | *Green Chemistry* | 457 | 38.1 |
| 3 | Bar et al. (2009) | Green synthesis of AgNPs using latex of *Jatropha curcas* | *Colloid Surf A: Physicochem Eng Asp* | 437 | 43.7 |
| 4 | Nadagouda et al. (2008) | Green synthesis of AgNPs and PdNPs at room temperature using coffee and tea extracts | *Green Chemistry* | 348 | 31.6 |
| 5 | Makarov et al. (2014) | Green nanotechnologies: Synthesis of metal NPs using plants | *Acta Naturae* | 320 | 64.0 |
| 6 | Sangeetha et al. (2009) | Green synthesis of zinc oxide NPs by *Aloe barbadensis miller* leaf extract: Structure and optical properties | *Mater Res Bull* | 265 | 33.1 |
| 7 | Dipankar et al. (2012) | The green synthesis, characterization and evaluation of the biological activity of AgNPs synthesized from *Iresine herbstii* leaf aqueous extract | *Colloid Surf B: Biointerfaces* | 208 | 29.7 |
| 8 | Edison et al. (2012) | Instant green synthesis of AgNPs using *Terminalia chebula* fruit extract and evaluation of their catalytic activity on reduction of methylene blue | *Process Biochem* | 200 | 28.6 |
| 9 | Prakash et al. (2013) | Green synthesis of AgNPs from leaf extract of *Mimusops elengi* Linn for enhanced antibacterial against multi-drug resistant clinical isolates | *Colloid Surf B: Biointerfaces* | 190 | 31.7 |
| 10 | Ahmed et al. (2016) | Green synthesis of AgNPs using *Azadirachta indic*a aqueous leaf extract | *Radiat Res Appl Sci* | 180 | 60.0 |
| 11 | Dubey et al. (2010) | Green synthesis and characterization of AgNPs and AuNPs using leaf extract of *Rosa rugosa* | *Colloid Surf A: Physicochem Eng* | 178 | 19.8 |
| 12 | Smitha et al. (2009) | Green synthesis of AuNPs using *Cinnamomum zeylanicum* leaf broth | *Spectroc Acta Pt A: Molec Biomolec Spectr* | 173 | 17.3 |
| 13 | Jagtap et al. (2013) | Green synthesis of AgNPs using *Artocarpus heterophyllus* Lam. seed extract and its antibacterial activity | *Ind Crop Prod* | 169 | 28.2 |

(continued)

**Table 1.5** (continued)

| Order | Reference | Topic | Journals | TC | TC/ year |
|---|---|---|---|---|---|
| 14 | Yang et al. (2010) | Green synthesis of palladium NPs using broth of *Cinnamomum camphora* leaf | *J Nanopart Res* | 165 | 18.3 |
| 15 | Aromal et al. (2012) | Green synthesis of AuNPs using *Trigonella foenum graecum* and its size dependant catalytic activity | *Spectroc Acta Pt A: Molec Biomolec Spectr* | 162 | 23.1 |
| 16 | Li et al. (2012) | Fungus mediated green synthesis of AgNPs using *Aspergillus terreus* | *Int J Mol Sci* | 160 | 22.9 |
| 17 | Singh et al. (2010) | A green biogenic approach for the synthesis of AuNPs and AgNPs using *Zingiber officinale* | *DIG J Nanomater Biostruct* | 155 | 17.2 |
| 18 | Saxena et al. (2012) | Green synthesis of AgNPs using aqueous solution of *Ficus benghalensis* leaf extract and characterization of their antibacterial activity | *Mater Lett* | 153 | 21.9 |
| 19 | Sun et al. (2014) | Green synthesis of AgNPs using tea leaf extract and evaluation of their stability and antibacterial activity | *Colloid Surf A: Physicochem Eng Asp* | 148 | 29.6 |
| 20 | Wang et al. (2014) | Green synthesis of Fe NPs using *Eucalyptus* leaf extract and their treatment of eutrophic wastewater | *Sci Total Environ* | 143 | 28.6 |
| 21 | Ibrahim et al. (2015) | Green synthesis and characterization of AgNPs using banana peel extract and their antimicrobial activity against representative microorganisms | *J Radiat Res Appl Sci* | 139 | 34.8 |
| 22 | Zargar et al. (2011) | Green synthesis and antibacterial effect of AgNPs using *Vitex negundo* L. | *Molecules* | 138 | 17.2 |
| 23 | Kora et al. (2010) | Gum Kondagogu (*Cochlospermum gossypium*): A template for green synthesis and stability of AgNPs with antibacterial application | *Carbohydr Polym* | 137 | 15.2 |
| 24 | Dhand et al. (2016) | Green synthesis of AgNPs using Coffea arabica seed extract and its antibacterial activity | *Mater Sci Eng C: Mater Biol Appl* | 134 | 44.7 |
| 25 | Kumar et al. (2011) | Green synthesis of AuNPs with *Zingiber officinale* extract: Characterization and blood compatibility | *Process Biochem* | 132 | 16.5 |

*TC* total citation, *TC/year* total citation

there is a need to revamp this flourishing technology to commercial mass production [35].

In addition to this, cadmium nanoparticles referred to as quantum dots (a semiconductor metalloid crystal with an estimated size of 2–100 nm) have exhibited favourable hope in the identification and therapeutic management of cancer coupled with targeted drug delivery as a result of their adjustable size fluorescence with the effortless operation in tissue targeting, but various data available on the pharmacology and toxicity of cadmium NPs (quantum dots) need to be addressed so as not to penetrate the biological domain in nanoform since cadmium contamination in our environment can bring about the risk of new cancer growth because vulnerability to cadmium has been linked to tumours in the kidney, lung, liver, prostate and urinary bladder in man [36].

## 1.10 Conclusion

Biogenic synthesis of metal oxide NPs had been an extremely attractive area of research over a period of 10 years. Several components of natural extracts like bacteria, fungi, yeast and plant extracts have been used for the bio-fabrication of NPs. Observation reached in this study revealed an international increase in research related to green synthesis nanoparticle as evidenced in the Lokta's analysis with the goodness of fit depicting that scientific productivity in this field correlates with Lokta's law signifying that the number of publication related to this field will be on the increase.

## References

1. Duraipandiyan V, Ayyanar M, Ignacimuthu S (2006) Antimicrobial activity of some ethnomedicinal plants used by Paliyar tribe from Tamil Nadu, India. BMC Complement Altern Med 6(1):35
2. Verma S, Singh SP (2008) Current and future status of herbal medicines. Vet World 1(11):347
3. Ai J, Biazar E, Jafarpour M, Montazeri M, Majdi A, Aminifard S, Zafari M, Akbari HR, Rad HG (2011) Nanotoxicology and nanoparticle safety in biomedical designs. Int J Nanomed 6:1117
4. Jain N, Bhargava A, Majumdar S, Tarafdar JC, Panwar J (2011) Extracellular biosynthesis and characterization of silver nanoparticles using Aspergillus flavus NJP08: a mechanism perspective. Nanoscale 3(2):635–641
5. Kulkarni N, Muddapur U (2014) Biosynthesis of metal nanoparticles: a review. J Nanotechnol 2014:Article ID 510246
6. Arya A, Gupta K, Chundawat TS, Vaya D (2018) Biogenic synthesis of copper and silver nanoparticles using green alga Botryococcus braunii and its antimicrobial activity. Bioinorg Chem Appl. Article ID 7879403, 1–9
7. Larayetan R, Ojemaye MO, Okoh OO, Okoh AI (2019) Silver nanoparticles mediated by *Callistemon citrinus* extracts and their antimalaria, antitrypanosoma and antibacterial efficacy. J Mol Liquids 273:615–625
8. Ekundayo TC, Okoh AI (2018) A global bibliometric analysis of Plesiomonas-related research (1990–2017). PLoS One 13(11):e0207655

9. Olisah C, Okoh OO, Okoh AI (2019) Global evolution of organochlorine pesticides research in biological and environmental matrices from 1992 to 2018: a bibliometric approach. Emerg Contam 5:157–167
10. Olisah C, Okoh OO, Okoh AI (2018) A bibliometric analysis of investigations of polybrominated diphenyl ethers (PBDEs) in biological and environmental matrices from 1992–2018. Heliyon 4(11):e00964
11. Sa'ed HZ, Waring WS, Al-Jabi SW, Sweileh WM (2017) Global cocaine intoxication research trends during 1975–2015: a bibliometric analysis of web of science publications. Subst Abuse Treat Prev Policy 12(1):6. s13011-017-0090-9
12. Sun J, Guo Y, Scarlat MM, Lv G, Yang XG, Hu YC (2018) Bibliometric study of the orthopaedic publications from China. Int Orthop 42(3):461–468
13. Siamaki S, Geraei E, Zare-Farashbandi F (2014) A study on scientific collaboration and co-authorship patterns in library and information science studies in Iran between 2005 and 2009. J Educ Health Promot 3:99
14. Cabral BP, Fonseca MD, Mota FB (2018) The recent landscape of cancer research worldwide: a bibliometric and network analysis. Oncotarget 9(55):30474
15. Lotka AJ (1926) The frequency distribution of scientific productivity. J Wash Acad Sci 16 (12):317–323
16. Cañas-Guerrero I, Mazarrón FR, Pou-Merina A, Calleja-Perucho C, Díaz-Rubio G (2013) Bibliometric analysis of research activity in the "Agronomy" category from the Web of Science, 1997–2011. Eur J Agron 50:19–28
17. Zhang J, Yu Q, Zheng F, Long C, Lu Z, Duan Z (2016) Comparing keywords plus of WOS and author keywords: a case study of patient adherence research. J Assoc Inf Sci Technol 67 (4):967–972
18. Rotimi L, Ojemaye MO, Okoh OO, Sadimenko A, Okoh AI (2019) Synthesis, characterization, antimalarial, antitrypanocidal and antimicrobial properties of gold nanoparticle. Green Chem Lett Rev 12(1):61–68
19. Saquib Q, Faisal M, Al-Khedhairy AA, Alatar AA (eds) (2018) Cellular and molecular toxicology of nanoparticles. Springer, New York
20. Gonzalez-Brambila CN, Reyes-Gonzalez L, Veloso F, Perez-Angón MA (2016) The scientific impact of developing nations. PLoS One 11(3):e0151328
21. Adams J (1998) Benchmarking international research. Nature 396(6712):615
22. King DA (2004) The scientific impact of nations. Nature 430(6997):311
23. May RM (1997) The scientific wealth of nations. Science 275(5301):793–796
24. National Agency for Science and Engineering Infrastructure (2019) Nanotechnology. https://www.naseni.org/nanotechnology.html
25. Qu Y, Zhang C, Hu Z, Li S, Kong C, Ning Y, Shang Y, Bai C (2018) The 100 most influential publications in asthma from 1960 to 2017: a bibliometric analysis. Respir Med 137:206–212
26. Zyoud SH, Fuchs-Hanusch D (2017) A bibliometric-based survey on AHP and TOPSIS techniques. Expert Syst Appl 78:158–181
27. Li T, Ho YS, Li CY (2008) Bibliometric analysis on global Parkinson's disease research trends during 1991–2006. Neurosci Lett 441(3):248–252
28. Liu X, Zhang L, Hong S (2011) Global biodiversity research during 1900–2009: a bibliometric analysis. Biodivers Conserv 20(4):807–826
29. Zhang L, Wang MH, Hu J, Ho YS (2010) A review of published wetland research, 1991–2008: ecological engineering and ecosystem restoration. Ecol Eng 36(8):973–980
30. Peng Y, Lin A, Wang K, Liu F, Zeng F, Yang L (2015) Global trends in DEM-related research from 1994 to 2013: a bibliometric analysis. Scientometrics 105(1):347–366
31. Hirsch JE (2005) An index to quantify an individual's scientific research output. Proc Natl Acad Sci U S A 102(46):16569–16572
32. Mo Z, Fu HZ, Ho YS (2018) Highly cited articles in wind tunnel-related research: a bibliometric analysis. Environ Sci Pollut Res 25(16):15541–15553

33. Iravani S (2011) Green synthesis of metal nanoparticles using plant. Green Chem 3 (10):2638–2650
34. Zhang B, Misak H, Dhanasekaran PS, Kalla D, Asmatulu R (2011) Environmental impacts of nanotechnology and its products. In: Proceedings of the 2011 Midwest Section Conference of the American Society for Engineering Education. pp 1–9
35. Lu Y, Ozcan S (2015) Green nanomaterials: on track for a sustainable future. Nano Today 10 (4):417–420
36. Huff J, Lunn RM, Waalkes MP, Tomatis L, Infante PF (2007) Cadmium-induced cancers in animals and in humans. Int J Occup Environ Health 13(2):202–212

# Current Green Nanotechnology: The Case of Noble Metal Nanocomposites and Applications

2

Elias Emeka Elemike and Wisdom Ivwurie

**Abstract**

Noble metal nanoparticles are important class of nanomaterials which have contributed immensely to the development of nanotechnology. In recent times, the improvement on the properties and applications of the pure noble metal nanoparticles has shifted interest towards the development of their nanocomposites. The noble metals can form composite materials with polymers, cellulose, carbon materials and metal oxides. This chapter will focus on green synthesized nanocomposites of silver, gold and platinum with cellulose, different metal oxides, graphene oxides and polymers. The use of green methods such as plant extracts, microorganism biomolecules and industrial and agricultural wastes are interesting techniques that leads to formation of the nanoparticles with lesser or no toxicity compared to other methods. The different behaviours and applications of the nanocomposites in catalysis, water treatment, sensing and biomedicine would be studied. This work will offer newer perspectives towards the excellent synthesis and applications of the noble metal nanocomposites.

**Keywords**

Green synthesis · Nanocomposites · Noble metals · Carbon materials

## 2.1 Introduction

Nanotechnology has become an interesting science in recent days with nanoproducts widely circulating and being consumed. Over 70 beverages and food products contain nanomaterials according to Nanotechnology Consumer Product Inventory report [1]. Most medical therapy and diagnostics are also recently made easier

E. E. Elemike (✉) · W. Ivwurie
Department of Chemistry, Federal University of Petroleum Resources Effurun, Effurun, Nigeria

© Springer Nature Singapore Pte Ltd. 2020

Q. Saquib et al. (eds.), *Green Synthesis of Nanoparticles: Applications and Prospects*, https://doi.org/10.1007/978-981-15-5179-6_2

through nanotechnology. The world of electronics is also growing in smarter ways, with most of the innovation being made possible by the application of nanotechnology. There are several methods of obtaining nanoparticles which include the solution-based, vapour state and biological methods [2]. The solution-based method includes sonochemical method, solvothermal method, sol-gel, microemulsion, co-precipitation and microwave-assisted methods. The vapour state techniques comprise the laser ablation method, chemical vapour techniques, combustion method and template/surface-mediated synthesis, whereas the biological method involves plant-mediated synthesis, microorganism-assisted methods and agrowaste methods.

Nanomaterials have been majorly prepared by the bottom-up approach (chemical synthesis or solution-based techniques) which involves the use of reducing, surface-active and/or stabilizing agents such as $NaBH_4$, hydrazine and hydroxylamine and stabilizers including dopamine, trisodium citrate, ascorbic acid, gelatine, polyvinylpyrrolidone (PVP) and cetyl triammonium bromide (CTAB) [3]. These agents are toxic, and they pose great risk to the users of the products and also the environment. Their preparation and use are also against green chemistry principles.

The demand for nanoproducts makes it a veritable concern to limit the use of toxic methods or chemicals in producing them. The greener strategy that can employ water as a solvent of synthesis and environmentally friendly materials (such as plant parts, wastes, microorganisms or biomimetic agents) that are of less toxicity and can function as reducing/capping agents becomes a better option. The process should also be of low-cost, easy and save a lot of energy. Nanomaterials made through such means can confidently be applied in water treatment, environmental remediation, biomedicine and sustainable and renewable energy [4].

Microwave-assisted method of synthesizing nanomaterials is another trending green method. The microwave method is compatible with many materials, occurs within the shortest possible time, reduces wastes and can maintain homogeneity of the materials [5].

Nanomaterials have been used in food packaging, textiles and clothing, pharmaceutical formulations, antimicrobial treatment, dental care, electronics, tissue engineering, self-sterilizing polymer films, bone implant, water purification and other applications [6]. When the nanomaterials are made from toxic chemicals, there is a tendency of reaction and gradual release of the toxic substances into the material in use. Such situation leads to toxicity and can be reduced or avoided by current green nanotechnology principles.

Nanocomposites are novel materials which may involve the compounding of nanoparticles (metals, clays, metal oxides) with other materials such as polymers, cellulose and carbon materials to give new materials with improved and extra functions. Our main investigation in this work is to study the different green nanocomposites formed with noble metal nanoparticles and verify their properties and applications.

## 2.2 Noble Metal Nanoparticles

Nanoparticles of different shapes such as nanobelts, nanospheres and nanorods have been made, but it is challenging to synthetically control the formation of their morphologies. One of the few successes recorded is the green method of using vitamin B2 (riboflavin), vitamin B1 and vitamin C to obtain nanospheres, nanowires and nanorods in the presence of water [5]. In this case, vitamin B2 which is interestingly soluble in water functions both as reducing and capping agents. The substrates are also less toxic and biodegradable. However, there are many reports on the green synthesis of noble metal nanoparticles using plant extracts under the influence of water, but most of them give rise to nanospheres [7–12].

The use of plant extracts in nanosynthesis is due to the primary and secondary metabolites in them which can effectively reduce the metal salts and stabilize the nanoparticles. The sizes and morphologies of the synthesized nanoparticles are largely dependent on the concentration of the metal salts and extracts, reaction temperature, pH and time. This green process is widely gaining attention because it is facile, simple, eco-friendly, cheap and sustainable.

The green synthesized colloidal noble metals especially nanosilver are very well applied in antimicrobial formulations, wound dressings, anti-plasmodial, targeted drug delivery, anti-platelet, anti-cancer, sensing and imaging [8]. Due to their large surface area, they also have effective catalytic properties required to destroy toxic substances and some dangerous organic compounds [13]. The shortcoming experienced in the use of plant method of synthesis otherwise called the phytogenic method is the formation of polydisperse nanoparticles due to the presence of different components (flavonoids, alkaloids, saponins, phenols, etc.) in the plant extract. Seasonal variations can also affect the components of the plant, thereby making them inconsistent in behaviour towards nanoparticle synthesis.

Another green method of synthesis involving microorganisms has also been explored. Different microorganisms including bacteria, cyanobacteria, fungi, algae, yeast and actinomycetes have been used to prepare noble metal nanoparticles [14–16].

The microbial synthesis could be intracellular or extracellular. The intracellular method involves several steps of ultrasound treatment and other surfactant reactions that will release the synthesized nanoparticles, whereas the extracellular method is simple and encourages large-scale production [17]. The extracellular method simply involves the treatment of the organisms' culture supernatant with aqueous solutions of the metal salts to form the nanoparticles. The microbial or microgenic biosynthesis is an awesome process because it uses reductase enzymes to accumulate and detoxify metals with considerable monodispersity [15]. One of its disadvantages is that it involves long culturing time and maintenance of sterilized environment.

The use of fungi in microgenic synthesis or mycosynthesis seems more promising than bacteria due to more bioactive metabolites, huge accumulation and improved production associated with fungal organisms [15]. These microbes apply different mechanisms such as metal complexation, biosorption, changes in solubility, extracellular precipitation and oxidation-reduction towards the production of the

nanoparticles. The nanoparticles made by biological method are mostly applied in biomedicine since they are of lesser or no toxicity. However, they are also applied in diverse fields.

Nanoporous gold have been applied as electrode materials for supercapacitors due to their great conductivity and high surface area. Such electrode properties give access to the electrolytes which result in improved performance of the supercapacitors both in aqueous and non-aqueous electrolytes [18].

Nevertheless, microwave-assisted synthetic method is one of the interesting ways of obtaining and controlling the shapes of noble metal nanostructures giving shapes such as prisms, cubes and hexagons. Silver nanorods can be obtained in the absence of surfactants by mixing aqueous silver nitrate ($AgNO_3$) with polyethylene glycol and the reaction subjected to microwave irradiation at temperature of 100 °C and pressure of 280 psi for an hour [5].

The search for improvement on the activities of the monometallic nanoparticles has led to the synthesis of bimetallic noble metal nanoparticles. The bimetallic nanoparticles show enhanced catalytic and optoelectronic properties compared to the monometallic ones. It could therefore be said that the improved properties are due to synergy in the individual properties of the contributing metals which hitherto would also exhibit new and interesting behaviours [19].

These bimetallic nanoparticles could be in the form of core-shell or alloy nanoparticles depending on the synthetic procedures.

Hurtado et al. reported the synthesis of Ag-Au bimetallic nanospherical alloys by simply adding rongalite solution into an aqueous $AgNO_3$ [20]. After a while (approx. 10 min), ascorbic acid and sucrose were added, and there was evidence of metal salt reduction due to appearance of yellow colour. Furthermore, $HAuCl_4$ was added and stirred with appearance of an ochre tone indicating colloidal Ag-Au nanoalloys.

In a similar work by Elemike et al., Au-Ag bimetallic nanoalloys were also prepared in situ using *Solidago canadensis* leaf extract [21]. The bimetallic nanoparticles were seen to be electroactive when used as electrode materials without interfering with the electrolyte solution. Such behaviour explains their stability and therefore they could act as efficient electrocatalysts.

Blosi et al. have also reported the microwave-assisted green synthetic procedures of bimetallic nanoparticles using polyvinylpyrrolidone (PVP) as the chelating or stabilizing agent which ensured homogeneous particle nucleation and shorter reaction time [19]. It is interesting to note that in the microwave procedure, both alloy and core-shell morphologies can be obtained depending on the reaction conditions. It is therefore obvious that bimetallic nanoparticles have improved functionalities than their monometallic counterparts for applications especially in catalysis, medicine and photocatalysis.

## 2.3 Metal Oxides/Semiconductor Nanoparticles

In recent times, ZnO, $TiO_2$, $Fe_2O_3$ and $SnO_2$ are among the widely studied semiconductor nanoparticles with ZnO NPs being the most widely used [1].

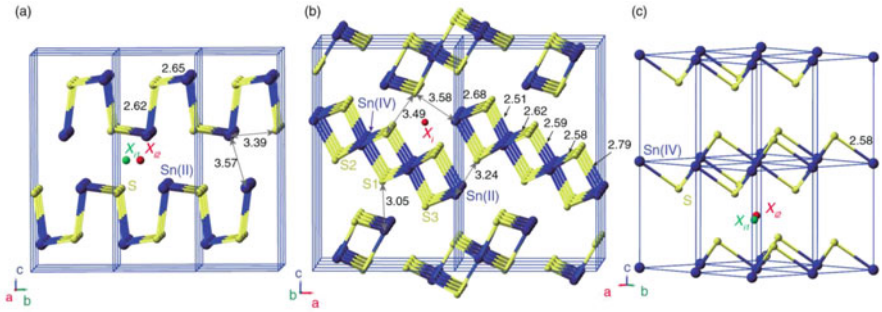


**Fig. 2.1** Crystal structures of (**a**) SnS, (**b**) $Sn_2S_3$ and (**c**) $SnS_2$. (Reprinted from American Physical Society 2016) [25]

CuO and $Cu_2O$ nanoparticles are other interesting semiconductors with vast applications in sensing, photovoltaics, catalysis, batteries and medicine [22]. CuO are preferably applied in magneto-resistance materials, catalysis, nanofluids and electrode materials, and whereas $Cu_2O$ are potentially applied in solar energy, photochemical production of hydrogen from water, generation of photocurrent, gas sensing, CO oxidation and photocatalysis [23]. The formation of any or both of the copper oxide nanoparticles depends on the reaction conditions. Park et al. are of the opinion that $Cu_2O$ can be converted to CuO when the pH of the reaction is increased [24].

Tin sulphide is another interesting semiconductor nanoparticle which is abundant and can exist in stable forms of SnS, $Sn_2S_3$ and $SnS_2$. SnS is preferably applied in thin-film photovoltaic cells due to its low bandgap energy of 1.1 eV which has high energy absorption capacity compared to the $SnS_2$ with bandgap of 2.3 eV. The $Sn_2S_3$ seems to have received the lowest attention among the three, but it is simply a combination of SnS and $SnS_2$. However, its property seems to relate more to SnS. The crystal structures as shown in Fig. 2.1 revealed the differences in the Sn-S bonds among others. In SnS, the Sn-S bond is longer which shows an expanded ionic radius of Sn(II) compared to Sn(IV) [25]. In addition, the coordination of the Sn (II) is by three S, and the Sn(IV) is by six S in an octahedral arrangement.

Green ZnO nanoparticles have been prepared using *Chlorella* microalgae and were further used in the degradation of dibenzothiophene (a sulphur-containing pollutant that could contain heavier petroleum fractions) [4]. From the reports, lower concentration of the green ZnO NPs can desulphurize the pollutant to about 97% efficiency.

Gao et al. have used ZnO nanoparticles as an antimicrobial agent in wound closure [26]. It promotes angiogenesis and blood clotting and induces deposition of collagen and proliferation of fibroblasts. Further in their report, the ZnO nanoparticles effectively exhibited adhesive behaviour for gelatine hydrogels, hydrogel/polymer and tissues. This ability simply shows that there is no need of incorporating the ZnO into hydrogels that have the same property as the skin in order to be used for wound healing or tissue engineering. $TiO_2$ nanoparticles also exhibit

such properties, and both ZnO and $TiO_2$ nanoparticles have been reported to be important components in cosmetics, food and drugs.

Two or more metal oxides can form a composite in two ways, either as a mixture of individual metal oxides to form binary or ternary oxides or multi-metal oxides with properties emanating from the synergy between the combining components. The sol-gel method is preferably used to form the individual binary oxides ($SnO_2$-$In_2O_3$) in a hybrid form instead of multi-metal oxides (Sn-$In_2O_3$) [2].

These semiconductors exhibit bandgap energy resulting from separation and charge transfer from valence band to conduction band. Such electronic movement creates hole leading to electron-hole (e−/h+) pairs which may undergo recombination. The situation further impedes the photoresponse of the semiconductor materials.

The coupling of two semiconductors could lead to hindered electron-hole recombination. In an $SnO_2$-$TiO_2$ nanocomposite system reported by Zhang et al. [27], there is an increased electron mobility effect due to $SnO_2$. Moreover, the conduction band edge of $SnO_2$ has more positive value than $TiO_2$ which results in movement of photo-excited electrons from $TiO_2$ to $SnO_2$ (in the conduction band region). Such movement suppresses recombination, thereby improving the light absorption and transformation effect of the semiconductor couple.

Since these nanomaterials are commercially being produced and used, one pertinent thing is their influence or toxicity towards organisms or environment. Human alveolar epithelial cells have been used to study the in vitro toxic behaviour of CuO, $TiO_2$, ZnO, $Fe_3O_4$, $Fe_2O_3$ and $CuZnFe_2O_4$. The results showed that pure $Fe_3O_4$ and $Fe_2O_3$ nanoparticles were not toxic, $TiO_2$ just triggered DNA damage and CuO induced a great proportion of cell death with DNA damage, whereas multi-metal oxide $CuZnFe_2O_4$ nanoparticles were strongly toxic and damaged DNA. The toxic behaviour of the nanomaterials could be due to some factors which centre around the amount of metal ions released during interaction with the living organisms and the induced production of reactive oxygen species (ROS).

The toxicity of some metal oxides could be reduced by doping with metals, using a chelator (diethylenetriaminepentaacetic acid) or incorporating into polymer solutions. Such reduces the release of the metal ions that causes the toxicity. A typical example is the distribution of Fe atoms around ZnO crystal structure which improved the stability and reduced the aqueous dissolution or release of the metal ions in biological media [2].

## 2.4 Polymer Nanomaterials

Polyaniline (PAni), polythiophene (PT), polypyrrole (PPy), polyacetylene (PA), polyphenylene (PP) and their derivatives are a group of materials that have sparked great interest in the study of nanotechnology due to their efficient processability, conductivity and tunable electronic and optical properties [28]. Due to these properties, they stand out as interesting materials for applications in optoelectronic and luminescence devices. Polyethylene glycol (PEG), polylactic acid (PLA) and

poly(lactic-co-glycolic acid) (PLGA) are also some group of synthetic polymers that are biocompatible and can easily form nanoparticles [29]. Polymeric nanoparticles are widely applied in pharmaceutics and biotechnology. They act as nanocarriers because of their interesting properties such as biodegradability, biocompatibility, nonimmunogenicity and nontoxicity [30].

It is always a difficult task to make nanomaterials of controllably the same size for use in industrial applications as when they differ even in few nanometres, they tend to have different functions. Sol-gel method has become a technique that could considerably control the size of nanoparticles for industrial applications. In the case of polymer nanomaterials, the monomers can be mixed, hydrolysed and subjected to polycondensation reactions.

It has been reported that some monomers can be dissolved in water-ethanol mixture with mild heating (75 °C) to give nanospheres of the same size using para-phenylenediamine as a catalyst. Moreover, nanoparticles of polybenzoxazine have been prepared without the introduction of any matrices or surfactants [31].

Polymeric nanoparticles have found wide application especially in biomedicine. They serve as drug carriers and can effectively deliver non-water-soluble drugs and prevent unstable compounds from degradation [29]. There are three major methods through which the polymer nanoparticles could be made to deliver drugs: encapsulation, adsorption and dispersion on the polymer matrix.

## 2.5 Cellulose and Nanocellulose

Cellulose fibres are porous materials with microfibrillated width of about 10–30 nm connected to each other in a three-dimensional manner. Cellulose is one of the most abundant polysaccharides with many hydroxyl groups and a biopolymer formed from glucose molecules connected by β-1,4-glycosidic linkages.

The chemical structure of cellulose is such that it exhibits unique properties including porosity, water retention, renewability, biocompatibility, infusibility and biodegradability. These properties enable them to act as platforms in different reactions and in the formation of composites [32].

Cellulose has been used in different applications like clothing, foods, papers, environmental remediation, energy, water treatment, solar cells, supercapacitors, pharmaceutics and healthcare.

There are both amorphous and crystalline portions of cellulose which occur in different proportions depending on the plant type [33]. It could therefore be said that nanocellulose or cellulose nanocrystals obtained from plants differ and may also be applied to specific purposes. The crystalline part is orderly packed, and it gives the cellulose its rigidity and strength, whereas the amorphous region gives flexibility of the bulk cellulose [34].

There are different types of cellulose which can be used in composites, and they include bacterial cellulose (BC), nanocrystalline or vegetable cellulose (VC) and nanofibrillated cellulose (NFC) or cellulose nanofibres. The major differences

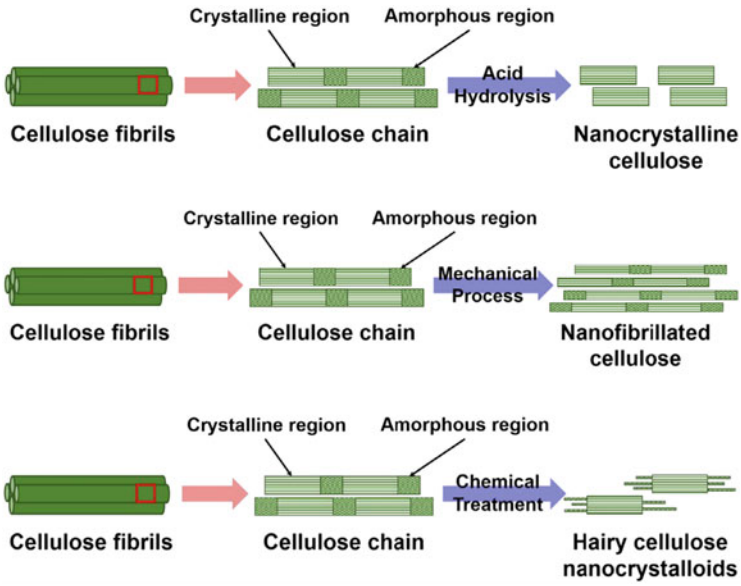


**Fig. 2.2** (**a**–**c**) Different types of nanocellulose showing the amorphous and crystalline regions. (Reprinted from Elsevier 2018) [34]

among them are their morphologies and mechanical behaviour; otherwise, they share the same structure and chemistry [35].

Nanocrystalline cellulose can also be called cellulose nanowhiskers or cellulose nanocrystals, and they are characterized by short rodlike shape of diameter 2–20 nm and length 100–500 nm. They are extracted by acid hydrolysis of the cellulose and are of high crystallinity. The nanofibrillated or cellulose nanofibres are obtained from the cellulose by mechanical means. It is longer than the nanocrystalline cellulose having larger surface area and numerous hydroxyl groups for easier surface functionalization and modification. Figure 2.2a, b shows the nanocrystalline and nanofibrillated cellulose, respectively.

Bacterial nanocellulose is formed through a bottom-up approach whereby sugars from bacteria such as *Gluconacetobacter xylinus* build up for some weeks. As a result, the formation of BC differs from the others which are formed by top-down approach of lignocellulosic materials. However, BC is the purest form of nanocellulose devoid of lignin, hemicellulose and pectin. There is a report in recent times on another type of nanocellulose called hairy cellulose nanocrystalloid (HCNC) [34]. It is obtained by chemical treatment of the cellulose (not acid hydrolysis or mechanical treatment) which solubilizes the amorphous part while the crystalline part remains. They are more like the nanocrystalline cellulose with protrusion at the ends of the crystalline part as shown in Fig. 2.2c. The different chemical treatments determine the nature of protrusion.

The chemical modification of cellulose has opened up opportunities of obtaining materials with promising properties [36]. Surface functionalization and modification

of nanocellulose encourage the addition of hydroxyl groups into substrates or replacement of the hydroxyl groups with other groups. One of the major effects is the formation of amphiphobic surface, a surface that takes care of both polar and non-polar media. Such surface enables properties including change in wettability, self-cleaning, anticorrosion and antibacterial. The replacement or modification of the hydroxyl groups may be by etherification, amidation, silylation and carbanylation for various applications.

Generally, nanocellulose has interesting and unique properties such as high thermal ability, high mechanical strength, lightweight and good transparency. They offer these properties to composite materials which improves their applicability.

Core-shell novel nanocomposite materials have been made by coating oxidized cellulose nanocrystals with intrinsically conductive polymer (ICP) or polypyrrole (PPy) [37]. This material exhibits functional properties greater than those of graphene and single- and multi-walled carbon nanotubes. Some of the properties are mechanical strength stronger than steel yet lighter in weight, printability which offers wide applications in flexible electronics, biodegradability and enlarged surface area with active groups and abundance. This material can therefore structurally act as a platform for impregnation of noble metal nanoparticles for other applications especially in biomedicine due to its green nature.

## 2.6 Carbon Nanomaterials

Graphene, a two-dimensional lattice structured $sp^2$ carbon material, has some important and exceptional properties which include the planar structure, high mechanical strength, unique conductivity and optical and electronic behaviour. The large surface area contributes to the graphene materials having great carrier capacity and mobility. Due to these properties, graphene in recent times has been greatly utilized in energy, supercapacitors, electronics, electrocatalysts, water splitting, photovoltaic cells and sensing materials [38].

However, their uses are not restricted to structural materials but have extended to bioapplications. They have found applications as chemotheranostics in cancer treatment, stem cell imaging and biosensing [39].

Graphite can be oxidized to graphene oxides using Hummers method (use of $KMnO_4$ and $H_2SO_4$) or Brodie and Staudenmaier methods ($KClO_3$ and $HNO_3$). The graphene oxide (GO) contains more hydroxyl groups at the base of the planar structures with some other groups such as carboxyl, carbonyl, phenol, lactone and quinone at the edges. Such groups have endowed the oxide with hydrophilic nature and made them to have some distinct properties from the graphene sheets. However, both graphene (graphite) and GO possess interesting electronic, thermal, electrochemical, mechanical and biocompatible properties. The oxygen and hydroxyl molecules in GO can further be reduced to rGO (reduced graphene oxide) using electrochemical, thermal, biological and chemical methods giving rGO improved properties. The properties depend on the parameters applied during reduction which

include the reducing agent, reduction reaction time, reaction and annealing temperature and time. In general, the application of the rGO determines the reduction methods to be used. For instance, biological reduced graphene oxide would be better applied in biological functions.

Carbon nanotubes are obtained from graphene, and they are long and cylindrical with size of about half the width of DNA [40]. There are single-walled carbon nanotubes (SWCNTs) and multi-walled carbon nanotubes (MWCNTs). The carbon nanotubes interestingly absorb near-infrared light waves and transmit them through cells without harming them, a property that has been used in nanomedicine. These nanotubes can be functionalized to have improved properties.

## 2.7 Nanocomposite Materials

Nanocomposites are materials made by the combination of two or more nanosized materials which could be either organic, inorganic or both for improved properties and applications. The obtained composite materials have the properties of the individual components and additional novel characteristics.

The processability and material characteristics of polymers, carbon materials (nanotubes, graphene), cellulose and metal oxides can be improved when their composites are made with metals or other materials.

The expensive nature of noble metals has necessitated their integration into other cheaper materials such as polymers, carbon materials and cellulose which seems to be a better way of improving their properties and applications at a minimal cost [41].

Nanocomposites are prepared the same way as the earlier mentioned methods of synthesizing nanoparticles including self-assembly, lithography, electrodeposition, Langmuir-Blodgett (LB) methods and hydrothermal, microwave and other greener techniques.

In the LB techniques, nanoparticles are synthesized on water surface and made as thin film which is later transferred to a polymer membrane. The nanoparticles (Ag, Au, Pt) offer optical responsibility to the nanocomposites, and their efficiency and applications depend on the interaction with the polymer under specific conditions. Different nanocomposite materials with noble metals are discussed in this work.

### 2.7.1 Noble Metal-Carbon Material Nanocomposites

The noble metal-carbon materials involve both noble metal-graphene-related nanocomposites and noble metal-carbon nanotubes. The material properties of the carbon materials are different which enables them to offer distinct characteristics when compounded with noble metals.

#### 2.7.1.1 Noble Metal-Graphene Nanocomposites

Graphene serves as templates for nucleation and growth of noble metal nanomaterials. The chemical synthetic strategy is the most popularly used synthetic

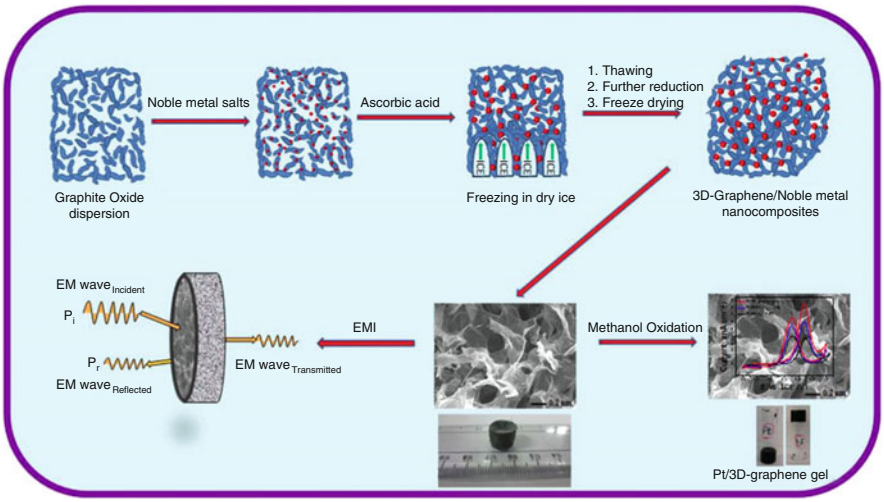


**Fig. 2.3** Fabrication of 3D graphene/noble metal nanocomposites using the freeze-casting method, for use in EMI shielding and as electrocatalyst in the oxidation of methanol. (Reprinted from scientific reports 2015) [38]

method whereby the metal precursor (e.g. $AgNO_3$, $HAuCl_4$, $H_2PtCl_6 \cdot 6H_2O$) is reduced together with GO sheets using agents as amines (hydroxylamine, octadecylamine, oleylamine), $NaBH_4$ and ascorbic acid [41]. Different morphologies of the noble metals, e.g. nanodots, nanowires, nanoseeds and nanosheets, can grow on the graphene depending on the reducing agents used; in other words, the structures or morphologies can be controlled. These chemical-mediated nanocomposites have shortcomings of application in biological substrates and environmental and therefore the advocacy for green procedures.

The noble metal-graphene nanohybrids can have added advantages over the individual nanoparticles due to combined properties from the individual components that make up the composites. Silver and gold nanoparticles have demonstrated great biological properties with less toxicity especially those made from green substrates. Therefore, such green synthesized nanoparticles when combined with graphene-based materials would exhibit highly desirable properties for bio-applications. They can also show improvement in their optical, electronic, sensing, catalytic and magnetic applications. The nature of the composite formation can be twofolds: (a) the nanoparticles can be decorated on the graphene surfaces and (b) they can be encapsulated and covered by the graphene. The difference lies in the relative size ratio of the nanoparticle diameter and the graphene sheets (lateral dimension) with the latter occurring when the nanoparticle sizes are larger [39].

Freeze-casting process can be used to prepare porous 3D graphene/noble metal nanocomposites as shown in Fig. 2.3. The method involves reaction of graphene oxide and the metal salt solution using reducing/stabilizing agent such as ascorbic

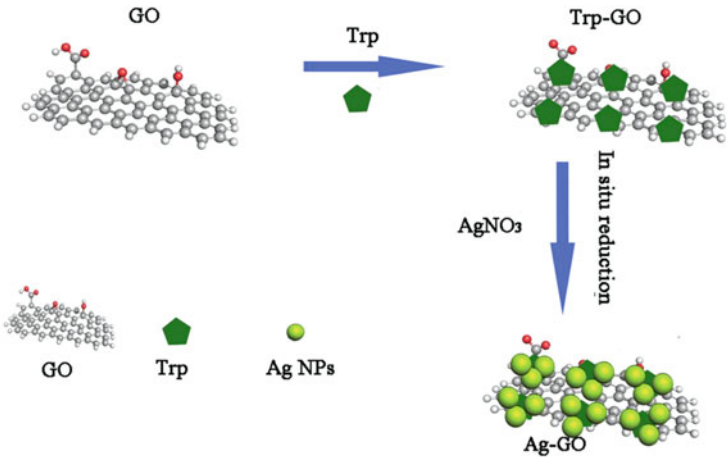


**Fig. 2.4** Synthetic pathway of decorating Ag on graphene oxide. (Reprinted from Elsevier 2014) [44]

acid. The freezing process then follows, and process time and temperature are important parameters to the formation of the 3D graphene.

Sahoo et al. have prepared 3D graphene/noble metal nanocomposites by the method of a cost-effective green process for electromagnetic interference (EMI) shielding and electrocatalytic oxidation of methanol [38]. The nanocomposites showed interesting stability, good electrocatalytic performance and abnormal poison tolerance better than such existing Pt/reduced graphene oxide nanocomposites. There is no doubt that the intercalation of the noble metals on graphene sheets leads to existence of electron clouds and increased $\pi$-$\pi$ interaction which enhances great electron transport and improves conductivity.

Graphene can serve as substrate for surface-enhanced Raman scattering (SERS), a property for sensitive and selective spectroscopic molecular detection even at very low concentrations but with some limitations involving particle aggregation leading to *p-p* interactive stacking [42, 43]. On the other hand, noble metal nanoparticles are also interesting candidates for highly sensitive detection due to SERS properties. Therefore, the decoration of the noble metal nanoparticles on GO leads to improved SERS properties that nullifies the aggregation effect of the GO.

Yang et al. [44] have reported the tryptophan-assisted synthesis of Ag-graphene oxide nanocomposites for improved SERS applications. The use of tryptophan with interesting functional groups as a reducing/stabilizing agent is a green procedure that avoids the chemical methods of toxic hydrazine and sodium borohydride. Figure 2.4 explains the synthetic pathway and the decoration of Ag on the GO.

GO-Ag nanocomposites have been used as an efficient photocatalytic material in the oxidation of cyclohexane, reduction of nitrobenzene to aniline and degradation of dyes (rhodamine B, methylene blue) and acetaldehyde, among others [45].

When silver nanoparticles are incorporated into materials with large surface area such as the 2D materials, the nanoparticles are properly dispersed on the material surface which prevents agglomeration [45]. However, active reaction sites are created on the nanocomposites which aids photocatalysis. Further photocatalytic mechanism which can be favoured by reduction in the rate of electron-hole recombination is experienced in the hybrid materials. Graphene oxide and reduced graphene oxide are better materials to act as platforms for incorporation of Ag than graphene sheets due to their dispersion ability and stability in both aqueous and non-aqueous media.

Bimetallic noble metal nanomaterials, including Pt-Ag, Au-Pt, Pd-Ag, Pt-Pd and Au-Pd, have also been incorporated into graphene to give interesting nanostructures and enhanced properties [41]. Pt-Pd bimetallic nanodendrites on graphene nanosheets have shown improved catalytic properties. Au-Pd nanoflowers have also been added by electrostatic interaction into an ionic liquid-grafted graphene sheets. These noble metal nanostructures decorated on graphene have shown promising applications in sensing of gas, biomolecules and chemicals and as catalysts in fuel cells. The graphene-noble metal nanocomposites are more effective in applications than the carbon black-noble metal composites, while the bimetallic metal-graphene nanostructures showed the most improved applications due to synergistic properties.

Raghavendra et al. have reported that core-shell $Pd_{core}@Au_{shell}$ decorated with reduced graphene oxide showed improved properties compared to the single metal-rGO nanocomposites [46]. The core-shell morphology immensely contributes to the enhanced behaviour of the nanocomposites as electrocatalysts in oxygen reduction reactions (ORR).

#### 2.7.1.2 Noble Metal-Carbon Nanotubes

Carbon nanotubes (CNTs) have interesting properties ranging from high chemical stability, electrical conductivity, large surface area, efficient mechanical strength and great thermal stability [47]. Noble metals on their own also exhibit unique optical, electronic and magnetic properties. The deposition of the nanoparticles on carbon nanotubes combines the properties of the different nanomaterials in interestingly new nanocomposites for efficient applications. The nanocomposite material exhibits characteristic interfacial interactions which determine their applications. The most interesting application of this group of nanocomposites is in the field of sensors and SERS in which the localized surface plasmon effect of the noble metals and the large surface area effect contributed by the nanotubes among other properties showed a stronger effect and multifold sensitivity.

The preparation of CNT-metal nanoparticle composites requires proper dispersion of the CNTs in a liquid media; otherwise poor dispersion may lead to some bottlenecks in the applications. Polymers can be incorporated into the aqueous media to serve as a non-covalent dispersion method. The function of the polymer materials is to provide good biocompatibility with the CNTs. In this regard, chitosan has been used to enhance the dispersion of multi-walled carbon nanotubes (MWCNTs) in

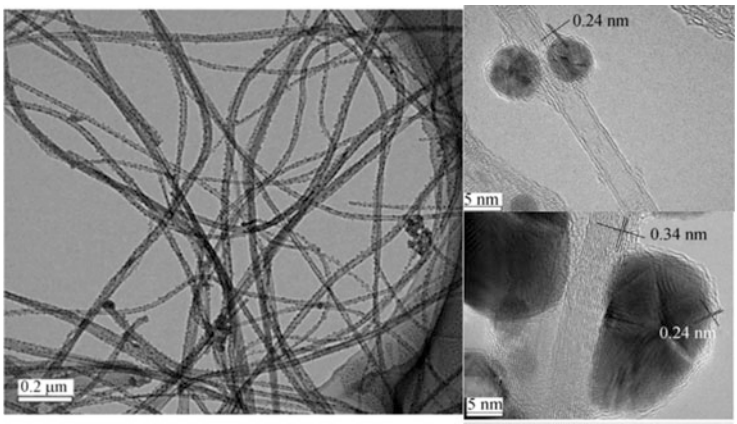


**Fig. 2.5** High-resolution TEM showing the deformed Ag nanocrystals on the MWCNTs. (With permission from Springer 2009) [48]

liquid media. Single-walled carbon nanotubes (SWCNTs) have also been dispersed in Nafion aqueous solution [47].

There is another interesting way of obtaining the metal nanoparticle-CNT hybrid nanocomposites referred to as "parasitical" method. This involves the in situ growth of the metal nanoparticles on the CNTs. The growth mechanism or rather the interaction of the different materials is an important phenomenon which affects the structure and properties of the nanocomposites [48].

Zhenxia et al. have reported that during the growth of Ag nanocrystals on MWCNTs, there was observed deformation as shown in Fig. 2.5, which the easiest possible explanation may be due to electrostatic interaction involved with the Ag and π-carbon networks [48].

Intrchom et al. have reported the interaction of carbon nanotube-noble metal hybrids when exposed to algae [49]. It was observed that the carbon nanotubes delay the release of Ag ion into the organisms. $AgNO_3$ alone released $Ag^+$ which led to recorded toxicity of the algae. However, the interaction of the nanocomposite recorded the secretion of polymeric substance which serves as a protective layer against toxicity. The CNT-Pt hybrid was less toxic compared to the CNT-Ag hybrid, but the effect still depends on the concentration. Figure 2.6a–d shows algae and the level of damage done on the algae by $Ag^+$ and the nanocomposites. There was tearing of the algal organisms by Ag, but the use of the nanocomposites on the organisms did not show much algal cellular disruption.

### 2.7.2 Noble Metal-Metal Oxide Nanocomposites

Metal oxides have good optical, electronic, redox and catalytic properties required for different applications, but their functional performance is limited. However, the incorporation of noble metals into the metal oxide leads to better performance of the

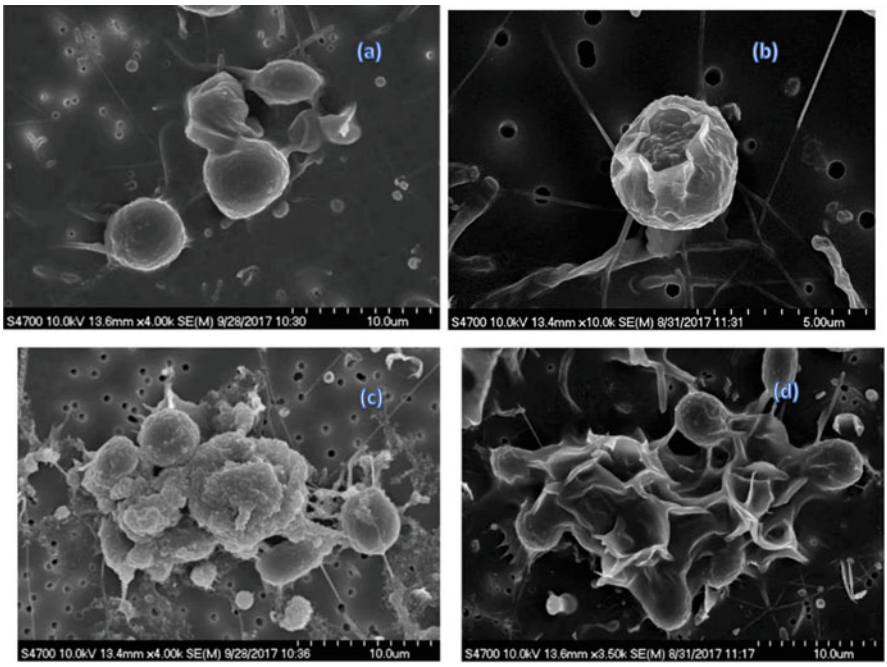


**Fig. 2.6** Appearance of algae cultures indicating (**a**) algae alone, (**b**) $Ag^+$ interaction with algae, (**c**) CNT-Ag and (**d**) CNT-Pt. (Reprinted from Scientific Reports 2018) [49]

nanocomposites with the formation of core-shell structure more effective in application than the surface doping modification technique [50]. Core-shell materials have been reported whereby the metal oxides or semiconductors serve as the shell materials and the noble metals become the core components. These structures have been verified to be active in applications including information storage and components of electronic circuits [51]. The stability of the silver nanoparticles has been improved by forming $SnO_2$ shell around them. This is simply because the metal oxides resist coagulation by forming electrosteric barrier around the surface of the particles [51].

Au-ZnO nanocomposites have been prepared using phytochemicals or biological method [52]. The gold salt, $HAuCl_4 \cdot 3H_2O$, was slowly introduced into the ZnO nanoparticles with a syringe and stirred, followed by the addition of the aqueous biological reducing agents (cumin seeds). The characterization techniques showed that the gold nanoparticles existed on the surface of the ZnO, whereas photocatalytic studies revealed the enhanced degradation of methylene blue by the composite compared to the ZnO alone.

Some other superior nanomaterials such as $Mo_2N/MoS_2/Ag$ have been prepared in recent times with self-lubricating and tribological properties [53].

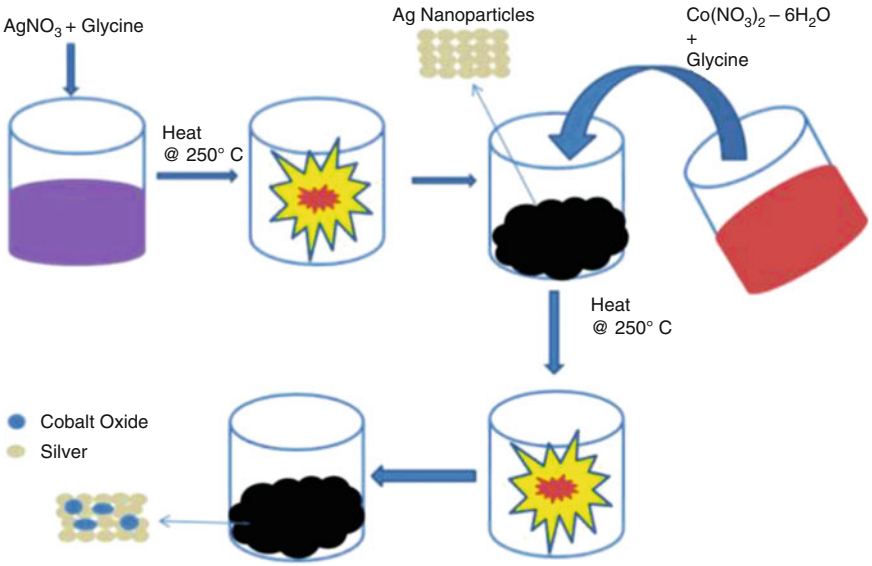


**Fig. 2.7** Green synthetic route of nanocomposites using biomimetic compounds. (Reprinted from ACS Omega, 2018) [56]

$MoS_2$ and Ag have also been incorporated into chitosan to form a nanocomposite by simple green process using ascorbic acid. The nanomaterials represent new electrocatalysts and electrochemical sensors especially for biological molecules [54].

$MoS_2$ is an interesting material that can have wide industrial applications due to its abundance, low cost, good stability and nontoxicity, but it could poorly act as good photocatalyst due to electron-hole pair recombination [55]. However, the combination of $MoS_2$ with noble metals suppresses the recombination phenomenon and positions the nanocomposites for efficient reactions and applications.

Ashok et al. have prepared Ag-$Co_3O_4$ nanomaterials for application as catalysts in electrochemical oxygen reduction and evolution reactions [56]. The cobalt oxide in the matrix improves the rate of adsorption and transport of oxygen whereas the Ag atoms activates the O-O bond splitting, improves the activity, stability, stronger performance and hastens the oxygen reduction reaction kinetics. Figure 2.7 shows a simple green synthesis of Ag-$Co_3O_4$ nanocomposites.

### 2.7.3 Noble Metal-Polymer Nanocomposites

The introduction of noble metal nanoparticles into polymers is an exciting and emerging field of composites that will serve as building blocks for fabrication of nanodevices. This type of composites is connected by covalent and coordination bonds and can easily form films. The bulk polymer materials have properties different from the thin films and thin surface layer configurations. This is a result

of the surface molecular motion and the interfacial interaction involved in the thin films and the layered structures of polymers [57]. However, the surfaces could be hard or soft, have different film thickness and experience different polymer-substrate interaction and thermal properties.

The incorporation of noble metal nanoparticles into polymers improves the conductivity of the polymers, and it is a good way of probing the dynamics and behaviour of the polymer surfaces. These noble metals appear in the form of nanoclusters (1–5 nm) and usually grow as spheres on the surface of the polymers. Bipyridyl-terminated poly(oxyethylene) could be grafted on Pd nanoparticles by simply stirring palladium(II) acetate in acetic acid solution [58]. The prepared metal-polymer composites still contained the polymeric ligand even after drying showing their stability. They are also soluble in methanol, $CH_2Cl_2$, acetone, $CHCl_3$ and water.

Polymers especially the conductive or conjugated polymers (CP) can easily be prepared in a composite with metals in order to enhance their conductivity and optical and electronic properties.

The electronic structure of the polymer, however, greatly affects the behaviour of the incorporated metals as well and enables adequate movement of electronic charges to active sites. The metal-polymer nanocomposites are majorly prepared by electrochemical deposition or electropolymerization methods [28]. This class of nanocomposites is interesting, and the synergy in their properties leads to improved applications. A greener procedure of fabricating this group of nanocomposite may involve the use of metal ion with higher reduction potential than the polymer. The $\pi$-conjugated polymer with electron-donating ability initiates the transfer of electrons to the metals [58]. This leads to the metal being reduced to zero-valent metal by the polymer without the addition of an extra reducing agent. Consequently, the polymer is oxidized since the metal is reduced as shown in the mechanism or pathway described in Fig. 2.8 [28].

Figure 2.9a is a generalized simultaneous in situ reduction of metal salts to their elemental forms and encapsulation by polymeric materials, whereas Fig. 2.9b shows the typical reduction and subsequent stabilization of Au nanoparticles by poly (dithiafulvene) polymer.

Polyaniline (PAni) is a conducting polymer considered as a *p*-type material which is of low cost, very stable and easily prepared and with vast applications. It has been applied in electronics, batteries, separation membranes, sensing, anticorrosion and anti-static coating [59]. Other interesting properties exhibited by PAni could be the photoluminescent properties due to the observed electronic states (polaron, conduction and defect bands) [60]. The nanocomposite of PAni with metal nanoparticles is an interesting way of enhancing their conductivity. The formed nanomatrix can have high sensitivity and selectivity and be well applied in sensing, catalysis and optoelectronics.

In another application, silver nanoparticles have been incorporated into biopolymers to form composites that are used for food packaging [61]. The composite materials have antimicrobial effect due to the nanosilver and would prevent microbial proliferation and oxidation and maintain stability.

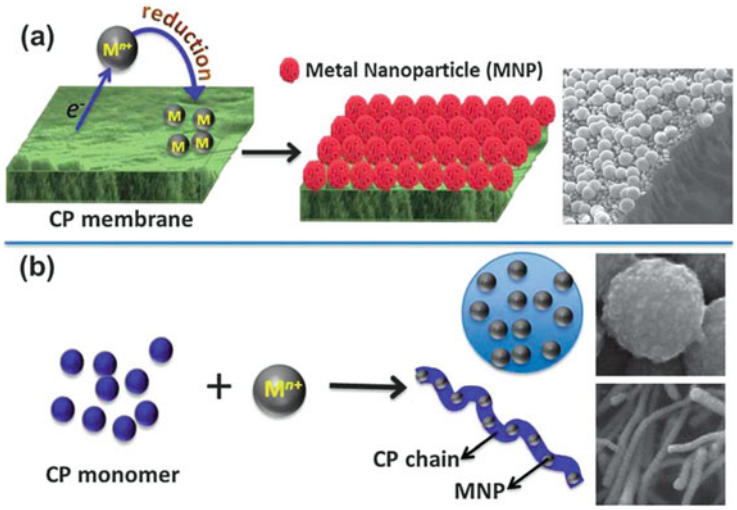


**Fig. 2.8** Grafting of metal nanoparticles on conjugated polymers. (**a**) shows that the surface of the polymer is decorated with the metals while (**b**) explains the integration of the metal nanoparticles into the polymer. (Reprinted from Chem. Soc. Rev., 2014, 43, 1349) [28]

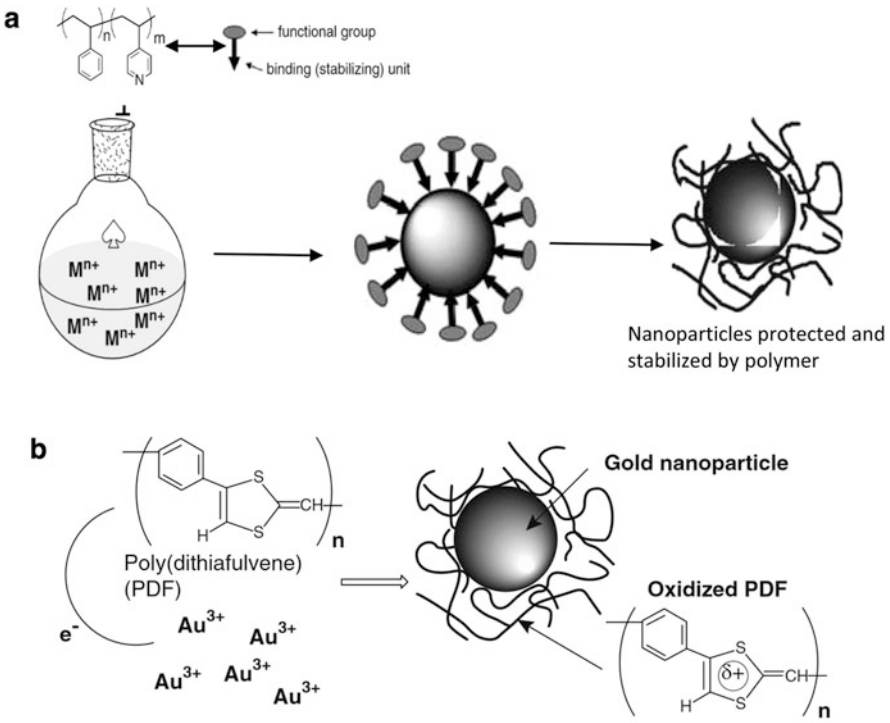


**Fig. 2.9** (**a**) Synthetic procedure of metal-polymer nanocomposites. (**b**) The stabilization of gold nanoparticles by poly(dithiafulvene) polymer

### 2.7.4 Noble Metal-Cellulose Nanocomposites

Cellulose is an awesome material that serves as an interesting support or matrix to noble metal nanoparticles. When noble metals are impregnated into cellulose fibres, it is expected that there will be ion-dipole type of electrostatic interactions. Such bonds are due to the interesting attraction of the electropositive noble metal towards the electron-rich nature of the cellulose with polar hydroxyl and ether groups [62]. The cellulose-Ag nanohybrids can also give rise to different types of scaffolds ranging from nanocrystals, fibres, films and hydrogels [6]. Cellulose-noble metal nanocomposites can be made by dissolving the microcrystalline cellulose in a solution of the noble metal nanoparticles followed by different fabrication techniques (casting, extrusion and electrospinning) depending on the application of the composites. The ratios of the cellulose to the noble metals can be varied to obtain material of diverse strength.

The chemical methods of using sodium borohydride, hydrazine, hydroxylamine, triethanolamine (TEA) and ascorbic acid including polyvinylpyrrolidone (PVP) or gelatine to reduce, stabilize and cap nanoparticles for possible entrapment into the cellulose nanofibres have become a common practice [35]. Their concentrations can be varied to obtain nanoparticles of various sizes. Trisodium citrate, ascorbic acid and gelatine could be classified as green reductants and stabilizers and better preferred to the chemical reductants since they are biomimetic compounds and less toxic.

In another green method, since the cellulose materials such as BC contain some functional groups that can exhibit both reducing and stabilizing properties, it follows that the hydrothermal treatment of the noble metal salts with the cellulose would lead to incorporation of the formed nanoparticles into the cellulose [35]. The incorporation of silver nanoparticles into cellulose materials is an interesting way of improving their optical, catalytic and antibacterial activities [3]. This type of composite materials has been applied in wound dressing, dental material, textiles and water purification.

### 2.7.5 Noble Metal-Carbon-Metal Oxide Nanocomposites

Graphene is a promising carbon material capable of serving as templates for metals and metal oxide nanocomposites. The simple reason may be due to the fascinating properties of graphene which include their high thermal and electrical conductivity, mobility and large surface area. These properties enable them to effectively transport electrons and could enhance photocurrent and photocatalytic properties. When noble metals are incorporated into metal oxides, there occur native defects and oxygen vacancies in the crystal lattices due to difference in ionic radius of the individual components [63]. The defects and vacancies in turn open up sites that can generate electrons when light energy falls on them. They also act as recombination centres which propel electrons into the metal oxides and graphene materials leading to charge carrier separation and reduction in recombination rate. In the report of

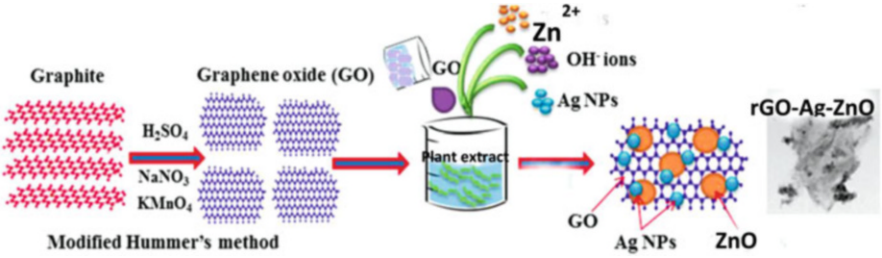


**Fig. 2.10** Green synthetic pathway for preparation of rGO-Ag-ZnO nanocomposites

Khurshid et al., the reduced graphene oxide (rGO) and Ag present in ZnO:Ag/rGO nanocomposite have led to improved mobility of charge carriers in the electrochemical system [64]. Such effect results in good optical response of the electrodes and therefore qualifies the nanocomposites for enhanced optoelectrochemical applications. In another report by Ata et al., they prepared Ag/ZnO/g-$C_3N_4$ nanocomposites by sonication method (which is an efficient green procedure) that have the capability to degrade methylene blue dye with efficiency of 98% in 20-min reaction time [65]. Dou et al. have performed similar experiment using microwave-assisted method in the preparation of Ag/ZnO/graphene nanocomposites [63]. Their reports revealed that the quantity of graphene in the composite materials affects their photocatalytic behaviour. About 99.6% degradation of methyl orange dye was observed under 80-min reaction time using 1 wt% graphene oxide in the composite whereby the 2 wt% gave 81.2% degradation.

Elemike et al. prepared rGO-Ag-ZnO nanocomposites by green methods using *Stigmaphyllon ovatum* aqueous plant extract [66]. The prepared nanocomposites showed some degree of photocatalytic degradation of methylene blue. Figure 2.10 shows the possible synthetic pathway followed during the preparation of the nanocomposites, whereas Fig. 2.11 explains the photocatalytic process and electron transfer reaction involved when the nanocomposites absorb radiation.

### 2.7.6 Applications of Nanocomposites as Antimicrobials

Among the noble metals, silver metal has age-long antibacterial properties, and it is less toxic in minute quantities. The loading of silver nanoparticles into polymers or non-metal surfaces to form composites is a good way of enhancing their properties especially the antimicrobial functions. In such manner, they can inculcate such property in wound healing, dental materials, textile materials and killing of bacteria in contaminated water.

Cellulose/Ag nanocomposites have been reported to have improved antimicrobial properties due to the controlled release of silver in the nanocomposite [3]. The OH platform in the cellulose is very rich in electron and therefore impacts favourably in stabilizing the nanocomposites in aqueous media through electrostatic interactions and hydrogen bonds. These properties of Ag NPs and cellulose in a composite

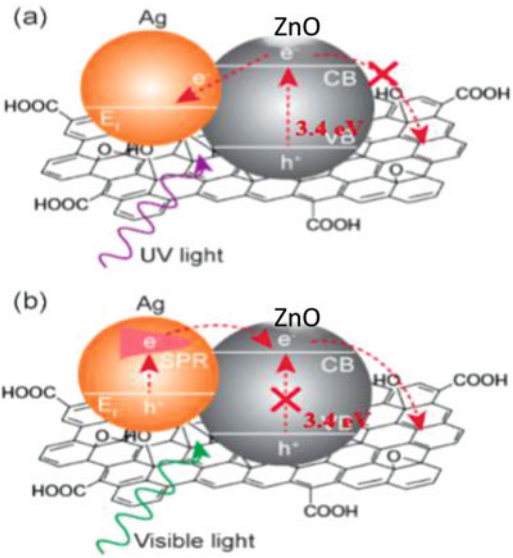


**Fig. 2.11** Possible electron transfer process involved in the nanocomposite. (**a**) shows the exposure of the nanomaterials to only UV light whereas (**b**) explains the absorption of visible light due to the surface plasmon exhibited by Ag, which enables the transfer of electrons thereby creating holes. (Reprinted from MDPI 2017) [67]

therefore contribute immensely towards their antibacterial behaviour. In a study done by Jadhav et al., it was reported that CuO NPs exhibited better antibacterial properties than the composites of Ag-CuO [68]. Ordinarily, one would have expected that the synergistic action of Ag and CuO should contribute to enhanced antibacterial behaviour. This therefore explains that the physicochemical properties of nanoparticles and nature of bacteria are determinants towards antibacterial behaviours. In another investigation, Ag-$SnO_2$ nanocomposites synthesized using *Saccharum officinarum* stem extract have shown remarked antibacterial properties [69].

Generally, there is no doubt that the noble metal nanoparticles synthesized by green method have extensively been used as antimicrobials especially nanosilver. Also, from the few review of their nanocomposites with polymers, cellulose and graphene, it is still evident that they act as templates for the anchoring of the nanoparticles and they affect slow release of the metal ions. These template materials are nontoxic, and they offer large surface area which improves the antimicrobial action of the nanocomposites.

### 2.7.7 Application of Nanocomposites in Water Treatment

Some aromatic compounds and dyes are greatly used in the chemical and petroleum industries. However, their effluents from bulk of the water pollutants need to be treated. For instance, cellulose ester can be obtained from cellulose acetate in the presence of nitrobenzene. Nitrobenzene is a dangerous and tough aromatic compound which is carcinogenic above the permissible level. It is also difficult to oxidize to less harmful forms. The semiconductor nanoparticles such as $TiO_2$ and ZnO show

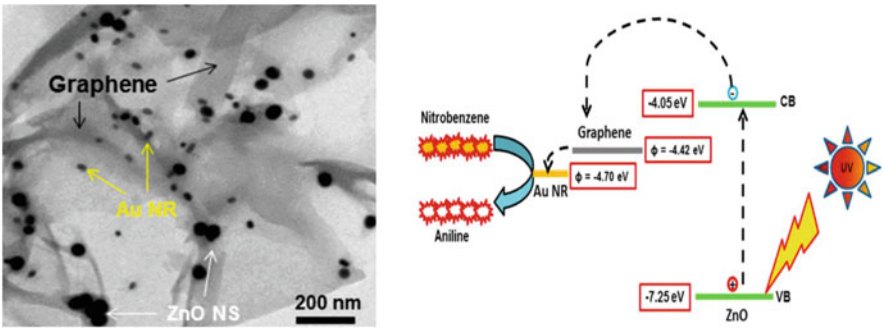


**Fig. 2.12** Structural view of Au-ZnO/graphene nanocomposites and their possible photocatalytic reaction (VB and CB are the valence and conduction band edge of ZnO, whereas $\phi$ is the work function of Au and graphene). (Reprinted with permission from ACS Environ. Sci. Technol. 2013, 47, 6688–6695) [70]

photoreduction of the nitrobenzene under UV irradiation, but their action is limited. They can be modified with other metals to be able to absorb in the visible region for improved photocatalytic efficiency. The choice of metals to dope the semiconductors is strategic as transition metals may result in low electron mobility and creation of electron holes due to discrete energy effect experienced in the photocatalysts [70]. In furtherance for the search of more effective photocatalysts, the noble metal-metal oxide nanoparticles can be decorated on graphene platform, and this technique has proved more promising. The graphene material has wide surface area and would enable effective electron transport. It also has good electrical conductivity and great charge transfer and undergoes $\pi$-$\pi$ interaction with the pollutant. The noble metals will ensure good charge separation, whereas the metal oxides absorb maximally in the UV region. The synergistic effect of the nanocomposite introduced by each of the components becomes a great factor to be considered in this type of material. During the photocatalytic reaction, more photogenerated electrons appear on the surface of the nanocomposite, and the reaction is more efficient in the absence of oxygen as they compete with these electrons [70]. Figure 2.12 describes the mechanism involved in the transfer of electrons and charges and subsequent photodegradation of organic pollutants.

### 2.7.8 Application of Nanocomposites in Electronics, Photovoltaic Cells, Sensing and Catalysis

There are several reports of noble metal composite materials having applications in sensing, solar cells and optoelectronic and electronic devices. Pd-doped $SnO_2$ and reduced graphene oxide have been used in $CH_4$ sensing, whereas Pd, Pt and Rh nanoparticles distributed on reduced graphene oxide serve as active electrode materials in electrochemical reduction of $NO_3^-$ and $NO_2^-$ [71, 72]. Conjugated polymers with nanoscale gold, silver, platinum and palladium particles are also

interesting materials for applications in gas sensors, biosensors and chemical sensors. Yang et al. have prepared polycrystalline one-dimensional Ag@$TiO_2$ core-shell nanowires with enhanced selectivity towards sensing of ammonia gas [50]. Further to their report, the mechanistic enhancement towards the gas sensing arises from the Schottky barrier effect existing at the AgNWs and $TiO_2$ nanoparticle interface.

In another application, green synthesized silver nanoparticles have been incorporated in $TiO_2$ nanoparticles to be used as photoanodes in dye-sensitized solar cells [73]. The plasmon behavioural effect of the modified electrode material was improved by the composite leading to higher power conversion efficiency. The synthetic method, the mechanism of nanoparticle incorporation and the material component of the nanocomposites are key factors that play significant roles towards the performance of the nanocomposites. Conducting polymers and graphene are electron-rich materials, and their composite forms with noble metals reduce their light scattering ability when exposed to radiation which makes them good optical materials. They are therefore attractive materials for applications in solar cell light absorbers, optoelectronic devices, sensors, surface-enhanced Raman spectroscopy, bandgap tuning, Bragg reflectors and laser technology [74]. The excellent conducting nature of graphene and carbon nanotube materials has also made them to be emerging materials in electronic applications which are improved in composite forms. Since graphene materials are transparent and flexible, they can be improved in nanocomposites, thereby becoming very important in modern technologies, such as video displays, touchscreen electronic devices and plastic solar cells [75]. The transport of electrons and charge transfer are improved in the composite materials than in the individual components of graphene and the metals [76].

Moreover, polymer-based nanocomposite materials are getting diverse applications in electronic devices including electroluminescent devices, smart windows, batteries, chemical sensors, electrocatalysis, field-effect transistors, memory devices and light-emitting diodes (LEDs) [77].

Noble metals are effective catalysts used in different chemical reactions. They can however be supported by carbon materials to be more efficient in their catalytic applications. In this regard, Pd/C nanocomposites have been used as catalysts in hydrogenation, hydrogenolysis and carbon-carbon bond formation. Hongkun and Chao have reported the catalytic reduction of hexacyanoferrate(III) using graphene-decorated Pd, Pt, Au and Ag NPs [78]. Zhao et al. have also reported that the bioinspired synthesized Fe3O4-Ag/rGO ternary nanohybrids exhibit more abundant nanopores and larger surface area which have influenced their exceptional catalytic properties [79]. Similarly Au nanoparticles were seeded on the surfaces of $Fe_3O_4$ hollow microspheres coated with polyethyleneimine-dithiocarbamates (PEI-DTC) to obtain nanocomposites that can effectively catalyse the reduction of 4-nitrophenol as shown in Fig. 2.13 [80].

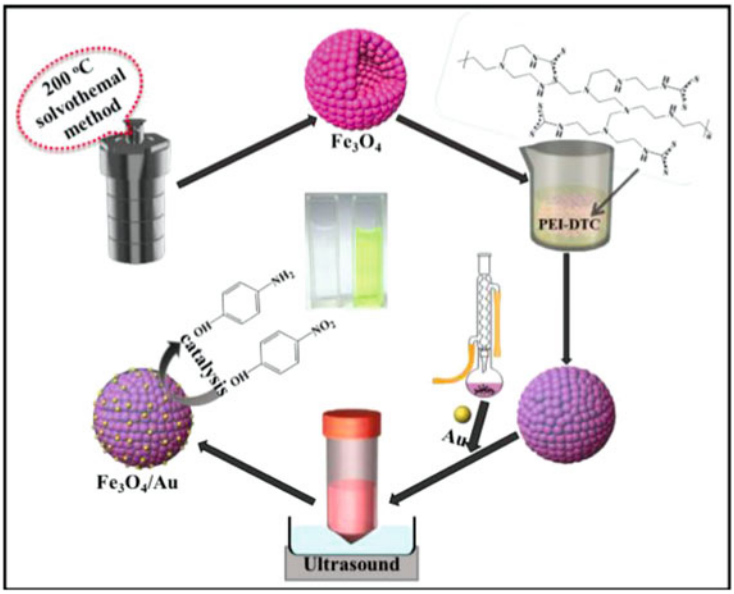


**Fig. 2.13** Synthesis of $Fe_3O_4$-Au nanocomposites and their application in catalytic reduction of 4-nitrophenol. (Reprinted from MDP1 2018) [80]

## 2.8 Conclusion

It is evident that the incorporation of noble metals into different materials such as polymers, metal oxides, graphene and cellulose gives nanocomposites improved functions. They have been majorly formed by chemical means which is easy and could control the distribution of the nanoparticles on the platform of the polymers, cellulose, graphene or semiconductors, but there is a big issue of chemical toxicity. The advocacy for green methods of nanofabrication is on the rise and promising as there have been successful works carried out using such techniques. The various green materials exploited so far include plant extracts (bark, leaves, root, fruit, stem, sap), microorganisms, agrowastes (fruit wastes, peels) and biomimetic compounds. Amidst the challenges in the formation, it is still believed that these nanocomposites are solutions to the emerging problems in electronics, catalysis, energy, medicine, environmental remediation and water purification. In the case of electronic devices, they may serve as solution to heat dissipation problems encountered in devices like computers, cell phones and others. Biomedicine is an area that has utilized the green nanomaterials more than any other application due to the biocompatibility nature and lower toxicity associated with the bioinspired nanomaterials. There are more opportunities and applications to the nanocomposite materials of noble metals with conducting polymers, cellulose, graphene and metal oxides. Therefore, research should be intensified in this area for improvement in the use of the nanocomposites.

**Acknowledgement** The authors sincerely acknowledge the management of Federal University of Petroleum Resources Effurun, Nigeria, led by Prof. Akii Ibhadode for their continued effort towards quality research.

**Declaration of Interest** The authors wish to state that this work does not represent any competing interest.

**Funding** This research did not receive funding from any organization.

## References

1. Abbasi-Oshaghi E, Mirzaei F, Mirzaei A (2018) Effects of ZnO nanoparticles on intestinal function and structure in normal/high fat diet-fed rats and CaCO-2 cells. Nanomedicine 13:2791–2816. https://doi.org/10.2217/nnm-2018-0202
2. Stankic S, Suman S, Haque F, Vidic J (2016) Pure and multi metal oxide nanoparticles: synthesis, antibacterial and cytotoxic properties. J Nanobiotechnol 14:1–20. https://doi.org/10.1186/s12951-016-0225-6
3. Fu L-H, Gao Q-L, Qi C, Ma M-G, Li J-F (2018) Microwave-hydrothermal rapid synthesis of cellulose/Ag nanocomposites and their antibacterial activity. Nanomaterials 8:978. https://doi.org/10.3390/nano8120978
4. Khalafi T, Buazar F, Ghanemi K (2019) Phycosynthesis and enhanced photocatalytic activity of zinc oxide nanoparticles toward organosulfur pollutants. Sci Rep 9:6866. https://doi.org/10.1038/s41598-019-43368-3
5. Nadagouda MN, Varma RS (2009) Risk reduction via greener synthesis of noble metal nanostructures and nanocomposites. In: Linkov I, Steevens J (eds) Nanomaterials: risks and benefits. NATO science for peace and security series C: environmental security. Springer, Dordrecht
6. Zhai L, Park J, Lee JY, Kim D, Kim J (2018) Synthesis, characterization, and antibacterial property of eco-friendly Ag/cellulose nanocomposite film. Int J Polym Mater Polym Biomater 67:420–426. https://doi.org/10.1080/00914037.2017.1342247
7. Fatimah I (2016) Green synthesis of silver nanoparticles using extract of Parkia speciosa Hassk pods assisted by microwave irradiation. J Adv Res 7:961–969. https://doi.org/10.1016/j.jare.2016.10.002
8. Keshari AK, Srivastava R, Singh P, Yadav VB, Nath G (2018) Antioxidant and antibacterial activity of silver nanoparticles synthesized by Cestrum nocturnum. J Ayurveda Integr Med 11:1–8. https://doi.org/10.1016/j.jaim.2017.11.003
9. Elemike EE, Fayemi OE, Ekennia AC, Onwudiwe DC, Ebenso EE (2017) Silver nanoparticles mediated by Costus afer leaf extract: Synthesis, antibacterial, antioxidant and electrochemical properties. Molecules 22:701. https://doi.org/10.3390/molecules22050701
10. Elemike EE, Onwudiwe DC, Ekennia AC, Ehiri RC, Nnaji NJ (2017) Phytosynthesis of silver nanoparticles using aqueous leaf extracts of Lippia citriodora: antimicrobial, larvicidal and photocatalytic evaluations. Mater Sci Eng C 75:980–989. https://doi.org/10.1016/j.msec.2017.02.161
11. Balashanmugam P, Durai P, Balakumaran MD, Kalaichelvan PT (2016) Phytosynthesized gold nanoparticles from C. roxburghii DC. leaf and their toxic effects on normal and cancer cell lines. J Photochem Photobiol B Biol 165:163–173. https://doi.org/10.1016/j.jphotobiol.2016.10.013
12. Nishanthi R, Malathi S, John Paul S, Palani P (2019) Green synthesis and characterization of bioinspired silver, gold and platinum nanoparticles and evaluation of their synergistic antibacterial activity after combining with different classes of antibiotics. Mater Sci Eng C 96:693–707. https://doi.org/10.1016/j.msec.2018.11.050

13. Salata OV (2004) Applications of nanoparticles in biology and medicine. J Nanobiotechnol 6: 1–6. https://doi.org/10.1186/1477-3155-2-12
14. Fang X, Wang Y, Wang Z, Jiang Z, Dong M (2019) Microorganism assisted synthesized nanoparticles for catalytic applications. Energies 12:190. https://doi.org/10.3390/en12010190
15. Ovais M, Khalil AT, Ayaz M, Ahmad I, Nethi SK, Mukherjee S (2018) Biosynthesis of metal nanoparticles via microbial enzymes: a mechanistic approach. Int J Mol Sci 19:1–20. https://doi.org/10.3390/ijms19124100
16. Patil MP, Do Kim G (2018) Marine microorganisms for synthesis of metallic nanoparticles and their biomedical applications. Colloids Surf B Biointerfaces 172:487–495. https://doi.org/10.1016/j.colsurfb.2018.09.007
17. Das VL, Thomas R, Varghese RT, Soniya EV, Mathew J, Radhakrishnan EK (2013) Extracellular synthesis of silver nanoparticles by the Bacillus strain CS 11 isolated from industrialized area. 3 Biotech 4:121–126. https://doi.org/10.1007/s13205-013-0130-8
18. Lang XY, Yuan HT, Iwasa Y, Chen MW (2011) Three-dimensional nanoporous gold for electrochemical supercapacitors. Scr Mater 64:923–926. https://doi.org/10.1016/j.scriptamat.2011.01.038
19. Blosi M, Ortelli S, Costa A, Dondi M, Lolli A, Andreoli S, Benito P, Albonetti S (2016) Bimetallic nanoparticles as efficient catalysts: facile and green microwave synthesis. Materials (Basel) 9:550. https://doi.org/10.3390/ma9070550
20. Britto Hurtado R, Cortez-Valadez M, Arizpe-Chávez H, Flores-Lopez N, Calderón-Ayala G, Flores-Acosta M (2017) Random alloy of Au-Ag bimetallic nanoparticles at room temperature—facile synthesis and vibrational properties. Gold Bull 50:85–92. https://doi.org/10.1007/s13404-017-0199-7
21. Elemike EE, Onwudiwe DC, Fayemi OE, Botha TL (2019) Green synthesis and electrochemistry of Ag, Au, and Ag–Au bimetallic nanoparticles using golden rod (Solidago canadensis) leaf extract. Appl Phys A Mater Sci Process 125:42. https://doi.org/10.1007/s00339-018-2348-0
22. Lan T, Fallatah A, Suiter E, Padalkar S (2017) Size controlled copper (I) oxide nanoparticles influence sensitivity of glucose biosensor. Sensors 17:1944. https://doi.org/10.3390/s17091944
23. Zayyoun N, Bahmad L, Laânab L, Jaber B (2016) The effect of pH on the synthesis of stable $Cu_2O$/CuO nanoparticles by sol–gel method in a glycolic medium. Appl Phys A Mater Sci Process 122:3–8. https://doi.org/10.1007/s00339-016-0024-9
24. Park JC, Kim J, Kwon H, Song H (2009) Gram-scale synthesis of $Cu_2O$ nanocubes and subsequent oxidation to CuO hollow nanostructures for lithium-ion battery anode materials. Adv Mater 21:803–807. https://doi.org/10.1002/adma.200800596
25. Kumagai Y, Burton LA, Walsh A, Oba F (2016) Electronic structure and defect physics of tin sulfides: SnS. Phys Rev Appl 6:014009. https://doi.org/10.1103/PhysRevApplied.6.014009
26. Gao Y, Han Y, Cui M, Tey HL, Wang L, Xu C (2017) ZnO nanoparticles as an antimicrobial tissue adhesive for skin wound closure. J Mater Chem B 5:4535–4541. https://doi.org/10.1039/c7tb00664k
27. Zhang Z, Ma Y, Bu X, Wu Q, Hang Z, Dong Z, Wu X (2018) Facile one-step synthesis of $TiO_2$/Ag/$SnO_2$ ternary heterostructures with enhanced visible light photocatalytic activity. Sci Rep 8:1–11. https://doi.org/10.1038/s41598-018-28832-w
28. Xu P, Han X, Zhang B, Du Y, Wang HL (2014) Multifunctional polymer-metal nanocomposites via direct chemical reduction by conjugated polymers. Chem Soc Rev 43:1349–1360. https://doi.org/10.1039/c3cs60380f
29. Calzoni E, Cesaretti A, Polchi A, Di Michele A, Tancini B, Emiliani C (2019) Biocompatible polymer nanoparticles for drug delivery applications in cancer and neurodegenerative disorder therapies. J Funct Biomater 8:1–15. https://doi.org/10.3390/jfb10010004
30. Kumari RM, Sharma N, Gupta N, Chandra R, Nimesh S (2018) Synthesis and evolution of polymeric nanoparticles. In: Design. Dev New Nanocarriers. pp 401–438. https://doi.org/10.1016/B978-0-12-813627-0.00011-9

31. Zhao J, Gilani MRHS, Liu Z, Luque R, Xu G (2018) Facile surfactant-free synthesis of polybenzoxazine-based polymer and nitrogen-doped carbon nanospheres. Polym Chem 9:4324–4331. https://doi.org/10.1039/C8PY00911B
32. Li Y, Tian J, Yang C, Hsiao BS (2018) Nanocomposite film containing fibrous cellulose scaffold and Ag/$TiO_2$ nanoparticles and its antibacterial activity. Polymers (Basel) 10:1052. https://doi.org/10.3390/polym10101052
33. Paulo J, Morais S, De Freitas M, De M, De Souza M, Dias L, Magalhães D, Ribeiro A (2013) Extraction and characterization of nanocellulose structures from raw cotton linter. Carbohydr Polym 91:229–235. https://doi.org/10.1016/j.carbpol.2012.08.010
34. Phanthong P, Reubroycharoen P, Hao X, Xu G (2018) Nanocellulose: extraction and application. Carbon Resour Convers 1:32–43. https://doi.org/10.1016/j.crcon.2018.05.004
35. Pinto RJB, Neves MC, Neto CP, Trindade T (2012) Composites of cellulose and metal nanoparticles. In: Ebrahimi F (ed) Nanocomposites – new trends and developments. IntechOpen, pp 73–96. https://doi.org/10.5772/50553
36. Emam HE, Shaheen TI (2019) Investigation into the role of surface modification of cellulose nanocrystals with succinic anhydride in dye removal. J Polym Environ 27:2419–2427. https://doi.org/10.1007/s10924-019-01533-9
37. Akhlaghi SP, Berry RM, Tam KC (2015) Modified cellulose nanocrystal for vitamin C delivery. AAPS PharmSciTech 16:306–314
38. Sahoo PK, Aepuru R, Panda HS, Bahadur D (2015) Ice-templated synthesis of multifunctional three dimensional graphene/noble metal nanocomposites and their mechanical, electrical, catalytic, and electromagnetic shielding properties. Sci Rep 5:1–12. https://doi.org/10.1038/srep17726
39. Yin PT, Shah S, Chhowalla M, Lee K (2015) Design, synthesis, and characterization of graphene—nanoparticle hybrid materials for bioapplications. Chem Rev 115:2483–2531. https://doi.org/10.1021/cr500537t
40. Khan T, Gurav P (2018) PhytoNanotechnology: enhancing delivery of plant based anti-cancer drugs. Front Pharmacol 8:1002. https://doi.org/10.3389/fphar.2017.01002
41. Tan C, Huang X, Zhang H (2013) Synthesis and applications of graphene-based noble metal nanostructures. Mater Today 16:29–36. https://doi.org/10.1016/j.mattod.2013.01.021
42. Qian Z, Cheng Y, Zhou X, Wu J, Xu G (2013) Fabrication of graphene oxide/Ag hybrids and their surface-enhanced Raman scattering characteristics. J Colloid Interface Sci 397:103–107. https://doi.org/10.1016/j.jcis.2013.01.049
43. Nguyen TA, Lee SW (2016) Hierarchical Au nanostructure electrodeposited on graphene oxide—modified ITO glass as an ultrasensitive SERS substrate. Mater Res Bull 83:550–555. https://doi.org/10.1016/j.materresbull.2016.07.005
44. Yang B, Liu Z, Guo Z, Zhang W, Wan M, Qin X, Zhong H (2014) In situ green synthesis of silver-graphene oxide nanocomposites by using tryptophan as a reducing and stabilizing agent and their application in SERS. Appl Surf Sci 316:22–27. https://doi.org/10.1016/j.apsusc.2014.07.084
45. Parvathi P, Jose A, Kalarikkal N, Thomas S (2018) Silver-attached reduced graphene oxide nanocomposite as an eco-friendly photocatalyst for organic dye degradation. Res Chem Intermed 44:5597–5621. https://doi.org/10.1007/s11164-018-3443-8
46. Raghavendra P, Vishwakshan Reddy G, Sivasubramanian R, Sri Chandana P, Subramanyam Sarma L (2018) Reduced graphene oxide-supported Pd@Au bimetallic nano electrocatalyst for enhanced oxygen reduction reaction in alkaline media. Int J Hydrog Energy 43:4125–4135. https://doi.org/10.1016/j.ijhydene.2017.07.199
47. Chang H, Hsu P, Tsai Y (2012) Ag/Carbon nanotubes for surface-enhanced Raman scattering. In: Kumar CSSR (ed) Raman spectroscopy for nanomaterials characterization. Springer, Berlin, pp 119–136. https://doi.org/10.1007/978-3-642-20620-7
48. Zhenxia W, Xinnian LI, Cuilan REN, Zhenzhong Y, Jiankang ZHU, Wenyun LUO, Fang X (2009) Growth of Ag nanocrystals on multiwalled carbon nanotubes and Ag-carbon nanotube

interaction. Sci China Ser E Technol Sci 52:3215–3218. https://doi.org/10.1007/s11431-009-0278-y
49. Intrchom W, Thakkar M, Hamilton RF, Holian A (2018) Effect of carbon nanotube-metal hybrid particle exposure to freshwater algae Chlamydomonas reinhardtii. Sci Rep 6:1–11. https://doi.org/10.1038/s41598-018-33674-7
50. Yang X, Fu H, Zhang L, An X, Xiong S, Jiang X, Yu A (2019) Enhanced gas sensing performance based on the fabrication of polycrystalline Ag@$TiO_2$ core-shell nanowires. Sens Actuat B Chem 286:483–492. https://doi.org/10.1016/J.SNB.2019.01.096
51. Zhang N, Liu S, Xu Y, Yan Y, Wang T, Li X, Pang H, Xue H, Zheng X, Yan X et al (2018) Synthesis and evaluation of optical and antimicrobial properties of Ag-$SnO_2$ nanocomposites. J Alloys Compd 2018:4133–4143. https://doi.org/10.1021/acssuschemeng.6b03114
52. Choudhary MK, Kataria J, Sharma S (2018) Novel green biomimetic approach for preparation of highly stable Au-ZnO heterojunctions with enhanced photocatalytic activity. ACS Appl Nano Mater 1(4):1870–1878. https://doi.org/10.1021/acsanm.8b00272
53. Aouadi SM, Paudel Y, Luster B, Stadler S, Kohli P, Muratore C, Hager C, Voevodin AA (2008) Adaptive $Mo_2N$/$MoS_2$/Ag tribological nanocomposite coatings for aerospace applications. Tribol Lett 29:95–103. https://doi.org/10.1007/s11249-007-9286-x
54. Xia X, Zheng Z, Zhang Y, Zhao X, Wang C (2014) Synthesis of Ag-MoS2/chitosan nanocomposite and its application for catalytic oxidation of tryptophan. Sensors Actuators B Chem 192:42–50. https://doi.org/10.1016/j.snb.2013.10.096
55. Wu J, Zhou Y, Nie W, Chen P (2018) One-step synthesis of Ag 2 S/Ag@MoS2 nanocomposites for SERS and photocatalytic applications. J Nanopart Res 20:1–13
56. Ashok A, Kumar A, Matin MA, Tarlochan F (2018) Synthesis of highly efficient bifunctional Ag/$Co_3O_4$ catalyst for oxygen reduction and oxygen evolution reactions in alkaline medium. ACS Omega 3:7745–7756. https://doi.org/10.1021/acsomega.8b00799
57. Zaporojtchenko V, Strunskus T, Erichsen J, Faupel F (2001) Embedding of noble metal nanoclusters into polymers as a potential probe of the surface glass transition. Macromolecules 34:1125–1127. https://doi.org/10.1021/ma0008600
58. Naka K, Chujo Y (2009) Nanohybridized synthesis of metal nanoparticles and their organization. In: Muramatsu A, Miyashita T (eds) Nanohybridization of organic-inorganic materials. Advances in Materials Research, vol 13. Springer, Berlin, Heidelberg
59. Sarmah S, Kumar A (2013) Electrical and optical studies in polyaniline nanofibre-$SnO_2$ nanocomposites. Bull Mater Sci 36:31–36. https://doi.org/10.1007/s12034-013-0431-x
60. Jian K-S, Chang C-J, Wu JJ, Chang Y-C, Tsay C-Y, Chen J-H, Horng T-L, Lee G-J, Karuppasamy L, Anandan S, Chen C-Y (2019) High response CO sensor based on a polyaniline/$SnO_2$ nanocomposite. Polymers 11:184. https://doi.org/10.3390/polym11010184
61. Dairi N, Ferfera-Harrar H, Ramos M, Garrigós MC (2019) Cellulose acetate/AgNPs-organoclay and/or thymol nano-biocomposite films with combined antimicrobial/antioxidant properties for active food packaging use. Int J Biol Macromol 121:508–523. https://doi.org/10.1016/j.ijbiomac.2018.10.042
62. He J, Kunitake T, Nakao A (2003) Facile in situ synthesis of noble metal nanoparticles in porous cellulose fibers. Chem Mater 15:4401–4406. https://doi.org/10.1021/cm034720r
63. Dou P, Tan F, Wang W, Sarreshteh A, Qiao X, Qiu X, Chen J (2015) One-step microwave-assisted synthesis of Ag/ZnO/graphene nanocomposites with enhanced photocatalytic activity. J Photochem Photobiol A Chem 302:17–22. https://doi.org/10.1016/j.jphotochem.2014.12.012
64. Khurshid F, Jeyavelan M, Hudson MSL, Nagarajan S (2019) Ag-doped ZnO nanorods embedded reduced graphene oxide nanocomposite for photo-electrochemical applications. R Soc Open Sci 6:181764
65. Ata S, Shaheen I, Ghafoor S, Sultan M, Majid F (2018) Diamond & related materials graphene and silver decorated ZnO composite synthesis, characterization and photocatalytic activity evaluation. Diam Relat Mater 90:26–31. https://doi.org/10.1016/j.diamond.2018.09.015
66. Elemike EE, Onwudiwe DC, Wei L, Chaogang L, Zhiwei Z (2019) Synthesis of nanostructured ZnO, AgZnO and the composites with reduced graphene oxide (rGO-AgZnO ) using leaf extract

of Stigmaphyllon ovatum. J Env Chem Eng 7:103190. https://doi.org/10.1016/j.jece.2019.103190
67. Alsharaeh EH, Bora T, Soliman A, Ahmed F, Bharath G, Ghoniem MG, Abu-salah KM, Dutta J (2017) Sol-gel-assisted microwave-derived synthesis of anatase Ag/$TiO_2$/GO nanohybrids toward efficient visible light phenol degradation. Catalysts 7:1–11. https://doi.org/10.3390/catal7050133
68. Jadhav MS, Kulkarni S, Raikar P, Barretto DA, Vootla SK, Raikar US (2018) Green biosynthesis of CuO & Ag-CuO nanoparticles from Malus domestica leaf extract and evaluation of antibacterial, antioxidant and DNA cleavage activities. New J Chem 42:204–213. https://doi.org/10.1039/c7nj02977b
69. Sinha T, Adhikari PP, Bora R (2017) Green and environmentally sustainable fabrication of Ag-$SnO_2$ nanocomposite and its multifunctional efficacy as photocatalyst and antibacterial and antioxidant agent. ACS Sustain Chem Eng 56:4645–4655. https://doi.org/10.1021/acssuschemeng.6b03114
70. Roy P, Periasamy AP, Liang C, Chang H (2013) Synthesis of graphene-ZnO-Au nanocomposites for efficient photocatalytic reduction of nitrobenzene. Environ Sci Technol 47(12):6688–6695. https://doi.org/10.1021/es400422k
71. Nasresfahani S, Sheikhi MH, Tohidi M, Zarifkar A (2017) Methane gas sensing properties of Pd-doped $SnO_2$/reduced graphene oxide synthesized by a facile hydrothermal route. Mater Res Bull 89:161–169. https://doi.org/10.1016/j.materresbull.2017.01.032
72. Sun C, Li F, An H, Li Z, Bond AM, Zhang J (2018) Facile electrochemical co-deposition of metal ( Cu, Pd, Pt, Rh ) nanoparticles on reduced graphene oxide for electrocatalytic reduction of nitrate/nitrite. Electrochim Acta 269:733–741. https://doi.org/10.1016/j.electacta.2018.03.005
73. Saravanan S, Kato R, Balamurugan M, Kaushik S, Soga T (2017) Efficiency improvement in dye sensitized solar cells by the plasmonic effect of green synthesized silver nanoparticles. J Sci Adv Mater Devices 2:418–424. https://doi.org/10.1016/j.jsamd.2017.10.004
74. Folarin OM, Sadiku ER, Maity A (2011) Polymer-noble metal nanocomposites: review. Int J Phys Sci 6:4869–4882
75. Jones WE, Chiguma J, Johnson E, Pachamuthu A, Santos D (2010) Electrically and thermally conducting nanocomposites for electronic applications. Materials (Basel) 3:1478–1496. https://doi.org/10.3390/ma3021478
76. Basu S, Hazra SK (2017) Graphene–noble metal nano-composites and applications for hydrogen sensors. Carbon 3:29. https://doi.org/10.3390/c3040029
77. Tyagi M, Tyagi D (2014) Polymer nanocomposites and their applications in electronics industry. Int J Electron Electr Eng 7:603–608
78. He H, Gao C (2011) Graphene nanosheets decorated with Pd, Pt, Au, and Ag nanoparticles: synthesis, characterization, and catalysis applications. Sci China Chem 54:397–404. https://doi.org/10.1007/s11426-010-4191-9
79. Zhao S, Jiang H, Li J, Meng X, Chao T, Zhang Z, Zhang P, Gao Y, Cao D (2018) Amorphizing of Ag nanoparticles under bioinspired one-step assembly of $Fe_3O_4$-Ag/rGO hybrids via self-redox process with enhanced activity. Appl Organomet Chem 32:e4428. https://doi.org/10.1002/aoc.4428
80. Chen Y, Zhang Y, Kou Q, Liu Y, Han D, Wang D, Sun Y, Zhang Y, Wang Y, Lu Z, Chen L, Yang J, Xing S (2018) Enhanced catalytic reduction of 4-nitrophenol driven by $Fe_3O_4$-Au magnetic nanocomposite interface engineering: from facile preparation to recyclable application. Nanomaterials 8:353. https://doi.org/10.3390/nano8050353

# Role of Solvent System in Green Synthesis of Nanoparticles

3

Khursheed Ali, Tijo Cherian, Saher Fatima, Quaiser Saquib, Mohammad Faisal, Abdulrahman A. Alatar, Javed Musarrat, and Abdulaziz A. Al-Khedhairy

**Abstract**

Nanoscale structures have acquired large scale of scientific interests, leading them as an effective bridging medium between bulk size and atomic/molecular structures. Therefore, in recent past, scientists from multidisciplinary fields have inclined their interest to devise novel methods/protocols/designs to develop reliable, sustainable, eco-friendly nontoxic and biodegradable nanostructures. In order to maintain the sustainability of the method, synthesis of nanostructures using green chemistry is also liable to keep abreast with defined solvent system which concerns the economic and environmental issues such as cost-effectiveness, safety, and health impact. Therefore, in view of 12 principles defined as green chemistry prerequisites, this chapter presents an overview on different types of solvents which fundamentally can be categorized as green solvents.

**Keywords**

Solvent system · Green solvent · Green chemistry · Nanoparticles

K. Ali · T. Cherian · S. Fatima
Department of Agricultural Microbiology, Faculty of Agricultural Sciences, Aligarh Muslim University, Aligarh, Uttar Pradesh, India

Q. Saquib · A. A. Al-Khedhairy
Department of Zoology, College of Science, King Saud University, Riyadh, Saudi Arabia

M. Faisal · A. A. Alatar
Department of Botany & Microbiology, College of Science, King Saud University, Riyadh, Saudi Arabia

J. Musarrat (✉)
Department of Agricultural Microbiology, Faculty of Agricultural Sciences, Aligarh Muslim University, Aligarh, Uttar Pradesh, India

School of Biosciences and Biotechnology, Baba Ghulam Shah Badshah University, Rajouri, India

© Springer Nature Singapore Pte Ltd. 2020

Q. Saquib et al. (eds.), *Green Synthesis of Nanoparticles: Applications and Prospects*, https://doi.org/10.1007/978-981-15-5179-6_3

## 3.1 Introduction

The term "nanoparticles" (NPs) is defined as the most fundamental component of synthesized nanoscale materials [1], with at least one dimension is <100 nm, bearing a peculiar configuration of atoms (0.2–90%) on the surfaces [2] and constant size-dependent physicochemical properties (i.e. melting point, surface area, optical property, mechanical strength, magnetic behaviour, surface plasmon resonance (SPR) and quantum confinement) as compared to their bulk counterparts [3]. Owing to these extraordinary properties, NPs have been considered as building blocks of the next-generation optoelectronics, electronics, theranostics, nanomedicines, and biochemical sensors [4, 5]. Therefore, nanoscale structures are debated immensly as an effective bridging medium between bulk size and atomic/molecular structures [6]. Consequently, multidisciplinary researchers are investigating the processess to develop a reliable, sustainable, eco-friendly nontoxic and biodegradable nanoscale materials, which can represent the desired characteristics. Also, over the past decade, it has been researched that a subtle but systematic change in the traditional synthesis methods can result in desired functioning of nanoscale product formation, while evading the associated limitations. For instance, pH, ingredients and temperature of reaction mixture can directly control the size, morphology, and stability [7, 8] and kinetics of interaction of metal ions with reducing agents during nucleation and stabilization of NPs synthesis [9]. Bjornmalm et al. [10] have also affirmed that synthesis protocols can yield significantly advanced as well as specifically programmed NPs for biomedical, optical, and electronic applications. Nevertheless, inspired from the unique properties of nanoscale materials, biologists, chemists, physicists and engineers came together to form a multidisciplinary quorum for nanosynthesis within the premises of sustainable/green chemistry [11, 12]. Thus, the designing of naive atoms, elements and molecules to novel nanomaterials has gained tremendous pace. Such materials own programmed structure, functional, and green prerequisites such as less toxic, eco-friendly, functionally stable in the wide spectrum of vicinity of action and cost-effective scaling up have now become indispensable to produce a sustainable regime of nanomedicines, electronics, sensors, nanoscale bio-structures, energy capture, storage devices, and consumer products, respectively.

A notable elevation in demand of NPs with desired efficiency and properties at low cost and minimum environmental risk has however given the birth to the term "green nanosynthesis". In fact, this term represents a strong embracement with the principles of green chemistry. Strictly, the concept of green nanosynthesis is based on the principles of green chemistry. However, it is always crucial and hence discussed exclusively to categorize a product, reactant and solvent as green. On the other hand, in order to make synthetic procedures greener, the core pursuits of green chemistry comprehensively framed the principles that encourage the incorporation of adequate solvents/liquid media, reactants, energy and purification system in nanosynthesis. In details, Anastas and Warner [13] advised 12 principles of green chemistry which are as follows: (1) safe chemical design; (2) renewable

feedstock; (3) less hazardous synthesis; (4) safer solvent and auxiliaries; (5) waste prevention; (6) energy efficiency; (7) atom economy; (8) catalysis; (9) reduced use of derivatives; (10) design for degradation; (11) real-time analysis; and (12) inherently safe chemistry to ascertain the greenness of matter of interest. Therefore, following the 12 principle criteria the procedures and reactants involved in green nanosynthesis must meet the following parameters; (1) constant and large-scale availability; (2) non-competitiveness and constant price ensuring the sustainability of the process; (3) recyclability/eco-friendliness; (4) low-energy consumption; (5) synthesis with high atom economy; (6) negligible toxicity; (7) biodegradability, i.e. should not produce toxic metabolites; (8) extraordinary viscosity, polarity and density compared to common one; (9) thermal and (electro)chemical stability; (10) non-flammability; (11) safe and non-hazardous, i.e. easy to transport and store; and (12) renewability. In the present scenario, it is practically challenging to define how a solvent system, a nanomaterial and a synthetic procedure can accurately be designated as a green/sustainable chemistry practice. Contrarily, the traditional solvents, such as organic and aliphatic/aromatic hydrocarbons and halogenated (chlorinated) inorganic chemicals, have been characterized as highly toxic (by oral and inhalation routes) and are often associated with chronic negative effects, such as mutagenicity, teratogenicity, and carcinogenicity [14], which entails that the selection of a solvent itself is not a simple matter.

On the other side, plenty of viewpoints support how a synthesis procedure falls in the category of green practices. For instance, the synthesis of NPs is named as green synthesis due to the utilization of the reactants which are aligned to the criteria of green chemistry in their synthesis procedures. Fundamentally, via green route, NPs formation is strictly associated with the environmental regulation, control, clean-up and remediation process, which therefore directly uplift their eco-friendliness. Thus, some green components such as prevention of waste, reduction of pollution, use of safer (or nontoxic) solvents, as well as renewable feedstock are particularly addressed while experimenting a green synthesis protocol. Therefore, the idea of "green solvents" was conceived to minimize the hazardous environmental impact, which is often associated with the type of solvent.

Precisely, through bottom-up/self-assembly approach, atoms, molecules or the clusters get configured as NPs [15], via cost-effective wet synthesis methods, such as chemical [16], electrochemical [17], sonochemical [18] and polyol reduction [19]. In this way, the formation of NPs originates from individual atom which however involves either cost-effective chemicals or bio-compatible reducing agents [20]. This approach provides a better scope to configure NPs with less surface imperfection and more homogeneous chemical composition by encompassing (1) metal ion reduction, (2) nucleation, and (3) particle growth in some kind of solvent process. Thus, in particular, solvents used in the synthesis, purification, and separation of nanomaterials received great attention due to their environmental risks [21]. The greener aspects of a solvent prompted a universal reflection towards its environmental adequateness including its economic value, prevention of waste, minimization of toxic and hazardous substances, safety and health issues. Fundamentally, dielectric constant, dipole moment, ability to accept or donate electron pairs or protons,

cohesive pressure and numerous solubility and spectroscopic parameters of a solvent play vital role in the relative solvency behaviour of a specific solvent [22, 23]. An apparent affirmative note can be taken from Yang et al. [24], who also suggested that the polarity of a solvent is significantly important to determine the structural configuration, interpenetration and topology net. More strictly, the inter-/intra-cohesion of solvent molecule is primarily associated with the polarity of solvents, and so a polar solvent often is a cohesive one. Besides these, Hildebrand [25] has also used the cohesiveness of solvents while creating one of the first scales of solvent polarity, noting that liquids were miscible if the difference in the square root of the cohesive pressure is less than 3.4. Nanosynthesis and environmental health both factors have been considered by the nanotechnologists to define how a nanosynthetic process is regarded as green nanosynthesis within the ambit of 12 principles of green chemistry (Fig. 3.1) [21].

## 3.2 Concept of Green Synthesis of NPs

The nature acts like a large "bio-laboratory" comprising of plants, algae, fungi, yeast, etc., identified as a viable source of naturally occurring biomolecules, which provides a bio-inspired green route for the production of pure and nanoscale metal and metal oxide particles [26]. Indeed, intra- or extracellular biological entities such as proteins, carbohydrates and nucleic acids possessing functional groups including thiol (-SH), hydroxyl (-OH), carboxyl (-COO), imidazole ($C_3N_2H_4$), amino ($-NH_2$) and imino (=NH) groups with high affinity to bind metal ions yield an excellent bio-reducing green solvent/medium for metal ion reduction to nanostructures [27]. On the other hand, green extracts of plant biomass (such as leaf, root, stem, bark, etc.) also contain a variety of bioactive polyphenols, proteins, sugars, flavonoids, alkaloids, flavonones and terpenoids, which may play an important role in the metal ion reduction and stabilization of NPs [28]. However, the bio-inspired synthesis of Ag and Au NPs have successfully marked the green route of NP bio-fabrication through microorganisms and plants, employing *Pseudomonas stutzeri* AG259 and alfalfa plant biomass, respectively [29, 30]. In recent years, a huge demand of nanomaterial production in industries like biomedical, paints, pharmaceuticals, electronics, etc. has encouraged the use of plant biomass as a viable and renewable green resource, as compared to the tedious culturing and maintenance of microbial cells [31]. Hence, bio-inspired synthesis of nanomaterials via green route of plants has emerged as an innovative, safe, inexpensive, and environment-friendly approach [32].

Despite the facile and one-pot synthesis protocol, the method of green extract-mediated synthesis of NPs faces challenges with respect to mono-dispersity, desired size, and surface morphology. Also, the varied composition and structural versatility of phytoconstituents in the extracts of different plant origins pose certain problems in the synthesis of NPs [33]. Besides, the elucidation of exact mechanism of NPs synthesis using crude extracts of plant and plant biomass is critical. This has led many researchers to further simplify the process of NPs synthesis by focusing on

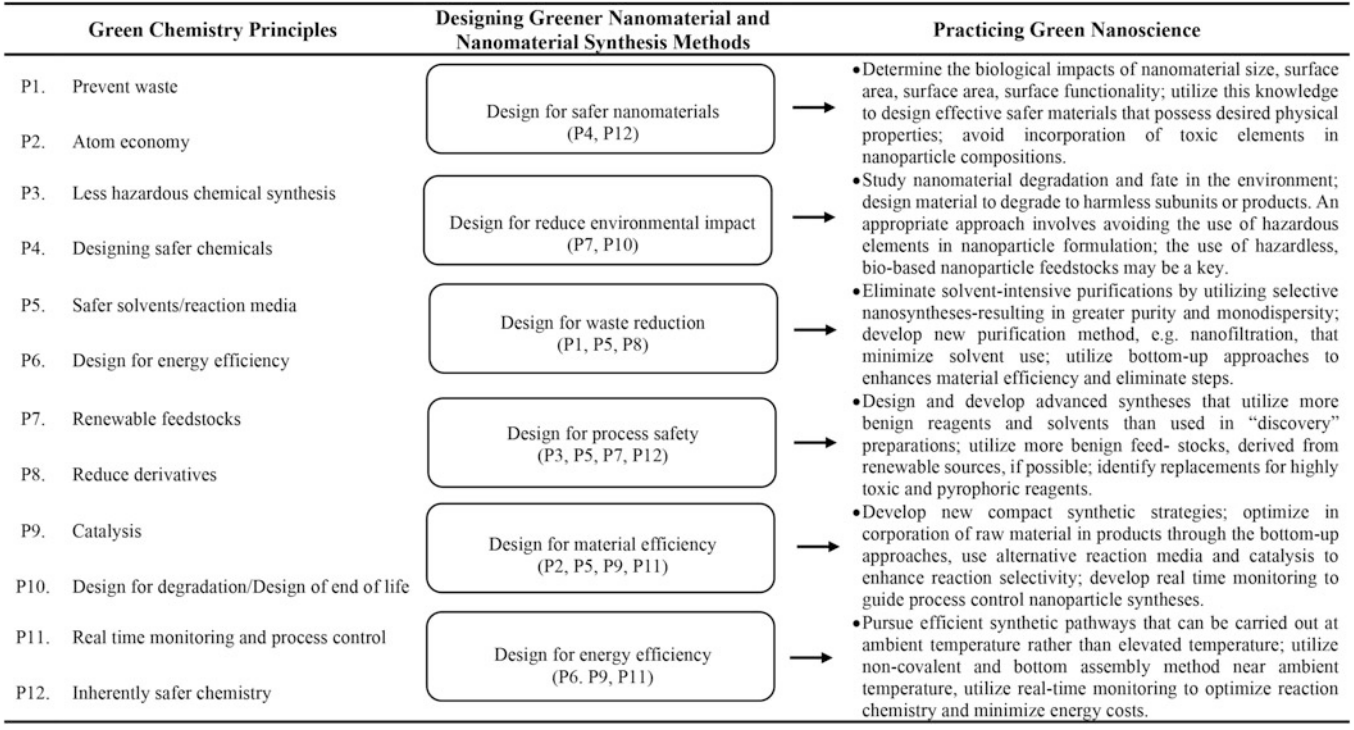


**Fig. 3.1** Translating the 12 green chemistry principles for application in the practice of green nanoscience. The principles are listed, in abbreviated form, along with the general approaches to designing greener nanomaterials and nanomaterial production methods and specific examples of how these approaches are being implemented in green nanoscience. Within the figure, PX, where X) 1–12, indicates the applicable green chemistry principle. (Adapted with permission from ref. [21]. Copyright 2007 American Chemical Society)

isolation of particular antioxidant phytoconstituents, which come into play during bio-fabrication of NPs as a reducing, capping and stabilizing agent. Earlier, a few studies have predicted the possible role of polyphenols and flavonoids for the synthesis and stabilization of NPs [34]. Isolated phytoconstituents such as terpenoids and sugars from *Diospyros kaki* [35] and *Ocimum sanctum* [36]; tannins, alkaloids, flavanols, phenols, glycosides and proteins from *Anacardium occidentale* [37]; flavones from *Cinnamomum camphora* leaf [38]; and polyols from *Artemisia annua* leaf extracts [39] have acted as green solvents directly in the reduction and stabilization of a variety of metal ions to metal and metal oxide NPs. Aromal and Philip [40] have suggested that the control over morphology and size of NPs can be achieved by adjusting the concentration of green reducing and capping agents.

## 3.3 Concept of Solvent and Green Solvent

The word "solvent" however refers to a variety of ubiquitous auxiliary substances, yet it is conceptually defined as an external liquid medium or an agent holding extraordinary solvency for a number of solutes and chemicals [41]. Indeed, the solvency of solvents and dissolution of solutes are decisive parameters while a chemical reaction proceeds. Thus, an ideal solvent is expected to offer excellent solvency towards a wide range of solutes. Within the composition landscape, most of the solvents either exist as a single molecule solution (e.g. water, methanol, ethanol, *n*-butanol and iso-propanol) or a blend of miscellaneous components (e.g. by-products of fodder industry, extracts obtained from different parts of plant and animals) in liquid state [42]. While, the traditional solvents viz. organic and aliphatic/aromatic hydrocarbons and halogenated (chlorinated) inorganic chemicals have been used in the synthetic processes. Though, they have been characterized as highly toxic (when entered orally and via inhalation) and are often associated with chronic negative effects, such as mutagenicity, teratogenicity and carcinogenicity [14]. Hence, there aroused a universal reflection that the selection of a solvent itself is not as simple as it appears. Therefore, keeping in view the prominent merits of green solvents generating functional, tailored nanoscale structures while evading the deleterious by-products and maintaining the efficacy of chemical reactions; the 12 principles of green/sustainable chemistry prescribed by Anastas and Warner at the US Environmental Protection Agency (USEPA) [13] has to be adapted entirely to make the nanosynthetic procedures green.

Thus, these exciting environment-friendly principles of green chemistry attracted the researchers associated to different disciplines of science and industrial sectors to develop customized nanosynthetic designs intending solely to minimize or even eliminate the hazardous impacts of resulting products [43]. Indeed, green solvents were introduced in the context of being versatile green alternatives to conventional solvents. Inspired from the central idea of green approaches, i.e. environmental health, the quest for safe and comparatively less or nontoxic alternative solvents was begun to define. On the other hand consideration on the efficacy of synthetic events (e.g. reduction, capping and stabilization) come into play during fabrication

or self-assembling of nanostructures. Overall, it can be articulated that the idea of green synthesis of NPs was established to devise alternative methods/procedures which firmly offer eco-friendly, less energy-consuming and non-hazardous generation of nanoscale materials. Precisely, the state-of-the-art use of alternative green reaction media for sustainable, bio-compatible and functional synthesis of NPs involves a wide variety of solvents including water, ionic liquids (ILs), supercritical carbon dioxide (Sc-$CO_2$), supercritical water (Sc-W) and bio-based benign solvents (e.g. crude extracts of plants or explants, microbial cells and animal tissues). Thus, in recent times, green synthesis of NPs is now deemed as a focused subdiscipline within the landscape of nanotechnology and hence deserves special concern. Therefore, it is rightly conceived that the inception of green nanosynthesis paved the way for a more careful and conscientious use of safer and non-hazardous solvents, accentuating the core theme "use of safer solvents and auxiliaries" as they are critical fractions of synthetic protocols providing medium for the disbanding of precursor molecules, promotion of optimum thermal effects, reactant relocation and dispersion of final products [44, 45]. However, the involvement of naturally occurring reducing cum capping and stabilizing solvents, such as green extracts obtained from the plants, explants, microbial and human cells have been adapted directly [46]. Overall, the 12 principles of green chemistry are highly appealing set of guidelines for green synthesis of NPs via self-assembly approach, as it proceeds under very low energy input when compared to the both top-down mechanochemical and solvent-based self-assembly approaches [47].

## 3.4 Significance of Solvent in Nanosynthesis

Commonly, a simple chemical reaction constitutes around 80% solvent of the total volume [48]. Likewise, in wet green nanosynthetic pursuits, a liquid phase is required for metal ion reduction, nucleation, ordering of atoms into particles, growth of the particles to nanoscaled dimensions and stabilization of nascent NPs [49]. Specifically, nucleation of the new phase and growth of nascent nanocrystals occur in the presence of an effective reducing, capping and stabilizing agent, which is dissolved in a suitable solvent that hinders NPs agglomeration and prevents their growth beyond a certain size. Besides these, a wet nanotechnological reaction is also subjected to optimization by conditioning the physicochemical parameters (such as heat and pH) in wide range to achieve optimal rate of nanoformation. Consequently, it is envisioned that a solvent system in green synthesis of NPs acts as a multifunctional reagent. Strictly, the need of solvent is not merely a condition for the reaction. Rather, it also offer a favourable environment to establish a better inter- or intra-species reactant contact, while they undergo transition states. Despite these, a solvent is not directly responsible for the composition of a product, nor it is the active component of a formulation; however, it is considered to be a fundamental module which provides necessary medium for the activation of components/reactants for reaction.

## 3.5 Water as a Green Solvent

Except for the principles of sustainable chemistry, till date, no exact set of rules has been defined to ensure the green aspects of a solvent; hence, the immediate conditions of a reaction are solely considered [50]. Water has been acknowledged as a universal solvent and is deemed an ideal and suitable solvent system for synthetic processes. According to Sheldon [51], "the best solvent is no solvent, and if a solvent is desirable then water is ideal". Since the beginning of NPs synthesis, usage of water as a prime solvent for the synthesis of various NPs has been first preferred, as it is the cheapest and most commonly accessible and available solvent on earth. Most of the ionic compounds dissociate well resulting in decreased ion-ion attractive forces, thereby causing their free movement in solution. Nevertheless, water at different temperatures and at 10 MPa pressure has excellent solvency towards nearly all inorganic compounds than any other solvent due to its extraordinary physicochemical characteristics as highlighted in Table 3.1. Thus, water can be defined as a safest and most environmental friendly solvent. The greener concerns of water include all 12 principle of green chemistry. Strictly, a solvent like water can be characterized by its dipole moment and relative permittivity ($\varepsilon_r$), which is a measure of solute-solvent interactions, as well as by its polarizability $\pi^*$. For water at ambient conditions (25 °C), all these three parameters have high values 1.85, 78.5 and 1.12, respectively [52]. Furthermore, the solvency of water is greatly relied on its solvatochromic Kamlet-Taft parameters [53] which reflects its ability to donate ($\alpha$ 51.2 at 25 °C) and accept ($\beta$ 50.37 at 25 °C) hydrogen bonds. In green nanosynthesis, water is the most convenient, eco-friendly and cheapest solvent for ionic as well as polar compounds. Therefore, molecules of water dissolute nearly all inorganic compounds. It can even dissolve some organic moieties like sugars and proteins. Thus, water has become the first-choice solvent for aqueous extraction and synthesis reaction [54, 55]. Similarly, in green nanosynthesis, water plays a crucial role during evolution of crystal structure precisely at nucleation and growth phases [56, 57] by encompassing via sub-phases, namely, elemental distribution within metal particles [55, 58], self-assembly [59], particle aggregation and coalescence [60], and formation of pores in nanomaterials, respectively [61]. However, prior to the beginning of green nanosynthesis procedures, most of the nanotechnologists were using pure water as a primary green solvent for the extraction of secondary green solvents from animals, microbial and plant cell extracts to reduce the metal ions into NPs. In this context, an array of plant extracts have been obtained using water as a primary green solvent, and so the obtained extracts were employed as a secondary green solvents as a multifunctional (reducing, capping and stabilizing) agent for the synthesis of Ag NPs via green route (Table 3.2).

**Table 3.1** Physicochemical of liquid water at different temperatures and at 10 MPa pressure [120]

| Property | 25 °C | 100 °C | 150 °C | 200 °C | 250 °C | 300 °C |
|---|---|---|---|---|---|---|
| Density, $\rho$ (g/dm$^3$) | 1001 | 962.9 | 922.3 | 870.9 | 805.7 | 715.3 |
| Dynamic viscosity, $\eta$ (mPa s) | 0.89 | 0.28 | 0.18 | 0.14 | 0.11 | 0.09 |
| Self-diffusion coefficient, $D$ ($m_2$/s)[a] [121, 122] | $2.30 \times 10^{-9}$ | $8.36 \times 10^{-9}$ | $14.2 \times 10^{-9}$ | $21.5 \times 10^{-9}$ | $30.4 \times 10^{-9}$ | $40.4 \times 10^{-9}$ |
| Surface tension, $\gamma$ (N/m)[a] | 0.072 | 0.059 | 0.049 | 0.038 | 0.026 | 0.014 |
| Relative permittivity, $\varepsilon_r$ | 78.8 | 55.9 | 44.4 | 35.1 | 27.3 | 20.3 |
| Dissociation constant, p$K$w[b] [123] | 13.99 | 12.25 | 11.64 | 11.31 | 11.20 | 11.34 |
| Specific heat capacity, $C_p$ (kJ/kg K) | 4.15 | 4.19 | 4.28 | 4.45 | 4.79 | 5.68 |

**Table 3.2** Plant extract-based solvents and characteristics of green synthesized Ag NPs

| Plants | Size (nm) | Source of green extract | Shape | References |
|---|---|---|---|---|
| *Alternanthera dentata* | 50–100 | Leaves | Spherical | [124] |
| *Acorus calamus* | 31.83 | Rhizome | Spherical | [125] |
| *Boerhaavia diffusa* | 25 | Whole plant | Spherical | [126] |
| *Tea extract* | 20–90 | Leaves | Spherical | [127] |
| *Tribulus terrestris* | 16–28 | Fruit | Spherical | [128] |
| *Cocos nucifera* | 22 | Inflorescence | Spherical | [128] |
| *Calotropis procera* | 19–45 | Plant | Spherical | [129] |
| *Vitex negundo* | 5 and 10–30 | Leaves | Spherical and face-centered cubic (fcc) | [130] |
| *Melia dubia* | 35 | Leaves | Spherical | [131] |
| *Thevetia peruviana* | 10–30 | Latex | Spherical | [132] |
| *Eclipta prostrata* | 35–60 | Leaves | Triangles, pentagons, hexagons | [133] |
| *Nelumbo nucifera* | 25–80 | Leaves | Spherical, triangular | [134] |
| *Acalypha indica* | 20–30 | Leaves | Spherical | [135] |
| *Allium sativum* | 4–22 | Leaves | Spherical | [136] |
| *Aloe vera* | 50–350 | Leaves | Spherical, triangular | [137] |
| *Memecylon edule* | 20–50 | Leaves | Triangular, circular, hexagonal | [138] |
| *Nelumbo nucifera* | 25–80 | Leaves | Spherical, triangular | [134] |
| *Datura metel* | 16–40 | Leaves | Quasilinear superstructures | [139] |

## 3.6 Bio-based Green Solvents

According to the principles of green chemistry, concerns about a reaction can be ascertained by screening the synthesis design, chemical used as solvents and reactants, and solvents used in the separation and purification. Consequently, to underscore green properties of a nanosynthesis processes likely involve at least 2 out of the 12 green chemistry principles:

1. The synthetic approaches should generate products with little or no toxicity to human health and environment.
2. The use of auxiliary substances (e.g. solvents, separation agents, etc.) must be obtained from non-competitive renewable eco-friendly resources.

The bio-based benign solvents such as lactic acid, levulinic acid, furfural, 5-hydroxymethylfurfural or γ-valerolactone [62] from renewable feedstock are in agreement with green chemistry principles. In the same line, ILs, low-melting organic solvents and non-flammable fluid over a wide temperature range are also able to dissolve many polymers including cellulose [63], chitin [64], chitosan [65], polyvinyl chloride [66] and polystyrene [67], which are reported insoluble in the conventional solvents. The renewable resources of precursors used as building blocks of ILs such as amino acids and amino alcohols from proteins; sugars from cellulose, chitin, starch and other polysaccharides; aromatic aldehydes from lignin; and a diverse group of other compounds such as fatty acids from vegetable or algae-derived oils, etc. support the green aspects of IL solvents. Therefore, bio-based solvents can suitably be applied for green synthesis of nanomaterials owing to the potential of their reducing and stabilizing matrix for a range of metal cations [68].

In the light of the above background, it can be articulated that there are two major solvent systems: (1) water as a primary green solvent and (2) bio-based solvent/formulation which is deemed as a secondary/auxiliary solvent component. Besides water, the greener concern of bio-based ILs rely on their renewability and widely available resource as feedstocks and biorefineries, while conventional ILs are synthesized from petroleum-derived starting materials [69]. More specifically, ILs have emerged as one of the best green media for green synthesis of NPs which indeed offers comprehensive solubility towards a wide range of bio-based solvents playing precisely as a solvent for reducing, stabilizing and capping agent of metal NPs. Moreover, the rate and equilibrium of the reaction have also been found influenced by dielectric constant with the attainment of narrow size distribution of the NPs by supercritical hydrothermal synthesis [70]. On the other hand, ILs are ion-laced with melting points below 100 °C and are tagged as "room-temperature ionic liquids". Metallic NPs such as gold (Au), silver (Ag), aluminium (Al), tellurium (Te), ruthenium (Ru), iridium (Ir) and platinum (Pt) have been synthesized in IL media served dually as reductant and as protective agent [71–74]. Lazarus et al. [75] synthesized both smaller isotropic spherical and large-sized anisotropic hexagonal shaped Ag NPs in ILs (BmimBF4) employing ILs as an alternative for water without mechanical stirring. A comparative study regarding the synthesis of manganese oxide ($Mn_3O_4$) NPs using imidazolium and oleylamine ILs was conducted by Bussamara et al. [76], illustrating the formation of NPs (9.9 ± 1.8 nm) with improved dispersity in ILs than oleylamine (12.1 ± 3.0 nm). A phase preparation technique for growth and formation of small-sized crystalline Au and Pt NPs was developed by Kim et al. [77], using thiol-functionalized ILs (TFILs) as a stabilizing agent. Dupont et al. [78] synthesized 2 nm sized $Ir^0$ NPs by $Ir^I$ reduction using 1-*n*-butyl-3-methylimidazolium hexafluorophosphate, suggesting the efficacy of IL media for the fabrication and modulation of recyclable biphasic catalytic systems for hydrogenation reactions (Table 3.3).

**Table 3.3** Some examples of green solvents and nanoparticle synthesis

| Sr. no. | Name of solvent | Source functionalization of solvents | Stabilized nanoparticle | References |
|---|---|---|---|---|
| 1 | Ionic liquids | Glucose | Cr (0) | [140] |
| 2 | Ionic liquids | Cellulose | Ru (0) | [141] |
| 3 | Bio-based | Indium chloride and gallium chloride | $Cu(In_{1-x}Ga_x)Se_2$ | [142] |
| 4 | Deep eutectic solvent | 2-Aminopyridines, aldehydes and alkynes | $CuFeO_2$ | [143] |
| 5 | Aqueous solvent | Peptides | Pd | [144] |
| 6 | Deep eutectic solvent | Ethylene glycol/choline chloride | $Mn_3O_4$ | [145] |
| 7 | Deep eutectic solvent | Choline chloride/urea | Pt | [49] |
| 8 | Ionic liquids | 1-*n*-butyl-3-methylimidazolium hexafluorophosphate | $Ir^0$ and $Rh^0$ | [146] |
| 9 | Supercritical water | – | $WO_3$ | [88] |
| 10 | Supercritical $CO_2$ | – | MWCNTs | [87] |

## 3.7 Supercritical Fluids

Supercritical fluid (SCF) technology significantly contributes in greening a broad spectrum of synthetic and separation processes while reserving green aspects such as (1) no organic solvent and (2) complete solvent recycling. Besides, Adschiri et al. [79] have demonstrated supercritical water-light-gas (Sc-W-$O_2$/$H_2$, etc.) system is an excellent green solvent for hydrothermal crystallization of metal oxide particles with defined morphologies such as barium hexaferrite ($BaFe_{12}O_{19}$). Thus, it is apparent that the SCFs originally are novel hybrids of gas and liquid, exhibiting unique properties of a green medium for chemical reactions and separations [80–82]. SCFs are also able to dissolve various solutes as a liquid and yet hold gaseous properties such as low viscosity, elevated diffusivity and zero surface tension. Extraordinarily, SCFs are feasible to get mixed with gases, while the solvency can be programmed by tuning the pressure and temperature. Beyond these, the aforementioned characteristics suggest that SCFs are attractive media for the target delivery of reactant molecules to the target areas such as high aspect ratios, complicated surfaces and poorly wettable substrates to attain remarkable uniformity and homogeneity. Furthermore, Sc-$CO_2$ has been extensively studied as a green medium for chemical reactions and separations [80], whereas $CO_2$ is one of the most feasible supercritical, non-hazardous inert fluids [83, 84], synthesizing Ag and Cu NPs in its supercritical state [85], suggesting a decline in the solubility of metal oxides around the critical point, leading to super saturation, formation and configuration of NPs

[70]. For example, the study of Ye et al. [86] demonstrates that a simple hydrogen reduction of metal β-diketone precursors using Sc-$CO_2$ as a green medium resulted in a rapid, one-step formation of functionalized multi-walled carbon nanotubes (MWCNTs) with palladium (Pd), rhodium (Rh) and Ru catalyst NPs (Table 3.3). Similarly, Sc-W has also been appreciated as green solvent system for several synthetic reactions [87]. Kim et al. [88] work is also very appealing showing the synthesis of crystalline tungsten oxide ($WO_3$) and tungsten blue oxide NPs in Sc-W system. Further, near-edge X-ray absorption fine structure (NEXAFS) results confirmed that Sc methanol was much better as compared to glycerol hydrothermal reduction, employed in the reduction of $WO_3$. ZnS nanoneedles with average diameter and length as 100 nm and 3 μm, respectively, were fabricated by sulphidation of zinc plates in $H_2S$ by employing $H_2S/H_2O$ SCFs as green solvent [89]. Thus, inspiring such comprehensive merits of Sc-$CO_2$ solutions and Sc-W, many SCF-based approaches have been developed for the synthesis of nanomaterials [90–94]. Sc-$CO_2$ solutions (e.g. Sc-$CO_2$/ethanol) were also regarded as green reaction media, which allowed the range of precursors to be extended to commonly used inorganic salts (e.g. metal nitrates) [95, 96], and a large number of metal oxides, including $Eu_2O_3$ [97], $Co_3O_4$ [98], $Al_2O_3$ [99], $Fe_2O_3$ [100], $ZrO_2$ [101], $CeO_2$ and $La_2O_3$ [102], $Mn_3O_4$ [103], $Cr_2O_3$ [104] and $SnO_2$ [105], were successfully decorated on CNTs, producing a series of metal oxide/CNT composites.

## 3.8 Deep Eutectic Solvents

Deep eutectic solvents (DESs) has been regraded as an alternative class of ionic fluids which embrace the principles of green chemistry by the fact that they are typically less expensive, more synthetically accessible (typically from bulk commodity chemicals using solvent/waste-free processes), nontoxic and biodegradable [106, 107]. The DESs can be obtained from eco-friendly renewable feedstocks such as choline, chloride and carbohydrates or amino acids. DESs contain at least two organic molecular components, namely, Lewis/Bronsted acid and base, which act as hydrogen bond donor and acceptor, respectively [108–110]. Overall, it can be argued that the DESs represent a sustainable class of nascent solvents and hence are considered as green solvents such as glycerol, glymes, poly(ethylene glycol), supercritical fluids and room-temperature ionic liquids (RTILs). However, DESs are not entirely RTILs but are composed of molecular components instead of ions dominantly [111]. The customization of physicochemical characteristics is the hallmark of DESs which in fact widens the scope to control their interfacial behaviour. The charged components of DESs are envisioned to attune the nucleation and growth mechanisms by charge neutralization, modification of reduction potentials and dictating growth along programmed/desired crystallographic directions [49]. The bio-compatibility of DESs has warranted the fascinating potential for designing biomolecular architectures in these novel media. Nevertheless, taken together, greening the solvents and nanosynthetic processes, DESs play a role as designer solvents while producing pre-designed/desired nanoscale structures such

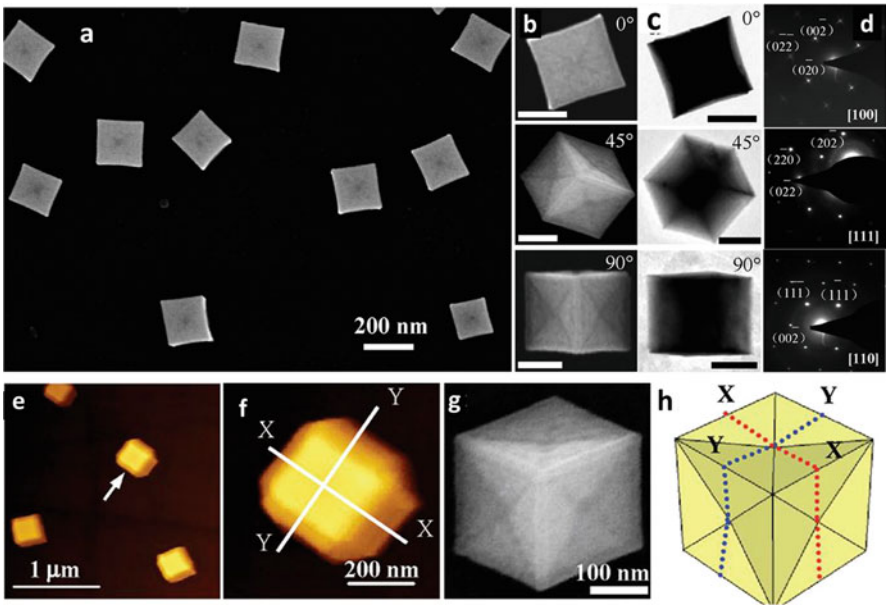


**Fig. 3.2** (**a**) SEM images of concave THH Pt NCs electrodeposited on glass carbon disk in 19.3 mM H2PtCl6/DES solution at 80 °C by a programmed electrodeposition method and (**b**) SEM and (**c**) TEM images of concave THH Pt NCs tilted 0, 45, and 90 to illustrate the concave faces. Scale bar of the inset is 100 nm. (**d**) selected area electron diffraction (SAED) patterns of concave THH Pt NCs oriented along the [99, 109, 110] directions. (**e**) Typical AFM images of concave THH Pt NCs shown in panel a, (**f**) magnified AFM image of concave THH Pt NCs indicated by the white arrow, (**g**) SEM and (**h**) model images of a concave THH Pt NCs. (Reproduced with permission from ref. [114]. Copyright 2012 American Chemical Society)

as NPs with controlled size and defined morphology, metal-organic nanocomposites, colloidal assemblies and porous and DNA/RNA template-based NPs [49]. In the light of the aforementioned breakthroughs, the multifunctional role of DESs in green nanosynthesis system can further be explored explicitly. The DESs are able to direct the nanosynthesis acting as supramolecular template, metal/carbon source, sacrificial agent (e.g. ammonia release from urea) and/or redox agent, all in the absence of formal stabilizing ligand [112]. Overall, DESs provide a wide scope for advanced nanostructure construction within low-water solvent.

Within the landscape of DESs, Wei et al. [113] have demonstrated an efficient and tactful electrochemical deposition route for Pt nanoflowers (∼200 nm) with sharp crystalline petals in DESs, namely, reline (1:2 choline chloride/urea) at 80 °C. In the same way, Wei et al. [114] successfully constructed shape-controlled concave tetrahexahedral (THH) Pt nanocrystals enclosed by {910} and vicinal high-index facets in DESs (Fig. 3.2).

Later, Hammons et al. [115] employed ultrasmall-angle X-ray scattering that supported electrochemical deposition and stabilization of Pd NPs in the same

DESs reline medium. The NPs formed via electrodeposition approach in DESs reline encompass the assembling of nanocrystals into two-dimensional superstructures due to simultaneous layer-by-layer deposition of a net positive charge over anionic layer. Dong et al. [116] prepared excellent photocatalytic single-crystalline mesoporous ZnO nanosheets (10 nm thick) in the same green DESs, i.e. reline, as green antisolvent procedure. Ethaline (1:2 choline chloride/ethylene glycol) is considered as another well-explored green DES used as solvent for polycrystalline gold nanowire network (NWN) synthesis at 40 °C [117]. Besides, the study of Mamajanov et al. [118] demonstrated that the DESs can also play a crucial role while engineering the secondary nanostructures of nucleic acids such as duplex, triplex and G-quadruplex. Querejeta-Fernandez et al. [119] investigated that the pathway underlying the nanoscale growth and self-assembly of nascent lead sulphide (PbS) nanocrystals into star-like superstructures within a DES encompasses the (1) formation of relatively loose and polydisperse octahedral PbS (30 nm) agglomerate, (2) self-assembly of octahedral meso-crystals of PbS (100–500 nm), (3) assembly into hyperbranched microstructures, (4) transformation of hyperbranched PbS microstructures into six armed stars and (5) top-down degradation of superstructures into short NPs, respectively. Nonetheless, the above breakthroughs entail the story of DESs employed as a successful solvent system in nanosynthesis while embracing the principle of green chemistry.

## 3.9 Conclusion

Overall, synthetic protocol of a nanoscale structure holds various green chemistry concerns with environment, which are presumably expected to affect its potential applications directly. Besides the synthetic/manufacturing designs and participant precursors, the solvent system or liquid phase is the critical factor which in parallel addresses the fundamental greener aspect of environmental safety, renewability and risks or conflicts associated with consumers. Thus, in order to ascertain whether a synthetic process is green, it must require to meet the set of prescribed standards. The exploitation of different liquid phases, for example, water, and bio-based solvents (DESs, ILs and supercritical liquids) in green nanotechnologies hopefully inspires more scientists to develop further green solvent-based nanomaterials. Systematic customization/manipulation of solvents will certainly open new avenues for comprehensively sustainable nanomaterial preparation.

**Acknowledgments** The authors extend their appreciation to the International Scientific Partnership Program (ISPP) at King Saud University (https://doi.org/10. 13039/501100002383) for funding this research work through ISPP# 0031.

## References


1. Horikoshi S, Serpone N (eds) (2013) Microwaves in nanoparticle synthesis: fundamentals and applications. Wiley, Weinheim
2. Ramsurn H, Gupta RB (2013) Nanotechnology in solar and biofuels. ACS Sus Chem Eng 1:779–797
3. Padmanabhan P, Kumar A, Kumar S et al (2016) Nanoparticles in practice for molecular-imaging applications: an overview. Acta Biomater 41:1–16
4. Hahn MA, Singh AK, Sharma P et al (2011) Nanoparticles as contrast agents for in-vivo bioimaging: current status and future perspectives. Anal Bioanal Chem 399:3–27
5. Kameya Y, Hanamura K (2011) Enhancement of solar radiation absorption using nanoparticle suspension. Sol Energy 85:299–307
6. Ariga K, Li J, Fei J et al (2016) Nano architectonics for dynamic functional materials from atomic-/molecular-level manipulation to macroscopic action. Adv Mater 28:1251–1286
7. Ali K, Ahmed B, Dwivedi S, Saquib Q et al (2015) Microwave accelerated green synthesis of stable silver nanoparticles with *Eucalyptus globulus* leaf extract and their antibacterial and antibiofilm activity on clinical isolates. PLoS One 10:e0131178
8. Ali K, Dwivedi S, Azam A et al (2016) *Aloe vera* extract functionalized zinc oxide nanoparticles as nanoantibiotics against multi-drug resistant clinical bacterial isolates. J Colloid Interface Sci 472:145–156
9. Bastus NG, Merkoçi F, Piella J et al (2014) Synthesis of highly monodisperse citrate-stabilized silver nanoparticles of up to 200 nm: kinetic control and catalytic properties. Chem Mater 26:2836–2846
10. Bjornmalm M, Thurecht KJ, Michael M et al (2017) Bridging bio-nano science and cancer nanomedicine. ACS Nano 11:9594–9613
11. Schmidt G, Malwitz MM (2003) Properties of polymer-nanoparticle composites. Curr Opin Colloid Interface Sci 8:103–108
12. Schmid G, Corain B (2003) Nanoparticulated gold: syntheses, structures, electronics, and reactivities. Eur J Inorg Chem 2003:3081–3098
13. Anastas PT, Warner JC (1998) Green chemistry. Frontiers. 640
14. Huang B, Lei C, Wei C, Zeng G (2014) Chlorinated volatile organic compounds (Cl-VOCs) in environment-sources, potential human health impacts, and current remediation technologies. Environ Int 71:118–138
15. Wan J, Zhang C, Zeng G et al (2016) Synthesis and evaluation of a new class of stabilized nano-chlorapatite for Pb immobilization in sediment. J Hazard Mater 320:278–288
16. Sun J, Wang X, Sun J et al (2006) Photocatalytic degradation and kinetics of Orange G using nano-sized Sn (IV)/$TiO_2$/AC photocatalyst. J Mol Catal Chem 260:241–246
17. Yang K, Feng L, Shi X et al (2013) Nano-graphene in biomedicine: theranostic applications. Chem Soc Rev 42:530–547
18. Wang SF, Gu F, Lu MK (2006) Sonochemical synthesis of hollow PbS nanospheres. Langmuir 22:398–401
19. Saade J, de Araujo CB (2014) Synthesis of silver nanoprisms: a photochemical approach using light emission diodes. Mater Chem Phys 148:1184–1193
20. Ahmed B, Hashmi A, Khan MS et al (2018) ROS mediated destruction of cell membrane, growth and biofilms of human bacterial pathogens by stable metallic AgNPs functionalized from bell pepper extract and quercetin. Adv Powder Technol 29:1601–1616
21. Dahl JA, Maddux BL, Hutchison JE (2007) Toward greener nanosynthesis. Chem Rev 107:2228–2269
22. Adams DJ, Dyson PJ, Tavener SJ (2005) Chemistry in alternative reaction media. Wiley, Chichester
23. Reichardt C (1988) Solvents and solvent effects in organic chemistry, 2nd edn. Wiley-VCH, Weinheim

24. Yang Y, Hu C, Abu-Omar MM (2012) Conversion of glucose into furans in the presence of $AlCl_3$ in an ethanol-water solvent system. Bioresour Technol 116:190–194
25. Snyder LR (1974) Classification of the solvent properties of common liquids. J Chromatogr 92:223–230
26. Sharma JK, Srivastava P, Akhtar MS et al (2015) α-$Fe_2O_3$ hexagonal cones synthesized from the leaf extract of *Azadirachta indica* and its thermal catalytic activity. New J Chem 39:7105–7111
27. Lin LQ, Wu WW, Huang JL et al (2013) Catalytic gold nanoparticles immobilized on yeast: from biosorption to bioreduction. Chem Eng J 225:857–864
28. Haroon M, Zaidi A, Ahmed B et al (2019) Effective inhibition of phytopathogenic microbes by eco-friendly leaf extract mediated silver nanoparticles (AgNPs). Indian J Microbiol 59:273–287
29. Klaus T, Joerger R, Olsson E et al (1999) Silver-based crystalline nanoparticles, microbially fabricated. Proc Natl Acad Sci U S A 96:13611–13614
30. Gardea-Torresdey J, Tiemann K, Gamez G et al (1999) Gold nanoparticles obtained by bio-precipitation from gold (III) solutions. J Nano Res 1:397–404
31. Ali K, Ahmed B, Ansari SM et al (2019) Comparative in situ ROS mediated killing of bacteria with bulk analogue, Eucalyptus leaf extract (ELE)-capped and bare surface copper oxide nanoparticles. Mater Sci Eng C 100:747–758
32. Ali K, Ahmed B, Khan MS et al (2018) Differential surface contact killing of pristine and low EPS Pseudomonas aeruginosa with *Aloe vera* capped hematite (α-$Fe_2O_3$) nanoparticles. J Photochem Photobiol B 188:146–158
33. Cherian T, Ali K, Fatima S et al (2019) Myristica fragrans bio-active ester functionalized ZnO nanoparticles exhibit antibacterial and antibiofilm activities in clinical isolates. J Microbiol Method 166:105716
34. Tamuly C, Hazarika M, Bordoloi M et al (2014) Biosynthesis of Ag nanoparticles using pedicellamide and its photocatalytic activity: an eco-friendly approach. Spectr Acta A 132:687–691
35. Song JY, Kwon EY, Kim BS (2010) Biological synthesis of platinum nanoparticles using Diospyros kaki leaf extract. Bioprocess Biosyst Eng 33:159–164
36. Soundarrajan C, Sankari A, Dhandapani P (2012) Rapid biological synthesis of platinum nanoparticles using Ocimum sanctum for water electrolysis applications. Bioprocess Biosyst Eng 35:827–833
37. Sheny D, Philip D, Mathew J (2013) Synthesis of platinum nanoparticles using dried Anacardium occidentale leaf and its catalytic and thermal applications. Spectr Acta A 114:267–271
38. Yang X, Li Q, Wang H et al (2010) Green synthesis of palladium nanoparticles using broth of *Cinnamomum camphora* leaf. J Nano Res 12:1589–1598
39. Edayadulla N, Basavegowda N, Lee YR (2015) Green synthesis and characterization of palladium nanoparticles and their catalytic performance for the efficient synthesis of biologically interesting di-(indolyl)-indolin-2-ones. J Ind Eng Chem 21:1365–1372
40. Aromal SA, Philip D (2012) Green synthesis of gold nanoparticles using Trigonella foenum-graecum and its size-dependent catalytic activity. Spectrochim Acta A Mol Biomol 97:1–5
41. Linak E, Bizzari SN (2013) Global solvents: opportunities for greener solvents. London, IHS Markit
42. Brennan L, Owende P (2010) Biofuels from microalgae—a review of technologies for production, processing, and extractions of biofuels and co-products. Renew Sust Energ Rev 14:557–577
43. Tundo P, Esposito V (eds) (2008) Green chemical reactions. Springer, Dordrecht
44. Constable DJ, Jimenez-Gonzalez C, Henderson RK (2007) Perspective on solvent use in the pharmaceutical industry. Org Proc Res Dev 11:133–137
45. Shanker U, Jassal V, Rani M et al (2016) Towards green synthesis of nanoparticles: from bio-assisted sources to benign solvents. A review. Int J Environ Anal Chem 96:801–835

46. Duan N, Geng X, Ye L et al (2016) A vascular tissue engineering scaffold with core-shell structured nano-fibers formed by coaxial electrospinning and its biocompatibility evaluation. Biomed Mater 11:035007
47. Maksimovic M, Omanovic-Miklicanin E (2017) Towards green nanotechnology: maximizing benefits and minimizing harm. In: CMBEBIH 2017. Springer, Singapore, pp 164–170
48. Jimenez-Gonzalez C, Curzons AD, Constable DJ et al (2004) Cradle-to-gate life cycle inventory and assessment of pharmaceutical compounds. Int J Life Cycle Assess 9:114–121
49. Wagle DV, Zhao H, Baker GA (2014) Deep eutectic solvents: sustainable media for nanoscale and functional materials. Account Chem Res 47:2299–2308
50. Gu Y, Jerome F (2013) Bio-based solvents: an emerging generation of fluids for the design of eco-efficient processes in catalysis and organic chemistry. Chem Soc Rev 42:9550–9570
51. Sheldon RA (2005) Green solvents for sustainable organic synthesis: state of the art. Green Chem 7:267–278
52. Plaza M, Turne C (2015) Pressurized hot water extraction of bio-actives. TrAC Trend Anal Chem 71:39–54
53. Jessop PG, Jessop DA, Fu D et al (2012) Solvatochromic parameters for solvents of interest in green chemistry. Green Chem 14:1245–1259
54. Kus NS (2012) Organic reactions in subcritical and supercritical water. Tetrahedron 4:949–958
55. Kruse A, Vogel H (2010) Chemistry in near- and supercritical water. In: Leitner W, Jessop PG (eds) Handbook of green chemistry: supercritical solvents. Wiley-VCH Verlag GmbH & Co. KGaA, Weinheim, p 457475
56. Thiruvenkadam S, Izhar S, Yoshida H, Danquah MK, Harun R (2015) Process application of subcritical water extraction (SWE) for algal bio-products and biofuels production. Appl Energy 154:815–828
57. Pollet P, Davey EA, Uren˜a-Benavides EE, Eckert CA, Liotta CL (2014) Solvents for sustainable chemical processes. Green Chem 16:10341055
58. Prat D, Wells A, Hayler J et al (2016) CHEM21 selection guide of classical- and less classical-solvents. Green Chem 18:288–296
59. Ebigwai JK, Edu EA, Itam EH et al (2012) Activity of crude cold-water extract of the culinary-medicinal oyster mushroom, Pleurotus ostreatus (Jacq: Fr.) P. Kumm. (higher Basidiomycetes), and timolol maleate on induced ocular hypertension. Int J Med Mushrooms 14(5):467–470
60. Reis SF, Rai DK, Abu-Ghannam N (2012) Water at room temperature as a solvent for the extraction of apple pomace phenolic compounds. Food Chem 135:1991–1998
61. Qian L, Wang S, Xu D et al (2016) Treatment of municipal sewage sludge in supercritical water: a review. Water Res 89:118131
62. Gallezot P (2012) Conversion of biomass to selected chemical products. Chem Soc Rev 41:1538–1558
63. Swatloski RP, Spear SK, Holbrey JD et al (2002) Dissolution of cellulose with ionic liquids. J Am Chem Soc 124:4974–4975
64. Kadokawa JI (2013) Ionic liquid as useful media for dissolution, derivatization, and nanomaterial processing of chitin. Green Sustain Chem 3:19–25
65. Xiao F, Zhao F, Mei D et al (2009) Nonenzymatic glucose sensor based on ultrasonic-electrodeposition of bimetallic PtM (M=Ru, Pd and Au) nanoparticles on carbon nanotubes–ionic liquid composite film. Biosens Bioelectron 24:3481–3486
66. Glas D, Hulsbosch J, Dubois P et al (2014) End-of-life treatment of poly (vinyl chloride) and chlorinated polyethylene by dehydrochlorination in ionic liquids. ChemSusChem 7:610–617
67. Winterton N (2006) Solubilization of polymers by ionic liquids. J Mater Chem 16:4281–4293
68. Rak MJ, Friscic T, Moores A (2014) Mechanochemical synthesis of Au, Pd, Ru and Re nanoparticles with lignin as a bio-based reducing agent and stabilizing matrix. Faraday Discuss 170:155–167

69. Hulsbosch J, De-Vos DE, Binnemans K et al (2016) Biobased ionic liquids: solvents for a green processing industry? ACS Sustain Chem Eng 4:2917–2931
70. Sue K, Adschiri T, Arai K (2002) Predictive model for equilibrium constants of aqueous inorganic species at subcritical and supercritical conditions. Ind Eng Chem Res 41:3298–3306
71. Er H, Yasuda H, Harada M et al (2017) Formation of silver nanoparticles from ionic liquids comprising *N*-alkylethylene diamine: effects of dissolution modes of the silver (I) ions in the ionic liquids. Colloids Surf Physicochem Eng Asp 522:503–513
72. Srivastava V (2014) In-situ generation of Ru nanoparticles to catalyze $CO_2$ hydrogenation to formic acid. Catal Lett 144:1745–1750
73. Vollmer C, Redel E, Abu-Shandi K et al (2010) Microwave irradiation for the facile synthesis of transition-metal nanoparticles (NPs) in ionic liquids (ILs) from metal-carbonyl precursors and Ru-, Rh-, and Ir-NP/IL dispersions as biphasic liquid-liquid hydrogenation nanocatalysts for cyclohexene. Chem Eur J 6:3849–3858
74. Zhang H, Cui H (2009) Synthesis and characterization of functionalized ionic liquid-stabilized metal (gold and platinum) nanoparticles and metal nanoparticle/carbon nanotube hybrids. Langmuir 25:2604–2612
75. Lazarus LL, Riche CT, Malmstadt N, Brutchey RL (2012) Effect of ionic liquid impurities on the synthesis of silver nanoparticles. Langmuir 28:15987–15993
76. Bussamara R, Melo WWM, Scholten JD, Migowski P, Marin G, Zapata MJ, Machado G, Teixeira SR, Novak MA, Dupont J (2013) Controlled synthesis of $Mn_3O_4$ nanoparticles in ionic liquids. Dalton Trans 42:14473
77. Kim KS, Demberelnyamba D, Lee H (2004) Size-selective synthesis of gold and platinum nanoparticles using novel thiol-functionalized ionic liquids. Langmuir 20:556–560
78. Dupont J, Fonseca GS, Umpierre AP et al (2002) Transition-metal nanoparticles in imidazolium ionic liquids: recyclable catalysts for biphasic hydrogenation reactions. J Am Chem Soc 124:4228–4229
79. Adschiri T, Hakuta Y, Arai K (2000) Hydrothermal synthesis of metal oxide fine particles at supercritical conditions. Ind Eng Chem Res 39:4901–4907
80. Darr JA, Poliakoff M (1999) New directions in inorganic and metal-organic coordination chemistry in supercritical fluids. Chem Rev 99:495–542
81. Cansell F, Chevalier B, Demourgues A et al (1999) Supercritical fluid processing: a new route for materials synthesis. J Mater Chem 9:67–75
82. Wai CM, Hunt FH, Smart NG, Lin Y (2000) US Patent No. 6,132,491. US Patent and Trademark Office, Washington, DC
83. Furstner A, Lutz A, Karsten B et al (2001) Olefin metathesis in supercritical carbon dioxide. J Am Chem Soc 123:9000–9006
84. Wittmann K, Wisniewski W, Mynott R et al (2001) Supercritical carbon dioxide as solvent and temporary protecting group for rhodium-catalyzed hydroaminomethylation. Chem Eur J 7:4584–4589
85. Ohde H, Hunt F, Wai CM (2001) Synthesis of silver and copper nanoparticles in a water-in-supercritical-carbon dioxide microemulsion. Chem Mater 13:4130–4135
86. Ye XR, Lin Y, Wang C et al (2004) Supercritical fluid synthesis and characterization of catalytic metal nanoparticles on carbon nanotubes. J Mater Chem 14:908–913
87. Pollet P, Eckert CA, Liotta CL (2011) Solvents for sustainable chemical processes. WIT Trans Ecol Environ 154:21–31
88. Kim M, Lee BY, Ham HC et al (2016) Facile one-pot synthesis of tungsten oxide ($WO_{3-x}$) nanoparticles using sub and supercritical fluids. J Super Fluids 111:8–13
89. Fedyaeva ON, Antipenko VR, Vostrikov AA (2014) Conversion of sulfur-rich asphaltite in supercritical water and effect of metal additives. J Super Fluid 88:105–116
90. Eckert CA, Knutson BL, Debenedetti PG (1996) Supercritical fluids as solvents for chemical and materials processing. Nature 383:313
91. Pai RA, Humayun R, Schulberg MT et al (2004) Mesoporous silicates prepared using preorganized templates in supercritical fluids. Science 303:507–510

92. Bag S, Trikalitis PN, Chupas PJ et al (2007) Porous semiconducting gels and aerogels from chalcogenide clusters. Science 317:490–493
93. Lucky RA, Charpentier PA (2008) A one-step approach to the synthesis of $ZrO_2$-modified $TiO_2$ nanotubes in supercritical carbon dioxide. Adv Mater 20:1755–1759
94. Zhang J, Ohara S, Umetsu M et al (2007) Colloidal ceria nanocrystals: a tailor-made crystal morphology in supercritical water. Adv Mater 19:203–206
95. Liu Z, Han B (2009) Synthesis of carbon-nanotube composites using supercritical fluids and their potential applications. Adv Mater 21:825–829
96. Liu Z, Wang J, Zhang J et al (2004) In situ $Eu_2O_3$ coating on the walls of mesoporous silica SBA-15 in supercritical ethane + ethanol mixture. Micropor Mesopor Mater 75:101–105
97. Fu L, Liu ZM, Liu YQ et al (2004) Coating carbon nanotubes with rare earth oxide multiwalled nanotubes. Adv Mater 16:350–352
98. Fu L, Liu ZHIMIN, Liu Y et al (2005) Beaded cobalt oxide nanoparticles along carbon nanotubes: towards more highly integrated electronic devices. Adv Mater 17:217–221
99. Fu L, Liu YQ, Liu ZM (2006) Carbon nanotubes coated with alumina as gate dielectrics of field-effect transistors. Adv Mater 18:181–185
100. Sun Z, Yuan H, Liu Z et al (2005) A highly efficient chemical sensor material for H2S: $\alpha$-$Fe_2O_3$ nanotubes fabricated using carbon nanotube templates. Adv Mater 17:2993–2997
101. Sun Z, Zhang X, Na N et al (2006) Synthesis of ZrO-carbon nanotube composites and their application as chemiluminescent sensor material for ethanol. J Phys Chem 110:13410–13414
102. Sun Z, Zhang X, Han B et al (2007) Coating carbon nanotubes with metal oxides in a supercritical carbon dioxide-ethanol solution. Carbon 45:2589–2596
103. An G, Yu P, Xiao M et al (2008) Low-temperature synthesis of $Mn_3O_4$ nanoparticles loaded on multi-walled carbon nanotubes and their application in electrochemical capacitors. Nanotechnology 19:275709
104. An G, Zhang Y, Liu Z et al (2007) Preparation of porous chromium oxide nanotubes using carbon nanotubes as templates and their application as an ethanol sensor. Nanotechnology 19:035504
105. Sun Z, Liu Z, Han B et al (2007) Supercritical carbon dioxide-assisted deposition of tin oxide on carbon nanotubes. Mater Lett 61:4565–4568
106. Khandelwal S, Tailor YK, Kumar M (2016) Deep eutectic solvents (DESs) as eco-friendly and sustainable solvent/catalyst systems in organic transformations. J Mol Liquid 215:345–386
107. Francisco M, van den Bruinhorst A, Kroon MC (2013) Low-transition-temperature mixtures (LTTMs): a new generation of designer solvents. Angew Chem Int Ed 52:3074–3085
108. Carriazo D, Serrano MC, Gutierrez MC et al (2012) Deep-eutectic solvents playing multiple roles in the synthesis of polymers and related materials. Chem Soc Rev 41:4996–5014
109. Smith EL, Abbott AP, Ryder KS (2014) Deep eutectic solvents (DESs) and their applications. Chem Rev 114:11060–11082
110. Zhang Q, Vigier KDO, Royer S et al (2012) Deep eutectic solvents: syntheses, properties and applications. Chem Soc Rev 41:7108–7146
111. Abbott AP, Boothby D, Capper G et al (2004) Deep eutectic solvents formed between choline chloride and carboxylic acids: versatile alternatives to ionic liquids. J Am Chem Soc 126:9142–9147
112. Cooper ER, Andrews CD, Wheatley PS et al (2004) Ionic liquids and eutectic mixtures as solvent and template in synthesis of zeolite analogues. Nature 430:1012
113. Wei L, Fan YJ, Wang HH et al (2012) Electrochemically shape-controlled synthesis in deep eutectic solvents of Pt nanoflowers with enhanced activity for ethanol oxidation. Electrochim Acta 76:468–474
114. Wei L, Fan YJ, Tian N et al (2011) Electrochemically shape-controlled synthesis in deep eutectic solvents—a new route to prepare Pt nanocrystals enclosed by high-index facets with high catalytic activity. J Phys Chem 116:2040–2044

115. Hammons JA, Muselle T, Ustarroz J et al (2013) Stability, assembly, and particle/solvent interactions of Pd nanoparticles electrodeposited from a deep eutectic solvent. J Phys Chem 117:14381–14389
116. Dong JY, Lin CH, Hsu YJ et al (2012) Single-crystalline mesoporous ZnO nanosheets prepared with a green antisolvent method exhibiting excellent photocatalytic efficiencies. Cryst Eng Comm 14:4732–4737
117. Chirea M, Freitas A, Vasile BS et al (2011) Gold nanowire networks: synthesis, characterization, and catalytic activity. Langmuir 27:3906–3913
118. Mamajanov I, Engelhart AE, Bean HD et al (2010) DNA and RNA in anhydrous media: duplex, triplex, and G-quadruplex secondary structures in a deep eutectic solvent. Angew Chem Int Ed 49:6310–6314
119. Querejeta-Fernandez A, Hernandez-Garrido JC, Yang H et al (2012) Unknown aspects of self-assembly of PbS microscale superstructures. ACS Nano 6:3800–3812
120. Hartonen K, Riekkola ML (2017) Water as the first-choice green solvent. In: The application of green solvents in separation processes. Elsevier, Amsterdam, pp 19–55
121. Yoshida K, Matubayasi N, Nakahara M (2008) Self-diffusion coefficients for water and organic solvents at high temperatures along the coexistence curve. J Chem Phys 129:214501
122. Holz M, Heil SR, Sacco A (2000) Temperature-dependent self-diffusion coefficients of water and six selected molecular liquids for calibration in accurate 1H NMR PFG measurements. Phys Chem Chem Phys 2:4740–4742
123. Bandura AV, Lvov SN (2006) The ionization constant of water over wide ranges of temperature and density. J Phys Chem Ref Data 35:15–30
124. Nakkala JR, Mata R, Gupta AK et al (2014) Green synthesis and characterization of silver nanoparticles using Boerhaavia diffusa plant extract and their antibacterial activity. Ind Crop Prod 52:562–566
125. Nakkala JR, Mata R, Gupta AK et al (2014) Biological activities of green silver nanoparticles synthesized with Acorous calamus rhizome extract. Eur J Med Chem 85:784–794
126. Suna Q, Cai X, Li J et al (2014) Green synthesis of silver nanoparticles using tea leaf extract and evaluation of their stability and antibacterial activity. Colloid Surf A Physicochem Eng Asp 444:226–231
127. Nabikhan A, Kandasamy K, Raj A et al (2010) Synthesis of antimicrobial silver nanoparticles by callus and leaf extracts from saltmarsh plant, Sesuvium portulacastrum L. Colloid Surf B 79:488–493
128. Mariselvam R, Ranjitsingh AJA, Nanthini AUR, Kalirajan K, Padmalatha C, Selvakumar PM (2014) Green synthesis of silver nanoparticles from the extract of the inflorescence of Cocos nucifera (Family: Arecaceae) for enhanced antibacterial activity. Spectr Acta A Mol Biomol Spectr 129:537–541
129. Gondwal MA, Pant GJ (2013) Biological evaluation and green synthesis of silver nanoparticles using aqueous extract of *Calotropis procera*. Int J Pharm Biol Sci 4:635–643
130. Zargar M, Hamid AA, Bakar FA et al (2011) Green synthesis and antibacterial effect of silver nanoparticles using *Vitex negundo* L. Molecules 16:6667–6676
131. Kathiravan V, Ravi S, Kumar SA (2011) Synthesis of silver nanoparticles from Melia dubia leaf extract and their in vitro anticancer activity. Spectr Acta A Mol Biomol Spectr 130:116–121
132. Rupiasih NN, Aher A, Gosavi S et al (2013) Green synthesis of silver nanoparticles using latex extract of Thevetia peruviana: a novel approach towards poisonous plant utilization. J Phys Conf Ser 423:1–8
133. Rajakumar G, Rahuman AB (2011) Larvicidal activity of synthesized silver nanoparticles using Eclipta prostrata leaf extract against filariasis and malaria vectors. Acta Trop 118:196–203
134. Santhoshkumar T, Rahuman AA, Rajakumar G et al (2011) Synthesis of silver nanoparticles using Nelumbo nucifera leaf extract and its larvicidal activity against malaria and filariasis vectors. Parasitol Res 108:693–702

135. Krishnaraj C, Muthukumaran P, Ramachandran R et al (2014) *Acalypha indica* Linn: biogenic synthesis of silver and gold nanoparticles and their cytotoxic effects against MDA-MB-231, human breast cancer cells. Biotechnol Rep 4:42–49
136. Ahamed M, Khan M, Siddiqui M et al (2011) Green synthesis, characterization and evaluation of biocompatibility of silver nanoparticles. Phys E Low Dimen Syst Nanostruct 43:1266–1271
137. Chandran S, Chaudhary M, Pasricha R et al (2006) Synthesis of gold nanotriangles and silver nanoparticles using *Aloe vera* plant extract. Biotechnol Prog 22:577–583
138. Elavazhagan T, Arunachalam KD (2011) Memecylon edule leaf extract mediated green synthesis of silver and gold nanoparticles. Int J Nanomedicine 6:1265–1278
139. Kesharwani J, Yoon KY, Hwang J et al (2009) Phytofabrication of silver nanoparticles by leaf extract of Datura metel: hypothetical mechanism involved in synthesis. J Bionanosci 3:39–44
140. He J, Zhang Y, Chen EYX (2013) Chromium (0) nanoparticles as effective catalyst for the conversion of glucose into 5-hydroxymethylfurfural. ChemSusChem 6:61–64
141. Ignatyev IA, Van-Doorslaer C, Mertens PG et al (2010) Reductive splitting of cellulose in the ionic liquid 1-butyl-3-methylimidazolium chloride. ChemSusChem 3:91–96
142. Al-Juhaiman L, Scoles L, Kingston D et al (2010) Green synthesis of tunable Cu ($In_{1-x}Gax$) $Se_2$ nanoparticles using non-organic solvents. Green Chem 12:1248–1252
143. Lu J, Li XT, Ma EQ et al (2014) Superparamagnetic $CuFeO_2$ nanoparticles in deep eutectic solvent: an efficient and recyclable catalytic system for the synthesis of imidazo[1,2-a] pyridines. ChemCatChem 6:2854–2859
144. Pacardo DB, Sethi M, Jones SE (2009) Biomimetic synthesis of Pd nanocatalysts for the Stille coupling reaction. ACS Nano 3:1288–1296
145. Karimi M, Eshraghi MJ (2017) One-pot and green synthesis of $Mn_3O_4$ nanoparticles using an all-in-one system (solvent, reactant and template) based on ethaline deep eutectic solvent. J Alloy Comp 696:171–176
146. Fonseca GS, Umpierre AP, Fichtner PF et al (2003) The use of imidazolium ionic liquids for the formation and stabilization of Ir0 and Rh0 nanoparticles: efficient catalysts for the hydrogenation of arenes. Chem Eur J 9:3263–3269

# Surface Engineering Techniques Associated with Stability, Biocompatibility, and Toxicity of Nanoparticles

4

Khursheed Ali, Tijo Cherian, Saher Fatima, Quaiser Saquib, Mohammad Faisal, Abdulrahman A. Alatar, Javed Musarrat, and Abdulaziz A. Al-Khedhairy

**Abstract**

Originally surface engineering encompasses an array of state-of-the-art techniques and methods which address the challenges associated with surface fortification, strongholds, and other elements of defense systems. Hence, the surface engineering of nanoparticles (NPs) manufactured for the desired applications is the hallmark of their functional abilities. The compatibility of a wide range of biological system at NPs exposure is described in terms of degree of toxicity and stability of nanoformulations while preserving their characteristic applications. In recent times, nanotechnology has markedly transformed the traditional chemical and physical manufacturing process into green nanotechnology by incorporating the less hazardous and less toxic biogenic reactants for the green production of NPs. Taken together, the stability, biocompatibility, and toxicity of NPs and the applicability of a variety of biogenic materials in surface engineering of NPs have been summarized in this chapter.

K. Ali · T. Cherian · S. Fatima
Department of Agricultural Microbiology, Faculty of Agricultural Sciences, Aligarh Muslim University, Aligarh, Uttar Pradesh, India

Q. Saquib (✉) · A. A. Al-Khedhairy
Department of Zoology, College of Science, King Saud University, Riyadh, Saudi Arabia

M. Faisal · A. A. Alatar
Department of Botany & Microbiology, College of Science, King Saud University, Riyadh, Saudi Arabia

J. Musarrat
Department of Agricultural Microbiology, Faculty of Agricultural Sciences, Aligarh Muslim University, Aligarh, Uttar Pradesh, India

School of Biosciences and Biotechnology, Baba Ghulam Shah Badshah University, Rajouri, India

© Springer Nature Singapore Pte Ltd. 2020

Q. Saquib et al. (eds.), *Green Synthesis of Nanoparticles: Applications and Prospects*, https://doi.org/10.1007/978-981-15-5179-6_4

**Keywords**

Surface functionalization · Green stabilizers · Conjugated copolymers · Biological medium

## 4.1 Nanotechnology: A General Background

Nanotechnology is a science which overlaps the boundaries of various fields including but not limited to engineering, chemistry, and bioscience. The nanotechnology broadly deals with the synthesis of various shaped or structured nanomaterials (NMs) with distinct morphological features, chemical composition, and dispersibility [1]. The NMs or more specifically the nanoparticles (NPs) are synthesized by numerous methods including chemical, physical, and biological either using top-down or bottom-up approach [2]. These NPs have been proved as prospective materials for the use of humans and to maintain the sustainability of environment by their applications in agriculture, industry, biomedical, nutrition, food processing, and various other consumer products [3]. Apart from the chemical and physical approaches in nanotechnology, the development of "green nanotechnology," and thus green production of NPs on the other hand, has markedly transformed the current manufacturing processes. Due to this, the green nanotechnology has reasonably protected environmental eminence by reducing pollution and conserving innate resources [4].

The production of eco-friendly and safe NPs could have been possible by adopting the principles of "green chemistry" in nanotechnology. The green chemistry is an outbranch of classical chemistry which underlines the credentials of "a chemical philosophy" encouraging designs and procedures with a prime aim on reducing and eliminating the usage and generation of hazardous products and by-products [5, 6]. With the application of "green principles," there has been an overall reduction in the usage of toxic solvents by using the improved raw materials, adjusted reaction parameters, enhanced energy efficiency, use of renewable sources, and product designing without posing threat to the human health and environment [7, 8]. However, despite all the merits of green NPs, the stability, and longer persistence of NPs in the environment, interaction between NPs and organisms particularly useful microflora and plants and their fate in biological systems remains an important aspect of nanotoxicology [9].

Successful applications of NPs in various fields such as catalysis, electronics, biomedicals, material production, wastewater purification, and many other interdisciplinary fields are critically acclaimed and sharply scrutinized. The applicability of such NPs depends on their structural artifacts such as morphological features (size, shape, and geometry) and chemical properties (elemental composition and surface chemistry) [10], thus expanding the array of properties required for the development of various eco-friendly routes for the generation of NPs bearing various physicochemical features significant to the desired setting [11].

### 4.1.1 Functionalization of Metallic NPs

The high reactivity of well-surfaced NPs engineered by aggregation confers undesirable strength and irreversibility, but the process reduces surface area to volume ratio as well as the interfacial energy which leads to weakened particle reactivity [12, 13]. Due to these, the paramount issue of NPs stability is a serious concern especially during transportation, storage, and the overall life cycle [13]. The majority of stabilizing methods involves dispersant molecules. Including the surfactants and polyelectrolytes, altering the surface physicochemistry along with the generation of tremendous residual waste, occupying considerable (>50%) mass fraction of particle system, subsequently posing a deleterious and adverse impact on the environment [14]. Therefore, the search for environmentally inert and safe stabilizing pathways with the application of biocompatible and nontoxic stabilizers is urgently needed to overcome such issues which restrict biocompatibility of NPs. In this context, various natural stabilizers have been identified to prevent particle aggregation, functionalize NPs, and bypass the severe reaction conditions and lethal impacts, which are unfit and deleterious for both biological and biochemical applications of NPs [15, 16]. Some of the major green stabilizers include polyphenols, vitamins (B, C, D, K), enzymes, low molecular weight organic acids, biopolymers, and silica. These compounds were credited in full-swing operations for the stabilization of synthesized NPs and devoid any unwanted ramifications on the overall equilibria of environment and biological systems.

### 4.1.2 Recovery and Reuse of Nanoparticles

With the importance and applicability of NPs in varied fields, it is the need of the hour to functionalize/stabilize the metal NPs to make the process of recovery and reuse more economic for their utilization. As an example, over the last decade, heterogeneous supports of magnetic nano-cores have revolutionized the metal and dye recovery, drug conjugation, protein and cellular separations, and enzyme immobilization. Such unique advantages paved way for easy recoverability, elevated efficiency, cost-effectiveness, and rapidity in contrast to other nano-counterparts [4, 17]. This also eliminates the pre- and post-reaction need of solvent swelling and catalyst filtration [18, 19].

## 4.2 Green Stabilizers

In order to enhance the biocompatibility and chemical reactivity of NPs, while keeping its eco-friendly nature preserved, which is however absent in other NPs produced via lethal chemical stabilizers, application of green stabilizers is encouraged [20]. Green stabilizers include moderate or low molecular weight organic moieties such as monomers/polymers of carbohydrates, organic acids such as citric acid, flavonoids, and terpenoids either in purified form or occurring naturally

in a mixture of other reductants/oxidants [20–23]. The role of some polymeric compounds as nano-stabilizers is discussed in the following sections.

### 4.2.1 Biodegradable Polymers

These can be extracted or derived from various natural sources such as corn grain, plant cellulose and oils, chitosan, gelatin, thermoplastic starch, and polylactides or from petro-chemical products including polyesters and co-polyesters of aliphatic and aromatic compounds. Some of the biodegradable polymers can be obtained from bacterial cells in the form of small monomers or mixtures of biomass, which have been successfully employed to NPs as surface-active polymers. These polymers strongly adhere due to Van der Waals forces of attraction occurring between surface of NPs and monomeric units of polymer chain. Hence, the surface energy is decreased, as compared to native NPs due to the bonding of polymers on NPs surface leading to their stabilization [24, 25]. Also, in this process, the block polymers have been proved to be more effective stabilizers than homopolymers owing to their efficient phase separation, higher surface reactivity, elasticity, selectivity, and resistance [26].

#### 4.2.1.1 Polylactides (PLA) and Conjugated Copolymers

The PLA is a biodegradable aliphatic polyester derived from plant sources like corn starch or sugarcane. Due to its thermoplastic, stable, biocompatible, yet biodegradable nature, it is suitable for biomedical purposes such as tissue engineering and drug delivery [27]. PLA-conjugated polymer-stabilized metal NPs are used in magnetic cell separation, hyperthermia treatment of tumor, and target-specific drug delivery [28, 29]. In an earlier study, Wassel et al. [30] reported that UV irradiation and gradient temperature method of NPs stabilization, which involves di-block poly(D,L-lactide-co-glycolide) and triblock poly(lactide-b-siloxane-b-lactide) copolymers in organic solvent stabilizes the spherical shaped magnetic NPs with nil or poor aggregation over a tested timeframe. Later on, Ragheb and Riffle [28] demonstrated the role of pH in the degradation of copolymers which is important for the complete adsorption of copolymer onto the surface of magnetic NPs. Another classical example is the gold (Au) NPs stabilized by phase separation approach which are extensively developed and utilized in biological and medical fields due to their biocompatibility, smaller size, and surface chemistry [31, 32]. Moreover, a preparation-cum-stabilization procedure was formulated by Qiu et al. [27], involving the dissolution of NPs precursor in aqueous media which were subsequently transferred to organic phase ($N(C_8H_{17})_4Br$ in toluene) under vigorous stirring resulted in Au NPs being spherical predominantly. These Au NPs also demonstrated their stability in weakly polar or non-polar organic solvents such as toluene and chloroform.

#### 4.2.1.2 Polysaccharides

Polysaccharides are yet another important stabilizer for NPs. These are unbranched (linear) or branched polymeric carbohydrate chains, linked together via the

glycosidic bonds, and hence they provide NPs a significant surface modification using ingrained carbohydrate chemistry and allow tailored surface functionality of metal NPs [33].

### Carboxymethyl Cellulose (CMC)

Among the polysaccharides, cellulose is one of the most plentiful natural biopolymers. After its modification to sodium (Na) carboxymethyl cellulose (CMC), it has found immense quest of applications in various technologies, biomedical applications, antimicrobial coatings, biolabeling, and food packaging due to its properties of exerting high sensitivity and lesser toxicity [13, 34]. For instance, iron (Fe) NPs have found stabilized using CMC in aqueous solutions irrespective of the temperature used. On the contrary, the stabilization of Au, Pd, and Pt was not promising when attempted with CMC due to their inability to chelate with carboxyl ($-COO^-$) groups of CMC [13, 35]. Also, Nadagouda and Varma [35] fabricated homogeneously colored metal nanocomposites by employing microwave irradiation method using CMC both as reducing and capping agents. Moreover, Cu-CMC composite, spherical indium (In) and Fe NPs embedded uniformly in CMC, and cubical Ag NPs were also synthesized [35]. Stable spherical Fe NPs prepared via reduction by sodium borohydride ($NaBH_4$) in water were found similar in size to those generated by microwave irradiation. In another study, the CMC along with ascorbic acid reduced and stabilized Pd NPs in aqueous solution at a temperature gradient ranging from 22 to 95 °C which showed spherical nanostructures with 10% increase in size, as compared to NPs reduced by conventional methods [36]. He et al. [34] also stabilized Pd NPs using CMC and reported greater surface catalysis of CMC-Pd NPs for the degradation of trichloroethene (TCE) in aqueous solutions. Similarly, Liu et al. [37] stabilized faceted but spherical Pt NPs by CMC which were initially reduced by $NaBH_4$. The CMC-Pt NPs were found stabilized for about 9 months. Furthermore, the size and stability of metal NPs are highly dependent on the molar ratio of polymer like CMC and metal concentration with additive roles of pH of the reaction mixture and concentration of cations such as $Na^+$ and $Ca^{2+}$ in water [34]. However, Liu et al. [37] reported that no observable effect of CMC concentration was seen on the size of Pt NPs, while it significantly decreased the size of CMC-stabilized Pd NPs with simultaneous increase in temperature [34, 36].

### Chitosan

Chitosan (2-amino-2-deoxy-b-β-glucan) being a deacylated derivative of chitin is hydrophilic and nontoxic in nature. Hence, its derivatives are widely used in biosensor development, pharmaceutical and food industry, drug delivery, and wastewater treatment [36, 38–40]. Due to its multifarious uses, chitosan has been attempted to be used as eco-friendly stabilizer of metallic NPs. Wang and Cui [39] stabilized Au NPs by chitosan. The amino ($-NH_2$) and hydroxyl (-OH) groups of chitosan in the presence of luminol resulted in the formation of spherical Au NPs of mean size as 18 nm (chitosan or luminal alone) and nanoflowers of 10 nm (chitosan + luminol) in 2% acetic acid solution. Likewise, the synthesis of chitosan-stabilized Ag NPs was reported by Murugadoss et al. [41], with overall yield of NPs ranging

from 70 to 98% which were then exploited in C-C coupling reactions. Wei et al. [38] also documented the synthesis of single-crystal chitosan-Au NPs with regular shaped micro-sized nanosheets at high salt concentrations (8–12 mM), while a large number of Au NPs of size 50 nm were produced at smaller salt concentrations (<8 mM). Wang et al. [42] proposed the synthesis of chitosan-ninhydrin (CHIT-NH) bioconjugate in 2% acetic acid solution at 37 °C, resulting in highly branched but spherical assemblies having a mean diameter of 18 nm which was stable for longer period of time. This biological method increases the effectivity and limits the use of reducing agent.

#### Other Polysaccharides

Other polysaccharides include dextran (a D-glucopyranosyl polysaccharide polymer) which has good biocompatibility, hydrophilicity, and nontoxicity is used in coating of various polymeric as well as metallic NPs. In this context, Jiang et al. [43] used a complex of ammonium hydroxide ($NH_4OH$), urea, and dextran (pH 10–11), producing narrow size NPs of 25.3 nm in comparison with those obtained via conventional co-precipitation method. In a study, Philip [44] exemplified the functionalization of Au NPs in aqueous solution of honey (major source of fructose, glucose, and amino acids) at room temperature, which resulted in unstable triangular NPs at lower honey concentrations, whereas stable spherical NPs were generated with an average size of 15 nm at higher concentrations of honey. Theoretically, fructose, glucose, gluconic acid, vitamin C, sucrose, and enzymes play a major role in the reduction and simultaneous stabilization of NPs. However, the exact mechanism of reduction/stabilization remains unclear and warrants further research. The utilization of polysaccharides with a comprehensive outlook on different preparatory methods for Ag NPs and their application as antibacterial agent has been reviewed by Sharma et al. [45].

### 4.2.1.3 Polyethylene Glycol (PEG) and Block Copolymers

Apart from the other polymers, the polyethylene glycol (PEG) and other block copolymers have captivated much consideration due to their cost-effectiveness, nil toxic impact, hydrophilicity, and tunable properties [46]. PEGylated metal NPs provide a wide range of biomedical and chemical uses such as contrasting agent in diagnosis for computed tomography [47], colloidal biosensors, semiconductors [48, 49], and catalysis [50]. Nadagouda and Varma [35] have reported synthesis of various NPs such as Ag, Fe, and Pt and their stabilization by PEG using one-pot synthesis by mixing aqueous metal salt solutions with PEG (300 g/mol) at room temperature followed by microwave irradiation at 100 °C/280 psi pressure for 1 h evading usage of any surfactants or reducing agents. Sawoo et al. [51] suggested that the PEG concentration is the major factor in controlling the size and morphology during the stabilization of metal NPs with an optimum amount reaching at surface saturation of NPs with PEG. The literature suggests that the NPs have predominantly been prepared at higher PEG concentrations, while nucleation of nanorods with NPs has been observed at low PEG concentrations. Huang et al. [50] postulated the assistance of organic solvents in the stabilization of metal NPs with homopolymer of

PEG by dissolving certain amounts of metal salts with solvents such as *n*-heptane, toluene, etc. with various concentrations of PEG under pressurized hydrogen for desired time period. In an earlier study, Nakao et al. [52] reported the stabilization of Pd NPs by PS-PEG which also exhibited redox reaction of selected organic compounds under aerobic and aqueous conditions yielding up to 99% of NPs. Furthermore, the thermodynamic stability of a metal NPs is due to the steric stabilization by composition and density of block copolymer, polymer-metal ratio, and reducing agent used such as hydrogen and $NaBH_4$ [40, 53, 54]. Interestingly, Huang et al. [50] also reported the ability of block copolymers of PEG as efficient stabilizers for NPs but only in non-polar organic solvents used at high temperature. The non-polar nature of PEG and higher temperature render the copolymers miscible with metal NPs which bind to metals in the core providing easier separation of PEGylated NPs from the reaction mixture. On the other hand, Sidorov et al. [55] postulated water-assisted stabilization of metal NPs by using branched copolymer of PEG, where only one part of copolymer stabilized the NPs.

#### 4.2.1.4 Enzymes

Over the years, enzymes have successfully catalyzed many biological reactions and hence emerged as a reasonable choice for processes including bioremediation, bio-catalysis, biosensing, and biomedical applications. While possessing the aforesaid potential, the enzymes have also reduced the energy and raw material consumption with almost nil or very low generation of waste and toxic by-products [56, 57]. Moreover Scott et al. [56] have defined initiation or reduction sites present on enzyme-metal NPs which in turn enables efficient stabilization and controlled size of NPs, thereby expanding perceptive methods of biomimetic NPs synthesis.

The effective stabilization of metal NPs by glutathione reductase from *E. coli* via interactions of NPs with active sites of cysteine molecule has been reported [56]. It was a major breakthrough for biomimetic synthesis of NPs which further directed the reduction of metal ions to metal NPs via specific adsorption of metal to the active sites of enzymes. In addition, different oxidase enzymes have also been used as stimulant for the production of stable metal NPs. In this regard, Willner et al. [58] reported the acetylcholinesterase (AChE) enzyme-mediated synthesis of gold nanowires, addition of glucose enhanced the growth of NPs ranging from 2–3 nm to 10–30 nm in just 10 min. Karam et al. [59] used a homodimer glycoprotein glucose oxidase (GOx) for the stabilization of Pt NPs (4 nm) in the presence of hydrogen to fabricate biosensor having the ability to detect oxidation of $H_2O_2$ and glucose. Moreover, enzymes have been effectively utilized both as reducing agent and stabilizer in NPs synthesis which adhered covalently or non-specifically to NPs [60]. Rangnekar et al. [61] reported that α-amylase simultaneously mediated synthesis and surface functionalization of spherical shaped Au NPs at pH 7.0 (37 °C) for 2 days. The resulted Au NPs retained activity of α-amylase over an extended period of time for starch digestion. In a study, Brennan et al. [60] stabilized Au NPs using lipase obtained from *Thermomyces lanuginosus*, while Gole et al. [62] studied the production of aspartic protease-stabilized Au NPs extracted from fungus *Aspergillus satoi*. Eby et al. [63] synthesized spherical lysozyme-Au NPs efficient to be used in

biology or medicine, via lysozyme monolayer-protected Au NPs providing excellent stability.

#### 4.2.1.5 Other Stabilizers

Numerous protocols have been discussed for the synthesis of engineered NPs such as synthesis via organic solvents or capping agents [64, 65], for creating electrosteric and electrostatic repulsions between individual particles which prevents their aggregation and thus sedimentation in solutions [66–68]. The vital objective of organic coating is stabilization of NPs without aggregation in or at certain stages of growth of NPs. Different types of engineered nanostructures have been produced which varied in size and shape such as nanorods, nano-tubes, quasi-spheres, nano-discs, nano-cubes, nano-prisms, and triangular nano-plates [69, 70]. The Ag NPs are one of the most studied among NPs for their different shapes and morphologies which are illustrated in Fig. 4.1 [71]. The synthesized NPs are generally coated with capping agents such as polysaccharides, citric acid, proteins, surfactants, polymers, and natural organic matter (NOM) [72, 73] and inorganic ligands like chloride, sulfide, carbonate, and borate [74, 75]. The activity and fate of the core-shell NPs are usually

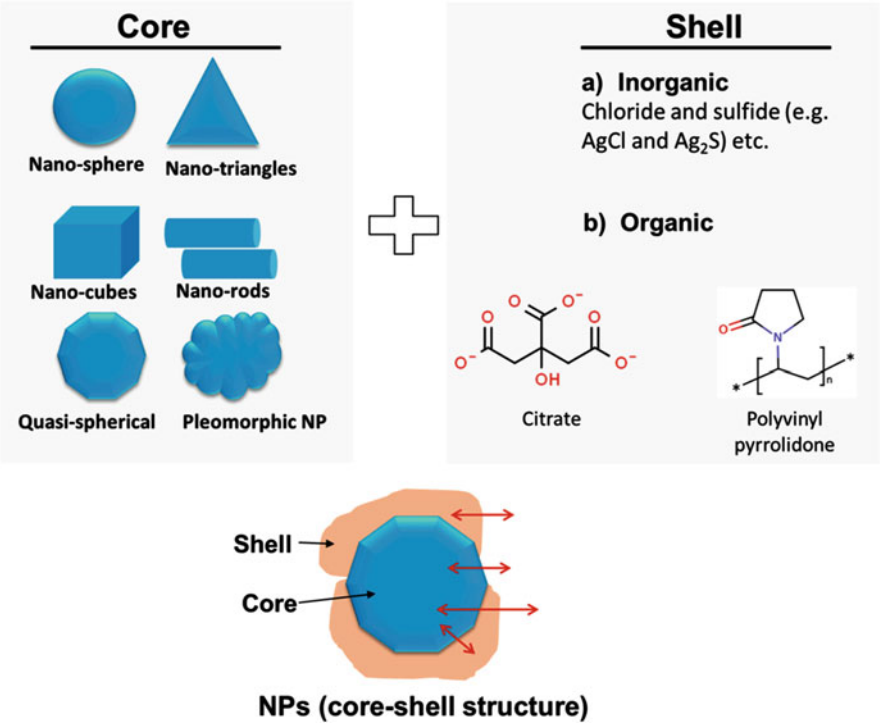


**Fig. 4.1** Typical core-shell structure of a NP that might be released into the environment. Double arrows in red represent the reactions that occur between the shell or the core with the environment and also at the interface between core and shell

determined by the properties of shell formed around the NP core consisting of reduced metal atoms (Fig. 4.1).

Among the organic capping agents used for NP synthesis, citric acid is the most commonly used (Fig. 4.1) [76], followed by oleic acid [77]; polysaccharides such as sophorolipids, maltose, and GA [78]; and surfactants such as cetyltrimethylammonium bromide, sodium dodecyl sulfate, and Tween 80. Proteins like bovine serum albumin, low molecular weight fatty acids, and polymers like dodecanethiol, thiol-modified oligonucleotides, polyethyleneimine, polyacrylamide, polyvinyl alcohol, poly(diallyldimethylammonium chloride), and polyvinylpyrrolidone (PVP) [79, 80] are also used as NP surface modifiers for their effective stabilization. Studies have shown that organic matter such as fulvic and humic acids are also able to form stable NPs [81].

### Importance of Stability

The ever-increasing demand of nano-enabled products for various industrial and domestic end uses, and their release from those products into the environment has raised alarm on human health effects as well as toxicity to primary producers of terrestrial ecosystems [82, 83]. NPs when released into the environment are expected to interact with the biological systems due to the presence of organic ligands, ion channels/pumps, and low pH. Considerable amounts of selenium (Se) and photochemistry in the near-skin regions may also be involved in the transformation of metal NPs, for instance, Ag NPs (Fig. 4.2) [84], such as the dissolution of ions from NPs in the gastrointestinal (GI) tract and inhalation and ingestion of NPs.

Interestingly, selenide ions are known to rapidly exchange sulfide ions in $Ag_2S$ films and $Ag_2S$-NPs, for example, the dermal connective tissue in argyria proteins was found to have silver-rich granules containing S and Se [85]. Loeschner et al. [86] in a study detected the presence of NPs prepared from Ag, S, and Se in the intestine of rat. Further, $Ag^+$ possess greater affinity toward proteins and thiols, and therefore Ag-protein and Ag-thiol complexes are easily formed which results in the immobilization of Ag as Ag NPs in the near-skin region (Fig. 4.2) [87].

In aqueous conditions, various processes such as aggregation (homo or hetero), redox reactions, flocculation, dissolution of ions, and adsorption of NOM and sulfidation play an important role in the transformation of NPs (Fig. 4.3) [71, 88, 89]. The surface functionalization or capping of NPs determines the stability and transport of NPs in the environment. The radiation-based processes like phototransformation, photoreduction, and photo-oxidation of organic matter produce hydroxylated or oxygenated hydrophilic species. Such processess are critical for the stability of NPs. Some other environmental parameters including pH, ionic strength, dissolved amounts of oxygen and sulfide, type of coating material, light, bio-colloids, clays, and NOM such as fulvic and humic acid also influence the stability of NPs in soil as well as aquatic system.

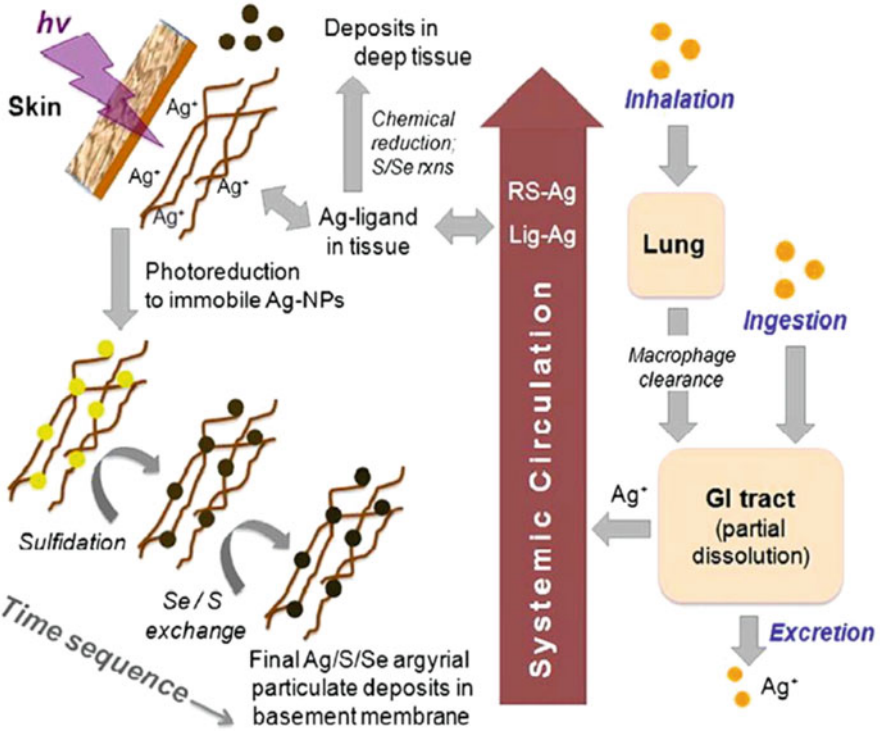


**Fig. 4.2** Summary of the biological transformations of Ag NPs and conceptual model for formation of argyrial deposits. The Ag/S/Se argyrial particulate is proposed to be the result of gastric dissolution, ion uptake, circulatory thiol transport, and photoreduction to immobile secondary particles of zerovalent silver followed by sulfidation and Se/S exchange reactions. $Ag^+$ complexes may be secondarily reduced in deep tissues at slower rates by non-photochemical processes. (Reproduced with permission from ref. [84], Copyright 2012 American Chemical Society)

## 4.3 Factors Influencing the Stability of NPs

### 4.3.1 Biological Medium

Over the past years, an urgent emphasis has been laid upon the stability of NPs in biological media for understanding their fate on human system and environment. Generally, the stability of NPs is appraised on the basis of changes in surface plasmon resonance (SPR) as it was discussed for PVP-coated Ag NPs [90]. In that study, the formulations of CM-1 (OECD, pH 6.9), CM-10 (OECD, pH 7.3), NM-1 (pH 6.9), NM-10 (pH 7.4), SM-1 (pH 7.0), and SM-10 (pH 7.2) and chloride ion ($Cl^-$) of OECD media at identical ionic strength were substituted with nitrate ($NO_3^{2-}$) and sulfate ($SO_4^{2-}$) ions, respectively. PVP-Ag NPs were found stable for about 21 days showing no considerable decline in its absorbance with a minor

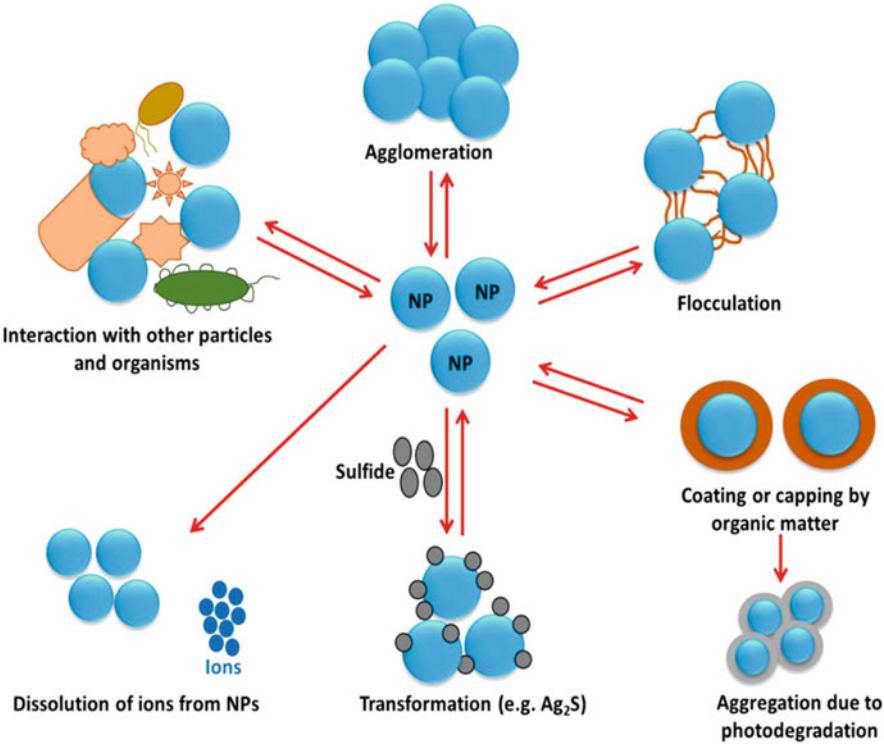


**Fig. 4.3** Major forms of NP transformation in soil and aquatic environment

peak area reduction up to 8–13% in aqueous media. A similar study on citrate- and PEG-stabilized Ag NPs reported major decrease in the SPR of Ag NPs. In all media studied, the sum loss in SPR peak area of citrate-Ag NPs was experiential between 0 and 3 days. In CM-10, the decreased absorbance was found to be about 40% in 21 days with no qualitative changes in SPR spectra. Relatively, SM-10 and NM-10 were found with a continuous absorbance decrease at 390–393 nm with simultaneous peak broadening from 470 to 550 nm. Interestingly, TEM micrographs exhibited no apparent changes in the shape of PVP- and PEG-Ag NPs in SM-10 and NM-10, whereas citrate-stabilized Ag NPs showed extensive modifications in the shape from spherical to triangular and hexagonal. The standard OECD medium used in contact studies caused agglomeration of Ag NPs, resulting in alternations in shape, morphology, and levels of Ag NPs in contrast to well-dispersed particles without OECD medium [91].

The effect of pH on the stability of organic-capped Ag NPs in culture media at 50 °C [92] showed decreased intensities of SPR peaks at pH 2 and 3. The rate was faster in SPR peak disappearance at pH 4 and 10. No absorbance decrease was observed at pH 7 and 9. In bovine serum albumin (BSA) capping of Ag NPs, no decrease in absorbance was observed except at pH 4 and 10 with its stability due to

the steric effect branching from BSA molecules of size 66 kDa. Starch-layered Ag NPs were found to be exceptionally more stable except for pH 10, as compared to citrate- and BSA-Ag NPs. The disappearance of Ag NP signal at pH 10 could be due to the reaction of Ag atoms bound to Ag NP surface under basic conditions [92]. The compositional effects of electrolyte such as alkali chlorides (NaCl, LiCl) and potassium halides (KBr, KCl, and KI) were also studied in case of citrate-coated Ag NPs [92]. A decrease of ~10–20% in SPR peak of Ag NPs in alkali chlorides was noted up to 3 days which remained unchanged with change in type of metal ion. In contrast, there were distinct effects of different halide ions: the decrease in the rate of SPR peak increased in the following order: $Cl^- < Br^- < I^-$. A complete decrease in KI solution was observed for <10 h attributing to oxidative decomposition of the surfaces of Ag NPs and their aggregation induced by halide ions [93].

### 4.3.2 Natural Organic Matter (NOM)

The NOM involved in the determination of fate and transport of NPs in aquatic environments [94, 95] consists of numerous molecules, and its composition varies with type of water chemistry, source materials, and biogeochemical processes [95, 96]. Since the volumes of NOM are higher in magnitude than engineered NPs, their fate and properties are greatly affected. Scientific findings regarding interactions between NPs and NOM like fulvic acid and humic acid have been reported to provide stabilization due to charge and steric effects of synthesized NPs [97], via slowdown of proton relaxation. Besides, proteins as constituents of NOM also stabilize NPs. For instance, casein produces stable Ag NPs with no agglomeration which depends on the NOM's concentration and pH of the solution [98, 99]. The Fourier transform infrared (FTIR) spectroscopic analysis suggests the participation of amide I (C=O stretch at 1600–1700 $cm^{-1}$) and amide II (C-N stretch and N-H deformation at 1530–1560 $cm^{-1}$) linkages with the presence of negative charge on NP surface confirmed by zeta potential.

### 4.3.3 Ionic Medium

Several studies have been undertaken to investigate the effects of ionic strength and surrounding electrolyte composition on NPs stability [100–102]. Different parameters such as electrophoretic mobility, zeta potential ($\zeta$), aggregation kinetics, hydro-dynamicity, critical coagulation concentration, particle size, and attachment efficiency have been determined for the detailed understanding on the influence of different ionic species on the stability of different coated NPs [103, 104]. The effect of ionic strength in $AgNO_3$ medium at different pH revealed that with an increase in ionic strength, the measured hydro-dynamicity increases for both uncoated $H_2$-Ag NPs and electrostatic well-stabilized citrate- and borohydride-Ag NPs, suggesting appreciable decrease in the thickness of diffused layer with a simultaneous increase in ionic strength, thereby increasing the possibility of particle settlement and

aggregation. Both ionic strength and pH demonstrated their influence on the aggregates of BPEI-Ag NPs which were more distinct at pH $< 7$ than pH $\geq 7$. Both electrostatic and steric repulsions stabilized the BPEI-Ag NPs with varied pH values [105].

The revise on $H_2^-$, citrate-, and $NaBH_4$-Ag NPs under various electrolytes of similar ionic strengths exhibited no significant change in HDD induced by $Cl^-$ ion due to the formation of steady negatively charged AgCl nano-colloids, but 0.01 M $Ca^{2+}$ aggregated them. The values of ionic strength, pH, and electrolyte type were found to have no promising influence on the aggregation of PVP-Ag NPs. In another study conducted by Li et al. [106], the aggregation of Tween 80 and SDS-Ag NPs in $NaNO_3$, $CaCl_2$, and NaCl were investigated with their kinetics of aggregation in different electrolytes found to be well consistent with Derjaguin-Landau-Verwey-Overbeek (DLVO) theory.

### 4.3.4 Dissolved Oxygen

In aqueous medium, a possibility exists of the release of metal ions due to dissolved oxygen-mediated oxidation. An orderly approach dealing majorly with the kinetics of metallic (e.g., $Ag^+$) ions released from citrate-Ag NPs was reported under unlike conditions (such as size of the particle, Ag NP concentration, pH, and oxygen) [107–109]. The amount of $Ag^+$ ions released by dissolved oxygen with Ag NPs of different size of particles as a time function has been reported [110]. The rate of released $Ag^+$ revealed first-order kinetics with an appreciable increase in the rate of $Ag^+$ ion release in case of all particle sizes with concentration increase from 300 to 600 μg $l^{-1}$. The released $Ag^+$ ions were found to be lower in large-sized particles exhibiting the rate of release to be inversely proportional to the size of the particle. Miscible salts of marine water had minor effects on the release of $Ag^+$ ions. Hydrogen peroxide ($H_2O_2$), the transitional product of dissolution of Ag NPs (size 10 nm), induces the latter by 100 times faster than in case of oxygen [108]. A recent analysis carried out on exposing citrate-, PVP-, and tannic acid-Ag NPs (sizes 5 nm, 10 nm, and 50 nm, respectively) to lake and river water reported the rapid solubility [111]. The dissolution of Ag NPs under oxygenic conditions was expected to take place in 6–125 days for completion of citrate-Ag NPs into $Ag^+$ in the environment. Therefore, the dissolution rate was slow, and NPs were found participating in other processes like settlement, aggregation, and interaction with living biota of the environment.

### 4.3.5 Luminosity

A few studies conducted for analyzing the changes in Ag NPs due to irradiation of sunlight and artificial light [106, 112] revealed that NPs under conservative fluorescent light irradiation and laser pulse excitation generate fragments of small particles fusing to form large spheres [113, 114]. The photo-induced fusion and fragmentation

change the morphological features along with the available total surface area of NPs due to the transformation processes like photo-sensed fragmentation, fusion, and reduction. In studies related to bare Ag NPs and citrate-Ag NPs, Li et al. [106] reported the dissolved Ag concentrations were found to be 24.5 and 28.4 μg $l^{-1}$ at dark conditions, respectively, while the values under light were found as 24.5 and 28.0 μg $l^{-1}$. The characteristic SPR peak of GA-Ag NPs (6 and 25 nm) at wavelength of 400 nm sharply decreased in less than 4 days of sunlight treatment [112], with TEM micrographs suggesting particle aggregation into larger ones. In comparison, PVP-capped and Tween-capped Ag NPs were found to be stable under light irradiation with the former one well-dispersed in the solution [106, 112]. Similar results were also reported in the case of irradiated PVP-Ag NPs which is explicated by the disparities in the binding energies of core coatings of Ag NPs. A novel technique of photo-oxidation of individual particles of Ag NPs was reported by the method of spatial modulation spectroscopy [115], in which real-time pathways of morphological and optical changes were observed. The reaction of $H_2O_2$ with citrate-capped Ag NPs has also been studied [116], in which their reactivity was different from Ag NPs generated under in situ conditions from the reduction of ionic $Ag^+$ by $O_2^{\cdot -}$. Other studies have also been carried out demonstrating the NP formation (especially Ag NPs) under irradiations of UV light and sunlight inducing the reduction of ionic $Ag^+$ to Ag NPs in presence of crude organic matter in the solution [117]. The fixed state concentration of NPs depends on the competitive rates of the reactions that are dependent on pH and size of the particle. The following reaction may occur during the interaction of Ag NPs with $O_2^{\cdot -}$ and $H_2O_2$:

$$\text{Intermediate} + H_2O_2 \rightarrow Ag^+ + O_2^{\cdot -} \quad k_1 > 1.0 \times 10^7\,M^{-1}s^{-1} \tag{4.1}$$

$$Ag^+ + O_2^{\cdot -} \rightarrow Ag\,NP + O_2 \quad k_2 = 6.45 \times 10^1\,M^{-1}s^{-1} \tag{4.2}$$

$$Ag\,NPs + O_2^{\cdot -} \rightarrow Ag\,NP^* + O_2 \quad k_3 = 1.0 \times 10^{10}\,M^{-1}s^{-1} \tag{4.3}$$

$$Ag\,NP^{\#} + O_2^{\cdot -} \rightarrow Ag\,NP + O_2^{\cdot -} \quad k_4 = 2.0 \times 10^9\,M^{-1}s^{-1} \tag{4.4}$$

$$Ag\,NP^{\#} + Ag^+ \rightarrow Ag\,NP + Ag\,NP \quad k_5 = 7.0 \times 10^{10}\,M^{-1}s^{-1} \tag{4.5}$$

$$Ag\,NPs + O_2 \rightarrow Ag^+ + O_2^{\cdot -} \quad k_6 < 0.01\,M^{-1}s^{-1} \tag{4.6}$$

where "*k*" is the reaction rate constant.

## 4.4 Toxicity of NPs

The toxicity of metals and their ions have been known since time immemorial [118], but the understanding of toxicity of their nanoforms and mechanisms still remains an inscrutable theory. Some of the suggested mechanisms can be listed as (1) direct damage to the cell membrane by NPs, (2) disruption in the processes of ATP production, (3) DNA replication by metal ions released by NPs, (4) vacillations in

gene expression, and (5) ROS generation by NPs [119–121]. Feng et al. [122] reported the disruption and block of microbial respiratory chain in the region of enzyme cytochrome oxidase and nicotinamide adenine dinucleotide ($NAD^+$/NADH) by Ag ions, while Rainnie et al. [123] reported the inhibition of oxidation of compounds like glucose, glycerol, succinate, etc. due to Ag ions in *E. coli*.

### 4.4.1 Cyto- and Geno-Toxicity

In recent years, studies pertaining to NPs toxicity have been documented underlining [120, 124] several processes such as (1) increased levels of ROS, (2) diminutions in the levels of intracellular glutathione, (3) decreased potentials of mitochondrial membrane of organisms [125], and (4) inflammations in lung epithelial cells and macrophages [120]. Rahman et al. [126] reported upregulation of several genes responsible for oxidative stress in mouse brain. In general, the process of toxicity is affected by a variety of parameters like stability, purity, and surface functionalities. For instance, chitosan-capped Ag NPs possess antimicrobial activity with nontoxicity toward the eukaryotic cell [127]. The production of ROS induced by NPs is one of the major reasons of spontaneous DNA damage with short-lived hydroxyl radical ($^{\cdot}OH$), possessing high reactivity toward DNA via the means of cross-linking of intra- and inter-strands and DNA-protein interactions [128]. AshaRani et al. [129] reported ATP reduction in human glioma (U251) and human lung (IMR90) cells on exposure to Ag NPs, whereas Hsin et al. [130] reported the activation of cytochrome c release, c-Jun N-terminal kinases (JNK) (phosphorylation), Bax translocation, cleavage of p53, and poly(ADP-ribose) polymerase on exposure to NPs.

### 4.4.2 Toxic Effects on Biotic Community

#### 4.4.2.1 Plant System

Transformation of NPs has been found in food chains due to the ingestion and utilization of plant parts by both humans and animals. Various plants such as *Cucurbita pepo*, *Phaseolus radiatus*, *Hordeum vulgare*, *Sorghum bicolor*, *Lolium perenne*, *Lolium multiflorum*, *Linum usitatissimum*, *Solanum lycopersicon*, and *Allium cepa* have been studied at length for their interactions with NPs [131–137]. Stampoulis et al. [138] quantified the Ag concentration in the plant shoots of zucchini (*Cucurbita pepo*) to be 4.7 times higher in magnitude when exposed to 10–1000 mg $l^{-1}$ Ag NPs to that of bulk Ag at the same concentration. In contrast, when plants of *Brassica juncea* were exposed to Ag NPs, no accumulation of Ag in any form was observed [139]. Lee et al. [140] documented the energy dispersive spectroscopy (EDS) peaks for the confirmation of the presence of Ag in root cells of *Sorghum bicolor* and *Phaseolus radiatus*. Overall, the uptake, accumulation, and translocation of NPs depend on the species of plant and size, composition, type, and aggregation state of NPs [141–144].

#### 4.4.2.2 Bacteria

Extensive and detailed literature on the toxicity of NPs to different bacterial species are available. Species of *Escherichia coli*, *Nitrosomonas europaea*, *Bacillus subtilis*, *Pseudomonas fluorescens*, and *Pseudomonas aeruginosa* have been studied at stretch pertaining to their toxicity models [145–149]. The microbial technique of colony-forming units and variations in the optical densities allow the conception of growth curves and calculation of MICs (minimum inhibitory concentrations) for the analysis of viability and cultivability of bacteria. Electron microscopic study and fluorescently labeled probes have also been employed for the study of morphological changes and ROS (reactive oxygen species) formation along with Raman spectroscopic peaks, mass spectrometry, FTIR, and quantitative PCR for the visualization of observational changes in outer membranes and bacterial genes [150–152]. For instance, Shahverdi et al. [153] and Neal [154] reported the penetrability of NPs into the bacterial cell membranes, causing an increase in the respiratory disturbances and permeability, leading to cell lysis followed by the interaction of released NPs with thiol groups of proteins resulting in the inactivation of vital enzymes and affecting DNA replication. Fabrega et al. [155] examined the Ag NPs' effect on the growth patterns of *P. fluorescens* under different conditions (organic matter, pH, and concentration). Apart from bacterial growth inhibition, NPs were found to be involved in the change of composition of bacterial communities in natural waterbodies upon exposure [156]. Several studies stressed on inactivation and influence of specific ions on Gram-positive and Gram-negative species by organic NPs have been performed [157, 158]. The structural arrangement of cell wall decides the degrees of NP toxicity: cell wall of Gram-positive consists of thick layer of about 20–50 nm of peptidoglycan (PG), appended to teichoic acid in contrast to that of Gram-negative ones with slim PG layer enclosed in outer membrane, resistant to both chemo- and hydrophobic compounds [159–162]. Therefore, the transportation of NPs into the bacterial cell is more stalled in Gram-negative bacteria than Gram-positive ones [157]. Yuan et al. [146] reported coating-dependent damage to the cell wall of *N. europaea* ATCC 19718.

In a study, the role of particle size of Ag NPs and oxygen was investigated against *E. coli* [148, 163]. Under anoxygenic conditions, 158 mg $l^{-1}$ of PEG-Ag NPs (5 nm) and 195 mg $l^{-1}$ of PEG-Ag NPs (11 nm) showed no toxic effects on *E. coli* [148]. The Ag NP concentrations used were about three orders of amount higher than minimum lethal concentration (MLC) of $Ag^{+}$ ions (0.025 mg $l^{-1}$) under similar conditions [163]. Under aerobic environment, enhanced toxicity to *E. coli* was observed, conferred upon by aerial Ag NP dissolution by releasing $Ag^{+}$ ions and enhancing Ag NP toxicity. The particle size effects for PEG- and PVP-Ag NPs is illustrated in Fig. 4.4 [148]. Under oxygenic environment, the oxidative dissolution of crystal cores increased the soluble silver ion concentration; thereby, small-sized Ag NPs releasing more soluble $Ag^{+}$ ions increase the toxicity with EC50 values with increased particle size, further indicating the size-dependent toxicity. The addition of $Cl^{-}$, $S^{2-}$, phosphate, and cysteine decrease the toxicity [163]. The role of NP sulfidation was examined by exposure of *E. coli*, in which sulfidation process of

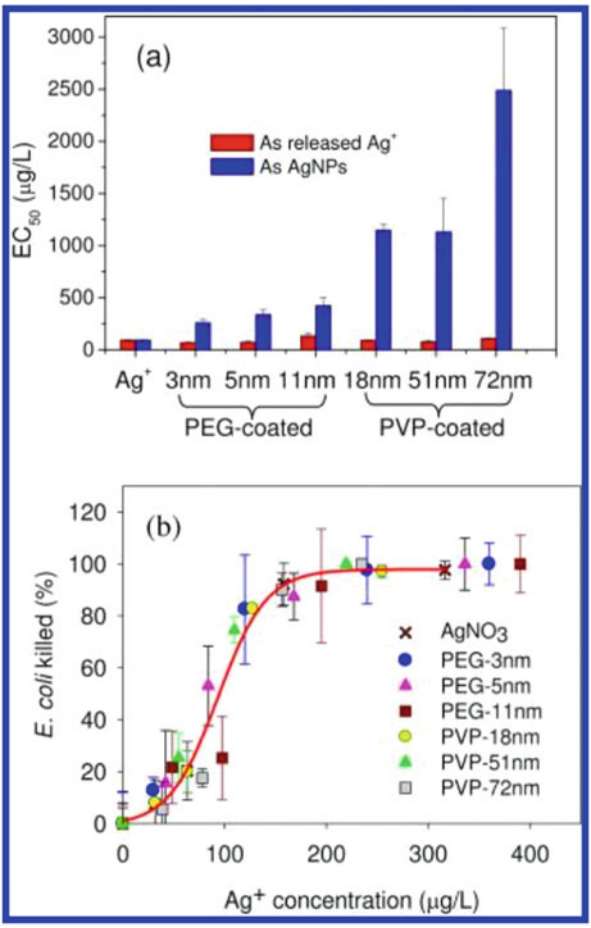


**Fig. 4.4** Dose-response of *E. coli* vulnerable to various air-exposed Ag NPs. EC50 increases with the increasing particle size (**a**), suggesting size-dependent toxicity. This is an indirect effect associated with $Ag^+$ release (smaller Ag NPs release more $Ag^+$ and are more toxic). Antibacterial activity expression as a function of the concentration of the released $Ag^+$ was statistically indistinguishable from the dose response patterns of cells exposed to $Ag^+$ (added as $AgNO_3$) ($p > 0.05$), illustrating that the released $Ag^+$ is the critical factor of antibacterial activity (**b**). (Reproduced with permission from ref. [148], Copyright 2012 American Chemical Society)

monodispersed particles was observed with partial sulfidization of polydispersed particles, retaining potential toxic effects of NPs [164].

#### 4.4.2.3 Terrestrial and Aquatic Life Forms

Numerous enthused patterns on the effect and fate of NPs have been studied for the estimation of porched concentrations of NPs for their eco-toxicological effects on the biota of terrestrial and aquatic environments [165–167]. NPs in soil and aquatic phases generally enter the body via mouth, gills, and gut of animals, resulting in their alternations. Shape, size, ionic dissolution, and surface charge are some of the key parameters determining the conclusion of NPs exposure to zebrafish (*Danio rerio*) and its embryos [168]. The contact study of citrate-Ag NPs to *D. rerio* has shown Ag NP accumulation in the bodies of embryo, associated with downregulation of genes involved in patterns of cell growth, differentiation, and proliferation, with crystal defects at atomic or sub-atomic levels in Ag NP toxic models to medaka and embryos

of zebrafish [169, 170]. Kwok et al. [166] reported differential toxicities of GA-, PVP-, and citrate-Ag NPs to Japanese medaka, with highest toxicity exhibited by GA-coated Ag NPs, confirming that $Ag^+$ species are 3–10 times more toxic than Ag NPs when $AgNO_3$ and Ag NPs with the same masses were exposed separately. Many other aquatic organisms (*Pseudokirchneriella subcapitata*, *Oncorhynchus mykiss*, *D. rerio*, *Squalus acanthias*, *Ceriodaphnia dubia*, *Caenorhabditis elegans*, *Nereis diversicolor*) have also been examined [171–173].

Algae, as an important photosynthetic member of aquatic ecosystem, play an important role as food source. A few literary studies on NP-algae interactions have been reported [174–176]. An exemplary work by Burchardt et al. [177] on the effects of Ag NPs in diatom *Thalassiosira pseudonana* and cyanobacterium *Synechococcus* sp. showed induced differential effects of Ag NP exposure due to size, preparation and stability, its aggregation state, and speciation of the released $Ag^+$ ions.

In recent times, detailed investigations on Ag NP toxicity in *Daphnia magna* have been undertaken along with microcosm experiments consisting of freshwater sediments and two aquatic plants (*Egeria densa* and *Potamogeton diversifolius*) and GA- and PVP-capped Ag NPs for toxicity tests [178–180]. The findings of microcosm Ag NP experiments on two aquatic organisms, *D. magna* and *D. rerio*, have been reported. The different water matrices were designated as water (W), water + plants (WP), water + sediments (WS), and water + plants + sediments (WPS). In PVP- and GA-coated Ag NP treatment, no significant effect on matrices was seen with lower mortality in zebrafish observed for WPS and WP matrices as compared to W matrix. In *D. magna*, the WPS and WS results were the same as that of W matrix. However, WP matrix illustrated significant mortality differences inferring that plant plays a defensive role against toxic effects induced by PVP- and GA-capped Ag NPs. The toxicity tests were also conducted by exposing zebrafish to salt concentrations of $AgNO_3$. Overall, the results clearly elucidate that the plant systems (alone or in combination with sediments) provide defense against NP toxicity.

The effect of NPs on soil ecosystem has been examined using earthworms as indicator organisms [181–183], underlining as well as examining the parameters of growth, avoidance behavior, apoptotic bioavailability, gene expression, mortality, and reproduction. Silver accumulation in earthworm was found to be lower in artificial soil than sandy soil. PVP-capped Ag NPs of different sizes had adverse effects on the rate of reproduction [77], with its toxicity of lower magnitude than of $Ag^+$ ion. Patterns of gene expression were found to be similar in earthworm *Eisenia fetida* when exposed to PVP-coated Ag NPs and $AgNO_3$ in natural soils [184]. Significant similarity was observed with respect to the relationships of enzyme catalase and heat shock protein (HSP70) expression to Ag soil concentration, indicating similar toxic mechanisms of $Ag^+$ ions and Ag NPs, suggesting short-term or acute toxicity of Ag NPs [184]. The study on *Drosophila melanogaster* with mannitol-Ag NPs exhibited the toxic effect at 20 mg $l^{-1}$ with 50% of tested flies shelled or blocked at pupae stage, thus unsuccessful in completing their developmental cycle [185]. The long-term exposure to Ag NPs (5 mg $l^{-1}$) affected the fertility rates of *Drosophila* in the first three filial generations. Nevertheless, the fecundity rate of

flies in succeeding generations increased up to the level of control sample, validating the adaptableness of flies to long-term exposures of Ag NPs.

## References


1. Kumar V, Yadav SK (2009) Plant-mediated synthesis of silver and gold nanoparticles and their applications. J Chem Technol Biotech 84:151–157
2. Ahmed B, Khan MS, Saquib Q et al (2018) Interplay between engineered nanomaterials (ENMs) and edible plants: a current perspective. In: Phytotoxicity of nanoparticles. Springer, Cham, pp 63–102
3. Dwivedi S, Saquib Q, Ahmad B et al (2018) Toxicogenomics: a new paradigm for nanotoxicity evaluation. In: Cellular and molecular toxicology of nanoparticles. Springer, Cham, pp 143–161
4. Virkutyte J, Varma RS (2011) Green synthesis of metal nanoparticles: biodegradable polymers and enzymes in stabilization and surface functionalization. Chem Sci 2:837–846
5. Shi S, Chen F, Ehlerding EB, Cai W (2014) Surface engineering of graphene-based nanomaterials for biomedical applications. Bioconjugate Chem 25:1609–1619
6. Anastas PT, Warner JC (1998) Principles of green chemistry. In: Green chemistry: theory and practice. Oxford University Press, New York, pp 29–56
7. Dahl JA, Maddux BL, Hutchison JE (2007) Toward greener nanosynthesis. Chem Rev 107:2228–2269
8. Karn B (2008) Research on nanotechnology applications: green nanotechnology for past, present, and preventing future problems. NanoECO, Monte Verita, Switzerland
9. Cherian T, Ali K, Fatima S et al (2019) Myristica fragrans bio-active ester functionalized ZnO nanoparticles exhibit antibacterial and antibiofilm activities in clinical isolates. J Microbiol Methods 166:105716
10. Paris JL, Mannaris C, Cabanas MV et al (2018) Ultrasound-mediated cavitation-enhanced extravasation of mesoporous silica nanoparticles for controlled-release drug delivery. Chem Eng J 340:2–8
11. Lyon PC, Gray MD, Mannaris C et al (2018) Safety and feasibility of ultrasound-triggered targeted drug delivery of doxorubicin from thermosensitive liposomes in liver tumours (TARDOX): a single-centre, open-label, phase 1 trial. Lancet Oncol 19:1027–1039
12. Pomogailo AD, Kestelman VN (2006) Metallopolymer nanocomposites, vol 81. Springer, Berlin
13. He F, Zhao D, Liu J et al (2007) Stabilization of Fe-Pd nanoparticles with sodium carboxymethyl cellulose for enhanced transport and dechlorination of trichloroethylene in soil and groundwater. Ind Eng Chem Res 46:29–34
14. Stubbs D, Gilman P (2007) Nanotechnology applications in environmental health: big plans for little particles. Oak Ridge Center for Advanced Studies, Oak Ridge
15. Nadagouda MN, Castle AB, Murdock RC et al (2010) In vitro biocompatibility of nanoscale zerovalent iron particles (NZVI) synthesized using tea polyphenols. Green Chem 12:114–122
16. Moulton MC, Braydich-Stolle LK, Nadagouda MN et al (2010) Synthesis, characterization and biocompatibility of "green" synthesized silver nanoparticles using tea polyphenols. Nanoscale 2:763–770
17. Lu AH, Salabas EE, Schuth F (2007) Magnetic nanoparticles: synthesis, protection, functionalization, and application. Angew Chem Int Ed 46:1222–1244
18. Baruwati B, Varma RS (2009) High value products from waste: grape pomace extract-a three-in-one package for the synthesis of metal nanoparticles. ChemSusChem 2:041–1044
19. Polshettiwar V, Varma RS (2009) Nanoparticle-supported and magnetically recoverable palladium (Pd) catalyst: a selective and sustainable oxidation protocol with high turnover number. Org Bio Chem 7:37–40

20. Ali K, Ahmed B, Khan MS et al (2018) Differential surface contact killing of pristine and low EPS Pseudomonas aeruginosa with *Aloe vera* capped hematite ($\alpha$-$Fe_2O_3$) nanoparticles. J Photochem Photobiol B 188:146–158
21. Ali K, Dwivedi S, Azam A et al (2016) *Aloe vera* extract functionalized zinc oxide nanoparticles as nano antibiotics against multi-drug resistant clinical bacterial isolates. J Colloid Interface Sci 472:145–156
22. Ali K, Ahmed B, Dwivedi S et al (2015) Microwave accelerated green synthesis of stable silver nanoparticles with *Eucalyptus globulus* leaf extract and their antibacterial and antibiofilm activity on clinical isolates. PLoS One 10:e0131178
23. Ali K, Ahmed B, Ansari SM et al (2019) Comparative in situ ROS mediated killing of bacteria with bulk analogue, Eucalyptus leaf extract (ELE)-capped and bare surface copper oxide nanoparticles. Mater Sci Eng C 100:747–758
24. Ray SS, Bousmina M (2005) Biodegradable polymers and their layered silicate nanocomposites: in greening the 21st century materials world. Prog Mater Sci 50:962–1079
25. Rozenberg BA, Tenne R (2008) Polymer-assisted fabrication of nanoparticles and nanocomposites. Prog Pol Sci 33:40–112
26. Christodoulakis K, Palioura D, Anastasiadis S et al (2009) Metal nanocrystals embedded within polymeric nanostructures: effect of polymer-metal compound interactions. Topic Catal 52:394–411
27. Qiu H, Rieger J, Gilbert B et al (2004) PLA-coated gold nanoparticles for the labeling of PLA biocarriers. Chem Mater 16:850–856
28. Ragheb RT, Riffle JS (2008) Synthesis and characterization of poly (lactide-b-siloxane-b-lactide) copolymers as magnetite nanoparticle dispersants. Polymer 49:5397–5404
29. Bensaid F, du Thillaye BO, Amgoune AP et al (2013) Y-shaped mPEG-PLA cabazitaxel conjugates: well-controlled synthesis by organocatalytic approach and self-assembly into interface drug-loaded core–corona nanoparticles. Biomacromolecules 14:189–1198
30. Wassel RA, Grady B, Kopke RD et al (2007) Dispersion of super paramagnetic iron oxide nanoparticles in poly (d, l-lactide-co-glycolide) microparticles. Colloid Surf A Phys Engr Asp 292:25–130
31. Tam JM, Tam JO, Murthy A (2010) Controlled assembly of biodegradable plasmonic nanoclusters for near-infrared imaging and therapeutic applications. ACS Nano 4:2178–2184
32. Hosta-Rigau L, Olmedo I, Arbiol J et al (2010) Multifunctionalized gold nanoparticles with peptides targeted to gastrin-releasing peptide receptor of a tumor cell line. Biocon Chem 21:1070–1078
33. Habibi Y, Dufresne A (2008) Highly filled bionanocomposites from functionalized polysaccharide nanocrystals. Biomacromolecules 9:1974–1980
34. He F, Liu J, Roberts CB et al (2009) One-step "green" synthesis of Pd nanoparticles of controlled size and their catalytic activity for trichloroethene hydrodechlorination. Ind Engr Chem Res 48:6550–6557
35. Nadagouda MN, Varma RS (2007) Synthesis of thermally stable carboxymethyl cellulose/metal biodegradable nanocomposites for potential biological applications. Biomacromolecules 8:2762–2767
36. Liu J, He F, Gunn TM et al (2009) Precise seed-mediated growth and size-controlled synthesis of palladium nanoparticles using a green chemistry approach. Langmuir 25:7116–7128
37. Liu X, Hu Q, Fang Z et al (2008) Magnetic chitosan nanocomposites: a useful recyclable tool for heavy metal ion removal. Langmuir 25:3–8
38. Wei D, Qian W, Shi Y et al (2007) Mass synthesis of single-crystal gold nanosheets based on chitosan. Carbohydr Res 342:2494–2499
39. Wang W, Cui H (2008) Chitosan-luminol reduced gold nanoflowers: from one-pot synthesis to morphology-dependent SPR and chemiluminescence sensing. J Phys Chem C 112:10759–10,766

40. Laurent S, Forge D, Port M (2008) Magnetic iron oxide nanoparticles: synthesis, stabilization, vectorization, physicochemical characterizations, and biological applications. Chem Rev 108:2064–2110
41. Murugadoss A, Goswami P, Paul A et al (2009) 'Green' chitosan bound silver nanoparticles for selective C–C bond formation via in situ iodination of phenols. J Mol Cat Chem 304:153–158
42. Wang Y, Li YF, Huang CZ (2009) A one-pot green method for one-dimensional assembly of gold nanoparticles with a novel chitosan-ninhydrin bioconjugate at physiological temperature. J Phys Chem 113:4315–4320
43. Jiang W, Yang HC, Yang SY (2004) Preparation and properties of superparamagnetic nanoparticles with narrow size distribution and biocompatible. J Magnet Mag Mater 283:210–214
44. Philip D (2009) Honey mediated green synthesis of gold nanoparticles. Spectr Acta A Mol Biomol Spectr 73:650–653
45. Sharma VK, Yngard RA, Lin Y (2009) Silver nanoparticles: green synthesis and their antimicrobial activities. Adv Colloid Interface Sci 45:83–96
46. Ma X, Jiang T, Han B (2008) Palladium nanoparticles in polyethylene glycols: efficient and recyclable catalyst system for hydrogenation of olefins. Cat Commun 9:70–74
47. Kim D, Park S, Lee JH et al (2007) Antibiofouling polymer-coated gold nanoparticles as a contrast agent for in vivo X-ray computed tomography imaging. J Am Chem Soc 129:7661–7665
48. Zhang G, Yang Z, Lu W et al (2009) Influence of anchoring ligands and particle size on the colloidal stability and in vivo biodistribution of polyethylene glycol-coated gold nanoparticles in tumor-xenografted mice. Biomaterials 30:1928–1936
49. Otsuka H, Nagasaki Y, Kataoka K et al (2003) PEGylated nanoparticles for biological and pharmaceutical applications. Adv Drug Del Rev 55:403–419
50. Huang TS, Wang YH, Jiang JY et al (2008) PEG-stabilized palladium nanoparticles: an efficient and recyclable catalyst for the selective hydrogenation of 1, 5-cyclooctadiene in thermoregulated PEG biphase system. Chin Chem Lett 19:102–104
51. Sawoo S, Srimani D, Dutta P et al (2009) Size controlled synthesis of Pd nanoparticles in water and their catalytic application in C-C coupling reactions. Tetrahedron 65:4367–4374
52. Nakao R, Rhee H, Uozumi Y (2005) Hydrogenation and dehalogenation under aqueous conditions with an amphiphilic-polymer-supported nanopalladium catalyst. Org Lett 7:163–165
53. Babu K, Dhamodharan R (2009) Synthesis of polymer grafted magnetite nanoparticle with the highest grafting density via controlled radical polymerization. Nanoscale Res Lett 4:1090–1102
54. Li D, He Q, Li J (2009) Smart core/shell nanocomposites: intelligent polymers modified gold nanoparticles. Adv Colloid Interface Sci 149:28–38
55. Sidorov SN, Bronstein LM, Valetsky PM, Hartmann J, Cölfen H, Schnablegger H, Antonietti M (1999) Stabilization of metal nanoparticles in aqueous medium by polyethyleneoxide–polyethyleneimine block copolymers. J Colloid Interface Sci 212:197–211
56. Scott D, Toney M, Muzikar M (2008) Harnessing the mechanism of glutathione reductase for synthesis of active site bound metallic nanoparticles and electrical connection to electrodes. J Am Chem Soc 130:865–874
57. Rokhina EV, Lens P, Virkutyte J (2009) Low-frequency ultrasound in biotechnology: state of the art. Trends Biotechnol 27:298–306
58. Willner I, Baron R, Willner B (2006) Growing metal nanoparticles by enzymes. Adv Mater 18:1109–1120
59. Karam P, Xin Y, Jaber S et al (2008) Active Pt nanoparticles stabilized with glucose oxidase. J Phys Chem C 112:13846–13850
60. Brennan JL, Hatzakis NS, Tshikhudo TR et al (2006) The creation of functional hybrids of lipases and gold nanoparticles. Bioconjugate Chem 17:1373–1375

61. Rangnekar A, Sarma TK, Singh AK et al (2007) Retention of enzymatic activity of α-amylase in the reductive synthesis of gold nanoparticles. Langmuir 23:5700–5706
62. Gole A, Dash C, Soman C et al (2001) On the preparation, characterization, and enzymatic activity of fungal protease-gold colloid bioconjugates. Bioconjugate Chem 12:684–690
63. Eby DM, Schaeublin NM, Farrington KE (2009) Lysozyme catalyzes the formation of antimicrobial silver nanoparticles. ACS Nano 3:984–994
64. Ravindran A, Chandran P, Khan SS (2013) Biofunctionalized silver nanoparticles: advances and prospects. Colloid Surf B 105:342–352
65. Faramarzi MA, Sadighi A (2013) Insights into biogenic and chemical production of inorganic nanomaterials and nanostructures. Adv Colloid Interface Sci 189–190:1–20
66. Hotze EM, Phenrat T, Lowry GV (2010) Nanoparticle aggregation: challenges to understanding transport and reactivity in the environment. J Environ Qual 39:1909–1924
67. Phenrat T, Saleh N, Sirk K et al (2008) Stabilization of aqueous nanoscale zerovalent iron dispersions by anionic polyelectrolytes: adsorbed anionic polyelectrolyte layer properties and their effect on aggregation and sedimentation. J Nanopart Res 10:795–814
68. Siskova K, Becicka O, Masek V et al (2012) Spacer-free SERRS spectra of unperturbed porphyrin detected at 100 fM concentration in Ag hydrosols prepared by modified Tollens method. J Raman Spectrosc 43:689–691
69. Liu G, Eichelsdoerfer DJ, Rasin B (2013) Delineating the pathways for the site-directed synthesis of individual nanoparticles on surfaces. Proc Natl Acad Sci U S A 110:887–891
70. Ringe E, Zhang J, Langille MR et al (2012) Correlating the structure and localized surface plasmon resonance of single silver right bipyramids. Nanotechnology 23:444005
71. Levard C, Hotze EM, Lowry GV et al (2012) Environmental transformations of silver nanoparticles: impact on stability and toxicity. Environ Sci Technol 46:6900–6914
72. Sanghi R, Verma P (2009) Biomimetic synthesis and characterization of protein capped silver nanoparticles. Bioresour Technol 100:501–504
73. Gigault J, Hackley VA (2013) Differentiation and characterization of isotopically modified silver nanoparticles in aqueous media using asymmetric-flow field flow fractionation coupled to optical detection and mass spectrometry. Anal Chim Acta 763:57–66
74. Delay M, Dolt T, Woellhaf A et al (2011) Interactions and stability of silver nanoparticles in the aqueous phase: influence of natural organic matter (NOM) and ionic strength. J Chromatogr A 1218:4206–4212
75. Piccapietra F, Sigg L, Behra R (2012) Colloidal stability of carbonate-coated silver nanoparticles in synthetic and natural freshwater. Environ Sci Technol 46:818–825
76. Poynton HC, Lazorchak JM, Impellitteri CA et al (2012) Toxicogenomic responses of nanotoxicity in *Daphnia magna* exposed to silver nitrate and coated silver nanoparticles. Environ Sci Technol 46:6288–6296
77. Bala T, Swami A, Prasad BLV et al (2005) Phase transfer of oleic acid capped NicoreAgshell nanoparticles assisted by the flexibility of oleic acid on the surface of silver. J Colloid Interf Sci 283:422–431
78. Kasture MB, Patel P, Prabhune A A et al (2008). Synthesis of silver nanoparticles by sophorolipids: Effect of temperature and sophorolipid structure on the size of particles. J Chem Sci 120:515–520
79. Mathew TV, Kuriakose S (2013) Studies on the antimicrobial properties of colloidal silver nanoparticles stabilized by bovine serum albumin. Colloid Surf B: Biointerf 101:14–18
80. Teerasong S, Jinnarak A, Chaneam S et al (2017) Poly (vinyl alcohol) capped silver nanoparticles for antioxidant assay based on seed-mediated nanoparticle growth. Talanta 170:193–198
81. Dubas, Stephan T, Vimolvan Pimpan (2008) Humic acid assisted synthesis of silver nanoparticles and its application to herbicide detection. Mater Lett 62: 2661–2663
82. Lapresta FA, Fernandez A, Blasco J (2012) Nanoecotoxicity effects of engineered silver and gold nanoparticles in aquatic organisms. Trends Anal Chem 32:40–59

83. Sharma VK, Siskova KM, Zboril R et al (2014) Organic-coated silver nanoparticles in biological and environmental conditions: fate, stability and toxicity. Adv Colloid Interface Sci 204:15–34
84. Liu J, Wang Z, Liu FD et al (2012) Chemical transformations of nano silver in biological environments. ACS Nano 6:9887–9899
85. Bowden LP, Royer MC, Hallman JR et al (2011) Rapid onset of argyria induced by a silver-containing dietary supplement. J Cutan Pathol 38:832–835
86. Loeschner K, Hadrup N, Qvortrup K et al (2011) Distribution of silver in rats following 28 days of repeated oral exposure to silver nanoparticles or silver acetate. Particle Fibre Toxicol 2011:8
87. Leung BO, Jalilehvand F, Mah V et al (2013) Silver (I) complex formation with cysteine, penicillamine, and glutathione. J Phys Chem C 52:4593–4602
88. Delay M, Frimmel FH (2012) Nanoparticles in aquatic systems. Anal Bioanal Chem 402:583
89. Lowry GV, Espinasse BP, Badireddy AR (2012) Long-term transformation and fate of manufactured Ag nanoparticles in a simulated large-scale freshwater emergent wetland. Environ Sci Technol 46:7027–7036
90. Tejamaya M, Romer I, Merrifield RC et al (2012) Stability of citrate PVP, PVP, and PEG coated silver nanoparticles in ecotoxicology media. Environ Sci Technol 46:7011–7017
91. Romer I, White TA, Baalousha M et al (2011) Aggregation and dispersion of silver nanoparticles in exposure media for aquatic toxicity tests. J Chromatogr 1218:4226–4233
92. MacCuspie RI (2011) Colloidal stability of silver nanoparticles in biologically relevant conditions. J Nanopart Res 13:2893–2908
93. Espinoza MG, Hinks ML, Mendoza AM (2012) Kinetics of halide induced decomposition and aggregation of silver nanoparticles. J Phys Chem 116:8305–8313
94. Aiken GR, Hsu-Kim H, Ryan JN (2011) Influence of dissolved organic matter on the environmental fate of metals, nanoparticles, and colloids. Environ Sci Technol 45:3196–3201
95. Furman O, Usenko S, Lau BLT (2013) Relative importance of the humic and fulvic fractions of natural organic matter in the aggregation and deposition of silver nanoparticles. Environ Sci Technol 47:1349–1356
96. Unrine JM, Colman BP, Bone AJ et al (2012) Biotic and abiotic interactions in aquatic microcosms determine fate and toxicity of Ag nanoparticles. Aggregation and dissolution. Environ Sci Technol 46:6915–6924
97. Lau BLT, Hockaday WC, Ikuma K et al (2013) A preliminary assessment of the interactions between the capping agents of silver nanoparticles and environmental organics. Colloid Surf Physicochem Eng Asp 435:22–27
98. Rafey A, Shrivastavaa KBL, Iqbal SA et al (2011) Growth of Ag-nanoparticles using aspartic acid in aqueous solutions. J Colloid Interfaces Sci 354:190–195
99. Ashraf S, Abbasi AZ, Pfeiffer C et al (2013) Protein-mediated synthesis, pH-induced reversible agglomeration, toxicity and cellular interaction of silver nanoparticles. Colloids Surf B Biointerfaces 102:511–518
100. MacCuspie RI, Rogers K, Patra M et al (2011) Challenges for physical characterization of silver nanoparticles under pristine and environmentally relevant conditions. J Environ Monit 13:1212–2126
101. Stamplecoskie KG, Scaiano JC (2012) Silver as an example of the applications of photochemistry to the synthesis and uses of nanomaterials. Photochem Photobiol 88:762–768
102. Thio BJR, Montes MO, Mahmoud MA et al (2012) Mobility of capped silver nanoparticles under environmentally relevant conditions. Environ Sci Technol 46:6985–6991
103. Holthoff H, Egelhaaf SU, Borkovec M et al (1996) Coagulation rate measurements of colloidal particles by simultaneous static and dynamic light scattering. Langmuir 12:5541–5549
104. Chen KL, Elimelech M (2006) Aggregation and deposition kinetics of fullerene ($C_{60}$) nanoparticles. Langmuir 22:10994–101001

105. El Badawy AM, Luxton TP, Silva RG et al (2010) Impact of environmental conditions (pH, ionic strength, and electrolyte type) on the surface charge and aggregation of silver nanoparticles suspensions. Environ Sci Technol 44:1260–1266
106. Li X, Lenhart JJ, Walker HW (2012) Aggregation kinetics and dissolution of coated silver nanoparticles. Langmuir 28:1095–1104
107. Liu J, Sonshine DA, Shervani S et al (2010) Controlled release of biologically active silver from nanosilver surfaces. ACS Nano 4:6903–6913
108. Ho C, Wong C, Yau SK et al (2011) Oxidative dissolution of silver nanoparticles by dioxygen: a kinetic and mechanistic study. Chem Asian J 6:2506–2511
109. Kittler S, Greulich C, Diendorf J et al (2010) Toxicity of silver nanoparticles increases during storage because of slow dissolution under release of silver ions. Chem Mater 22:4548–4554
110. Zhang W, Yao Y, Sullivan N et al (2011) Modeling the primary size effects of citrate coated silver nanoparticles on their ion release kinetics. Environ Sci Technol 45(10):4422–4428
111. Dobias J, Bernier-Latmani R (2013) Silver release from silver nanoparticles in natural waters. Environ Sci Technol 47:4140–4146
112. Cheng Y, Yin L, Lin S et al (2011) Toxicity reduction of polymer stabilized silver nanoparticles by sunlight. J Phys Chem 115:4425–4432
113. Tripathy SK (2008) Nanophotothermolysis of poly-(vinyl) alcohol capped silver particles. Nanoscale Res Lett 3:164–167
114. Kamat PV, Flumiani M, Hartland GV (1998) Picosecond dynamics of silver nanoclusters. Photo ejection of electrons and fragmentation. J Phys Chem B 102:3123–3128
115. Grillet N, Manchon D, Cottancin E et al (2013) Photooxidation of individual silver nanoparticles: a real-time tracking of optical and morphological changes. J Phys Chem C 117:2274–2282
116. He D, Garg S, Waite TD (2012) $H_2O_2$-mediated oxidation of zero-valent silver and resultant interactions among silver nanoparticles, silver ions, and reactive oxygen species. Langmuir 28:10266–10275
117. Yin Y, Liu J, Jiang G (2012) Sunlight-induced reduction of ionic Ag and Au to metallic nanoparticles by dissolved organic matter. ACS Nano 6:7910–7919
118. Berger TJ, Spadaro JA, Bierman R et al (1976) Antifungal properties of electrically generated metallic ions. Antimicrob Agents Chemother 10:856–860
119. Ostro B, Lipsett M, Reynolds P et al (2010) Long-term exposure to constituents of fine particulate air pollution and mortality: results from the California teachers study. Environ Health Perspect 118:363–369
120. Teow Y, Asharani PV, Hande MP (2011) Health impact and safety of engineered nanomaterials. Chem Commun 47:7025–7038
121. Wiley B, Sun Y, Xia Y (2007) Synthesis of silver nanostructures with controlled shapes and properties. Acc Chem Res 40:1067–1076
122. Feng QL, Wu J, Chen GQ (2000) A mechanistic study of the antibacterial effect of silver ions on *Escherichia coli* and *Staphylococcus aureus*. J Biomed Mater Res 52:662–668
123. Rainnie DJ, Bragg PD (1973) The effect of iron deficiency on respiration and energy coupling in *Escherichia coli*. J Gen Microbiol 77:339–3349
124. Puzyn T, Rasulev B, Gajewicz A (2011) Using nano-QSAR to predict the cytotoxicity of metal oxide nanoparticles. Nat Nanotechnol 6:175
125. Ahmed B, Dwivedi S, Abdin MZ et al (2017) Mitochondrial and chromosomal damage induced by oxidative stress in $Zn^{2+}$ ions, ZnO-bulk and ZnO-NPs treated Allium cepa roots. Sci Rep 7:40685
126. Rahman MF, Wang J, Patterson TA et al (2009) Expression of genes related to oxidative stress in the mouse brain after exposure to silver-25 nanoparticles. Toxicol Lett 187:15–21
127. Travan A, Pelillo C, Donati I et al (2009) Non-cytotoxic silver nanoparticle-polysaccharide nanocomposites with antimicrobial activity. Biomacromolecules 10:1429–1435
128. Sharma VK (2013) Oxidation of amino acids, peptides, and proteins. Wiley, New Jersey

129. AshaRani PV, Mun GLK, Hande MP et al (2009) Cytotoxicity and genotoxicity of silver nanoparticles in human cells. ACS Nano 3:279–290
130. Hsin Y, Chen C, Huang S et al (2008) The apoptotic effect of nano silver is mediated by a ROS- and JNK-dependent mechanism involving the mitochondrial pathway in NIH3T3 cells. Toxicol Lett 179:130–139
131. Miralles P, Church TL, Harris AT (2012) Toxicity, uptake, and translocation of engineered nanomaterials in vascular plants. Environ Sci Technol 46:9224–9239
132. Lee WM, Kwak JI, An YJ (2012) Effect of silver nanoparticles in crop plants Phaseolus radiatus and *Sorghum bicolor*: media effect on phytotoxicity. Chemosphere 86:491–499
133. El-Temsah YS, Joner EJ (2012) Impact of Fe and Ag nanoparticles on seed germination and differences in bioavailability during exposure in aqueous suspension and soil. Environ Toxicol 27:42–49
134. Patlolla AK, Berry A, May L et al (2012) Genotoxicity of silver nanoparticles in *Vicia faba*: a pilot study on the environmental monitoring of nanoparticles. Int J Environ Res Pub Health 9:1649–1662
135. Yin L, Cheng Y, Espinasse B et al (2011) More than the ions: the effects of silver nanoparticles on *Lolium multiflorum*. Environ Sci Technol 45:2360–2367
136. Ahmed B, Khan MS, Musarrat J (2018) Toxicity assessment of metal oxide nano-pollutants on tomato (*Solanum lycopersicon*): a study on growth dynamics and plant cell death. Environ Pollut 240:802–816
137. Ahmed B, Shahid M, Khan MS et al (2018) Chromosomal aberrations, cell suppression and oxidative stress generation induced by metal oxide nanoparticles in onion (Allium cepa) bulb. Metallomics 10:1315–1327
138. Stampoulis D, Sinha SK, White JC (2009) Assay-dependent phytotoxicity of nanoparticles to plants. Environ Sci Technol 43:9473–9479
139. Haverkamp RG, Marshall AT (2009) The mechanism of metal nanoparticle formation in plants: limits on accumulation. J Nanopart Res 11:1453–1463
140. Lee WM, Kwak JI, An YJ (2012) Effect of silver nanoparticles in crop plants Phaseolus radiatus and Sorghum bicolor: media effect on phytotoxicity. Chemosphere 86:491–499
141. Rico CM, Majumdar S, Duarte-Gardea M et al (2011) Interaction of nanoparticles with edible plants and their possible implications in the food chain. J Agric Food Chem 59:3485–3498
142. Maurer-Jones MA, Gunsolus IL, Murphy CJ et al (2013) Toxicity of engineered nanoparticles in the environment. Anal Chem 85:3036–3049
143. Musante C, White JC (2012) Toxicity of silver and copper to *Cucurbita pepo*: differential effects of nano and bulk-size particles. Environ Toxicol 27:510–517
144. Bandyopadhyay S, Peralta-Videa JR, Gardea-Torresdey JL (2013) Advanced analytical techniques for the measurement of nanomaterials in food and agricultural samples: a review. Environ Eng Sci 30:118–125
145. Suresh AK, Pelletier DA, Wang W et al (2010) Silver nanocrystallites: biofabrication using *Shewanella oneidensis*, and an evaluation of their comparative toxicity on gram-negative and gram-positive bacteria. Environ Sci Technol 44:5210–5215
146. Yuan Z, Li J, Cui L et al (2013) Interaction of silver nanoparticles with pure nitrifying bacteria. Chemosphere 90:1404–1411
147. Arnaout CL, Gunsch CK (2012) Impacts of silver nanoparticle coating on the nitrification potential of *Nitrosomonas europaea*. Environ Sci Technol 46:5387–5395
148. Xiu Z, Zhang Q, Puppala HL et al (2012) Negligible particle-specific antibacterial activity of silver nanoparticles. Nano Lett 12:4271–4275
149. Kim SW, Baek Y, An Y (2011) Assay-dependent effect of silver nanoparticles to *Escherichia coli* and *Bacillus subtilis*. Appl Microbiol Biotechnol 92:1045–1052
150. Patel IS, Premasiri WR, Moir DT et al (2008) Barcoding bacterial cells: a SERS-based methodology for pathogen identification. J Raman Spectrosc 39:1660–1672

151. Wigginton NS, De-Titta A, Piccapietra F et al (2010) Binding of silver nanoparticles to bacterial proteins depends on surface modifications and inhibits enzymatic activity. Environ Sci Technol 44:2163–2168
152. Silva BFD, Perez S, Gardinalli P et al (2011) Analytical chemistry of metallic nanoparticles in natural environments. TrAC Trends Anal Chem 30:528–540
153. Shahverdi AR, Fakhimi A, Shahverdi HR et al (2007) Synthesis and effect of silver nanoparticles on the antibacterial activity of different antibiotics against *Staphylococcus aureus* and *Escherichia coli*. Nanomedicine 3:168–171
154. Neal AL (2008) What can be inferred from bacterium-nanoparticle interactions about the potential consequences of environmental exposure to nanoparticles? Ecotoxicology 17:362–371
155. Fabrega J, Fawcett SR, Renshaw JC et al (2009) Silver nanoparticle impact on bacterial growth: effect of pH, concentration, and organic matter. Environ Sci Technol 43:7285–7290
156. Das P, Xenopoulos MA, Williams CJ et al (2012) Effects of silver nanoparticles on bacterial activity in natural waters. Environ Toxicol Chem 31:122–130
157. Jin X, Li M, Wang J et al (2010) High-throughput screening of silver nanoparticle stability and bacterial inactivation in aquatic media: influence of specific ions. Environ Sci Technol 44:7321–8328
158. Kvitek L, Panacek A, Prucek R et al (2011) Antibacterial activity and toxicity of silver-nano silver versus ionic silver. J Phys Conf Ser 304:012029
159. Yuan Z, Chen Y, Li T (2013) Reaction of silver nanoparticles in the disinfection process. Chemosphere 93:619–625
160. Hajipour MJ, Fromm KM, Akbar AA et al (2012) Antibacterial properties of nanoparticles. Trends Biotechnol 30:499–511
161. Suresh AK, Pelletier DA, Doktycz MJ (2013) Relating nanomaterial properties and microbial toxicity. Nanoscale 5:463–474
162. Scott JR, Barnett TC (2006) Surface proteins of gram-positive bacteria and how they get there. Annu Rev Microbiol 60:397–423
163. Xiu ZM, Ma J, Alvarez PJJ (2011) Differential effect of common ligands and molecular oxygen on antimicrobial activity of silver nanoparticles versus silver ions. Environ Sci Technol 45:9003–9008
164. Reinsch BC, Levard C, Li Z et al (2012) Sulfidation of silver nanoparticles decreases *Escherichia coli* growth inhibition. Environ Sci Technol 46:6992–7000
165. Batley GE, Kirby JK, McLaughlin MJ (2013) Fate and risks of nanomaterials in aquatic and terrestrial environments. Acc Chem Res 46:1854–1862
166. Kwok KWH, Auffan M, Badireddy AR et al (2012) Uptake of silver nanoparticles and toxicity to early life stages of Japanese medaka (*Oryzias latipes*): Effect of coating materials. Aquat Toxicol 120–121:59–66
167. Holden PA, Nisbet RM, Lenihan HS et al (2012) Ecological nanotoxicology: integrating nanomaterial hazard considerations across the subcellular, population, community, and ecosystems levels. Acc Chem Res 46:813–822
168. Lee KJ, Browning LM, Nallathamby PD et al (2012) In vivo quantitative study of sized-dependent transport and toxicity of single silver nanoparticles using zebrafish embryos. Chem Res Toxicol 25:1029–1046
169. Kashiwada S, Ariza ME, Kawaguchi T et al (2012) Silver nanocolloids disrupt medaka embryogenesis through vital gene expressions. Environ Sci Technol 46:6278–6287
170. George S, Lin S, Ji Z et al (2012) Surface defects on plate shaped silver nanoparticles contribute to its hazard potential in a fish gill cell line and zebrafish embryos. ACS Nano 6:3745–3759
171. Kennedy AJ, Chappell MA, Bednar AJ et al (2012) Impact of organic carbon on the stability and toxicity of fresh and stored silver nanoparticles. Environ Sci Technol 46:10772–10780

172. McLaughlin J, Bonzongo JJ (2012) Effects of natural water chemistry on nano silver behavior and toxicity to *Ceriodaphnia dubia* and *Pseudokirchneriella subcapitata*. Environ Toxicol Chem 31:168–175
173. Yang X, Gondikas AP, Marinakos SM et al (2012) Mechanism of silver nanoparticle toxicity is dependent on dissolved silver and surface coating in *Caenorhabditis elegans*. Environ Sci Technol 46:1119–1127
174. Perreault F, Bogdan N, Morin M et al (2012) Interaction of gold nanoglycodendrimers with algal cells (Chlamydomonas reinhardtii) and their effect on physiological processes. Nanotoxicology 6:109–120
175. Dash A, Singh AP, Chaudhary BR et al (2012) Effect of silver nanoparticles on growth of eukaryotic green algae. Nano Micro Lett 4:158–165
176. Turner A, Brice D, Brown MT (2012) Interactions of silver nanoparticles with the marine macroalga, *Ulva lactuca*. Ecotoxicology 21:148–154
177. Burchardt AD, Carvalho RN, Valente A et al (2012) Effects of silver nanoparticles in diatom *Thalassiosira pseudonana* and *Cyanobacterium synechococcus* sp. Environ Sci Technol 46:11336–11344
178. Bone AJ, Colman BP, Gondikas AP et al (2012) Biotic and abiotic interactions in aquatic microcosms determine fate and toxicity of Ag nanoparticles: part 2-toxicity and Ag speciation. Environ Sci Technol 46:6925–6933
179. Blinova I, Niskanen J, Kajankari P et al (2012) Toxicity of two types of silver nanoparticles to aquatic crustaceans *Daphnia magna* and *Thamnocephalus platyurus*. Environ Sci Pollut Res 2012:1–8
180. Zhao C, Wang W (2013) Regulation of sodium and calcium in *Daphnia magna* exposed to silver nanoparticles. Environ Toxicol Chem 32:913–919
181. Schlich K, Klawonn T, Terytze K et al (2013) Effects of silver nanoparticles and silver nitrate in the earthworm reproduction test. Environ Toxicol Chem 32:181–188
182. Hu C, Li M, Wang W et al (2012) Ecotoxicity of silver nanoparticles on earthworm *Eisenia fetida*: responses of the antioxidant system, acid phosphatase and ATPase. Toxicol Environ Chem 94:732–741
183. Coutris C, Hertel-Aas T, Lapied E et al (2012) Bioavailability of cobalt and silver nanoparticles to the earthworm *Eisenia fetida*. Nanotoxicology 6:186–195
184. Tsyusko OV, Hardas SS, Shoults-Wilson WA et al (2012) Short-term molecular-level effects of silver nanoparticle exposure on the earthworm, *Eisenia fetida*. Environ Pollut 171:249–255
185. Panacek A, Prucek R, Safarova D, Dittrich M, Richtrova J, Benickova K, Zboril R, Kvitek L (2011) Acute and chronic toxicity effects of silver nanoparticles (NPs) on Drosophila melanogaster. Environ Sci Technol 45(11):4974-4979

# Role of Light in the Improvement of Nanoparticle Synthesis

5

Dai Phat Bui, Hoang The Vinh Tran, Thi Minh Cao, and Viet Van Pham

**Abstract**

This chapter compares the properties of different light sources. A comprehensive comparison reports the advantages and disadvantages of chemical reduction and photoreduction methods. The role of light in the nanoparticle formation mechanism is proposed with the evidence from previous studies. Interestingly, the factors affecting the properties of nanoparticles, such as light sources, photoreduction time, and chemical concentration, are reviewed and evaluated. This chapter also provides examples of the synthesis of nanoparticles via the photoreduction method. In addition, a comprehensive comparison discriminates the chemical reduction and photoreduction methods with clear examples of their advantages and disadvantages. Finally, the potential of the photoreduction method is described to support the readers' perspective in the green synthesis of nanomaterials.

**Keywords**

Light source · Photosynthesis · Photoreduction · Nanoparticles · Synthesis scale

D. P. Bui · H. T. V. Tran · V. Van Pham (✉)
Faculty of Materials Science and Technology, University of Science, VNU-HCM, Ho Chi Minh City, Vietnam
e-mail: pvviet@hcmus.edu.vn

T. M. Cao
Ho Chi Minh City University of Technology (HUTECH), Ho Chi Minh City, Vietnam

© Springer Nature Singapore Pte Ltd. 2020

Q. Saquib et al. (eds.), *Green Synthesis of Nanoparticles: Applications and Prospects*, https://doi.org/10.1007/978-981-15-5179-6_5

## 5.1 Overview of Light and Light Source

### 5.1.1 Light and Classification of Light Source

Light is an electromagnetic radiation, which can be described as both a wave and a particle. It accounts for many processes of life, including metabolism, photosynthesis, responsiveness, and so on [1, 2]. Light mainly includes visible light, ultraviolet light, and infrared light, as shown in Fig. 5.1 [3, 4]. The visible light is usually defined as having wavelengths in the range of 400–700 nanometers (nm), while those of the ultraviolet light and the infrared light are shorter than 400 nm and higher than 700 nm, respectively [5]. Therein, only the visible light could be seen by human eyes.

There are two sources of light, including natural light and artificial light. The natural light mainly comes from the Sun, while the artificial light comes from incandescent/filament, fluorescent/discharge, light-emitting diodes (LEDs), and laser, as shown in Fig. 5.2 [6]. In artificial light, there are many light sources, for example, Mercury lamp (HBO), Xenon (XBO) lamp, argon ion laser, and helium-neon (HeNe) laser. Some characteristics of these light sources have been indicated in Table 5.1. The classification of the light sources that based on wavelength of electromagnetic spectrum can be classified to UV range, visible light, infrared light, etc. (Table 5.2).

### 5.1.2 Properties and Applications of Light

The natural light significantly contributes to the water cycle, agriculture development, vitamin D synthesis of humans and animals, and antibacterial resistance

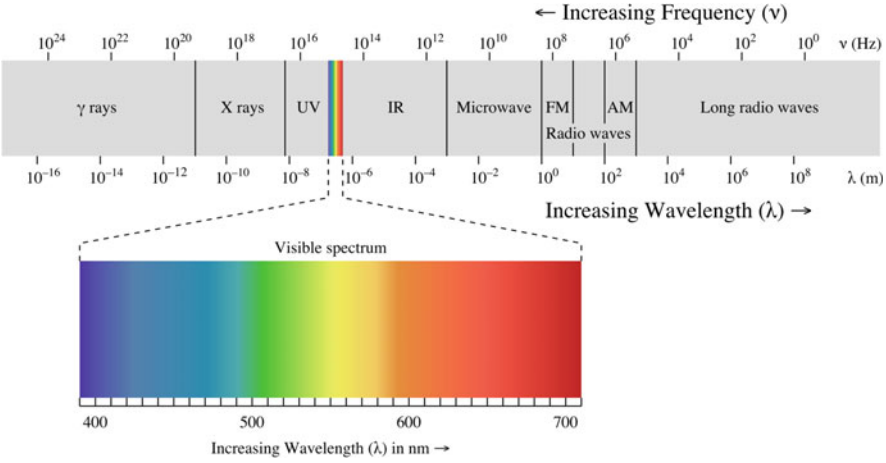


**Fig. 5.1** Electromagnetic spectrum, with the visible portion highlighted

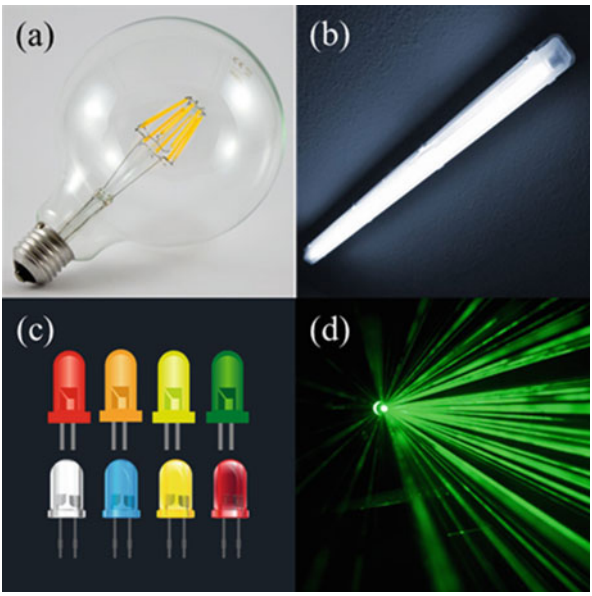


**Fig. 5.2** Artificial light with different lamps: filament (**a**), fluorescent (**b**), and LEDs (**c**) and laser source (**d**)

**Table 5.1** Comparisons of some lamps with their emission wavelength, power, estimated price, and lifetime [7]

| Light source | Wavelength (nm) | Power | Price | Lifetime (h) |
|---|---|---|---|---|
| Mercury (HBO) lamp | Peaks: 313, 334, 365, 406, 435, 546, 578 | 100 W | ~$170 | 200 |
| Xenon (XBO) lamp | From 400 to 800 | 75 W | ~$200 | 400 |
| Argon ion laser | Lines: 351, 364, 457, 476, 488, 514 | 50–100 mW | >$5000 | 6000 |
| Helium-neon (HeNe) laser | Lines: 543, 594, 633 | 1.5–10 mW | >$1500 | 40,000 |

[1, 2]. The artificial light plays an essential role in synthetic and analytical chemistry. Firstly, it is used in spectroscopy techniques such as photoluminescence, Raman, and UV-Vis spectroscopy to analyze optical properties, defects in materials, or chemical compounds. Secondly, it is used to conduct photochemical synthesis/photosynthesis and generate alternative energy [9]. Along with advantages compared to the solar light, the conventional artificial light sources reveal their disadvantages such as excessive heat production, short lifetime, and expensive equipment, as shown in Table 5.3.

**Table 5.2** The physical characteristics of the light sources [8]

| Class | | Frequency | Wavelength | Energy |
|---|---|---|---|---|
| Ionizing radiation | Gamma rays | 300 EHz | 1 pm | 1.24 MeV |
| | Hard X-rays | 30 EHz | 10 pm | 124 keV |
| | Soft X-rays | 3 EHz | 100 pm | 12.4 keV |
| | | 300 PHz | 1 nm | 1.24 keV |
| | Extreme ultraviolet | 30 PHz | 10 nm | 124 eV |
| | Near ultraviolet | 3 PHz | 100 nm | 12.4 eV |
| Visible | Near infrared | 300 THz | 1 μm | 1.24 eV |
| | Mid infrared | 30 THz | 10 μm | 124 meV |
| | Far infrared | 3 THz | 100 μm | 12.4 meV |
| Microwaves and radio waves | Extremely high frequency | 300 GHz | 1 mm | 1.24 meV |
| | | 30 GHz | 1 cm | 124 μeV |
| | Super high frequency | 3 GHz | 1 dm | 12.4 μeV |
| | Ultrahigh frequency | 300 MHz | 1 m | 1.24 μeV |
| | Very high frequency | 30 MHz | 10 m | 124 neV |
| | High frequency | 3 MHz | 100 m | 12.4 neV |
| | Medium frequency | 300 kHz | 1 km | 1.24 neV |
| | Low frequency | 30 kHz | 10 km | 124 peV |
| | Very low frequency | 3 kHz | 100 km | 12.4 peV |
| | Ultralow frequency | 300 Hz | 1000 km | 1.24 peV |
| | Super low frequency | 30 Hz | 10,000 km | 124 feV |
| | Extremely low frequency | 3 Hz | 100,000 km | 12.4 feV |

**Table 5.3** Advantages and disadvantages of common light sources

| | | |
|---|---|---|
| Mercury (HBO) lamp | Advantages | Multiple spectra peaks, incoherent source, reasonable price, compact light-emitting surface |
| | Disadvantages | Excessive heat production, short lifetime, ozone production, excitation and emission filters required, difficult to modulate |
| Xenon (XBO) lamp | Advantages | Broadband spectrum, incoherent source, reasonable price, compact light-emitting surface |
| | Disadvantages | Excessive heat production, short lifetime, ozone production, excitation and emission filters required, difficult to modulate |
| Lasers | Advantages | Monochromatic spectral lines, high power per spectral line, relatively long lifetime, compact light-emitting surface |
| | Disadvantages | Excessive heat production, high price, coherent source, emission filters required, high voltage required, difficult to modulate |

## 5.2 Role of Light in Green Synthesis of Nanoparticles

To synthesize NPs, methods such as chemical reduction, biosynthesis, sonochemistry, and physical chemistry are often used [10, 11]. However, these traditional methods have shown negative effects on the environment by producing toxic intermediates. For this reason, photoreduction, known as a green method, has attracted the interest of a lot of researchers in recent decades. In this chapter, the green synthesis of NPs is emphasized. The next section compares both chemical-induced and photo-induced synthesis.

### 5.2.1 Chemical-Induced Synthesis

Chemical-based methods could be bottom-up processes or top-down processes (Fig. 5.3a) [14]. The bottom-processes relate to the chemical formation of nanomaterials from ions. In contrast, the top-down processes relate to the control

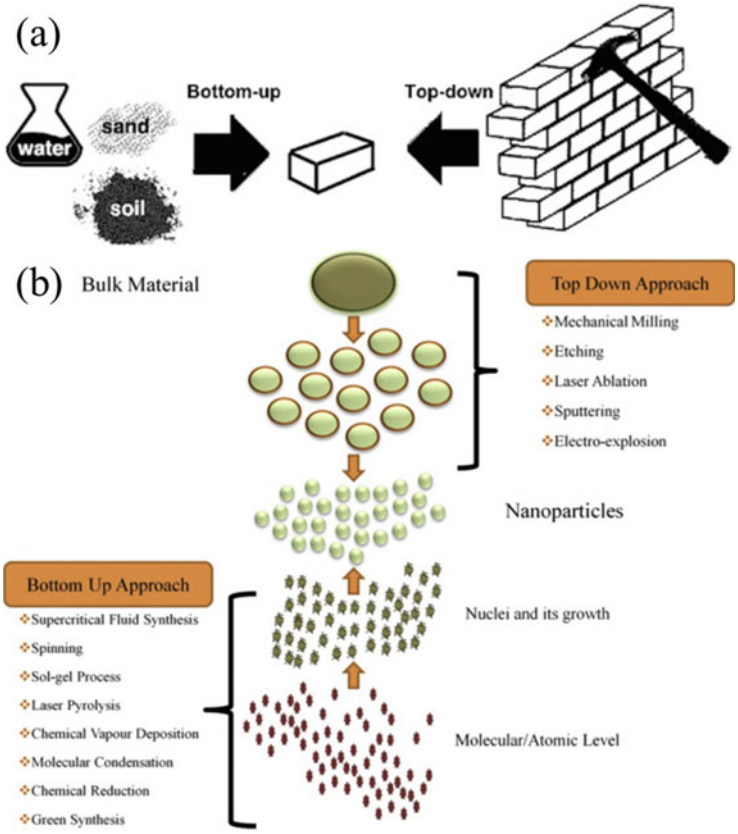


**Fig. 5.3** Illustration of the concepts of bottom-up and top-down methods (**a**) [12] and synthesis of nanomaterials (NPs) via top-down and bottom-up approaches (b) [13]

of temperature, pressure, reaction time, and pH for the formation of nanostructures after breaking bigger units. For chemical-based methods, the nanostructures could be controlled in size and shape by using organic (polyols, vinyl polymers) or inorganic (sodium salts, hydrazine) chemical agents (Fig. 5.3b). The experiment could be conducted in a simple or extremely complicated way. For example, aldehydes reduce the $Ag^+$ cations to Ag NPs, or the mixture of $NaBH_4$, citrate, cetrimonium bromide (CTAB), and ascorbic acid at different ratios to form Ag nanorods, nanowires, nanoprisms, and nanotriangles. Unfortunately, these methods not only increase the cost of synthesizing nanomaterials but also cause potential problems to the environment due to chemicals' toxicity [15].

The chemical reduction method is the usage of chemical agents to reduce metal ions which play the role of nuclei, and over these nuclei, NPs growth will occur. For convenience, the chemical methods conducting in liquid form are also called wet chemical methods. The initial solution contains salts of metals such as $HAuCl_4$, $H_2PtCl_6$, $AgNO_3$, and so on [16, 17]. Then, the metal deionizing agents such as citric acid, ascorbic acid (vitamin C), sodium borohydride ($NaBH_4$), ethanol ($C_2H_6O$), ethylene glycol ($C_2H_6O_2$), hydroquinone, and gallic acid are added into the initial solution to reduce cations to metals [16, 17]. The reaction mechanism of the formation of metal NPs via chemical reduction method is presented according to Eq. (5.1). For this method, photon energy will transform polyols (polyvinylpyrrolidone (PVP), Ethylene glycol) to aldehydes, then these aldehydes will reduce salts to metals as the case of forming Ag and $Cu_2O$ from $[Ag(NH_3)_2]OH$ and $Cu(OH)_2$, respectively.

$$m\mathrm{Me}^{n+} + n\mathrm{Red} \rightarrow m\mathrm{Me}^0 + n\mathrm{Ox} \tag{5.1}$$

where $Me^{n+}$ is the metal ions, $n^+$ is oxidation number, Red is reducing agent, Me is the metal atoms, and Ox is oxidation production. The metal atoms synthesized by the reduction method are essentially insoluble, resulting in the slow aggregation of particles. This is represented by Eq. (5.2).

$$x\mathrm{Me}^0 \rightleftarrows \left(\mathrm{Me}_x^0\right)_{\mathrm{em}} \tag{5.2}$$

The formation of NPs could be described in three steps. Firstly, there are tiny metal clusters. Secondly, the medium-sized nuclei either split or grow to become stable. Finally, the nuclei reach a critical size and separate from solutions in the form of solid particles (Eqs. 5.3–5.6).

$$\left(\mathrm{Me}_x^0\right)_{\mathrm{em}} + y\mathrm{Me}^0 \rightarrow \left(\mathrm{Me}_{x+y}^0\right)_{\mathrm{nucl}} \tag{5.3}$$

$$\left(\mathrm{Me}_n^0\right)_{\mathrm{nucl}} + m\mathrm{Me}^0 \rightarrow \left(\mathrm{Me}_{n+m}^0\right)_{\mathrm{pp}} \tag{5.4}$$

$$\left(\mathrm{Me}^0\right)_{\mathrm{pp}} + n\mathrm{Me}^0 \rightarrow \left(\mathrm{Me}^0\right)_{\mathrm{p}} \tag{5.5}$$

$$m\left(\mathrm{Me}^0\right)_{\mathrm{pp}} \rightarrow \left(\mathrm{Me}^0\right)_{\mathrm{p}} \tag{5.6}$$

### 5.2.2 Photo-Induced Synthesis

Photo-induced synthesis is an eco-friendly approach and more effective than the chemical-induced method. These methods include photophysical and photochemical processes. The photophysical process is a top-down process deploying laser, microwave, or electron beam to break the materials into nano-fragments or nanomaterials at different dimensions [18]. It could bring many advantages, such as promptitude, homogeneity, and clean. However, this photophysical process requires a wide range of expensive instruments and a highly clean reaction environment, which will affect its cost as well as wide application [15]. The photochemical process is a bottom-up process using UV, visible light, or solar light for the synthesis of nanomaterials from ions. It has promised more advantages in ecology, cost, and property.

The photochemical process could be described as follows. Firstly, the salt as a precursor is combined with alcohol (ROH) under light irradiation. Then, the photon energy transforms alcohol into radicals and aldehydes, while reducing salts to metals. The photoreduction mechanism is based on the electronic movement from the solvent molecule under the action of excitation light, as shown in Eqs. (5.7–5.10) and Fig. 5.4.

$$\mathrm{Me}^+ + \mathrm{H_2O} \xrightarrow{h\nu} \mathrm{Me}^0 + \mathrm{H}^+ + \mathrm{HO}^{\cdot} \tag{5.7}$$

$$\mathrm{Me}^+ + \mathrm{RCH_2OH} \xrightarrow{h\nu} \mathrm{Me}^0 + \mathrm{H}^+ + \mathrm{R{\cdot}CHOH} \tag{5.8}$$

$$\mathrm{Me}^+ + \mathrm{R{\cdot}CHOH} \xrightarrow{h\nu} \mathrm{Me}^0 + \mathrm{H}^+ + \mathrm{RCHO} \tag{5.9}$$

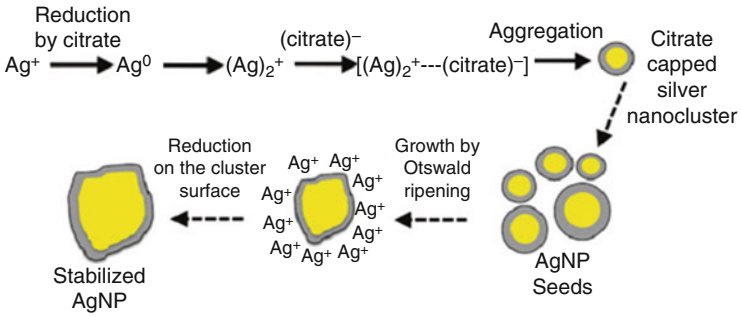


**Fig. 5.4** Nucleation and mechanism of formation of Ag NPs under a reducing agent called citrate [19]

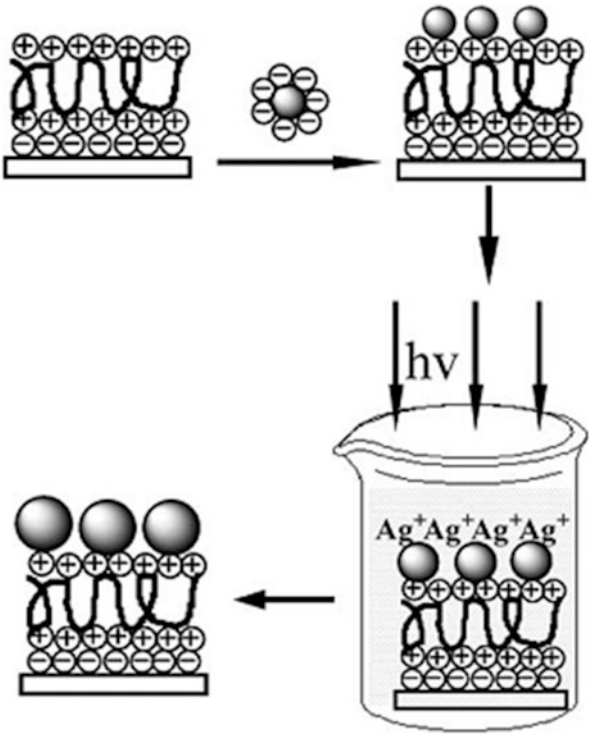


**Fig. 5.5** Schematic of Ag NPs film fabrication mechanism by the photoreduction method with the help of thioglycolic acid [20]

$$n\mathrm{Me}^0 \rightarrow \mathrm{Me\,NP} \tag{5.10}$$

In the case of producing metals, such as Ag NPs, on a substrate, thioglycolic acid ($HSCH_2COOH$) is used as a supporting agent, as shown in Fig. 5.5. In detail, the substrate surface is soaked with thioglycolic acid, then mixed with $AgNO_3$ solution, and under the excitation of UV light produced $Ag^+$ ions. These ions are then bonded to the substrate surface and form Ag NPs film.

Along with the direct photoreduction, recently, the formation of noble metal NPs has been synthesized by the indirect photoreduction process. In this process, the polymer, silica, cells, inorganic materials, such as $TiO_2$, ZnO, $SnO_2$, and so on have been used as the membrane to improve the efficiency of the reduction process through the indirect reduction. In this process, metal ions look for sensitive substances (such as polymer films, glass, cells, inorganic materials such as $TiO_2$, ZnO) to bond and receive additional electrons on the surface of this agent to form NPs. Therefore, in some cases, these agents will exist in the sample after the end of the experiment, and at the same time, we must find a way to remove them from the product.

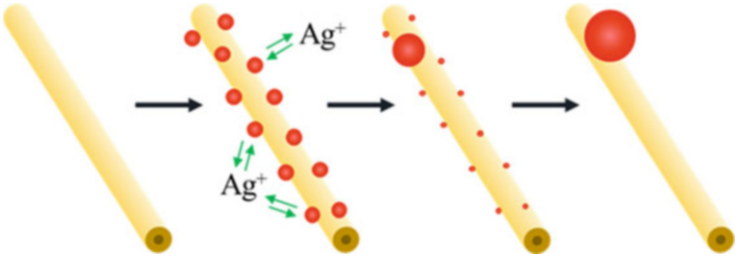


**Fig. 5.6** Mechanism of adhesion of Ag NPs onto the $TiO_2$ surface

It has been previously reported that the synthesis of Ag NPs loaded on the $TiO_2$ surface with initial precursors is $AgNO_3$ salt and $TiO_2$ powder. Firstly, the electron-hole pairs will be generated when a semiconductor template is irradiated with light having photon energy larger than the template's bandgap (Eq. 5.11). Finally, these pairs will react with cations from salts to produce nanometals as in Eqs. (5.12–5.16) [21]

$$TiO_2 \xrightarrow{h\nu} TiO_2(e^- + h^+) \tag{5.11}$$

$$AgNO_3 \rightarrow Ag^+_{ads} + NO^-_3 \tag{5.12}$$

$$e^- + Ti^{IV}_{surf} \rightarrow Ti^{III}_{surf} \tag{5.13}$$

$$Ti^{III}_{surf} + Ag^+_{ads} \rightarrow Ti^{IV}_{surf} + Ag^0 \tag{5.14}$$

$$Ag^0_{ads} + Ag^+_{ads} \rightarrow Ag^+_{2ads} \tag{5.15}$$

$$Ag^+_{ads} + Ti^{III}_{surf} \rightarrow Ag^0_{2ads} \xrightarrow[Ti^{III}]{nAg^+} Ag^0_n\,(\text{cluster}) \tag{5.16}$$

Therein, Ag atoms and $Ag_2{}^+$ radicals are the first products of the reduction process in the electrolyte. They will be on the surface of $TiO_2$, causing the process of charge transport and forming Ag clusters, as shown in Fig. 5.6. During the reaction process, electrons are attracted and trapped in the Ag cluster and vice versa; at the same time, holes recombine on the Ti surface (Eq. 5.17).

$$Ti^{III}_{surf} + h^+_{ads} \rightarrow Ti^{IV}_{surf} \tag{5.17}$$

#### 5.2.2.1 Effect of Light Sources

This section discusses the role of different lights in the synthesis of nanomaterials. Typically, the UV light has supported the synthesis of crystalline nanoparticles (NPs) such as γ-manganese oxide (γ-$MnO_2$), cobalt oxide hydroxide (CoOOH),

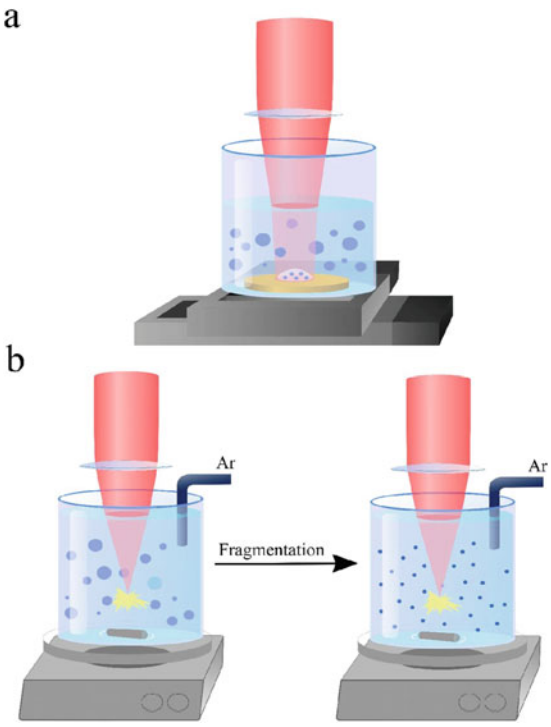


**Fig. 5.7** (**a**) Schematics of laser ablation setup. A laser beam is focused on the surface of the TiN target, which is placed in the vessel filled with a liquid. The vessel is mounted on a moving translation stage to avoid ablation from the same area of the target. (**b**) Schematic of laser fragmentation setup to minimize size dispersion of NPs. Ar bubbling used optionally to remove dissolved oxygen [23]

and cerium oxide ($CeO_2$) hierarchical nanoarchitectures [22]. The assistance of light has reduced synthesis time, crystallinity, and morphology control. Along with UV light irradiation, the femtosecond laser has shown its advantages in the synthesis of the ultrapure and size-tunable TiN NPs, as shown in Fig. 5.7 [23]. The experimental process is shown in Fig. 5.7, and the radiation from a femtosecond laser (Yb:KGW, $\lambda$: 1025 nm, $f$: 1–100 kHz) was focused onto a TiN target placed on the bottom of a glass vessel filled with deionized water or acetone to initiate ablation of material. The femtosecond laser shows its potential in reducing the size of TiN NPs to a uniform size of about 4 nm.

The photoreduction process can produce relatively uniform Ag NPs with the advantages of simplicity, low cost, and eco-friendly nature [18, 21, 24–28]. Besides, this method also is considered as a green process because it uses only photo-assistance without any additional toxic substances [28–30]. But this method depends on a high-power UV lamp, or long-time UV exposure, or chemical reducing agents such as $NaBH_4$, acrylic, $NH_3 \cdot 2H_2O$, and benzoin [18, 19, 31–33] which limit its application on the industrial scale. Therefore, it is needed to overcome the high power consumption and decrease toxic chemical problems. One prominent solution is to optimize the ratio of the reactants to maximize the yield of the reduction with a low-intensity UV light and control additional reducing chemicals as shown in Fig. 5.8 [34].

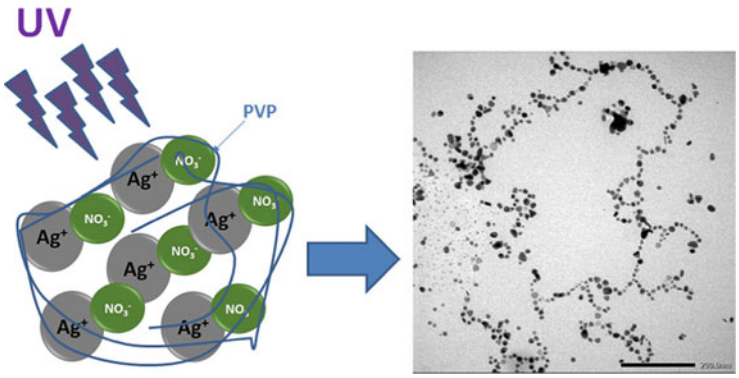


**Fig. 5.8** An improved green synthesis method via a photoreduction process using low-power UV light [34]

**Table 5.4** Changes in morphology of nanoparticles under different excitation light

| Metal | Morphology | Wavelength | Ref. |
|---|---|---|---|
| Ag | Nanoparticle | 405 nm | Stamplecoskie and Scaiano [35] |
| | Nanorod | 720 nm | |
| | Nanotriangle | 590/627 nm | |
| | Nanohexagon | 505 nm | |
| Au | Nanoparticle | 473 nm | Nadal et al. [36] |
| | Nanorod | 253 nm | Abdelrasoul et al. [37] |
| | Nanohexagon | 250–490 nm | Taubert et al. [38] |
| Cu | Nanoparticle | 365 nm | Miyagawa et al. [39] |

The use of light with different wavelengths is also useful to control the size and shape of nanomaterials. To illustrate, the irradiation with different wavelengths in the range of 400–700 nm could form Ag NPs (405 nm), nanopentagons (455 nm), nanohexagons (505 nm), nanotriangles (590/627 nm), and nanorods (720 nm). The materials' size will also be different with the changing irradiation time of wavelength by only 1–10 nm. For a clear overview, the experimental parameters for the synthesis of NPs of some noble metals are described as shown in Table 5.4.

### 5.2.2.2 Effect of Irradiation Time

In most studies, the more the photoreduction time, the greater the number of Ag NPs formed. Precursors 0.2 mM of $AgNO_3$, 0.2 mM of 2-hydroxy-4′-(2-hydroxy-ethoxy)-2-methyl-propiophenone (Irgacure-2959®, I-2959), and 1 mM of sodium citrate were irradiated by a UV light with the wavelength of 320 nm. The more the photoreduction time, the higher the plasmon peak characteristic surface of Ag NPs at 404 nm, as shown in Fig. 5.9. In a report of Sudeep et al., the particle size increases with the duration of photolysis, thus providing a simple experimental parameter to control the particle size as shown in Fig. 5.10 [40]. The plasmonic peak increases,

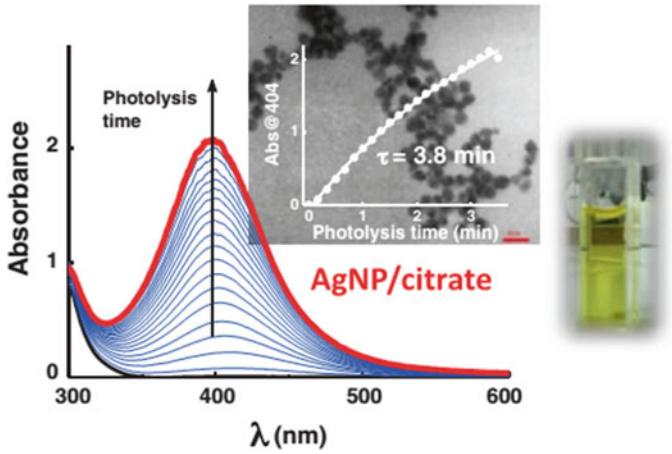


**Fig. 5.9** The absorption spectrum of the nano Ag solution when photosynthesis time changes

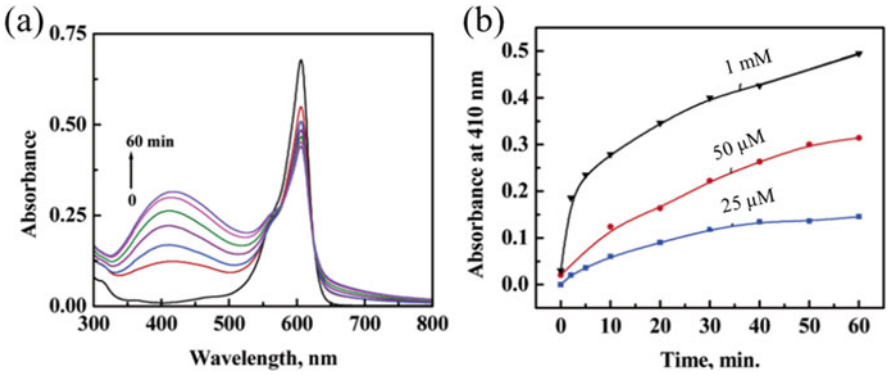


**Fig. 5.10** (**a**) Absorption spectra of Ag NPs versus irradiation time in toluene/ethanol mixture (1:1) and the absorbance at 410 nm of samples containing 25 μM, 50 μM, and 1 mM $AgNO_3$ versus time of visible light irradiation [40]

while the typical peak of thionine dye at 590 nm tends to decrease (Fig. 5.10a). The increase of $AgNO_3$ concentration is accounted for the increase in absorbance of the plasmonic peak of Ag NPs (Fig. 5.10b).

The results are similar when using a laser instead of a UV light. Shweta Verma et al. used a second harmonic Nd:YAG laser (YG980, Quantel), the wavelength of 532 nm, pulse duration of 9 ns, and pulse repetition rate of 10 Hz, as shown in Fig. 5.11 [41]. The light-based synthesized Ag has a surface plasmon resonance over a broad range of wavelengths. The morphology of Ag NPs was also affected by laser irradiation, as shown in Fig. 5.11 [42]. Firstly, the triangular Ag formed in 10 mM of citrate after 30 min of laser irradiation (Fig. 5.11a). Secondly, the spherical particle

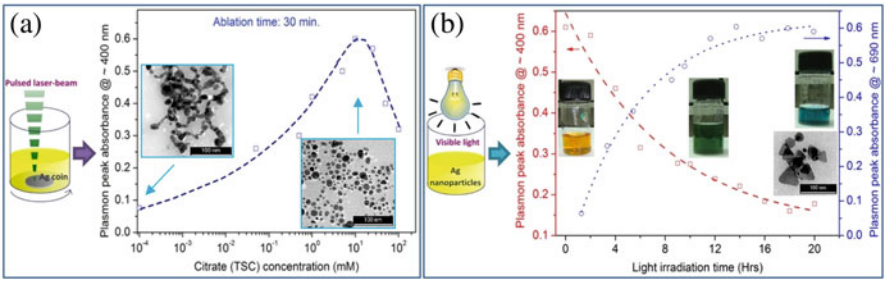


**Fig. 5.11** The intensity of Ag NPs plasmon resonance peaks versus citrate concentration (a) and irradiation time (b) by [41]

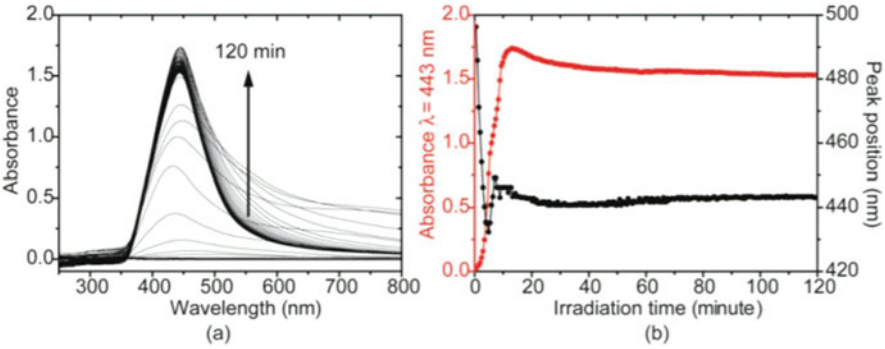


**Fig. 5.12** (**a**) The evolution of UV-visible absorption spectra of Au50 NPs during the irradiation with femtosecond laser for 120 min. (**b**) The absorbance change at lamda = 443 nm and peak position as a function of irradiation time [44]

of Ag with the plasmonic peak at 400 nm decreased after 12 h. Finally, the nanoplate Ag was formed with the evidence that the plasmonic peak at 600 nm increased (Fig. 5.11b).

In the synthesis of bimetallic alloy, Yuliati Herbani et al. experimented with a mixture of solutions of Ag and Au ions in the presence of ammonia without any dispersant in 2 h [43]. Figure 5.12a shows the experimental results related to the absorption spectra change of the mixture solution of Au and Ag ions during the formation of binary Au-Ag alloy NPs by femtosecond laser. The formation of the binary alloy was surveyed by observing the change of the absorption spectrum at the exciting wavelength. As shown in Fig. 5.12b, the shift in absorption in Au-Ag solution with a ratio of 1:1 was observed at wavelength 443 nm to investigate the density of alloy NPs. In general, the formation process reacted very quickly in the first 20 min and reached the maximum absorption, before reaching the equilibrium.

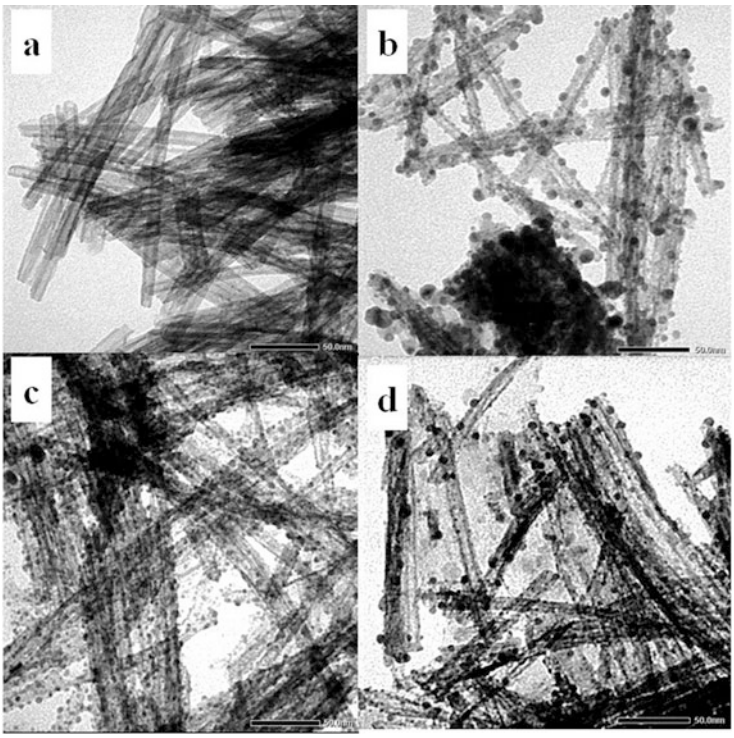


**Fig. 5.13** TEM images of $TiO_2$ nanotubes (**a**) and Ag/$TiO_2$ nanotubes according to precursor concentration $AgNO_3$ (**b**–**d**) [45]

### 5.2.2.3 Effect of Precursors Concentration

The concentration of precursors was investigated by a recent study that after the UV light photoreduction, the amount of Ag increases when the concentration of the $AgNO_3$ precursor increases [45]. The morphology of productions is depicted in Fig. 5.13. The results show that the formation of Ag NPs loaded on $TiO_2$ nanotubes has affected significantly when $AgNO_3$ concentration increases; in detail, the $AgNO_3$ concentration decides the size and distribution of Ag NPs on $TiO_2$ nanotubes surface.

In addition, Pillai et al. proposed that $Ag^+$ ions are reduced to form Ag NPs with citrate in solution [46]. In this case, because citrate is a reducing agent, the color of the mixed solution ($AgNO_3$ and sodium citrate) will change after UV irradiation. This result shows the formation of Ag seed and stability of Ag NPs with the reduction by citrate. During this formation, the development of Ag NPs is suitable with the growth by *Ostwald ripening* model, therein *Ostwald ripening* leads to the dissolution of smaller solid grains, diffusion of the solute through the liquid, and the re-precipitation of the solid onto large grains [47–49].

## 5.3 Prospects of Using Light Assistance for Green Synthesis of Nanoparticles

The photoreduction method demonstrated its efficiency in synthesizing NPs due to short synthesis time, easily controlled morphology, and so on. However, synthesized materials are demanding high stability of NPs as well as a high-yield green process that increases the synthesis efficiency without harmful chemicals. It is necessary to find optimization parameters of wavelengths and chemicals ratio for synthesizing NPs at low power consumption and a modest production cost.

Another concern regarding this method is to reduce reducing and capping agents. Many studies have shown that the stability of NPs can increase by increasing the concentration of reducing agents, preserving them at low temperatures, or using surfactants. For instance, Vera Pinto et al. [50] reported that the Ag NPs in the aqueous medium would be more stable when stored at $4.0 \pm 2.0$ °C and the use of tri-sodium citrate increased the stability of Ag NPs against oxidation. A compelling report of Ram Prasad [51] also indicated that the stability of Ag NPs depends on a high concentration of reductant.

Producing NPs at a massive scale is also necessary. As mentioned above, the principle of photoreduction is based on the direct formation of metal NPs under the effect of appropriate light. Unfortunately, in the aqueous phase, the light is easily absorbed by solvents, leading to energy wastage. That increases the expense and limits the synthesis of NPs on a massive scale.

## References

1. Chen X, Liu L, Yu PY, Mao SS (2011) Increasing solar absorption for photocatalysis with black hydrogenated titanium dioxide nanocrystals. Science 331:746–750. https://doi.org/10.1126/science.1200448
2. Liu W, Wang M, Xu C, Chen S (2012) Facile synthesis of g-$C_3N_4$/ZnO composite with enhanced visible light photooxidation and photoreduction properties. Chem Eng J 209:386–393. https://doi.org/10.1016/j.cej.2012.08.033
3. Vainshtein LA (1988) Electromagnetic waves. Izdatel Radio Sviaz, Moscow
4. Zwinkels J (2014) Light, electromagnetic spectrum. In: Luo R (ed) Encyclopedia of color science and technology. Springer, Berlin, pp 1–8. https://doi.org/10.1007/978-3-642-27851-8_204-1
5. Kirk JTO (1994) Light and photosynthesis in aquatic ecosystems. Cambridge University Press, London. https://doi.org/10.1017/cbo9780511623370
6. Weisbuch C (2018) Historical perspective on the physics of artificial lighting. C R Phys 19:89–112. https://doi.org/10.1016/j.crhy.2018.03.001
7. Young IT, Garini Y, Dietrich HR, van Oel W, Lung GL (2004) LEDs for fluorescence microscopy. In: Three-dimensional and multidimensional microscopy: image acquisition and processing XI. International Society for Optics and Photonics, pp 208–215
8. Elert G (1998) The electromagnetic spectrum, the physics hypertextbook. Hypertextbook.com
9. Solís-López M, Durán-Moreno A, Rigas F, Morales A, Navarrete M, Ramírez-Zamora R (2014) Assessment of copper slag as a sustainable Fenton-type photocatalyst for water disinfection. In: Ahuja S (ed) Water reclamation and sustainability. Elsevier, Amsterdam, pp 199–227

10. Iravani S, Zolfaghari B (2013) Green synthesis of silver nanoparticles using Pinus Eldarica bark extract. Biomed Res Int 2013:639725. https://doi.org/10.1155/2013/639725
11. Mokhtari N, Daneshpajouh S, Seyedbagheri S, Atashdehghan R, Abdi K, Sarkar S, Minaian S, Shahverdi HR, Shahverdi AR et al (2009) Biological synthesis of very small silver nanoparticles by culture supernatant of Klebsiella pneumonia: the effects of visible-light irradiation and the liquid mixing process. Mater Res Bull 44:1415–1421. https://doi.org/10.1016/j.materresbull.2008.11.021
12. Pacioni NL, Borsarelli CD, Rey V, Veglia AV (2015) Synthetic routes for the preparation of silver nanoparticles. In: Silver nanoparticle applications. Engineering materials, pp 13–46. https://doi.org/10.1007/978-3-319-11262-6_2
13. Khanna P, Kaur A, Goyal D (2019) Algae-based metallic nanoparticles: synthesis, characterization and applications. J Microbiol Methods 163:105656. https://doi.org/10.1016/j.mimet.2019.105656
14. Iqbal P, Preece JA, Mendes PM (2012) Nanotechnology: the "top-down" and "bottom-up" approaches. In: Steed JW, Atwood JL (eds) Supramolecular chemistry. Wiley, Hoboken, NJ. https://doi.org/10.1002/9780470661345.smc195
15. Lu Z, Meng M, Jiang Y, Xie J (2014) UV-assisted in situ synthesis of silver nanoparticles on silk fibers for antibacterial applications. Colloids Surf A Physicochem Eng Asp 447:1–7. https://doi.org/10.1016/j.colsurfa.2014.01.064
16. Kemp MM et al (2009) Synthesis of gold and silver nanoparticles stabilized with glycosaminoglycans having distinctive biological activities. Biomacromolecules 10:589–595. https://doi.org/10.1021/bm801266t
17. Wang H, Qiao X, Chen J, Ding S (2005) Preparation of silver nanoparticles by chemical reduction method. Colloids Surf A Physicochem Eng Asp 256:111–115. https://doi.org/10.1016/j.colsurfa.2004.12.058
18. Courrol LC, de Oliveira Silva FR, Gomes L (2007) A simple method to synthesize silver nanoparticles by photo-reduction. Colloids Surf A Physicochem Eng Asp 305:54–57. https://doi.org/10.1016/j.colsurfa.2007.04.052
19. Harada M, Inada Y, Nomura M (2009) In situ time-resolved XAFS analysis of silver particle formation by photoreduction in polymer solutions. J Colloid Interface Sci 337:427–438
20. Jia H, Zeng J, Song W, An J, Zhao B (2006) Preparation of silver nanoparticles by photo-reduction for surface-enhanced Raman scattering. Thin Solid Films 496:281–287
21. Pham VV, Phan BT, Mott D, Maenosono S, Truong TS, Cao MT, Le VH (2018) Silver nanoparticle loaded $TiO_2$ nanotubes with high photocatalytic and antibacterial activity synthesized by photoreduction method. J Photochem Photobiol A 352:106–112. https://doi.org/10.1016/j.jphotochem.2017.10.051
22. King'ondu CK et al (2011) Light-assisted synthesis of metal oxide hierarchical structures and their catalytic applications. J Am Chem Soc 133:4186–4189. https://doi.org/10.1021/ja109709v
23. Popov AA et al (2019) Laser-synthesized TiN nanoparticles as promising plasmonic alternative for biomedical applications. Sci Rep 9:1194. https://doi.org/10.1038/s41598-018-37519-1
24. Gong Y et al (2017) Solar light assisted green synthesis of photoreduced graphene oxide for the high-efficiency adsorption of anionic dyes. RSC Adv 7:53362–53372
25. Kumar SSD, Houreld NN, Kroukamp EM, Abrahamse H (2018) Cellular imaging and bactericidal mechanism of green-synthesized silver nanoparticles against human pathogenic bacteria. J Photochem Photobiol B 178:259–269
26. Nguyen THN, Nguyen TD, Cao MT, Pham VV (2020) Fast and simple synthesis of triangular silver nanoparticles under the assistance of light. Colloids Surf A Physicochem Eng Asp 594:124659. https://doi.org/10.1016/j.colsurfa.2020.124659
27. Sato-Berrú R, Redón R, Vázquez-Olmos A, Saniger JM (2009) Silver nanoparticles synthesized by direct photoreduction of metal salts. Application in surface-enhanced Raman spectroscopy. J Raman Spectrosc 40:376–380
28. Sharma VK, Yngard RA, Lin Y (2009) Silver nanoparticles: green synthesis and their antimicrobial activities. Adv Colloid Interf Sci 145:83–96

29. Alvarez RA et al (2016) Vibrational properties of gold nanoparticles obtained by green synthesis. Phys E 84:191–195
30. Rocha-Rocha O et al (2017) Green synthesis of Ag-Cu nanoalloys using Opuntia ficus-indica. J Electron Mater 46:802–807
31. Abyaneh MK, Paramanik D, Varma S, Gosavi S, Kulkarni S (2007) Formation of gold nanoparticles in polymethylmethacrylate by UV irradiation. J Phys D Appl Phys 40:3771
32. Callegari A, Tonti D, Chergui M (2003) Photochemically grown silver nanoparticles with wavelength-controlled size and shape. Nano Lett 3:1565–1568
33. Xu G-n, Qiao X-l, Qiu X-l, Chen J-g (2008) Preparation and characterization of stable monodisperse silver nanoparticles via photoreduction. Colloids Surf A Physicochem Eng Asp 320:222–226. https://doi.org/10.1016/j.colsurfa.2008.01.056
34. Pham VV, Truong TS, Nguyen HNB, Cao MT (2018) An improved green synthesis method and Escherichia Coli antibacterial activity of silver nanoparticles. J Photochem Photobiol B 182:108–114
35. Stamplecoskie KG, Scaiano JC (2010) Light emitting diode irradiation can control the morphology and optical properties of silver nanoparticles. J Am Chem Soc 132:1825–1827. https://doi.org/10.1021/ja910010b
36. Nadal E, Barros N, Glénat H, Laverdant J, Schmool DS, Kachkachi H (2017) Plasmon-enhanced diffraction in nanoparticle gratings fabricated by in situ photo-reduction of gold chloride doped polymer thin films by laser interference patterning. J Mater Chem C 5:3553–3560. https://doi.org/10.1039/c7tc00061h
37. Abdelrasoul GN, Cingolani R, Diaspro A, Athanassiou A, Pignatelli F (2014) Photochemical synthesis: effect of UV irradiation on gold nanorods morphology. J Photochem Photobiol A 275:7–11. https://doi.org/10.1016/j.jphotochem.2013.10.008
38. Taubert A, Arbell I, Mecke A, Graf P (2006) Photoreduction of a crystalline Au(III) complex: a solidstate approach to metallic nanostructures. Gold Bull 39:205–211. https://doi.org/10.1007/bf03215555
39. Miyagawa M, Yonemura M, Tanaka H (2016) Lustrous copper nanoparticle film: photodeposition with high quantum yield and electric conductivity. Chem Phys Lett 665:95–99. https://doi.org/10.1016/j.cplett.2016.10.057
40. Sudeep PK, Kamat PV (2005) Photosensitized growth of silver nanoparticles under visible light irradiation: a mechanistic investigation. Chem Mater 17:5404–5410. https://doi.org/10.1021/cm0512777
41. Verma S, Rao BT, Srivastava AP, Srivastava D, Kaul R, Singh B (2017) A facile synthesis of broad plasmon wavelength tunable silver nanoparticles in citrate aqueous solutions by laser ablation and light irradiation. Colloids Surf A Physicochem Eng Asp 527:23–33. https://doi.org/10.1016/j.colsurfa.2017.05.003
42. Lee SH, Jun BH (2019) Silver nanoparticles: synthesis and application for nanomedicine. Int J Mol Sci 20(4):865. https://doi.org/10.3390/ijms20040865
43. Herbani Y, Nakamura T, Sato S (2010) Femtosecond laser-induced formation of gold-rich nanoalloys from the aqueous mixture of gold-silver ions. J Nanomater 2010:1–9. https://doi.org/10.1155/2010/154210
44. Herbani Y, Nakamura T, Sato S (2016) Spectroscopic monitoring on irradiation-induced formation of AuAg alloy nanoparticles by femtosecond laser. In: AIP conference proceedings, vol 1. AIP Publishing, p 030005
45. Pham VV, Phan BT, Cao MT, Le VH (2017) Controlled formation of silver nanoparticles on $TiO_2$ nanotubes by photoreduction method. J Nanosci Nanotechnol 17:1497–1503. https://doi.org/10.1166/jnn.2017.12645
46. Pillai ZS, Kamat PV (2004) What factors control the size and shape of silver nanoparticles in the citrate ion reduction method? J Phys Chem B 108:945–951. https://doi.org/10.1021/jp037018r
47. Spanos G, Reynolds W (2014) Microstructure of metals and alloys. In: Laughlin D, Hono K (eds) Physical metallurgy. Elsevier, Amsterdam, pp 1073–1112

48. Vetter T, Iggland M, Ochsenbein DR, Hänseler FS, Mazzotti M (2013) Modeling nucleation, growth, and ostwald ripening in crystallization processes: a comparison between population balance and kinetic rate equation. Cryst Growth Des 13:4890–4905. https://doi.org/10.1021/cg4010714
49. Walstra P (2005) Emulsions. In: Lyklema J (ed) Fundamentals of interface and colloid science, vol 5. Elsevier, Amsterdam, pp 8.1–8.94
50. Pinto VV, Ferreira MJ, Silva R, Santos HA, Silva F, Pereira CM (2010) Long time effect on the stability of silver nanoparticles in aqueous medium: effect of the synthesis and storage conditions. Colloids Surf A Physicochem Eng Asp 364:19–25. https://doi.org/10.1016/j.colsurfa.2010.04.015
51. Prasad R (2014) Synthesis of silver nanoparticles in photosynthetic plants. J Nanoparticles 2014:1–8. https://doi.org/10.1155/2014/963961

# Application of Nanomaterials for Cancer Diagnosis and Therapy

6

Shaofei Wang, Yubin Li, and Dianwen Ju

**Abstract**

The extensive application of nanoparticles in diverse fields, ranging from agricultural, environmental, computational, and industrial sciences to pharmaceutical and biomedical sciences, is expected to revolutionize many aspects of human life. With the continuous development of nanotechnology, the medical application of nanomaterials has gained increasing interests from both academic and industrial communities. Various functionalized nanomaterials, such as molecular imaging biomarkers and biosensors, drug carriers, biological devices, and nanomedicine, are designed and developed for specific medical purposes. In this chapter, we will give a brief introduction to nanotechnology and nanomaterials and their biomedical applications in cancer diagnosis and therapy; summarize their unique properties for cancer diagnostic and therapeutic applications; enumerate repre-

Shaofei Wang and Yubin Li contributed equally to this work.

S. Wang
Department of Cellular and Genetic Medicine, School of Basic Medical Sciences, Fudan University, Shanghai, People's Republic of China

Y. Li
Department of Neurology, Xinqiao Hospital, Third Military Medical University (Army Medical University), Chongqing, People's Republic of China

Department of Dermatology, Perelman School of Medicine, University of Pennsylvania, Philadelphia, PA, USA

Corporal Michael J. Crescenz VA Medical Center, Philadelphia, PA, USA

D. Ju (✉)
Department of Biological Medicine and Shanghai Engineering Research Center of Immunotherapeutics, School of Pharmacy, Fudan University, Shanghai, People's Republic of China
e-mail: dianwenju@fudan.edu.cn

© Springer Nature Singapore Pte Ltd. 2020

Q. Saquib et al. (eds.), *Green Synthesis of Nanoparticles: Applications and Prospects*, https://doi.org/10.1007/978-981-15-5179-6_6

sentative functionalized nanomaterials developed for biomedical applications, in particular their advantages and disadvantages for applications in early cancer detection and diagnosis as well as therapeutic drug discovery and delivery; and discuss the challenges and prospects for future exploitations of these nanomaterials.

**Keywords**

Nanotechnology · Nanomaterials · Cancer diagnosis · Cancer therapy · Drug delivery

## Abbreviations

| | |
|---|---|
| CNTs | Carbon nanotubes |
| CT | Computed tomography |
| EPR | Enhanced permeability and retention |
| IONPs | Iron oxide nanoparticles |
| MRI | Magnetic resonance imaging |
| MSNs | Mesoporous silica nanoparticles |
| MWCNT | Multi-walled nanotubes |
| OI | Optical imaging |
| PAMAM | Poly(amidoamine) |
| PDT | Photodynamic therapy |
| PEG | Polyethylene glycol |
| PET | Positron emission computed tomography |
| PLGA | Poly(lactic-co-glycolic acid) |
| PTT | Photothermal therapy |
| QDs | Quantum dots |
| SPECT | Single-photon emission computed tomography |
| SPIONPs | Superparamagnetic iron oxide nanoparticles |
| SWCNT | Single-walled nanotubes |
| US | Ultrasonography |

## 6.1 Introduction

Cancer is one of the leading causes of mortality worldwide due to the lack of strategies for early diagnosis and effective therapy. Clinical imaging techniques, including optical imaging (OI), X-ray computed tomography (CT), ultrasonography (US), magnetic resonance imaging (MRI), positron emission computed tomography (PET), and single-photon emission computed tomography (SPECT) as well as hybrid dual-imaging technologies, are currently available to visualize the morphology of primary tumors and the presence of distant metastasis in cancer patients.

However, commonly used imaging contrasts and tracers have a series of disadvantages and limitations such as nonspecific distribution, insufficient sensitivity, rapid elimination, and undesirable adverse reactions. Meanwhile, it is generally recognized that the difficulty in early and accurate detection of cancer has been a major challenge in cancer diagnosis and treatment for the reason that current available imaging techniques fail to detect minimal precancerous or cancerous lesions. Moreover, the lack of selectivity and specificity of the conventional cancer therapies including chemotherapy, radiotherapy, and combination therapy poses a fundamental challenge for cancer treatment because of severe side effects. Therefore, in order to improve overall survival rate and life quality of cancer patients, there is an urgent need to develop novel technologies for early diagnosis and targeted therapy on the basis of specific makers of cancer.

In the past decades, with the rapid development of nanotechnology, nanomaterials have attracted considerable attention for agricultural, environmental, computational, industrial, and biomedical applications due to their unique and superior optical, electrical, magnetic, and catalytic properties. Recent advances in nanoscience and nanotechnology have promoted the development of various functionalized nanomaterials such as molecular imaging biomarkers and biosensors, drug carriers, and nanomedicine that are suitable for cancer diagnostic and therapeutic applications [1–3]. Nanoparticles show significant potentials for cancer diagnosis and therapy due to their nanoscale size, high loading capacity, tailorable and functionalizable surface property, and controllable and sustainable release pattern. Notably, the enhanced permeability and retention (EPR) effect, owing to the special anatomical and pathophysiological characteristics of solid tumors, preferentially facilitates the penetration and accumulation of the nanomaterials in cancerous tissues [4, 5]. More importantly, selective and specific delivery of cancer diagnostic or therapeutic agents can be carefully manipulated by modulating the size, shape, structure, and composition of nanoparticles during synthesis process and subsequent surface modification of nanomaterials by cancer-targeting ligands or addition of stimuli-responsive drug release elements so as to alter the pharmacokinetics (absorption, distribution, metabolism, and excretion) of the nanoparticles.

To date, various functionalized nanomaterials have been exploited for biomedical applications and thus revolutionized the conventional cancer diagnosis and therapy. Nanoprobes with high payload capacity, enhanced imaging capability, and excellent photostability can be conveniently prepared by optimization of nanomaterials, assembly of signal components into the nanoparticles, and subsequent functional modification of surface groups for specific targeting, thus enabling the targeted delivery of optical imaging agents to tumor sites and thereby overcoming the disadvantages of traditional diagnosis, in particular the lack of sensitivity and specificity. The EPR effect [4, 5] of nanomaterials in solid tumors makes it possible for nanoprobes to accumulate and maintain long-term retention at tumor sites, giving rise to sustained signal for cancer diagnosis. Notably, advances in nanotechnology will possibly realize real-time, high-contrast, high temporal resolution cancer imaging and therefore provide novel approaches for early detection and ensure timely treatment and accurate evaluation of therapeutic efficacy of cancer. Moreover,

nanomedicines largely overcome the shortcomings of conventional cancer therapy, including low bioavailability, nonspecific biodistribution, acquired drug resistance, and undesired adverse effects. Besides, the versatile nanostructure, composition, and functionalization of nanomaterials make them ideal carriers of high dose of anti-cancer agents or imaging probes in their inner cavity and high density of targeting ligands on their surface to the tumor sites, thus enabling integration of cancer diagnosis and therapy by utilizing multifunctional nanomaterials.

In this chapter, we will highlight the biomedical applications of nanomaterials in cancer diagnosis and therapy. First, we will summarize the common advantages of nanomaterials for cancer diagnostic and therapeutic applications. Second, we will enumerate the representative functionalized nanomaterials in different categories and highlight their unique properties suitable for early cancer detection and diagnosis as well as therapeutic anti-cancer drug discovery and delivery. Third, we will discuss the challenges and limitations for applications of these nanomaterials for cancer diagnostic and therapeutic applications.

## 6.2 Advantages of Nanomaterials for Cancer Diagnostic and Therapeutic Applications

Attributing to the intrinsic properties of nanoparticles such as nanoscale size and high surface-to-volume ratio and unique properties such as other tunable physicochemical characteristics, the most prominent advantages of nanomaterials for cancer diagnosis and therapy include the improvement of solubility and stability, high loading capacity and efficiency, passive targeting and active targeting, and controllable and sustainable drug release. Therefore, nanomaterial-based delivery systems and nanomedicines have a series of advantages over small-molecule imaging probes and anti-cancer drugs for cancer diagnostic and therapeutic applications, such as improved in vivo solubility and stability, extended blood circulation time, and decreased clearance rate that allow for sustained cancer imaging and anti-cancer drug delivery. It is possible to improve both the pharmacokinetics and pharmacodynamics and thus optimize the efficacy of existing diagnostic and therapeutic agents by loading them into nanocarriers. Moreover, nanomaterials with both diagnostic and therapeutic potentials, also called nanotheranostics, can be engineered and applied to improve the accumulation and retention of both contrast and therapeutic agents at the disease sites and to realize controllable release of payloads and to avoid the rapid development of drug resistance. In particular, with highly tunable physicochemical characteristics to be engineered as cancer-targeting and stimuli-responsive devices, nanomaterials can serve as ideal candidates to selectively fight against cancerous cells without affecting normal cells, thus overcoming unwanted toxicity and side effects caused by conventional diagnosis and therapy.

### 6.2.1 Improvement of Solubility and Stability

The poor stability and solubility of anti-cancer pharmaceuticals has been a major challenge for efficient cancer therapy for the reason that high hydrophobicity and low solubility seem to be the intrinsic properties of anti-cancer agents such as cisplatin, camptothecin [6], etoposide, paclitaxel [7], tamoxifen, and doxorubicin. Meanwhile, the lack of solubility of numerous drug candidates with potent anti-cancer activity identified through high-throughput screening techniques hinders their further research and development as clinical anti-cancer therapeutics. Fortunately, nanomaterials offer the possibility of encapsulation and transportation of poorly soluble anti-cancer drugs to protect bioactive molecules from enzyme degradation, thereby promoting the apparent solubility and improving the bioavailability of cancer therapeutics. In the past decades, liposomes and dendrimers are extensively explored for solubilizing and stabilizing various anti-cancer drugs with poor solubility and limited bioavailability. Moreover, encapsulating anti-cancer compounds that are vulnerable to enzymatic cleavage into nanomaterials or coupling anti-tumor molecules with synthetic polymers can efficiently avoid their degradation by biological enzyme system, thus extending the in vivo half-life and prolonging the action time of biodegradable anti-cancer therapeutics. For instance, anti-cancer agents including siRNAs or proteins that are easily degradable by RNase in the plasma and trypsin in the stomach, respectively, can evade being degraded by encapsulation and transportation by functionalized nanocarriers.

### 6.2.2 High Loading Capacity and Efficiency

Thanks to the inherent property of high surface-to-volume ratio, nanoscale materials possess relative high loading capacity over macromolecular carriers. For example, carbon nanotube drug delivery systems have been extensively investigated as drug carriers for encapsulating and transporting anti-cancer drugs or molecules through both internal cavity and external surface. Besides, self-assembled vesicular nanocarriers such as liposomes possess the capability to load with both hydrophilic and hydrophobic compounds in their inner aqueous core and lipid bilayer membrane, respectively. More importantly, nanotechnology largely facilitates the combination regimens that are commonly practiced in cancer diagnosis and therapy due to the high loading capacity of nanomaterials. Notably, it is convenient to encapsulate and transport multiple anti-cancer pharmaceuticals to the tumor sites by engineering them into a single nanoplatform in order to achieve synergistic anti-cancer effects and avoid the development of drug resistance. Moreover, nanomaterials enable the simultaneous delivery of cancer diagnostic and therapeutic agents at the cancerous pathological sites and thus realize the targeting and imaging as well as detection and treatment of cancer at the same time. For instance, multifunctionalized magnetic nanoparticles enable not only contrast-enhanced magnetic resonance imaging but also targeted drug delivery, controllable drug release, and thermal therapy of glioblastoma [8].

### 6.2.3 Passive and Active Cancer Targeting

Nanoparticles, due to their controllable size and tunable surface modification, can be designed to target cancerous sites by two major mechanisms: passive targeting and active targeting [9–11] (Fig. 6.1). One the one hand, nanomaterials tend to accumulate in cancerous pathological sites with abnormal leaky vasculature and poor lymphatic drainage via the EPR effect [4, 5]. On the other hand, nanomaterials facilitate active targeted delivery of diagnostic and therapeutic agents into tumorous areas by surface modification with specific ligands to recognize the receptors or antigens specifically expressed or overexpressed on cancerous cells. Moreover, active targeting, on the basis of the specific interactions between ligands modified on the surface of nanocarriers and the receptors expressed on the cancerous cells, can preferably promote the initial ligation of nanoparticles with cancer-specific biomarkers and subsequent internalization of nanocarriers via receptor-mediated endocytosis [12]. Therefore, various ligands against tumor-specific biomarkers, including folate [13], transferrin [14], antibody or antibody fragment [15–18], protein, peptide, and aptamer [19], are conjugated with nanoparticles and exploited for cancer targeting to promote selective delivery of diagnostic and therapeutic

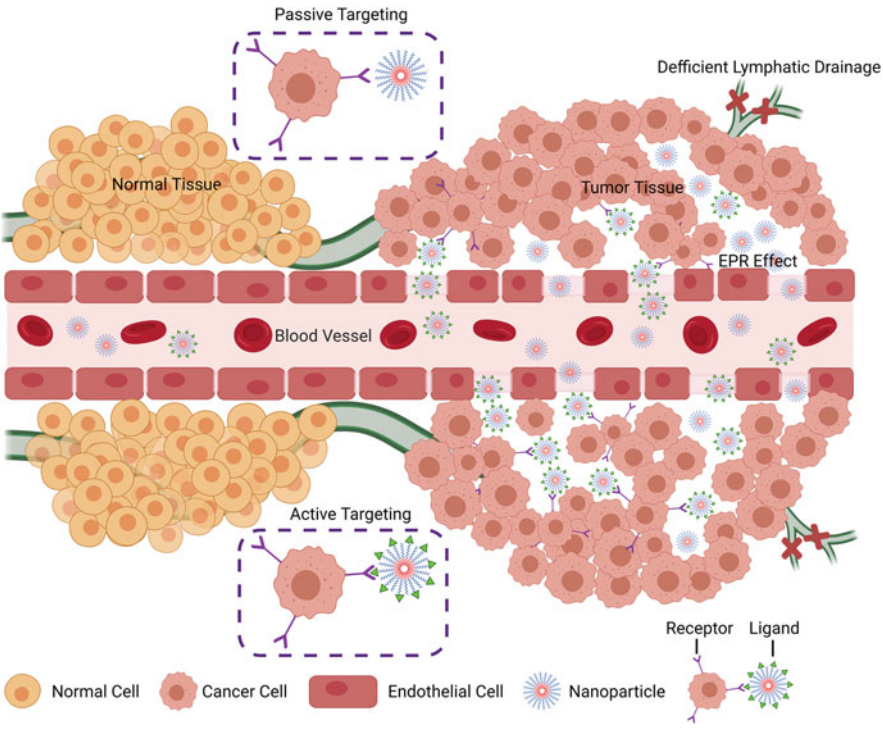


**Fig. 6.1** Schematic illustration of passive targeting and active targeting by functionalized nanomaterials

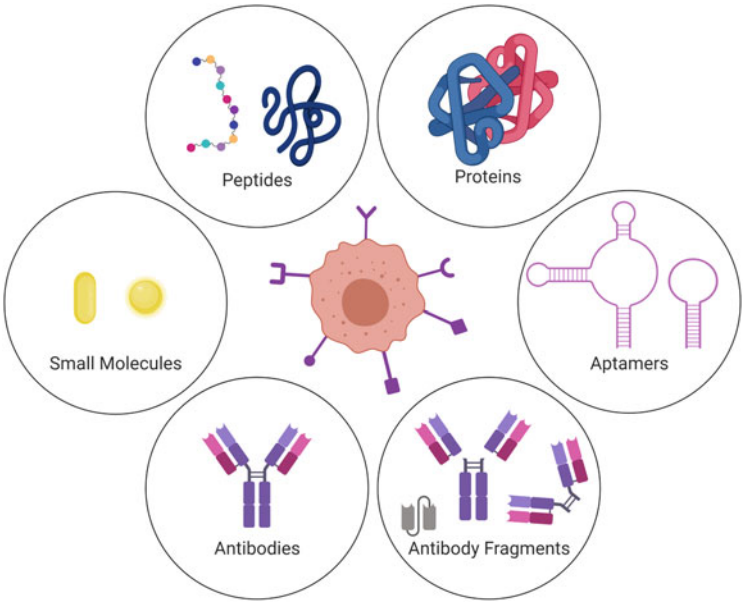


**Fig. 6.2** Schematic illustration of ligands for cancer active targeting

agents to cancerous sites (Fig. 6.2). For instance, in order to achieve active targeting of HER2-positive breast cancer, anti-HER2 immunoliposomes constructed by conjugating HER2-specific monoclonal antibody fragments to liposomes are utilized to facilitate the binding and internalization of the nanomedicines by HER2-overexpressing cancerous cells [17]. Nanoparticles are highly tunable and modifiable to facilitate loaded diagnostic and therapeutic agents to pass through biologic barriers, to recognize tumor-specific molecules, to mediate molecular interactions, and to be preferably internalized by cancerous cells. However, it should be noted that functionalization of the nanoparticles with high molecular weight ligands such as antibodies, proteins, and aptamers probably increases the hydrodynamic radius and thus alters the biotransport kinetics and intratumoral distribution of modified nanomaterials. Besides, molecular weight and surface property of ligands as well as the ligand-receptor affinity and ligand density will probably affect the active targeting of malignancy.

### 6.2.4 Controllable and Sustainable Release of Payloads

Nanosized carriers can conveniently be designed to realize controllable or sustainable release of diagnostic and therapeutic agents at designated sites in response to various stimuli. These stimuli can be classified into endogenous stimuli mainly including acidic pH, hypoxia, and enzyme in the tumor microenvironment or even overexpression of certain biomolecules within cancerous tissues and exogenous

physical stimuli such as light, temperature, ultrasound, and magnetic and electric fields. On the one hand, pH-sensitive [20], redox-sensitive [21], enzyme-sensitive [22], and thermo-sensitive [23] nanoplatforms are engineered to release their payloads in response to acidic pH [24], elevated reducing condition, overexpressed enzymes, and hyperthermia in the tumor microenvironment upon delivery to the pathological sites. On the other hand, the multifunctionalized nanocarriers can also be designed to respond to external stimuli (e.g., light, heat, magnetic or electric field, and ultrasound) to realize site-specific drug release and exert selective anti-cancer effects. Therefore, the advantage of stimuli-responsive nanoplatforms for cancer diagnosis and therapy is that the release of imaging probes and anti-cancer agents can be precisely controlled by the alteration of pH, redox [25], enzyme, and temperature or even overexpression of certain biomolecules in cancerous tissues or the application of external stimuli such as light, temperature, ultrasound, and magnetic and electric fields, thereby minimizing systemic toxicities and adverse effects. For instance, the theranostic nanomedicine can be engineered to get controlled and sustained release of diagnostic or therapeutic agents and to overcome the limitations of conventional cancer chemotherapy including the lack of selectivity and acquaintance of resistance.

## 6.3 Classification and Application of Nanomaterials in Cancer Diagnosis and Therapy

Generally, functionalized nanomaterials for cancer diagnostic and therapeutic applications can be roughly classified into two major categories: inorganic nanomaterials (e.g., metallic nanoparticles, silica-based nanoparticles, quantum dots, carbon-based nanoparticles, and magnetic nanoparticles) and organic nanoparticles (e.g., lipid-based nanoparticles, protein-based or peptide-based nanoparticles, synthetic polymer-based nanoparticles, polymeric micelles, dendritic polymers). Universal and unique properties of representative organic and inorganic nanomaterials applied in cancer diagnosis and therapy are summarized in this section.

### 6.3.1 Inorganic Nanoparticles

Inorganic nanoparticles possess a series of characteristics (in particular their distinct imaging modalities, unique magnetic properties, and photothermal capabilities) that are not common in organic counterparts such as lipid- and polymer-based nanoparticles. Therefore, inorganic nanoparticles, especially multifunctional gold nanoparticles, mesoporous silica nanoparticles, quantum dots, carbon nanotubes, and magnetic nanoparticles, have been extensively investigated for cancer theranostic applications to address unique challenges currently existing in clinical settings. Herein, we review the representative inorganic nanoplatforms as well as their opportunities for cancer diagnostic and therapeutic applications.

#### 6.3.1.1 Metallic Nanoparticles (e.g., Gold Nanoparticles)

Due to their unique and tunable optical properties and electronic properties, gold nanoparticles are representative metallic nanoparticles being extensively investigated in cancer bioimaging, photothermal therapy (PTT), and photodynamic therapy (PDT). In particular, given their distinct surface plasmon resonance properties absorbing and converting specific light into localized heat to ablate cancerous cells, gold nanoparticles have already become ideal platforms for both cancer imaging and PTT. Notably, gold nanoparticles possess high affinity with thiol groups, which make them flexible for surface modifications with various functional moieties such as specific targeting ligands, stabilizing coating materials, smart stimuli-responsive linkers, bioimaging agents, and therapeutic cargos (e.g., photosensitizers, proteins [26], peptides [27], siRNA [28], and chemotherapeutic drugs [29]). Gold nanoparticles of diverse structures, mainly including gold nanospheres, nanorods, nanocages, and nanoshells, have already emerged as attractive nanoplatforms for photosensitizer delivery [30]. Moreover, diverse functional components can be simultaneously integrated into gold nanoparticles to fabricate multifunctional nanoplatforms for cancer diagnostic and therapeutic applications. Besides, gold nanoparticles fabricated with polymers [31], magnetic nanoparticles [32], mesoporous silica nanoparticles [33], or carbon nanotubes [34] have been increasingly investigated as hybrid multifunctional nanomaterials for therapeutic applications.

#### 6.3.1.2 Silica-Based Nanoparticles (e.g., Mesoporous Silica Nanoparticles)

Mesoporous silica nanoparticles (MSNs) emerge as multifunctional delivery platforms due to their excellent chemical and thermal stability, high loading capacity, ready availability [35], eminent biocompatibility [36], tunable and controllable morphology and porosity, and versatile and modifiable surface functionalization [37]. The unique porous architecture of MSNs allows for the construction of stimuli-responsive devices enabling the controlled and ordered release of encapsulated payloads (including both cancer diagnostic and therapeutic agents) in response to certain internal stimuli in the tumor microenvironment as well as external stimuli such as light, temperature, magnetic field, and ultrasound. Specifically, owing to the exceptional porous structure of MSNs, molecules or even nanoparticles can be conveniently grafted onto the pore entrances as caps to completely retain both hydrophobic and hydrophilic payloads within the hollow cavity of MSNs via stimuli-sensitive linkers. Upon exposure to corresponding stimuli, the molecules or nanoparticles anchored on the pore outlets of MSNs are disassembled, thereby leading to the release of the entrapped payloads. Notably, diverse gatekeeper molecules [38] such as peptides [39], polymers [40], proteins [41], and inorganic nanoparticles [42] have been anchored to the nanopores of the MSNs via various stimuli-sensitive elements. For instance, a reversible pH-responsive nanoplatform based on MSNs was assembled by anchoring metal-oxide magnetic nanoparticles onto the nanopore entrances of MSNs by boronate ester linkers [43] for targeted delivery of therapeutic agents to pathological sites with

low pH such as cancerous tissues. In recent years, the silica-based nanoparticles are extensively investigated in preclinical studies and clinical trials for cancer therapeutic and diagnostic applications, thus resulting in the development of MSNs as novel multifunctional theranostic nanoplatforms [37, 44–49]. Besides, to avoid aggregation and improve colloidal stability of bare MSNs due to the abundance of silanol groups on the outer surface, the nanoparticles can be functionalized with hydrophilic moieties such as PEG and lipid layers or other charged groups to provoke steric or electrostatic repulsion, respectively.

#### 6.3.1.3 Quantum Dots (QDs)

QDs, as semiconducting fluorescent nanocrystals exhibiting unique and favorable photophysical and electronic properties including tunable fluorescent wavelength, broad excitation and narrow emission spectra, high florescence yields and low photobleaching, sharp and symmetrical fluorescent peak, and large Stokes shift [50], have been extensively investigated as noninvasive imaging probes for biomedical applications in cancer imaging and diagnosis. The advantages of QDs make them an ideal class of florescent probes over traditional organic fluorophores of low specificity, stability, and signal penetration [51]. With flexible surface chemistry for functionalization and conjugation, QDs can be modified by covalently bonding to certain targeting ligands such as antibodies, peptides, and aptamers as well as therapeutic drugs for targeted drug delivery to specific cancerous sites, thereby integrating cancer imaging and drug delivery into single nanoplatform [52]. For instance, various multifunctional QD-based nanosystems conjugated with aptamer and doxorubicin were developed for synchronous selective cancer imaging and drug delivery and therapy [53]. Moreover, QDs also provide a suitable nanoplatform for multimodal cancer imaging by conjugation with multiple ligands that specifically recognize different cancer biomarkers [54] or hybridization with other nanomaterials that possess unique optical properties [55].

#### 6.3.1.4 Carbon-Based Nanoparticles (e.g., Carbon Nanotubes)

Carbon nanotubes (CNTs), classified as single-walled nanotubes (SWCNT) and multi-walled nanotubes (MWCNT), are hollow cylindrical nanostructures composed of one or more seamless graphene sheets. The needle-like morphology of carbon nanotubes facilitates their cellular internalization by the target cells and subsequent release of the payloads such as drugs, nucleic acids, and imaging agents. Carbon nanotubes can be easily conjugated with targeting ligands such as antibodies [56], aptamers [57], proteins [58], and peptides [59] to further increase their affinity and specificity to cancerous cells. The surface of CNTs can be functionalized by covalent conjugation or non-covalent interaction with therapeutic molecules and targeting ligands. With considerable external surface areas, CNTs have been used as multifunctional nanocarriers with high loading capacity for the delivery of chemotherapeutics such doxorubicin, camptothecin, carboplatin, cisplatin, and paclitaxel. Notably, due to their unique electrical, thermal, and spectroscopic properties, CNTs have been increasingly regarded as a versatile nanosystem for application in cancer detection and drug delivery and therapy. Particularly, CNTs exhibit

thermodynamic properties that render them attractive candidates for application as noninvasive carriers and mediators for photothermal therapy and photodynamic therapy to directly destroy cancerous tissues without affecting normal tissues [60–63].

#### 6.3.1.5 Magnetic Nanoparticles (e.g., Iron Oxide Nanoparticles)

Magnetic nanoparticles, a class of nanomaterials with unique physical properties in response to external magnetic fields, possess considerable biomedical potentials in noninvasive magnetic resonance imaging (MRI), controllable drug delivery, and hyperthermia therapy for cancer diseases [64, 65]. Notably, due to their intrinsic and exclusive high magnetic susceptibility, magnetic nanoparticles can be conveniently manipulated by applying an external magnetic field to realize controlled release of imaging probes or anti-cancer drugs to a desired target site at a specific rate, thus overcoming the side effects caused by conventional cancer diagnostic and therapeutic methods. Interestingly, after the nanoparticles are targeted to the cancer cells, it is possible to heat the tumor by oscillating the applied magnetic field for hyperthermia therapy. With excellent enhanced proton relaxation capabilities, magnetic nanoparticles can be used as contrast agents for MRI to improve imaging technique resolution, thus emerging as powerful imaging probes for cancer detection and diagnosis. For instance, biocompatible multifunctional magnetic iron oxide nanoparticles (IONPs) or superparamagnetic iron oxide nanoparticles (SPIONPs) are ideal theranostic platforms for the development of imaging-guided targeted cancer drug delivery and therapy [66]. It should be noted that appropriate surface modifications by coating with suitable materials and conjugating to cancer-targeted moieties are indispensable to improve physical and chemical stability and enhance selective and specific delivery of IONPs for biomedical applications in cancer diagnosis and therapy.

### 6.3.2 Organic Nanoparticles

#### 6.3.2.1 Lipid-Based Nanoparticles (e.g., Liposomes)

Liposomes are spherical vesicles with an internal aqueous core and one or more external lipid bilayers assembled by amphiphilic lipid molecules such as phospholipid and cholesterol and thus recognized as promising nanoplatforms for biomedical applications for their ready availability, prominent biocompatibility, and biodegradability. The liposome-based nanoplatforms facilitate the uptake and internalization of payloads via endocytosis following their adhesion and fusion with the bilayer of the phospholipid membranes of cancer cells, which can be further tailored by alteration of lipid composition and modification with protective steric stabilizer polyethylene glycol (PEG) [67]. Moreover, to overcome the lack of selectivity and minimize adverse effects, the liposomes can be functionalized by surface modification with specific ligands such as antibodies and antibody fragments [68] for active cancer targeting. Triggered-release liposomes can be engineered by inclusion of stimuli-sensitive elements or devices into the liposomes. Notably, due to their unique

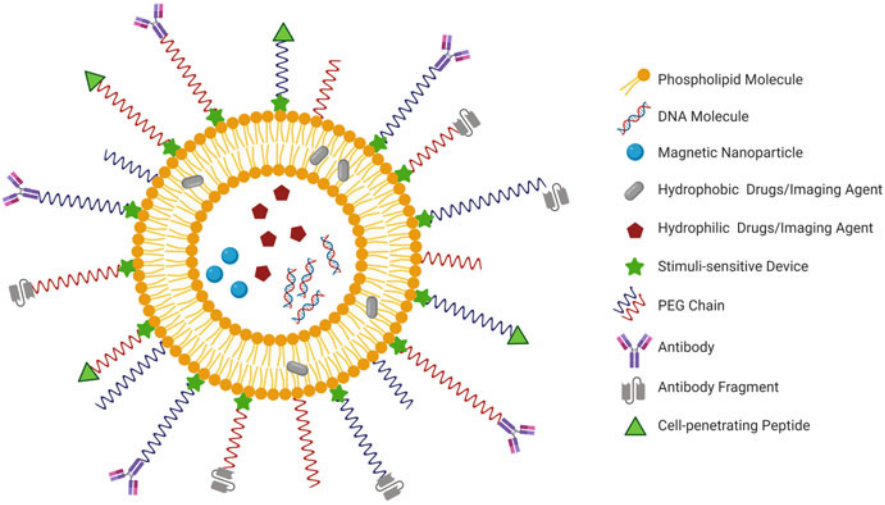


**Fig. 6.3** Schematic illustration of multifunctional liposomes

structure, liposomes enable not only the encapsulation of hydrophilic agents into the inner aqueous core but also the accommodation of hydrophobic molecules between the lipid bilayers, thus providing a nanoplatform for the simultaneous delivery of a wide range of cancer diagnostic and therapeutic agents with distinct physicochemical properties. Various hydrophilic chemotherapeutic compounds, such as doxorubicin, paclitaxel, and cisplatin, have been successfully formulated as liposomes for drug delivery to improve stability and solubility, prolong circulation time, and enhance selective cancer targeting. For instance, Doxil® [69], a clinical available PEGylated liposome-based nanomedicine containing doxorubicin, has been formulated and approved for the treatment of metastatic ovarian cancer, AIDS-related Kaposi's sarcoma, and multiple myeloma. Besides, cancer imaging devices can also be easily assembled by incorporation of fluorescent probes into the liposomes (Fig. 6.3).

#### 6.3.2.2 Protein- or Peptide-Based Nanoparticles (e.g., Albumin-Based Nanoparticles)

Protein- or peptide-based nanoparticles are a class of biocompatible and biodegradable nanoparticles composed of natural proteins or peptides. Albumin, as a versatile carrier protein, is the most widely and commonly used protein for the preparation of protein-based nanoparticles. Due to high availability, biocompatibility, and biodegradability, in particular the lack of immunogenicity and toxicity of albumin, albumin-based nanoparticles have been regarded as ideal candidates for cancer drug delivery. Abraxane [70], an albumin-bound paclitaxel nanoparticle that has been approved for the treatment of metastatic breast cancer, non-small cell lung cancer, and adenocarcinoma of the pancreas, further proves the safety of albumin-based nanoparticles. Drug release from albumin-based nanoparticles can be naturally controlled by mechanism based on protease degradation. Albumin-based

nanoparticles can be properly modified or fabricated to incorporate cancer-specific targeting ligands to optimize drug delivery efficiency. Notably, with abundant reactive functional groups (e.g., thiol, amino, and carboxyl) on their surface, albumin-based nanoparticles are amenable to various surface modifications that allow for the attachment of drugs and cancer-targeting ligands. For instance, albumin-based nanoparticles modified by covalently linking to avidin molecules and subsequently conjugated with biotinylated HER2 antibody can be constructed to realize selective targeting to cancerous cells with HER2 overexpression [71].

#### 6.3.2.3 Synthetic Polymer-Based Nanoparticles (e.g., PLGA [72])

Polymeric nanoparticles fabricated from amphiphilic copolymers, in particular poly (lactic-co-glycolic acid) (PLGA) that has been approved by FDA as effective drug carriers, possess tremendous potential as drug delivery platforms for the development of cancer nanomedicines due to its superior biocompatibility and biodegradability, high drug-loading efficiency, and controllable and sustainable release properties [73]. Notably, the fabrication or formulation of anti-cancer biomacromolecules such as proteins and nucleic acids that are vulnerable to enzymatic and chemical degradation into polymeric nanoparticles enables more controllable and sustainable drug delivery for cancer therapy. Due to their relative small size and facile surface modification, PLGA nanoparticles make it possible to circumvent multiple physiological barriers such as brain-blood barriers [74] and cell membranes and to release anti-cancer drugs at specific cancerous sites. Moreover, the biodegradable PLGA-based nanoplatforms could be designed by incorporating stimuli-responsive devices to realize controlled or triggered release of anti-cancer drugs [75, 76]. PLGA-based nanoparticles have been widely used as carriers for the delivery of small-molecule anti-cancer drugs such as docetaxel, doxorubicin, and paclitaxel to prolong circulation time, enhance specific targeting, or avoid rapid elimination. By modification of the nanoparticle surface with functional groups such as targeting molecules, anti-cancer drugs loaded to PLGA nanoparticles can be directed to the desired cancerous sites. For instance, with hydrophilic PEG as modifiers and short peptides as targeting molecules, the functionalized PLGA nanoparticles can be used as drug delivery vehicles to specifically target the αvβ3 integrin on cancer cells [77].

#### 6.3.2.4 Polymeric Micelles

Polymeric micelles, typically formed by self-assembled amphiphilic copolymers with an inner hydrophobic core and an outer hydrophilic shell, have emerged as a multifunctional nanoplatform for the delivery of poorly water-soluble anti-cancer compounds. Due to this unique core-shell nanostructure, polymeric micelles possess two distinct advantages as delivery carriers. On the one hand, the hydrophobic core of polymeric micelles serves as a reservoir for encapsulation and accommodation of drugs with poor aqueous solubility. On the other hand, the hydrophilic shell acts as a physical shield to minimize degradation and opsonin adsorption, thus contributing to largely improved in vivo stability and extended blood circulation time. Hydrophobic core-forming components with a broad range of structural diversity and polarity,

such as poly(propylene oxide), poly(lactic acid), and poly(L-lysine), are used for fabricating polymeric micelles, thus enabling the encapsulation and solubilization of a wide range of poorly water-soluble imaging or chemotherapeutic agents. PEG and its conjugates are the most widely and commonly used hydrophilic components to construct polymer micelles with good biocompatibility. However, it should be noted that assembly of polymeric micelles by PEG can largely be limited by its undesirable immunological response, unpredictable pharmacokinetics profile, and unfavorable biological degradability. Besides, it is relatively convenient to fabricate multifunctional nanoparticles for cancer diagnosis and therapy by incorporating cancer imaging, targeting, and therapeutic agents into a single nanoplatform of polymeric micelles. For instance, by incorporating stimuli-responsive modules and conjugating cancer-specific targeting ligands, polymeric micelles can be conferred with active targeting and controllable release properties, making it possible to selectively deliver various hydrophobic chemotherapeutic drugs to the cancerous tissues.

#### 6.3.2.5 Dendritic Polymers (e.g., PAMAM Dendrimers)

Dendritic polymers are a class of highly and repetitively branched nanosized macromolecules with three-dimensional tree-like architectures. Dendritic polymers are typically composed of three basic structural elements, including a focal core constituted of a single atom or molecule, an interior dendritic structure with consecutive and repetitive layers (also called as generations), and an exterior surface with abundant terminal functional groups enabling the anchoring of multiple therapeutic agents, targeting modules, imaging moieties, and biocompatible groups. Notably, with well-defined and controlled size and structure and high monodispersity, dendrimers offer a promising nanoplatform for the flexible drug loading of chemotherapeutic agents and anti-cancer macromolecules, either by covalently conjugating to terminal multifunctional groups of exterior surface or physically encapsulating into internal cavities via hydrophobic or electrostatic interactions. Meanwhile, various gene materials, such as plasmids and nucleic acids, can be complexed with dendritic polymers by electrostatic interaction. For instance, poly(amidoamine) (PAMAM) dendrimers are one of the most commonly and intensively investigated dendritic polymers for cancer diagnostic and therapeutic applications. Owing to their potential to interact with phosphate groups of nucleic acids to form transfection complexes, PAMAM dendrimers with numerous amino groups on the surface [78] have been intensively instigated as vectors used in gene therapy for cancerous diseases. Besides, it should be noted that cationic dendrimers should be modified by acetylation or PEGylation for biomedical applications, for the reason that their positively charged surface groups tend to interact with negative biological membranes and lead to low biocompatibility and high cytotoxicity.

## 6.4 Challenges and Prospects

A series of technical and regulatory challenges, such as nanomaterial characterization, quality control, security concerns [79], and regulatory issues, need to be addressed to ensure the successful translation of nanotechnology to practical clinical applications in cancer diagnosis and therapy. Notably, although substantial efforts have been devoted to surface modification of multifunctional nanomaterials with coating materials and targeting ligands, unwanted biological interactions between nanoparticles and normal tissues are still inevitable. On the one hand, it is not possible for the coating materials to maintain long-term stability in the viable and complex internal environments. On the other hand, it is not feasible to identify receptors or antigens that are exclusively expressed on cancerous cells but not on normal cells for specific targeting. It is imperative to have an in-depth understanding of interactions between nanoparticles and biological systems. Therefore, nowadays it is still too early to predict the success of nanotechnology in cancer diagnosis and therapy before some fundamental challenges concerning the biomedical applications of nanoparticles are properly addressed.

Regardless of the currently existing challenges for the application of nanomaterials in cancer diagnosis and therapy, multifunctional nanoparticles, for their distinctive advantages over conventional delivery systems, have emerged as a promising strategy to realize synergistic diagnostic, therapeutic, or theranostic effects for oncologic diseases. Nowadays multifunctional nanoparticles with superior capability to simultaneously achieve multiple functionalities including imaging, targeting, stimuli responsiveness, and therapeutics are designed and fabricated for biomedical purposes [80]. Moreover, multifunctional nanoparticles can also be fabricated by integrating inorganic and organic nanomaterials to exploit the unique properties and advantages of both categories of nanomaterials, thus enabling in vivo cancer-specific biomarker detection, real-time tumor tracking and monitoring, controllable drug release, targeted diagnosis and treatment, and cancer hyperthermia. A more comprehensive understanding and intensive investigation of functional nanoparticles will push the frontiers of their biomedical applications and ultimately lead to their use in cancer detection, imaging, diagnosis, and therapy.

**Acknowledgments** Financial supports were provided by the National Natural Science Foundation of China (81901232, 81773620) and Shanghai Sailing Program (20YF1402800).

## References

1. Davis ME, Chen ZG, Shin DM (2008) Nanoparticle therapeutics: an emerging treatment modality for cancer. Nat Rev Drug Discov 7(9):771–782. https://doi.org/10.1038/nrd2614
2. Nam J, Won N, Bang J, Jin H, Park J, Jung S, Jung S, Park Y, Kim S (2013) Surface engineering of inorganic nanoparticles for imaging and therapy. Adv Drug Deliv Rev 65(5):622–648. https://doi.org/10.1016/j.addr.2012.08.015

3. Peer D, Karp JM, Hong S, Farokhzad OC, Margalit R, Langer R (2007) Nanocarriers as an emerging platform for cancer therapy. Nat Nanotechnol 2(12):751–760. https://doi.org/10.1038/nnano.2007.387
4. Hobbs SK, Monsky WL, Yuan F, Roberts WG, Griffith L, Torchilin VP, Jain RK (1998) Regulation of transport pathways in tumor vessels: role of tumor type and microenvironment. Proc Natl Acad Sci U S A 95(8):4607–4612. https://doi.org/10.1073/pnas.95.8.4607
5. Maeda H, Wu J, Sawa T, Matsumura Y, Hori K (2000) Tumor vascular permeability and the EPR effect in macromolecular therapeutics: a review. J Control Release 65(1–2):271–284
6. Takahashi A, Ohkohchi N, Yasunaga M, Kuroda J, Koga Y, Kenmotsu H, Kinoshita T, Matsumura Y (2010) Detailed distribution of NK012, an SN-38-incorporating micelle, in the liver and its potent antitumor effects in mice bearing liver metastases. Clin Cancer Res 16 (19):4822–4831. https://doi.org/10.1158/1078-0432.CCR-10-1467
7. Ooya T, Lee J, Park K (2003) Effects of ethylene glycol-based graft, star-shaped, and dendritic polymers on solubilization and controlled release of paclitaxel. J Control Release 93 (2):121–127
8. Yao J, Hsu CH, Li Z, Kim TS, Hwang LP, Lin YC, Lin YY (2015) Magnetic resonance nanotheranostics for glioblastoma multiforme. Curr Pharm Des 21(36):5256–5266. https://doi.org/10.2174/1381612821666150923103307
9. Bertrand N, Wu J, Xu X, Kamaly N, Farokhzad OC (2014) Cancer nanotechnology: the impact of passive and active targeting in the era of modern cancer biology. Adv Drug Deliv Rev 66:2–25. https://doi.org/10.1016/j.addr.2013.11.009
10. Byrne JD, Betancourt T, Brannon-Peppas L (2008) Active targeting schemes for nanoparticle systems in cancer therapeutics. Adv Drug Deliv Rev 60(15):1615–1626. https://doi.org/10.1016/j.addr.2008.08.005
11. Perrault SD, Walkey C, Jennings T, Fischer HC, Chan WC (2009) Mediating tumor targeting efficiency of nanoparticles through design. Nano Lett 9(5):1909–1915. https://doi.org/10.1021/nl900031y
12. Sahay G, Alakhova DY, Kabanov AV (2010) Endocytosis of nanomedicines. J Control Release 145(3):182–195. https://doi.org/10.1016/j.jconrel.2010.01.036
13. Low PS, Henne WA, Doorneweerd DD (2008) Discovery and development of folic-acid-based receptor targeting for imaging and therapy of cancer and inflammatory diseases. Acc Chem Res 41(1):120–129. https://doi.org/10.1021/ar7000815
14. Wang J, Tian S, Petros RA, Napier ME, Desimone JM (2010) The complex role of multivalency in nanoparticles targeting the transferrin receptor for cancer therapies. J Am Chem Soc 132 (32):11306–11313. https://doi.org/10.1021/ja1043177
15. Mamot C, Drummond DC, Noble CO, Kallab V, Guo Z, Hong K, Kirpotin DB, Park JW (2005) Epidermal growth factor receptor-targeted immunoliposomes significantly enhance the efficacy of multiple anticancer drugs in vivo. Cancer Res 65(24):11631–11638. https://doi.org/10.1158/0008-5472.CAN-05-1093
16. Nielsen UB, Kirpotin DB, Pickering EM, Hong K, Park JW, Refaat Shalaby M, Shao Y, Benz CC, Marks JD (2002) Therapeutic efficacy of anti-ErbB2 immunoliposomes targeted by a phage antibody selected for cellular endocytosis. Biochim Biophys Acta 1591(1–3):109–118. https://doi.org/10.1016/s0167-4889(02)00256-2
17. Park JW, Hong K, Kirpotin DB, Colbern G, Shalaby R, Baselga J, Shao Y, Nielsen UB, Marks JD, Moore D, Papahadjopoulos D, Benz CC (2002) Anti-HER2 immunoliposomes: enhanced efficacy attributable to targeted delivery. Clin Cancer Res 8(4):1172–1181
18. Zhou Y, Drummond DC, Zou H, Hayes ME, Adams GP, Kirpotin DB, Marks JD (2007) Impact of single-chain Fv antibody fragment affinity on nanoparticle targeting of epidermal growth factor receptor-expressing tumor cells. J Mol Biol 371(4):934–947. https://doi.org/10.1016/j.jmb.2007.05.011
19. Poolsup S, Kim CY (2017) Therapeutic applications of synthetic nucleic acid aptamers. Curr Opin Biotechnol 48:180–186. https://doi.org/10.1016/j.copbio.2017.05.004

20. Qu D, Xue JW, Mo R, Ju CY, Jin X, Zhang C (2015) Extracellular pH-sensitive mixed micelles for prostate tumor targeted anticancer drug delivery. J Control Release 213:e14. https://doi.org/10.1016/j.jconrel.2015.05.019
21. Chen G, Wang Y, Xie R, Gong S (2017) Tumor-targeted pH/redox dual-sensitive unimolecular nanoparticles for efficient siRNA delivery. J Control Release 259:105–114. https://doi.org/10.1016/j.jconrel.2017.01.042
22. He H, Sun L, Ye J, Liu E, Chen S, Liang Q, Shin MC, Yang VC (2016) Enzyme-triggered, cell penetrating peptide-mediated delivery of anti-tumor agents. J Control Release 240:67–76. https://doi.org/10.1016/j.jconrel.2015.10.040
23. Guo Y, Zhang Y, Ma J, Li Q, Li Y, Zhou X, Zhao D, Song H, Chen Q, Zhu X (2018b) Light/magnetic hyperthermia triggered drug released from multi-functional thermo-sensitive magnetoliposomes for precise cancer synergetic theranostics. J Control Release 272:145–158. https://doi.org/10.1016/j.jconrel.2017.04.028
24. Obata Y, Tajima S, Takeoka S (2010) Evaluation of pH-responsive liposomes containing amino acid-based zwitterionic lipids for improving intracellular drug delivery in vitro and in vivo. J Control Release 142(2):267–276. https://doi.org/10.1016/j.jconrel.2009.10.023
25. Guo X, Cheng Y, Zhao X, Luo Y, Chen J, Yuan WE (2018a) Advances in redox-responsive drug delivery systems of tumor microenvironment. J Nanobiotechnol 16(1):74. https://doi.org/10.1186/s12951-018-0398-2
26. El-Sayed IH, Huang X, El-Sayed MA (2006) Selective laser photo-thermal therapy of epithelial carcinoma using anti-EGFR antibody conjugated gold nanoparticles. Cancer Lett 239 (1):129–135. https://doi.org/10.1016/j.canlet.2005.07.035
27. Tkachenko AG, Xie H, Coleman D, Glomm W, Ryan J, Anderson MF, Franzen S, Feldheim DL (2003) Multifunctional gold nanoparticle-peptide complexes for nuclear targeting. J Am Chem Soc 125(16):4700–4701. https://doi.org/10.1021/ja0296935
28. Giljohann DA, Seferos DS, Prigodich AE, Patel PC, Mirkin CA (2009) Gene regulation with polyvalent siRNA-nanoparticle conjugates. J Am Chem Soc 131(6):2072–2073. https://doi.org/10.1021/ja808719p
29. Wang F, Wang YC, Dou S, Xiong MH, Sun TM, Wang J (2011) Doxorubicin-tethered responsive gold nanoparticles facilitate intracellular drug delivery for overcoming multidrug resistance in cancer cells. ACS Nano 5(5):3679–3692. https://doi.org/10.1021/nn200007z
30. Blaszkiewicz P, Kotkowiak M (2018) Gold-based nanoparticles systems in phototherapy—current strategies. Curr Med Chem 25(42):5914–5929. https://doi.org/10.2174/0929867325666181031120757
31. Chen T, Xu S, Zhao T, Zhu L, Wei D, Li Y, Zhang H, Zhao C (2012) Gold nanocluster-conjugated amphiphilic block copolymer for tumor-targeted drug delivery. ACS Appl Mater Interfaces 4(11):5766–5774. https://doi.org/10.1021/am301223n
32. Hoskins C, Min Y, Gueorguieva M, McDougall C, Volovick A, Prentice P, Wang Z, Melzer A, Cuschieri A, Wang L (2012) Hybrid gold-iron oxide nanoparticles as a multifunctional platform for biomedical application. J Nanobiotechnol 10:27. https://doi.org/10.1186/1477-3155-10-27
33. Zhang Z, Wang L, Wang J, Jiang X, Li X, Hu Z, Ji Y, Wu X, Chen C (2012) Mesoporous silica-coated gold nanorods as a light-mediated multifunctional theranostic platform for cancer treatment. Adv Mater 24(11):1418–1423. https://doi.org/10.1002/adma.201104714
34. Minati L, Antonini V, Dalla Serra M, Speranza G (2012) Multifunctional branched gold-carbon nanotube hybrid for cell imaging and drug delivery. Langmuir 28(45):15900–15906. https://doi.org/10.1021/la303298u
35. Tang F, Li L, Chen D (2012) Mesoporous silica nanoparticles: synthesis, biocompatibility and drug delivery. Adv Mater 24(12):1504–1534. https://doi.org/10.1002/adma.201104763
36. Asefa T, Tao Z (2012) Biocompatibility of mesoporous silica nanoparticles. Chem Res Toxicol 25(11):2265–2284. https://doi.org/10.1021/tx300166u
37. Mai WX, Meng H (2013) Mesoporous silica nanoparticles: a multifunctional nano therapeutic system. Integr Biol 5(1):19–28. https://doi.org/10.1039/c2ib20137b

38. Wen J, Yang K, Liu F, Li H, Xu Y, Sun S (2017) Diverse gatekeepers for mesoporous silica nanoparticle based drug delivery systems. Chem Soc Rev 46(19):6024–6045. https://doi.org/10.1039/c7cs00219j
39. de la Torre C, Mondragon L, Coll C, Sancenon F, Marcos MD, Martinez-Manez R, Amoros P, Perez-Paya E, Orzaez M (2014) Cathepsin-B induced controlled release from peptide-capped mesoporous silica nanoparticles. Chemistry 20(47):15309–15314. https://doi.org/10.1002/chem.201404382
40. Tan L, Yang MY, Wu HX, Tang ZW, Xiao JY, Liu CJ, Zhuo RX (2015) Glucose- and pH-responsive nanogated ensemble based on polymeric network capped mesoporous silica. ACS Appl Mater Interfaces 7(11):6310–6316. https://doi.org/10.1021/acsami.5b00631
41. Li LL, Xie M, Wang J, Li X, Wang C, Yuan Q, Pang DW, Lu Y, Tan W (2013) A vitamin-responsive mesoporous nanocarrier with DNA aptamer-mediated cell targeting. Chem Commun 49(52):5823–5825. https://doi.org/10.1039/c3cc41072b
42. Liu R, Zhang Y, Zhao X, Agarwal A, Mueller LJ, Feng P (2010) pH-responsive nanogated ensemble based on gold-capped mesoporous silica through an acid-labile acetal linker. J Am Chem Soc 132(5):1500–1501. https://doi.org/10.1021/ja907838s
43. Gan Q, Lu X, Yuan Y, Qian J, Zhou H, Lu X, Shi J, Liu C (2011) A magnetic, reversible pH-responsive nanogated ensemble based on Fe3O4 nanoparticles-capped mesoporous silica. Biomaterials 32(7):1932–1942. https://doi.org/10.1016/j.biomaterials.2010.11.020
44. Phillips E, Penate-Medina O, Zanzonico PB, Carvajal RD, Mohan P, Ye Y, Humm J, Gonen M, Kalaigian H, Schoder H, Strauss HW, Larson SM, Wiesner U, Bradbury MS (2014) Clinical translation of an ultrasmall inorganic optical-PET imaging nanoparticle probe. Sci Transl Med 6(260):260ra149. https://doi.org/10.1126/scitranslmed.3009524
45. Radu DR, Lai CY, Jeftinija K, Rowe EW, Jeftinija S, Lin VS (2004) A polyamidoamine dendrimer-capped mesoporous silica nanosphere-based gene transfection reagent. J Am Chem Soc 126(41):13216–13217. https://doi.org/10.1021/ja046275m
46. Benezra M, Penate-Medina O, Zanzonico PB, Schaer D, Ow H, Burns A, DeStanchina E, Longo V, Herz E, Iyer S, Wolchok J, Larson SM, Wiesner U, Bradbury MS (2011) Multimodal silica nanoparticles are effective cancer-targeted probes in a model of human melanoma. J Clin Invest 121(7):2768–2780. https://doi.org/10.1172/JCI45600
47. Giri S, Trewyn BG, Stellmaker MP, Lin VS (2005) Stimuli-responsive controlled-release delivery system based on mesoporous silica nanorods capped with magnetic nanoparticles. Angew Chem 44(32):5038–5044. https://doi.org/10.1002/anie.200501819
48. Kramer R, Friedricn T (2005) Structure of functional modules from energy-transducing complexes in prokaryotes: examples for molecular machines. J Mol Microbiol Biotechnol 10(2–4):73–75. https://doi.org/10.1159/000091555
49. Pohl JF, Judkins J, Meihls S, Lowichik A, Chatfield BA, McDonald CM (2010) Cystic fibrosis and celiac disease: both can occur together. Clin Pediatr. https://doi.org/10.1177/0009922810388512
50. Wegner KD, Hildebrandt N (2015) Quantum dots: bright and versatile in vitro and in vivo fluorescence imaging biosensors. Chem Soc Rev 44(14):4792–4834. https://doi.org/10.1039/c4cs00532e
51. Jaiswal JK, Mattoussi H, Mauro JM, Simon SM (2003) Long-term multiple color imaging of live cells using quantum dot bioconjugates. Nat Biotechnol 21(1):47–51. https://doi.org/10.1038/nbt767
52. Zrazhevskiy P, Sena M, Gao X (2010) Designing multifunctional quantum dots for bioimaging, detection, and drug delivery. Chem Soc Rev 39(11):4326–4354. https://doi.org/10.1039/b915139g
53. Savla R, Taratula O, Garbuzenko O, Minko T (2011) Tumor targeted quantum dot-mucin 1 aptamer-doxorubicin conjugate for imaging and treatment of cancer. J Control Release 153(1):16–22. https://doi.org/10.1016/j.jconrel.2011.02.015
54. Peng CW, Tian Q, Yang GF, Fang M, Zhang ZL, Peng J, Li Y, Pang DW (2012) Quantum-dots based simultaneous detection of multiple biomarkers of tumor stromal features to predict

clinical outcomes in gastric cancer. Biomaterials 33(23):5742–5752. https://doi.org/10.1016/j.biomaterials.2012.04.034
55. Jing L, Ding K, Kershaw SV, Kempson IM, Rogach AL, Gao M (2014) Magnetically engineered semiconductor quantum dots as multimodal imaging probes. Adv Mater 26 (37):6367–6386. https://doi.org/10.1002/adma.201402296
56. Lee PC, Chiou YC, Wong JM, Peng CL, Shieh MJ (2013) Targeting colorectal cancer cells with single-walled carbon nanotubes conjugated to anticancer agent SN-38 and EGFR antibody. Biomaterials 34(34):8756–8765. https://doi.org/10.1016/j.biomaterials.2013.07.067
57. Zhang H, Hou L, Jiao X, Yandan J, Zhu X, Hongji L, Chen X, Ren J, Xia Y, Zhang Z (2014) In vitro and in vivo evaluation of antitumor drug-loaded aptamer targeted single-walled carbon nanotubes system. Curr Pharm Biotechnol 14(13):1105–1117
58. Ren J, Shen S, Wang D, Xi Z, Guo L, Pang Z, Qian Y, Sun X, Jiang X (2012) The targeted delivery of anticancer drugs to brain glioma by PEGylated oxidized multi-walled carbon nanotubes modified with angiopep-2. Biomaterials 33(11):3324–3333. https://doi.org/10.1016/j.biomaterials.2012.01.025
59. Hu S, Wang T, Pei X, Cai H, Chen J, Zhang X, Wan Q, Wang J (2016) Synergistic enhancement of antitumor efficacy by PEGylated multi-walled carbon nanotubes modified with cell-penetrating peptide TAT. Nanoscale Res Lett 11(1):452. https://doi.org/10.1186/s11671-016-1672-6
60. Burke A, Ding X, Singh R, Kraft RA, Levi-Polyachenko N, Rylander MN, Szot C, Buchanan C, Whitney J, Fisher J, Hatcher HC, D'Agostino R Jr, Kock ND, Ajayan PM, Carroll DL, Akman S, Torti FM, Torti SV (2009) Long-term survival following a single treatment of kidney tumors with multiwalled carbon nanotubes and near-infrared radiation. Proc Natl Acad Sci U S A 106(31):12897–12902. https://doi.org/10.1073/pnas.0905195106
61. Chakravarty P, Marches R, Zimmerman NS, Swafford AD, Bajaj P, Musselman IH, Pantano P, Draper RK, Vitetta ES (2008) Thermal ablation of tumor cells with antibody-functionalized single-walled carbon nanotubes. Proc Natl Acad Sci U S A 105(25):8697–8702. https://doi.org/10.1073/pnas.0803557105
62. Kam NW, O'Connell M, Wisdom JA, Dai H (2005) Carbon nanotubes as multifunctional biological transporters and near-infrared agents for selective cancer cell destruction. Proc Natl Acad Sci U S A 102(33):11600–11605. https://doi.org/10.1073/pnas.0502680102
63. Singh R, Torti SV (2013) Carbon nanotubes in hyperthermia therapy. Adv Drug Deliv Rev 65 (15):2045–2060. https://doi.org/10.1016/j.addr.2013.08.001
64. Gao J, Gu H, Xu B (2009) Multifunctional magnetic nanoparticles: design, synthesis, and biomedical applications. Acc Chem Res 42(8):1097–1107. https://doi.org/10.1021/ar9000026
65. Kim KS, Kim J, Lee JY, Matsuda S, Hideshima S, Mori Y, Osaka T, Na K (2016) Stimuli-responsive magnetic nanoparticles for tumor-targeted bimodal imaging and photodynamic/hyperthermia combination therapy. Nanoscale 8(22):11625–11634. https://doi.org/10.1039/c6nr02273a
66. Hu Y, Mignani S, Majoral JP, Shen M, Shi X (2018) Construction of iron oxide nanoparticle-based hybrid platforms for tumor imaging and therapy. Chem Soc Rev 47(5):1874–1900. https://doi.org/10.1039/c7cs00657h
67. Duzgune, scedil, Nir S (1999) Mechanisms and kinetics of liposome-cell interactions. Adv Drug Deliv Rev 40(1–2):3–18
68. Wicki A, Rochlitz C, Orleth A, Ritschard R, Albrecht I, Herrmann R, Christofori G, Mamot C (2012) Targeting tumor-associated endothelial cells: anti-VEGFR2 immunoliposomes mediate tumor vessel disruption and inhibit tumor growth. Clin Cancer Res 18(2):454–464. https://doi.org/10.1158/1078-0432.CCR-11-1102
69. Barenholz Y (2012) Doxil®—the first FDA-approved nano-drug: lessons learned. J Control Release 160(2):117–134. PMID: 22484195
70. Green MR, Manikhas GM, Orlov S, Afanasyev B, Makhson AM, Bhar P, Hawkins MJ (2006) Abraxane, a novel Cremophor-free, albumin-bound particle form of paclitaxel for the treatment of advanced non-small-cell lung cancer. Ann Oncol 17(8):1263–1268. PMID: 16740598

71. Wartlick H, Michaelis K, Balthasar S, Strebhardt K, Kreuter J, Langer K (2004) Highly specific HER2-mediated cellular uptake of antibody-modified nanoparticles in tumour cells. J Drug Target 12(7):461–471. https://doi.org/10.1080/10611860400010697
72. Kulkarni RK, Moore EG, Hegyeli AF, Leonard F (1971) Biodegradable poly(lactic acid) polymers. J Biomed Mater Res 5(3):169–181. https://doi.org/10.1002/jbm.820050305
73. Kamaly N, Yameen B, Wu J, Farokhzad OC (2016) Degradable controlled-release polymers and polymeric nanoparticles: mechanisms of controlling drug release. Chem Rev 116 (4):2602–2663. https://doi.org/10.1021/acs.chemrev.5b00346
74. Wohlfart S, Gelperina S, Kreuter J (2012) Transport of drugs across the blood-brain barrier by nanoparticles. J Control Release 161(2):264–273. https://doi.org/10.1016/j.jconrel.2011.08.017
75. Hu K, Zhou H, Liu Y, Liu Z, Liu J, Tang J, Li J, Zhang J, Sheng W, Zhao Y, Wu Y, Chen C (2015) Hyaluronic acid functional amphipathic and redox-responsive polymer particles for the co-delivery of doxorubicin and cyclopamine to eradicate breast cancer cells and cancer stem cells. Nanoscale 7(18):8607–8618. https://doi.org/10.1039/c5nr01084e
76. Wu J, Zhang J, Deng C, Meng F, Cheng R, Zhong Z (2017) Robust, responsive, and targeted PLGA anticancer nanomedicines by combination of reductively cleavable surfactant and covalent hyaluronic acid coating. ACS Appl Mater Interfaces 9(4):3985–3994. https://doi.org/10.1021/acsami.6b15105
77. Graf N, Bielenberg DR, Kolishetti N, Muus C, Banyard J, Farokhzad OC, Lippard SJ (2012) α(V)β(3) integrin-targeted PLGA-PEG nanoparticles for enhanced anti-tumor efficacy of a Pt (IV) prodrug. ACS Nano 6(5):4530–4539. PMID: 22584163
78. Astruc D, Boisselier E, Ornelas C (2010) Dendrimers designed for functions: from physical, photophysical, and supramolecular properties to applications in sensing, catalysis, molecular electronics, photonics, and nanomedicine. Chem Rev 110(4):1857–1959. https://doi.org/10.1021/cr900327d
79. Dobrovolskaia MA, McNeil SE (2007) Immunological properties of engineered nanomaterials. Nat Nanotechnol 2(8):469–478. https://doi.org/10.1038/nnano.2007.223
80. Yao X, Niu X, Ma K, Huang P, Grothe J, Kaskel S, Zhu Y (2017) Graphene quantum dots-capped magnetic mesoporous silica nanoparticles as a multifunctional platform for controlled drug delivery, magnetic hyperthermia, and photothermal therapy. Small 13(2):1602225. https://doi.org/10.1002/smll.201602225

# Marine Resources for Biosynthesis and Surface Modification of Anticancer Nanoparticles

7

Sreeranjini Pulakkat and Vandana B. Patravale

**Abstract**

In the recent past, there has been a marked increase in the research utilizing nature as a "bio-laboratory" for eco-friendly synthesis of nanoparticles with controlled morphologies and unique properties. Several biotemplates sourced from plants, microorganisms, marine ecosystem, etc., have been explored for the biosynthesis of metallic and metal oxide nanoparticles. These bionanoparticles have been utilized for a diverse range of applications including catalysis, solar energy, water treatment, nanotherapeutics, drug delivery, diagnostics, etc. This chapter deals with the use of marine resources for the development of bionanoparticles for anticancer applications. The marine ecosystem provides abundant bioactives that may have a significant impact in the development of pharmaceutical and nanotechnology products. Marine algae and microorganisms have been widely studied for their natural ability to sequester metal ions and synthesize inorganic nanoparticles either intracellularly or extracellularly. Marine polysaccharides represent a new class of biomaterials that is still underutilized and have the potential to act as reducing as well as stabilizing agents influencing the surface properties of the biosynthesized nanoparticles. They also have been explored for surface modification of prepared nanoparticles for conferring biocompatibility and surface functionality. The exact mechanism of biosynthesis of nanoparticles using different marine resources is yet to be elucidated. In addition, although these green nanoparticles have been reported to have inherent biocompatibility and selective toxicity to cancer cells, a mechanistic approach to unravel their exact mode of action, comprehensive toxicity studies, and clinical trials are warranted before they can be put to clinical use.

S. Pulakkat · V. B. Patravale (✉)
Department of Pharmaceutical Sciences and Technology, Institute of Chemical Technology, Mumbai, India
e-mail: vb.patravale@ictmumbai.edu.in

© Springer Nature Singapore Pte Ltd. 2020

Q. Saquib et al. (eds.), *Green Synthesis of Nanoparticles: Applications and Prospects*, https://doi.org/10.1007/978-981-15-5179-6_7

**Keywords**

Marine nanoparticles · Anticancer · Green synthesis · Marine algae · Polysaccharides · Microbial biosynthesis

## 7.1 Introduction

### 7.1.1 Why Green Synthesis?

The use of nanoparticles in healthcare has the potential to provide more efficient and affordable diagnosis, customized treatments, and follow-up of several debilitating diseases [1, 2]. Several techniques that have been reported for the synthesis of nanoparticles can be broadly classified as top-down and bottom-up approaches. The top-down methods for the synthesis of nanoparticles are ball milling, microcontact printing, lithography, etc., while the commonly used bottom-up approaches include chemical reduction, self-assembly, pyrolysis, sol–gel processing, etc. [3]. However, these methods involve costly, toxic, and nonbiodegradable reagents as stabilizing and reducing agents, which may accumulate in the environment in solid, liquid, or gaseous forms, thereby limiting the applications of these nanoparticles. The removal of residual organic solvents in the chemical synthesis methods from the final nanoparticle-based formulations can often be tedious. Further, majority of these methods are very expensive and cumbersome, have low material conversion rates, and involve the use of high energy, and therefore, an alternative method using biological agents for the synthesis of nanoparticles is the need of the hour. Further, the nanoparticles can easily enter the human body, cross natural barriers, and interact with biomolecules in the blood or within organs, tissues, or cells. Hence, great caution is to be exercized with regard to the accumulation and long-term adversities of these engineered nanomaterials to the environment and human beings [4, 5]. In this regard, the green synthesis of nanoparticles poses as a safer, eco-friendly, simple, energy-efficient, and low-cost alternative.

Green nanotechnology, which involves eco-friendly preparation of nanoparticulate systems by avoiding the use of hazardous chemicals and solvents, has been mostly explored for the synthesis of different metal and metal oxide nanoparticles. Environmentally safe reducing agents, stabilizing or capping agents, and solvents are among the principal criteria involved in the bottom-up green synthesis of nanoparticles. Several biomolecules sourced from plant extracts, seaweeds, algae, bacteria, viruses, fungi, and animal-derived polysaccharides, such as chitin and silk, have been explored for their natural potential to reduce metallic ions into neutral atoms without the use of hazardous chemicals. Biosynthesis of nanoparticles is an energy-efficient process and eliminates the need for high temperature, pressure, or energy. The pH, temperature, substrate concentration, enzyme activity, sonication, reaction time, and many other factors can be modified to control the nucleation and crystal growth as well as the final shape and size of the

nanoparticles. Majority of the reducing agents used in the green synthesis of nanoparticles also act as capping agents, thereby rendering biocompatibility and stability to the metal nanoparticles. Biosynthesis of metal nanoparticles like gold, silver, copper, cobalt, palladium, platinum, etc., and metal oxide/salt nanoparticles like titanium oxide, copper oxide, zinc oxide, lead sulfide, iron oxide, nickel oxide, magnesium oxide, etc., have been reported so far. The size and shape of the synthesized nanoparticles determine their fundamental electronic, optical, magnetic, and catalytic properties [6–10].

The exact mechanism of biosynthesis of nanoparticles is yet to be elucidated. However, several compounds like terpenoids, phenolics, flavonoids, enzymes, sugars, proteins, pigments, alkaloids, and other reducing agents present in the plant extracts and microbial cells have been reported to trigger the reduction of metal ions to nanoparticles. In microbial-mediated nanoparticle synthesis, the electrostatic interaction between the bacterial cell wall and metal ions in addition to the intracellular or cell surface enzymes plays a role in the nanoparticle synthesis [11, 12]. In addition, peptides such as phytochelatins have been reported to be synthesized in response to heavy metal stress in plants [13], bacteria [14], and fungi [15]. They are involved in sequestering metal ions and stabilizing the synthesized nanoparticles [16]. Nevertheless, the major drawback for the biological synthesis of nanoparticle is that the exact mechanism of nanoparticle synthesis is to be elucidated to ensure scalability and reproducibility of the processes. Further, the slow microbial growth and biosynthesis under natural conditions may increase the duration of nanoparticle synthesis.

### 7.1.2 Marine-Based Biosynthesis of Nanoparticles

Marine bio-nanotechnology is a less explored but exciting area of research that holds great promise in the field of nanotechnology. Most of the research work on biosynthesis of metal, metal sulfide, and metal oxide nanoparticles has been based on terrestrial plants and organisms. The diverse marine environment is a rich source of bioactive reducing agents, precursor molecules (silica, calcium, chitosan), and stabilizing agents (polysaccharides, lipids, and peptides) that may find vast applications in the field of pharmaceutical and biotechnology product development. Owing to the fact that the marine ecosystem is totally different from terrestrial ecosystem, the biomolecules like polyphenols, flavonoids, alkaloids, tannins, enzymes, peptides, etc., sourced from marine ecosystem would differ in their capability to sequester metal ions, reduce them, and stabilize the formed nanoparticles. Several marine organisms including bacteria, cyanobacteria, yeasts, fungi, sponges, etc., in addition to algae, mangroves, and seagrasses have been studied for biosynthesis of nanoparticles. These marine-based biogenic nanoparticles were then investigated for their antimicrobial, anticancer, and antifungal properties, with the major chunk of the research being directed toward evaluation of antimicrobial properties [17–22].

Considering the enhanced utility of nanoparticles in anticancer applications, the antioxidant properties and the apoptotic potential of marine-based biogenic nanoparticles need to be explored in detail, and the exact mechanism of action needs to be discovered. It is believed that most of the biogenic nanoparticles cause generation of reactive oxygen species (ROS), which activate the caspase 3 enzyme that triggers apoptosis. Further, the increased oxidative stress can cause oxidation of glutathione, an antioxidant that prevents cell damages due to ROS [23]. However, exact mechanisms might change with respect to the different marine sources and the synthesis conditions. Some of the marine-based biogenic nanoparticles investigated for anticancer applications have been discussed in the following sections.

## 7.2 Biosynthesis of Anticancer Nanoparticles Using Marine Algae

Marine algae are eukaryotic, oxygenic photoautotrophs and are rich sources of biomolecules including polysaccharides, polyphenols, carotenoids, protein, and other phytochemicals, which act as effective metal-reducing agents and capping agents. They are broadly classified into microalgae (e.g., phytoplanktons that remain suspended in the water) and macroalgae or seaweeds (plant-like organisms with size ranging from a few centimeters to several meters). They are also classified based on the algal body or thallus pigmentation into brown algae, red algae (predominantly marine based), and green algae (marine and fresh water based). Algae-derived biomolecules are promising candidates for the biosynthesis of different metallic and metal oxide nanoparticles. Although several algae have been investigated for intracellular or extracellular biosynthesis of different nanoparticles, the exact mechanism of synthesis or the factors to control the size and shape of the products are not yet fully understood. Similar to microbial mediated biosynthesis, the electrostatic interaction between the metal ions and negatively charged cell surface leading to sequestering of the metal ions on the cell wall and further reduction by cellular enzymes/biocatalysts into nanoparticles is thought to be applicable to algae-mediated biosynthesis also. The synthesis method, in most cases, is a straightforward room temperature process involving mixing of a metal salt solution with an aqueous solution of algal extract. The mono or divalent metal ions get reduced to their zerovalent states and undergo subsequent nucleation and growth to form nanoparticles indicated by a color change in the reaction mixture. The algal biomolecules also act as surfactants on specific crystal facets and influence the size, morphology, and physicochemical properties of the final nanoparticles [24]. Currently, the role of experimental parameters like concentration of algal extract and metal salt, pH, reaction time, and temperature is being investigated; however, the role of specific biomolecules and their individual influence in nanoparticle growth and properties need to be studied further. Among the various metal nanoparticles, gold and silver nanoparticles have been extensively investigated for antibacterial, anticancer, and anti-fungicidal applications [24, 25]. The following

section describes the studies exploring anticancer applications of algae-mediated biogenic nanoparticles.

The extract of an edible marine brown alga, *Ecklonia cava*, has been reported as an effective reducing and capping agent for biosynthesis of silver nanoparticles and has been widely investigated for its antimicrobial, antioxidant, and anticancer activities [26]. Biosynthesized, spherical silver nanoparticles having an average size of 43 nm were prepared using an aqueous extract of *Ecklonia cava*. They demonstrated a significant antibacterial activity against *Escherichia coli* and *Staphylococcus aureus* and a strong apoptotic activity against human cervical cancer cells, HeLa cells ($IC_{50}$ value, 59 μg/mL) [27]. In another study, a wide range of seaweeds (*Ulva fasciata*, *Corallina elongata*, *Gelidium crinale*, *Laurencia obtusa*, *Cystoseira myrica*, *and Turbinaria turbinata*) were evaluated for their ability to produce silver nanoparticles, and the antitumor efficiency of different concentrations of such biosynthesized nanoparticles was evaluated on Ehrlich ascites carcinoma (EAC) cells. Silver nanoparticles biosynthesized by *Turbinaria turbinata* exhibited the highest cytotoxicity against EAC in vitro [28]. These nanoparticles of 8–16 nm size were then evaluated for their in vivo anticancer effect against Ehrlich cell carcinoma (ECC) in mice. A dose-dependent reduction in tumor size and reduction in elevated white blood cell count in tumor-bearing mice were observed when treated with these biogenic silver nanoparticles [29]. In a similar study, anticancer efficacy of different concentrations of silver nanoparticles biosynthesized by various blue green algae (*Anabaena oryzae*, *Nostoc muscorum*, *and Calothrix marchica*) was analyzed on EAC cells, and the nanoparticles biosynthesized using *Calothrix marchica* showed highest anticancer activity [30]. *Padina tetrastromatica* is another seaweed which was utilized for the green synthesis of near spherical silver nanoparticles of 30–40 nm for anticancer applications against breast cancer MCF-7 cells [31]. Biosynthesized silver nanoparticles prepared using red seaweed *Pterocladiella capillacea* showed bactericidal activity and concentration-dependent cytotoxicity in human hepatocellular cancer cell line, Hep G2, indicating that the alkaloids present in the algae may contribute to the cytotoxic effects [32]. Another red alga, *Gracilaria corticata*, was employed for the green synthesis of silver nanoparticles, which were then studied for antimicrobial (against Gram-positive and Gram-negative bacteria, fungal species) and anticancer (against HeLa cells) applications [33].

*Sargassum* is a genus of brown macroalgae that have been widely explored for the biosynthesis of silver nanoparticles. Govindaraju et al. employed *Sargassum vulgare* to synthesize 10 nm-sized silver nanoparticles and studied their anticancer efficacy against human myeloblastic leukemic cells (HL60) and cervical cancer cells (HeLa). The study established the potential of such nanoparticles as a prophylactic agent in cancer treatment along with the usual chemotherapy regime [34]. The same group also demonstrated the extracellular synthesis of silver nanoparticles of size 30–40 nm from *Sargassum ilicifolium*. Antibacterial activity against five clinical pathogens and the in vitro toxicity against a brine shrimp, *Artemia salina*, were established in the study [35]. In another study, the methanolic extract of the seaweed *Sargassum polycystum* was used for the synthesis of silver nanoparticles of size

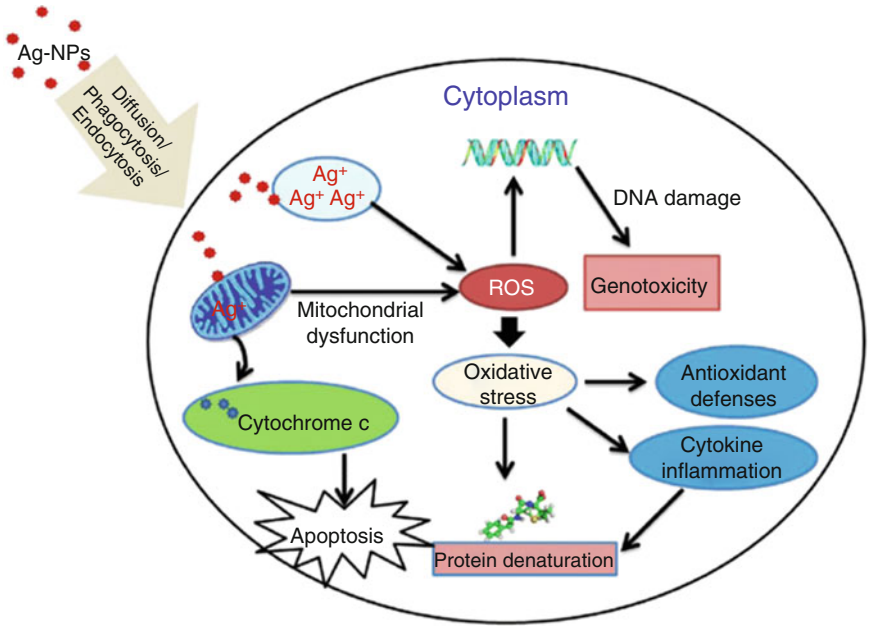


**Fig. 7.1** Possible mechanisms of cellular uptake and cytotoxicity of silver nanoparticles. (Reprinted with permission from Akter M, Sikder MdT, Rahman MdM, Ullah AKMA, Hossain KFB, Banik S, et al. A systematic review on silver nanoparticles-induced cytotoxicity: Physico-chemical properties and perspectives. Journal of Advanced Research. 2018 Jan 1;9:1–16. [23])

5–7 nm, and their antimicrobial and anticancer effects were analyzed. The bioactive component in the crude extract was identified as fatty acids, which along with the nanoparticles exerted anticancer activity in breast cancer cell line, MCF-7 [36]. Devi et al. developed silver nanoparticles using aqueous extracts of the macroalga *Sargassum longifolium* and observed that these nanoparticles showed a dose-dependent cytotoxicity against Hep-2 cell line [37]. They also studied the cytotoxic activity of silver nanoparticles synthesized using the seaweed *Hypnea* sp. as a function of the nanoparticle dimensions. Smaller nanoparticles exerted higher cytotoxicity in human colon adenocarcinoma cells, HT-29 [38].

The possible mechanisms of cellular uptake and cytotoxicity induced by silver nanoparticles are depicted in Fig. 7.1.

Apart from silver, majority of the research on green synthesis of metallic nanoparticles has been focused on the preparation of gold nanoparticles. Some of the challenges inherent to current cancer treatment modalities may be overcome using gold nanoparticles, for instance, they can be utilized for radiation dose enhancement or hyperthermia-induced radio-sensitization. Single-celled green and blue-green algae like *Spirulina platensis* and *Tetraselmis kochinensis* have been reported to exhibit strong binding toward tetra-chloro-aurate/silver ions, which get bound to the algal surface and subsequently reduced to gold/silver nanoparticles, respectively [39, 40]. Biosynthesized gold nanoparticles of size 15 nm were prepared

using an aqueous extract of the red seaweed *Corallina officinalis* as the reducing and stabilizing agent. The polyphenol content of the algae along with the gold nanoparticles brought about dose-dependent cytotoxicity and necrosis in breast cancer cells, MCF-7 [41]. In another study, brown seaweed *Padina gymnospora* was used to fabricate gold nanoparticles of size 8–21 nm, and the cytotoxic efficacy of the prepared nanoparticles was studied in liver cancer (HepG2) and lung cancer (A549) cell line. A specific cell toxicity in liver cancer cells was observed via DNA fragmentation while the lung cancer cells were less affected. Thus, further studies are warranted to elucidate the exact mechanism by which gold nanoparticles inhibit specific cancer cell progression [42]. Another brown macroalga, *Cystoseira baccata*, was also used to synthesize spherical, stable, polycrystalline gold nanoparticles with a mean diameter of $8.4 \pm 2.2$ nm. In vitro cytotoxicity studies of these nanoparticles using colon cancer cell lines HT-29 and Caco-2, as well as normal fibroblast cell line PCS-201-010, revealed their potential to treat colon rectal cancer [43]. Several studies utilizing the *Sargassum* genus of brown algae for preparation of gold nanoparticles have also been reported. Stable nanoparticles of gold were prepared by treating aqueous gold precursor with the aqueous extract of *Sargassum muticum* that acts as both reducing and capping agent [44]. In another study, spherical gold nanoparticles of size 35 nm and zeta potential −27 mV were biosynthesized using *Sargassum swartzii*. These nanoparticles exhibited a dose-dependent apoptotic activity against human cervical carcinoma (HeLa) cells [45]. In yet another study, *Sargassum glaucescens* extract was used to prepare and stabilize gold nanoparticles of size 4 nm, and their cytotoxic activity was analyzed in cervical (HeLa), liver (HepG2), breast (MDA-MB-231), and leukemia (CEM-ss) cell lines. The nanoparticles showed dose- and time-dependent cytotoxicity via intrinsic apoptotic pathway in all cancer cell lines while remaining nontoxic to the normal human mammary epithelial cells (MCF-10A) [46].

Brown algae from *Sargassum* genus were also utilized for the biosynthesis of metal oxide nanoparticles. Different seaweeds such as *Caulerpa peltata*, *Hypnea valencia*, and *Sargassum myriocystum* were screened for their ability to synthesize zinc oxide nanoparticles extracellularly. Water-soluble fucoidan pigments present in *Sargassum myriocystum* extract were found to be responsible for reduction and stabilization of zinc oxide nanoparticles [47]. Namvar et al. identified the bioactive materials like amino, sulfate, carboxyl, and hydroxyl groups in extract of *Sargassum muticum* for the biosynthesis of zinc oxide nanoparticles. The particles with a hexagonal morphology with size ranging from 3 to 57 nm were analyzed for their cytotoxicity in murine cancer cells (CT-26, WEHI-3, 4T1, and CRL-1451) and normal fibroblast cells (3T3). Further, the nanoparticles had selective toxicity against leukemia cell line, WEHI-3, but no adverse effect on normal fibroblast cells [48]. The same group evaluated the antiangiogenic and apoptotic properties of these zinc oxide nanoparticles on human liver cancer cell line (HepG2), which were found to be efficient at all concentration and time of incubation. Hence, these nanoparticles may be proposed as a supplemental drug in cancer treatment for decreasing angiogenesis and inducing apoptosis after in-depth in vivo analysis [49]. They also attempted in situ biosynthesis of zinc oxide/hyaluronan

nanocomposite using aqueous *Sargassum muticum* extract. The cytotoxic analysis of the nanocomposite carried out in pancreatic adenocarcinoma (PANC-1), ovarian adenocarcinoma (CaOV-3), colonic adenocarcinoma (COLO205), and acute promyelocytic leukemia (HL60) cells revealed that the composite was most toxic to the HL60 cells while it did not have any adverse effect in normal human lung fibroblast (MRC-5) cell line [50]. Ferric oxide nanoparticles having a cubic morphology of size 18 ± 4 nm were also prepared by a one-step biosynthetic method using *Sargassum muticum* extract. The authors identified the amino, carboxyl, and hydroxyl functional groups present in the polysaccharide algal walls to act as both reducing agent and capping agent. Subsequent in vitro studies revealed that these nanoparticles induced cell cycle arrest and apoptosis by activating caspase-3 and caspase-9 in a time-dependent fashion in human cell lines for leukemia (Jurkat), breast cancer (MCF-7), cervical cancer (HeLa), and liver cancer (HepG2) [51].

The different metal/metal oxide nanoparticles synthesized using marine algae and evaluated for their anticancer efficacy are summarized in Table 7.1.

## 7.3 Biosynthesis of Anticancer Nanoparticles Using Marine Microbes

Marine microorganisms, which account for 98% of ocean biomass, include bacteria, cyanobacteria, actinobacteria, yeast, and fungi. These tiny organisms are found abundantly in the marine ecosystem and easily adapt to extreme environments involving a range of acidity, alkalinity, temperatures, and salinity. Several metal-tolerant microorganisms have been known for their potential to synthesize metallic nanoparticles, either extracellularly or intracellularly. In intracellular biosynthesis, the microbial cell wall, owing to its negative charge, electrostatically interacts with the cationic metal ions. Further, the cell wall enzymes facilitate the reduction of these metal ions to nanoparticles, which then diffuse into the cell interior. Extracellular biosynthesis of metal nanoparticles involves a NADH-dependent reductase enzyme that supplies electrons and gets oxidized to $NAD^+$. This transfer of electrons from NADH results in the bioreduction of metal ions into metal nanoparticles (Fig. 7.2) [19, 22, 52].

Marine cyanobacteria are among the most primitive, photoautotrophic marine bacteria. They have been explored for the biosynthesis of metal nanoparticles owing to their ability to produce water-soluble fluorescent pigments and phycobiliproteins. Different functional groups, such as hydroxyl group, carboxyl anions, amino acids, and intracellular proteins, have been identified to be involved in the intracellular biosynthesis [53, 54]. Geetha et al. utilized marine cyanobacteria *Gloeocapsa* sp. for the intracellular synthesis of gold nanoparticles. The nanoparticles were of spherical and triangular shape having size less than 100 nm. The antitumor activity of the gold nanoparticles was studied in HeLa cells, and the $IC_{50}$ value calculated was 250 mg [55]. Another cyanobacterium isolated from deep sea water, *Pseudomonas aeruginosa* (JQ989348), was used for synthesis of silver nanoparticles. These particles having size between 13 and 76 nm showed high antimicrobial activity

**Table 7.1** Different algae species used for biosynthesis of anticancer metal/metal oxide nanoparticles

| Marine alga | Nanosystem | Study details and reference |
|---|---|---|
| *Ecklonia cava* | Silver nanoparticles | Biosynthesis and further analysis of antibacterial, antioxidant, and anticancer activity of 43-nm-sized spherical nanoparticles [27] |
| *Turbinaria turbinata* | Silver nanoparticles | Biosynthesis followed by in vitro and in vivo cytotoxicity of 8–16-nm-sized nanoparticles [28, 29] |
| *Padina tetrastromatica* | Silver nanoparticles | Biosynthesis and anticancer activity of near spherical nanoparticles of size 30–40 nm [31] |
| *Pterocladiella capillacea* | Silver nanoparticles | Biosynthesis and analysis of bactericidal and antitumor activity of 12 nm-sized nanoparticles [32] |
| *Gracilaria corticata* | Silver nanoparticles | Biosynthesis and evaluation of antibacterial and anticancer activity of nanoparticles [33] |
| *Sargassum vulgare* | Silver nanoparticles | Biosynthesis and anticancer efficacy of nanoparticles of size 10 nm [34] |
| *Sargassum ilicifolium* | Silver nanoparticles | Extracellular synthesis and evaluation of antibacterial and antitumor activity of nanoparticles of size 30–40 nm [35] |
| *Sargassum polycystum* | Silver nanoparticles | Biosynthesis and further analysis of antimicrobial and anticancer effects of nanoparticles of size 5–7 nm [36] |
| *Sargassum longifolium* | Silver nanoparticles | Biosynthesis and cytotoxicity analysis of cubical nanoparticles having size 30 nm [37] |
| *Hypnea* sp. | Silver nanoparticles | Biosynthesis and evaluation of bactericidal and cytotoxicity activity of spherical nanoparticles with size 10–20 nm [38] |
| *Corallina officinalis* | Gold nanoparticles | Biosynthesis and anticancer efficacy of nanoparticles of size 15 nm [41] |
| *Padina gymnospora* | Gold nanoparticles | Biosynthesis and antitumor efficacy of 8–21-nm-sized nanoparticles [42] |
| *Cystoseira baccata* | Gold nanoparticles | Biosynthesis and antitumor efficacy of spherical, polycrystalline nanoparticles of size 6–10 nm [43] |
| *Sargassum swartzii* | Gold nanoparticles | Biosynthesis and cytotoxicity analysis of spherical nanoparticles having size 35 nm [45] |
| *Sargassum glaucescens* | Gold nanoparticles | Biosynthesis and antitumor efficacy of 4 nm sized nanoparticles [46] |
| *Sargassum muticum* | Zinc oxide nanoparticles | Biosynthesis and further analysis of antiangiogenic and apoptotic properties [48, 49] |
| | Zinc oxide/ hyaluronan nanocomposite | In situ biosynthesis and cytotoxicity analysis of nanocomposite [50] |
| | Ferric oxide nanoparticles | Biosynthesis and cytotoxicity analysis of cubic nanoparticles having size 18 ± 4 nm [51] |

against *Escherichia coli*, *Vibrio cholerae*, *Aeromonas* sp., and *Corynebacterium* sp. They also had notable activity against biofilm-forming bacteria like *P. aeruginosa* and *Staphylococcus aureus*. Further, in vitro toxicity assay using human cervical cancer cells revealed that these nanoparticles have excellent

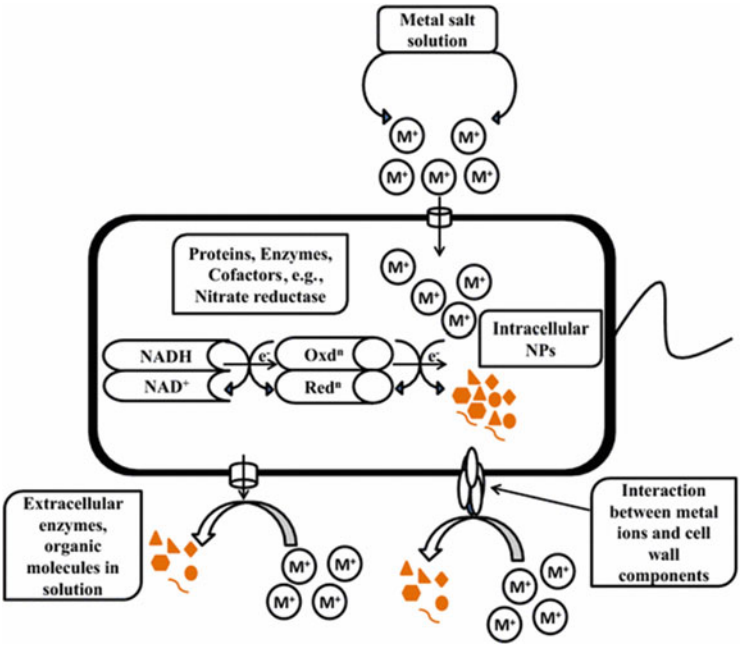


**Fig. 7.2** Possible mechanisms of biosynthesis of metal nanoparticles by microorganisms. (Reprinted with permission from Salunke BK, Sawant SS, Lee S-I, Kim BS. Microorganisms as efficient biosystem for the synthesis of metal nanoparticles: current scenario and future possibilities. World Journal of Microbiology and Biotechnology. 2016 Apr 2;32(5):88. [12])

cytotoxicity [56]. In another study, 15 marine bacteria were evaluated for their potential for biosynthesis of silver nanoparticles, and the most promising *Pseudomonas* sp. was further investigated. The biosynthesized nanoparticles were analyzed for their antibacterial, antifungal, antifouling, antioxidant, and bioremediation activities. In vitro cytotoxicity studies in HepG-2, MCF-7, and CaCo-2 cell lines revealed that the nanoparticles had the highest inhibitory activity against MCF-7 and HepG-2 cells. The differences in cytotoxicity were attributed to the variation in nanoparticle–cell surface interaction and subsequent disturbances in cell composition with cell type [57].

Marine actinobacteria, which play a pivotal role in breaking down organic compounds and recycling the organic matter, have also been investigated for potential biosynthesis of metallic nanoparticles. Manivasagan et al. studied the biosynthesis and characterization of gold nanoparticles using *Nocardiopsis* sp. *MBRC-1* isolated from the marine sediment samples. The prepared nanoparticles of size 45 nm showed excellent antimicrobial, antifungal, as well as dose-dependent anticancer activity against HeLa cells [58]. The same group also developed gold nanoparticles biosynthesized using another actinobacteria *Nocardiopsis* sp. *MBRC-48* and evaluated its antimicrobial, antioxidant, and anticancer activity. The synthesized nanoparticles had an average size of 11.57 ± 1.24 nm and were

spherical in shape. They exhibited good antimicrobial activity against pathogens like *Bacillus subtilis*, *Pseudomonas aeruginosa*, *Escherichia coli*, *Staphylococcus aureus*, *Candida albicans*, *Aspergillus niger*, *A. fumigatus*, *and A. brasiliensis.* Further, they showed strong antioxidant activity and dose-dependent cytotoxicity against cervical cancer cell line, HeLa, via apoptosis [59].

Hamed and group studied several actinomycetes isolates from sediment of the Suez Gulf, Egypt, for their ability for extracellular biosynthesis of gold nanoparticles. In one study, isolate M8 out of nine isolates was selected and identified as *Streptomyces griseus* and utilized for the biosynthesis of gold nanoparticles. These nanoparticles possessed significant antimicrobial activity against Gram-positive and Gram-negative bacteria. Further in vitro cytotoxicity studies revealed that the bionanoparticles exhibited a significant degree of anticancer activity against colon carcinoma cells (HCT-116) and breast carcinoma cells (MCF-7) [60]. In another study, the most potent isolate among 41 actinomycetes tested was identified as *Streptomyces rochei* MHM13 and used for the biosynthesis of silver nanoparticles. These biosynthesized nanoparticles of size 18–27 nm significantly inhibited the growth of several pathogenic bacteria and also possessed antifouling properties. The in vitro cytotoxicity studies were conducted in different cell lines, viz., hepatocellular carcinoma (HepG-2), breast carcinoma (MCF-7), colon carcinoma (HCT-116), prostate carcinoma (PC-3), lung carcinoma (A-549), intestinal carcinoma (CaCo), larynx carcinoma (HEP-2), and cervical carcinoma (HeLa). The nanoparticles had reasonable anticancer activity against Hep-G2, HCT-116, A-549, MCF-7, and PC-3 cell lines, while the CACO, HEP-2, and HeLa cells were resistant toward the cytotoxic activity [61]. In yet another work, the fermentation parameters controlling the production of bioactive metabolites by marine *Streptomyces cyaneus* strain Alex-SK121 were optimized, and the cell-free supernatant was used for the biosynthesis of spherical gold nanoparticles having size 6.5–20 nm. Antibacterial studies of the nanoparticles exhibited good activity against Gram-positive and Gram-negative pathogenic bacteria. Further studies in human breast and liver carcinoma cells showed that the biosynthesized particles had excellent antioxidant and antitumor activity [62]. Subbaiya et al. synthesized silver nanoparticles using actinomycetes isolated from marine soil sample and identified as *Streptomyces atrovirens*. These bionanoparticles showed profound anticancer activity in MCF-7 breast cancer cells in a dose-dependent manner and induced cell morphological changes as revealed by acridine orange and ethidium bromide double staining methods [63]. *Streptomyces* sp., well-known for its ability to produce several novel secondary metabolites, was studied for optimization of the use of a novel fucoidanase for the green synthesis of gold nanoparticles. The biosynthesized nanoparticles exhibited a dose-dependent cytotoxicity against HeLa cells with an $IC_{50}$ value of 350 μg/mL at 24 h and 250 μg/mL at 48 h [64]. *Streptomyces* sp. was also used as a reducing agent for the biosynthesis of zinc oxide nanoparticles. These nanoparticles were evaluated for their antibacterial activity against *E. coli* and *Bacillus subtilis* as well as cytotoxicity against A549 lung cancer cells [65].

*Enterococcus* sp. is another marine bacterium which was studied for the green synthesis of gold nanoparticles. These nanoparticles were spherical in shape having

size 6–13 nm and exhibited significant anticancer activity against liver cancer (HepG2) and lung cancer (A549) cells at 100-μg concentration [66]. Extracellular biosynthesis of silver nanoparticles has also been reported using culture supernatant of *Enterococcus* sp. The developed spherical nanoparticles in the size range of 10–80 nm showed enhanced antimicrobial activity when used in combination with marketed antibiotics. Further in vitro cytotoxicity analysis in liver cancer (HepG2) and lung cancer (A549) cells revealed the potential of these nanoparticles to inhibit cell growth [67]. The bacterium *E. coli* (VM1), isolated from marine sediments, was also exploited for its capability of biosynthesis of silver nanoparticles. The in vitro anticancer assay done in human lung cancer cells (A549), human cervical cancer cells (HeLa), and normal (Vero) cells showed dose-dependent cytotoxicity of silver nanoparticles. Loss of membrane integrity, cell shrinkage, and reduced cell concentrations, typical of apoptosis, were observed in all cells; however, the extent of cellular toxicity was more in cancer cells compared to normal cells [68].

Marine fungi have also been explored for green synthesis of metal nanoparticles, and the fungal proteins have been reported to play a vital role in the synthesis and stability of the nanoparticles. The cell-free filtrates of different fungal species (*Aspergillus flavus* SP-3, *Trichoderma gamsii* SP, *Trichoderma gamsii* SP-4, *Talaromyces flavus* SP-5, and *Aspergillus oryzae* SP-6) isolated from marine sediments were used for the biosynthesis of silver nanoparticles. The silver nanoparticles synthesized using *Trichoderma gamsii* SP-4 had the maximum antibacterial, antifungal, and antioxidant activity. It was observed that the biosynthesized nanoparticles had a concentration-dependent activity when tested in Hep2 cell line [69].

Table 7.2 summarizes the wide variety of marine microbes that were used for the biosynthesis of metal/metal oxide nanoparticles investigated for anticancer applications.

## 7.4 Biosynthesis of Anticancer Nanoparticles Using Other Marine Sources

The callus extract of the sand dune plant, *Citrullus colocynthis*, was used to synthesize silver nanoparticles, which when tested on human epidermoid larynx carcinoma cells (HEp-2) showed anticancer property with an $IC_{50}$ value of 500 nM [70]. In another study, gold nanoparticles were synthesized using an extract derived from upcycling sea wastes by jellyfish as the reducing agent. The nanoparticles were spherical and triangular in shape and exhibited significant cytotoxicity against HeLa cancer cells through AKT and ERK downregulation but not against normal cells like NIH-3T3 and Raw 264.7 cells [71].

**Table 7.2** Marine microbes used for biosynthesis of anticancer metal/metal oxide nanoparticles

| Marine microorganism | Nanoparticle | Study details and reference |
|---|---|---|
| Cyanobacteria *Gloeocapsa* sp. | Gold nanoparticles | Intracellular synthesis and antitumor activity of spherical and triangular shaped nanoparticles of size less than 100 nm [55] |
| Cyanobacteria *Pseudomonas aeruginosa* | Silver nanoparticles | Biosynthesis followed by antibacterial and anticancer activity of nanoparticles of size 13–76 nm [56] |
| Cyanobacteria *Pseudomonas* sp. | Silver nanoparticles | Biosynthesis and analysis of antibacterial, antifungal, antifouling, antioxidant, and antitumor effect of spherical nanoparticles of size 3–22 nm [57] |
| Actinobacteria *Nocardiopsis* sp. *MBRC-1* | Gold nanoparticles | Biosynthesis and analysis of antimicrobial, antifungal, as well as anticancer activity of nanoparticles of size 45 nm [58] |
| Actinobacteria *Nocardiopsis* sp. *MBRC-48* | Gold nanoparticles | Extracellular biosynthesis and analysis of antimicrobial, antioxidant, and anticancer effects of spherical nanoparticles of size 12 nm [59] |
| Actinobacteria *Streptomyces griseus* | Gold nanoparticles | Biosynthesis and evaluation of antimicrobial and cytotoxic efficacy of nanoparticles [60] |
| Actinobacteria *Streptomyces rochei* MHM13 | Silver nanoparticles | Biosynthesis and analysis of antibacterial, antifouling, and antitumor activities of nanoparticles of size 18–27 nm [61] |
| Actinobacteria *Streptomyces cyaneus* | Gold nanoparticles | Biosynthesis and evaluation of antibacterial, antioxidant, and antitumor activity of spherical nanoparticles of size 6–20 nm [62] |
| Actinobacteria *Streptomyces atrovirens* | Silver nanoparticles | Biomimetic synthesis and cytotoxicity of nanoparticles [63] |
| Actinobacteria *Streptomyces* sp. | Zinc oxide nanoparticles | Biosynthesis and evaluation of antibacterial and anticancer activity of spherical nanoparticles of size 20–50 nm [65] |
| *Enterococcus* sp. | Gold nanoparticles | Biosynthesis and cytotoxicity of spherical nanoparticles of size 6–13 nm [66] |
| | Silver nanoparticles | Extracellular biosynthesis and evaluation of antibacterial and anticancer activity of 10–80-nm-sized spherical nanoparticles [67] |
| *Escherichia coli* (VM1) | Silver nanoparticles | Biosynthesis and cytotoxicity of nanoparticles [68] |
| Fungi *Trichoderma gamsii* SP-4 | Silver nanoparticles | Biosynthesis and evaluation of antibacterial, antifungal, antioxidant, and anticancer activity [69] |

## 7.5 Surface Modification and Biocompatibility of Biosynthesized Nanoparticles

Most of the metal/metal oxide nanoparticles developed via green synthesis have been reported to be nontoxic and biocompatible in normal cell lines, but highly toxic in cancer cell lines. However, a few studies noted an interesting observation that both cancerous and normal cells did not show metal nanoparticle-mediated cytotoxicity. For instance, Patra et al. reported that the silver and gold nanoparticles synthesized using leaf extracts did not show any cytotoxic effect in the range of 0.3–2.5 μM on different cancer and normal cell lines unless conjugated or loaded with an anticancer drug [72]. In another study, the gold nanoparticles synthesized using microbial filtrates were found to be biocompatible when tested for in vitro cytotoxicity on normal 3T3-L1, H9c2, and cancerous HepG2 cell lines in the concentration range of 0.01–1000 μg/mL [73]. Thus, it is possible that the cytotoxicity of biosynthesized nanoparticles would not only depend on the particle size, surface area, and reactivity but also on the source and mechanism of biosynthesis of nanoparticles.

In order to avoid aggregation and impart stability in addition to ensuring biocompatibility of green nanoparticles, it is important to select environment-friendly stabilizing agents and functionalization pathways. Biosynthesis of metallic nanoparticles using natural polysaccharides as stabilizing and reducing agents can be considered as a promising approach in this regard. Metallic precursors are reduced to zerovalent state, followed by the nucleation and nanocrystals growth in a typical bottom-up synthesis. Polysaccharides can be employed as the hosts that combine with guest metallic precursor ions/nanoparticles through noncovalent bonding causing a change in the order of free energy which enables stabilization, morphological control, and kinetic growth of the nanoparticles. The stereogenic centers of polysaccharides also aid in the anchoring resulting in homogeneous and biocompatible nanoparticles [74].

Marine polysaccharides including sulfated polysaccharides from algae, polysaccharides derived from the exoskeleton of marine crustaceans like chitin and chitosan, and exopolysaccharides produced by marine microorganisms have been explored for biosynthesis of nanoparticles as well as imparting biocompatibility, stability, and surface functionality. Chitosan has been widely explored as a reducing agent and a stabilizer in the biosynthesis of metallic nanoparticles, facilitating surface modification and thus improving stability. Chitosan exhibits high biocompatibility and acts as an effective adjuvant permitting efficient interaction and permeation across the cellular membranes. The charge transfer from polar groups present in chitosan aids in the reduction of metal ions, whereas the electrostatic forces between metal ions and the amino groups in chitosan play a vital role in the formation and stabilization of metal nanoparticles [21]. Chitosan-derived polysaccharide solution was used for biosynthesis of silver nanoparticles, which exhibited high antibacterial activities toward both Gram-negative and Gram-positive bacteria and in vitro cytotoxicity via apoptosis against HepG2 (hepatocellular carcinoma), Lu (lung carcinoma), KB (epidermic carcinoma), and MCF-7 (breast carcinoma) cancer cells [75]. In another study, chitosan–silver bionanocomposite

was prepared, and it was observed that chitosan augmented the antimicrobial efficacy of silver nanoparticles [76]. Highly stable cationic chitosan-stabilized gold nanoparticles were also prepared, and the effect of adding tripolyphosphate into chitosan solution on the size and shape of nanoparticles was also studied. Addition of tripolyphosphate resulted in spherical and polygonal gold nanoparticles with a bimodal size distribution [77].

Polysaccharides extracted from marine algae have also been used as biocompatible reducing and stabilizing agents. Laminarin, fucoidan, and alginates are extracted from marine brown algae; carrageenans, agarose, and porphyran are sulfated polysaccharides extracted from red algae, while ulvan is isolated from green algae [21]. Fucoidans have been used for the biosynthesis of metal nanoparticles and utilized for anticancer, antiangiogenic, anti-inflammatory, and drug delivery applications. For instance, biosynthesized silver nanoparticles using seaweed polysaccharide fucoidan were developed and further coated with chitosan to form an electrolyte complex on the surface conferring stability. The developed nanoparticles showed significant microbial inhibition and anticancer activity in human cervical cancer cells (HeLa) [78]. Similarly, fucoidan-mimetic glycopolymer was used for surface modification of gold nanoparticles which conferred selective toxicity of these nanoparticles against human colon cancer cell lines (HCT116) in comparison with mouse fibroblast cell lines (NIH3T3) [79]. Fucoidan was also used as a coating material to prepare stable formulations of poly(isobutylcyanoacrylate) nanoparticles, which were found to be cytotoxic to J774 macrophage and NIH3T3 fibroblast cell lines. Similar fucoidan-coated poly(isobutylcyanoacrylate) core-shell nanoparticles were also used for loading miRNA against cardiovascular diseases [80]. Fucoidan being an anticancer agent itself was reported to show synergistic anticancer and photothermal effects in HeLa, A549, and K562 cells when coated onto copper sulfate nanoparticles via layer-by-layer method [81]. Multifunctional doxorubicin-loaded fucoidan capped gold nanoparticles were also developed for drug delivery and photoacoustic imaging [82].

Carrageenan is another biopolymer obtained from marine red algae that was investigated for the biosynthesis of metal/metal oxide nanoparticles. In situ synthesis and stabilization of magnetite nanoparticles attempted using κ, ι, and λ carrageenans have been reported. The presence of carrageenan resulted in smaller particles and prevented oxidation of the magnetite nanoparticles by determining oxygen diffusion rates through the medium [83]. Carrageenan oligosaccharides have also been employed as a reducing and capping agent to prepare gold nanoparticles, which exhibited significant cytotoxicity in colon (HCT-116) and breast cancer (MDA-MB-231) cells [84]. Porphyran extracted from algae was also used as a reducing agent for one pot, green synthesis of gold nanoparticles, which were then used as a carrier for the delivery of an anticancer drug [85]. In another study, in vitro cytotoxicity and in vivo subacute oral toxicity of gold nanoparticles biosynthesized using the sulfated polysaccharide porphyran were studied. The in vitro cytotoxicity analysis of porphyran-reduced gold nanoparticles in normal monkey kidney cell line revealed their nontoxic nature [86]. Another polysaccharide that was explored for green synthesis is laminarin, a storage compound obtained from the brown alga *Turbinaria*

*ornata*. Silver nanoparticles biosynthesized using laminarin were analyzed for their free radical scavenging activities and cytotoxicity against retinoblastoma Y79 cell lines. These nanoparticles were found to induce apoptosis as evidenced by flow cytometry and DNA fragmentation study [87]. Thus, marine polysaccharides comprise a new class of materials that are highly stable, biocompatible, biodegradable, economical, and abundant. Most of the research involving these polysaccharides is at the laboratory level. After detailed in vivo and clinical evaluations, they can be put to use for large-scale production of bionanoparticles for a host of applications in the biomedical, food, and pharmaceutical industries.

## 7.6 Conclusions

Research in the field of green synthesis of nanomaterials is in a highly investigative phase for a wide variety of applications including therapeutics, drug delivery, biosensors, catalysis, etc. Owing to their inherent biocompatibility and selective toxicity to cancer cells, they have been widely explored for the treatment and diagnosis of cancer; however, their clinical applications are yet to be realized via clinical trials. Marine ecosystem offers abundant resources in terms of marine algae, microorganisms, and polysaccharides, which can be utilized for biosynthesis of nanomaterials. A thorough understanding of the mechanism of biosynthesis and their mode of action in addition to systematic comparison with conventional chemical counterparts is necessary to tailor the size and shape of nanoparticles as well as their intended application. In addition, surface modifications in overcoming key physiological barriers in vivo are also vital in the effective targeting of these nanoparticles to cancer cells. Furthermore, a comprehensive acute and chronic toxicity analysis of these nanoparticles is the need of the hour to establish their safety and rule out any long-term hazards associated with their use.

Currently, green synthesis possesses some limitations in terms of residues of polysaccharides, flavonoids, alkaloids, enzymes, etc., being attached to the nanoparticle surface even after purification. Similarly, contamination by pathogens in case of biosynthesis involving microorganisms could be a concern, and hence, the downstream processing of these nanoparticles also demands attention. Another limitation is the adsorption of protein on the nanoparticle surface or the protein corona effect in biological fluids that defines the nanoparticle–cell interaction. Considering these factors, proper optimization for large-scale industrial biosynthesis of nanoparticles and economic analysis in comparison with the conventionally used chemical methods will result in great strides toward sustainability and environment-friendly research.

## References

1. Pelaz B, Alexiou C, Alvarez-Puebla RA, Alves F, Andrews AM, Ashraf S et al (2017) Diverse applications of nanomedicine. ACS Nano 11(3):2313–2381

2. Patra JK, Das G, Fraceto LF, Campos EVR, Rodriguez-Torres MDP, Acosta-Torres LS et al (2018) Nano based drug delivery systems: recent developments and future prospects. J Nanobiotechnol 16:71
3. Paliwal R, Babu RJ, Palakurthi S (2014) Nanomedicine scale-up technologies: feasibilities and challenges. AAPS PharmSciTech 15(6):1527–1534
4. Patel P, Shah J (2017) Safety and toxicological considerations of nanomedicines: the future directions. Curr Clin Pharmacol 12(2):73–82
5. Viswanath B, Kim S (2017) Influence of nanotoxicity on human health and environment: the alternative strategies. In: de Voogt P (ed) Reviews of environmental contamination and toxicology. Springer, Cham, pp 61–104. https://doi.org/10.1007/398_2016_12
6. Das RK, Pachapur VL, Lonappan L, Naghdi M, Pulicharla R, Maiti S et al (2017) Biological synthesis of metallic nanoparticles: plants, animals and microbial aspects. Nanotechnol Environ Eng 2:18
7. Kumar S, Lather V, Pandita D (2015) Green synthesis of therapeutic nanoparticles: an expanding horizon. Nanomedicine 10(15):2451–2471
8. Kharissova OV, Dias HVR, Kharisov BI, Pérez BO, Pérez VMJ (2013) The greener synthesis of nanoparticles. Trends Biotechnol 31(4):240–248
9. Thakkar KN, Mhatre SS, Parikh RY (2010) Biological synthesis of metallic nanoparticles. Nanomedicine 6(2):257–262
10. Kulkarni N, Muddapur U (2014) Biosynthesis of metal nanoparticles: a review. J Nanotechnol 15:2014
11. Mukherjee P, Ahmad A, Mandal D, Senapati S, Sainkar SR, Khan MI et al (2001) Fungus-mediated synthesis of silver nanoparticles and their immobilization in the mycelial matrix: a novel biological approach to nanoparticle synthesis. Nano Lett 1(10):515–519
12. Salunke BK, Sawant SS, Lee S-I, Kim BS (2016) Microorganisms as efficient biosystem for the synthesis of metal nanoparticles: current scenario and future possibilities. World J Microbiol Biotechnol 32(5):88
13. Cobbett CS (2000) Phytochelatin biosynthesis and function in heavy-metal detoxification. Curr Opin Plant Biol 3(3):211–216
14. Pages D, Rose J, Conrod S, Cuine S, Carrier P, Heulin T et al (2008) Heavy metal tolerance in Stenotrophomonas maltophilia. PLoS One 3(2):e1539
15. Guimarães-Soares L, Pascoal C, Cássio F (2007) Effects of heavy metals on the production of thiol compounds by the aquatic fungi Fontanospora fusiramosa and Flagellospora curta. Ecotoxicol Environ Saf 66(1):36–43
16. Liu F, Kang SH, Lee Y-I, Choa Y, Mulchandani A, Myung NV et al (2010) Enzyme mediated synthesis of phytochelatin-capped CdS nanocrystals. Appl Phys Lett 97(12):123703
17. Asmathunisha N, Kathiresan K (2013) A review on biosynthesis of nanoparticles by marine organisms. Colloids Surf B Biointerfaces 103:283–287
18. Baker S, Harini BP, Rakshith D, Satish S (2013) Marine microbes: invisible nanofactories. J Pharm Res 6(3):383–388
19. Manivasagan P, Nam SY, Oh J (2016) Marine microorganisms as potential biofactories for synthesis of metallic nanoparticles. Crit Rev Microbiol 42(6):1007–1019
20. Vijayan SR, Santhiyagu P, Ramasamy R, Arivalagan P, Kumar G, Ethiraj K et al (2016) Seaweeds: a resource for marine bionanotechnology. Enzyme Microb Technol 95:45–57
21. Manivasagan P, Oh J (2016) Marine polysaccharide-based nanomaterials as a novel source of nanobiotechnological applications. Int J Biol Macromol 82:315–327
22. Patil MP, Kim G-D (2018) Marine microorganisms for synthesis of metallic nanoparticles and their biomedical applications. Colloids Surf B Biointerfaces 172:487–495
23. Akter M, Sikder MT, Rahman MM, Ullah AKMA, Hossain KFB, Banik S et al (2018) A systematic review on silver nanoparticles-induced cytotoxicity: physicochemical properties and perspectives. J Adv Res 9:1–16

24. Fawcett D, Verduin JJ, Shah M, Sharma SB, Poinern GEJ (2017) A review of current research into the biogenic synthesis of metal and metal oxide nanoparticles via marine algae and seagrasses. J Nanosci 2017:15
25. El-Sheekh MM, El-Kassas HY (2016) Algal production of nano-silver and gold: their antimicrobial and cytotoxic activities: a review. J Genet Eng Biotechnol 14(2):299–310
26. Athukorala Y, Kim K-N, Jeon Y-J (2006) Antiproliferative and antioxidant properties of an enzymatic hydrolysate from brown alga, Ecklonia cava. Food Chem Toxicol 44(7):1065–1074
27. Venkatesan J, Kim S-K, Shim MS (2016) Antimicrobial, antioxidant, and anticancer activities of biosynthesized silver nanoparticles using marine algae Ecklonia cava. Nanomaterials (Basel) 6(12):235
28. Khalifa KS, Hamouda RA, Hamza DHA (2016) In vitro antitumor activity of silver nanoparticles biosynthesized by marine algae. Dig J Nanomater Bios 11(1):213–221
29. El Bialy EB, Hamouda RA, Khalifa KS, Hamza DHA (2017) Cytotoxic effect of biosynthesized silver nanoparticles on ehrlich ascites tumor cells in mice. Int J Pharmacol 13(2):134–144
30. Khalifa KS, Hamouda RA, Hamza HA (2016) Antitumor activity of silver nanoparticles biosynthesized by micro algae. J Chem Pharm Res 8(3):1–6
31. Selvi BCG, Madhavan J, Santhanam A (2016) Cytotoxic effect of silver nanoparticles synthesized from Padina tetrastromaticaon breast cancer cell line. Adv Nat Sci Nanosci 7 (3):035015
32. El Kassas HY, Attia AA (2014) Bactericidal application and cytotoxic activity of biosynthesized silver nanoparticles with an extract of the red seaweed Pterocladiella capillacea on the HepG2 cell line. Asian Pac J Cancer Prev 15(3):1299–1306
33. Poornima S, Valivittan K (2015) Synthesis, characterization, antimicrobial activity and anticancerous efficacy (HeLa cell lines) by Gracilaria corticata mediated synthesized silver nanoparticles. Int J Curr Res Multidiscip 1(6):1–18
34. Govindaraju K, Krishnamoorthy K, Alsagaby SA, Singaravelu G, Premanathan M (2015) Green synthesis of silver nanoparticles for selective toxicity towards cancer cells. IET Nanobiotechnol 9(6):325–330
35. Kumar P, Selvi SS, Prabha AL, Rani LM, Suganthi P, Devi BS et al (2012) Antibacterial activity and in vitro cytotoxicity assay against brine shrimp using silver nanoparticles synthesized from Sargassum ilicifolium. Dig J Nanomater Bios 7940:1447–1455
36. Thangaraju N, Venkatalakshmi RP, Chinnasamy A, Kannaiyan P (2012) Synthesis of silver nanoparticles and the antibacterial and anticancer activities of the crude extract of Sargassum polycystum C. Agardh Nano Biomed Eng 4(2):89–94
37. Devi JS, Bhimba BV, Peter DM (2013) Production of biogenic silver nanoparticles using Sargassum longifolium and its applications. Indian J Mar Sci 42(1):125–130
38. Devi JS, Bhimba BV (2012) Silver nanoparticles: antibacterial activity against wound isolates & in vitro cytotoxic activity on Human Caucasian colon adenocarcinoma. Asian Pac J Trop Dis 2:S87–S93
39. Govindaraju K, Basha SK, Kumar VG, Singaravelu G (2008) Silver, gold and bimetallic nanoparticles production using single-cell protein (Spirulina platensis) Geitler. J Mater Sci 43 (15):5115–5122
40. Senapati S, Syed A, Moeez S, Kumar A, Ahmad A (2012) Intracellular synthesis of gold nanoparticles using alga Tetraselmis kochinensis. Mater Lett 79:116–118
41. El-Kassas HY, El-Sheekh MM (2014) Cytotoxic activity of biosynthesized gold nanoparticles with an extract of the red seaweed Corallina officinalis on the MCF-7 human breast cancer cell line. Asian Pac J Cancer Prev 15(10):4311–4317
42. Singh M, Kumar M, Manikandan S, Chandrasekaran N, Mukherjee A, Kumaraguru AK (2014) Drug delivery system for controlled cancer therapy using physico-chemically stabilized bioconjugated gold nanoparticles synthesized from marine macroalgae, Padina gymnospora. J Nanomed Nanotechnol S5:009

43. González-Ballesteros N, Prado-López S, Rodríguez-González JB, Lastra M, Rodríguez-Argüelles MC (2017) Green synthesis of gold nanoparticles using brown algae Cystoseira baccata: its activity in colon cancer cells. Colloids Surf B Biointerfaces 153:190–198
44. Namvar F, Azizi S, Ahmad MB, Shameli K, Mohamad R, Mahdavi M et al (2015) Green synthesis and characterization of gold nanoparticles using the marine macroalgae Sargassum muticum. Res Chem Intermediat 41(8):5723–5730
45. Dhas TS, Kumar VG, Karthick V, Govindaraju K, Shankara Narayana T (2014) Biosynthesis of gold nanoparticles using Sargassum swartzii and its cytotoxicity effect on HeLa cells. Spectrochim Acta A 133:102–106
46. Ajdari Z, Rahman H, Shameli K, Abdullah R, Abd Ghani M, Yeap S et al (2016) Novel gold nanoparticles reduced by Sargassum glaucescens: preparation, characterization and anticancer activity. Molecules 21(3):123–123
47. Nagarajan S, Arumugam Kuppusamy K (2013) Extracellular synthesis of zinc oxide nanoparticle using seaweeds of gulf of Mannar, India. J Nanobiotechnol 11(1):39
48. Namvar F, Rahman HS, Mohamad R, Azizi S, Tahir PM, Chartrand MS et al (2015) Cytotoxic effects of biosynthesized zinc oxide nanoparticles on murine cell lines. Evid Based Complement Alternat Med 2015:593014
49. Sanaeimehr Z, Javadi I, Namvar F (2018) Antiangiogenic and antiapoptotic effects of green-synthesized zinc oxide nanoparticles using Sargassum muticum algae extraction. Cancer Nanotechnol 9(1):3
50. Namvar F, Azizi S, Rahman HS, Mohamad R, Rasedee A, Soltani M et al (2016) Green synthesis, characterization, and anticancer activity of hyaluronan/zinc oxide nanocomposite. Onco Targets Ther 9:4549–4559
51. Namvar F, Rahman HS, Mohamad R, Baharara J, Mahdavi M, Amini E et al (2014) Cytotoxic effect of magnetic iron oxide nanoparticles synthesized via seaweed aqueous extract. Int J Nanomedicine 9:2479–2488
52. Gahlawat G, Choudhury AR (2019) A review on the biosynthesis of metal and metal salt nanoparticles by microbes. RSC Adv 9(23):12944–12967
53. Gunasekaran M (2011) Biosynthesis and characterization of silver nanoparticles using marine cyanobacterium, Oscillatoria willei NTDM01. Dig J Nanomater Biostruct 6(2):385–390
54. Xie J, Lee JY, Wang DIC, Ting YP (2007) Silver nanoplates: from biological to biomimetic synthesis. ACS Nano 1(5):429–439
55. Geetha S, SathakkathulZariya J, Aarthi R, Blessie H (2014) Green synthesis of gold nanoparticle using marine cyanobacteria Gloeocapsa sp and the antitumor potential. J Chem Pharm Sci 4:172–174
56. Ramalingam V, Rajaram R, PremKumar C, Santhanam P, Dhinesh P, Vinothkumar S et al (2014) Biosynthesis of silver nanoparticles from deep sea bacterium Pseudomonas aeruginosa JQ989348 for antimicrobial, antibiofilm, and cytotoxic activity. J Basic Microbiol 54 (9):928–936
57. Hassan WMS, Abd El-latif HH (2018) Characterization and applications of the biosynthesized silver nanoparticles by marine Pseudomonas sp. H64. J Pure Appl Microbiol 12(3):1289–1299
58. Manivasagan P, Venkatesan J, Senthilkumar K, Sivakumar K, Kim S-K (2013) Biosynthesis, antimicrobial and cytotoxic effect of silver nanoparticles using a novel Nocardiopsis sp. MBRC-1. BioMed Res Int 2013:287638
59. Manivasagan P, Alam MS, Kang K-H, Kwak M, Kim S-K (2015) Extracellular synthesis of gold bionanoparticles by Nocardiopsis sp. and evaluation of its antimicrobial, antioxidant and cytotoxic activities. Bioproc Biosys Eng 38(6):1167–1177
60. Hamed M, Abdelftah LS (2019) Biosynthesis of gold nanoparticles using marine Streptomyces griseus isolate (M8) and evaluating its antimicrobial and anticancer activity. Egypt J Aquat Biol Fish 23(1):173–184
61. Abd-Elnaby HM, Abo-Elala GM, Abdel-Raouf UM, Hamed MM (2016) Antibacterial and anticancer activity of extracellular synthesized silver nanoparticles from marine Streptomyces rochei MHM13. Egypt J Aquat Res 42(3):301–312

62. El-Batal AI, Al Tamie MSS (2015) Biosynthesis of gold nanoparticles using Marine Streptomyces cyaneus and their antimicrobial, antioxidant and antitumor (in vitro) activities. J Chem Pharm Res 7(7):1020–1036
63. Subbaiya R, Saravanan M, Priya AR, Shankar KR, Selvam M, Ovais M et al (2017) Biomimetic synthesis of silver nanoparticles from Streptomyces atrovirens and their potential anticancer activity against human breast cancer cells. IET Nanobiotechnol 11(8):965–972
64. Manivasagan P, Oh J (2015) Production of a novel fucoidanase for the green synthesis of gold nanoparticles by Streptomyces sp. and its cytotoxic effect on HeLa cells. Mar Drugs 13 (11):6818–6837
65. Balraj B, Senthilkumar N, Siva C, Krithikadevi R, Julie A, Potheher IV et al (2017) Synthesis and characterization of zinc oxide nanoparticles using marine Streptomyces sp. with its investigations on anticancer and antibacterial activity. Res Chem Intermediat 43(4):2367–2376
66. Rajeshkumar S (2016) Anticancer activity of eco-friendly gold nanoparticles against lung and liver cancer cells. J Genet Eng Biotechnol 14(1):195–202
67. Rajeshkumar S, Malarkodi C, Vanaja M, Annadurai G (2016) Anticancer and enhanced antimicrobial activity of biosynthesizd silver nanoparticles against clinical pathogens. J Mol Struct 1116:165–173
68. Maharani V, Sundaramanickam A, Balasubramanian T (2016) In vitro anticancer activity of silver nanoparticle synthesized by Escherichia coli VM1 isolated from marine sediments of Ennore southeast coast of India. Enzyme Microb Technol 95:146–154
69. Anand Bibin G, Thomas CKN, Prakash S, Kumar CS (2015) Biosynthesis of silver nanoparticles by marine sediment fungi for a dose dependent cytotoxicity against HEp2 cell lines. Biocatal Agric Biotechnol 4(2):150–157
70. Satyavani K, Gurudeeban S, Ramanathan T, Balasubramanian T (2012) Toxicity study of silver nanoparticles synthesized from Suaeda monoica on Hep-2 cell line. Avicenna J Med Biotechnol 4(1):35–39
71. Ahn E-Y, Hwang SJ, Choi M-J, Cho S, Lee H-J, Park Y (2018) Upcycling of jellyfish (Nemopilema nomurai) sea wastes as highly valuable reducing agents for green synthesis of gold nanoparticles and their antitumor and anti-inflammatory activity. Artif Cells Nanomed Biotechnol 46(sup2):1127–1136
72. Patra S, Mukherjee S, Barui AK, Ganguly A, Sreedhar B, Patra CR (2015) Green synthesis, characterization of gold and silver nanoparticles and their potential application for cancer therapeutics. Mater Sci Eng C 53:298–309
73. Kalpana D, Srikanth K, Tirupathi Pichiah PB, Cha YS, Lee YS (2014) Synthesis, characterization and in vitro cytotoxicity of gold nanoparticles using cultural filtrate of low shear modeled microgravity and normal gravity cultured K. pneumoniae. Macromol Res 22(5):487–493
74. Wang C, Gao X, Chen Z, Chen Y, Chen H (2017) Preparation, characterization and application of polysaccharide-based metallic nanoparticles: a review. Polymers 9(12):689
75. Tran HV, Tran LD, Ba CT, Vu HD, Nguyen TN, Pham DG et al (2010) Synthesis, characterization, antibacterial and antiproliferative activities of monodisperse chitosan-based silver nanoparticles. Colloids Surf A Physicochem Eng Asp 360(1):32–40
76. Paulkumar K, Gnanajobitha G, Vanaja M, Pavunraj M, Annadurai G (2017) Green synthesis of silver nanoparticle and silver based chitosan bionanocomposite using stem extract of Saccharum officinarum and assessment of its antibacterial activity. Adv Nat Sci Nanosci 8 (3):035019
77. Huang H, Yang X (2004) Synthesis of chitosan-stabilized gold nanoparticles in the absence/presence of tripolyphosphate. Biomacromolecules 5(6):2340–2346
78. Venkatesan J, Singh SK, Anil S, Kim S-K, Shim MS (2018) Preparation, characterization and biological applications of biosynthesized silver nanoparticles with chitosan-fucoidan coating. Molecules 23(6):1429
79. Tengdelius M, Gurav D, Konradsson P, Påhlsson P, Griffith M, Oommen OP (2015) Synthesis and anticancer properties of fucoidan-mimetic glycopolymer coated gold nanoparticles. Chem Commun 51(40):8532–8535

80. Antunes JC, Benarroch L, Moraes FC, Juenet M, Gross M-S, Aubart M et al (2019) Core-shell polymer-based nanoparticles to deliver MiR-155-5p to endothelial cells. Mol Ther Nucleic Acids 17:210–222. https://doi.org/10.1016/j.omtn.2019.05.016
81. Jang B, Moorthy MS, Manivasagan P, Xu L, Song K, Lee KD et al (2018) Fucoidan-coated CuS nanoparticles for chemo-and photothermal therapy against cancer. Oncotarget 9 (16):12649–12661
82. Manivasagan P, Bharathiraja S, Bui NQ, Jang B, Oh Y-O, Lim IG et al (2016) Doxorubicin-loaded fucoidan capped gold nanoparticles for drug delivery and photoacoustic imaging. Int J Biol Macromol 91:578–588
83. Daniel-da-Silva AL, Trindade T, Goodfellow BJ, Costa BFO, Correia RN, Gil AM (2007) In situ synthesis of magnetite nanoparticles in carrageenan gels. Biomacromolecules 8 (8):2350–2357
84. Chen X, Zhao X, Gao Y, Yin J, Bai M, Wang F (2018) Green synthesis of gold nanoparticles using carrageenan oligosaccharide and their in vitro antitumor activity. Mar Drugs 16(8):277
85. Venkatpurwar V, Shiras A, Pokharkar V (2011) Porphyran capped gold nanoparticles as a novel carrier for delivery of anticancer drug: in vitro cytotoxicity study. Int J Pharm 409(1):314–320
86. Venkatpurwar V, Mali V, Bodhankar S, Pokharkar V (2012) In vitro cytotoxicity and in vivo sub-acute oral toxicity assessment of porphyran reduced gold nanoparticles. Toxicol Environ Chem 94(7):1357–1367
87. Remya RR, Rajasree SRR, Suman TY, Aranganathan L, Gayathri S, Gobalakrishnan M et al (2018) Laminarin based AgNPs using brown seaweed Turbinaria ornata and its induction of apoptosis in human retinoblastoma Y79 cancer cell lines. Mater Res Express 5(3):035403

# Green Synthesis of Nanoparticles and Their Application in Cancer Therapy

8

Valeria De Matteis, Mariafrancesca Cascione, Loris Rizzello, Eva Liatsi-Douvitsa, Azzurra Apriceno, and Rosaria Rinaldi

**Abstract**

Biological systems such as yeasts, fungi, bacteria and plant extracts are recently used as natural sources to synthetize nanoparticles (NPs). These green alternatives to traditional chemical routes have different advantages derived from the use of phytochemicals, carbohydrates and other biomolecules. The possibility to employ organisms as 'chemical factories' using neutral pH and low temperatures makes them a powerful eco-friendly tool to synthetize nanomaterials. In particular, plants are the best candidates for the large-scale biosynthesis of metallic NPs such as silver (Ag NPs) and gold nanoparticles (Au NPs) having unique physicochemical properties particularly suitable in the field of cancer therapy. In this chapter, we carefully analyse the main green methods to synthetize metallic NPs, with a particular focus on the use of plants or their derivatives. The role of nontoxic capping and reducing agents and safe solvents and their influence on the NP formations are investigated, especially regarding their size and shape. Successively, the assessment of their anticancer properties in vitro and in vivo together with a life cycle assessment (LCA) is

V. De Matteis (✉) · M. Cascione · R. Rinaldi
Department of Mathematics and Physics "Ennio De Giorgi", University of Salento, Lecce, Italy
e-mail: valeria.dematteis@unisalento.it

L. Rizzello
Department of Chemistry, University College London (UCL), London, UK

Institute for Bioengineering of Catalonia (IBEC), The Barcelona Institute of Science and Technology, Barcelona, Spain

E. Liatsi-Douvitsa
Department of Chemistry, University College London (UCL), London, UK

A. Apriceno
Institute for Bioengineering of Catalonia (IBEC), The Barcelona Institute of Science and Technology, Barcelona, Spain

© Springer Nature Singapore Pte Ltd. 2020

Q. Saquib et al. (eds.), *Green Synthesis of Nanoparticles: Applications and Prospects*, https://doi.org/10.1007/978-981-15-5179-6_8

discussed. Also, we report some recent examples on how metallic nanoparticles can be used as self-propelling system, an interesting topic pioneering the concept of nano-robot able to respond and move towards specific stimuli. We finally report the use of green and stimuli-responsive polymeric nanovesicles, mainly used in drug delivery applications.

**Keywords**

Green synthesis · Metallic nanoparticles · Liposomes · Polymersomes · Nanobots

## 8.1 Introduction

The unique physicochemical properties of nanoparticles (NPs) due to the large surface area, quantum confinement and high surface energy [1] make them a suitable platform in a large variety of applications ranging from industrial [2] and food [3] to cosmetics [4] and medicine [5]. NPs can be synthetize by different routes, which are physical, chemical or biological following 'top-down' and 'bottom-up' approaches [6]. The first method allows to obtain objects from a bulk material (lithography), while the bottom-up starts from atoms to obtain monodispersed materials with few defects [7].

The common physical methods are evaporation-condensation [8], laser ablation [9], thermal decomposition [10], arc discharge [11] and ultrasonic spray pyrolysis [12] that have the advantage of not using hazardous solvents, but on the other hand, they required expensive and large instrumentations with a consequent energy consumption, heat generation and long times to reach thermal stability [13]. The chemical routes are more suitable to obtain NPs, especially those used in nanomedicine applications where stable, monodispersed NPs with tunable size are required [14]. Chemical reduction [15], microemulsion [16], sonochemical [17], sol-gel [18] and electrochemical synthetic [19] methods are the common chemical routes to obtain NPs; these procedures are low cost, and typically, they require fast steps [20]. However, the use of toxic and hazardous solvents represents a serious problem for potential adverse effects on living organisms and environment [21]. The concept of 'green chemistry' designed by the Environmental Protection Agency (EPA) was applied with the scope to reduce the toxic reagents and to decrease the waste after materials synthesis [22]. In this optic, green nanotechnology is environment-friendly, simple and cost-effective chemical route that did not require expensive equipment; in addition, it is easy to scale up and permit to obtain different kind of NPs [23, 24]. A large number of NPs free from toxic solvents generated with green nanotechnology have successfully been used in various applications [25]. In particular, metallic NPs such as palladium, iron, gold, silver and zinc oxide were quickly synthetized, thanks to the easy reduction of metallic ions in aqueous solutions [26]. The phytocompound-enriched plant extracts (polyphenols, alkaloids, phenolic compounds, polyols, enzymes, proteins and terpenoids) are the principal molecules involved in metal salt reduction from positive oxidation state to zero, which induce NP's achievement in the range of 1–100 nm acting as reducing agent

[27, 28]. The physicochemical properties of NPs (size, shape, surface charge, etc.) are strictly dependent on the extract biomolecules that also influence the reaction speed [29]. In fact, it is observed that the fast reduction of salt allows to obtain small NPs; on the contrary, a slow reaction induces the formation of bigger materials [30]. Indeed, the biological agents work also as capping and stabilizing tolls; in this way, the external addition of these two agents is needless [23].

The green route is usually a one-step procedure; the obtained NPs resulting more stable, thanks to the elimination of some parameters that characterize the 'conventional' routes such as pressure, pH and high temperature [31].

Metallic NPs in solution were first discovered by Faraday, whereas Mie explained their plasmonic properties observing the colour change in NP solution [32]. In addition, these kinds of NPs showed quantum confinement and specific electronic structure [33]. The most common green synthetized metallic NPs are silver NPs (Ag NPs) because of the easy reduction from monovalent $Ag^{+}$ to $Ag^{0}$ [34]; Ag NPs highlight the highest plasmon excitation efficiency [35], and they are mostly used as antibacterial [36] and anticancer tools [37]. Gold nanoparticles (Au NPs) are often applied in many fields, especially in nanomedicine, due to their properties to absorb light in infrared spectrum, making them suitable agents in thermal therapy for cancer treatments [38, 39].

## 8.2 Natural Sources to Synthetize Silver and Gold Nanoparticles (Ag NPs and Au NPs)

In general, the natural sources useful to synthetize NPs can be (Fig. 8.1):

(a) *Bacteria*
(b) *Fungi*
(c) Yeasts and *algae*
(d) Plants

### 8.2.1 Bacteria

*Bacteria* are potential biofactories for NP synthesis, especially for Ag NPs [40]. Depending on the NP localization, the synthesis can be intracellular or extracellular, and the NADH-dependent nitrate reductase enzyme plays an important role in metallic ion reduction [41]. In addition, the presence of amines, carboxylic group and several types of biomolecules stabilizes the NPs, preventing the agglomeration phenomena [42].

*Bacteria* resistant to Ag can accumulate a lot of Ag in the cell wall (c.a. 25 %), suggesting their potential employment in industrial recovery [43].

Ag NPs with different physicochemical properties were synthetized using *Pseudomonas stutzeri* [44], *Bacillus megaterium* [45], *Escherichia coli* [46] and *Klebsiella pneumoniae* [47]. *Staphylococcus aureus* was employed to achieve Ag NPs as

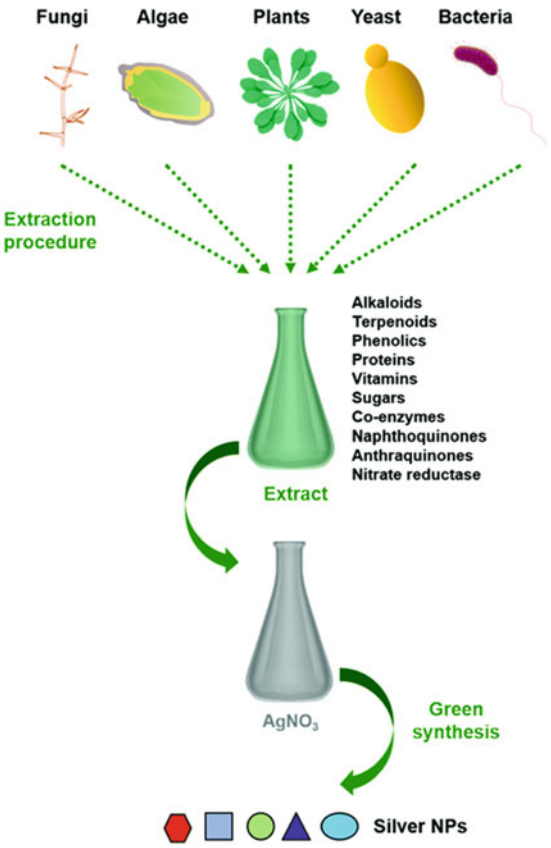


**Fig. 8.1** Schematic green synthesis method to obtain Ag NPs with different physicochemical properties. (Published by The Royal Society of Chemistry [30])

well as *Bacillus licheniformis* [48]. *Enterococcus faecium* was used to synthetize Ag NPs due to its ability in sugar production such as galactose, mannose and glucose contributing in redox reaction [49]. Spherical Au NPs were achieved by *Escherichia coli DH5α* using tetrachloroauric acid ($HAuCl_4$) [50].

### 8.2.2 Fungi

*Fungi* are good living systems for large-scale production of NPs due to the ease and cost efficiency of growth and easy set-up equipment in the laboratory compared to bacteria [51]. *Fungi*-mediated synthesis of NPs can occur by in vivo and in vitro methods. In the in vivo methods, the NPs are synthesized inside the mycelia where the toxic metal ions are internalized [52]; the formation of NPs is more advantageous for mycelia because it reduces the adverse effects induced by ions [53]. In vitro methods were performed using fungal cell-free extracts [54].

The enzyme nitrate reductase in culture filtrate was used in the reduction of $Ag^+$ by *Penicillium fellutanum* [55] as well as *Aspergillus niger* [56] that produced small Ag NPs extracellularly combining the action of reductase enzyme and quinine, which triggered the electron transfer [57]. In addition, the surface of fungus can be a good platform for $Ag^+$ confinement and consequently a suitable surface to obtain Ag NPs overcoming their synthesis in solution [58]. This phenomenon can occur due to the negative charge of carboxylic groups constituting wall proteins that help the Ag nuclei formation [55]. Biomass of *Aspergillus flavus* was used to synthetize spherical Ag NPs (7.13 nm) by Bhangale et al. [59] as well as Vigneshwaran et al. [60] that reported a similar synthesis of NPs with a size of $8.92 \pm 1.61$. Ag NPs and Au NPs can be synthesized by *Fusarium oxysporum* [61], *Aspergillus terreus* [62], *Phanerochaete chrysosporium* [63], *Fusarium solani* [64] [11], *Penicillium fellutanum* [65] and *Epicoccum nigrum* [66].

Molnár et al. [67] used three different routes to achieve AuNPs using extracellular and intracellular fractions and fungi autolysate of 29 thermophilic fungi. The fungi strain and the experimental conditions permit to obtain different sizes of AuNPs. The extract of saprophytic straw mushroom fungus, *Verticillium luteo,* was employed to achieve Au and Ag NPs by extracellular synthetic route [68].

### 8.2.3 Yeast and Algae

In general, the yeast strains are more suitable to synthesize NPs with respect to *bacteria* due to the easiness to control their rapid growth in laboratories using simple nutrients [69]. A lot of studies have been conducted to investigate the synthesis of metallic NPs.

Some yeast like *Schizosaccharomyces pombe* and *Candida glabrata* were used to synthetize Ag NPs and Au NPs [70]. Extracellular synthesis of Ag NPs was performed by a silver-tolerant yeast strain MKY3 [71], using 1 mM of soluble Ag in the log phase of growth obtaining NPs with an average diameter of 2–5 nm. Mourato et al. [72] used extremophilic yeasts isolated from acid mine drainage in Portugal to obtain well-dispersed Ag NPs (20 nm) and AuNPs (20–100 nm) with controlled size and plasmonic properties. The yeast was able to synthetize both metal NPs, but the molecules released are able to reduce only $Ag^+$. Therefore, both NPs were stable, indicating the presence of capping agents on their surface. Using different concentration of $HAuCl_4$ and *Yarrowia lipolytica* cells [73] in log stage of growth was possible to obtain AuNPs and nanoplates: the ratio between metallic salts and cells concentration allowed to achieve different sizes of NPs.

Many studies have reported the use of *algae* to obtain NPs. Small monodispersed Au NPs (5 nm) were obtained using a blue-green alga, *Spirulina platensis*, through a protein-mediated process [74]. *Sargassum wightii*, a brown seaweed, was used to synthetize stable Au NPs with a size ranging from 8 to 12 nm; in addition, the same *alga* was able to form Ag NPs [75].

### 8.2.4 Plants

The synthesis of green NPs, especially Au NPs and Ag NPs, using plants (inactivated plant tissues, plant extracts and living plants) is currently under investigation. The great advantage is to achieve large quantity of nanomaterials with cheap instrumentations and without the use of solvents due to the presence of reducing and capping agents in extracts [76]. The presence of polyphenols in plant extracts and active biomolecules (e.g. vitamins, tannins, proteins, amino acids, enzymes, organic acids and polysaccharides) was responsible for NP formation [77].

### 8.2.5 Living Plants and Biomass

A lot of studies reported the use of plant biomass or part of plants from *Arabidopsis halleri* [78] and *Thlaspi caerulescens* [79] in detoxification and accumulation of heavy metals; these plant properties make them a promising tool for the contaminant removal by an eco-friendly approach. The formation of Au and Ag NPs in *Medicago sativa* plants was demonstrated for the first time by Gardea-Torresdey et al. [80] using the uptake of Au and Ag from solid media. In the case of AuNPs, plants were grown in $AuCl_4^-$ media obtaining NPs in crystalline state and different shapes (cubic and icosahedral NPs).

Rod-shaped AuNPs were achieved by wheat biomass using potassium tetrachloroaurate $K(AuCl_4)$ (0.3 mM) at room temperature and a specific range of pH (2–6) reducing Au (III) to Au (0) obtaining decahedral, hexagonal, tetrahedral, icosahedral and rod-shaped NPs [81].

Decahedral and icosahedral shaped Au NPs were synthetize using *Pelargonium graveolens* leaves exposed to chloroaurate ions ($HAuCl_4$.). The fast reduction of Au ions allowed to obtain NPs having an average size of 20–40 nm after 60 min of reaction [82]. The biomass of *Cinnamomum camphora* leaves with aqueous solution of $AgNO_3$ or $HAuCl_4$ precursors at room temperature was suitable to obtain AgNPs (from 55 to 80 nm) and triangular or spherical AuNPs with the possibility to customize the size tuning the biomass concentration [83]. At the higher concentration of the same biomass (0.5 grams) in the presence of $HAuCl_4$, the shape underwent a transition from triangular to spherical shape of Au NPs. Harris et al. [84] investigated the Ag NPs production by *Brassica juncea* using 1000 ppm of $AgNO_3$ for 72 h that internalized ca. 12.4 wt % of Ag, whereas *Medicago sativa* accumulated 13.6 wt % after 10,000 ppm of $AgNO_3$ for 24 h. In both procedures, roughly spherical Ag NPs with a size of 50 nm were achieved.

### 8.2.6 Plant Extracts

Many researches used plant extracts to obtain metallic NPs and their successive application in many fields. Generally, the addition of plant extracts on $AgNO_3$ aqueous solution induced the reduction of $Ag^+$ [85]. The *Alternanthera dentata*

extracts permitted the rapid synthesis of spherical Ag NPs, having a size less than 100 nm, that exhibited antibacterial activity [86]. Smaller Ag NPs (15–50 nm) were achieved by Krishnaraj et al. [87] from *Acalypha indica* as well as those obtained from orange peel (*Citrus sinensis*) with a size of 6 nm [88]. Olive leaf extracts from *Olea europaea* were used to obtain Ag NPs observing that an increase of pH and temperature allowed to obtain spherical Ag NPs (20–25 nm) with a strong antibacterial ability against *Staphylococcus aureus*, *Pseudomonas aeruginosa* and *Escherichia coli* [89]. Similar size range was obtained using *Coffea arabica* seed extract in the presence of $AgNO_3$ [90]. Shankar et al. [91] synthetized bimetallic core-shell NPs Au/Ag by simultaneous reduction of aqueous $Ag^+$ and $AuCl_4^-$ by *Azadirachta indica* broth. The obtained Ag NPs were polydispersed and spherical, with a diameter of 5–35 nm, whereas the Au NPs showed planar structures with, in most cases, triangular shape.

Recently, good Au NPs were obtained using aqueous solution of *Sansevieria roxburghiana* leaf extract in the presence of $HAuCl_4$ (2 mM) at low reaction temperature (40 °C). The authors achieved different shapes of NPs (spherical, triangular, hexagonal, rod and decahedral) that were useful to degrade organic pollutants such as 4-nitrophenol, acridine orange, congo red, bromothymol blue, phenol red and methylene blue [92]. Boomi et al. [93] obtained different sizes of AuNPs from *Coleus aromaticus* leaf extract at three different temperatures (30 °C, 60 °C and 100 °C) in order to apply them in cotton fabric showing UV protection and cytotoxic effects on human liver cancer (HepG2) cell lines.

Kasthuri et al. [94] used *Lawsonia inermis* (henna) to produce anisotropic Au and quasi-spherical Ag NPs exploiting the high concentration of apiin, a flavonoid that enriched this plant. The apiin is characterized by hydroxyl and carbonyl groups that not only acted as reducing agents of metal salts but also functionalized the NP surface contributing to make them stable up to 3 months. Ag NPs with a size between 15 and 500 nm were achieved by *Pinus densiflora*, *Diospyros kaki*, *Ginkgo biloba*, *Magnolia kobus* and *Platanus orientalis* [95]. The authors obtained Au NPs from *Magnolia kobus* and *Diospyros kaki* extracts having a size of 5–300 nm at different shape within a few minutes and a reaction temperature of 95 °C. In this work, it was demonstrated that an increase of temperature allowed a faster rate of NP production and, at the same time, a reduction of NP size. AuNPs from *Magnolia kobus* extract were analysed by Fourier-transform infrared spectroscopy (FTIR), which shows peaks related to metabolites and proteins that were absorbed on NP surface. Jafarizad et al. [96] used *Mentha* and *Pelargonium* plant extracts to achieve Au NPs. Prior, the authors conducted gas chromatography–mass spectrometry (GC-MS) analysis on extracts to define the components and found isoeugenol and spathulenol in *Mentha* extract and phenolic acids, tannins and flavonoids in *Pelargonium:* these molecules represented the reducing agents due to their hydroxyl functional groups. The effect of NP stabilization was also verified by the presence of C=C bonds in monoterpene and sesquiterpene and carboxylic groups. Ag NPs (60–80 nm) were obtained using callus extract of *Carica papaya*; also in this case, active biomolecules and proteins acted as suitable tools for the synthesis and stabilization of NPs [97]. Eya et al. [98] obtained Ag NPs from *Stachytarpheta*

*cayennensis*, a ligneous weed abundant in saponins, carbohydrates, flavonoids and terpenoids. The NPs obtained within 5 min were characterized by the presence of pure Ag and AgCl nanocrystallites, with an average diameter of 13 nm and 20 nm for Ag and AgCl, respectively. In addition, a lot of natural and synthetic polymers (PEG, PVA, starch, chitosan, sodium alginate, gum acacia) were able to reduce metallic ions in solution [23]. Spherical and monodisperse Ag NPs with a size of 3 nm were obtained using *Gum kondagogu* (a polysaccharide derived from *Cochlospermum gossypium*): its hydroxyl and carboxylate chemical groups were involved in the synthesis of Ag NPs [99].

In all the synthetic routes described above, two steps (nucleation and growth) were verified: the manipulation of these opens new scenario to obtain customized NPs in terms of size, morphology and surface charge. In this way, capping and reducing agents together with the reaction solvent play an important role to obtain monodispersed green NPs [100].

## 8.3 Green Capping Agents

Capping agents were used to stabilize colloidal NPs due to their ability to control size and shape/morphology and to protect the surface from agglomeration phenomena. In the colloidal chemical routes, many kinds of capping agents such as polyethylenimine (PEI), cetyl trimethylammonium bromide (CTAB), polyethylene glycol (PEG), oleic acid (OA), polyvinylpyrrolidone (PVP) and polyvinyl alcohol (PVA) were used: in most cases, they were toxic due to their corrosive, irritant and harmful nature. In addition, these agents were environmentally and economically unfavourable [23].

Biomolecules are biocompatible and environment-friendly with respect to typical capping agent, and in addition, their molecular recognition properties make them optimal tools to control the morphology of NPs [101]. Biomolecules such as proteins and peptides as capping agents were adsorbed in the NP formation process affecting the reaction dynamic and the growth in different directions. In this way, a controllable green synthesis occurred when the capping agent adsorption was adjustable [102]. For example, the pentapeptide cysteine-alanine-leucine-aspargine-aspargine (CALNN) was used by Jia et al. [103] to set up a one-step preparation of peptide-coated Au NPs with tunable size exhibiting good stability. Also small molecules can be used in the green NP synthesis; therefore, their use is subordinated to the presence of organic capping agents that must be cleaned before applications; these limitations make small molecules not completely adapted for green routes [104].

The use of polysaccharides constituting of D-glucose is appropriated in the field of green chemistry due to their solubility in water without any toxic agents and easy purification: this can occur, thanks to the few interactions between the NPs and polysaccharide [105]. The latter presented a double behaviour in the synthetic route because they can be capping agent and reduction agent: AgNPs were obtained by Raveendran et al. [106] using starch as capping and reducing agent preventing $AgNO_3$ from aggregation. The limitation, in this case, was the high temperature of

reaction that required a solubility increase permitting NP formation. However, the complete functionalization of capping agent was obtained using few temperatures. To overcome this restriction, dextran was employed as capping agent due to its high biocompatible nature. Carré-Rangel et al. [107] synthetized Ag NPs by the use of $AgNO_3$ solution enriched with dextrans characterized by different molecular weights acting as stabilizing and reducing agent. NPs achieved were spherical having an average size ranging from 1 to 10 nm.

### 8.3.1 Reducing Agents

Chemical reduction is the most used technique to obtain NPs employing toxic and reactive reducing agents such as hydrazine ($N_2H_4$), formaldehyde and sodium borohydride ($NaBH_4$) [108].

In general, the addition of reducing agents in the reaction solution is superior with respect to the effective stoichiometric requirement; the agent remains in the solution bypassing their activity [23].

Another suitable reagent used for NP synthesis is $H_2$, a cleanest alternative to the agents mentioned above. Albeit its great advantages, its combustibility and high pressure required to work limit its employment in laboratory and industry for safety issues [109]. In this optic, the discovery of new green molecules acting as reducing agents is a new challenge to eliminate hazardous materials substituted by safe alternatives such as polysaccharides (e.g. D-glucose) [110]. These organic molecules having polar nature contain hydroxyl groups that are involved in metal ion reduction; in addition, they do not show adverse effects in living cells [111]. Starch and amylose can be used as reducing agents [112]. In particular, amylose, a polyhydroxylated macromolecule, formed dynamic supramolecular association which led to induce the aggregation, complexation and reduction of ions [113]. Semi-monodispersed Au NPs were obtained by D-glucose with a controlled pH value range that was able to reduce $Au^{3+}$ in a controlled manner [114].

As reported above, the polysaccharides could act as both reducing and capping agents allowing the precursor reduction in order to obtain high controlled NPs. In the case of Au, the plants or plant extract concentration influenced the NP morphology in a strong manner; the growth step was instead managed by pH and reaction temperature [115].

### 8.3.2 Solvents

Solvents play a pivotal role in the synthesis of NPs due to their intrinsic properties to transfer reactants and heat, to dissolve capping and reducing agents and finally to disperse NPs. The most used solvents are organic solvents that are toxic for living organisms emphasizing, at the same time, the problem of environment toxicity and recycling [85].

In addition, the volatility of these compounds increases air pollution and risk for worker exposure: in this contest, the green solvent alternative is actually under investigation.

Starting from the assumption that 'the best solvent is no solvent and if a solvent is needed then water is preferred' [116], water is the most innocuous substance on the planet with non-inflammable nature and high thermal capacity. In addition, it can be used for wide chemical reactions including carbon-carbon bond as well as reductions, oxidations [117] and dehydration reactions [118].

$CO_2$ is studied for its energy-efficient properties (superior to water) and is environment sustainable due to its abundance; it is also achieved from waste materials derived from other processes. Under supercritical phases, $CO_2$ presents a comparable density with the common organic solvents; in addition, the easy tunable $CO_2$ pressure gives great control in terms of selectivity and rate of NP synthesis [119].

Ohde and co-worker [120] synthetized Ag NPs by chemical reduction using supercritical fluid $CO_2$ microemulsion; the formation of the NPs was followed by high-pressure fibre-optic reactor equipped with a CCD array UV–vis spectrometer. The critical step that induces the NP formation was the diffusion and distribution phenomena of the reducing agent oxidized form between the micellar core and supercritical $CO_2$.

Esumi et al. [121] reported the synthesis of $1.0 \pm 0.3$ nm AuNPs in a single phase of $scCO_2$ using triphenylphosphine gold(I) perfluorooctanoate (TPauFO). The NPs obtained were finally dispersed in ethanol.

Another green solvent is represented by supercritical water having a critical temperature of 373 °C and a pressure of 22.1 MPa. Due to its nonpolar feature, this solvent was used to dissolve nonpolar organics and, in a typical hydrothermal route, is obtained in water and is autoclaved [122, 123]. Using this method, the dielectric constant of water has a great effectiveness on solubility, reaction rate and equilibrium which are the factors that influenced the NP synthesis as demonstrated by Sue et al. [124]. They showed the strong dependence of dielectric constant with solubility in metal oxide NP synthesis. Near supercritical point, the authors demonstrated that the solubility of materials was strongly dependent on the variation of dielectric constant. Around supercritical point, the solubility of metal oxide decreased inducing the formation of small-sized nanoparticles.

## 8.4 Life Cycle Assessment (LCA)

Life cycle assessment (LCA) is a helpful tool to measure the potential environmental impacts of nanomaterials during their life cycles [125]. The ISO 14040 (2006) [126, 127] has described the LCA process in four steps [128]:

1. Goal and scope definition
2. Inventory analysis
3. Impact assessment
4. Interpretation

In the case of NPs, they have unique physicochemical properties that are different from conventional materials, and a lot of authors analysed the employment of LCA in nanotechnology field [129, 130]. Moreover, these studies often focused on the NP assessment in input flow parameters such as material, energy and water consumption, but the output flows regarding the distribution in environment were ignored.

The eco-friendly green synthesis with the implementation of biomass was analysed by Sierra et al. [131] that described the impact induced by the green synthesis of Ag NPs achieved by leaf extracts from plants. The authors quantified the inputs and outputs (mass and energy) of the system following the methodology reported in literature. They concluded the study underlining the need of several steps for reaction optimization, in particular the washing step and consequently the need of emission reduction. On the other hand, the green NPs appeared less toxic and biocompatible.

Pati et al. [132] conducted a comparative LCA of Au NP synthesis using three conventional reducing agents and 13 green reducing agents. The embodied energy in Au was responsible for energy footprinting in Au NP synthesis. Consequently, an environment impact can be found also in green route; therefore, these adverse effects were yield and reaction time dependent. The results obtained do not recommend a great method with respect to the other, though the use of plant-derived agents was suitable to achieve Au NPs for biomedical applications. On the contrary, the conventional method permitted to allow greater monodispersion and controlled size than green route. In general, as well as to find green methods suitable for the synthesis of nanomaterials, it is essential to know the life cycle from the beginning to the end of a material. In this way, the use of LCA as a preliminary study before proceeding with the scale-up of a particular procedure could place the foundations for the NP production in a conscious manner.

## 8.5 Anticancer Activity of Green Ag NPs and Au NPs

Nowadays, cancer remains one of the world's main causes of death. Surgical interventions, chemotherapeutic drugs and radiation therapies are the current cancer treatments; nevertheless, these therapeutic approaches are toxic also to healthy cells, increasing side effects on patients [133]. In order to overcome these, the scientific research aims to develop new therapeutic methods, including the use of NPs. Among different kinds of NPs, Au NPs own unique optical properties and electrochemical stability; for this reason, the application of Au NPs in biological and medical fields are widely examined [134]. The extensive use of Au NPs in biomedical applications motivated the development of bio- and green synthesis approach to obtain them, in order to reduce the use of chemical reagents [135].

The cytotoxic effects of green synthetized Au NPs in several cancer cell lines were exploited to test their effectiveness as anticancer tools. Baharara et al. [136] evaluated the in vitro cytotoxic effects induced in human cervical carcinoma cells (HeLa) and bone marrow stromal cells (BMSCs), as normal cells, by green synthetized Au NPs. These NPs were obtained using extracts of *Zataria multiflora*

leaves. The cells were exposed to different concentrations (0–400) μg/mL of Au NPs for 48 h, and using MTT assay, the authors reported cell viability reduction of ~ 50% with respect to the unexposed cells using a concentration of 100 μg/mL of Au NPs. In addition, at the highest concentration, the died cells drastically increased. The exposure to 100 μg/mL of Au NPs, boosted the cellular caspase-3/9 activation in cells respect to the untreated samples.

The results showed the cytotoxic effects on HeLa cells using Au NPs at concentration up to 400 μg/mL. NPs reduced cellular viability in a concentration-dependent manner, activating apoptosis process as demonstrated by fluorescence study. BMSCs underwent similar effects only at the higher NPs concentration tested in the study.

The eco-friendly Au NPs anticancer activity was investigated in three human colorectal cancer cell lines: HT-29, Caco-2, and HCT 116.

In detail, González-Ballesteros et al. [137] achieved Au NPs using brown *alga Cystoseira baccata* showing a significant viability reduction in HT-29 and Caco-2 cell lines after 48 h of NP exposure at different concentrations: 400, 200, 100 and 50 μM. In addition, the apoptosis onset was estimated by flow cytometry using Annexin V-FITC and propidium iodide (PI) in order to characterize the phospholipids distribution and the permeability of the plasma membrane. The authors showed a high percentage of cells in early apoptosis. These phenomenon was more evident in Caco-2 than HT-29 cells, whereas the rate of late apoptosis became higher in HT-29. Moreover, a non-significant % of cells in late apoptosis/necrosis was detected when comparing untreated and treated PSC-201-010 fibroblasts: the latter were used as normal counterpart in this study. After the optimization of one-pot and size-controlled synthesis of diastase-stabilized Au NPs, Maddinedi et al. [138] performed the viability assay on HTC116. They demonstrated a dose dependent toxic effect. These results were confirmed in human liver cancer cell line (HepG2).

Breast adenocarcinoma cell line (MCF-7) and HepG2 cells were used by Muthukumar et al. [139]. They synthetized spherical and triangular shaped Au NPs using plant leaf extracts derived from *Carica papaya* (CP) and *Catharanthus roseus* (CR) and from the combination of these two extracts (CPCRM). The MTT test, conducted on the cells after 24 h of exposure at different concentrations of CP, CR, CPCRM (10, 50, 100, 150 and 250 μg), showed an increase of cell mortality in both cell lines in a dose-dependent manner. Moreover, the 3T3 fibroblast cell line were used to test the bicompatibility of Au NPs (250 μg/mL); rhe results obtained suggested the safety of Au NPs. The green Au NP cytotoxicity was also evaluated in breast cancer cell lines. Hoshyar and colleagues [140] developed a one-step crocin-mediated synthesis of Au NPs examining their anticancer potential on MCF-7 cells, using MTT, LDH and neutral red assays at different concentration of crocin (0–3 mg/mL) at two time points (24 and 48 h). In all cases, the authors reported a reduction in terms of viability and proliferation, concluding that crocin-Au NPs potentially constrain cancer cell proliferation in a time- and dose-dependent manner.

Anticancer impact on triple negative breast cancer cell line (MDA-MB 231) of green synthetized Au NPs by aqueous neem of *Azadirachta indica* fruit extract was evaluated. A Two capping agents, namely monomeric surfactant hexadecyltrimethylammonium chloride (CTAC) and dimeric counterion coupled gemini surfactant (COCOGS) was used [141]. The authors demonstrated that the bio-synthesized Au NPs inhibited cancer cell proliferation through the apoptosis pathways activation triggered by loss of mitochondrial membrane potential and caspases production. These effects were dose dependent (0.4–25 nM), particularly evident using COCOGS Au NPs after 24 h.

Considering that the Au NP treatment on normal 3T3 cells did not affect cellular physiology, the authors concluded that the COCOGS Au NPs could be employed as cancer therapeutic tools. Kajani et al. [142] used aqueous and ethanolic *Taxus baccata* extracts to synthetise green Au NPs. The authors investigated the potential anticancer effects on breast (MCF-7), ovary (Caov-4) and cervix (HeLa) cell lines comparing the results with non-cancerous (fibroblast) cells. In detail, after 48 h and 72 h of Au NPs incubation using several concentrations (2, 4, 8, 16 and 20 μg/mL), the authors quantified the alteration in terms of viability percentage alteration and the caspases activation. The results indicated the cell death trigger by apoptosis and by necrosis in a time and dose dependent manner. In another experimental work [143], the increase of pancreatic cancer cell (PANC-1) disruption following the incubation to 25 μg/mL and 50 μg/mL of green Au NPs derived from the *Scutellaria barbata* after 24 h was reported. The authors reported the dose-dependent down-regulation of Bid and Bcl-2 protein expression and, simultaneously, an up-regulation of Bax and caspase 3/9 compared to control cells. Biosynthesized Au NPs and Ag NPs from *Commelina nudiflora* aqueous leaf extracts were tested by Kuppusamy et al. [144] in colon cancer cell (HTC-116). The exposure of HTC-116 to these NPs induced cell viability reduction using 100 μg/mL and 200 μg/mL after 24 h: the adverse effects were stimulated by up-regulation of pro-apoptotic gene expression (PUMA). Wang et al. [145] achieved a one-step biosynthesis of *Dendropanax* Ag NPs (D-Ag NPs) and *Dendropanax* Au NPs (D-Au NPs) using the crude extract of *D. morbifera Léveille* leaves. The cytotoxicity of D-Ag NPs and D-Au NPs (100 μg/mL) was tested in human keratinocyte cell line (HaCaT) and human lung cancer cell (A549), in terms of viability and nuclear morphology alteration.

All evidences suggested a promising anticancer property of D-Ag NPs, whereas D-Au NPs did not induced cytotoxic effects in HaCaT and A549 cells. Another green synthetic procedure was proposed by Nakkala et al. [146]. The authors used *Gymnema sylvestre* extract as reducing agent to produce Ag NPs (GYAg NPs) and Au NPs (GYAu NPs): these NPs were successively used to expose HeLa derivative (Hep2) cells at different concentrations (10, 30, 60, 90, 120, 150, 180, 210 and 250 μg/mL) up to 24 h in order to investigate their potential anticancer effect. In this study, HaCaT cells were used as health control.

A stronger antiproliferative capability, severe morphological alterations and increased ROS levels were obtained due to Ag NP application in comparison with GYAu NPs; instead, negligible effects were recorded in normal HaCaT cells. Patra

et al. [147] produced b-Au NP and b-Ag NP, using *Butea monosperma* (BM) leaf extracts. b-Au NP and b-Ag NP were biocompatible in normal endothelial cells (HUVEC, ECV-304) as well as cancer cell lines (B16F10, MCF-7, HNGC2, A549) using 4, 10 and 20 μM of NP concentrations. However, b-Au NPs and b-Ag NPs conjugated with doxorubicin (DOXO) at concentration of 0.25 μM, they triggered a drastic inhibition of cancer cell proliferation, with respect to free drug.

After 48 h of exposure, the cell viability decreased when the b-Au-500-DOX and b-Ag-750-DOX concentrations increased, concluding that b-Au-500 and b-Ag-750 could be useful for drug delivery strategies in cancer treatments. Ag NPs (60 μg/mL) obtained from walnut (*Juglans regia* L.) husk extracts were used to test anticancer activity on MCF-7. Authors showed a 40 % of viability reduction, whereas it was less than 20 % in non-cancerous cell line (L-929). Interestingly, commercial Ag NPs used at same concentration (60 μg/mL) induced a viability decrease in MCF-7 [148]. The aqueous extract of *Nepeta deflersiana* plants was used by Al-Sheddi and colleagues [149] to prepare Ag NPs (ND-Ag NPs). The exposure of HeLa cells to Ag NPs (10–50 μg/mL) induced a significant increase of ROS and lipid peroxidation activation; at same time, a reduction of glutathione and metalloproteins levels was showed.

In addition, ND-Ag NPs blocked Sub-G1 cell cycle phase and they activated the apoptotic/necrotic cellular death processes highlighting the potential anticancer effect of ND-Ag NPs on cervical cancer cells. Sreekanth and co-workers [150] evaluated the anti-tumoral effects on cervical cancer cells provoked by green Ag NPs achieved by *Saccharina japonica* extracts. Sulforhodamine B (SRB) assay and 2′,7′-dichlorodihydrofluorescein diacetate (DCFH-DA) assay were performed to quantify cell proliferation and ROS amount. HeLa cells were exposed to 0.001, 0.01, 0.02, 0.04, 0.08, 0.16 and 0.32 mg/mL of AgNPs up to 24 h showing the ROS levels increase and the reduction of cell proliferation. These evidences, along with fluorescent studies, confirmed that Ag NPs induced apoptosis, suggesting further applications in nanomedicine.

The pigment phycocyanin, extracted from *Nostoc linckia*, was used as reducing agent for Ag NPs production. Ag NPs were tested on MCF-7 showing cytotoxic activity due to the cell viability reduction depending on NPs concentration. In human lung fibroblast (WI38) and human amnion (WISH) cell lines (used as controls), no significant cell death was observed. The cytotoxic potential against cancer cells was also confirmed by El-Naggar et al. [151] that performed in vivo studies using albino adult Swiss male mice model. The experimental results demonstrated that Ag NPs administration boosted the loss of cell membrane integrity in Ehrlich ascites carcinoma bearing mice EAC cells, suggesting the possible application of Ag NPs as anticancer tool. The presented results demonstrated the impact of Ag and Au NPs on tumour cells, inducing apoptosis by different metabolic pathways activation (Fig. 8.2). These evidences encourage their involvement in pharmacological strategies aimed to contrast cancer proliferation and, consequently, the metastatic progression. Then, the green synthesis of metallic NPs can be a powerful tool to achieve stable nano-objects without additional toxic risks induced by the presence of chemical reagents usually derived from conventional approaches.

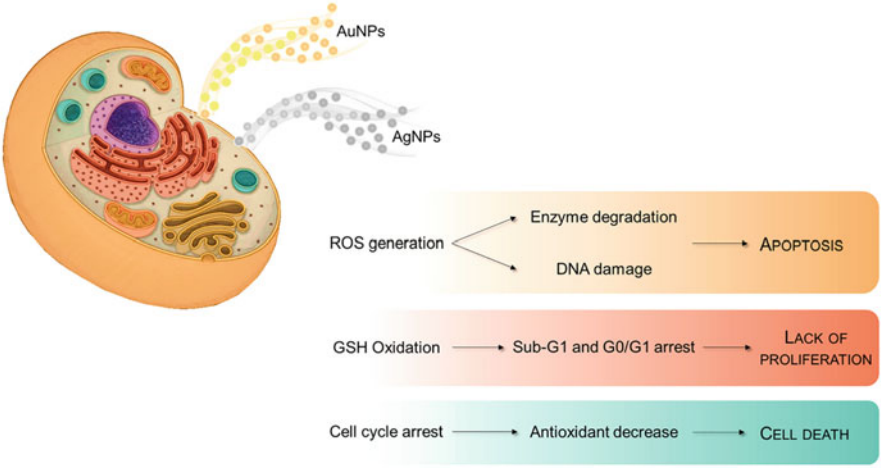


**Fig. 8.2** Schematic representation of cytotoxic effects induced by plasmonic NPs (Ag NPs and Au NPs) in cells

## 8.6 Nanovesicles: Cell-Mimicking Platforms

The metal NPs described in the previous sections represent a perfect tool in applications like plasmonics, imaging or theranostic. In this paragraph, we will introduce a different class of NPs that are based either on polymers, or natural silk-derived proteins, chitosan and DNA. These NPs have one peculiar feature that makes them different from their metallic counterpart. These are vesicles indeed, which means they possess a hollow core where molecules can be entrapped. Historically, the first vesicles successfully used for drug delivery were the liposomes [152], namely, an assembly of natural phospholipids surrounding an aqueous lumen. However, liposomes come with several limitations, often associated with the labile nature of their building blocks. For example, the ability of phospholipids to form vesicles is the direct result of the ratio of hydrophobic and hydrophilic groups. Any modification (e.g. ligand conjugation or PEGylation) will alter this balance, shifting the self-assembly towards micellar structures, hence losing the ability to encapsulate molecules and to successfully deliver their cargo. Moreover, micellar forming amphiphiles have higher critical assembly concentrations, and the assembly integrity is not conserved during the inevitable dilution process following administration in model organisms. That is why liposomes can only be partially modified with essential motifs to enhance in vivo circulation and targeting [153, 154]. Also, the phospholipids lack the ability to control their disassemble upon specific stimuli, and this hinders a correct release upon cell uptake [155, 156].

For several years, scientists and engineers have attempted developing alternatives to liposomes, and several synthetic surrogates have been proposed so far [157–159]. In the last decades, this effort has been combined with polymer science, and

today, we can engineer polymeric vesicles using amphiphilic copolymers. These vesicles, appropriately named as polymersomes (polymer- and -some, from the Greek word which means 'body of'), share the same ability of liposomes to encapsulate and release both water insoluble and soluble drugs [160–162]. Polymersomes have been proposed as a platform for drug delivery systems for the first time since the late 1990s to deliver hydrophilic and/or hydrophobic therapeutic and diagnostic agents. These assemblies are formed by amphiphilic block copolymers, which possess a largely increased chain length over lipids (up to several orders of magnitude). This leads to chain entanglement in their final assemblies, thus ultimately strengthening them. Additionally, these macromolecules exhibit a significantly lower critical aggregation concentration (CAC) over lipids. Therefore, there are virtually no free single block copolymer chains in solution, which could interchange with those forming assembled structures [163]. The rate of single chain exchange between block copolymer assemblies is also defined as ergodicity, meaning that liposomes are ergodic and block copolymer assemblies are non-ergodic [164].

Polymersomes have indeed enhanced stability and chemical versatility of polymer assemblies. As an example, shear viscosity of polymersome membrane was estimated 500 times higher than the one evaluated for lipid membranes [165]. Their relatively robust membrane and colloidal stability, along with a significant biocompatibility and easy ligand conjugation methods, make polymersomes the first candidates for therapeutic drug delivery in cancer clinical treatments. In addition, they represent an optimal choice as imaging tools in non-invasive diagnostic approaches. Figure 8.3 summarizes the features of both liposomes and polymersomes.

However, one of the most important characteristics of polymersomes is their vesicular nature, which means they possess an aqueous core surrounded by a bilayer of amphiphile. This is the same concept as compartmentalization, peculiar characteristics of living systems, which makes them a valid construct for studying proto- or artificial cell systems [166]. Compartmentalization is, in fact, the separation of a cell, or organelle, from its outer environment with a lipid bilayer membrane and is key to life in that it enables complex, multi-step reactions to happen in a highly efficient manner. Polymersomes, because of their characteristics, represent a unique opportunity to mimic the natural cell membrane and design self-assembled systems that begin to exhibit characteristics of life [166]. In an effort to mimic the responsiveness of natural cell membranes, polymersomes have been engineered to exhibit temperature-, pH-, chemical-, and light-responsive behaviour. However, many of them have been assembled starting from synthetic polymers, many of them being either not compatible or not degradable.

In this section of the chapter, we will highlight some different strategies to create efficient delivery vesicles made by natural products, which can represent a good alternative to synthetic polymers. We summarized three main categories, namely, delivery platforms made by silk-derived proteins, chitosan and DNA-origami nanoparticles. The great advantage of these NPs is that they are designed to still preserve some responsiveness (e.g. to pH and temperature) while maintaining a high

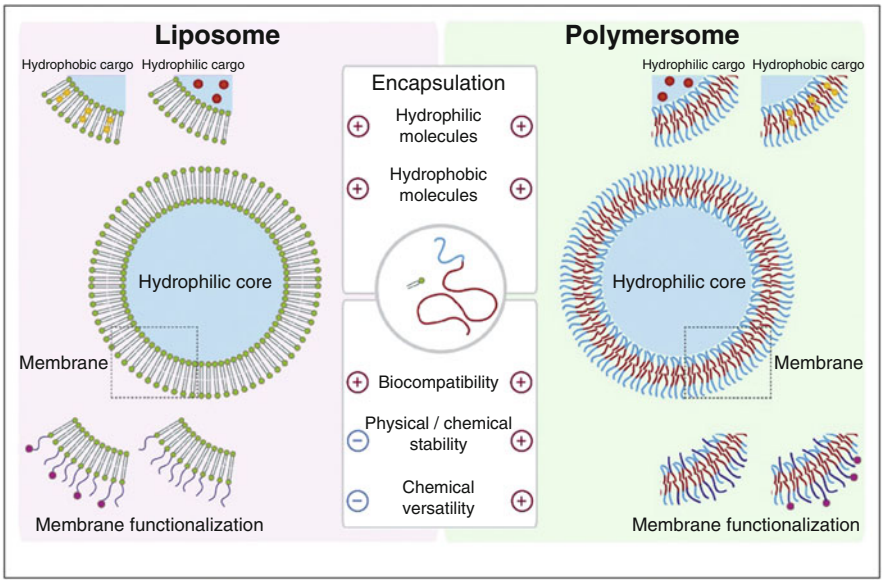


**Fig. 8.3** Schematic representation of liposomes (left) versus polymersomes (right). Polymersomes are synthetic analogues of liposomes, and they comprise amphiphilic block copolymer membrane. While most properties are similar for both carriers, polymersomes exhibit a high versatility and an enhanced stability. (Reprinted from Publication [163] Copyright (2014), with permission from Elsevier)

biocompatibility due to the nature-inspired product they are made of. Inevitably, this also means that their clinical translation can be much easier compared to their polymeric counterpart.

All the NPs discussed in this part belong to the big category of passive nanosystems, which means these NPs passively diffuse within a body upon injection, or alternatively they follow a Brownian random motion in the solvent they are dispersed. Of course, such characteristics is typical of all the NPs produced by the scientific community so far. However, very recently we observed a complete new class of nanovesicles having a new feature, namely, the possibility of self-propelling and move not in Brownian motion, but following a specific trajectory. These are self-propelling nanoparticles, also baptized as 'nanobots' or 'nanoids', and represent indeed the last generation of devices that can move towards or against a flow or gradient of molecules. In the last part of this section, we will describe such a complete new nanosystem that we believe can revolutionize the way we will design the next generation of nanoparticles for biomedical application. Also, in this case, attention will be given to present safe and/or biodegradable systems where the clinical translation can be accomplished.

### 8.6.1 Nature-Inspired Nanovesicles for Drug Delivery: The Best Way to Clinically Translate Lab-Derived Nanotechnologies

We are witnessing a growing trend in the use of NPs, specifically nanovesicles, in potential clinical applications. The scientific literature is indeed full of work claiming how much NPs are ideal candidates for the treatment of a countless number of human diseases. One example is cancer treatment, which has hijacked a lot of attention in an effort to replace the current use of chemotherapies. In 1995, the year when the first cancer nanomedicine, Doxil, was approved by the Food and Drug Administration (FDA), only 23 manuscripts appeared in a PubMed search for 'NPs for cancer' keywords. Now, over 25,000 manuscripts can be found using those same keywords. Based on the clinicaltrials.gov database, a total of 75 cancer nanomedicines are under clinical investigation involving 190 clinical trials [167]. Nevertheless, it is crucial mentioning that according to a very recent survey (August 2019), only 15 NP-based cancer nanomedicine therapies have been successfully translated into real clinical applications [167] despite decades of efforts, claim and huge amount of money invested.

The next question is then: why this unsuccess? What stops cancer (or any other disease) nanomedicine during its journey to success? There are several reasons:

(a) There is an insufficient understanding of NP interactions with biological components. It is established that upon injections all the NPs are prone to be covered during time by plasma proteins—the so called protein corona—that will change the physicochemical properties of the same nano-objects and influence their stability, metabolism, clearance and immune response [168, 169].
(b) A sustainable production of clinical grade NPs with high quality to meet Good Manufacturing Practice standards is another big hurdle for developing nanomedicine.
(c) Despite the formal toxicology evaluations for all products entering clinical trial, toxicity-related clinical failures still occur for NPs. For instance, in 2016, Mirna Therapeutics halted phase 1 trial for MRX34 after one-fifth of patients experienced severe immune-related adverse events [170]. This probably has to do with the fact that we are still lacking proper toxicological evaluation of nanoparticles.
(d) The NPs have very poor pharmacokinetics, which means that most of the injected material is removed by the mononuclear phagocyte system (MPS) within minutes or hours, hindering efficacious, site-specific delivery. This also contributes to the non-specific distribution of nanomaterials in healthy organs [171].
(e) It has been demonstrated that the accumulation in the tumour site is very low. A recent analysis of 117 cancer NP papers from the past 10 years found that only 0.7% of the administered NP is delivered to a solid tumour, presenting a great challenge for cancer nanomedicine [172].
(f) Last, but not least at all, the material used for the production of nanovesicles is produced using synthetic procedures that will hinder their real translation into

the clinic. Alternatively, NPs are made by non-degradable material that will be accumulated within the body and might cause accumulation-related diseases.

With respect to this last point, recent works have focused on adopting green production processes or, even better, green materials to produce nano-delivery systems. One of the most interesting is surely the silk, and one of its main constituent proteins is sericin, because it combines biocompatibility together with no immunogenicity, mechanical strength and ordering. Sericin, one of the two main proteins of silk, has been, for example, employed in the production of tumour-targeting NPs [173]. This biocompatible material, exceptionally rich in functional groups, has been conjugated with the standard chemotherapy based on DOXO. The hydrophilicity of sericin and the hydrophobicity of DOXO allow the conjugate to self-assemble in an aqueous environment. The construct is smartly designed to incorporate a pH-responsive bridge (hydrazone bond) between the protein and the drug. Hence, the system is completely stable during the body circulation at physiological pH, while it only disassembles and releases the DOXO in the acidic lysosomal environment (pH 5) upon tumour cell uptake. Moreover, the conjugate is further coupled to folate, allowing for receptor-mediated endocytosis in folate-receptor positive cancer cells.

Another interesting class is represented by genetically engineered polymers composed of the combination of mechanically unique silk and elastin [174]. These have been demonstrated to have the ability to form nanostructures and to incorporate at the same time model anticancer drugs. As demonstrated, the ratio between the two proteins plays a crucial role on the self-assembly capabilities of these biopolymers. When the elastin concentration become predominant with respect to silk content to the polymer, it exists predominantly free in solution. However, upon an increase of temperature, or the addition of a hydrophobic drug (i.e. doxorubicin), the chains aggregate into micellar conformations. However, evaluated as a drug delivery platform, this micellar nanostructure released a small amount of DOXO only in the presence of proteases. Thus, it appears that the platform would benefit from incorporating pH-sensitive moiety, even though it must be stated that it possesses an important thermal responsiveness.

Another interesting example is represented by thixotropic silk hydrogels which have been evaluated as a platform for the localized delivery of cancer therapeutics [175]. These nanofiber hydrogels self-assemble in a complete green all-aqueous approach. The silk content and the crystallinity of the system can be controlled to achieve a sustainable release of the model drug doxorubicin. These DOXO-loaded hydrogels exhibited pH-dependent drug release, again crucial for the delivery of payloads only upon cell uptake. The great advantage of this system is that it possesses good injectability and showed high DOXO release at pH 4.5 (pH sensitivity) in vitro. Within the first 6 days, free DOXO and DOXO-loaded hydrogels have comparable toxicity, and DOXO-loaded hydrogels inhibited cell growth throughout the incubation (10 days) in vivo.

In addition to silk and its main protein constituent, chitosan has been also proposed as valid constituent for the production of green vesicles for drug delivery.

Chitosan and ATP have been proved to self-assemble into spherical aggregates through electrostatic interactions [176]. Chitosan is both interacting with the negatively charged ATP and forming the positively charged outer hydrophobic corona. The ratio between the polymers and the charges present has been proved to influence the stability of the system. The pH also plays a crucial role in the stability of this system (i.e. at pH 7, it precipitates shortly after assembly). The great advantage of this system is that it is based on an abundant polysaccharide as well as on natural polyelectrolyte ATP (hydrophobic adenine/four negative charges). It is a biocompatible system indeed, it presents pH-dependent stability, and it is enzyme responsive.

A combination of chitosan and silk fibroin has been also used as surface modifiers for liposomes [177]. The resultant liposome had a multilamellar structure and displayed cargo release (calcein) predominantly at pH 6.5–6. The complexation of the modifiers was higher at this pH, and thus, they compressed the liposomal membrane at a higher extent inducing calcein release.

In similar attempts, a drug-polymer conjugate (prodrug) has been proved to form micelles of ~63 nm in aqueous solution [178]. The attachment between chitosan-stearic acid and the model drug (again DOXO) is a disulphide bridge that upon exposure in a reducing environment breaks resulting in drug release. In this case, the advantage of the system is that there is less drug leaking than in the case with physically entrapped cargos. The DOXO and the stearic acid play the role of the hydrophobic block connected to the hydrophilic biopolymer chitosan. The stearic-chitosan polymer is stable as a nanoparticle also when DOXO is not attached. Part of the DOXO is also exposed on the surface of the nanoparticle, while the chitosan monomer has structural similarity with *N*-acetylglucosamine (present in nuclear membranes), and this makes the system a good candidate for nuclear delivery.

A last class of NPs we will be considering here is based on DNA origami, which combines a general biocompatibility together with the possibility of programmable production, as well as precise and accurate responsiveness. One remarkable example is a DNA nano-robot explored for the delivery of cancer therapeutics [179]. This sophisticated construct responds to a specific molecular trigger by altering its conformation from a hollow tube to a flat sheet (origami) exposing its cargo (thrombin). This reordering is driven by the binding of aptamer functionalities to the nucleolin marker present on the tumour endothelial vasculature. These intelligent DNA origami-based systems inhibit the tumour growth by interfering the tumour blood supply through in loco exposure of thrombin.

Another DNA origami capsule has been designed to open and/or close in response to variation of pH. In this example, a Hoogsteen triplex (polypurine-polypyrimidine) is formed at a low pH that holds the capsule together. At a higher pH (i.e. intracellular pH of cancer cells), the capsules open exposing the anchored cargo. Here, Au NPs and horseradish peroxidase (HRP) are used as models. In particular, HRP shows enhanced activity at pH 6.4 (closed state of the capsule)

indicating that the nanocapsule is porous and accessible to small molecules but the entry of larger molecules is hindered.

### 8.6.2 Active and Self-Propelling Nanoparticles: Towards a New Generation of Nanobots

The possibility to customize NP formulations down to a molecular level has interestingly matched fundamental phenomena, like macro- and microorganism survival mechanisms, resulting in ad hoc engineered nano-objects able to reproduce and model biologically relevant events. In order to survive, in fact, *bacteria*, sperm cells and uni- or multicellular organisms need to sense and promptly react to environmental changes [180]. This adaptation process, most of the time, requires the generation of directed movement: most bacterial species move towards nutrients or away from toxins according to different mechanism [181]. This migration towards chemical sources often plays a crucial role in the evolution of many biological processes [182].

The translation of these primary phenomena into artificial nanoscale systems has initiated the concept of active matter. NPs are active when are able to self-propel, thanks to the transformation of external energy into mechanical work that generates oriented motion [183]. The external energy here is intended to have the same role that environmental stimuli have on biological entities like bacteria, and obviously different energy sources (temperature, magnetic fields, adhesion forces, chemical gradients) may drive the migration (thermotaxis, magnetotaxis, haptotaxis, chemotaxis) [184].

The development of such objects capable of self-migration when micro- or nano-dimensions are involved is still challenging, as the physical principles of propulsion are different at very small scales. Brownian effect, in fact, can impact the motility of active nanomotors through the continuous collisions with the solvent molecules as result of thermal fluctuations, randomizing and re-orienting any directionality. Moreover, water behaves like a viscous liquid at the nanoscale, hindering the navigation of very small objects [185]. Under these conditions, a body can self-propel exclusively when the flow field over its surface is perturbed. This state is achieved by imposing boundary conditions like altering the body shape to displace the fluid around (swimmers) or generating a gradient that results in a phoretic slip velocity (squirmers) [186].

In the former case, the object performs a non-reciprocal movement [186], and in this sense, nature offers several examples of this resolution such as providing prokaryotes and eukaryotes with designated appendices and protrusions [187, 188] (Fig. 8.4a, b). Common bacteria like *Escherichia coli*, in fact, achieve propulsion by non-time-reversible motion of long flagella, and this asymmetric shape of the body is fundamental to generate the motion in a desired direction [189]. This strategy has been rather considered for the design of artificial nano-swimmers, and several studies have indicated their potentiality for biological and biomedical applications [190]. Schwarz et al. [191] proposed the design of metal-coated polymer magnetic

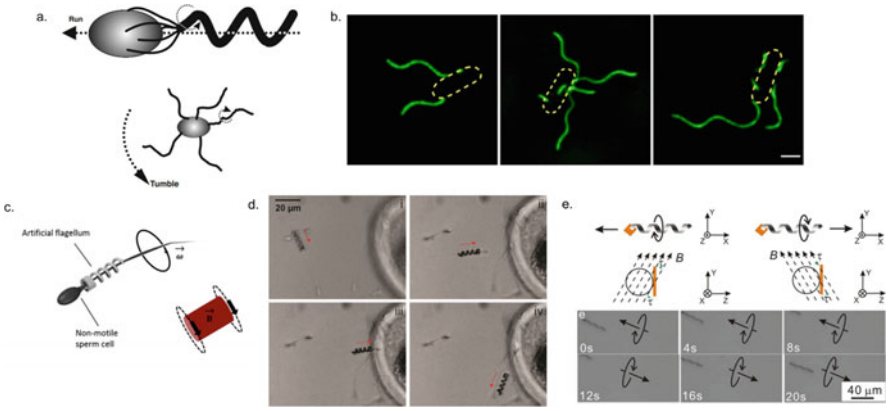


**Fig. 8.4** Micro- and nano-object self-propulsion (or swimming) through body shape alteration. Schematic representation (**a**) and representative super-resolution fluorescent images (**b**) of *E. coli* flagella. *E. coli* bacteria swim by rotating their five flagella anticlockwise; a clockwise inversion of the flagella rotational direction breaks the bundle and leads the tumbling. (Figure **a** reprinted (adapted) with permission from [184] Copyright (2018) American Chemical Society. Figure **b** adapted from [188]). Schematic representation (**c**) and video frames (**d**) of magnetic microhelices that assist the capture and the delivery of a sperm cell to the oocyte. (Figure **c** reprinted from [191] with the permission of AIP Publishing. Figure **d** reprinted (adapted) from [192] Copyright (2016) American Chemical Society). (**e**) Control of a left-handed artificial bacterial flagella motion forward and backward through a magnetic field with a strength of 2.0 mT. (Reprinted from [193] with the permission of AIP Publishing)

microhelices through Direct Laser Writing for the synthesis of effective spermbots. The helix navigation could be easily controlled in fluidic channels where the physiological environment was recreated, and, more surprisingly, the ability to capture, transport and deliver sperm cells to the oocyte was reported (Fig. 8.4c, d) [191, 192].

Artificial bacterial flagella (ABF) functionalized with plasmid DNA (pDNA)-loaded lipoplexes have concurrently showed to perform single-cell gene delivery in vitro to human embryonic kidney (HEK 293) [194]. Here, the accurate control of micro-motor propulsion with micrometer precision in 3D is essentially tuned by biocompatible magnetic fields. Specifically, ABF always have a magnetic portion; thus, when the orientation of the applied rotating magnetic field varies, the magnetic moment of the motors undergoes magnetic restoring torque and tends to align with the current field resulting in the rotation of the magnetic part. The helical or tail, consequently, spins or oscillates leading to the propulsion [193, 195] (Fig. 8.4e). Furthermore, hybrid nanowire motors provided with flexible filaments have emerged as self-propelling systems [196]. Gao et al. [197] reported the synthesis of a flexible multisegment Pt-Au-Agflex-Ni with Pt-Au and Au-Agflex moieties responsible for the catalytic and magnetic propulsions, respectively.

Autonomous propulsion has been successfully imparted on nano-objects through alteration of their local environment with the generation of gradients, a concept very well-known as phoretic transport. Phoresis generally refers to the motion of particles due to short-range interactions with a local gradient that can generate fluid motion at

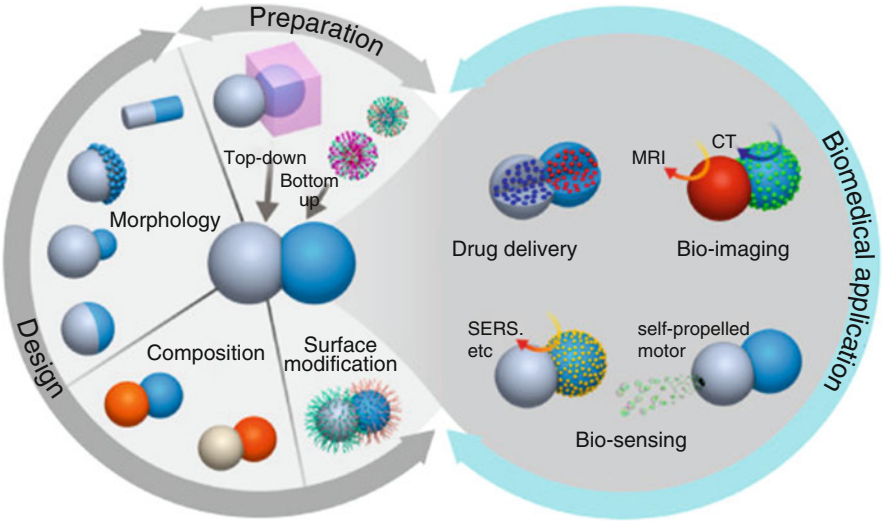


**Fig. 8.5** Design, synthesis and biomedical application of Janus particles. (Reprinted from [212], Copyright (2019), with permission from Elsevier)

the particle surface [198]. When the particles are able to produce these gradients by themselves, phoretic effects can create self-propelled motion [199]. In this circumstance, a gradient is generated in an asymmetric manner, e.g. through chemical surface reactions or by emitting or absorbing heat, producing consequently an asymmetric concentration field near the particle, which results in a surface slip flow. This flow provides hydrodynamic stress necessary to overcome viscous resistance and induce propulsion [200].

As a certain level of asymmetry is required to get propulsion, the final object configuration has been extensively investigated through the modification of material composition and/or alteration of surface and shape profile [200, 201].

So far, a great number of studies have reported the development of self-propelling NPs with different geometric forms (e.g. rods [202] and sphere [203]), different propulsion mechanisms (e.g. bubble propulsion [204] or self-phoresis [205]), different material compositions and different surface functionalization (e.g. Janus [206] or enzyme-powered particles [207]) and different activating gradients (e.g. chemical [208], temperature [209] (Fig. 8.2i), magnetic [210] and light gradients [211]).

Janus particles (JPs) are a perfect example to understand how asymmetry is fundamental to achieve self-propulsion. The application of JPs in the biomedical field is explored such as drug delivery, bio-imaging and bio-sensing. These particles are composed of two or more elements that differ in their chemical or physical properties and that can selectively and specifically interact with the surroundings generating the force necessary for the navigation [212] (Fig. 8.5).

The concrete use of autonomous NPs has found in biomedicine the best application to invest efforts in [196, 213, 214], thanks to their combination with

biodegradable and biocompatible polymeric materials [215] and the ability for some of them of self-destruction after the completion of their task through disassembling into safe products [216].

The first example of nanomotors used to deliver drug carriers was published as proof of concept in 2010 by Kagan et al. [217]. As previously reported with the delivery of polystyrene NPs [218], self-propelled Au-PT bimetallic rods, powered with hydrogen peroxide, have proved to load, transport and release poly-D,L-lactic-co-glycolic acid (PLGA) biodegradable polymeric particles and liposomes containing doxorubicin. The cargo was captured, thanks to a weak magnetic attraction between the motor nickel portion and the iron oxide encapsulated within PLGA, while a fast change in the direction of the nanowire permitted the payload release, since the drag force imposed on the NP overcome the magnetic attraction. In 2015, the first artificial poly(3,4-ethylenedioxythiophene) (PEDOT)/zinc (Zn)-based micro-wire has been tested in vivo using an acid-driven propulsion into the stomach that allowed an enhanced binding and retention of the motors [219]. Among the various chemical reactions used to fuel nanomotors, enzymatic-driven catalysis became one of the most interesting alternatives to induce self-propulsion, thanks to the fuel biocompatibility, bioavailability and versatility [220]. Interacting with a specific substrate to form products, enzyme diffusive behaviour increases in a substrate concentration-dependent manner, and the transformation of chemical energy into mechanical work generates forces comparable to that characteristic of motor protein [221]. A very interesting analysis has been recently proposed disclosing how the navigation of micro- and nanomotors propelled through enzymatic asymmetrically distributed reactions is regulated by several factors: the size and shape of the motors, the enzyme distribution that, in turn, determines the motion dynamics (enhanced diffusion or ballistic motion for particles in the nanometers or micrometers range, respectively) and the intrinsic biochemical properties of the enzyme [220]. Even though the mechanisms behind this diffusion enhancement are still not fully understood and different possible hypotheses have been suggested [207], powering the nano-motors with enzymatic reactions has shown successful tumour targeting. Hortelao et al. recently reported the synthesis of pristine mesoporous silica NPs (MSNs) coated with polyethylene glycol (PEG) and functionalized with anti-FGFR3 antibody that penetrate bladder cancer spheroids, thanks to urease catalytic reaction [222]. The presence of the enzyme and the antibody improved spheroids internalization by three- and fourfold, respectively, when compared with the bare mesoporous particles and prevented cancer cell proliferation. Besides chemical reactions, other sources have been used to power synthetic machines. A temperature-sensitive poly(N-isopropylacrylamide) (PNIPAM) polymer brush was chemically grown onto bowl-shaped polymeric vesicles, known as stomatocytes, used to entrap platinum NPs (PtNPs) [209]. The polymer brush here worked as a controlling valve, thanks to the lower critical solution temperature (LCST) above which the brushes collapsed and formed a hydrophobic layer on the opening of the stomatocyte. In this way, with the variation of the external temperature, the aperture was opened or closed accordingly, preventing the hydrogen peroxide to react with the platinum and, consequently, stopping the movement.

The development of artificial motors at very small scales able to sense locally the environmental changes and regulate their navigation as function of these variations is a notable step forward in the current research and particularly in the biomedical scenario. A lot of engineered systems present incredible performances in targeted therapy and drug delivery. However, the complete characterization of these systems in more complex environment and full comprehension of their mechanisms are challenges that remain still open.

## References


1. Gatoo MA, Naseem S, Arfat MY, Dar AM, Qasim K, Zubair S (2014) Physicochemical properties of nanomaterials: implication in associated toxic manifestations. Biomed Res Int 2014:1
2. Stark WJ, Stoessel PR, Wohlleben W, Hafner A (2015) Industrial applications of nanoparticles. Chem Soc Rev 44:5793–5805
3. Xu L, Liu Y, Bai R, Chen C (2010) Applications and toxicological issues surrounding nanotechnology in the food industry. Pure Appl Chem 82(2):349–372
4. Raj S, Jose S, Sabitha M (2012) Nanotechnology in cosmetics: opportunities and challenges. J Pharm Bioallied Sci 4(3):186–193
5. Marzo JL, Jornet JM, Pierobon M (2019) Nanotechnology derived nanotools in biomedical perspectives: an update. Curr Drug Targets 20(8):800–807
6. Wang Y, Xia Y (2004) Bottom-up and top-down approaches to the synthesis of monodispersed spherical colloids of low melting-point metals. Nano Lett 4(10):2047–2050
7. Iqbal P, Preece JA, Mendes PM (2012) Nanotechnology: the "top-down" and "bottom-up" approaches. In: Gale PA, Steed JW (eds) Supramolecular chemistry.
8. Wolfrum C, Peukert W (2012) Experimental study of metal nanoparticle synthesis by an arc evaporation/condensation process. J Nanopart Res 14:1–16
9. Amendola V, Meneghetti M (2009) Laser ablation synthesis in solution and size manipulation of noble metal nanoparticles. Phys Chem Chem Phys 11:3805–3821
10. Odularu AT (2018) Metal nanoparticles: thermal decomposition, biomedicinal applications to cancer treatment, and future perspectives. Bioinorg Chem Appl 2018:Article ID 9354708
11. Chaitoglou S, Sanaee MR, Bertran E (2014) Arc-discharge synthesis of iron encapsulated in carbon nanoparticles for biomedical applications. J Nanomater 2014:1
12. Tsai SC, Song YL, Tsai CS et al (2004) Ultrasonic spray pyrolysis for nanoparticles. J Mater Sci 3(9):3647–3657
13. De Matteis V, Cascione M, Toma CC, Leporatti S (2018) Silver nanoparticles: synthetic routes, in vitro toxicity and theranostic applications for cancer disease. Nanomaterials 8(5):pii: E319
14. Zhang XF, Liu ZG, Shen WGS (2016) Silver nanoparticles: synthesis, characterization, properties, applications, and therapeutic approaches. Int J Mol Sci 13(17):9
15. Kim S-W, Chung H-E, Kwon J-H, Yoon H-G, Kim W (2010) Facile synthesis of silver chloride nanocubes and their derivatives. Bull Kor Chem Soc 31(10):2918–2922
16. Viger ML, Live LS, Therrien OD, Boudreau D (2008) Reduction of self-quenching in fluorescent silica-coated silver nanoparticles. Plasmonics 3(1):33–40
17. Guo W, Lin Z, Wang X, Song G (2003) Sonochemical synthesis of nanocrystalline $TiO_2$ by hydrolysis of titanium alkoxides. Microelectr Eng 66:95–101
18. Rahman IA, Padavettan V (2012) Synthesis of silica nanoparticles by sol-gel: size-dependent properties, surface modification, and applications in silica-polymer nanocomposites—a review. J Nanomater 2012:1

19. Rodrıguez-Sanchez L, Blanco MC, López-Quintela MA (2000) Electrochemical synthesis of silver nanoparticles. J Phys Chem B 104:9683–9688
20. Heuer-Jungemann A, Feliu N, Bakaimi I, Hamaly M, Alkilany A, Chakraborty I, Masood A, Casula MF, Kostopoulou A, Eunkeu O, Susumu K, Stewart MH, Medintz IL, Stratakis E, Parak WJ, Kanaras AG (2019) The role of ligands in the chemical synthesis and applications of inorganic nanoparticles. Chem Rev 119(8):4819–4880
21. Farooqi ZH, Khalid R, Begum R, Farooq U, Wu Q, Wu W et al (2019) Facile synthesis of silver nanoparticles in a crosslinked polymeric system by in situ reduction method for catalytic reduction of 4-nitroaniline. Environ Technol 40(15):2027–2036
22. Collins TJ (1997) Green chemistry. In: Macmillan encyclopedia of chemistry. Simon and Schuster, Macmillan, New York, pp 691–697
23. Duan H, Wang D, Li Y (2015) Green chemistry for nanoparticle synthesis. Chem Soc Rev 44:5778–5792
24. Jime VM (2013) The greener synthesis of nanoparticles. Trends Biotechnol 31(4):240–248
25. Singh J, Dutta T, Kim K-H, Rawat M, Samddar P, Kumar P (2018) Green' synthesis of metals and their oxide nanoparticles: applications for environmental remediation. J Nanobiotechnol 16:84
26. Shah M, Fawcett D, Sharma S, Tripathy SK (2015) Green synthesis of metallic nanoparticles via biological entities. Materials (Basel) 8(11):7278–7308
27. Gopisetty MK, Szerencsés B (2018) Biosynthesized silver and gold nanoparticles are potent antimycotics against opportunistic pathogenic yeasts and dermatophytes. Int J Nanomedicine 13:695–703
28. Dauthal P, Mukhopadhyay M (2016) Noble metal nanoparticles: plant-mediated synthesis, mechanistic aspects of synthesis, and applications. Ind Eng Chem Res 55(36):9557–9577
29. Limo MJ, Sola-rabada A, Boix E, Thota V, Westcott ZC, Puddu V et al (2018) Interactions between metal oxides and biomolecules: from fundamental understanding to applications. Chem Rev 118:11118–11193
30. Roy A, Bulut O, Some S, Mandal AK, Yilmaz MD (2019) Green synthesis of silver nanoparticles: biomolecule-nanoparticle organizations targeting antimicrobial activity. RSC Adv 9:2673–2702
31. Pal G, Rai P, Pandey A (2019) Green synthesis of nanoparticles: a greener approach for a cleaner future [Internet]. Green synthesis, characterization and applications of nanoparticles. Elsevier Inc. pp 1–26. https://doi.org/10.1016/B978-0-08-102579-6.00001-0
32. Daniel M, Astruc D (2004) Gold nanoparticles: assembly, supramolecular chemistry, quantum-size-related properties, and applications toward biology, catalysis, and nanotechnology. Chem Rev 104:293–346
33. Lue J (2001) A review of characterization and physical property studies of metallic nanoparticles. J Phys Chem Solids 62:1599–1612
34. Dargo H, Ayaliew A, Kassa H (2017) Synthesis paradigm and applications of silver nanoparticles (AgNPs ): a review. Sustain Mater Technol 13:18–23. https://doi.org/10.1016/j.susmat.2017.08.001
35. Mlalila NG, Swai HS, Hilonga A, Kadam DM (2016) Antimicrobial dependence of silver nanoparticles on surface plasmon resonance bands against Escherichia coli. Nanotechnol Sci Appl 10:1–9
36. Rizzello L, Pompa PP (2014) Nanosilver-based antibacterial drugs and devices: mechanisms, methodological drawbacks, and guidelines. Chem Soc Rev 43:1501–1518
37. De Matteis V, Cascione M, Toma CC, Leporatti S (2018) Morphomechanical and organelle perturbation induced by silver nanoparticle exposure. J Nanoparticle Res 20(10):14
38. De Matteis V, Cascione M, Cristina C, Rinaldi R (2019) Engineered gold nanoshells killing tumor cells: new perspectives. Curr Pharm Des 25:1–13
39. Huang X, El-sayed MA (2015) Plasmonic photo-thermal therapy (PPTT). Alexandria J Med 47(1):1–9

40. Iravani S (2018) Bacteria in nanoparticle synthesis: current status and future prospects. Int Sch Res Not, Article ID 359316, 18 p
41. Rafique M, Sadaf I, Rafique MS, Tahir M (2017) A review on green synthesis of silver nanoparticles and their applications. Artif Cells Nanomed Biotechnol 45(7):1272–1291
42. Hulkoti NI, Taranath TC (2014) Biosynthesis of nanoparticles using microbes—a review. Colloids Surf B Biointerfaces 121:474–483
43. Pooley FD (1982) Bacteria accumulate silver during leaching of sulphide ore minerals. Nature 296:642–643
44. Prabhu S, Poulose EK (2012) Silver nanoparticles: mechanism of antimicrobial action, synthesis, medical applications, and toxicity effects. Int Nano Lett 2:32
45. Saravanan M, Vemu AK, Barik SK (2011) Rapid biosynthesis of silver nanoparticles from Bacillus megaterium (NCIM 2326) and their antibacterial activity on multi drug resistant clinical pathogens. Colloids Surf B Biointerfaces 1(88):325–331
46. Nanda A, Saravanan M (2009) Biosynthesis of silver nanoparticles from Staphylococcus aureus and its antimicrobial activity against MRSA and MRSE. Nanomedicine 5:452–456
47. Malarkodi C, Rajeshkumar S, Vanaja M, Paulkumar K (2013) Eco-friendly synthesis and characterization of gold nanoparticles using Klebsiella pneumoniae. J Nanostruct Chem 3 (30):1–7
48. El-Shanshoury AE-RR, ElSilk SE, Ebeid M (2011) Extracellular biosynthesis of silver nanoparticles using Escherichia coli ATCC 8739, Bacillus subtilis ATCC 6633, and Streptococcus thermophilus Esh1 and their antimicrobial activities. ISRN Nanotechnol 2011:Article ID 385480
49. Saravanan C, Rajesh R, Kaviarasan T, Muthukumar K, Kavitake D, Shetty PH (2017) Synthesis of silver nanoparticles using bacterial exopolysaccharide and its application for degradation of azo-dyes. Biotechnol Reports. 15:33–40
50. Du L, Jiang H, Liu X, Wang E (2007) Biosynthesis of gold nanoparticles assisted by Escherichia coli DH5α and its application on direct electrochemistry of hemoglobin. Electrochem Commun 9(5):1165–1170
51. Molnár Z, Bódai V, Szakacs G, Erdélyi B, Fogarassy Z (2018) Green synthesis of gold nanoparticles by thermophilic filamentous fungi. Sci Rep 3943:1–12
52. El-Sonbaty SM (2013) Fungus-mediated synthesis of silver nanoparticles and evaluation of antitumor activity. Cancer Nano 4:73–79
53. Siddiqi KS, Husen A (2016) Fabrication of metal nanoparticles from fungi and metal salts: scope and application. Nanoscale Res Lett 11:98. https://doi.org/10.1186/s11671-016-1311-2
54. Chowdhury S, Basu A, Kundu S (2014) Green synthesis of protein capped silver nanoparticles from phytopathogenic fungus Macrophomina phaseolina (Tassi) Goid with antimicrobial properties against multidrug-resistant bacteria. Nanoscale Res Lett 9(365):1–11
55. Kathiresan K, Manivannan S, Nabeel M, Dhivya B (2009) Studies on silver nanoparticles synthesized by a marine fungus, Penicillium fellutanum isolated from coastal mangrove. Colloids Surf B Biointerfaces 71:133–137
56. Kathiresan K, Alikunhi NM, Pathmanaban S, Nabikhan A, Kandasamy S (2010) Analysis of antimicrobial silver nanoparticles synthesized by coastal strains of Escherichia coli and Aspergillus niger. Can J Microbiol 56:1050–1059
57. Gade A, Bonde P, Ingle A, Marcato P, Duran N, Rai M (2008) Exploitation of Aspergillus niger for synthesis of silver nanoparticles. J Biobaased Mater Bioenergy 2:243–247
58. Costa LP, Cunegundes MC, Ferraz CM, Araújo JV, Tobias FL (2017) Extracellular biosynthesis of silver nanoparticles using the cell-free filtrate of nematophagous fungus Duddingtonia flagrans. Int J Nanomedicine 12:6373–6381
59. Bhangale H, Sarode K, Patil A, Patil DI (2016) Microbial synthesis of silver nanoparticles using Aspergillus flavus and their characterization. In: Techno-Societal 2016, Int Conf Adv Technol Soc Appl

60. Vigneshwaran N, Ashtaputre N, Varadarajan P, Nachane R, Paralikar K, Balasubramanya R (2007) Biological synthesis of silver nanoparticles using the fungus Aspergillus flavus. Mater Lett 61:1413–1418
61. Birla SS, Gaikwad SC, Gade AK, Rai MK (2013) Rapid synthesis of silver nanoparticles from Fusarium oxysporum by optimizing physicocultural conditions. Sci World J 2013:Article ID 796018
62. Li G, He D, Qian Y, Guan B, Gao S, Cui Y, Yokoyama K, Wang L (2011) Fungus-mediated green synthesis of silver nanoparticles using Aspergillus terreus. Int J Mol Sci 13:466–476
63. Vigneshwaran N, Kathe AA, Varadarajan PV et al (2006) Biomimetics of silver nanoparticles by white rot fungus, Phaenerochaete chrysosporium. Colloid Surf B 53:55–59
64. Ingle A, Rai M, Gade A et al (2009) Fusarium solani: a novel biological agent for the extracellular synthesis of silver nanoparticles. J Nanopart Res 11:2079–2085
65. Kathiresan K, Manivannan S, Nabeel MA et al (2009) Studies on silver nanoparticles synthesized by a marine fungus, Penicillium fellutanum isolated from coastal mangrove sediment. Colloid Surf B 71:133–137
66. Sheikhloo Z, Salouti MKFB (2011) Biological synthesis of gold nanoparticles by fungus Epicoccum nigrum. J Clust Sci 22:661–665
67. Molnár Z, Bódai V, Szakacs G, Erdélyi B, Fogarassy Z, Sáfrán G et al (2018) Green synthesis of gold nanoparticles by thermophilic flamentous fungi. Sci Rep 8:3943
68. Philip D (2009) Biosynthesis of Au, Ag and Au–Ag nanoparticles using edible mushroom extract. Spectrochim Acta Part A Mol Biomol Spectrosc 73:374–381
69. Moghaddam AB, Namvar F, Moniri M, Tahir P, Azizi S, Mohamad R (2015) Nanoparticles biosynthesized by fungi and yeast: a review of their preparation, properties, and medical applications. Molecules 20:16540–16565
70. Golinska P, Wypij M, Ingle AP (2014) Biogenic synthesis of metal nanoparticles from actinomycetes: biomedical applications and cytotoxicity. Appl Microbiol Biotechnol 98:8083–8097
71. Ahmad A, Senapati S, Sergeev GB, Moriarty P, Applications B (2003) Extracellular synthesis of silver nanoparticles by a silver-tolerant yeast strain MKY3. Nanotechnology 14:95–100
72. Mourato A, Lino AR (2011) Biosynthesis of crystalline silver and gold nanoparticles by extremophilic yeasts. Bioinorg Chem Appl 8:Article ID 546074
73. Pimprikar PS, Joshi SS, Kumar AR, Zinjarde SS, Kulkarni SK (2009) Biointerfaces influence of biomass and gold salt concentration on nanoparticle synthesis by the tropical marine yeast Yarrowia lipolytica. Colloids Surf B Biointerfaces 74:309–316
74. Suganya KSU, Govindaraju K, Kumar VG, Dhas TS, Karthick V, Singaravelu G et al (2015) Blue green alga mediated synthesis of gold nanoparticles and its antibacterial efficacy against Gram positive organisms. Mater Sci Eng C 47:351–356. https://doi.org/10.1016/j.msec.2014.11.043
75. Singaravelu G, Arockiamary JS, Kumar VG, Govindaraju K (2007) A novel extracellular synthesis of monodisperse gold nanoparticles using marine alga, Sargassum wightii Greville. Colloids Surf B Biointerfaces 57:97–101
76. Links DA (2011) Green synthesis of metal nanoparticles using plants. Green Chem 13:2638–2650
77. Parandhaman T, Dey D, Das SK (2019) Biofabrication of supported metal nanoparticles: exploring the bioinspiration strategy to mitigate. Green Chem 21:5469–5500
78. Hall JL (2002) Cellular mechanisms for heavy metal detoxification and tolerance. J Exp Bot 53 (366):1–11
79. Milner MJ, Kochian LV (2008) Investigating heavy-metal hyperaccumulation using Thlaspi caerulescens as a model system. Ann Bot 102:3–13
80. Gardea-Torresdey JL, Parsons JG, Gomez E, Peralta-Videa J, Troiani HE, Santiago P, Jose Yacaman M (2002) Formation and growth of Au nanoparticles inside live alfalfa plants. Nano Lett 2:24397–24401

81. Armendariz V, Parsons JG, Lopez ML, Peralta-Videa JR, Jose-Yacaman M, Gardea-Torresdey JL (2009) The extraction of gold nanoparticles from oat and wheat biomasses using sodium citrate and cetyltrimethylammonium bromide, studied by x-ray absorption spectroscopy, high-resolution transmission electron microscopy, and UV–visible spectroscopy. Nanotechnology 20(10):105607
82. Shankar SS, Ahmad A, Sastry M (2003) Bioreduction of chloroaurate ions by geranium leaves and its endophytic fungus yields gold nanoparticles of different shapes. J Mater Chem 13:1822–1826
83. Huang J, Li Q, Sun D, Lu Y (2007) Biosynthesis of silver and gold nanoparticles by novel sundried Cinnamomum camphora leaf. Nanotechnology 18:105104
84. Harris AT, Bali R (2008) On the formation and extent of uptake of silver nanoparticles by live plants. J Nanopart Res 10:691–695
85. Beach ES, Cui Z, Anastas PT (2009) Green chemistry: a design framework for sustainability. Energy Environ Sci 2:1038–1049
86. Kumar DA, Palanichamy V, Roopan SM (2014) Green synthesis of silver nanoparticles using Alternanthera dentata leaf extract at room temperature and their antimicrobial activity. Spectrochim Acta Part A Mol Biomol Spectrosc 127:168–171
87. Krishnaraj C, Jagan E, Rajasekar S, Selvakumar P, Kalaichelvan P, Mohan N (2010) Synthesis of silver nanoparticles using Acalypha indica leaf extracts and its antibacterial activity against water borne pathogens. Colloids Surfaces B Biointerfaces 76:50–56. 76: 50–56
88. Veeraputhiran V (2013) Bio-catalytic synthesis of silver nanoparticles. Int J Chem Tech Res 5:255–2562
89. Khalil MMH (2014) Green synthesis of silver nanoparticles using olive leaf extract and its antibacterial activity. Arab J Chem 7(6):1131–1139. https://doi.org/10.1016/j.arabjc.2013.04.007
90. Dhand V, Soumya L, Bharadwaj S, Chakra S, Bhatt D, Sreedhar B (2016) Green synthesis of silver nanoparticles using Coffea arabica seed extract and its antibacterial activity. Mater Sci Eng C 58:36–43
91. Shankar SS, Rai A, Ahmad ASM (2004) Rapid synthesis of Au, Ag, and bimetallic Au core-Ag shell nanoparticles using Neem (Azadirachta indica) leaf broth. J Colloid Interface Sci 275 (2):496–502
92. Kumar I, Mondal M, Meyappan V, Sakthivel N (2019) Green one-pot synthesis of gold nanoparticles using Sansevieria roxburghiana leaf extract for the catalytic degradation of toxic organic pollutants. Mater Res Bull 117:18–27. https://doi.org/10.1016/j.materresbull.2019.04.029
93. Boomi P, Ganesan RM, Poorani G, Prabu HG, Ravikumar S, Jeyakanthan J (2019) Biological synergy of greener gold nanoparticles by using Coleus aromaticus leaf extract. Mater Sci Eng C 99:202–210. https://doi.org/10.1016/j.msec.2019.01.105
94. Kasthuri J, Veerapandian S, Rajendiran N (2009) Biological synthesis of silver and gold nanoparticles using apiin as reducing agent. Colloids Surf B Biointerfaces 68:55–60
95. Song JY, Kim BS (2009) Rapid biological synthesis of silver nanoparticles using plant leaf extracts. Bioprocess Biosyst Eng 32(1):79–84
96. Jafarizad A, Safaee K, Gharibian S, Omidi Y, Ekinci D (2015) Biosynthesis and in-vitro study of gold nanoparticles using Mentha and Pelargonium extracts. Procedia Mater Sci 11:224–230. https://doi.org/10.1016/j.mspro.2015.11.113
97. Mude N, Ingle A, Gade A, Rai M (2009) Synthesis of silver nanoparticles using callus extract of Carica papaya—a first report. J Plant Biochem Biotechnol 18(1):83–86
98. Eya F, Olivier J, Mbeng A, Ebongue CO, Schlüsener C, Kök□am Ü et al (2019) Stachytarpheta cayennensis aqueous extract, a new bioreactor towards silver nanoparticles for biomedical applications. J Biomater Nanobiotechnology 10:102–119
99. Kora AJ, Sashidharb RB, Arunachalama J (2010) Gum kondagogu (Cochlospermum gossypium): a template for the green synthesis and stabilization of silver nanoparticles with antibacterial application. Carbohydr Polym 82(3):670–679

100. Gour A, Jain NK (2019) Advances in green synthesis of nanoparticles. Artif Cells Nanomed Biotechnol 47(1):844–851
101. Sharma D, Kanchi S, Bisetty K (2019) Biogenic synthesis of nanoparticles: a review. Arab J Chem 12(8):3576–3600
102. Qi C, Musetti S, Fu L, Zhu Y, Huang L (2019) Biomolecule-assisted green synthesis of nanostructured calcium phosphates and their biomedical applications. Chem Soc Rev 48 (10):2698–2737
103. Jia Y, Yan X, Guo X, Zhou G, Liu P, Li Z (2019) One step preparation of peptide-coated gold nanoparticles with tunable size. Materials (Basel) 12:2107
104. You H, Yang S, Ding B, Yang H (2013) Synthesis of colloidal metal and metal alloy nanoparticles for electrochemical energy applications. Chem Soc Rev 42:2880–2904
105. Boury B, Plumejeau S (2015) Metal oxides and polysaccharides: an efficient hybrid association for materials chemistry. Green Chem 17:72–88
106. Raveendran P, Fu J, Wallen SL, Hill C, Carolina N (2003) Completely "green" synthesis and stabilization of metal nanoparticles. JACS 125:13940–13941
107. Carré-Rangel L, Alonso-Nuñez G, Espinoza-Gómez H, Flores-López LZ (2015) Green synthesis of silver nanoparticles: effect of dextran molecular weight used as stabilizing-reducing agent. J Nanosci Nanotechnol 15(12):9849–9855
108. Maribel Guzman MA, Dille J, Godet S, Rousse C (2018) Effect of the concentration of NaBH4 and N2H4 as reductant agent on the synthesis of copper oxide nanoparticles and its potential antimicrobial applications. Nano Biomed Eng 10(4):392–405
109. Lu L, An X (2015) Silver nanoparticles synthesis using $H_2$ as reducing agent in toluene—supercritical $CO_2$ microemulsion. J Supercrit Fluids 99:29–37. https://doi.org/10.1016/j.supflu.2014.12.024
110. Kvı L, Vec R (2006) Silver colloid nanoparticles: synthesis, characterization, and their antibacterial activity. J Phys Chem B 110:16248–16253
111. Liu J, Qin G, Raveendran P, Ikushima Y (2006) Facile "green" synthesis, characterization, and catalytic function of b-D-glucose-stabilized Au nanocrystals. Chemistry 12(8):2131–2138
112. Vasileva P, Donkova B, Karadjova I, Dushkin C (2011) Synthesis of starch-stabilized silver nanoparticles and their application as a surface plasmon resonance-based sensor of hydrogen peroxide. Colloids Surf A Physicochem Eng Asp 382(1):203–210
113. Chairam S, Poolperm C, Somsook E (2009) Starch vermicelli template-assisted synthesis of size/shape-controlled nanoparticles. Carbohydr Polym 75(4):694–704. https://doi.org/10.1016/j.carbpol.2008.09.022
114. Engelbrekt C, Sørensen KH, Zhang J, Welinder AC, Jensen PS, Ulstrup J (2009) Green synthesis of gold nanoparticles with starch—glucose and application in bioelectrochemistry. J Mater Chem 19:7839–7847
115. Dumur F, Guerlin A, Dumas E, Bertin D, Gigmes D, Mayer CR (2011) Controlled spontaneous generation of gold nanoparticles assisted by dual reducing and capping agents. Gold Bull 44:119–137
116. Sheldon RA, Sheldon R (2005) Green solvents for sustainable organic synthesis: state of the art. Green Chem 7:267–278
117. Li CJ (2005) Organic reactions in aqueous media with a focus on carbon-carbon bond formations: a decade update. Chem Rev Aug 105(8):3095–3165
118. Manabe K, Iimura S, Sun X (2002) Dehydration reactions in water. Brønsted acid—surfactant-combined catalyst for ester, ether, thioether, and dithioacetal formation in water. JACS 124 (40):11971–11978
119. Leitner W (2002) Supercritical carbon dioxide as a green reaction medium for catalysis. Acc Chem Res 35(9):746–756
120. Ohde H, Hunt F, Wai CM (2001) Synthesis of silver and copper nanoparticles in a water-in-supercritical-carbon dioxide microemulsion. Chem Mater 9:4130–4135
121. Esumi K, Sarashina S, Yoshimura T (2004) Synthesis of gold nanoparticles from an organometallic compound in supercritical carbon dioxide. Langmuir 14:5189–5191

122. Pollet P, Davey EA, Eckert CA, Liotta CL (2014) Solvents for sustainable chemical processes. Green Chem 16:1034–1055
123. Adschiri T, Lee Y-W, Goto M, Takami S (2011) Green materials synthesis with supercritical water. Green Chem 13:1380–1390
124. Sue K, Adschiri T, Arai K (2002) Predictive model for equilibrium constants of aqueous inorganic species at subcritical and supercritical conditions. Ind Eng Chem Res 41:3298–3306
125. Klöpffer W, Curran MA, Frankl P, Heijungs R et al (2006) Nanotechnology and life cycle assessment. a systems approach to nanotechnology and the environment. Synthesis of results obtained at a workshop. In: Nanotechnology and life cycle assessment workshop. Woodrow Wilson Int Cent Sch Washington, DC
126. International Standardisation Organisation (ISO), European Standard EN ISO 14′044 G (2006) Environmental management—life cycle assessment—requirements and guidelines
127. International Standardization Organization (ISO), European Standard EN ISO 14′040 G (2006) Environmental management—life cycle assessment—principles and framework
128. Salieri B, Turner DA, Nowack B, Hischier R (2018) Life cycle assessment of manufactured nanomaterials: where are we? NanoImpact 10:108–120. https://doi.org/10.1016/j.impact.2017.12.003
129. Gavankar S, Suh S, Keller AF (2012) Life cycle assessment at nanoscale: review and recommendations. Int J Life Cycle Assess 17:295–303
130. Kim HC, Fthenakis V (2013) Life cycle energy and climate change implications of nanotechnologies. A critical review. J Ind Ecol 17:528–541
131. Sierra MJ, Herrera AP, Ojeda KA (2018) Life cycle analysis of the synthesis of eco-friendly metallic nanoparticles. Contemp Eng Sci 11(25):1227–1234
132. Pati P, Mcginnis S, Vikesland P (2014) Life cycle assessment of "green" nanoparticle synthesis methods. Environ Eng Sci 31(7):410–420
133. Chauhan VP, Jain RK (2013) Strategies for advancing cancer nanomedicine. Nat Mater 12 (11):958–962. http://www.nature.com/doifinder/10.1038/nmat3792
134. Shukla R, Bansal V, Chaudhary M, Basu A, Bhonde RR, Sastry M (2005) Biocompatibility of gold nanoparticles and their endocytotic fate inside the cellular compartment: a microscopic overview. Langmuir 21(23):10644–10654
135. Rajeshkumar S (2016) Anticancer activity of eco-friendly gold nanoparticles against lung and liver cancer cells. J Genet Eng Biotechnol 14(1):195–202
136. Baharara J, Ramezani T, Divsalar A, Mousavi M, Seyedarabi A (2016) Induction of apoptosis by green synthesized gold nanoparticles through activation of caspase-3 and 9 in human cervical cancer cells. Avicenna J Med Biotechnol 8(2):75–83
137. González-Ballesteros N, Prado-López S, Rodríguez-González JB, Lastra M, Rodríguez-Argüelles MC (2017) Green synthesis of gold nanoparticles using brown algae Cystoseira baccata: its activity in colon cancer cells. Colloids Surf B Biointerfaces 153(1):190–198
138. Maddinedi SB, Mandal BK, Ranjanb S, Dasgupta N (2015) Diastase assisted green synthesis of size-controllable gold nanoparticles. RSC Adv 5:26727–26733
139. Muthukumar T, Sudhakumari R, Balaji S, Aravinthan A, Sastry TP, Kim J-H (2016) Green synthesis of gold nanoparticles and their enhanced synergistic antitumor activity using HepG2 and MCF7 cells and its antibacterial effects. Process Biochem 51(3):384–391
140. Hoshyar R, Khayati GR, Poorgholami M, Kaykhaii M (2016) A novel green one-step synthesis of gold nanoparticles using crocin and their anti-cancer activities. J Photochem Photobiol B Biol 159:237–242
141. Siddiq AM, Thangam R, Madhan B, Alam MS (2019) Green (gemini) surfactant mediated gold nanoparticles green synthesis: effect on triple negative breast cancer cells. Nano-Struct Nano-Objects 2019:1003
142. Kajani AA, Bordbar A-K, Zarkesh Esfahani SH, Razmjou A (2016) Gold nanoparticles as potent anticancer agent: green synthesis, characterization, and in vitro study. RSC Adv 6 (68):63973–63983

143. Wang L, Xu J, Yan Y, Liu H, Karunakaran T, Li F (2019) Green synthesis of gold nanoparticles from Scutellaria barbata and its anticancer activity in pancreatic cancer cell (PANC-1). Artif Cells Nanomed Biotechnol 47(1):1617–1627
144. Kuppusamy P, Ichwan SJA, Al-Zikri PNH et al (2016) In vitro anticancer activity of Au, Ag nanoparticles synthesized using Commelina nudiflora L. aqueous extract against HCT-116 colon cancer cells. Biol Trace Elem Res 173:297
145. Wang C, Mathiyalagan R, Kim YJ, Castro-Aceituno V, Singh P, Ahn S, Wang D, Yang DC (2016) Rapid green synthesis of silver and gold nanoparticles using Dendropanax morbifera leaf extract and their anticancer activities. Int J Nanomedicine 10(11):3691–3701
146. Nakkala JR, Mata R, Bhagat E, Rani SS (2015) Green synthesis of silver and gold nanoparticles from Gymnema sylvestre leaf extract: study of antioxidant and anticancer activities. J Nanopart Res 17:151
147. Patra S, Mukherjeea S, Baruia AK et al (2015) Green synthesis, characterization of gold and silver nanoparticles and their potential application for cancer therapeutics. Mater Sci Eng C 53:298–309
148. Khorrami S, Zarrabi A, Khaleghi M, Danaei M, Mozafari MR (2018) Selective cytotoxicity of green synthesized silver nanoparticles against the MCF-7 tumor cell line and their enhanced antioxidant and antimicrobial properties. Int J Nanomedicine 13:8013–8024
149. Al-Sheddi ES, Farshori NN, Al-Oqail MM, Al-Massarani SM, Saquib Q, Wahab R, Musarrat J, Al-Khedhairy AA, Siddiqui MA (2018) Anticancer potential of green synthesized silver nanoparticles using extract of nepeta deflersiana against human cervical cancer cells (HeLA). Bioinorg Chem Appl 2018:12
150. Sreekanth TVM, Pandurangan M, Kim DH, Lee YR (2016) Green synthesis: in-vitro anticancer activity of silver nanoparticles on human cervical cancer cells. J Clust Sci 27:671
151. El-Naggar NE, Hussein MH, El-Sawah AA (2017) Bio-fabrication of silver nanoparticles by phycocyanin, characterization, in vitro anticancer activity against breast cancer cell line and in vivo cytotxicity. Sci Rep 7:10844
152. Angelico R, Ceglie A, Sacco P, Colafemmina G, Ripoli M, Mangia A (2014) Phyto-liposomes as nanoshuttles for water-insoluble silybin—phospholipid complex. Int J Pharm 471 (1–2):173–181. https://doi.org/10.1016/j.ijpharm.2014.05.026
153. Marqués-gallego P, de Kroon AIPM (2014) Ligation strategies for targeting liposomal nanocarriers. Biomed Res Int 2014:129458
154. Brown S, Khan DR (2012) The treatment of breast cancer using liposome technology. J Drug Deliv 2012:212965
155. Du J, Tang Y, Lewis AL, Armes SP (2005) pH-sensitive vesicles based on a biocompatible zwitterionic diblock copolymer. JACS 127:17982–17983
156. Smart TP, Mykhaylyk OO, Ryan A, Battaglia G (2009) Polymersomes hydrophilic brush scaling relations. Soft Matter 5:3607–3610
157. Holowka EP, Pochan DJ, Deming TJ (2005) Charged polypeptide vesicles with controllable diameter. JACS 6(6):12423–12428
158. Koide A, Kishimura A, Osada K, Jang W, Yamasaki Y (2006) Semipermeable polymer vesicle (PICsome) self-assembled in aqueous medium from a pair of oppositely charged block copolymers: physiologically stable micro-/nanocontainers of water-soluble macromolecules. JACS 128:5988–5989
159. Al-jamal WT, Kostarelos K (2011) Liposomes: from a clinically established drug delivery system to a nanoparticle platform for theranostic nanomedicine. Acc Chem Res 44 (10):1094–1104
160. Discher DE, Eisenberg A (2002) Polymer vesicles. Science 297:967
161. Discher DE, Ahmed F (2006) Polymersomes. Annu Rev Biomed Eng 8:323–341
162. Discher BM, Won Y, Ege DS, Lee JC, Bates FS, Discher DE et al (1999) Polymersomes: tough vesicles made from diblock copolymers. Science 284:1143–1147
163. Gaitzsch J, Chierico L, Battaglia G (2014) Novel aspects of encapsulation and delivery using polymersomes. Curr Opin Pharmacol 1:104–111

164. Davis HT, Bates FS (2003) Molecular exchange in PEO—PB micelles in water. Macromolecules 36:953–955
165. Dimova R, Pouligny B, Dietrich C (2000) Pretransitional effects in dimyristoylphosphatidylcholine vesicle membranes: optical dynamometry study. Biophys J 79(1):340–356. https://doi.org/10.1016/S0006-3495(00)76296-5
166. Mason AF, Thordarson P (2017) Polymersomes as protocellular constructs. J Polym Sci A Polym Chem 55:3817–3825
167. He H, Liu L, Morin EE, Liu M, Schwendeman A (2019) Survey of clinical translation of cancer nanomedicines—lessons learned from successes and failures. Acc Chem Res 52 (9):2445–2461
168. Shi J, Kantoff PW, Wooster R, Farokhzad OC (2017) Cancer nanomedicine: progress, challenges and opportunities. Nat Rev Cancer 17(1):20–37
169. Albanese A, Tang PS, Chan WCW (2012) The effect of nanoparticle size, shape, and surface chemistry on biological systems. Annu Rev Biomed Eng 14:1–16
170. Mirna therapeutics halts phase 1 clinical study of MRX34. https://www.businesswire.com/news/home/20160920006814/en/Mirna-Therapeutics-Halts-Phase-1-Clinical-Study
171. Blanco E, Shen H, Ferrari M (2015) Principles of nanoparticle design for overcoming biological barriers to drug delivery. Nat Biotechnol 33(9):941–951
172. Wilhelm S, Tavares AJ, Dai Q, Ohta S, Audet J, Dvorak HF, Chan WCW (2016) Analysis of nanoparticle delivery to tumours. Nat Rev Mater 1(5):16014
173. Huang L, Tao K, Liu J, Qi C, Xu L, Chang P, Gao J, Shuai X, Wang G, Wang Z, Wang L (2016) Design and fabrication of multifunctional sericin nanoparticles for tumor targeting and pH-responsive subcellular delivery of cancer chemotherapy drugs. ACS Appl Mater Interfaces 8:6577–6585
174. Xia X, Xu Q, Hu X, Qin G, Kaplan DL (2011) Tunable self-assembly of genetically engineered silk—elastin-like protein polymers. Biomacromolecules 12:3844–3850
175. Wu H, Liu S, Xiao L, Dong X, Lu Q, Kaplan DL (2016) Injectable and pH-responsive silk nano fiber hydrogels for sustained anticancer drug delivery. ACS Appl Mater Interfaces 8:17118–17126
176. Kang Y, Wang C, Liu K, Wang Z, Zhang X (2012) Enzyme-responsive polymeric supra-amphiphiles formed by the complexation of chitosan and ATP. Langmuir 28:14562–14566
177. Hong Y-J, Kim J-C (2015) Complexation-triggerable liposome mixed with silk protein and chitosan. J Biomater Sci Polym Ed 26(12):766–779
178. Su Y, Hu Y, Du Y, Huang X, He J, You J et al (2015) Redox-responsive polymer—drug conjugates based on doxorubicin and chitosan oligosaccharide—g—stearic acid for cancer therapy. Mol Pharm 12:1193–1202
179. Li S, Jiang Q, Liu S, Zhang Y, Tian Y, Song C et al (2018) A DNA nanorobot functions as a cancer therapeutic in response to a molecular trigger in vivo. Nat Biotechnol 36(3):258–264. https://doi.org/10.1038/nbt.4071
180. Wadhams GH, Armitage JP (2004) Making sense of it all: bacterial chemotaxis. Nat Rev Mol Cell Biol 5:1024–1037
181. Micali G (2016) Bacterial chemotaxis: information processing, thermodynamics, and behavior. Curr Opin Microbiol 30:8–15
182. Wong-Ng J, Celani A, Vergassola M (2018) Exploring the function of bacterial chemotaxis. Curr Opin Microbiol 45:16–21
183. Khadka U, Holubec V, Yang H, Cichos F (2019) Active particles bound by information flows. Nat Commun 9:3864
184. You MY, Ming SK, Gua CCXM (2018) Intelligent micro/nanomotors with taxis. Acc Chem Res 51(12):3006–3014
185. Williams BJ, Anand SV, Rajagopalan J, Saif MT (2014) A self-propelled biohybrid swimmer at low Reynolds number. Nat Commun 5:3081
186. Purcell EM (1977) Life at low Reynolds number. Am J Phys 45:3

187. Qiu T, Lee T, Mark AG, Morozov KI, Mu R, Mierka O et al (2014) Swimming by reciprocal motion at low Reynolds number. Nat Commun 5:5119
188. Zhao Z, Zhao Y, Zhuang X, Lo W, Baker MAB, Lo C et al (2018) Frequent pauses in Escherichia coli flagella fluorescence imaging. Nat Commun 9:1885. https://doi.org/10.1038/s41467-018-04288-4
189. Kumar MS, Philominathan P (2010) The physics of flagellar motion of E. coli during chemotaxis. Biophys Rev 2(1):13–20
190. Ali J, Cheang UK, Martindale JD, Jabbarzadeh M, Fu HC, Jun Kim M (2017) Bacteria-inspired nanorobots with flagellar polymorphic transformations and bundling. Sci Rep 7 (1):14098
191. Schwarz L, Medina-Sanchez M, Schmidt OG (2017) Hybrid biomicromotors. Appl Phys Rev 4:031301
192. Medina-Sánchez M, Schwarz L, Meyer AK, Hebenstreit F, Schmidt OG (2016) Cellular cargo delivery: toward assisted fertilization by sperm-carrying micromotors. Nano Lett 16 (1):555–561
193. Zhang L, Abbott JJ, Dong L, Kratochvil BE, Bell D, Nelson BJ et al (2014) Artificial bacterial flagella: fabrication and magnetic control. Appl Phys Lett 64107(94):2007–2010
194. Qiu F, Fujita S, Mhanna R, Zhang L, Simona BR, Nelson BJ (2015) Magnetic helical microswimmers functionalized with lipoplexes for targeted gene delivery. Adv Funct Mater 25:1666–1671
195. Wang S, Liu X, Wang Y, Xu D, Liang C (2019) Biocompatibility of artificial micro/nanomotors for use in biomedicine. Nanoscale 11:14099–14112
196. Gao W, de Ávila BE, Zhang L, Wang J (2018) Targeting and isolation of cancer cells using micro/nanomotors. Adv Drug Deliv Rev 1:94–101
197. Gao W, Manesh KM, Hua J, Sattayasamitsathit S, Wang J (2011) Hybrid nanomotor: a catalytically/magnetically powered adaptive nanowire swimmer. Small 7(14):2047–2051
198. Moran JL, Posner JD (2017) Phoretic self-propulsion. Annu Rev Fluid Mech 49:511–540
199. You A, Be MAY, In I (2016) Diffusiophoretic self-propulsion of colloids driven by a surface reaction: the sub-micron particle regime for exponential and van der Waals interactions. Phys Fluids 25(1):12001(2013)
200. Popescu MN, Tasinkevych M, Stark H, Das S, Cacciuto A (2007) Designing phoretic micro- and nano-swimmers. New J Phys 9:127
201. Ibrahim Y, Golestanian R, Liverpool TB (2018) Shape dependent phoretic propulsion of slender active particles. Phys Rev Fluids 3(3):033101
202. Sa S (2016) Bubble-free propulsion of ultrasmall tubular nanojets powered by biocatalytic reactions. J Am Chem Soc 138:13782–13785
203. Wheat PM, Marine NA, Moran JL, Posner JD (2010) Rapid fabrication of bimetallic spherical motors. Langmuir 294(20):13052–13055
204. Gao W, Sattayasamitsathit S, Orozco J, Wang J (2013) Efficient bubble propulsion of polymer-based microengines in real-life environments. Nanoscale 5:8909–8914
205. Wang S, Wu N (2014) Selecting the swimming mechanisms of colloidal particles: bubble propulsion versus self-diffusiophoresis. Langmuir 30:3477–3486
206. Pourrahimi AM, Pumera M (2018) Multifunctional and self-propelled spherical Janus nano/micromotors: recent advances. Nanoscale 10:16398–16415
207. Zhao X, Gentile K, Mohajerani F, Sen A (2018) Powering motion with enzymes. Acc Chem Res 51:2373–2381
208. Stark H (2018) Artificial chemotaxis of self-phoretic active colloids: collective behavior published as part of the accounts of chemical research special issue “fundamental aspects of self-powered”. Acc Chem Res 51:2681–2688
209. Tu Y, Peng F, Sui X, Men Y, White PB, van Hest JCM, Wilson DA (2017) Self-propelled supramolecular nanomotors with temperature-responsive speed regulation. Nat Chem 9:480–486

210. Ming W, Jeong X, Guo C, Liu C, Chun S, Juinn D et al (2019) Motion control of biohybrid microbots under low Reynolds number environment: magnetotaxis. Chem Eng Process Process Intensif 141:107530. https://doi.org/10.1016/j.cep.2019.107530
211. Mou F, Li Y, Chen C, Li W, Yin Y, Ma H et al (2015) Single-component $TiO_2$ tubular microengines with motion controlled by light-induced bubbles. Small 21:2564–2570
212. Su H, Price CH, Jing L, Tian Q, Liu J, Qian K (2019) Janus particles: design, preparation, and biomedical applications. Mater Today Bio 4:100033. https://doi.org/10.1016/j.mtbio.2019.100033
213. Medina-Sánchez M, Xu H, Schmidt OG (2018) Micro- and nano-motors: the new generation of drug carriers. Ther Deliv 9(4):303–316
214. Chen Z, Xia T, Zhang Z, Xie S, Wang T, Li X (2019) Enzyme-powered Janus nanomotors launched from intratumoral depots to address drug delivery barriers. Chem Eng J 375:122109
215. Wu Z, Wu Y, He W, Lin X, Sun J, He Q (2013) Self-propelled polymer-based multilayer nanorockets for transportation and drug release. Angew Chem Int Ed 52:7000–7003
216. Chen C, Karshalev E, Li J, Soto F, Castillo R, Campos I, Mou F, Guan J, Wang J (2016) Transient micromotors that disappear when no longer needed. ACS Nano 10 (11):10389–10396
217. Kagan D, Laocharoensuk R, Zimmerman M, Clawson C, Balasubramanian S, Kang D et al (2010) Rapid delivery of drug carriers propelled and navigated by catalytic nanoshuttles. Small 23:2741–2747
218. Sundararajan S, Lammert PE, Zudans AW, Crespi VH, Sen A (2008) Catalytic motors for transport of colloidal cargo. Nano Lett 8(5):1271–1276
219. Gao W, Dong R, Thamphiwatana S, Li J, Gao W, Zhang L et al (2015) Artificial micromotors in the mouse's stomach: a step toward in vivo use of synthetic motors. ACS Nano 1:117–123
220. Patiño T, Arqué X, Mestre R, Palacios L, Sánchez S (2018) Fundamental aspects of enzyme-powered micro- and nanoswimmers. Acc Chem Res 51:2662–2671
221. Dey KK, Zhao X, Tansi BM, Golestanian R, Sen A (2015) Micromotors powered by enzyme catalysis. Nano Lett 15:8311–8315
222. Nanomotors U, Carrascosa R, Murillo-cremaes N, Patin T, Hortela AC (2019) Targeting 3D bladder cancer spheroids with urease-powered nanomotors. ACS Nano 13:429–439

# Gold Nanoparticles: Biogenic Synthesis and Anticancer Application

9

Maheshkumar Prakash Patil and Gun-Do Kim

**Abstract**

The fastest growing nanotechnology in recent years has attracted increasing interest in the field of nanoparticle research, in particular, synthesis of nanoparticles and their biomedical application. In green chemistry, using plant, microorganisms, and algae for gold nanoparticle (AuNP) synthesis has constantly expanding knowledge based on experimentation and a better understanding of its challenges. The biogenic synthesis process of AuNPs is ecofriendly, inexpensive, and time saving. At present, there seems to be focused interest in the applications of AuNPs to the management and treatment of cancer. The exciting experimental knowledge gave evidence that biogenic AuNPs show no toxicity on normal cells and significant cytotoxicity on numerous cancer cells. Here, we highlight and discussed about biogenic synthesis of AuNPs, general characterization methods, and biogenic-AuNP application in cancer treatment.

**Keywords**

Anticancer activity · Biogenic synthesis · Gold nanoparticles · Plant extract · Microorganisms

M. P. Patil
Research Institute for Basic Sciences, Pukyong National University, Busan, Republic of Korea

G.-D. Kim (✉)
Department of Microbiology, College of Natural Sciences, Pukyong National University, Busan, Republic of Korea
e-mail: gundokim@pknu.ac.kr

© Springer Nature Singapore Pte Ltd. 2020

Q. Saquib et al. (eds.), *Green Synthesis of Nanoparticles: Applications and Prospects*, https://doi.org/10.1007/978-981-15-5179-6_9

## 9.1 Introduction

Nanotechnology has become one of the most important technologies in the area of science and technology. Materials in nanoscale (100 nm or less) show unique properties compared to their bulk form [1]. Nanobiotechnology is a new field that focuses on the use of biological agents for manipulation of materials at the nanometer scale for advance biotechnology [2]. The synthesis of AuNPs using microorganisms and plants has been reported for their green, nontoxic, safe, time-saving, and inexpensive methodology [3, 4]. AuNPs are of great interest due to their physicochemical properties that are governed by their shape, size, and distribution [5]. Smaller AuNPs with large surface area to volume ratio are widely accepted, which leads to improved biological activity compared to their bulk form [6, 7]. Because of unique physicochemical properties, AuNPs are of particular interest for a number of applications including antimicrobial, anticancer, drug carrier, medical diagnostic imaging, and cancer detection [4, 7, 8]. Recently, biogenic synthesis of AuNPs was reported successfully, and their applications in biomedicine make huge impact in healthcare sector in treating various chronic diseases. Hence, biogenic synthesis of AuNPs is considered as building blocks of the forthcoming generation to control various diseases. This review focuses on biogenic synthesis of AuNPs using plants and microorganisms and their anticancer application.

### 9.1.1 Classical Approach for Gold

Anciently, the gold metal is known as a symbol of power and wealth. The gold is used in different forms to improve the human health ever since [9]. In the nineteenth century, gold had a reputation as a "nervine," a therapy for nervous disorder [10]. Even today, AuNPs are very useful to human health applications [11].

### 9.1.2 Different Methods for AuNP Synthesis

Different methods are reported for synthesis of AuNPs, such as physical, chemical, and biological. Figure 9.1 represents involvement of few methods under each group of synthesis methods. Mostly, physical methods apply top-bottom approach in which the nanoparticles are generally produced by size reduction from an appropriate starting material. In this method, use of high level energy and heat makes this method non-eco-friendly and also utilizes more time and cost [12, 13]. Likewise, chemical and biological methods apply bottom-up approach in which the nanoparticles are produced from smaller entities, such as by joining atoms, molecules, and smaller nanoparticles. Chemical methods utilize hazardous chemicals, and this method is also expensive and harmful to the environment and human beings [14, 15]. The AuNPs synthesized through physical and chemical methods have less biocompatibility. Biogenic synthesis of AuNPs has been reported

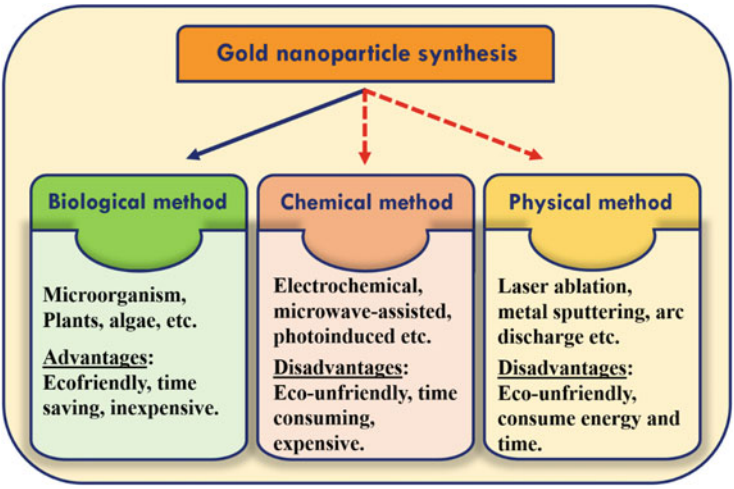


**Fig. 9.1** Different methods of gold nanoparticle synthesis

by using different plants, microorganisms, and algae, and the AuNPs synthesized by this method show biocompatibility [16].

### 9.1.3 Bio-Reduction

Plant extracts contain different biomolecules such as proteins, amino acids, enzymes, and sugars [16]. These biomolecules are involved in the reduction of gold salt to AuNPs. In the case of microorganisms, various reductase enzymes play an important role in the reduction of metal salt to nanoparticles with a nanoscale size [17]. An array of biogenic protocols for AuNPs synthesis has been reported using microorganism's biomass, supernatants, and derived components [18, 19].

### 9.1.4 Characterization

The significance of nanoparticles is dependent on their size, shape, and chemical composition. The characterization of nanoparticles is carried out by different methods. Few important techniques with their important role are listed in Table 9.1.

## 9.2 Biogenic Methods for AuNP Synthesis

In recent years, biogenic synthesis of AuNPs has emerged as an attractive alternative to traditional synthesis method. The use of biological entities such as plants, bacteria, fungi, and algae for AuNPs synthesis has been reported as a green chemistry and

**Table 9.1** The use of different techniques and their purpose in characterization of gold nanoparticles

| Techniques | Use | Refs. |
|---|---|---|
| UV-visible spectroscopy (UV-vis) | It is used to measure the extinction of light passing through a sample; it provides information about absorption, reflection, and luminescence properties of nanoparticles. This technique helps to observe the reduction of ions into nanoparticles. The UV-vis absorbance is very sensitive to the size, shape, concentration, and agglomeration of nanomaterials | Abdelhalim et al. [20]; Haiss et al. [21] |
| Transmission electron microscopy (TEM) | To determine the crystallographic structure of nanomaterials at an atomic scale. It is also useful for quantitative measurement of nanomaterials including their size, grain size, lattice type, size distribution, and size homogeneity | Asadabad and Eskandari [22] |
| Atomic force microscopy (AFM) | It is used to observe the surface of a nanomaterial at atomic scale, 2D and 3D with high resolution. AFM can give better idea about size of nanoparticles | Hoo et al. [23]; Yang et al. [24] |
| Selected area (electron) diffraction (SAED) | SAED is a crystallographic technique and can be performed inside a TEM microscope. This technique helps in the characterization of crystal structure of nanomaterials, whether the crystals are single or polycrystalline | Smitha et al. [25] |
| Dynamic light scattering spectroscopy (DLS) | It is useful to determine the size and size distribution of nanomaterials typically in the submicron region, lower than 1 nm | Hoo et al. [23] |
| Zeta potential (ZP) measurement | ZP is used to measure the electrostatic potential at the electrical layer on the surface of nanoparticles in solution | Clogston and Patri [26] |
| Field emission-scanning electron microscopy (FE-SEM) | This technique is useful to observe the surface topology (shape and size), composition, and dispersion of nanoparticles | Yao and Kimura [27] |
| Energy-dispersive X-ray (EDX) spectroscopy | EDX can be performed inside a FE-SEM microscope. It is applied to determine the near surface elements and their proportion at different position | Mishra et al. [28] |
| X-ray diffraction spectroscopy (XRD) | XRD reveals the structural properties of nanomaterials. It provides information about phase and crystallinity of nanoparticles. It is also a useful tool to calculate nanoparticle size using Debye-Scherrer formula. | Tian et al. [29] |
| Fourier transform infrared spectroscopy (FTIR) | FTIR is used to determine the interaction of reducing and stabilizing agents on the surface of nanomaterials. It also determines the chemical bonding in materials and functional molecules grafted on nanomaterial surface | Baudot et al. [30] |

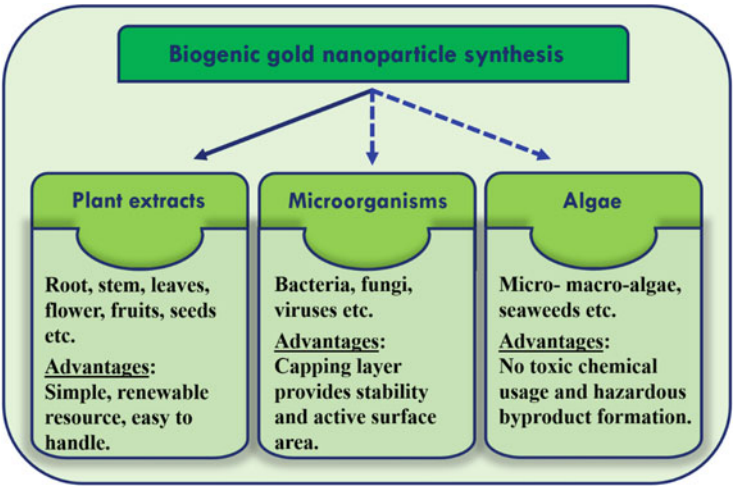


**Fig. 9.2** Biogenic method for synthesis of AuNPs

facile methodology [6, 7]. Figure 9.2 indicates the involvement of different sources in biogenic method for AuNP synthesis.

### 9.2.1 Plant-Mediated Synthesis of AuNPs

Synthesis of AuNPs using different plants and plant part is very cost-effective and thus can be used as an economic and valuable alternative for the large-scale production. The production of AuNPs using plant extracts can be performed by simply mixing them with a gold salt solution, and reaction can done at room temperature or specified temperature [31]. The synthesized AuNPs are characterized by different analytical techniques and checked for their biomedical applications. Figure 9.3 presents a schematic stepwise work flow for synthesis of AuNPs using plant extracts.

Phytonanotechnology is the biogenic synthesis of nanoparticles using plant resources. Different plant parts such as root, stem, leaf, galls, flower, fruits, and seeds have been reported for the synthesis of AuNPs as an eco-friendly, rapid, facile, stable, and cost-effective method. Plant extract-mediated AuNPs had advantages, including biocompatibility, scalability, and synthesis using water as solvent, as a reducing medium. Table 9.2 presents the synthesis of AuNPs using various plant species and their parts and also includes morphological features of synthesized nanoparticles and their anticancer activity on cancer cells.

#### 9.2.1.1 Root as a Source for AuNP Synthesis

The plant root extract used as a reducing agent to synthesize AuNPs was reported. Root of red ginseng was stated to contain biomolecules such as ginsenosides or

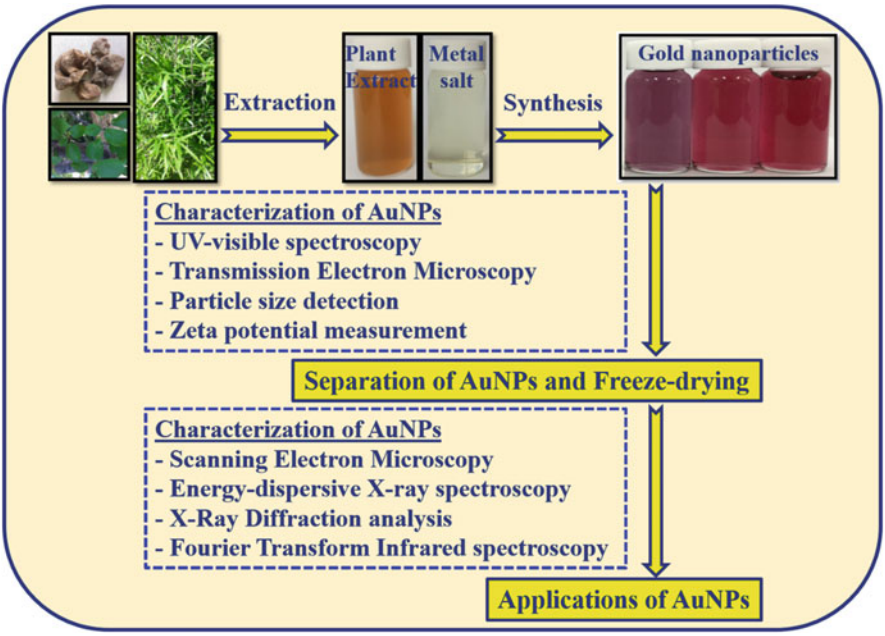


**Fig. 9.3** Schematic presentation of gold nanoparticle synthesis using plant extracts

polysaccharides, flavones, pyran derivatives, and amino acids which are involved in AuNP formation by an eco-friendly method [52]. *Angelica pubescens* Maxim root extract was prepared in water and reported for AuNP synthesis as a biogenic method. The different functional groups O-H, C-H, and C=C indicate alcohol, alkanes, and phenolic compounds, respectively, which are the responsible compounds in capping of AuNPs [53]. Similarly, root extract of *Zingiber officinale* was used to synthesize AuNPs, and the presence of functional groups such as C=C and C=O indicates as a capping material [54]. The molecular studies on biogenic synthesis of AuNPs are complex and not yet fully understood.

#### 9.2.1.2 Stem as a Source for AuNP Synthesis

Biogenic synthesis of AuNPs by using stem-bark extract was reported, and the morphologically different shape and size of AuNPs have been obtained by altering concentration of metal salt, plant extract, reaction time, and temperature. *Cassia fistula* stem-bark extract contains secondary metabolites, such as lupeol, beta-sitosterol, and hexacosanol, which could be responsible for reduction of gold ions to polydisperse with triangular and rectangular AuNPs [55]. Formation of polydisperse nanoparticles in biogenic synthesis using plant extract is mainly due to the presence of various phytochemicals [6, 17]. Bark extract of *Saraca indica* was reported for synthesis of AuNPs; different concentrations of bark extract are responsible for the variation of size of AuNPs [56]. Increasing concentration of *S. indica* bark extract results in decreasing size of AuNPs, which is due to increased

**Table 9.2** Synthesis and application of biogenic gold nanoparticles from plants ($IC_{50}$–50% inhibition of cell viability, *ND* not determined, *NA* not applicable)

| Plant | Plant tissue for extraction | AuNP size (nm) | Shape | Anticancer effect on cell line | $IC_{50}$ conc. (μg/ml) | Ref. |
|---|---|---|---|---|---|---|
| *Pleuropterus multiflorus* | Root | 104.8 | Spherical | A549 | ND | Castro-Aceituno et al. [32] |
| *Morinda citrifolia* | Root | 12.17–38.26 | Triangular, spherical | NA | NA | Suman et al. [33] |
| *Glycyrrhiza uralensis* | Root | 15–20 | Spherical | MCF-7 | ND | Huo et al. [34] |
| *Nerium oleander* | Stem bark | 10–100 | Spherical | MCF-7 | 74.04 | Barai et al. [35] |
| *Plumbago zeylanica* | Stem bark | 10–25 | Spherical | DLA | ND | Velammal et al. [36] |
| *Guazuma ulmifolia* | Bark | 20–25 | Spherical | NA | NA | Karthika et al. [37] |
| *Sasa borealis* | Leaves | 1–30 | Oval, spherical | AGS | 120 | Patil et al. [38] |
| *Nigella arvensis* | Leaves | 3–37 | Spherical | H1299 and MCF-7 | 10 and 25 | Chahardoli et al. [39] |
| *Backhousia citriodora* | Leaves | 8.40 ± 0.084 | Spherical | MCF-7 and HepG2 | 116.65 and 108.21 | Khandanlou et al. [40] |
| *Rhus chinensis* | Galls | 20–40 | Oval, spherical | MKN-28, Hep3B, and MG-63 | About 150 | Patil et al. [31] |
| *Pistacia integerrima* | Galls | 20–200 | Spherical | NA | NA | Islam et al. [41] |
| *Lonicera japonica* | Flower | 10–40 | Spherical, triangular, hexagonal | HeLa | 400 | Patil et al. [42] |
| *Moringa oleifera* | Flower | 3–5 | Spherical | A549 | ND | Anand et al. [43] |
| *Couroupita guianensis* | Flower | 7–48 | Spherical, triangular, tetragonal, pentagonal | HL-60 | 5.14 μM | Geetha et al. [44] |
| *Punica granatum* | Fruit | 5–20 | Triangular, spherical | HeLa | 62.5 | Lokina et al. [45] |

(continued)

**Table 9.2** (continued)

| Plant | Plant tissue for extraction | AuNP size (nm) | Shape | Anticancer effect on cell line | $IC_{50}$ conc. (μg/ml) | Ref. |
|---|---|---|---|---|---|---|
| *Hovenia dulcis* | Fruit | ~ 20 | Spherical, hexagonal | NA | NA | Basavegowda et al. [46] |
| *Actinidia deliciosa* | Fruit | 2–20 | Spherical | HCT116 | ND | Naraginti and Li [47] |
| *Vitis vinifera* | Seed | ~50 ± 5 | Spherical | A431 | 24.2 μM | Nirmala et al. [48] |
| *Elettaria cardamomum* | Seed | 15.2 | Spherical | HeLa | ND | Rajan et al. [49] |
| *Abies spectabilis* | Entire aerial parts | 20–200 | Spherical | T24 | 20 | Wu et al. [50] |
| *Commelina nudiflora* L. | Whole plant | 24–150 | Triangular, spherical | HCT-116 | 200 | Kuppusamy et al. [51] |

concentration of phytochemical contents. Similar observations are noted for AuNPs produced using bark extract of *Mimusops elengi*; the phenolic compounds are responsible for reduction of gold ions to AuNPs and also responsible for formation of different sizes of AuNPs [57].

#### 9.2.1.3 Leaf as a Source for AuNP Synthesis

The extract of plant leaves contains different biomolecules, particularly phenolic compounds, amines, alkaloids, flavonoids, and proteins that are involved in the formation of AuNPs. Rapid synthesis of AuNPs at room temperature using leaf extract of *Rosa rugosa* was reported [58]; the smaller AuNP formation at lower concentration of chloroauric acid and comparatively larger AuNP formation at higher concentration of gold ions were observed, and also increasing zeta potential (negative) value (−12.3 to −30 mV) was observed for the AuNPs synthesized at increasing pH (2 to 10). As the time of reaction increases, the absorbance peak also increases, which indicates improvement of nanoparticle yield [59]. In another study, in the AuNP synthesis using aqueous extract of *Chenopodium album* leaves, the increase in rate of the conversion of gold ions into AuNPs at higher temperature is observed [60].

#### 9.2.1.4 Flowers as a Source for AuNP Synthesis

Only few reports are available on synthesis of AuNPs using flower extract. Flowers contain alkaloids, flavonoids, phenolic compounds, aromatic amines, and alcohols; all these phytochemicals are good reducing agents and useful in green chemistry for synthesis of metallic nanoparticles. Recently, successfully synthesized AuNPs at room temperature within 1–2 h using aqueous flower extract from ornamental plant *Mirabilis jalapa* [61]. Similarly, medicinal plant *Carthamus tinctorius* L. was also reported for AuNP synthesis at room temperature, in the dark for 3–4 h [62]. Ethanol extract of *Nyctanthes arbortristis* was used for nanoparticle synthesis; spherical AuNPs were synthesized at room temperature, and it was observed that the biomolecules adsorbed on surface provided long-term stability [63].

#### 9.2.1.5 Fruit as a Source for AuNP Synthesis

Fruit extract from *Tribulus terrestris* was applied for AuNP synthesis. It has been reported that using 1 mM and 2 mM chloroauric acid, anisotropic 7 nm and 55 nm AuNPs, respectively, are formed. The different size of AuNP formation is due to the key role of phytochemicals [64]. A folk medicinal fruit of *Couroupita guianensis* was reported for eco-friendly synthesis of anisotropic AuNPs within a shorter period of time (5 min) [65]. Likewise, Kokum fruit aqueous extract also was reported for facile synthesis of AuNPs; increasing temperature of reaction response makes the process of formation of AuNPs faster [66]. Fruit extract of *Citrus maxima* contains polypeptide or proteins with amino and thiol groups that strongly bind to gold ions, and it triggers nucleation and growth of AuNPs; at the end, the polypeptide or proteins could make a covering layer on the surface of AuNPs and could provide stability by preventing agglomeration [67].

#### 9.2.1.6 Seeds as a Source for AuNP Synthesis

The seeds of *Trigonella foenum-graecum* (fenugreek) are rich with bioactive molecules including phenol, lignin, flavonoids, saponins, and vitamins. The synthesis of nearly spherical AuNPs by using seed extract was reported, and it was concluded that the concentration of seed extract and reaction pH are important factors in size distribution of AuNPs [68]. Polysaccharides and glycoproteins are high molecular glycosylated compounds present in seeds of *Abelmoschus esculentus*. The seed extract was used for synthesis of AuNPs and functional group O-H containing phyto-compounds observed in synthesized AuNPs [69]. Similarly, essential oil containing cumin's seeds was reported for formation of AuNPs; nanoplate formation at lower temperature and monodispersed spherical nanoparticles were observed at higher temperature [70].

### 9.2.2 Microorganism-Mediated Synthesis of AuNPs

At present, there is a growing need to develop sustainable route for AuNP synthesis without harming the environment and other living things. Biogenic methods using microorganisms including bacteria and fungi for the synthesis of AuNPs have been recognized as facile, viable, and eco-friendly compared to physical and chemical methods. Microorganisms have ability to detoxify and accumulate metals due to different reductase enzymes and reduce metal salt to metal nanoparticles. Microorganisms are potential biofactories for AuNP synthesis; specifically, in microbial synthesis of nanoparticles either intracellularly or extracellularly, experimental methods utilize microbial biomass, media supernatants, and microbial extracts. Among the different methods, extracellular synthesis of AuNPs is more preferable because it eliminates downstream processing for recovery of intracellularly synthesized AuNPs, which need several steps such as cell lysis, centrifugation, purification, and others. An overview on the microorganism-mediated synthesis of AuNPs and their anticancer effect on different cell lines is given in Table 9.3.

#### 9.2.2.1 Mechanism of Microbial Synthesis of AuNPs

The complete mechanism for the synthesis of nanoparticles using microorganism has not been reported yet. This is because different reducing agents from microorganisms interact differently in formation of nanoparticles. Many bacteria and fungi produce metal nanoparticles either intracellularly or extracellularly with different biomolecules. Schematic presentation of intracellular and extracellular synthesis of AuNPs is given in Fig. 9.4.

In intracellular synthesis of nanoparticles, the positively charged metal ions electrostatically are attracted to negatively charged cell wall, and then these ions are transported in the cell; in this case, cell wall plays an important role. In the microbial cell, the enzymes present on cell wall play a key role in formation of nanoparticles, and these synthesized nanoparticles get diffused off through the cell wall. A stepwise intracellular synthesis of AuNPs by *Rhizopus oryzae* explains that the Au(III) ions initially bind to cell surface and are then transported into cytoplasm

**Table 9.3** Synthesis and application of biogenic gold nanoparticles from microorganisms ($IC_{50}$–50% inhibition of cell viability, *ND* not determined, *NA* not applicable)

| Microorganism | AuNP synthesis | AuNP size (nm) | Shapes | Anticancer effect on cell line | $IC_{50}$ conc. (μg/ml) | Ref. |
|---|---|---|---|---|---|---|
| Bacteria | | | | | | |
| *Rhodococcus* sp. | Intracellular | 5–15 | Spherical | NA | NA | Ahmad et al. [71] |
| *Bacillus subtilis 168* | Intracellular | ~20 | Spherical | NA | NA | Southam and Beveridge [72] |
| *Enterococcus* sp. | Extracellular | 6–13 | Spherical | HepG2, A549 | ND | Rajeshkumar [73] |
| *Nocardiopsis* sp. MBRC-48 | Extracellular | 11.57 ± 1.24 | Spherical | HeLa | 300 | Manivasagan et al. [74] |
| *Streptomyces cyaneus* | Extracellular | 31.2 | Spherical | MCF-7 and HepG2 | 64.3 and 76.7 | El-Batal et al. [75] |
| Fungus | | | | | | |
| *Fusarium oxysporum* | Extracellular | 20–40 | Spherical, triangular | NA | NA | Mukherjee et al. [76] |
| *Verticillium* sp. | Intracellular | ~20 | Spherical, triangular, hexagonal | NA | NA | Mukherjee et al. [77] |
| *Penicillium brevicompactum* | Extracellular | 20–50 | Spherical, triangular, hexagonal | C2C12 | ND | Mishra et al. [78] |
| *Yarrowia lipolytica* | Intracellular | 9–27 | Spherical, triangular, hexagonal | NA | NA | Pimprikar et al. [79] |
| *Candida albicans* | Extracellular | 20–40 and 60–80 | Spherical and non-spherical | NA | NA | Chauhan et al. [80] |

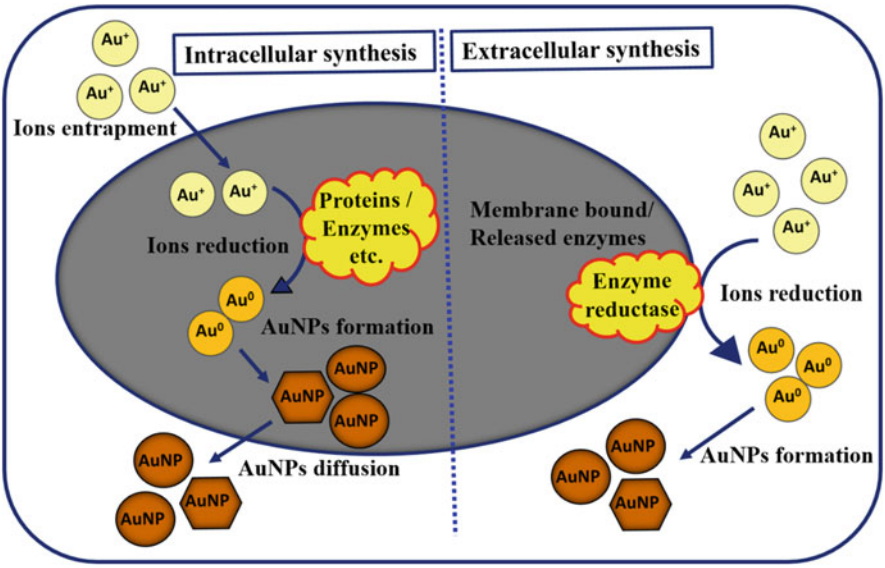


**Fig. 9.4** Schematic presentation of microbial intracellular and extracellular synthesis of gold nanoparticles

and reduced by cytoplasmic proteins to form intermediate Au(I)-protein complexes and finally AuNPs [81]. However, it is unclear whether the diffusion of Au(III) ions through membrane occurs via passive biosorption or bioaccumulation. The latter might be caused by Au(III) ion toxicity, which increases the porosity of cell membrane. The enzymatic reduction mechanism of Au(III) is essentially the same for intracellular and extracellular AuNPs [82]. Likewise, intracellular synthesis of AuNPs by *Verticillium* sp. also explains the stepwise mechanism such as gold ion trapping, reduction, and capping [77].

Different bacteria and fungi are reported for extracellular synthesis of AuNPs, but an exact mechanism is not established yet. The common underlying mechanism involved in synthesis is the reduction of gold ions to AuNPs; it is considered that the enzymes produced and secreted by bacteria or fungi play a key role in the reduction of gold ions, followed by nanoparticle nucleation, growth of nanoparticles, and finally formation of AuNPs. It is generally accepted that the extracellular synthesis of AuNPs is due to nitrate reductase activity. In viable cells, gold ions are reduced by NADH/NADPH oxidoreductase either in the cytoplasm or in the cell surface. The bacterium *Rhodopseudomonas capsulata* secretes cofactor NADH/NADH-dependent enzyme and is reported for extracellular synthesis of AuNPs [83]. The gold ion reduction was found to be initiated by electron transfer from NADH to NADH-dependent reductase as an electron carrier; Au(III) obtains electron and forms Au(0) and finally forms AuNPs. A similar mechanism, which involves an NADPH-dependent reductase enzyme that reduces Au(III) to Au(0), was reported for AuNPs synthesized using *Stenotrophomonas maltophilia* [84].

#### 9.2.2.2 Bacteria as a Source for AuNP Synthesis

Bacteria are the most abundant microorganisms on the earth and play an important role in the environment. In the last decades, microbial synthesis of nanoparticles attracted researchers, and different groups of bacteria were reported including Actinobacteria, Proteobacteria, Cyanobacteria, and many more. Primary report for the bacteria-mediated AuNPs was investigated in *Bacillus subtilis* [85]. Extracellular synthesis of AuNPs was observed after 24 h incubation at 37 °C by using cell-free supernatant of *Pseudomonas aeruginosa* [86]. Likewise, the proteobacterium *Shewanella oneidensis* was also reported for synthesis of smaller (2–50 nm) AuNPs [87]. The cell biomass of *S. oneidensis* was inoculated in the chloroauric acid at 30 °C; a spherical, homogenous extracellular formation of AuNPs was observed due to reducing agents present in the bacterial cell membrane. A thermophilic bacterium, *Geobacillus* sp. strain ID17, was reported for intracellular synthesis of AuNPs [88]. Living cells were inoculated with chloroauric acid; intracellularly, accumulation of AuNPs was observed by TEM. Synthesized AuNPs were quasi-hexagonal with a size about 5–50 nm, and it was concluded that reductase activity (NADH dependent) was involved in synthesis. Similarly, cell-free supernatant of thermophilic *Geobacillus stearothermophilus* was reported for synthesis of monodispersed AuNPs [89]. The proteins secreted by the bacterium in the media were involved in the formation and capping of AuNPs.

#### 9.2.2.3 Fungi as a Source for AuNP Synthesis

Several unicellular or multicellular fungi have been reported for the accumulation and biogenic synthesis of AuNPs either intracellularly or extracellularly, described in Table 9.3. Compared to bacterial synthesis of AuNPs, fungal synthesis is more facile because fungi produce extracellular enzymes which is easy to handle to collect fungal biomass or supernatant. Recently, extracellular and intracellular synthesis of AuNPs using *Trichothecium* sp. was reported [90]; it was observed that the fungal biomass produces extracellular AuNPs (5–200 nm) with different shapes (triangular, hexagonal, rod, and spherical) under stationary phase and biomass with chloroaurate ions under shaking condition produces intracellular AuNPs (10–25 nm). The formation of intracellular AuNPs is smaller than extracellular AuNPs, and the formation of different shapes of extracellularly synthesized AuNPs is due to the rate of synthesis or released enzymes or proteins in the solution by fungi. The filamentous fungus *Neurospora crassa* was reported for synthesis of intracellular AuNPs. The formation of AuNPs within the cells was mostly spherical with an average size of 11 nm observed [91]. In another study, mycelia-free filtrate medium from *Aspergillus niger* [92] and *Aspergillus terreus* [93] was used for extracellular synthesis of gold nanocrystals; the formation of different shapes and sizes of AuNPs is dependent on environmental variables including concentration of chloroauric acid, reaction temperature, and pH of the reaction solution.

### 9.2.3 Algae-Mediated Synthesis of AuNPs

The group of microorganisms that belongs to plant kingdom, namely, algae, which is an important part of biodiversity, was also reported for bioaccumulation and synthesis of AuNPs. Recently reported micro- and macroalgae for synthesis of AuNPs are listed in Table 9.4. The mechanism for extra- or intracellular synthesis of AuNPs by algae is reported similar to fungi and bacteria [101]. The general steps involved in algae-mediated synthesis of AuNPs include preparation of algal biomass/supernatant/cell extract in water or any other solvent. Another step is preparation of different concentration of chloroauric acid solution. And, the final step includes inoculation of algal biomass/supernatant/cell extract with different concentration of chloroauric acid solution, and synthesis can be performed at different temperature, with or without light and shaking. The extracellular synthesis of nanoparticles is due to the presence of active biomolecules of algae such as polysaccharides, pigments, proteins, and many more [102, 103].

#### 9.2.3.1 Microalgae as Source for AuNP Synthesis

Intracellular synthesis of AuNPs using biomass of microalgae *Euglena gracilis* has been reported recently [104]. The microalgae synthesize intracellular AuNPs through different steps such as uptake of gold ions, reduction of Au(III) to Au (0) and subsequently AuNP formation, and at the end release of as-produced AuNPs into culture media. An aqueous extract from dried alga *Gracilaria corticata* was reported for extracellular synthesis of AuNPs [105]. The synthesized AuNPs were about 45–57 nm. Likewise, unicellular *Chlorella vulgaris* extract was utilized for production of AuNPs at room temperature [106]. A protein with approximately 28 kDa was isolated from *C. vulgaris* which is responsible for reduction of gold ions

**Table 9.4** Synthesis and application of biogenic gold nanoparticles from algae ($IC_{50}$–50% inhibition of cell viability, *ND* not determined, *NA* not applicable)

| Algae | | AuNP synthesis | AuNPs size (nm) | Shapes | Ref. |
|---|---|---|---|---|---|
| *Tetraselmis suecica* | Microalgae | NA | 51–120 | Spherical | Shakibaie et al. [94] |
| *Tetraselmis kochinensis* | Microalgae | Intracellular | 5–35 | Spherical | Senapati et al. [95] |
| *Chlorella vulgaris* | Microalgae | Intracellular | 40–60 | Spherical/ polyhedral | Luangpipat et al. [96] |
| *Sargassum wightii* Greville | Macroalgae | Extracellular | 8–12 | Spherical | Singaravelu et al. [97] |
| *Padina gymnospora* | Macroalgae | Extracellular | 53–67 | Spherical | Singh et al. [98] |
| *Ecklonia cava* | Macroalgae | NA | 30 ± 0.25 | Spherical, triangular | Venkatesan et al. [99] |
| *Prasiola crispa* | Macroalgae | NA | 5–25 | Spherical | Sharma et al. [100] |

to AuNPs, and it was also observed that the protein plays a key role in controlling AuNP shape and size.

#### 9.2.3.2 Macroalgae as Source for AuNP Synthesis

The dried biomass and ethanolic extract of red alga *Galaxaura elongata* were reported for synthesis of AuNPs [107]. *G. elongata* is a rich source of fucoxanthin, phycoerythrin, proteins, polysaccharides, phenols, flavonoids, and terpenes; all these biomolecules could take part in AuNP formation. Similarly, water extract of dried *Sargassum muticum* was prepared and mixed with gold ion solution; within 30 min at 45 °C, formation of AuNPs was observed [108]. Synthesized nanoparticles that were spherical with a mean size of 5.42 ± 1.18 nm were observed. The algal (*Rhizoclonium fontinale* and *Ulva intestinalis*) biomass was exposed to gold ion solution with different pH; intracellular formation of AuNPs was observed after 72 h incubation at 20 °C [109]. Intracellularly synthesized AuNPs were collected from algal cells by breaking cells by ultra-sonication and purified by centrifugation. The choice of alga and reaction parameters (pH) is important for obtaining desired AuNPs.

## 9.3 Factors Influencing the Formation of AuNPs

There are several advantages of a biogenic AuNP synthesis, but still formation of different shapes and sizes of nanoparticles remains a challenge. Therefore, recently, many researchers attempted studies on controlling shape and size of AuNPs. The reaction parameters such as reaction time, temperature, pH, concentration of metal salt, and type of biogenic agents play an important role in formation of AuNPs and controlling their size and shape [6, 17]. Controlled size, shape, and stability of nanoparticles can be achieved by altering the reaction parameters in biogenic AuNP synthesis process, which is schematically presented in Fig. 9.5.

For instance, quasi-spherical AuNPs of smaller size formation using *Coffea arabica* at higher pH (e.g., pH > 10) were observed, while lower pH (e.g., pH < 5) of the reaction produces irregular shapes and bigger AuNPs [110]. Similarly, monodispersed AuNPs with smaller size were extracellularly synthesized using *Aspergillus terreus* by improving the reaction conditions, including salt concentration, pH, incubation temperature, and time [93]. In the case of living microorganism for intracellular nanoparticle synthesis, possible maximum or optimized temperature for optimized growth is recommended because enzymes responsible for formation of AuNPs are more active [88]. The reaction pH is a significant factor in the formation of AuNPs; at lower pH, phytochemicals may be denatured and may have an effect on formation of AuNPs and their size, shape, and yield [42]. The acidic pH is not recommended for nanoparticle synthesis because of lower yield, aggregation, and formation of polydisperse nanoparticles. Another important factor in controlling morphology of AuNPs is concentration of reducing agents. For instance, flower extract of *Nyctanthes arbor-tristis* with different concentrations was reported for AuNP synthesis. At higher concentration, formation of AuNPs indicates fast

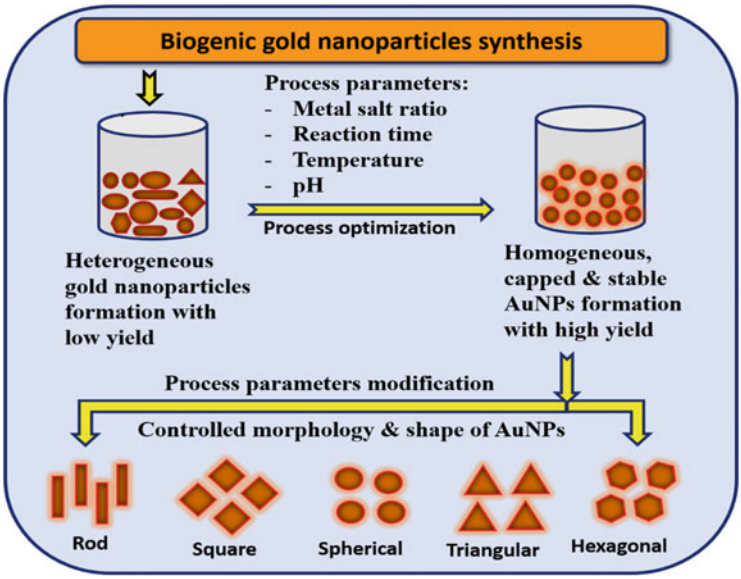


**Fig. 9.5** Involvement of different parameters in production of monodispersed, stable, and high-yield biogenic gold nanoparticles

reduction process, formation of monodispersed nanoparticles, and higher yield, while at lower concentration, polydisperse and lower yield is reported [63]. In another study, pH 6 and pH 7 are recommended for stable AuNP synthesis using fenugreek seed extract [68]. Increasing reaction temperature usually results in enhancement of reaction rate and enhances yield of nanoparticles. Other examples of shape-controlled biogenic synthesis of AuNPs were reported, which include formation of spherical [38, 74], triangular [90, 111], hexagonal [58, 78], octahedral [72], and nano-rod AuNPs [107, 109].

## 9.4 Anticancer Application of Biogenic AuNPs

Cancer cells are known to be rapidly dividing cells characterized by numerous defects in cell proliferation cycle control. A programmed cell death is also known as apoptosis; apoptosis is initiated by two different pathways: first, extrinsic pathway which is also recognized as receptor-mediated pathway, activated by interaction between cell surface receptors and specific ligands, and, second, intrinsic pathway which is also recognized as mitochondrial pathway, conditioned by various receptor-independent stimuli that induce certain mitochondrial changes. In current era, cancer is known to be one of the major causes of death in the world. Recently, AuNPs have found significant interest in designing and their application in anticancer therapy. The overexpression of cancerous cells can be controlled by treating with AuNPs synthesized using plants and microorganisms [6]. Biocompatibility is the major

concern for nanoparticles in biomedical applications. Plant extract-derived AuNPs are nontoxic to normal cells but show significant cytotoxicity on cancer cells only [31, 112]. The anticancer effect of AuNPs depends on interaction between AuNPs and cancer cells [113], cellular uptake or endocytosis [114], shape, size [115], and concentration of nanoparticles [40].

In cytoplasm, the photosynthesized AuNPs induce the production of reactive oxygen species (ROS), which has the capacity to induce apoptosis. For instance, increased ROS production was observed in the MCF-7 cells treated with *Nerium oleander* stem bark extract-mediated AuNPs [35]. The A431 (skin cancer) cells show disruption and loss of mitochondrial membrane potential after treatment with *Vitis vinifera* seed extract-mediated AuNPs, which is due to enhanced production of ROS in the cell [48]. Eventually, AuNPs can reach the nucleus and cause breakdown or fragmentation of genomic DNA and activate apoptosis [44, 116]. The caspase-8 activation leads to induction of apoptosis through extrinsic pathway which was observed in colon cancer (Caco-2) cells treated with AuNPs synthesized using brown alga *Cystoseira baccata* [117]. In another research, the key regulatory proteins associated with cancer, namely, p53 (proapoptotic protein) and Bcl-2 (antiapoptotic protein), in human breast adenocarcinoma (MCF-7) cells were regulated by Palm pollen extract-mediated AuNPs. In the AuNP-treated cells, increased level of protein p53 and decreased level of protein Bcl-2 were observed, which is responsible for death of MCF-7 cells through induction of apoptosis [118]. Likewise, *Commelina nudiflora* extract-mediated AuNPs show anticancer activity on colon cancer (HCT-116) cells through cell growth arrest in the sub-G1 cell cycle phase and also upregulation of proapoptotic genes (PUMA and caspase-3, caspase-8, caspase-9) [51].

## 9.5 Challenges and Limitations

Even though there are benefits of biogenic synthesis of AuNPs, there are yet many limitations and challenges to be solved before it can be applied in a large scale. Major challenges in biogenic synthesis of AuNPs include morphology or size/shape-controlled synthesis because of different reducing phytochemical composition of plant extract and different reducing enzymes or proteins of microorganisms (bacteria, fungi, and algae). Another limitation in the use of microorganisms for biogenic synthesis of AuNPs is microorganisms need very specific growth condition and to maintain purity. In case of microbial intracellularly synthesized AuNPs, additional steps are needed to collect nanoparticles such as breakdown of cell membrane and removal of unreacted microbial cell constituents by centrifugation. In addition, the stability of synthesized AuNPs is also a major challenge as during storage of AuNPs, they get aggregated or change their physicochemical properties.

## 9.6 Concluding Remarks and Prospects

The potential of using AuNPs in different fields increases the need to produce them on an industrial scale and in stable formulation with eco-friendly process. Therefore, huge efforts are being made toward exploring plants, microorganisms, and algal resources and implementing biogenic methods with advantages including the following: cost-effective, facile, nontoxic, and eco-friendly; thus, biogenic synthesis of AuNPs has a great potential. Here, we summarized the biogenic synthesis of AuNPs using plant extracts, bacteria, fungi, and algae. The critical parameters in formation of AuNPs are also summarized. With the help of available literature, anticancer potential of biogenic AuNPs is also explored. However, there is still much work needed for improved biogenic synthesis of AuNPs. Specifically, to improve yield of AuNPs in biogenic synthesis method, finding out the exact mechanism for AuNP formation and controlling morphology of AuNPs still remain to be educated. The biocompatibility of synthesized AuNPs and their anticancer applications in animals need to be addressed.

**Acknowledgments** This research was supported by Basic Science Research Program through the National Research Foundation of Korea (NRF) funded by the Ministry of Education (2018R1D1A1B07043388).

## References

1. Salata OV (2004) Applications of nanoparticles in biology and medicine. J Nanobiotechnol 2 (1):3
2. Goodsell DS (2004) Bionanotechnology: lessons from nature. Wiley
3. Das SK, Das AR, Guha AK (2009) Gold nanoparticles: microbial synthesis and application in water hygiene management. Langmuir 25(14):8192–8199
4. Kumar V, Yadav SK (2009) Plant-mediated synthesis of silver and gold nanoparticles and their applications. J Chem Technol Biotechnol 84(2):151–157
5. Guo S, Wang E (2007) Synthesis and electrochemical applications of gold nanoparticles. Anal Chim Acta 598(2):181–192
6. Patil MP, Kim G (2017) Eco-friendly approach for nanoparticles synthesis and mechanism behind antibacterial activity of silver and anticancer activity of gold nanoparticles. Appl Microbiol Biotechnol 101(1):79–92
7. Patil MP, Kim G (2018) Marine microorganisms for synthesis of metallic nanoparticles and their biomedical applications. Colloids Surf B Biointerfaces 172:487–495
8. Khan A, Rashid R, Murtaza G, Zahra A (2014) Gold nanoparticles: synthesis and applications in drug delivery. Trop J Pharm Res 13(7):1169–1177
9. Berners-Price SJ (2011) Gold-based therapeutic agents: a new perspective. Bioinorganic Medicinal Chemistry 197–222
10. Richards DG, McMillin DL, Mein EA, Nelson CD (2002) Gold and its relationship to neurological/glandular conditions. Int J Neurosci 112(1):31–53
11. Giljohann DA, Seferos DS, Daniel WL, Massich MD, Patel PC, Mirkin CA (2010) Gold nanoparticles for biology and medicine. Angew Chem Int Ed 49(19):3280–3294
12. Kabashin AV, Meunier M (2003) Synthesis of colloidal nanoparticles during femtosecond laser ablation of gold in water. J Appl Phys 94(12):7941–7943

13. Liu X, Wang A, Yang X, Zhang T, Mou C, Su D, Li J (2008) Synthesis of thermally stable and highly active bimetallic au− ag nanoparticles on inert supports. Chem Mater 21(2):410–418
14. Jana NR, Gearheart L, Murphy CJ (2001) Wet chemical synthesis of high aspect ratio cylindrical gold nanorods. J Phys Chem B 105(19):4065–4067
15. Kawasaki H, Nishimura K, Arakawa R (2007) Influence of the counterions of cetyltrimethylammonium salts on the surfactant adsorption onto gold surfaces and the formation of gold nanoparticles. J Phys Chem C 111(6):2683–2690
16. Shah M, Fawcett D, Sharma S, Tripathy S, Poinern G (2015) Green synthesis of metallic nanoparticles via biological entities. Materials 8(11):7278–7308
17. Singh P, Kim Y, Zhang D, Yang D (2016a) Biological synthesis of nanoparticles from plants and microorganisms. Trends Biotechnol 34(7):588–599
18. Hulkoti NI, Taranath T (2014) Biosynthesis of nanoparticles using microbes—a review. Colloids Surf B Biointerfaces 121:474–483
19. Shankar PD, Shobana S, Karuppusamy I, Pugazhendhi A, Ramkumar VS, Arvindnarayan S, Kumar G (2016) A review on the biosynthesis of metallic nanoparticles (gold and silver) using bio-components of microalgae: formation mechanism and applications. Enzym Microb Technol 95:28–44
20. Abdelhalim MAK, Mady MM, Ghannam MM (2012) Physical properties of different gold nanoparticles: ultraviolet-visible and fluorescence measurements. J Nanomed Nanotechol 3 (3):178–194
21. Haiss W, Thanh NT, Aveyard J, Fernig DG (2007) Determination of size and concentration of gold nanoparticles from UV− Vis spectra. Anal Chem 79(11):4215–4221
22. Asadabad MA, Eskandari MJ (2015) Transmission electron microscopy as best technique for characterization in nanotechnology. Synth React Inorg, Met-Org, Nano-Met Chem 45 (3):323–326
23. Hoo CM, Starostin N, West P, Mecartney ML (2008) A comparison of atomic force microscopy (AFM) and dynamic light scattering (DLS) methods to characterize nanoparticle size distributions. J Nanopart Res 10(1):89–96
24. Yang H, Wang Y, Lai S, An H, Li Y, Chen F (2007) Application of atomic force microscopy as a nanotechnology tool in food science. J Food Sci 72(4):R65–R75
25. Smitha S, Philip D, Gopchandran K (2009) Green synthesis of gold nanoparticles using *Cinnamomum zeylanicum* leaf broth. Spectrochim Acta Part A 74(3):735–739
26. Clogston JD, Patri AK (2011) Zeta potential measurement. Characterization of nanoparticles intended for drug delivery. Humana press, pp. 63-70
27. Yao H, Kimura K (2007) Field emission scanning electron microscopy for structural characterization of 3D gold nanoparticle superlattices. Modern research and educational topics in microscopy; Méndez-Vilas, a., Díaz, J., Eds. Pp. 568-575
28. Mishra AN, Bhadauria S, Gaur MS, Pasricha R, Kushwah BS (2010) Synthesis of gold nanoparticles by leaves of zero-calorie sweetener herb (*Stevia rebaudiana*) and their nanoscopic characterization by spectroscopy and microscopy. Int J Green Nanotechnol 1(2): P118–P124
29. Tian S, Li Y, Li M, Yuan J, Yang J, Wu Z, Jin R (2015) Structural isomerism in gold nanoparticles revealed by X-ray crystallography. Nat Commun 6:8667
30. Baudot C, Tan CM, Kong JC (2010) FTIR spectroscopy as a tool for nano-material characterization. Infrared Phys Technol 53(6):434–438
31. Patil MP, Ngabire D, Thi HHP, Kim M, Kim G (2017) Eco-friendly synthesis of gold nanoparticles and evaluation of their cytotoxic activity on cancer cells. J Clust Sci 28 (1):119–132
32. Castro-Aceituno V, Abbai R, Moon SS, Ahn S, Mathiyalagan R, Kim Y, Kim Y, Yang DC (2017) *Pleuropterus multiflorus* (Hasuo) mediated straightforward eco-friendly synthesis of silver, gold nanoparticles and evaluation of their anti-cancer activity on A549 lung cancer cell line. Biomed Pharmacother 93:995–1003

33. Suman T, Rajasree SR, Ramkumar R, Rajthilak C, Perumal P (2014) The green synthesis of gold nanoparticles using an aqueous root extract of *Morinda citrifolia* L. Spectrochim Acta Part A 118:11–16
34. Huo Y, Singh P, Kim YJ, Soshnikova V, Kang J, Markus J, Ahn S, Castro-Aceituno V, Mathiyalagan R, Chokkalingam M (2018) Biological synthesis of gold and silver chloride nanoparticles by *Glycyrrhiza uralensis* and in vitro applications. Artif Cells, Nanomed, Biotechnol 46(2):303–312
35. Barai AC, Paul K, Dey A, Manna S, Roy S, Bag BG, Mukhopadhyay C (2018) Green synthesis of *Nerium oleander*-conjugated gold nanoparticles and study of its in vitro anticancer activity on MCF-7 cell lines and catalytic activity. Nano convergence 5(1):10
36. Velammal SP, Devi TA, Amaladhas TP (2016) Antioxidant, antimicrobial and cytotoxic activities of silver and gold nanoparticles synthesized using *Plumbago zeylanica* bark. J Nanostruct Chem 6(3):247–260
37. Karthika V, Arumugam A, Gopinath K, Kaleeswarran P, Govindarajan M, Alharbi NS, Kadaikunnan S, Khaled JM, Benelli G (2017) *Guazuma ulmifolia* bark-synthesized ag, au and ag/au alloy nanoparticles: photocatalytic potential, DNA/protein interactions, anticancer activity and toxicity against 14 species of microbial pathogens. J Photochem Photobiol B 167:189–199
38. Patil MP, Jin X, Simeon NC, Palma J, Kim D, Ngabire D, Kim N, Tarte NH, Kim G (2018) Anticancer activity of *Sasa borealis* leaf extract-mediated gold nanoparticles. Artif Cells, Nanomed Biotechnol 46(1):82–88
39. Chahardoli A, Karimi N, Sadeghi F, Fattahi A (2018) Green approach for synthesis of gold nanoparticles from *Nigella arvensis* leaf extract and evaluation of their antibacterial, antioxidant, cytotoxicity and catalytic activities. Artif Cells, Nanomed, Biotechnol 46(3):579–588
40. Khandanlou R, Murthy V, Saranath D, Damani H (2018) Synthesis and characterization of gold-conjugated *Backhousia citriodora* nanoparticles and their anticancer activity against MCF-7 breast and HepG2 liver cancer cell lines. J Mater Sci 53(5):3106–3118
41. Islam NU, Jalil K, Shahid M, Muhammad N, Rauf A (2015) *Pistacia integerrima* gall extract mediated green synthesis of gold nanoparticles and their biological activities. Arab J Chem 12:2310. https://doi.org/10.1016/j.arabjc.2015.02.014
42. Patil MP, Bayaraa E, Subedi P, Piad LLA, Tarte NH, Kim G (2019) Biogenic synthesis, characterization of gold nanoparticles using *Lonicera japonica* and their anticancer activity on HeLa cells. J Drug Delivery Sci Technol 51:83–90
43. Anand K, Gengan R, Phulukdaree A, Chuturgoon A (2015) Agroforestry waste *Moringa oleifera* petals mediated green synthesis of gold nanoparticles and their anti-cancer and catalytic activity. J Ind Eng Chem 21:1105–1111
44. Geetha R, Ashokkumar T, Tamilselvan S, Govindaraju K, Sadiq M, Singaravelu G (2013) Green synthesis of gold nanoparticles and their anticancer activity. Cancer Nanotechnol 4 (4):91
45. Lokina S, Suresh R, Giribabu K, Stephen A, Sundaram RL, Narayanan V (2014) Spectroscopic investigations, antimicrobial, and cytotoxic activity of green synthesized gold nanoparticles. Spectrochim Acta Part A 129:484–490
46. Basavegowda N, Idhayadhulla A, Lee YR (2014) Phyto-synthesis of gold nanoparticles using fruit extract of *Hovenia dulcis* and their biological activities. Ind Crop Prod 52:745–751
47. Naraginti S, Li Y (2017) Preliminary investigation of catalytic, antioxidant, anticancer and bactericidal activity of green synthesized silver and gold nanoparticles using *Actinidia deliciosa*. J Photochem Photobiol B 170:225–234
48. Nirmala JG, Akila S, Nadar MM, Narendhirakannan R, Chatterjee S (2016) Biosynthesized *Vitis vinifera* seed gold nanoparticles induce apoptotic cell death in A431 skin cancer cells. RSC Adv 6(85):82205–82218
49. Rajan A, Rajan AR, Philip D (2017) *Elettaria cardamomum* seed mediated rapid synthesis of gold nanoparticles and its biological activities. OpenNano 2:1–8

50. Wu T, Duan X, Hu C, Wu C, Chen X, Huang J, Liu J, Cui S (2019) Synthesis and characterization of gold nanoparticles from *Abies spectabilis* extract and its anticancer activity on bladder cancer T24 cells. Artif Cells Nanomed Biotechnol 47(1):512–523
51. Kuppusamy P, Ichwan SJ, Al-Zikri PNH, Suriyah WH, Soundharrajan I, Govindan N, Maniam GP, Yusoff MM (2016) In vitro anticancer activity of au, ag nanoparticles synthesized using *Commelina nudiflora* L. aqueous extract against HCT-116 colon cancer cells. Biol Trace Elem Res 173(2):297–305
52. Singh P, Kim YJ, Wang C, Mathiyalagan R, El-Agamy Farh M, Yang DC (2016b) Biogenic silver and gold nanoparticles synthesized using red ginseng root extract, and their applications. Artif Cells Nanomed Biotechnol 44(3):811–816
53. Markus J, Wang D, Kim Y, Ahn S, Mathiyalagan R, Wang C, Yang DC (2017) Biosynthesis, characterization, and bioactivities evaluation of silver and gold nanoparticles mediated by the roots of Chinese herbal *Angelica pubescens* maxim. Nanoscale Res Lett 12(1):46
54. Velmurugan P, Anbalagan K, Manosathyadevan M, Lee K, Cho M, Lee S, Park J, Oh S, Bang K, Oh B (2014) Green synthesis of silver and gold nanoparticles using *Zingiber officinale* root extract and antibacterial activity of silver nanoparticles against food pathogens. Bioprocess Biosyst Eng 37(10):1935–1943
55. Daisy P, Saipriya K (2012) Biochemical analysis of *Cassia fistula* aqueous extract and phytochemically synthesized gold nanoparticles as hypoglycemic treatment for diabetes mellitus. Int J Nanomedicine 7:1189–1202
56. Dash SS, Majumdar R, Sikder AK, Bag BG, Patra BK (2014) *Saraca indica* bark extract mediated green synthesis of polyshaped gold nanoparticles and its application in catalytic reduction. Appl Nanosci 4(4):485–490
57. Majumdar R, Bag BG, Ghosh P (2016) *Mimusops elengi* bark extract mediated green synthesis of gold nanoparticles and study of its catalytic activity. Appl Nanosci 6(4):521–528
58. Dubey SP, Lahtinen M, Sillanpää M (2010) Green synthesis and characterizations of silver and gold nanoparticles using leaf extract of *Rosa rugosa*. Colloids Surf A Physicochem Eng Asp 364(1–3):34–41
59. Elavazhagan T, Arunachalam KD (2011) *Memecylon edule* leaf extract mediated green synthesis of silver and gold nanoparticles. Int J Nanomedicine 6:1265–1278
60. Dwivedi AD, Gopal K (2010) Biosynthesis of silver and gold nanoparticles using *Chenopodium album* leaf extract. Colloids Surf A Physicochem Eng Asp 369(1–3):27–33
61. Vankar PS, Bajpai D (2010) Preparation of gold nanoparticles from *Mirabilis jalapa* flowers. Ind J Biochem Biophys 47(3):157–160
62. Nagaraj B, Malakar B, Divya T, Krishnamurthy N, Liny P, Dinesh R, Iconaru S, Ciobanu C (2012) Synthesis of plant mediated gold nanoparticles using flower extracts of *Carthamus tinctorius* L.(safflower) and evaluation of their biological activities. Dig J Nanomater Biostruct 7:1289–1296
63. Das RK, Gogoi N, Bora U (2011) Green synthesis of gold nanoparticles using *Nyctanthes arbortristis* flower extract. Bioprocess Biosyst Eng 34(5):615–619
64. Gopinath V, Priyadarshini S, MubarakAli D, Loke MF, Thajuddin N, Alharbi NS, Yadavalli T, Alagiri M, Vadivelu J (2016) Anti-*Helicobacter pylori*, cytotoxicity and catalytic activity of biosynthesized gold nanoparticles: multifaceted application. Arab J Chem 12 (1):33–40
65. Sathishkumar G, Jha PK, Vignesh V, Rajkuberan C, Jeyaraj M, Selvakumar M, Jha R, Sivaramakrishnan S (2016) Cannonball fruit (*Couroupita guianensis*, Aubl.) extract mediated synthesis of gold nanoparticles and evaluation of its antioxidant activity. J Mol Liq 215:229–236
66. Desai MP, Sangaokar GM, Pawar KD (2018) Kokum fruit mediated biogenic gold nanoparticles with photoluminescent, photocatalytic and antioxidant activities. Process Biochem 70:188–197

67. Yu J, Xu D, Guan HN, Wang C, Huang LK (2016) Facile one-step green synthesis of gold nanoparticles using *Citrus maxima* aqueous extracts and its catalytic activity. Mater Lett 166:110–112
68. Aromal SA, Philip D (2012) Green synthesis of gold nanoparticles using *Trigonella foenum-graecum* and its size-dependent catalytic activity. Spectrochim Acta Part A 97:1–5
69. Jayaseelan C, Ramkumar R, Rahuman AA, Perumal P (2013) Green synthesis of gold nanoparticles using seed aqueous extract of *Abelmoschus esculentus* and its antifungal activity. Ind Crop Prod 45:423–429
70. Sneha K, Sathishkumar M, Lee SY, Bae MA, Yun Y (2011) Biosynthesis of au nanoparticles using cumin seed powder extract. J Nanosci Nanotechnol 11(2):1811–1814
71. Ahmad A, Senapati S, Khan MI, Kumar R, Ramani R, Srinivas V, Sastry M (2003) Intracellular synthesis of gold nanoparticles by a novel alkalotolerant actinomycete, *Rhodococcus* species. Nanotechnol 14(7):824–828
72. Southam G, Beveridge TJ (1996) The occurrence of sulfur and phosphorus within bacterially derived crystalline and pseudocrystalline octahedral gold formed in vitro. Geochim Cosmochim Acta 60(22):4369–4376
73. Rajeshkumar S (2016) Anticancer activity of eco-friendly gold nanoparticles against lung and liver cancer cells. J Genet Eng Biotechnol 14(1):195–202
74. Manivasagan P, Alam MS, Kang K, Kwak M, Kim S (2015) Extracellular synthesis of gold bionanoparticles by *Nocardiopsis* sp. and evaluation of its antimicrobial, antioxidant and cytotoxic activities. Bioprocess Biosyst Eng 38(6):1167–1177
75. El-Batal A, Mona S, Al-Tamie M (2015) Biosynthesis of gold nanoparticles using marine *Streptomyces cyaneus* and their antimicrobial, antioxidant and antitumor (in vitro) activities. J Chem Pharm Res 7:1020–1036
76. Mukherjee P, Senapati S, Mandal D, Ahmad A, Khan MI, Kumar R, Sastry M (2002) Extracellular synthesis of gold nanoparticles by the fungus *Fusarium oxysporum*. Chem Bio Chem 3(5):461–463
77. Mukherjee P, Ahmad A, Mandal D, Senapati S, Sainkar SR, Khan MI, Ramani R, Parischa R, Ajayakumar P, Alam M (2001) Bioreduction of AuCl4− ions by the fungus, *Verticillium* sp and surface trapping of the gold nanoparticles formed. Angew Chem Int Ed 40(19):3585–3588
78. Mishra A, Tripathy SK, Wahab R, Jeong S, Hwang I, Yang Y, Kim Y, Shin H, Yun S (2011) Microbial synthesis of gold nanoparticles using the fungus *Penicillium brevicompactum* and their cytotoxic effects against mouse mayo blast cancer $C_2C_{12}$ cells. Appl Microbiol Biotechnol 92(3):617–630
79. Pimprikar P, Joshi S, Kumar A, Zinjarde S, Kulkarni S (2009) Influence of biomass and gold salt concentration on nanoparticle synthesis by the tropical marine yeast *Yarrowia lipolytica* NCIM 3589. Colloids Surf B Biointerfaces 74(1):309–316
80. Chauhan A, Zubair S, Tufail S, Sherwani A, Sajid M, Raman SC, Azam A, Owais M (2011) Fungus-mediated biological synthesis of gold nanoparticles: potential in detection of liver cancer. Int J Nanomedicine 6:2305–2319
81. Das SK, Liang J, Schmidt M, Laffir F, Marsili E (2012) Biomineralization mechanism of gold by zygomycete fungi *Rhizopus oryzae*. ACS Nano 6(7):6165–6173
82. Gupta S, Bector S (2013) Biosynthesis of extracellular and intracellular gold nanoparticles by *Aspergillus fumigatus* and *A. flavus*. Antonie Van Leeuwenhoek 103(5):1113–1123
83. He S, Guo Z, Zhang Y, Zhang S, Wang J, Gu N (2007) Biosynthesis of gold nanoparticles using the bacteria *Rhodopseudomonas capsulata*. Mater Lett 61(18):3984–3987
84. Nangia Y, Wangoo N, Goyal N, Shekhawat G, Suri CR (2009) A novel bacterial isolate *Stenotrophomonas maltophilia* as living factory for synthesis of gold nanoparticles. Microb Cell Factories 8(1):39
85. Beveridge TJ, Murray RG (1980) Sites of metal deposition in the cell wall of *Bacillus subtilis*. J Bacteriol 141(2):876–887
86. Husseiny M, El-Aziz MA, Badr Y, Mahmoud M (2007) Biosynthesis of gold nanoparticles using *Pseudomonas aeruginosa*. Spectrochim Acta Part A 67(3–4):1003–1006

87. Suresh AK, Pelletier DA, Wang W, Broich ML, Moon J, Gu B, Allison DP, Joy DC, Phelps TJ, Doktycz MJ (2011) Biofabrication of discrete spherical gold nanoparticles using the metal-reducing bacterium *Shewanella oneidensis*. Acta Biomater 7(5):2148–2152
88. Correa-Llantén DN, Muñoz-Ibacache SA, Castro ME, Muñoz PA, Blamey JM (2013) Gold nanoparticles synthesized by *Geobacillus* sp. strain ID17 a thermophilic bacterium isolated from Deception Island, Antarctica. Microb Cell Fact 12(1):75
89. Fayaz AM, Girilal M, Rahman M, Venkatesan R, Kalaichelvan P (2011) Biosynthesis of silver and gold nanoparticles using thermophilic bacterium *Geobacillus stearothermophilus*. Process Biochem 46(10):1958–1962
90. Ahmad A, Senapati S, Khan MI, Kumar R, Sastry M (2005) Extra−/intracellular biosynthesis of gold nanoparticles by an alkalotolerant fungus, *Trichothecium* sp. J Biomed Nanotechnol 1 (1):47–53
91. Castro-Longoria E, Vilchis-Nestor AR, Avalos-Borja M (2011) Biosynthesis of silver, gold and bimetallic nanoparticles using the filamentous fungus *Neurospora crassa*. Colloids Surf B Biointerfaces 83(1):42–48
92. Xie J, Lee JY, Wang DI, Ting YP (2007a) High-yield synthesis of complex gold nanostructures in a fungal system. J Phys Chem C 111(45):16858–16865
93. Balakumaran MD, Ramachandran R, Balashanmugam P, Mukeshkumar DJ, Kalaichelvan PT (2016) Mycosynthesis of silver and gold nanoparticles: optimization, characterization and antimicrobial activity against human pathogens. Microbiol Res 182:8–20
94. Shakibaie M, Forootanfar H, Mollazadeh-Moghaddam K, Bagherzadeh Z, Nafissi-Varcheh N, Shahverdi AR, Faramarzi MA (2010) Green synthesis of gold nanoparticles by the marine microalga *Tetraselmis suecica*. Biotechnol Appl Biochem 57(2):71–75
95. Senapati S, Syed A, Moeez S, Kumar A, Ahmad A (2012) Intracellular synthesis of gold nanoparticles using alga *Tetraselmis kochinensis*. Mater Lett 79:116–118
96. Luangpipat T, Beattie IR, Chisti Y, Haverkamp RG (2011) Gold nanoparticles produced in a microalga. J Nanopart Res 13(12):6439–6445
97. Singaravelu G, Arockiamary J, Kumar VG, Govindaraju K (2007) A novel extracellular synthesis of monodisperse gold nanoparticles using marine alga, *Sargassum wightii* Greville. Colloids Surf B Biointerfaces 57(1):97–101
98. Singh M, Kalaivani R, Manikandan S, Sangeetha N, Kumaraguru A (2013) Facile green synthesis of variable metallic gold nanoparticle using *Padina gymnospora*, a brown marine macroalga. Appl Nanosci 3(2):145–151
99. Venkatesan J, Manivasagan P, Kim S, Kirthi AV, Marimuthu S, Rahuman AA (2014) Marine algae-mediated synthesis of gold nanoparticles using a novel *Ecklonia cava*. Bioprocess Biosyst Eng 37(8):1591–1597
100. Sharma B, Purkayastha DD, Hazra S, Gogoi L, Bhattacharjee CR, Ghosh NN, Rout J (2014) Biosynthesis of gold nanoparticles using a freshwater green alga, *Prasiola crispa*. Mater Lett 116:94–97
101. Sharma A, Sharma S, Sharma K, Chetri SP, Vashishtha A, Singh P, Kumar R, Rathi B, Agrawal V (2016) Algae as crucial organisms in advancing nanotechnology: a systematic review. J Appl Phycol 28(3):1759–1774
102. Dahoumane SA, Mechouet M, Wijesekera K, Filipe CD, Sicard C, Bazylinski DA, Jeffryes C (2017) Algae-mediated biosynthesis of inorganic nanomaterials as a promising route in nanobiotechnology–a review. Green Chem 19(3):552–587
103. Kaplan D, Christiaen D, Arad SM (1987) Chelating properties of extracellular polysaccharides from *Chlorella* spp. Appl Environ Microbiol 53(12):2953–2956
104. Dahoumane SA, Yéprémian C, Djédiat C, Couté A, Fiévet F, Coradin T, Brayner R (2016) Improvement of kinetics, yield, and colloidal stability of biogenic gold nanoparticles using living cells of *Euglena gracilis* microalga. J Nanopart Res 18(3):79
105. Naveena BE, Prakash S (2013) Biological synthesis of gold nanoparticles using marine algae *Gracilaria corticata* and its application as a potent antimicrobial and antioxidant agent. Asian J Pharm Clin Res 6(2):179–182

106. Xie J, Lee JY, Wang DI, Ting YP (2007b) Identification of active biomolecules in the high-yield synthesis of single-crystalline gold nanoplates in algal solutions. Small 3(4):672–682
107. Abdel-Raouf N, Al-Enazi NM, Ibraheem IB (2017) Green biosynthesis of gold nanoparticles using *Galaxaura elongata* and characterization of their antibacterial activity. Arab J Chem 10: S3029–S3039
108. Namvar F, Azizi S, Ahmad MB, Shameli K, Mohamad R, Mahdavi M, Tahir PM (2015) Green synthesis and characterization of gold nanoparticles using the marine macroalgae *Sargassum muticum*. Res Chem Int 41(8):5723–5730
109. Parial D, Patra HK, Dasgupta AK, Pal R (2012) Screening of different algae for green synthesis of gold nanoparticles. Eur J Phycol 47(1):22–29
110. Bogireddy N, Pal U, Gomez LM, Agarwal V (2018) Size controlled green synthesis of gold nanoparticles using *Coffea arabica* seed extract and their catalytic performance in 4-nitrophenol reduction. RSC Adv 8(44):24819–24826
111. Waclawek S, Goncukova Z, Adach K, Fijalkowski M, Cernik M (2018) Green synthesis of gold nanoparticles using *Artemisia dracunculus* extract: control of the shape and size by varying synthesis conditions. Environ Sci Pollut Res Int 25(24):24210–24219
112. Vimalraj S, Ashokkumar T, Saravanan S (2018) Biogenic gold nanoparticles synthesis mediated by *Mangifera indica* seed aqueous extracts exhibits antibacterial, anticancer and anti-angiogenic properties. Biomed Pharmacother 105:440–448
113. Soenen SJ, Manshian B, Montenegro JM, Amin F, Meermann B, Thiron T, Cornelissen M, Vanhaecke F, Doak S, Parak WJ, De Smedt S, Braeckmans K (2012) Cytotoxic effects of gold nanoparticles: a multiparametric study. ACS Nano 6(7):5767–5783
114. Gong N, Chen S, Jin S, Zhang J, Wang PC, Liang XJ (2015) Effects of the physicochemical properties of gold nanostructures on cellular internalization. Regen Biomater 2(4):273–280
115. Pan Y, Neuss S, Leifert A, Fischler M, Wen F, Simon U, Schmid G, Brandau W, Jahnen-Dechent W (2007) Size-dependent cytotoxicity of gold nanoparticles. Small 3(11):1941–1949
116. Singh M, Kumar M, Manikandan S, Chandrasekaran N, Mukherjee A, Kumaraguru A (2014) Drug delivery system for controlled cancer therapy using physico-chemically stabilized bioconjugated gold nanoparticles synthesized from marine macroalgaem, *Padina gymnospora*. J Nanomed Nanotechnol Doi s5. https://doi.org/10.4172/2157-7439.S5-009
117. Gonzalez-Ballesteros N, Prado-Lopez S, Rodriguez-Gonzalez JB, Lastra M, Rodriguez-Arguelles MC (2017) Green synthesis of gold nanoparticles using brown algae *Cystoseira baccata*: its activity in colon cancer cells. Colloids Surf B Biointerfaces 153:190–198
118. Banu H, Renuka N, Faheem SM, Ismail R, Singh V, Saadatmand Z, Khan SS, Narayanan K, Raheem A, Premkumar K, Vasanthakumar G (2018) Gold and silver nanoparticles biomimetically synthesized using date palm pollen extract-induce apoptosis and regulate p53 and Bcl-2 expression in human breast adenocarcinoma cells. Biol Trace Elem Res 186 (1):122–134

# Toxicity of Green-made Bacteriogenic Silver Nanoparticles Against Bacterial Pathogens: A Critical Review

10

Adriano Magesky and Émilien Pelletier

**Abstract**

Silver has long time been used as a powerful antimicrobial agent against human pathogens. More recently, incorporating silver nanoparticles in medical tools has become an ultimate strategy to control bacterial biofilm colonization and avoid hospital-acquired diseases in immunocompromised patients. This continued effort has been now reoriented to the potential biomedical applications of the green silver nanoparticles. Besides, a green synthesis appears to be a safer, cheaper, and more effective method to produce a larger amount of silver nanoparticles (AgNPs). In this context, the bacteria-mediated synthesis of AgNPs has been largely used to make green silver nanoparticles (g-AgNPs) owing to the bacterial bioactive biomolecules and the natural capacity of bacteria strains to handle trace metals. We herein exhaustively evaluated the publications describing the production of g-AgNPs mostly using bacteria liquid extracts and their application as antibacterial agents in toxicity assays. *Actinobacteria*, *Proteobacteria*, and *Firmicutes* were the mostly used phyla to synthesize bacteriogenic g-AgNPs. Unfortunately, some technical flaws (undefined nominal concentrations, lack of silver quantification and kinetics of g-AgNP, unawareness of exposure media composition and bacteria biology) jeopardized the g-AgNP final assessment. Henceforth, only a few studies seemed to support a real efficacy of bacteriogenic g-AgNPs to cope on itself with pathogenic bacteria or associated with classical antibiotics bringing the so-called synergistic effect. We further indicated some points to be considered for testing green nanosilver in toxicity

A. Magesky (✉)
CHU de Québec-Université Laval, Québec-QC/Institut National de Santé Publique du Québec (INSPQ), Québec, QC, Canada
e-mail: adriano.da-silva-magesky@inspq.qc.ca

É. Pelletier
Institut des Sciences de la Mer de Rimouski (ISMER), Université du Québec à Rimouski, 310, allée des Ursulines Rimouski, QC, Canada

© Springer Nature Singapore Pte Ltd. 2020

Q. Saquib et al. (eds.), *Green Synthesis of Nanoparticles: Applications and Prospects*, https://doi.org/10.1007/978-981-15-5179-6_10

assays with bacteria and how g-AgNP toxicity mechanisms could be better assessed in single and multiple exposures.

**Keywords**

Green silver nanoparticles · Biogenic AgNPs · Antibacterial AgNPs · Green nanoparticles

## 10.1 Introduction

Bulk and colloidal silver have culturally a long history of being integrated in the medical practices to fight microbial infections. Back to those times, silver salts were largely used as antibacterial agents against conjunctivitis, gastroenteritis, gonorrhea, and syphilis [1]. Currently, silver ($Ag^0$) has been continuously incorporated as nanoscale particles in everyday life products and medical tools. To secure aseptic practices, medical tools highly susceptible to microbial colonization such as orthopedic implants, synthetic fibrous for sutures, catheters, bandages, surgical meshes, vascular prosthesis, etc. have been successfully fabricated with addition of nanosilver or other silver compounds [2]. As an example, incorporating 0.5% of silver nanoparticles (AgNPs) in acrylic bone cement can significantly reduce biofilm formation of *Staphylococcus epidermidis* and *S. aureus* and prevent colonization, proliferation, and infection [3].

Even though recent studies have shown that some Gram-negative bacteria may develop resistance to minimal inhibitory concentrations (MIC) of AgNPs (3.38 mg. $L^{-1}$) after chronic exposures, they are still viewed as powerful nanoweapons [4]. Thereby AgNP has been also amended with antibacterial molecules. It is postulated that mechanisms of chemically synthesized AgNPs against bacteria involve electrostatic attraction between nanoparticles and the cell wall, production of free radicals, changes in membrane permeability, disturbance of respiratory chain, leakage of intracellular organelles, interaction with thiol groups, further inhibition of protein synthesis, and interaction with phosphorus-containing molecules as DNA [5]. All effects aforementioned might be optimized when AgNPs are coated with biologically active molecules, coming from vascular plants, algae, or microorganisms [6]. In fact, new experiments have been trying to integrate effects of both green and chemically made AgNPs and antibiotics in multiple exposures by functionalizing AgNP surfaces to harm bacteria cells. Lately, the biosynthesis of the so-called green silver nanoparticles (g-AgNPs) represents a new approach in treatment efficiency of microbial diseases [6, 7]. As demonstrated by Divya et al. [8], 30–50 nm g-AgNP-30 μg.mL coating treatment of urinary catheter can significantly prevent biofilm formation by Gram-positive and Gram-negative bacteria known to cause urinary tract infections.

As a rule, a green synthesis of AgNPs by microbial routes basically relies on two approaches: extracellular and intracellular. The intracellular route relies on the

ability of cell enzymatic machinery to reduce $Ag^+$ ions accumulated in the intracellular milieu to precipitate $Ag^0$ in situ as nanocrystals. Once the cells reach the optimum time for harvesting, a complementary treatment allows the extraction of the g-AgNPs. On another hand, with the extracellular route, biomolecules released by growing bacteria, for example, are separated from their remaining biomass after centrifugation, and used later on to convert aqueous $AgNO_3$ into nano-colloidal green silver within 24 h. Sometimes the whole bacteria biomass is used as biological matrix to nano-Ag production. In this case, a release of intracellular organics and/or biomolecules on bacteria surface (as amino acids or exopolysaccharides, EPS) may act as reducing agents for some species [9, 10]. Once exposed to Ag, bacteria will depend on their defense mechanisms to control the metal uptake and manage its levels inside the cells. Extracellular polymeric substances produced by proteobacterium *Escherichia coli*, for example, are proved to reduce surrounding $Ag^+$ into AgNP through hemiacetal and aldehyde groups mitigating thus silver toxicity [11]. Nanoparticles can be also produced by redox reactions inside or outside the cells with involvement of NADH-dependent nitrate reductases, as it happens with marine *Streptomyces* sp. LK3 [12]. This mechanism has been found with cultures of betaproteobacterium *Alcaligenes faecalis* as well [8]. Another case is given by Lengke et al. [13] on the biomineralization of Ag by filamentous cyanobacteria *Plectonema boryanum* from silver (I) nitrate complex. The authors found that 560 mg.L-$AgNO_3$ was precipitated as AgNPs at cell surface (1–200 nm) and within cells (<10 nm) at 25 to 100 °C. In addition, the release of organics from dead cyanobacteria caused further precipitation of AgNPs in solution. In any case, a plethora of biomolecules available in the cell-free supernatant or on bacterial biomass mediate silver reduction and final capping of silver nanoparticles in vitro.

Herein we critically reviewed the studies dealing with the antibacterial properties of eco-friendly AgNPs produced by means of bacteria biomolecules. Experiments were carried out in typical assays for predicting acute toxicity (24–48 h) in agar or broth liquid media at 37 °C. The agar disc or well diffusion, and broth dilution were the mostly used methods to assess antibacterial effects in these studies. Unfortunately, some crucial information for experimental repeatability was often neglected in many reports. Likewise, the lack of chemical data related to soluble Ag and nanosilver forms was another drawback observed. If mechanisms controlling green nanosilver toxicity must be comprehended, the kinetics of g-AgNP dissolution and dispersion in exposure media have to be documented. On another hand, a remarkable outcome of all studies was the diversity of bacteria taxa used for green nano-Ag synthesis. By far, strains of phylum Actinobacteria have been involved for bio-mediated synthesis of AgNPs in about 50% of assays. Actinobacteria have high guanine + cytosine content, and are ubiquitous Gram-positive bacteria present in several ecosystems, especially in the marine environment. Harboring an array of biosynthetic gene clusters, they have an unsurpassed ability to synthesize secondary metabolites of industrial and pharmacological interest [14]. The genus *Streptomyces*

(Actinobacteria) is present in 77% of reviewed publications, followed by *Nocardiopsis* (15%) and *Rhodococcus* (8%).

In addition to Actinobacteria, two other bacterial phyla have been used as biological models: Proteobacteria and Firmicutes. Gammaproteobacteria lineage is primarily Gram-negative, as all the others found in Proteobacteria (as Alphaproteobacteria and Betaproteobacteria lineage). Gammaproteobacteria taxon was present at 39% of reported assays, and then Alphaproteobacteria and Betaproteobacteria were used at 15% each. While bacteria species from Gammaproteobacteria lineage are of medical, ecological, and scientific importance like those from genus *Pseudomonas;* members from Alphaproteobacteria adopt an intracellular lifestyle as plant or animal pathogens, or even as plant mutualists like nonnodulating *Bradyrhizobium* spp. [15]. Similarly, Betaproteobacteria clade represents a broad variety of habitats and metabolic strategies with members inhabiting oligotrophic groundwater ecosystems and constructed wetlands, or even opportunistically living in human body as *Alcaligenes faecalis*. Finally, we also registered some bacilli used as medium for AgNP synthesis. Genera *Bacillus*, *Aneurinibacillus*, and *Lactococcus* (Firmicutes) corresponded to 31% of the chosen experimental organisms. Species from Firmicutes have low guanine + cytosine content and mostly show Gram-positive stain. This phylum is known to comprise species largely abundant in soil and aquatic environments, inhabiting normal flora of mammalian intestines, or being pathogenic to plants, to animals; but especially to humans. The species *Lactococcus lactis*, as an example, has some special biochemical features making them very valuable to the food industry [16].

As previously mentioned, there is scarce chemical data to properly address mechanisms of antibacterial biosynthesized AgNPs. The understanding of toxicity mechanisms of g-AgNPs can get even more complicated when g-AgNPs are used together with antibiotics in order to elucidate their combined effects on bacteria growth. Few researchers have started testing the molecular interactions of g-AgNPs with antibiotics, but much work has yet to be done to clearly understand the complexity of such mechanisms when g-AgNPs are involved. Often times, the wanted synergistic effects of g-AgNP + drug ended up with unexpectedly negative effects and no enhanced inhibition. Therefore, the aim of this chapter is first to briefly review the information available on AgNP biosynthesis with bacteria extracts and mainly explore their toxicity effects against pathogenic bacteria. Then we discuss some mechanisms by which g-AgNPs might be operating against pathogenic bacteria in single exposures or when associated with antibiotics.

## 10.2 Antibacterial Effects of Green Nanosilver Produced by Extracts of Actinobacteria

From cell-free extracts of marine actinobacterium *Nocardiopsis* sp. (MBRC-1) isolated from marine sediment, Manivasagan et al. [17] synthesized mostly spherical and aggregated 30–90 nm g-AgNPs. These nanoparticles were enrobed by different biomolecules whose chemical profiles were obtained by Fourier transform infrared

(FT-IR) spectroscopy analysis. Spectra indicated the presence of -OH stretches, C-H groups related to alkanes, -C=C- from alkenes, and H:C-H bend of the alkyne group. After exposing *Escherichia coli*, *Bacillus subtilis*, *Enterococcus hirae*, *Pseudomonas aeruginosa*, *Shigella flexneri*, and *Staphylococcus aureus* to g-AgNPs (10–50 μg.mL) at 35 °C up to 24 h, growth inhibition ocurred in a concentration-dependent trend. The highest antibacterial activity was detected against *B. subtilis* and *P. aeruginosa*. Interestingly, growth inhibition zones by all microorganisms tested were only wider than those induced by amoxicillin (positive control, 30 μg.mL) once g-AgNPs exceeded 30 μg.mL. As a consequence, the minimum inhibitory concentration of g-AgNPs was always ~1.1-fold stronger for each bacteria tested than those used with a classic antibiotic molecule. Similarly, Rajivgandhi et al. [18] exposed a strain of methicillin-resistant coagulase-negative *Staphylococcus* sp. to well dispersed and roughly spherical 20–50 nm g-AgNPs (5–100 μg.mL) obtained from 20 g biomass of marine *Nocardiopsis* sp. GRG1 (KT235640) challenged with 1 mM (170 μg.mL) $AgNO_3$ at 28 °C within 6 days. These *Nocardiopsis* AgNPs showed N-H vibration motions of amides and amines and C-Cl moieties in alkyl halides by FT-IR. Only medium to large concentrations (50–100 μg.mL) of g-AgNPs prevented *Staphylococcus* sp. from growing at ~18 mm (50 μg.mL) and ~15 mm (100 μg.mL) within 24 h at 37 °C, contrarily to ceftazidime (positive control, 30 μg.mL).

Using 2 isolates of *Streptomyces rochei* (MHM13) from marine sediment, Abd-Elnaby et al. [19] obtained spherical 22–85 nm g-AgNPs. To reduce $Ag^+$ to nanosilver, 1 mM (170 μg.mL) of $AgNO_3$ (50 mL) was mixed with actinomycete supernatants (50 mL) at pH 8.5. After synthesis, capping agents of g-AgNPs held IR stretches for primary amines (N-H), alkanes (C-H), carbon dioxide (O=C=O), aliphatic ethers (C-O), halo compounds (C-Cl or C-Br), and bending for alkanes (C-H). From the stock solution of g-AgNPs obtained, 50 μL aliquots were injected to exposure media with growing bacteria. Unexpectedly, g-AgNPs of isolate 13 induced the maximum zones of inhibition (16–19 mm) against all bacteria tested, but especially against *Vibrio fluvialis;* while g-AgNPs of isolate 38 caused moderate zones of inhibition (13–18 mm) (see Adb-Elnaby et al. [19] in Table 10.1). *E. coli* and *P. aeruginosa* were not affected by isolate 38 g-AgNPs. Later on, the authors combined isolate 13 g-AgNPs with antibiotics (Table 10.1) to evaluate mixed chemical effects on *V. fluvialis*, *Vibrio damsel*, *Salmonella typhimurium*, and *Escherichia coli* at 37 °C overnight. As a result, the antimicrobial effects were in some way enhanced by all chemicals associated with nanosilver (for a more detailed discussion between g-AgNPs and antibacterial drug interactions, see Sect. 10.5). Notwithstanding, the newly produced stock solution of g-AgNP was used without any dialysis process to isolate nanoparticles from unreacted biomolecules and residual soluble Ag, which is an active antimicrobial metal. Furthermore, due to dilution effect caused by mixture of both silver stock solution and actinomycete liquid extract, it is difficult (even impossible) to estimate what were the final nominal concentrations of g-AgNPs actually tested.

Along similar lines, 100 μg.mL of nearly spherical 30 nm g-AgNPs produced from marine *Streptomyces violaceus* (MM72) extracts caused strong antibacterial

**Table 10.1** Summary of the main features of g-AgNP synthesis and exposure conditions of toxicity assays for Actinobacteria isolates used for biosynthesis of nanosilver

| Biological matrices used for green AgNPs synthesis | Microorganism habitat | AgNP size after biosynthesis | AgNP morphological features after biosynthesis | Supernatant/AgNP functional groups (FT-IR or $^{1}$HNMR spectral analysis) | Final nominal concentrations of g-AgNPs | Microorganisms exposed to g-AgNPs | Time of exposure and temperature | Drugs as positive controls |
|---|---|---|---|---|---|---|---|---|
| Cell-free supernatant of *Streptomyces albogriseolus* [20] | Mangrove sediment | 16.25 ± 1.6 nm | Agglomerated, almost spherical | NH, C-O ester groups, C=O, C=C=C (polyenes). Both proteins and polyenes | Not provided | *Staphylococcus aureus* (NCIM2672), *Bacillus cereus* (NCIM2458), and *Escherichia coli* (NCIM2809) | 24 h; room temperature | None |
| Cell-free supernatant of *Streptomyces* sp. (BDUKAS10) [21] | Mangrove sediment | 21–48 nm | Agglomerated, predominantly spherical | NH and -C=C- | Not provided | *Bacillus cereus* (MTCC1272), *Pseudomonas aeruginosa* (MTCC1688), and *Staphylococcus aureus* (MTCC96) | 14 h; 37 °C | None |
| Cell-free supernatant of *Nocardiopsis* sp. (MBRC-1) [17] | Marine sediment | 30–90 nm with an average of 45 ± 0.05 nm | Mostly spherical aggregates | OH, CH (alkanes), -C=C- (alkenes), C=C-H:CH (of the alkynes group) | 10, 20, 30, 40, and 50 μg. mL | *Escherichia coli*, *Bacillus subtilis*, *Enterococcus hirae*, *Pseudomonas aeruginosa*, *Shigella flexneri*, *and Staphylococcus aureus* | 24 and 48 h; 35 °C | Amoxicillin and nystatin (30 μg. mL) |
| Biomass of *Streptomyces naganishii* (MA7) [22] | Soil from a magnesite mine region | 5–50 nm | Mostly spherical | NH, C=O, $CH_3$-R, amide I, -COO, amide III, and -C-O-C- | 1000, 5000, and 10 000 μg. mL | *Pseudomonas* sp. P1, *Aeromonas* sp. P26, *Bacillus* sp. P31, *Bacillus* sp. P46, *Alcaligenes* sp. P47, *Micrococcus* sp. P56, *Staphylococcus* sp. PP3, *Micrococcus* sp. PP5, *Aeromonas* sp. PP6, *Alcaligenes* sp. PP8 | 24 h; 37 °C | Erythromycin, chloramphenicol, tetracycline, and vancomycin (concentrations not mentioned) |
| Cell-free solution of actinorhodin pigment extracted from *Streptomyces coelicolor* [23] | Soil | 28–50 nm | Irregular shape | Cyclic C-O-C, C=O, and OH | Not provided | *Staphylococcus aureus* (MRSA) | 18 h; 37 °C | Gentamicin (10 μg.Disc) and oxacillin (1 μg. Disc) |
| Grown culture of *Rhodococcus* sp. NCIM2891 [24] | Soil, water and eukaryotic cells (but in this case the strain was already isolated) | 10–50 nm | Stable and spherical | Amides I and II, aromatic and aliphatic amines, carbonyl | 30, 50, and 100 μg.mL | *Staphylococcus aureus*, *Klebsiella pneumoniae*, *Proteus vulgaris*, *Enterococcus faecalis*, *Pseudomonas aeruginosa*, and *Escherichia coli* | 50 h; _ | None |

| | | | | | | | | |
|---|---|---|---|---|---|---|---|---|
| Cell-free supernatant of *Streptomyces kasugaensis* (NH28/M338-M1) [25] | Terrestrial ecosystem (isolated from humic layer of pine soil) | 4–65 ± 9.7 nm, mean size of 13 nm | Polydispersed and spherical | Not determined | 1.25–200 μg.mL | *Salmonella infantis*, *Proteus mirabilis*, *Bacillus subtilis* (ATTC6633), *Staphylococcus aureus* (ATTC6338), *Klebsiella pneumoniae* (ATTC700603), *Pseudomonas aeruginosa* (ATTC10145), and *Escherichia coli* (ATTC8739) | 24 h; 37 °C | Not mentioned which one it was used |
| Cell-free supernatant of *Streptomyces rochei* (MHM13, isolates 13 and 38) [19] | Marine sediment | 22–85 nm | Spherical | NH (stretch primary amine), CH (stretch alkane), O=C=O (stretch carbon dioxide), C=C (stretch alkene), CH (bend alkane), C-O (stretch aliphatic ether), C-Cl, or C-Br (stretch halo compounds) | Not provided | *Bacillus subtilis*, *Staphylococcus aureus*, *Pseudomonas aeruginosa*, *Bacillus cereus*, *Salmonella typhimurium*, *Escherichia coli*, *Vibrio fluvialis*, *Vibrio damsela* | Overnight; 37 °C | Ciprofloxacin (5 μg.Disc), ampicillin (10 μg. Disc), streptomycin (10 μg.Disc), gentamicin (10 μg.Disc), tetracycline (10 μg.Disc), lincomycin (2 μg. Disc) |
| Cell-free culture supernatant of *Streptomyces exfoliatus* ICN25 [26] | Rhizome soil region (from an estuarine mangrove) | 10–40 nm | Aggregated with spherical and rod shapes | Major peaks in spectrum of AgNPs were observed at 3464.27, 3431.48, 2063.9, and 1637.62, and a minor peak was observed at 586.38 $cm^{-1}$, corresponding to protein components | 10 μg.mL | Methicillin-resistant *Staphylococcus aureus* (ATCC33591), methicillin-sensitive *Staphylococcus aureus* (ATCC29213), *Escherichia coli* (ATCC35218), *Pseudomonas aeruginosa* (ATCC27853), and *Klebsiella pneumoniae* (ATCCBAA-1705) | 24 h; 37 °C | None |
| Cell-free supernatant of *Streptomyces violaceus* (MM72) [27] | Marine coastal sediment | 10–60 nm, mean size of 30 nm | Well dispersed and mostly spherical | The presence of α-D-galactopyranose units, the sugar backbone components (glucose and galactose residues), and rhamnose residues | 100 μg.mL | *Escherichia coli*, *Pseudomonas aeruginosa*, *Staphylococcus aureus*, and *Bacillus subtilis* | 24 h; 28 °C | Tetracycline (concentrations not mentioned) |

(continued)

**Table 10.1** (continued)

| Biological matrices used for green AgNPs synthesis | Microorganism habitat | AgNP size after biosynthesis | AgNP morphological features after biosynthesis | Supernatant/AgNP functional groups (FT-IR or $^{1}$HNMR spectral analysis) | Final nominal concentrations of g-AgNPs | Microorganisms exposed to g-AgNPs | Time of exposure and temperature | Drugs as positive controls |
|---|---|---|---|---|---|---|---|---|
| Cell-free supernatant of *Streptomyces* sp. Al-Dhabi-87 [28] | Marine sediment | 10–17 nm | Slightly polydispersed, mostly agglomerated | Bands were detected at 1050.0, 1100, 1392.5, 1500, 1800, 1920, and 2900 $cm^{-1}$ in the FT-IR spectrum | Not provided | *Bacillus subtilis*, *Enterococcus faecalis* (ATCC29212), *Staphylococcus epidermis* (ATCC12228), *S. aureus* (ATCC29213, WC25V880854, V552, ATCC43300, TC7692), *Pseudomonas aeruginosa* (MDR4406, ATCC27853), *Klebsiella pneumoniae* (ATCC0063), *Escherichia coli* (ATCC25922, ESBL4345, ATCC35218), *Acinetobacter baumannii* (MDR4414, MDR4474, 4414, MDR4273, MDR7077, MRO3964), *Proteus mirabilis* (DR4753), *Enterococcus faecium* (VRETC773, VREUR83198) | 17 h; 37 °C | None |
| Cell-free supernatant of *Streptomyces olivaceus* (MSU3) [29] | Marine ecosystem | ~12 nm | Monodispersed and almost spherical in shape | C=CH, R-OH, C=N-OH, C-C, R-COOH, and R-$NH_2$ | 0.313, 0.625, 1.25, 2.5, 5, 10, and 20 μg.mL | *Streptococcus mutant* (NCIM2063), *Streptococcus pneumoniae* (ATCC49619), *Klebsiella pneumoniae* (ATCC10273), *Escherichia coli* (ATCC25922), *Enterobacter faecalis* (ATCC29212) | 24 h; 37 °C | Chloramphenicol (25 μg.mL) |
| Biomass of *Nocardiopsis* sp. GRG1 (KT235640) [18] | Marine ecosystem | 20–50 nm, mostly 35 nm | Well dispersed and spherical | NH vibration motions of amides and amines and C-Cl moieties in alkyl halides | 5, 50, and 100 μg.mL | Bacterial strain of methicillin-resistant coagulase-negative *Staphylococcus* sp. (MR-CoNS) | 24 h; 37 °C | Ceftazidime (30 μg.mL) |

activity against *Escherichia coli* and *Pseudomonas aeruginosa* (with ~16 mm of inhibition zone for each), whereas *Bacillus subtilis* and *Staphylococcus aureus* were less affected. Both showed ~10 and ~ 4 mm of growth inhibition at 28 °C within 24 h, respectively [27]. In this study, Gram-negative bacteria had higher sensitivity than the Gram-positive ones. With *Streptomyces violaceus* (MM72)-g-AgNPs, α-D-galactopyranose units as well as sugar backbone components (such as glucose and galactose residues) and rhamnose residues were depicted by proton nuclear magnetic resonance ($^1$HNMR) analysis. Reducing sugars are known to be actively involved in AgNP mineralization in bacteria. After reaction with dissolved silver, the bands corresponding to rhamnose and pyranose structures normally become much weaker in the FT-IR spectra, while the bands of carboxyl groups get much sharper and stronger in exopolysaccharides of *Escherichia coli*. It means that aldehyde groups in these sugars were oxidized to carboxyl groups by $Ag^+$ [11].

Smaller and dispersed 15 nm g-AgNPs have been also produced from marine *Streptomyces* strains [29]. After mixing 50 mL of 1 mM (170 μg.mL) $AgNO_3$ with 50 mL of cell filtrated of *Streptomyces olivaceus* (MSU3) at 28 °C in dark; spherical and monodispersed ~12.3 nm g-AgNPs were produced. Five major functional groups were found in FT-IR: alkynes (C=C-H), alcohol (-OH), oxime (C=N-OH), alkene (C=C), carboxyl (-COOH), and amine (-$NH_2$) with alkynes and alcohol being predominant. By testing several nominal concentrations of g-AgNPs (0.313–20 μg.mL) within 24 h at 37 °C, a strong antibacterial activity was confirmed against *Streptococcus pneumoniae* with 0.625 μg.mL (MIC, minimum inhibitory concentration) and $\leq$ 2.50 μg.mL (MBC, minimum bactericidal concentration) in a concentration-dependent manner. Other bacteria such as *Streptococcus mutans* (MIC 0.625 and MBC $\leq$ 5.00 μg.mL), *Klebsiella pneumoniae* (MIC 2.50 and MBC $\geq$ 5.00 μg.mL), *Escherichia coli* (MIC 1.25 and MBC $\leq$ 5.00 μg.mL), and *Enterobacter faecalis* (MIC 1.25 and MBC $\leq$ 2.50 μg.mL) were also affected. More evidences supporting that small g-AgNPs might have a potential to act as broad-spectrum agents against different bacteria species came out from Al-Dhabi et al. [28] experiments. Using *Streptomyces* sp. (Al-Dhabi-87) supernatant and 1–5 mM $AgNO_3$ suspension, slightly polydispersed 9.7–17.25 nm g-AgNPs were prepared. By high-resolution scanning electron microscope (HRSEM) analysis, these g-AgNPs looked rather clustered-like and united by the biomolecular coating. Using concentrations at mg.mL level, biocide efficiency of 9.7–17.25 nm g-AgNPs was registered with Gram-negative bacteria models (such as *Enterobacter faecalis* and *Staphylococcus aureus*) showing a MIC of 0.039 mg.mL each. Among drug-resistant pathogens as *Escherichia coli*, *Acinetobacter baumannii*, and *Proteus mirabilis*, g-AgNPs were also efficient with MIC values reaching 18.0 μg.mL. A second drug-tolerant strain of *A. baumannii* showed higher MIC values (39, 156, and 312 μg.mL) though. Against *Pseudomonas aeruginosa* drug-resistant strains, MIC value reached 39 μg.mL, whereas a 312 μg.mL g-AgNPs treatment prevented *Enterococcus faecium* strains from growing. According to the authors, MIC values were comparatively lower than streptomycin concentration for Gram-positive bacteria.

Microbe-assisted synthesis of g-AgNPs has been equally performed with supernatants of *Streptomyces* spp. isolated from mangrove sediments [20, 21]. While spherical and agglomerated *S. albogriseolus* 16.2 ± 1.6 nm g-AgNPs exhibited N-H groups, C-O ester groups, C=O, and C=C=C (polyenes) on their organic coating, *Streptomyces* sp. (BDUKAS10) 21–48 nm g-AgNPs held free N-H and -C=C-, groups aparently related to heterocyclic compounds present in proteins [20, 21]. These nanoparticles were visually clustered-like. Pathogenic bacteria treated with *Streptomyces* sp. (BDUKAS10) g-AgNPs went through some growth limitation compared to treatments of pure actinobacteria extracts using disc diffusion method on agar plates up to 14 h at 37 °C [21]. For instance, *Bacillus cereus* was negatively affected by pure cell-free *Streptomyces* sp. (BDUKAS10) extracts at 1.25-fold increase compared to 5% diluted cell-free extracts. Once treated with g-AgNPs, only 1.3-fold increase of growth inhibition was detected if compared to pure cell-free supernatant. Correspondingly, 1.7-fold increase of antibacterial effect was observed against *Staphylococcus aureus* when treated with non-diluted extracts in comparison to 5% diluted fractions. After g-AgNPs exposure, *Staphylococcus aureus* had 1.1-fold increase of growth disruption. The same effect was observed with *Pseudomonas aeruginosa*. Because no additional positive controls (as $Ag^+$ ions, chemically produced AgNPs, or antibiotics) were evaluated, it is challenging to estimate at which degree these g-AgNPs might effectively prevent bacterial growth. Without quantification of remaining free Ag and/or free antibacterial biomolecules in raw g-AgNP stock solutions after reduction process (1) or final silver concentrations measured in the exposure media (2), it is tricky to unequivocally attribute the toxicological effects of g-AgNPs against bacteria to the green nanosilver itself. By investigating *Streptomyces albogriseolus*-made 16.2 ± 1.6 nm g-AgNPs' antibacterial properties against *Bacillus cereus*, *Escherichia coli*, and *Staphylococcus aureus* using agar well diffusion methods, Samundeeswari et al. [20] showed that g-AgNPs were able to display antimicrobial activity against *S. aureus* at ~18.5 mm, followed by *E. coli* at ~16.5 mm and *B. cereus* at ~14 mm. Compared to positive controls (free Ag and pure supernatant extract of *S. albogriseolus*), zones of inhibition created by g-AgNPs appeared to be slightly wider than those induced by dissolved Ag and cell-free supernatant, so no significant differences were observed. Both controls showed considerable antimicrobial effects against bacterial strains, especially for *S. aureus*. It is interesting to note that after biosynthesis of g-AgNPs, the yield of nanosilver obtained by atomic absorption spectrophotometer (AAS) was about 73%. Hence, ~27% of dissolved silver likely remained in the stock solution or converted to silver oxides or silver sulfides with unknown antimicrobial activities.

Silver reduction by terrestrial *Streptomyces kasugaensis* (NH28/M338-M1) liquid extracts produced spherical and polydispersed ~13 nm g-AgNPs likely holding proteins on their organic shell [25]. Concentrations of raw solution of green nano-Ag (1.25–200 μg.mL) were tested against bacteria at 1 x $10^6$ CFU.mL (CFU, colony formation unity) final concentrations per well. The strongest antibacterial activity of g-AgNPs given by MIC was against *Staphylococcus aureus* (1.25 μg.mL), *Klebsiella pneumoniae* (1.25 μg.mL), *Proteus mirabilis* (1.25 μg.mL), and *Escherichia coli*

(1.25 μg.mL) followed by *Bacillus subtilis* (2.5 μg.mL), *Salmonella infantis* (10 μg.mL), and *Pseudomonas aeruginosa* (10 μg.mL) up to 24 h at 37 °C. The lowest MIC value (1.25 μg.mL) for growth inhibition was found against *S. aureus* (48% of inhibition), *K. pneumoniae* (29%), *P. mirabilis* (23%), and *E. coli* (14%). The MIC for *B. subtilis* 13 nm g-AgNP-treated was 2.5 μg.ml, whereas for *P. aeruginosa* and *S. infantis* 10 μg.mL inhibited bacteria at 8%. Expectedly, Iniyan et al. [26] recently found that rod-shaped, smaller, and highly aggregated g-AgNPs (3–12 nm)) synthesized from *Streptomyces exfoliatus* ICN25 were greatly functional against methicillin-resistant and methicillin-sensitive *Staphylococcus aureus* (ATCC33591 and ATCC29213, respectively), *E. coli*, *P. aeruginosa*, and *K. pneumoniae* at $10^5$–$10^6$ CFU.mL cells. These 3–12 nm g-AgNPs also taken directly from newly prepared raw solution led to a much lower MIC (1 μg.mL; ~15.5 mm of inhibition zone) against methicillin-resistant *S. aureus* compared to methicillin-sensitive *S. aureus* (2 μg.mL; ~6.33 mm), *E. coli* (2 μg.mL; ~5.83 mm), *P. aeruginosa* (2 μg.mL; ~12.5 mm), and *K. pneumoniae* (2 μg.mL; ~4.33 mm). Antimicrobial effects were dose-dependent. As it turned out, g-AgNPs' impact over bacterial strains was twofold higher than dissolved ion counterparts [26]. Culture supernatant itself exhibited considerable antibacterial properties with inhibition zones being only about 2 mm smaller than those zones cleared by g-AgNP treatment. This is quite predictable owing to the fact that *Streptomyces exfoliatus* is able to produce a β-lactamase inhibitory protein of molecular mass estimated to 17.5 kDa [30] and β-Lactam antibiotics are normally applied to inhibit the synthesis of the bacterial peptidoglycan layer. As for *K. pneumoniae,* no differences were detected. Conversely, rounded ~5–50 nm g-AgNPs (1000–10000 μg.mL) capped by biomolecules extracted from *Streptomyces naganishii* (MA7) mycelium showed some inhibition effect against biofilm of several strains of pathogenic bacteria growing in Luria-Bertani (LB) media well plates [22]. Such effects were not significantly higher compared to either dissolved silver or classic antibiotics throughout 24 h at 37 °C. *Staphylococcus aureus* was the most affected species with >12 mm of inhibition due to g-AgNP effect. Overall, silver toxicity arose in a concentration-dependent manner. In this experiment, g-AgNPs were previously separated by ultracentrifugation after synthesis and weighted per 100 mL. Main features of g-AgNP synthesis and exposure conditions of toxicity assays reported in papers reviewed in this section are summarized in chronological order in Table 10.1.

## 10.3 Antibacterial Effects of Green Nanosilver Produced by Extracts of Proteobacteria and Firmicutes

Bacterial species of Firmicutes and Proteobacteria have been isolated from marine ecosystem, plant tissues, soils, chemical effluents, and even milk; then used to fabricate g-AgNPs. A wide range of pathogenic bacteria was exposed to lower

concentrations of green nano-Ag compared to the experiments conducted with actinobacteria-made g-AgNPs. A summary of AgNP synthesis methods and exposure conditions for papers reviewed in this section is given in Table 10.2.

After a 24 h-mixing process of 100 mL cell-free supernatant of marine seaweed epibiont *Bacillus vallismortis* (SS7) (Firmicutes) with 1 mM $AgNO_3$ final concentration at 37 °C, partially polydispersed ~22.76 nm g-AgNPs emerged in the stock solution [40]. FT-IR spectrum of g-AgNPs showed biomolecules harboring primary and secondary amines, C-H, N-O, and halogen-alkanes (C-F and C-Cl) of methyl (–$CH_3$) and methylene (=$CH_2$) groups of proteins. Throughout a 48 h exposure at 37 °C, *Pantoea agglomerans* was the most affected biofilm-forming bacteria whose zones of inhibition ranged from ~5 mm (0.25 nM) to ~14 mm (1.25 nM). For testing, initial cell concentrations in each well were ~ 2 x $10^8$ cells.mL. Then *Pseudomonas aeruginosa* (~5–12 mm), *Vibrio alginolyticus* (~4–12 mm), *Escherichia coli* (~3–11 mm), *Serratia marcescens* (~3–10 mm), and *Aeromonas hydrophila* (~3–8 mm) were inhibited in a wide range of low nominal concentrations (0.027–0.16 μg.mL of green nano-Ag) as well. In terms of minimum inhibition concentration (MIC) of green nano-Ag, bacteriostatic effects were reached with 0.027 μg.mL in *P. agglomerans*, *P. aeruginosa*, and *V. alginolyticus* cultures, whereas for the other species tested MIC corresponded 0.054 μg.mL. The bactericidal effect was reached at higher doses only (0.054–0.82 μg.mL). In comparison, roughly spherical 35–58 nm g-AgNPs bioreduced by liquid and solid extracts of marine bacillus *Ochrobactrum anthropi* (CB2/JQ435714) were able to disrupt growth of *Staphylococcus aureus*, *Salmonella typhi*, *Salmonella paratyphi*, and *Vibrio cholerae* at ~15, ~14, ~15, and ~ 16 mm, respectively [35]. The authors mentioned that 108 μg.mL of soluble Ag (1 mM) was used as positive control and did not stop bacteria growth. It should be also noted that bacteria were exposed to both cell-free supernatant and mycelia-synthesized g-AgNPs in a single exposure with no final concentrations established.

Bacterial endophytes are known to be plant symbionts inhabiting plant tissues for the majority of their life cycle without detrimental interactions between symbiont and host [43]. For instance, they can create an endophytic microbiome in the roots mostly dominated by Proteobacteria, Actinobacteria, and in a lesser extent Firmicutes [44]. Isolated from *Coffea arabica* L. (Rubiaceae) tissues, the endophytic *Pseudomonas fluorescens* gave rise to multi-shaped 5–50 nm g-AgNPs by reduction of $Ag^+$ ions in bacteria cell-free extracts at different concentrations (0.5–2 mM) and temperatures (20–90 °C) [36]. Before synthesis, *P. fluorescens* strain was pre-screened twice by culturing it on media supplemented with $AgNO_3$. After a 72 h incubation, culture broth was centrifuged to obtain a supernatant challenged with 1 mM $AgNO_3$. With initial cell concentrations reaching 5 x $10^5$ CFU.mL in test chambers, pathogenic bacteria had colony formation decreased as a function of nominal concentrations up to 100 μg.mL within 24 h and at 37 °C. Alone both chemically prepared AgNPs and g-AgNPs showed similar results inhibiting bacteria growth. Minimum inhibitory concentrations varied from 31.25 to 250 μg.mL, and it seemed to be more effective against *Klebsiella pneumoniae* and less effective against *Escherichia coli*. Antibiotics kanamycin (a) and tetracycline were stronger than AgNPs and g-AgNPs for all bacteria tested. In fact, $AgNO_3$ treatment and

**Table 10.2** Summary of the main features of g-AgNP synthesis and exposure conditions of toxicity assays with Proteobacteria and Firmicutes isolates used for biosynthesis of nanosilver

| Biological matrices used for green AgNP synthesis | Microorganism habitat | AgNP size after biosynthesis | AgNP morphological features after biosynthesis | Supernatant/AgNP functional groups (FT-IR or $^{1}$HNMR spectral analysis) | Final nominal concentrations of g-AgNPs | Microorganisms exposed to g-AgNPs | Time of exposure and temperature | Drugs as positive controls |
|---|---|---|---|---|---|---|---|---|
| Liquid and solid extracts of *Alcaligenes faecalis* [31] | Soil from metal-rich dump sites near industrial city | 11 ± 2.9 nm | Monodispersed and spherical | NH, C-C, amide I (C-O stretching mode) and II (NH in-plane bending and CN) corresponding to heterocyclic compounds like proteins | 2.16, 54, 108, 216 μg.mL | *Escherichia coli*, *Pseudomonas aeruginosa*, *Bacillus cereus*, and *Staphylococcus aureus* | _ | Erythromycin and ampicillin (concentrations not mentioned) |
| Biomass of *Bacillus cereus* GX1 [32] | Leafs of *Garcinia xanthochymus* | 20–40 nm | Slightly aggregated and spherical | OH (carboxylic acid), NH (primary amines), C, N, and O | Not provided | *Escherichia coli* (ATCC25922), *Pseudomonas aeruginosa* (ATCC27853), *Staphylococcus aureus* (ATCC25923), *Salmonella typhi* (ATCC6539), *Klebsiella pneumoniae* (NCIM 2883) | _; 37 °C | Amoxicillin, streptomycin, and ofloxacin (concentrations not mentioned) |
| Cell-free supernatant of *Stenotrophomonas maltophilia* OS4 [33] | Soil samples from rhizosphere of sweet pea (*Pisum sativum*) | ~93 nm | Well dispersed, cubic in shape | Hydroxyl, amine, alkyl, CHO, C=O of amide groups, $COO^{-}$ of carboxylate groups, $SO_3^{-}$, carbonyl, -NH (amide linkages) | 12.5, 25, 50 μg per well | *Staphylococcus aureus*, *Escherichia coli*, and *Serratia marcescens* | 48 h; 35 ± 2 °C | Tetracycline (25 μg) |
| Cell-free supernatant of *Serratia nematodiphila* [34] | Chemical effluent | ~4 nm | Well dispersed and spherical | NH primary and secondary amines or amides, CH stretching of alkenes group, aromatic amine and nitro groups (N=O), C-O stretching, amide I and amide II, aromatic group residues | Not provided | *Bacillus subtilis* (2727), *Klebsiella planticola* (3053), *Pseudomonas aeruginosa* | 24 h; 37 °C | Kanamycin (concentrations not mentioned) |

(continued)

**Table 10.2** (continued)

| Biological matrices used for green AgNP synthesis | Microorganism habitat | AgNP size after biosynthesis | AgNP morphological features after biosynthesis | Supernatant/AgNP functional groups (FT-IR or $^{1}$HNMR spectral analysis) | Final nominal concentrations of g-AgNPs | Microorganisms exposed to g-AgNPs | Time of exposure and temperature | Drugs as positive controls |
|---|---|---|---|---|---|---|---|---|
| Liquid and solid extracts of *Ochrobactrum anthropi* (CB2/JQ435714) [35] | Seawater | 35–85 nm | More or less spherical | Not determined | Not provided | *Salmonella typhi*, *S. paratyphi*, *Vibrio cholerae*, and *Staphylococcus aureus* | 18–24 h; 37 °C | None |
| Cell-free supernatant of *Pseudomonas fluorescens* (CA417) [36] | *Coffea arabica* L. tissues | 5–50 nm, 20.66 nm in average | Polydispersed, spherical, near to spherical, hexagonal, and triangular | NH, C=O, C-H, hydroxyl, aromatic before synthesis; NH, hydroxyl, aromatic after synthesis | 10, 25–100 μg.mL | *Bacillus subtilis* (MTCC121), *Staphylococcus aureus* (MTCC7443), *Pseudomonas aeruginosa* (MTCC 7903), *Klebsiella pneumoniae* (MTCC7407), *Escherichia coli* (MTCC7410) | 24 h; 37 °C | Kanamycin (1 μg.mL) and tetracycline (concentration not mentioned) |
| Cell-free supernatant of *Aneurinibacillus migulanus* 141 [37] | *Mimosa pudica* L. tissues | 10–60 nm and 20–30 nm were mostly numerous (24 nm in average) | Polydispersed, spherical, oval, hexagonal, cubic, and triangular shapes | NH, C-N, C-H, carbonyl, aromatic, amino, secondary aliphatic groups | 25–100 μg.mL (micro broth dilution assay), 10 000 μg.mL (agar disc experiment) | *Bacillus subtilis* (MTCC121), *Escherichia coli* (MTCC7410), *Klebsiella pneumoniae* (MTCC7407), *Staphylococcus aureus* (MTCC7443), *Pseudomonas aeruginosa* (MTCC7903) | 24 h; 37 °C | Gentamicin (1 mg.mL) |
| Cell-free supernatant of *Bradyrhizobium japonicum* SDK276 [38] | Legume root-nodulating nitrogen-fixing bacteria; soil | 5–50 nm | Rod- and oval-shaped | O-H, C-O-C, C-O | 0.10, 0.25, 0.50, 1.00, 1.5, 2.0, 2.5 μg.mL | *Escherichia coli* (ATCC11229) and *Staphylococcus aureus* (ATCC6538) | 24 h; 37 °C | None |

| | | | | | | | | |
|---|---|---|---|---|---|---|---|---|
| Cell-free supernatant of *Lactococcus lactis* 56 [KY484989] [39] | Milk | 5–50 nm, mean size of 19 ± 2 nm | Spherical, aggregated | Amide I from C=O stretching vibration, amide II (NH, CN), likely arginine residues ($CN_3H_5^+$), carboxyl groups, glutamic and aspartic acid, amide II, deprotonated carboxyl, possibly methylene (-$CH_2$) groups, -$CH_3$, phenolic ring, hydroxyl groups (OH), C-O-C of acid lactic and its metabolites, C-H, C=O stretching vibrations of fatty acids, C-H vibrations of proteins, peptides, amino acids or lipids | 1.875, 7.5, and 15 μg per well | *Pseudomonas aeruginosa* ATCC10145, *Proteus mirabilis* ATCC25933, *Staphylococcus epidermidis* ATCC49461, *Staphylococcus aureus* ATCC29213 (methicillin-sensitive), and *S. aureus* ATCC6338 | 18 and 24 h; 35 °C | None |
| Biomass and cell-free supernatant *Bacillus vallismortis* (SS7) [40] | Marine ecosystem (isolated from surfaces of seaweed *Ulva lactuca*) | 22.76 ± 10.7 nm in average in the range of 5–50 nm | Narrowly polydispersed and spherical | Primary and secondary amines, CH, NO, halogen-alkanes (C-F and C-cl) of methyl and methylene | 0.027-0.16 μg. mL | *Pantoea agglomerans*, *Pseudomonas aeruginosa*, *Vibrio alginolyticus*, *Escherichia coli*, *Serratia marcescens*, *Aeromonas hydrophila* | 48 h; 37 °C | None |
| Cell-free supernatant of *Aeromonas* sp. THG-FG1.2 [41] | Soil | 8–16 nm | Aggregated and spherical | Not determined | 15 μg per well | *Bacillus cereus* (ATCC14579), *Bacillus subtilis* (KACC14741), *Staphylococcus aureus* (ATCC6538), *Escherichia coli* (ATCC10798), *Pseudomonas aeruginosa* (ATCC6538), *Vibrio parahaemolyticus* (ATCC33844), *Salmonella enterica* (ATCC13076) | 24 h; 28 °C | Erythromycin (15 μg), novobiocin (30 μg), lincomycin (15 μg), penicillin G (10 μg), vancomycin (30 μg), oleandomycin (15 μg) |

(continued)

**Table 10.2** (continued)

| Biological matrices used for green AgNP synthesis | Microorganism habitat | AgNP size after biosynthesis | AgNP morphological features after biosynthesis | Supernatant/AgNP functional groups (FT-IR or $^{1}$HNMR spectral analysis) | Final nominal concentrations of g-AgNPs | Microorganisms exposed to g-AgNPs | Time of exposure and temperature | Drugs as positive controls |
|---|---|---|---|---|---|---|---|---|
| Cell-free supernatant of *Pseudomonas* sp. (THG-LS1.4) [42] | Soil | 228 ± 2.4 nm with some reaching 10–40 nm | Polydispersed, some with irregular shape | OH, primary amines (NH), alkane (C-H), amine (CN), carbonyl (C=O), aromatic and aliphatic amines | 500 μg.mL (500 ppm) | *Bacillus cereus* (KACCC11240), *Staphylococcus aureus* (KCTC3881), *Candida tropicalis* (KCTC17762), *Vibrio parahaemolyticus* (KACC10763), *Salmonella enterica* (KACC10763), *Escherichia coli* (CCARM0237), *Pseudomonas aeruginosa* (KACC14021) | 24 h; 28 °C | Erythromycin (15 μg), novobiocin (30 μg), lincomycin (15 μg), penicillin G (10 μg), vancomycin (30 μg), oleandomycin (15 μg) |
| Growing culture of *Alcaligenes faecalis* (MGL-D10) [8] | Marine ecosystem (isolated from coral surfaces) | 30–50 nm | Spherical and polydispersed | OH, aromatic groups | 50 μg.mL, and 5–80 μg. mL | *Bacillus* sp., *Escherichia coli*, *Klebsiella pneumoniae*, *Pseudomonas aeruginosa, and Staphylococcus aureus* | 16–18 h; 37 °C | None |

supernatant single exposures did not succeed to prevent bacterial growth. Only *Staphylococcus aureus* growth was affected at ~6 mm by $Ag^+$ ion exposures with concentrations not precisely determined. Having both kanamycin (1 μg.mL) and g-AgNPs (10 μg.disc) in the same treatment led to combined effects defined as synergistic by Syed et al. [36] (for a more detailed discussion about such interactions, see the Sect. 10.5).

These same authors synthesized ~24 nm g-AgNPs from supernatant of the endophytic bacterium *Aneurinibacillus migulanus* 141 isolated from shameplant *Mimosa pudica* L. (Fabaceae) tissues [37]. Differently from previous methods used with gammaproteobacterium *P. fluorescens*, endophytic *A. migulanus* (Firmicutes) was pre-screened (1x) with a nutrient media previously amended with 170 μg.mL $AgNO_3$ at 37 °C. Then colonies went through a 72 h fermentation process before being centrifuged to obtain the cell-free extracts. Once again, the supernatant was mixed with 170 μg.mL $AgNO_3$ in order to obtain the g-AgNPs. The pathogenic bacteria were concentrated ~$5 \times 10^6$ CFU.mL at time 0 when challenged with a 25–100 μg.mL g-AgNPs range. Antibacterial activity, given by inhibition growth (in mm and MIC), was primarily found with *Pseudomonas aeruginosa* (~21 mm, 12.5 μg.mL), then *Escherichia coli* (~18 mm, 12.5 μg.mL), *Staphylococcus aureus* (~16 mm, 12.5 μg.mL), *Bacillus subtilis* (~19 mm, 12.5 μg.mL), and *Klebsiella pneumoniae* (~17 mm, 25 μg.mL). The positive control gentamicin (1 mg.mL) showed similar or stronger effects compared to g-AgNPs against all bacteria tested, except for *P. aeruginosa*. With a different approach, Sunkar and Nachiyar [32] managed to reduce 1 mM of dissolved silver solution into slightly aggregated and spherical 20–40 nm g-AgNPs from biomass of the endophytic bacterium *Bacillus cereus* GX1 isolated from leafs of yellow mangosteen *Garcinia xanthochymus* (Guttiferae). After bacteriogenic nanosilver treatment, only *S. aureus* and *E. coli* clearly showed a better growth inhibition (~22 mm and ~ 18 mm, respectively) compared to all antibiotics used. Other bacteria tested such as *P. aeruginosa*, *K. pneumoniae*, and *Salmonella typhi* showed growth inhibition as well, but often similar to at least one of the antibiotics tested (positive controls).

According to Rasulov et al. [38], legume root-nodulating nitrogen-fixing gammaproteobacterium *Bradyrhizobium japonicum* SDK276 isolated from the soil makes high and low molecular mass exopolysaccharides (EPS). Dissolved silver (10 M) was then reduced in a solution of EPS (100 mL) and stored for 2 months at ambient temperature before producing rod and oval-shaped ~5–50 nm g-AgNPs. No attempt to separate the nanoparticles from the remaining reducing solution seemed to be applied. While high molecular mass-EPS g-AgNPs (HMM-g-AgNPs) ranged from ~20 to 50 nm, low molecular mass-EPS g-AgNPs (LMM-g-AgNPs) had ~5–20 nm. Toxicological testing of green nanosilver (0.10–2.5 μg.mL) took place at 37 °C throughout 24 h against Gram-negative *Escherichia coli* and Gram-positive *Staphylococcus aureus*. Inhibition of bacterial growth occurred as a function of nominal concentrations used. LMM-g-AgNPs were more effective to reduce bacterial cell viability and growth though. With lower doses (1–2.5 μg.mL), inhibition zones generally reached ~16–32 mm with LMM-g-AgNPs, whereas for HMM-g-AgNPs ~6–22 mm was found for both species. *S. aureus* was the most sensitive

bacteria, and it had 70–75% of cells dead after 12 h in 2.0–2.5 μg.mL g-AgNP testing media. When exposed to 10–50 μg.mL g-AgNPs, *E. coli* cells started sharply dropping in number after 6 h. Using only high doses of LMM-g-AgNPs (10–50 μg.mL), cell viability of bacteria started to drop in a shorter period of time right after exposure (~2 h). In this case, the most effective concentration was 30 μg.mL. The best results found with LMM-g-AgNPs can possibly be explained by differences of solubility of both g-AgNPs in the exposure media [38].

Bacteria isolated from chemically polluted soils or industrial effluents have been also used to biofabricate AgNPs [31, 34]. Liquid and solid extracts of betaproteobacterium *Alcaligenes faecalis* inhabiting metal-rich dump sites near industrial areas were used to obtain spherical and monodispersed ~11 nm g-AgNPs [31]. In their study, increasing concentrations of g-AgNPs (2.16–216 μg.mL) were more efficient to block bacteria growth in culture media than Ag ions. Lowest concentrations of silver only stopped bacteria growing in g-AgNP exposure media. *Escherichia coli* growth was reduced in ~3.2 mm. A dose of 2.16 μg.mL AgNP also inhibited *Pseudomonas aeruginosa* growing at ~2.0 mm, *Bacillus cereus* at ~2.2 mm, and *Staphylococcus aureus* at ~1.5 mm. Additionally, 21.6 μg.mL nominal concentrations for both g-AgNPs and $Ag^+$ ions inhibited *E. coli* at ~12.5 mm/1.2 mm ratio for g-AgNPs/$Ag^+$, ~9.2/0.8 for *P. aeruginosa*, ~9.8/1.3 for *B. cereus*, and ~ 9.9/1.8 for *S. aureus*. Similar effects likely emerged with spherical 4 nm g-AgNPs synthesized from gammaproteobacterium *Serratia nematodiphila* liquid extracts [34]. Green nanosilver showed high antimicrobial effects against *P. aeruginosa* by preventing its growth at ~18 mm and *Bacillus subtilis* at ~17 mm within 24 h at 37 °C. Lower effects were found against *Klebsiella planticola*, with ~14 mm of inhibition zone detected. In both studies, raw 24–72 h preincubated ~108 μg.mL g-AgNP stock solutions were used.

Finally, cell-free supernatant of lactic acid bacterium *Lactococcus lactis* (Firmicutes) isolated from milk products and mixed with 170 μg.mL $AgNO_3$ formed spherical silver nanoparticles of 5–50 nm (19 nm in average) with antibacterial activity [39]. This fermentative bacterium can almost totally convert its carbon source into L-lactate from pyruvate through lactate dehydrogenase, which dominates the maximum enzymatic activity once *L. lactis* is exposed to high doses of sugar [16]. So the preparation of the Ag-reducing media involved a preincubation of inoculate in MH (Mueller–Hinton) broth medium in a bioreactor for 7 days at 26 °C. Following a centrifugation process, a supernatant was combined with dissolved silver and incubated again at 26 °C for another 7 days in the dark. After this process, the residual silver ions and biomolecules were washed out from silver biocolloids in a 3-day dialysis. *L. lactis* is a natural factory of many aromatic acetylated products such as diacetyl, acetaldehyde, and acetate that could likely have acted as Ag reducers. The newly made g-AgNPs exhibited a large amount of functional groups (see Table 10.2) and were poorly dispersible, as depicted by TEM micrographs. The most effective g-AgNP concentration to avoid pathogenic bacteria growth was 15 μg per well with inhibition zones varying from ~11 to 16 mm at 35 °C within 24 h. *Proteus mirabilis* was the least sensitive, whereas *Staphylococcus*

*epidermidis* was the most affected. The MIC for *Staphylococcus aureus*, *S. epidermidis*, and *P. mirabilis* was calculated to be ~3.125 μg.mL, and then 6.25 μg.mL for *P. aeruginosa* and 12.5 μg.mL for methicillin-sensitive *S. aureus* (MSSA) at 35 °C within 18 h. Surprisingly, with 200 μg.mL, *S. aureus* was resistant to nano-Ag and showed ~70.2 in cell density (CD) compared to less than ~9 CD in absorbance measurements. Unfortunately, with no positive controls, there was no estimation of toxicity compared to silver ions or antibiotics.

## 10.4 Assessing g-AgNPs Effects on Bacteria Models: Accomplishments, Pitfalls, and Challenges

### 10.4.1 Nominal Concentrations and Stock Solution Preparation

So far, the research conducted to biosynthesize green silver nanoparticles and evaluate their potential as antimicrobial agents was successful in obtaining a great variety of isolates of bacterial strains (Tables 10.1 and 10.2). Promising results regarding antibacterial properties of green nanosilver were obtained with pathogenic bacteria known to cause hospital-acquired infections. Notwithstanding, the lack of information about final nominal concentrations for the antimicrobial assays can be considered as a major drawback in several studies dealing with g-AgNP toxicity. The nominal concentration refers to the calculated amount of a chemical to be introduced in a test chamber, while the measured concentration is referring to the real amount of the test substance analyzed in the exposure media at a given time. More than 30% of the reviewed papers have inaccurately reported the g-AgNP nominal concentration as a volume (μL) taken from the stock solution, which is considered as the initial concentration, without any additional analysis. One must take into consideration that after reduction process of silver nitrate (usually ~1 mM of $AgNO_3$; or 170 μg.mL) by liquid or solid extracts of bacteria, the main stock solution of newly produced g-AgNPs will doubtlessly retain an unknown proportion of unreacted dissolved silver and metabolites/exudates. In addition, this unknown proportion will be changing with reaction time and incubation temperature. Sampling μL aliquots from the raw g-AgNP stock solution to be injected into the exposure media implies exposing bacteria to residual $Ag^+$ ions, g-AgNPs, and unreacted and unknown biomolecules all together. Therefore, without a final dialysis of reaction fluid to wash out dissolved ions and free reactive biomolecules from the colloidal nano-Ag, the final testing concentrations of g-AgNP will be likely biased, and it becomes impossible to compare claimed antibacterial activity of such mixture (or protocol) proposed by different authors.

### 10.4.2 The Green AgNP Morphology and its Toxicity Mechanisms

After isolation of bacterial strains, the two principal matrices for AgNP mineralization (supernatant and biomass) are separated as schematically illustrated in Fig. 10.1a–c. Generally, the multiple biomolecules in a cell-free liquid extract

drive the production of silver nanoparticles in a rapid process (~24 to 48 h) (Fig. 10.1d–f, Fig. 10.2). In this context, AgNP size is likely related to the incubation time, the ability of functional groups of biomolecules to catch $Ag^+$ ions along the process, and increasing $AgNO_3$ concentrations mixed with bacteria exudates [45]. Henceforth, FT-IR or $^1$HNMR spectral analysis of g-AgNPs has been performed in the majority of publications we analyzed. What has been revealed is that amines, amides, carbonyl, hydroxyl, and alcohol functions, as well as different hydrocarbons, are found in the coating of g-AgNPs. Even though bacteria extracellular synthesis has been the more frequently used technique to reduce silver, cell-fabricated g-AgNPs have an unexplored potential to be used as antibacterial agents in toxicity testing [24] (see Table 10.1 for a summary).

It has been postulated that several factors are actually governing the toxicity of chemically synthesized AgNPs towards bacteria including shape, concentration, size, zeta potential, pH of exposure media, presence of capping agents, and electrical charge of organic ligands coating AgNP surface. In fact, much of the AgNP identity is related to the corona composition and the way it interacts with cells and surrounding molecules dispersed in the exposure media. As a consequence, the molecular/protein composition of the corona is strongly influencing nanoparticle-cell interactions, its biological fate, and final functions as well [46]. Therefore, more studies focusing the corona identity (i.e., chemical characterization) of green nanosilver with experimental media and biological fluids are needed to first reveal which functional groups could optimize g-AgNP attachment to Gram-positive and Gram-negative bacteria and how drug delivery would target pathogenic bacteria with these particles. We can suggest that g-AgNPs will behave like chemically made organic-coated AgNPs. Nonetheless, not only soluble silver and nano-Ag form (as a single particle and/or aggregates) will impair bacteria cell, but also the byproducts of bacteria used as capping shell as well. For instance, Ferreyra Maillard et al. [47] showed that green nano-Ag produced by plant extracts had a high zeta potential and seemed to adhere to bacteria cell wall in tryptic soy broth (TSB) media at 37 °C up to 18 h. Green AgNPs disrupted bacterial envelope just 1 h after exposure. Overall, an increase in surface roughness, membrane disruption, and leakage of intracellular contents was mainly observed with Gram-negative *Escherichia coli*, whereas Gram-positive *Staphylococcus aureus* appeared to be less affected. The authors stated that aromatic/hydrophobic moieties from the main phenolic compounds in plant extract adsorbed on AgNPs would likely allow interactions with hydrocarbon chain of lipids on bacteria surface.

Final g-AgNP morphology will depend on the way chemical groups of bacterial exudates will handle dissolved ions during the reducing process (Fig. 10.2). Nonetheless, there is no information about the molecular weight of biomolecules capping these nanoparticles. In fact, capping biomolecules might play a crucial role on g-AgNPs toxicity considering (1) the interaction with exposure media (and its constituents like $Cl^-$ ions) and bacterial cell envelope, and (2) the kinetics involving leaching $Ag^+$ ions out of g-AgNP surface. It has been hypothesized that once exposed in liquid media, high molecular weight (65,000 Da) poly-allylamine-coated AgNPs released in a few hours a first layer of $Ag^+$ ions already entrapped by capping

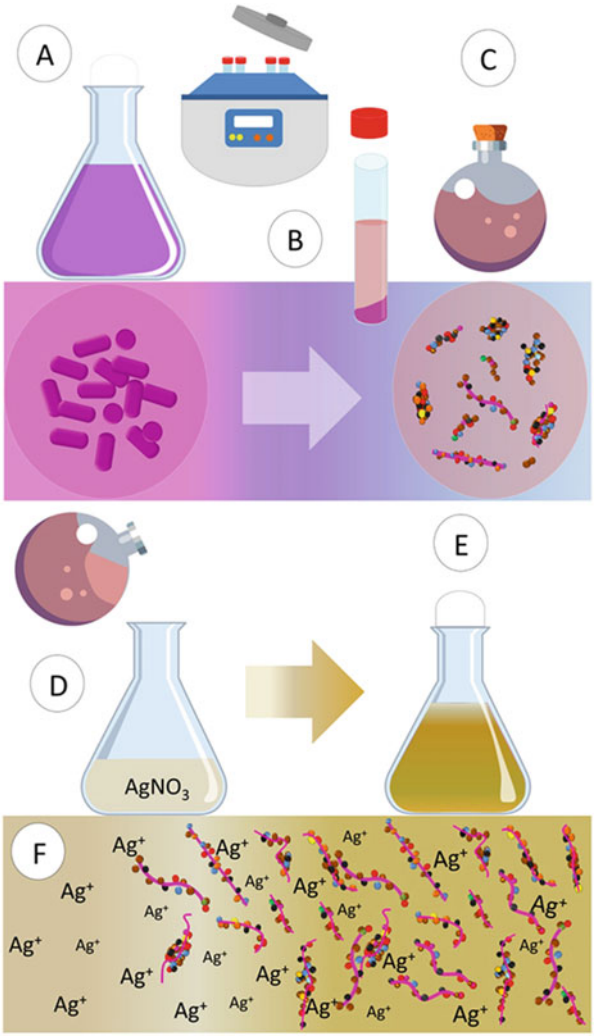


**Fig. 10.1** Schematic representation of procedures for green synthesis of silver nanoparticles. A- After isolation from the environment, bacteria are cultured in laboratory at around 30 °C. B- Centrifugation of broth cultures is a crucial step to obtain the biological matrix for green synthesis of AgNP. The matrix may be the bacterial biomass or the cell-free supernatant (presented in D-F ). Nucleation of dispersed ions may occur on the bacteria surface (when the biomass is resuspended into a new solution) or by means of free exudates dispersed in the solution (for cell-free supernatants). C- A cell-free extract is often used to mineralize soluble Ag into AgNP. Biomolecules of cultured bacteria are then studied by FT-IR or $^{1}$HNMR spectral analysis to depict functional groups likely responsible for reducing silver and lately capping the newly produced nanoparticles. D, E, and F- In many studies, 170 µg.mL $AgNO_3$ (1 mM) is mixed with bacteria supernatant in a wide range of temperatures (20–37 °C), and at different reaction times (1 h to ~6 days) to biomineralize Ag. Unreacted products (silver ions and biomolecules) likely remain in the final g-AgNP solution if a separation process is not applied

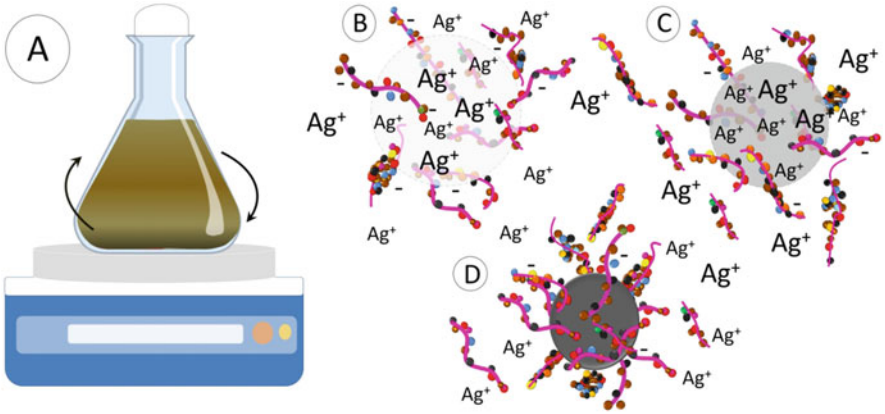


**Fig. 10.2** Silver reduction in a cell-free bacterial supernatant after mixing both $AgNO_3$ and bacterial supernatant (following Fig. 10.1). A- The visible color change in the $AgNO_3$ + bacteria supernatant solution is an indicator of the reduction of soluble silver into g-AgNP. It is known that several factors govern this process such as organic function of free biomolecules in solution, pH, composition of medium, metallic salt concentration, and temperature. B and C- In solution, reducing agents such as NADH, NADH-dependent reductases, proteins, exopolysaccharides (EPS), and other molecules can mediate $Ag^+$ silver loading in AgNP. D- EPS with reducing sugars can chelate, reduce, and stabilize metal ions by several functional groups. Polyanionic groups such as hydroxyl, carboxyl, phosphoric groups, and amino end groups have been suggested as main sites for soluble Ag reduction into nano-Ag

polymers [48]. As time goes on, the dissolution of Ag core slowly takes place under mediation of AgNP organic layer. Another example is given by the nanofibrillated cellulose used as antimicrobial agent in association with g-AgNPs where $Ag^+$ ions' release time is prolonged due to efficient in situ immobilization of nanosilver by carboxyl groups [49]. As demonstrated by the authors, silver nanoparticles were reduced by dialdehyde nanofibrillated celluloses by means of silver mirror reaction between the aldehyde groups and $[Ag(NH_3)_2]^+$, generating three carboxyl groups per unit in the molecular chain. As it follows, the reduced AgNPs were then firmly anchored by the carboxylate groups on the surface of fibers. Experiments carried out by Baygar et al. [50] with surgical sutures coated by *Streptomyces griseorubens*-made 30–50 nm g-AgNPs released an increasing amount of silver up to 2.93 μg.L after 21 days in phosphate-buffered saline (PBS). The Ag-coated material limited *Escherichia coli* and *Staphylococcus aureus* growing in agar, but no clear quantification was presented.

Bacteriogenic silver nanoparticles have been reported to be in a wide range size (4 to 85 nm, or even large particules reaching ~220 nm), and mostly spherical. However, the shape of all g-AgNP-types can vary from rod-shaped, oval, spherical, roughly spherical, or less frequently quadrangular (Tables 10.1 and 10.2). As it has

been pointed out by Vetchinkina et al. [51], when increasing incubation time, the ultrasmall g-AgNPs tend to disappear, and the larger ones will rise in number. As a general rule, the longer the incubation time, the larger will likely be the g-AgNPs, which is an expected observation. Accordingly, sticking g-AgNPs and formation of agglomerates also increase with reaction time [51]. Because a large part of these capping exudates could be amino-polysaccharides, they might have a crucial role in keeping AgNPs aggregated and/or partially dispersed after synthesis. The way small g-AgNPs combined with large aggregates will provoke toxicity in bacterial cells remains a mechanism poorly discussed so far. Moreover, AgNPs with different shapes might exhibit different antimicrobial properties probably because they give rise to many degrees of nanoparticle-cell membrane interactions leading to cell damage [6]. However, how exactly AgNP shape would affect toxicity towards microbial cells is still a matter of debate.

### 10.4.3 The Influence of the Exposure Media Features on g-AgNP Toxicity

Finding out how g-AgNPs behave in agar or liquid broth is another piece of the puzzle to understand their toxicity. Work by Oves et al. [33] has scrutinized the release kinetics of cubic and well-dispersed 93 nm g-AgNPs obtained from gammaproteobacterium *Stenotrophomonas maltophilia* OS4 liquid extracts. Their assays were performed with a dialysis bag suspended in a HEPES buffer solution over a period of 48 h. A slow release of Ag (~10%) was detected within a few hours; but after 12 h, ~70% of nano-Ag was already released; and at 48 h, 81% of g-AgNPs was dispersed in the medium. Interestingly, the smaller g-AgNPs were more rapidly dispersed than the bigger ones. Some variables such as oxygen diffusion and nano-Ag dispersion should have a significant impact on the results. First of all, dissolved oxygen is known to leach $Ag^+$ ions from nanosilver surface. Thus, antibacterial properties of nano-Ag will strongly depend on optimally displayed oxidized surfaces found in well-dispersed suspensions [44]. A limited diffusion rate of both g-AgNPs and free silver in the solid medium diminishes the amount of silver to readily react with bacteria [52]. As stated by Schumacher et al. [53], the handling of disc diffusion methods is quite simple and straightforward, but it requires appropriate diffusion. In other words, the density of the medium (which is defined by solubility, gelling agent's concentration, as well as the degree of polymerization), the molecular weight of capping agents; and the silver concentration (in terms of nominal concentrations and measured concentrations) will define how effective the g-AgNPs could act against bacteria.

The effect of $Cl^-$ ions must also be considered for green nanosilver toxicity assays with bacteria. The majority of antibacterial tests we reviewed were carried out within 24–48 h in agar diffusion methods (with discs or well plates), and sometimes in broth liquid media. As observed by Lok et al. [44], 9 nm AgNPs synthesized by borohydride reduction normally exhibit antibacterial effects in water or in buffered solutions, but they aggregate in commonly used culture media and biological buffers

having chloride and/or phosphate in their contents. As an example, Luria-Bertani liquid broth media (or lysogeny broth medium) contain high concentrations of $Cl^-$ ions (~ 5 g.L for Lennox or Luria medium and ~ 10 g.L for Miller formulation). In turn, chloride concentration in agar is around 0.5%. As a rule, $Cl^-$ ions can clearly interfere with silver $Ag^+$ concentration to form less soluble chloro complexes $(AgCl_x^{(x-1)})^-$ in the solution, affecting thus AgNP toxicity. Therefore, bactericidal activity interpreted as zone diameter or optical density measurement can be misinterpreted due to the presence of chloride in the medium. Working on silver fate in MH (Mueller-Hinton) agar, Tuncer and Seker [54] revealed that a clear local deposition of AgCl happened in a MIC antibacterial test of nanocomposites amended with dissolved silver (containing 29% Ag-$TiO_2$; titanium dioxide nanoparticles). This deposition was later involved by the bacteria-free zone, as depicted by a reflective optical microscope. In any case, the Cl/Ag ratio is considered as a governing factor of AgNP toxicity in exposure media with bacteria [55]. The rate of dissolution of AgNP will be strongly related to the solid AgCl/ $AgCl_x^{(x-1)-}$ ratio: as dissolution rate increases, $AgCl/AgCl_x^{(x-1)-}$ decreases. Using *Escherichia coli* as biological model, the reaction of $Cl^-$ ions on AgNP surfaces begins within 2h of exposure [55]. It results either in precipitation of AgCl or formation and dispersion of $AgCl_x^{(x-1)-}$-soluble forms. As Cl/Ag ratio increases, $AgCl_x^{(x-1)-}$-soluble species begin to dominate compared to solid AgCl. After 24 h of exposure, with lower initial concentrations of $Ag^+$ or AgNPs (~1.10–6 or 1.10–5 M) in 0.01–0.1 M NaCl-containing media, density of *E. coli* living cells remains close to 100%. Hence, it seems unlikely that high concentrations of dissolved silver (~34 to 170 μg.mL), used as positive controls in some experiments with g-AgNPs, failed to stop bacteria growth if we bear in mind that chloride ions have this critical influence on silver ion-mediated acute toxicity.

### 10.4.4 The Bacterial Model Used in the Toxicity Assays

According to Gordienko et al. [52], there is also another important limitation to be aware of in order to properly evaluate g-AgNP antibacterial activity: the growth phase of testing bacteria. A visible change in bacteria metabolism and cell structure in exponential and stationary phases is known to influence toxicity. Cultures of *Bacillus cereus*, *Pseudomonas aeruginosa*, and *Staphylococcus aureus* are proven to be more resistant to silver during exponential phase at 37 °C within 24 h. To date, it looks like the bacterial growth-stage aspect has been neglected in a majority of the studies reviewed in this report. Indeed, the combination of low to middle g-AgNP nominal concentrations and growth phases can show surprising results in bacteria species. *Rhodococcus* sp. 10–50 nm intracellularly produced-AgNP (10 μg. mL) seemed to be efficient to reduce *Klebsiella pneumoniae* activity only until 48 h of exposure [24]. The same concentration affected log phase of *Escherichia coli*, *Enterococcus faecalis*, *Staphylococcus aureus*, *Pseudomonas aeruginosa*, and *Proteus vulgaris* only delaying growth to ~20–30 h compared to controls. Later on, a 10 μg.mL g-AgNP treatment caused bacteriostatic effects in *Enterococcus faecalis*

and *Staphylococcus aureus* reaching to the stationary phase earlier than controls. Even with a 30 μg.mL exposure, some of these pathogens continued to grow after 50 h of incubation.

Noteworthy, some bacteria exhibit a natural resistance against silver nanoparticles; so the best exposure conditions (single or combined exposure, temperature range, acute or chronic treatment, and nominal concentration) should be pre-screened before testing. Thus, the biology of the species must be taken into account for toxicity assays. For instance, Rafińska et al. [56] observed that *Bacillus subtilis* displays different responses to silver in a short 24 h exposure at 37 °C. Briefly, four conditions were chosen as a function of silver chemical form and tetracycline combination: 1) 4–45 nm actinomycete-produced AgNPs [57] (6.25–200 μg.mL); 2) 4–45 nm g-AgNP + tetracycline (6.25–200 μg.mL and 0.25–128 μg.mL, respectively); 3) 4–45 nm g-AgNP functionalized with tetracycline (6.25–200 μg.mL); and 4) soluble silver (0.25–128 μg.mL). It was noted that MIC value for g-AgNPs was very high (200 μg.mL), while for functionalized g-AgNP with tetracycline, the value dropped to 50 μg.mL. At concentration of 12.5 μg.mL, silver ions seemed to provoke cell lysis. However, toxicity of ionic silver in low concentrations could be alleviated by interaction with compounds produced by *B. subtilis* cells. The mixture AgNP + tetracycline and the drug itself were the most effective treatments to induce intracellular reactive oxygen species production and impair *B. subtilis* growth. It was suggested that during incubation of *B. subtilis* culture with nanosilver, bacterial exudates expelled into the culture might have changed AgNP zeta potential, causing thus aggregation [56].

## 10.5 Bacteria-Green Nanosilver and Antibiotics Working Together: What Is the Deal?

There are current efforts to combine the effects of green nanosilver produced by bacterial extracts and classical drugs in an attempt to provide an alternative to cope with pathogenic bacteria that are very often resistant to antibiotics. Numerous cellular processes in bacteria are targeted by conventional antibiotics: ATP biosynthesis and $e^-$ transport, cell envelope structure, DNA replication and transcription, inhibition of folic acid metabolism, and disruption of 50S and 30S subunits of ribosomes. Chiefly, antibiotics basically change the metabolic state of bacteria, which leads to either death or stasis [58]. Moreover, once the bacterial metabolic state is changed by antibiotics, bacteria will be more susceptible to other chemicals (as nano-Ag or even other drugs).

As expected, some microorganisms appear to be more sensitive to g-AgNP + antibacterial drug combinations than others. Green nanosilver (~8–16 nm) obtained with liquid extracts of *Aeromonas* sp. THG-FG1.2 inhibited alone *Pseudomonas aeruginosa* (~16 mm), *Vibrio parahaemolyticus* (~16 mm), *Staphylococcus aureus* (~15.5 mm), *Bacillus cereus* (~13.5 mm), *Bacillus subtilis* (~13 mm), *Escherichia coli* (~13 mm), and *Salmonella enterica* (~11 mm) up to 24 h at 28 °C [41]. Combined effects of green nano-Ag and antibiotics (erythromycin and lincomycin) were

especially observed with bacteria *V. parahaemolyticus*. Accordingly, with erythromycin + g-AgNPs (15 µg + 15 µg per disc) or lincomycin + g-AgNPs (15 µg + 15 µg per disc); the bacteriostatic effects became onefold stronger to those coming out from the antibiotic acting alone. On the contrary, novobiocin or penicillin G + g-AgNP effects were diminished by the nanoparticles from ~29.5 to ~12.5 mm and ~ 45.5 to ~10.5 mm of *V. parahaemolyticus* inhibition zones, respectively. Drug-resistant *S. enterica*, *P. aeruginosa*, and *E. coli* displayed similar inhibition zones once treated with 6 different antibiotics and green nano-Ag, and in a g-AgNP single condition. Comparatively, ~228.7 nm-*Pseudomonas* sp.-made-green Ag composites associated with the same 6 antibiotics (erythromycin, novobiocin, vancomycin, lincomycin, penicillin G and oleandomycin) unleashed contrasting effects on *B. cereus*, *S. aureus*, *C. tropicalis*, *V. parahaemolyticus*, *E. coli*, *P. aeruginosa*, and *S. enterica* during a 24 h treatment at 28 °C [42]. The colloidal Ag solution, synthesized through $Ag^+$ reduction in supernatant of *Pseudomonas* sp. THG-LS1.4, was composed by larger Ag particles (~228.7 nm) and smaller (10–40 nm) Ag nanoparticles. Briefly, the protocol was as follows: small paper discs were soaked up with 500 µg.mL (500 ppm in 30 µL) of the green-made silver yield and then impregnated again with different antibiotics (10–30 µg.disc each) before being placed in the agar plates. Later on, clinical bacteria *P. aeruginosa*, *E. coli*, and *S. enterica* highly resistant strains to the 6 commercial antibiotics were sensitive to green AgNPs and exhibited inhibition zones reaching ~14.5 mm, ~13 mm, and ~ 11 mm, respectively. After a new set of treatments, it was suggested that synergistic effects possibly emerged when green nano-Ag slightly enhanced bacterial sensitivity to some of the antibiotics (see Table 10.2).

In this particular case as in many others we reviewed, it is questionable to consider such interactions emerging from g-AgNPs and antibiotics as a direct association. First, with no g-AgNP-cleaning up procedures after synthesis, both soluble and nano-Ag remained in solution. Secondly, silver concentration was extremely high (500 µg.mL). Thirdly, the inhibition zones from g-AgNP single exposure and antibiotic + g-AgNP treatments were very much alike and nonsignificant. As another example, a twofold increase against methicillin-resistant *Staphylococcus aureus* was documented by Manikprabhu and Lingappa [23] with 1 µg of oxacillin in agar, and freshly produced 28–50 nm g-AgNPs reduced from blue pigments of *Streptomyces coelicolor*. The synergistic effect might have been the result of multiple interacting factors as $Ag^+$, free pigments, active biomolecules, and green nanosilver. With equimolar concentrations of cyanobacterium *Oscillatoria limnetica*-made 3–18 nm g-AgNP 10 mg.mL and antibiotics (tetracycline or cefaxone at 10 mg.mL), Hamouda et al. [59] evaluated their antibacterial properties against *Escherichia coli* and *Bacillus cereus* by measuring inhibition growth in culture optical density with Luria-Bertani medium, and in a classical disc-diffusion method. By spectrophotometry, no significant differences were found with g-AgNP + cefaxone treatment compared to cefaxone itself or soluble Ag against both bacteria species. With the diffusion test, an antibacterial effect appeared, but neither g-AgNP

+ tetracycline nor g-AgNP + cefaxone conditions showed significant inhibition to be called synergistic.

Working with combined exposures of g-AgNP and antibiotics requires a very accurate experimental setup with objectives clearly formulated, and possible sources of errors comprehensively stated when comes time to interpret and discuss the results. So far, the studies dealing with g-AgNP produced by means of bacteria bioactive molecules and antibiotic combination employed ineffective (and often obsolete methods) to properly test their combined antibacterial proprieties. These studies also failed to fully explain their final results. Before such exposures, it is mandatory to anticipate (or in some cases to model) how the molecular structure of drugs would interact with silver and which testing doses should be used to assess bacterial sensitivity avoiding thus technical difficulties (as nanoparticle aggregation and precipitation). Often, a diffusion method with agar is used with antibiotic disc papers (5–30 μg) soaked up with raw solution of g-AgNPs. By using this simplistic exposition method, it is impossible to carefully calibrate the optimal dosage of drugs and AgNPs that cause real toxic effects in bacterial cells. Most probably, small changes in drug concentration and proportion can optimize or disrupt AgNP activity [56, 60, 61]. Very complex chemical and biochemical interactions between cell membranes, particulate/dissolved silver, and antibiotics are expected; and it gets even more complicated if no purification of the newly synthesized g-AgNP solution is performed before testing. In such a case, soluble silver, g-AgNPs, antibiotics, and unknown free bioactive molecules in solution will likely all interact with each other and bacteria in same time or in a stepwise chain of reactions (Fig. 10.3 A-C). With chloride and phosphate ions frequently found in agar or broth media composition, the equation achieves a new level of complexity.

From our exhaustive examination of published literature, we observed that several experiments seeking to obtain a synergistic effect with a co-exposure of g-AgNP + antibiotics failed to prove that such an effect was real. Many times, an antibiotic single treatment is first tested on bacteria as a "stand-alone drug control" using microbial strains known to be resistant to the given drug. Then, authors observe moderate or no effects, and confirm the resistance of strains. In the following step, the results of the exposure to the mixtures (antibiotic + g-AgNP) are described, and the synergistic effects are claimed only based on onefold (or less) increase of growth inhibition comparing to the antibiotic-alone condition in a basic ratio estimation. Oddly, g-AgNP antibacterial synergistic effect is estimated with $b$-$a$/$a$ x 100 formula (wherein $a$ is the drug effect and $b$ referred to g-AgNP + drug condition) that falls short to confirm such effects owing to the fact that it could just be an additive effect. A significant synergy in pharmacology is accepted when there is more than twofold deviation from concentration addition (dose addition) effects [62]. In other words, synergy rises up when mixtures obtain a minimum twofold difference between observed versus predicted effect concentrations, and a concentration addition as a reference model [62, 63]. Furthermore, synergism (also called superadditivity) for a drug pair not only relies on the agonist drug pair (herein g-AgNP and antibiotic), it depends on the ratio of the doses as well [63]. Hence, finding a range of dose ratios of two agonists is an additional step to bring synergistic interactions in a chemical

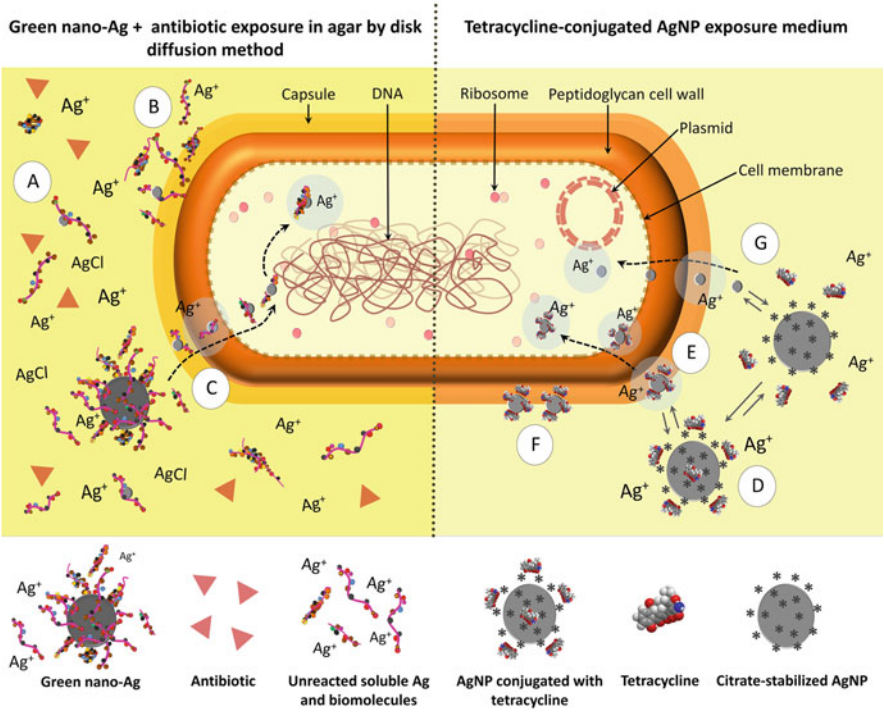


**Fig. 10.3** Schematic drawing of toxicity mechanisms of green silver nanoparticles (associated with antibiotic discs); and chemically produced tetracycline-conjugated AgNP against bacteria [60]. A- With an unfiltered solution of freshly produced g-AgNPs, a bacteria model will be exposed to soluble Ag, nanosilver, and bacteria exudates. By using antibiotic discs soaked with g-AgNP raw solution, an additional stressor will complexify green silver toxicity against bacteria. Considering the high levels of $Cl^-$ ions in agar (as in many other media), $Ag^+$ may precipitate as AgCl, which affects silver toxicity. B- Free bioactive bacterial biomolecules (previously separated from isolated strains) are an auxiliary agent to provoke joint toxicity with g-AgNPs on bacteria walls. C- Green nanosilver must behave like organic-coated AgNPs and easily penetrate in cells. By doing so, both interaction of the particle with cell structures and dissolution of Ag core will lead to nanotoxicity. D - A tetracycline-conjugated AgNP previously stabilized with citrate allows an increase of $Ag^+$ release. E and F- The presence of small amounts of tetracycline facilitates AgNP attachment to bacteria. Synergistic interactions will mainly occur following a principal pathway where a tetracycline + AgNP complex binds to bacteria and releases dissolved silver more than AgNP alone. G- Considered as a secondary and less likely pathway, AgNP alone would provoke toxicity by binding to bacteria and releasing $Ag^+$. The antibiotic molecule itself is not considered as a third pathway due to bacterial resistance to tetracycline

exposure. These relationships can be easily illustrated with a theoretical isobologram between g-AgNPs and an antibiotic causing low to higher effects in bacteria (Fig. 10.4).

Henceforth, in order to properly investigate the optimal synergism AgNP-drug ratio, an appropriate choice of dose combinations and the bacteria models must be

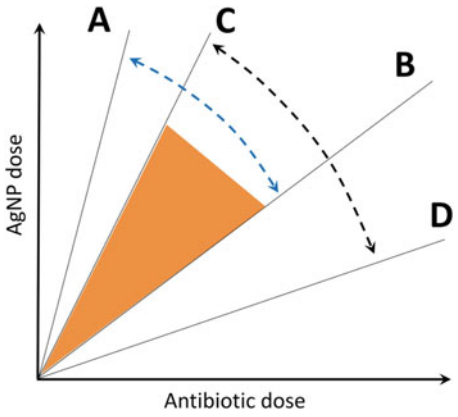


**Fig. 10.4** Synergistic interactions between nanosilver and antibiotics can be understood by a model predicting real synergism between two drugs (figure modified from [63]). To achieve a synergistic effect AgNP-antibiotic, it is necessary to optimize the drug combination dose ratio. Each axe represents the dose combinations of AgNPs and antibacterial drugs (dose ratios). The optimal synergistic dose will be found between a range of synergistic and subadditive doses. Synergism for a desired effect against bacteria will be determined for dose ratios between radial lines C and D (indicated by black arrowheads), while the subadditive effect is placed within the dose ratios between A and B (indicated by blue arrowheads). The intersection of these areas (orange triangle) represents the optimal set of ratios to reach a synergistic effect with no undesired side effects [63]

made as shown hereafter. Chemically produced citrate-stabilized 29.8 nm AgNPs (50 μM or 5.4 μg.mL) combined with tetracycline, enoxacin, kanamycin, and neomycin at different ratios (0.1–100 μM antibiotic/Ag) showed strong synergistic effects against drug-resistant *Salmonella* sp. [60]. The same outcome was not observed with ampicillin and penicillin. Even at lower doses of tetracycline, enoxacin, or kanamycin (~0.5 μM) in antibiotic + AgNP treatments, the inhibition was still observed. With 8–16 μM tetracycline + AgNPs, the inhibition reached nearly 100%. Quite the opposite, the AgNP itself was only able to inhibit 10% of *Salmonella* sp. growth in single treatments. The ratio of nano-Ag particles to *Salmonella* cells was ~73:1 in 0.108 μg.mL (1 μM) AgNP medium with ~1 x $10^7$ CFU.mL of bacteria cells. Testing 1 μM AgNPs for Ag binding to *Salmonella* cells (~1 × $10^7$ CFU.mL), the binding was 42.2% in the presence of 10 μM tetracycline; and it was not different when *Salmonella* cells increased to 4 × $10^7$ CFU.mL. Most strikingly, 50 μM AgNPs +1 μM tetracycline eliminated 90% of bacteria. Moreover, with a higher dose of tetracycline (10 μM), Ag-bacteria binding falls to 50%, but inhibition was still reaching 95%. Tetracycline molecules increased $Ag^+$ release from AgNPs to 14.5%, and once bacteria cells were present in AgNPs +10 μM tetracycline conditions, 18.2% of $Ag^+$ ions were leached away. In the presence of *Salmonella* only, $Ag^+$ is released at 12.1% (25% more than without bacteria cells). It can be concluded that some molecules such as tetracycline facilitate $Ag^+$ release [60] (Fig. 10.3 D-G). Noteworthy, aggregation of AgNPs emerged at

low antibiotic/AgNP molar ratios except for tetracycline. For a better comparison of mechanisms describing antibacterial effects of g-AgNP in exposure medium enriched with antibiotics (by disk diffusion method), and those observed with chemically synthesized AgNP + tetracycline molar combination (in aqueous solution); see Fig. 10.3.

Using the disc diffusion method, Railean-Pluragu et al. [61] tested a series of combinations with green synthesized AgNPs and classical antibiotics (kanamycin 5 μg, ampicillin 25 μg, neomycin 30 μg, streptomycin 25 μg) against Gram-negative *Salmonella infantis*, *Pseudomonas aeruginosa*, *Klebsiella pneumoniae*, and *Staphylococcus aureus*. The antibiotic disc was impregnated with 100 μg.mL g-AgNPs and placed into trypticase soy agar (TSA) plates. The 4–45 nm actinomycete-produced AgNPs were first properly separated from unreacted silver and bacterial exudates in a 3-day dialysis. A detailed study using flow cytometry showed that *Pseudomonas aeruginosa* was the most affected species by both g-AgNP single treatment (50 and 100 μg.mL) and streptomycin, neomycin, or kanamycin + g-AgNPs (12.5 μg.mL) exposures. After treatments, concentration of living cells was significantly lower than negative or positive controls. Such combinations were even less effective than g-AgNP single treatment in the *K. pneumoniae* case. Reduced doses of g-AgNPs (12.5 μg.mL) in single exposures were enough to significantly inhibit other bacteria such as *S. aureus* and *P. mirabilis*.

At the molecular level, g-AgNP and tetracycline combination seem to impair *Bacillus subtilis* metabolism [56] (Fig. 10.5). After a 2 h incubation in g-AgNP + tetracycline liquid medium, a sporulation process of *Bacillus subtilis* started. This condition was also triggered by g-AgNPs in single treatments. *Bacillus subtilis* is a rod-shaped bacteria known to go through sporulation process under inhospitable and lethal conditions to its normal vegetative forms. The coiling of bacterial DNA in g-AgNP single treatments after 6 h indicated the beginning of sporulation, with two cell populations present in the medium: a modified cell and a normal cell similar to the controls. Tetracycline-alone condition did not cause sporulation, but rather disintegrated cell cytoplasm after 2 h. In g-AgNP + tetracycline medium, cells were unable to complete the sporulation, which seems to be mostly due to tetracycline. Later on (4 h), cell-damaging condition was visible and it appeared in g-AgNP + tetracycline medium as well. Likewise, dissolved silver seems to contribute to toxicity: 12.5 μg.mL $Ag^{+}$-treated cells were severely damaged just after 2 h. With such combination, the sporulation is only induced by g-AgNPs, but tetracycline simultaneously avoided its completion.

Above published papers have shown promising results when g-AgNPs and antibiotics are added together to induce antibacterial effects, but some results are conflicting. Sometimes a green nano-Ag + antibiotic exposure can bring synergistic effects and detrimental effects to bacteria, but in other assays, these interactions may lead to nano-Ag aggregation and a reduced toxicity as well [60]. In order to accurately evaluate satisfactory synergistic effects of green nano-Ag and antibiotics in vitro, the following guidelines should be considered: (1) careful selection of the growing phase of bacteria cells [52]; (2) accurate preparation of g-AgNP inoculates including efficient dialysis of stock solution and determination of actual

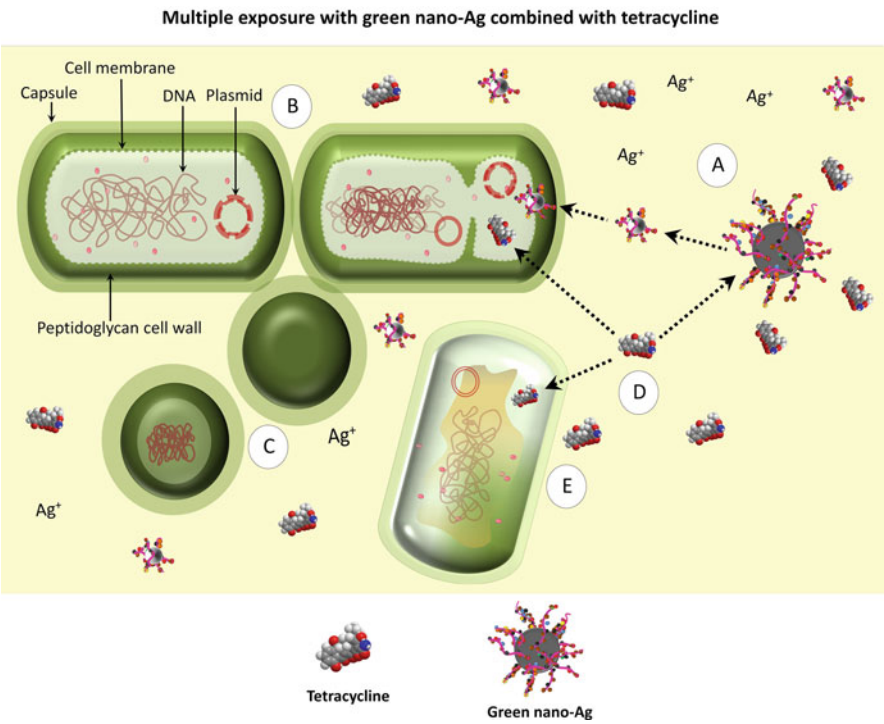


**Fig. 10.5** Schematic drawing of toxicity mechanisms of green silver nanoparticles combined with tetracycline (in solution) against *Bacillus subtilis*, and assessed in Mueller-Hinton broth medium [53]. A- The experiment began with a 2 h incubation in g-AgNP + tetracycline medium. B and C- The DNA coiling process indicated sporulation (from normal cell on the left to shrunken cell on the right; the spores below them). In g-AgNP single exposures, the same two cell types were observed. Sporulation began after 2h of exposure in the g-AgNP + tetracycline medium and in the g-AgNp single exposure. D and E- Tetracycline alone disintegrated cell cytoplasm. With g-AgNP mixed with tetracycline, cells do not complete the sporulation and started dying 4 h later. Dotted arrows represent possible pathways taken by tetracycline and g-AgNP. Due to dissolution of Ag core, soluble silver is also represented in the figure

concentrations of g-AgNPs); (3) running pre-screened low nominal concentrations of both green nano-Ag and antibiotics before testing [60]; (4) identification by FT-IR and NMR techniques of the main functional groups present in antibiotic molecules and green nano-Ag surfaces; and the exposure media constituents.

## 10.6 Final Thoughts

To date, most of the research dealing with green silver nanoparticles obtained by bacteria byproducts aimed to primarily describe the AgNP biosynthesis methods using a wide range of bacteria taxa and then eventually test the antibacterial potential

of g-AgNPs against pathogenic strains. The lack of analytical data, dialysis of green nano-Ag-stock solution, and g-AgNP kinetic experiments in so many reports is, however, a major setback. The pre-definition of final nominal concentrations is another crucial point to be taken into consideration if precision and accuracy are intended for such assays. Overall, FT-IR or $^{1}$HNMR spectral analysis provided a helpful dataset to progress forward new investigations of g-AgNP toxicity mechanisms. We suggest that g-AgNPs likely behave as chemically produced organic-coated AgNPs. By doing so, the g-AgNP-coating layer could have an important role in green nanosilver toxicity by mediating $Ag^{+}$ release and/or attaching nanoparticles to bacteria cells. But what about the capping biomolecules obtained from actinobacteria residues, for example? Do they just act as facilitators of Ag toxicity or directly interfere with bacteria metabolism as well? And which free biomolecules in bacteria supernatant interfere with g-AgNP solubility? Only by elucidating the complex interactions among silver forms, bacteria-capping agents, and antibiotics can the way be paved to a deeper understanding whether or not g-AgNPs might be really useful to treat bacterial infections in humans. There is no doubt these interactions are very complex, and progress of the knowledge at the molecular level would require the contribution of a number of sub-disciplines such as structural biochemistry, surface nanochemistry, and toxicokinetic modeling, among others.

## References

1. Medici S et al (2019) Medical uses of silver: history, myths, and scientific evidence. J Med Chem 62:5923–5943
2. Cohen M et al (2007) *In vitro* analysis of a nanocrystalline silver-coated surgical mesh. Surgical Infections (Larchmt) 8:397–403
3. Slane J et al (2015) Mechanical, material, and antimicrobial properties of acrylic bone cement impregnated with silver nanoparticles. Mater Sci Eng C 48:188–196
4. Panáček A et al (2018) Bacterial resistance to silver nanoparticles and how to overcome it. Nat Nanotechnol 13:65–71
5. Durán N et al (2015) Silver nanoparticles: a new view on mechanistic aspects on antimicrobial activity. Nanomedicine 12(3):789–799
6. Roy A et al (2019) Green synthesis of silver nanoparticles: biomolecule-nanoparticle organizations targeting antimicrobial activity. RSC Adv 9:2673–2702
7. Jelinkova P et al (2019) Nanoparticle-drug conjugates treating bacterial infections. J Control Release 307:166–185
8. Divya M et al (2019) Biogenic synthesis and effect of silver nanoparticles (AgNPs) to combat catheter-related urinary tract infections. Biocatal Agric Biotechnol 18:101037. https://doi.org/10.1016/j.bcab.2019.101037
9. Gahlawat G, Choudhury R (2019) A review on the biosynthesis of metal and metal salt nanoparticles by microbes. RSC Adv 9(12944):12944
10. Khan Z, Al-Thabaiti S (2019) Biogenic silver nanoparticles: green synthesis, encapsulation, thermal stability and antimicrobial activities. J Mol Liq 289:111102. https://doi.org/10.1016/j.molliq.2019.111102
11. Kang F et al (2013) Microbial extracellular polymeric substances reduce Ag+ to silver nanoparticles and antagonize bactericidal activity. Environ Sci Technol 48:316–322

12. Karthik L et al (2014) Streptomyces sp. LK3 mediated synthesis of silver nanoparticles and its biomedical application. Bioprocess Biosyst Eng 37:261–267
13. Lengke M et al (2007) Biosynthesis of silver nanoparticles by filamentous cyanobacteria from a silver (I) nitrate complex. Langmuir 23:2694–2699
14. Subramani R, Aalbersberg W (2012) Marine actinomycetes: an ongoing source of novel bioactive metabolites. Microbiol Res 167:571–580
15. Gano-Cohen K et al (2016) Nonnodulating Bradyrhizobium spp. modulate the benefits of legume-rhizobium mutualism. Appl Environ Microbiol 82:17. https://doi.org/10.1128/AEM.01116-16
16. Song AA-L et al (2017) A review on *Lactococcus lactis*: from food to factory. Microb Cell Factories 16:55. https://doi.org/10.1186/s12934-017-0669-x
17. Manivasagan P et al (2013) Biosynthesis, antimicrobial and cytotoxic effect of silver nanoparticles using a novel *Nocardiopsis* sp. MBRC-1. BioMed Res Int 2013: 287638. https://doi.org/10.1155/2013/287638
18. Rajivgandhi G et al (2019) Biosynthesized silver nanoparticles for inhibition of antibacterial resistance and biofilm formation of methicillin-resistant coagulase negative staphylococci. Bioorg Chem 89:103008
19. Abd-Elnaby HM et al (2016) Antibacterial and anticancer activity of extracellular synthesized silver nanoparticles from marine *Streptomyces rochei* MHM13. Egypt J Aquat Res 42:301–312
20. Samundeeswari A et al (2012) Biosynthesis of silver nanoparticles using actinobacterium *Streptomyces albogriseolus* and its antibacterial activity. Biotechnol Appl Biochem 59:503–507
21. Sivalingam P et al (2012) Mangrove *Streptomyces* sp. BDUKAS10 as nanofactory for fabrication of bactericidal silver nanoparticles. Colloids Surf B: Biointerfaces 98:12–17
22. Shanmugasundaram T et al (2013) A study of the bacterial, anti-fouling, cytotoxic and antioxidant properties of actinobacterially synthesized silver nanoparticles. Colloids Surf B: Biointerfaces 111:680–687
23. Manikprabhu D, Lingappa K (2013) Antibacterial activity of silver nanoparticles against methicillin-resistant *Staphylococcus aureus* synthesized using model *Streptomyces* sp. pigment by photo-irradiation method. J Pharm Res 6:255–260
24. Otari SV et al (2015) Intracellular synthesis of silver nanoparticle by actinobacteria and its antimicrobial activity. Spectrochim Acta A Mol Biomol Spectrosc 136:1175–1180
25. Skladlanowski M et al (2016) Evaluation of cytotoxicity, immune compatibility and antibacterial activity of biogenic silver nanoparticles. Med Microbiol Immunol 205:603–613
26. Iniyan AM et al (2017) *In vivo* safety evaluation of antibacterial silver chloride nanoparticles from *Streptomyces exfoliatus* ICN25 in zebrafish embryos. Microb Pathog 112:76–82
27. Sivasankar P et al (2018) Characterization, antimicrobial and antioxidant property of exopolysaccharide mediated silver nanoparticles synthesized by *Streptomyces violaceus* MM72. Carbohydr Polym 181:752–759
28. Al-Dhabi NA et al (2018) Characterization of silver nanomaterials derived from marine *Streptomyces* sp. Al-Dhabi-87 and its *in vitro* application against multidrug resistant and extent-spectrum beta-lactamase clinical pathogens. Nanomaterials 8:279
29. Sanjivkumar M et al (2019) Investigation on characterization and biomedical properties of silver nanoparticles synthesized by an actinobacterium *Streptomyces olivaceus* (MSU3). Biocatal Agric Biotechnol 17:151–159
30. Kang SG et al (2000) New β-lactamase inhibitory protein (BLIP-I) from *Streptomyces exfoliatus* SMF19 and its roles on the morphological differentiation. J Biol Chem 22:16851–16856
31. El-Deeb B, Mostafa NY, Altalhi A, Gherbawy Y (2013) Extracellular biosynthesis of silver nanoparticles by bacteria *Alcaligenes faecalis* with highly efficient anti-microbial property. Int J Chem Eng 30:1137–1144
32. Sunkar S, Nachiyar CV (2012) Biogenesis of antibacterial silver nanoparticles using the endophytic bacterium *Bacillus cereus* isolated from *Garcinia xanthochymus*. Asian Pac J Trop Biomed 2:953–959

33. Oves M et al (2013) Antibacterial and cytotoxic efficacy of extracellular silver nanoparticles biofabricated from chromium reducing novel O64 strain of *Stenotrophomonas maltophilia*. PLoS One 8:e59140
34. Malarkodi C et al (2013) Bactericidal activity of bio-mediated silver nanoparticles synthesized by *Serratia nematodiphila*. Drug Invention Today 5:119–125
35. Thomas R et al (2014) Antibacterial properties of silver nanoparticles synthesized by marine *Ochrobactrum* sp. Braz J Microbiol 45:1221–1227
36. Syed B et al (2016) Synthesis of silver nanoparticles by endosymbiont *Pseudomonas fluorescens* CA417 and their bacterial activity. Enzym Microb Technol 95:128–136
37. Syed B et al (2019) Synthesis and characterization of silver nanobactericides produced by *Aneurinibacillus migulanus* 141, a novel endophyte inhabiting *Mimosa pudica* L. Arab J Chem. 12(8) 3743-3752. https://doi.org/10.1016/j.arabjc.2016.01.005
38. Rasulov B et al (2016) Synthesis of silver nanoparticles on the basis of low and high molar mass exopolysaccharides of *Bradyrhizobium japonicum* 36 and its antimicrobial activity against some pathogens. Folia Microbiology 61:283–293
39. Railean-Plugaru V et al (2017) *Lactococcus lactis* as a safe and inexpensive source of bioactive silver composites. Appl Microbiol Biotechnol 101:7141–7153
40. Ramasubburayan R et al (2017) Synthesis of nano silver by a marine epibiotic bacterium *Bacillus vallismortis* and its potent ecofriendly antifouling properties. Environmental Nanotechnology, Monitoring and Management 8:112–120
41. Singh H et al (2017) Biosynthesis of silver nanoparticles using *Aeromonas* sp. THG-FG1.2 and its antibacterial activity against pathogenic microbes. Artificial cells, Nanomedicine, and Biotechnology 45:584–590
42. Singh H et al (2018) Extracellular synthesis of silver nanoparticles by *Pseudomonas* sp. THG-LS1.4 and their microbial application. Journal of Pharmaceutical Analysis 8:258–264
43. Kandel S et al (2017) Bacterial endophyte colonization and distribution within plants. Microorganisms 5:77. https://doi.org/10.3390/microorganisms5040077
44. Lok C-N et al (2017) Silver nanoparticles: partial oxidation and antibacterial activities. J Biol Inorg Chem 12:527–534
45. Htwe YZN et al (2019) Effect of silver nitrate concentration on the production of silver nanoparticles by green method. Mater Today Proc 17(3):568–573
46. Gunawan C et al (2014) Nanoparticle-protein corona complexes govern the biological fates and functions of nanoparticles. J Mater Chem B 2:2060–2083
47. Ferreyra Maillard A et al (2019) Studies on interactions of green silver nanoparticles with whole bacteria by surface characterization techniques. BBA-Biomembranes 1861:1086–1092
48. Bardaxoglou G et al (2017) High stability and very slow dissolution of bare and polymer coated silver nanoparticles dispersed in river and coastal waters. J Aquatic Pollut Toxicol 12:15
49. Li J et al (2019) Controlled release and long-term antibacterial activity of dialdehyde nanofibrillated cellulose/silver nanoparticle composites. ACS Sustainable Chemistry Engineering 7:1146–1158
50. Baygar T et al (2019) Antimicrobial characteristics and biocompatibility of the surgical sutures coated with biosynthesized silver nanoparticles. Bioorg Chem 86:254–258
51. Vetchinkina E et al (2019) Shape and size diversity of gold, selenium, and silica nanoparticles prepared by green synthesis using fungi and bacteria. Industrial & Engineering Chemistry Research DOI 58:17207. https://doi.org/10.1021/acs.iecr.9b03345
52. Gordienko MG et al (2019) Antimicrobial activity of silver salt and silver nanoparticles in different forms against microorganisms of different taxonomic groups. J Hazard Mater 378:120754
53. Schumacher A et al (2018) *In vitro* antimicrobial susceptibility testing methods: agar dilution to 3D tissue-engineered models. Eur J Clin Microbiol Infect Dis 37:187–208. https://doi.org/10.1007/s10096-017-3089-2

54. Tuncer M, Seker E (2011) Single step sol-gel made silver chloride on Titania xerogels to inhibit *E. coli* bacteria growth: effect of preparation and chloride ion on bactericidal activity. J Sol Gel Sci Technol 59:304–310
55. Levard C et al (2013) Effect of chloride on the dissolution rate of silver nanoparticles and toxicity to *E. coli*. Environ Sci Technol 47:5738–5745
56. Rafińska K et al (2019) Study of *Bacillus subtilis* response to different forms of silver. Science of Total Environment 661:120–129
57. Railean-Pluragu V et al (2016) Study of silver nanoparticles synthesized by acidophilic strain of Actinobacteria isolated from the *Picea sitchensis* forest soil. J Appl Microbiol 120:1250–1263
58. Stokes JM et al (2019) Bacterial metabolism and antibiotic efficacy. Cell Metab 30(6):251–259
59. Hamouda RA et al (2019) Characterization of silver nanoparticles derived from the cyanobacterium *Oscillatoria limnetica*. Scientific Rep 9:13071. https://doi.org/10.1038/s41598-019-49444-y
60. Deng H et al (2016) Mechanistic study of the synergistic antibacterial activity of combined silver nanoparticles and common antibiotics. Environ Sci Technol 50:8840–8848
61. Railean-Pluragu V et al (2016) Antimicrobial properties of biosynthesized silver nanoparticles studied by flow cytometry and related techniques. Electrophoresis 37:752–761
62. Cedergreen N (2014) Quantifying synergy: a systematic review of mixture toxicity studies within environmental toxicology. PLoS One 9(5):e96580
63. Tallarida RJ (2011) Quantitative methods for assessing drug synergism. Genes Cancer 2:1003–1008

# Green Synthesis of Selenium Nanoparticles (SeNPs) Via Environment-Friendly Biological Entities

11

Chunlan Xu

**Abstract**

Selenium (Se) is an essential trace element for human and animal health. Se nanoparticles (SeNPs) have gained extensive attention due to its unique biological properties. The green synthesis of SeNPs via environment-friendly biological entities is gaining importance to promote the application of SeNPs due to its security and efficiency compared to conventional physical and chemical methods. SeNPs exhibit attractive biological activities including antioxidant, antimicrobial, anti-inflammatory, and anticancer. Up to now, SeNPs have been tried to apply in biomedicine, nutritional supplement, biosensor, and environmental remediation. This chapter is aimed to provide an overview about the biosynthesis strategies, mainly biological effects and potential applications of SeNPs.

**Keywords**

Selenium nanoparticles · Antioxidant activity · Anticancer · Biosynthesis

## 11.1 Introduction

Green nanotechnology is a multidisciplinary field that has attracted considerable attention. Nanomaterials employing green nanotechnology have been widely applied in food, medicine, environment, etc. Therefore, the emergency of green nanotechnology has significantly changed our daily lives. Selenium (Se) as an

C. Xu (✉)
The Key Laboratory for Space Bioscience and Biotechnology, School of Life Sciences, Northwestern Polytechnical University, Xi'an, Shaanxi, China
e-mail: clxu@nwpu.edu.cn

© Springer Nature Singapore Pte Ltd. 2020

Q. Saquib et al. (eds.), *Green Synthesis of Nanoparticles: Applications and Prospects*, https://doi.org/10.1007/978-981-15-5179-6_11

essential trace element possesses unique biological functions. It usually exists in different chemical forms in nature. Se species exhibit different bioavailability and cytotoxicity effects [1]. Among them, selenium nanoparticles (SeNPs) have outstanding biological properties [2]. The results of safety evaluation based on cell and animal models indicated that the toxicity of Se species is ranked as follows: selenate > selenite > SeMet > SeNPs > lactomicroSe [3–5]. According to the current researches, the preparation process of SeNPs usually employed physical, chemical, and biological methods. By comparison, biosynthesis of SeNPs, the so-called green synthesis, has been recognized as a safe, low-cost, and eco-friendly approach [6, 7]. It is worth mentioning that biogenic SeNPs have broad application prospects owing to their unique physicochemical and biological properties. This chapter mainly focused on biosynthesis strategy of SeNPs, biological activities, and applications in biomedicine, food nutrition, and environmental restoration.

## 11.2 Biological Synthesis of SeNPs

These biological systems including bacteria, fungi, and plants possess the ability to transform selenite or selenate into elemental SeNPs. Biosynthesis of SeNPs is characterized by cost-effectiveness and eco-friendliness, which is considered to have great potential and advantages to replace traditional physical and chemical synthesis methods [6]. Biosynthesis of SeNPs by a novel green approach is often termed as "green synthesis" procedure. A variety of biological entities were employed to produce SeNPs [7]. Figure 11.1 shows the usually employed biological entities for the biosynthesis of SeNPs such as microbial, plant, algae, and biomimetic.

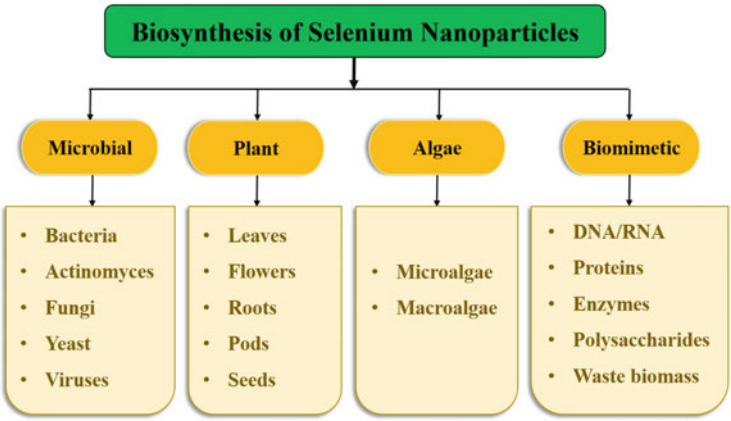


**Fig. 11.1** Biological entities were employed to synthesize SeNPs

### 11.2.1 Biological Synthesis of SeNPs by Plants

The biosynthesis of SeNPs employing plant extract has gained heightened research interest and is considered to be a green, economic, and eco-friendly way. Extracts from leaf, root, fruit, and seed have been used to synthesize SeNPs as stabilizers and/or reducing agents [8–12]. In general, the biological components in plant extracts such as polyphenols, ascorbic acid, alkaloids, terpenoids, carboxylic acids, polysaccharides, polyols, and flavonoids play a prominent role for the synthesis of SeNPs. Those bioactive substances were closely related to the transformation, encapsulation, and stabilization of SeNPs. Adding *Undaria pinnatifida* polysaccharides to the redox system composed of selenite and ascorbic acid is beneficial to the synthesis of size-controlled nano-Se [13]. Dried *Vitis vinifera* (raisin) contains bioactive components such as sugars, flavonoids, phenolic compounds, minerals, iron, vitamins, potassium, calcium, etc. [15]. Therefore, raisin extract was employed as a substrate for SeNPs [14]. Metabolites from plant extracts such as phenolics, flavonoids, and tannins play a crucial role in the process of SeNPs synthesis [16].

### 11.2.2 Biological Synthesis of SeNPs by Bacteria

The synthesis of SeNPs using bacteria has attracted wide attention due to its easy handling, fast growth rate, high efficiency, low cost, and environmental friendliness. On the other hand, the size and yield of NPs can be optimized. More and more studies have confirmed that a variety of bacteria possess the ability to transform the toxic selenite to the less toxic element Se and therefore have been employed to synthesize either intracellular or extracellular SeNPs with different size and morphology [17–21]. *Citrobacter freundii* Y9 exhibited high reduction efficiency of sodium selenite and synthesized SeNPs under both aerobic and anaerobic conditions [22]. Zhang et al. reported a cost-effective and eco-friendly biological approach for biogenic SeNPs synthesized by *Pseudomonas alcaliphila* [17]. The size and morphology of Se nanomaterials could be affected by various factors such as medium composition, pH, temperature, and initial selenite concentration [23]. Che et al. established the controllable synthesis approach of Se nanomaterials using *Lysinibacillus* sp. ZYM-1. The fabricated SeNPs using *Enterobacter* sp. strain were predominantly monodispersed and were stable for more than 2 months without significant aggregation. The bacterial proteins are believed to be responsible for the long-term stability of the biogenic SeNPs [24]. Our previous research indicated that SeNPs can be synthesized by *Lactobacillus casei* 393 and were accumulated intracellularly [3].

The synthesis process, characterization, and biological activity are shown in Fig. 11.2.

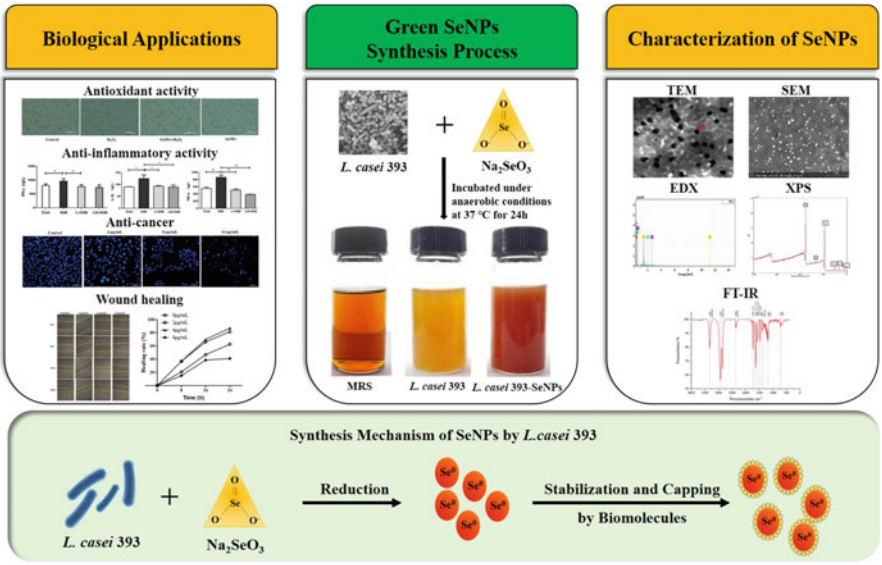


**Fig. 11.2** Synthesis of SeNPs using *Lactobacillus casei* 393: preparation, characterization, and their biological activities (adapted from Xu et al. [3])

### 11.2.3 Biological Synthesis of SeNPs by Fungi

Biosynthesis of NPs using fungi is also an eco-friendly and cost-effective process. Early studies demonstrated that several fungi such as *Candida albicans* [25], *Aspergillus parasiticus* [26], *Fusarium* sp. [27], *Mortierella* spp. [28], *Aureobasidium pullulans* [29], and *Aspergillus terreus* [30] can transform selenate and selenite to red SeNPs. Moreover, biogenic SeNPs accumulate intra- or extracellularly. The composition of the culture medium had a significant effect on the reduction of selenite [29]. The culture filtrate of *Alternaria alternata* exhibited the ability to reduce selenate to SeNPs [31]. Vetchinkina et al. first reported that organoselenium compound and inorganic sodium selenite can be reduced to SeNPs by edible basidiomycete *Lentinula edodes.* Moreover, the reduced SeNPs were accumulated in its mycelium [32]. Recently, Mosallam et al. established the green and simple synthesis method of SeNPs employing *Aspergillus oryzae*-fermented Lupin extract with gamma rays [33].

## 11.3 Beneficial Effects of SeNPs

### 11.3.1 Antioxidant Activity of SeNPs

One of the important biological activities of SeNPs is involved in the regulation of redox balance. Biogenic SeNPs using *Enterobacter cloacae* Z0206 exhibited strong antioxidant activity compared to SeMet and nano-Se prepared by chemical method, which attenuated oxidative stress-induced intestinal barrier damage [34]. Biogenic SeNPs synthesized by *K. pneumonia* could effectively alleviate testis oxidative damage caused by cisplatin [35]. SeNPs capped by *Lycium barbarum* polysaccharides exert high strong free radical scavenging activity [12]. Biogenic exopolysaccharide-capped SeNPs synthesized by *Bacillus paralicheniformis* SR14 suppressed the production of reactive oxygen species (ROS) and effectively protected against hydrogen peroxide ($H_2O_2$)-induced porcine jejunal epithelial cell oxidative damage [36]. The possible mechanism of SeNPs exhibits attractive antioxidant activity mainly manifested in the following aspects: (1) improved antioxidant defense, (2) improved bioenergetics, and (3) antioxidant effect [37]. Se is the important component of selenoproteins such as thioredoxin reductase (TrxR) and glutathione peroxidase (GPx). Many selenoproteins are involved in the redox status regulation and play a crucial role in protecting cells and tissues from oxidative damage. Suzuki et al. found that Se is absorbed, bound to albumin, and then transported to the liver for selenoprotein synthesis [38].

### 11.3.2 Anticancer Activity of SeNPs

Biogenic SeNPs exhibit higher anticancer activity, better biocompatibility, greater stability, and lower toxicity than inorganic and organic Se species and the chemically synthesized SeNPs [39, 40]. Biogenic SeNPs using *Bacillus licheniformis* JS2 can be cellularly internalized and induce ROS-mediated PC-3 cancer cell necroptosis [41]. SeNPs conjugated with transferrin promoted the generation of intracellular ROS and induced MCF-7 cell apoptosis through the activation of mitogen-activated protein kinase (MAPK) pathway [39]. It has also been reported that glucose-modified SeNPs triggered HepG2, MCF-7, A549, and Neuro-2a cell apoptosis [40]. The intracellular mechanisms of A375 cell apoptosis induced by SeNPs may be associated with mitochondrial dysfunction caused by oxidative stress. In addition, SeNPs are the promising form for delivery of anticancer drugs into cancer cells [42]. Nano-selenium may be further evaluated as a candidate for chemopreventive and chemotherapeutic agents in human cancers such as melanoma cancer [13]. SeNPs modified by sialic acid induced dose-dependent apoptotic cell death. Folate-chitosan-modified SeNPs could target cancer cells with the overexpression of folate receptor and then enter the cells and further induce the excessive production of ROS in cells, thus promoting cell apoptosis [43].

### 11.3.3 Antimicrobial Properties of SeNPs

NPs can inhibit pathogenic microorganisms and overcome drug resistance including decreased and slow drug uptake and efflux pumps, inactivating enzymes, biofilm formation, and intracellular bacterial parasitism [44]. Biogenic SeNPs synthesized by *Stenotrophomonas maltophilia* and *Bacillus mycoides* can inhibit the formation of biofilm and degrade glycocalyx, which was observed in both *P. aeruginosa* and *Candida* spp. [45]. Previous research demonstrated that the biofilm of clinical pathogens such as *S. aureus*, *P. aeruginosa*, and *P. mirabilis* could be effectively inhibited by biogenic SeNPs synthesized by *Bacillus* sp. MSh-1 [20]. Moreover, the antimicrobial activities of biogenic SeNPs against multidrug-resistant bacteria and pathogenic fungi including *Acinetobacter calcoaceticus*, *Staphylococcus aureus*, *Candida albicans*, and *Aspergillus flavus* were also described [33]. The biogenic SeNPs by *Enterococcus faecalis* prevented biofilm formation of *S. aureus*, which suggested that it was a promising and potential agent against *S. aureus* infections [46].

### 11.3.4 Anti-Inflammatory Activities of SeNPs

Previous researches demonstrated that SeNPs exhibited anti-inflammatory activities. The immunomodulatory activity was observed for SeNPs modified with the water-soluble derivative of *Ganoderma lucidum* polysaccharides [47]. Biogenic SeNPs by *L. plantarum* improved the immune responses and survival of mice in breast cancer murine model [48]. SeNPs modified with *Ulva lactuca* polysaccharide effectively alleviated colitis induced by dextran sodium sulfate (DSS), which may be associated with their inhibitory effects on NF-κB-mediated hyperinflammation signaling pathway [49]. Biogenic SeNPs by *Mycobacterium bovis* could induce an influential immune response against HB antigens [50]. In addition, the potential anti-inflammatory activity of SeNPs was found in irradiated rats [51]. The possible mechanisms of SeNPs exerting anti-inflammatory activity are as follows: p38 MAPKs and NF-κB signaling pathways were regulated in order to reduce the expression of inflammatory cytokines [37].

## 11.4 Applications of SeNPs

SeNPs prepared by green nanotechnology have been widely applied in biomedicine, biosensors, nutrition supplementation, environmental remediation, etc. (Fig. 11.3) due to their unique biological, physical, and chemical properties such as multiple effect, biocompatibility, stability and low toxicity, cost-effectiveness, and eco-friendliness. The details of various applications are further discussed in the following sections.

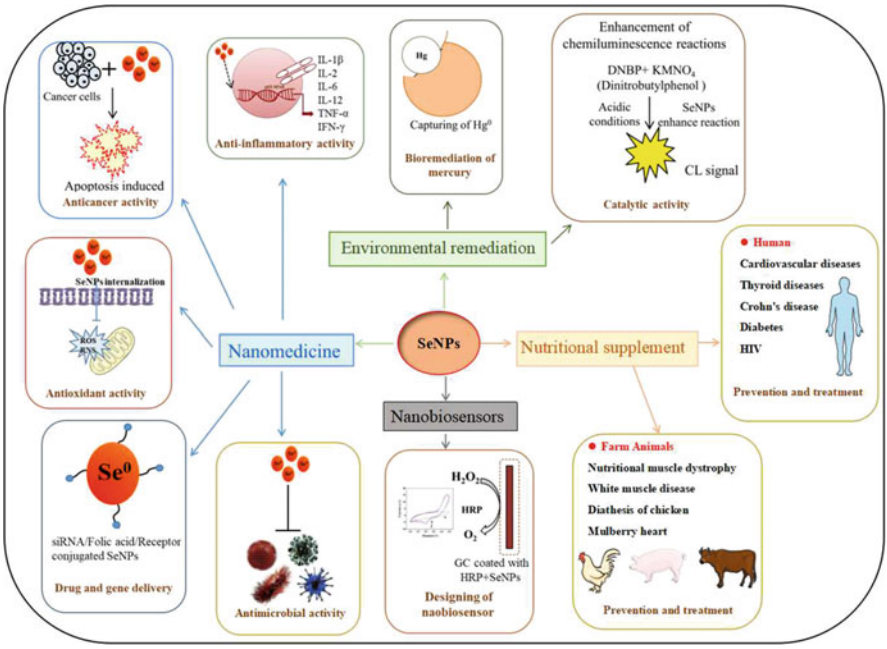


**Fig. 11.3** Applications of SeNPs (adapted from Wadhwani et al. [7] with appropriate modification)

### 11.4.1 Biomedicine

In recent years, SeNPs have been applied to oppose tumor, prevent diabetes, protect against liver damage, and reduce the toxic effects of drugs [39, 52–54]. Moreover, SeNPs are potential platform for drug and gene delivery. SeNPs decorated by chitosan conjugated with vasoactive intestinal peptide receptor 2 (VPAC2) agonist peptide exhibited selective activity against type 2 diabetes [55]. RGDfC-conjugated functionalized SeNPs have been reported to target delivery of siRNA against liver carcinoma [56]. Kalishwaralal et al. confirmed chitosan-modified SeNP films have shown promise as substrates for cellular behavior and as biocompatible film for cardiac tissue engineering applications [57]. Biogenic SeNPs were able to protect against hepatic injury induced by $CCl_4$ via enhancing the antioxidant capacity and relieving oxidative stress [58]. SeNPs synthesized by *Bacillus* sp. MSh-1 can be considered to treat the localized lesions typical of cutaneous leishmaniasis as a novel therapeutic agent [59]. In summary, SeNPs possess pleiotropic pharmacological activities. However, extensive safety evaluation experiments should be conducted before clinical transformation.

### 11.4.2 Biosensors

Nanomaterials possess conspicuous physicochemical characteristics such as photoelectric and semiconductor properties and have great potential and advantages in developing biosensors. Se is widely used in photocells, photographic exposure meters, semiconductor rectifiers, and in photocopy machines [17]. SeNPs also possess excellent photoelectric and semiconductor property. Prasad et al. established an eco-friendly and cost-effective approach for the synthesis of SeNPs using the crude enzyme isolated from *Bacillus pumilus* BAB-3706-fermented product. Moreover, biogenic SeNPs by the above method were with high surface area/volume ratio and could be made into low-cost and sensitive $H_2O_2$ biosensors [60]. Biogenic SeNPs by *Pseudomonas aeruginosa* JS-11 can be developed as a biosensor to assess nanotoxicity by monitoring the biological reduction process of $SeO_32$- treated with bacterial culture supernatant. The inhibition point of the reduction process can be considered as the toxicity end point [61]. Semiconductor monoclinic SeNPs by *Bacillus subtilis* have been used as enhancing and settled materials for $H_2O_2$ biosensor due to their high surface-to-volume ratio, good adhesive ability, and biocompatibility [62].

### 11.4.3 Environmental Remediation

As a worldwide problem, environmental pollution is becoming more and more serious and has attracted more and more attention. In recent years, researchers tried to employ SeNPs to treat air, water, and soil pollution based on their unique physical and chemical properties. Firstly, toxic Se species in the environment are removed by converting selenates and selenites into nontoxic elemental Se [63, 64]. On the other hand, SeNPs have been commonly used to treat groundwater and soil polluted by heavy metals or halogenated hydrocarbons. Jain et al. found that divalent cationic heavy metals such as $Zn^{2+}$ could be adsorbed onto BioSeNPs [65]. Hg0-contaminated surface and subsurface soils could be remediated by biogenic nano-$Se^0$ by *Citrobacter freundii* Y9, which was a cost-effective method [22]. Biogenic SeNPs were reported to exhibit photocatalytic activity of bromothymol blue and rhodamine B, which indicated that it could be useful in dye wastewater treatment [23, 66]. It is urgent to develop a bioreactor and establish an operational mode for SeNPs to effectively control and treat environmental pollution.

### 11.4.4 Nutritional Supplement

Se, as an essential micronutrient, is an important component of selenoprotein including selenoenzymes, which protect against free radical-induced cell and tissue oxidative damage [67, 68]. Se-enriched dietary supplement aroused great interest in pharmaceutical and food sciences [69]. Se supplementation is recommended for the diseases including HIV, Crohn's disease, cardiovascular disease, thyroid disease,

and kidney dialysis. Currently, the common forms of Se supplements mainly include sodium selenite, SeMet, or Se-enriched yeasts. SeNPs are considered to be a safe, economic, and efficient form of Se for exerting their biological activities [70–73]. The extent of absorption of NPs in the gastrointestinal tract depends on the size of their NPs. It was proven that NPs could be transported into the intestinal mucous layer covering the surface of the gastrointestinal tract [74]. After that, NPs penetrated into intestinal epithelial cells by passive or active transport [75]. Then, NPs were excreted from tissue cells by either transcytosis or exocytosis [76]. As a potential nutritional supplement, the dosage, form, and size of SeNPs should be further investigated.

## 11.5 Future Prospects of Biogenic SeNPs

Green nanotechnology attracted wide concerns because the nanoscale materials prepared by it were with unique physical, chemical, and biological properties. SeNPs were reported to possess antibacterial, anticancer, anti-inflammatory, and antioxidant activity. Moreover, SeNPs showed lower toxicity compared to other Se species. Biological entities that were employed microbial, plant, algae, and biomimetic supply a safe, clean, cost-effective, and eco-friendly approach to produce SeNPs compared to the physical and chemical techniques. Moreover, biogenic SeNPs have wide applicability in the field of nanomedicine, nanobiosensors, environmental remediation, and nutritional supplementation. However, it is still a challenge to develop eco-friendly and large-scale green technology for the synthesis of stable SeNPs with highly effective biological activity. In addition, further investigations should be carried out to decipher the mechanisms of synthesis and establish a tight control and manipulation of size and morphology of the SeNPs and reveal the biochemical or molecular mechanism of the antioxidant or anticancer properties and propose to harness these properties in a complex therapy.

## References

1. IP C, Hayes C, Budnick RM, Ganther HE (1991) Chemical form of selenium, critical metabolites, and cancer prevention. Cancer Res 51: 595–600
2. Zhang JS, Gao XY, Zhang LD et al (2001) Biological effects of a nano red elemental selenium. Biofactors 15:27–38
3. Xu CL, Qiao L. Guo Y et al (2018) Preparation, characteristics and antioxidant activity of polysaccharides and proteins-capped selenium nanoparticles synthesized by *Lactobacillus casei* ATCC 393. Carbohydr Polym 195: 576–585
4. Benko I, Nagy G, Tanczos B et al (2012) Subacute toxicity of nano-selenium compared to other selenium species in mice. Environ Toxicol Chem 31:2812–2820
5. Zhang JS, Wang HL, Yan XX et al (2005) Comparison of short-term toxicity between nano-se and selenite in mice. Life Sci 76:1099–1109
6. Husen A, Siddiqi KS (2014) Plants and microbes assisted selenium nanoparticles: characterization and application. J Nanobiotechnol 12:28

7. Wadhwani SA, Shedbalkar UU, Singh R et al (2016) Biogenic selenium nanoparticles: current status and future prospects. Appl Microbiol Biotechnol 100:2555–2566
8. Prasad KS, Patel H, Patel T et al (2013) Biosynthesis of se nanoparticles and its effect on UV-induced DNA damage. Colloids Surf B Biointerfaces 103:261–266
9. Prasad KS, Selvaraj K (2014) Biogenic synthesis of selenium nanoparticles and their effect on As (III)-induced toxicity on human lymphocytes. Biol Trace Elem Res 157: 275–283
10. Anu K, Singaravelu G, Murugan K et al (2017) Green-synthesis of selenium nanoparticles using garlic cloves (Allium sativum): biophysical characterization and cytotoxicity on vero cells. J Clust Sci 28:551–563
11. Ramamurthy CH, Sampath KS, Arunkumar P et al (2013) Green synthesis and characterization of selenium nanoparticles and its augmented cytotoxicity with doxorubicin on cancer cells. Bioprocess Biosyst Eng 36:1131–1139
12. Zhang WJ, Zhang J, Ding DJ (2018) Synthesis and antioxidant properties of Lycium barbarum polysaccharides capped selenium nanoparticles using tea extract. Artif Cells Nanomed Biotechnol 46:1463–1470
13. Chen TF, Wong YS, Zheng WJ et al (2008) Selenium nanoparticles fabricated in Undaria pinnatifida polysaccharide solutions induced mitochondria-mediated apoptosis in A375 human melanoma cells. Colloids Surf B Biointerfaces 67:26–31
14. Sharma G, Sharma AR, Bhavesh R et al (2014) Biomolecule-mediated synthesis of selenium nanoparticles using dried *Vitis vinifera* (raisin) extract. Molecules 19:2761–2770
15. Wu CD (2009) Grape products and oral health. J Nutr 139:1818S–1823S
16. Gunti L, Dass RS, Kalagatur NK (2019) Phytofabrication of selenium nanoparticles from Emblica officinalis fruit extract and exploring its biopotential applications: antioxidant, antimicrobial, and biocompatibility. Front Microbiol 10:931
17. Zhang WJ, Chen ZJ, Liu H et al (2011) Biosynthesis and structural characteristics of selenium nanoparticles by *Pseudomonas alcaliphila*. Colloids Surf B Biointerfaces 88:196–201
18. Yee N, Ma J, Dalia A et al (2007) Se (VI) reduction and the precipitation of se (0) by the facultative bacterium *Enterobacter cloacae* SLD1a-1: are regulated by FNR. Appl Environ Microbiol 73:1914–1920
19. Lampis S, Zonaro E, Bertolini C et al (2014) Delayed formation of zero-valent selenium nanoparticles by *Bacillus mycoides* SeITE01 as a consequence of selenite reduction under aerobic conditions. Microb Cell Factories 13:1–14
20. Shakibaie M, Forootanfar H, Golkari Y et al (2015) Anti-biofilm activity of biogenic selenium nanoparticles and selenium dioxide against clinical isolates of Staphylococcus aureus, Pseudomonas aeruginosa, and Proteus mirabilis. J Trace Elem Med Biol 29:235–241
21. Pouri S, Motamedi H, Honary S et al (2017) Biological synthesis of selenium nanoparticles and evaluation of their bioavailability. Braz Arch Biol Technol 60:e170452
22. Wang XN, Zhang DY, Pan XL et al (2017) Aerobic and anaerobic biosynthesis of nanoselenium for remediation of mercury contaminated soil. Chemosphere 170:266–273
23. Che L, Dong YX, Wu MH et al (2017) Characterization of selenite reduction by *Lysinibacillus* sp. ZYM-1 and Photocatalytic performance of biogenic selenium Nanospheres. ACS Sustain Chem Eng 5:2535–2543
24. Mollania N, Tayebee R, Narenji-Sani F (2016) An environmentally benign method for the biosynthesis of stable selenium nanoparticles. Res Chem Intermediat 42:4253–4271
25. Nickerson WJ, Falcone G (1963) Enzymatic reduction of selenite. J Bacteriol 85:763–771
26. Moss MO, Badii F, Gibbs G (1987) Reduction of biselenite to elemental selenium by Aspergillus parasiticus. Trans Br Mycol Soc 89:578–580
27. Ramadan SA, Razak AA, Yousseff YA (1988) Selenium metabolism in a strain of Fusarium. Biol Trace Element Res 18:161–170
28. Zieve R, Ansell PJ, Young TWK (1985) Selenium volatilization by *Mortierella* species. Trans Br Mycol Soc 84:177–179

29. Gharieb MM, Wilkinson SC, Gadd GM (1995) Reduction of selenium oxyanions by unicellular, polymorphic and filamentous fungi: cellular location of reduced selenium and implications for tolerance. J Industrial Microbiol 14:300–311
30. Zare B, Babaie S, Setayesh N et al (2013) Isolation and characterization of a fungus for extracellular synthesis of small selenium nanoparticles. Int J Nanomedicine 1:14–20
31. Sarkar J, Dey P, Saha S et al (2011) Mycosynthesis of selenium nanoparticles. Micro Nano Lett 6:599–602
32. Vetchinkina E, Loshchinina E, Kursky V et al (2013) Reduction of organic and inorganic selenium compounds by the edible medicinal basidiomycete Lentinula edodes and the accumulation of elemental selenium nanoparticles in its mycelium. J Microbiol 51:829–835
33. Mosallam FM, El-Sayyad GS, Fathy RM et al (2018) Biomolecules-mediated synthesis of selenium nanoparticles using *Aspergillus oryzae* fermented Lupin extract and gamma radiation for hindering the growth of some multidrug-resistant bacteria and pathogenic fungi. Microb Pathogenesis 122:108–116
34. Song DG, Cheng YZ, Li XX (2017) Biogenic nanoselenium particles effectively attenuate oxidative stress-induced intestinal epithelial barrier injury by activating the Nrf2 antioxidant pathway. ACS Appl Mater Inter 9:14724–14740
35. Rezvanfar MA, Rezvanfar MA, Shahverdi AR et al (2013) Protection of cisplatin-induced spermatotoxicity, DNA damage and chromatin abnormality by selenium nanoparticles. Toxicol Appl Pharmacol 266:356–365
36. Cheng YZ, Xiao X, Li XX et al (2017) Characterization, antioxidant property and cytoprotection of exopolysaccharide-capped elemental selenium particles synthesized by *Bacillus paralicheniformis* SR14. Carbohydr Polym 178:18–26
37. Khurana A, Tekula S, Saifi MA et al (2019) Therapeutic applications of selenium nanoparticles. Biomed Pharmacother 111:802–812
38. Suzuki Y, Hashiura Y, Matsumura K et al (2010) Dynamic pathways of selenium metabolism and excretion in mice under different selenium nutritional status. Metallomics 2:126–132
39. Huang Y, He L, Liu W et al (2013) Selective cellular uptake and induction of apoptosis of cancer-targeted selenium nanoparticles. Biomaterials 34:7106–7116
40. Nie TQ, Wu HL, Wong KH et al (2016) Facile synthesis of highly uniform selenium nanoparticles using glucose as the reductant and surface decorator to induce cancer cell apoptosis. J Mater Chem B 4:2351–2358
41. Sonkusre P, Cameotra SS (2017) Biogenic selenium nanoparticles induce ROS- mediated necroptosis in PC-3 cancer cells through TNF activation. J Nanobiotechnol 15:43
42. Sarin L, Sanchez VC, Yan A et al (2010) Selenium-carbon bifunctional nanoparticles for the treatment of malignant mesothelioma. Adv Mater 22:5207–5211
43. Yu B, Li XL, Zheng WJ et al (2014) PH-responsive cancer-targeted selenium nanoparticles: a transformable drug carrier with enhanced theranostic effects. J Mat Chem B 2:5409–5418
44. Pelgrift RY, Friedman AJ (2013) Nanotechnology as a therapeutic tool to combat micorbial resistance. Adv Drug Deliver Rev 65:1803–1815
45. Cremonini E, Zonaro E, Donini M et al (2016) Biogenic selenium nanoparticles: characterization, antimicrobial activity and effects on human dendritic cells and fibroblasts. Microb Biotechnol 9:758–771
46. Shoeibi S, Mashreghi M (2017) Biosynthesis of selenium nanoparticles using enterococcus faecalis and evaluation of their antibacterial activities. J Trace Elem Med Biol 39:135–139
47. Wang J, Zhang Y, Yuan Y et al (2014) Immunomodulatory of selenium nanoparticles decorated by sulfated Ganoderma lucidum polysaccharides. Food Chem Toxicol 68:183–189
48. Yazdi MH, Varastehmoradi B, Faghfuri E et al (2015) Adjuvant effect of biogenic selenium nanoparticles improves the immune responses and survival of mice receiving 4T1 cell antigens as vaccine in breast cancer murine model. J Nanosci Nanotechnol 15:10165–10172
49. Zhu C, Zhang S, Song C et al (2017) Selenium nanoparticles decorated with Ulva lactuca polysaccharide potentially attenuate colitis by inhibiting NF-κB mediated hyper inflammation. J Nanobiotechnol 15:20

50. Mavandadnejad F, Yazdi MH, Hassanzadeh SM et al (2018) Biosynthesis of SeNPs by *Mycobacterium bovis* and their enhancing effect on the immune response against HBs antigens: an in *vivo* study. IET Nanobiotechnol 12:57–63
51. EI-Ghazaly MA, Fadel N, Rashed E et al (2017) Anti-inflammatory effect of selenium nanoparticles on the inflammation induced in irradiated rats. Can J Physiol Pharmacol 95: 101–110
52. Kumar GS, Kulkarni A, Khurana A et al (2014) Selenium nanoparticles involve HSP-70 and SIRT1 in preventing the progression of type 1 diabetic nephropathy. Chem Biol Interact 223:125–133
53. Wang H, Wei W, Zhagn SY et al (2005) Melatonin-selenium nanoparticles inhibit oxidative stress and protect against hepatic injury induced by Bacillus Calmette-Guerin/ lipopolysaccharide in mice. J Pineal Res 39:156–163
54. Li Y, Li X, Wong YS et al (2011) The reversal of cisplatin-induced nephrotoxicity by selenium nanoparticles functionalized with 11-mercapto-1-undecanol by inhibition of ROS-mediated apoptosis. Biomaterials 32:9068–9076
55. Zhao SJ, Wang DH, Li YW et al (2017) A novel selective VPAC2 agonist peptide-conjugated chitosan modified selenium nanoparticles with enhanced anti-type 2 diabetes synergy effects. Int J Nanomedicine 12:2143
56. Xia Y, Lin Z, Li Y et al (2017) Targeted delivery of siRNA using RGDfC-conjugated functionalized selenium nanoparticles for anticancer therapy. J Mater Chem B 5:6941–6952
57. Kalishwaralal K, Jeyabharathi S, Sundar K et al (2018) A novel biocompatible chitosan–selenium nanoparticles (SeNPs) film with electrical conductivity for cardiac tissue engineering application. Mat Sci Eng C-Mater 92:151–160
58. Li BZ, Li D, Jing WX et al (2017) Biogenic selenium and its hepatoprotective activity. Sci Rep 7:15627
59. Beheshti N, Soflaei S, Shakibaie M et al (2013) Efficacy of biogenic selenium nanoparticles against *Leishmania major*: in *vitro* and in *vivo* studies. J Trace Elem Med Biol 27:203–207
60. Prasad KS, Vaghasiya JV, Soni SS et al (2015) Microbial selenium nanoparticles (SeNPs) and their application as a sensitive hydrogen peroxide biosensor. Appl Biochem Biotechnol 177:1386–1393
61. Dwivedi S, Alkhedhairy AA, Ahamed M et al (2013) Biomimetic synthesis of selenium nanospheres by bacterial strain JS-11 and its role as a biosensor for nanotoxicity assessment: a novel se-bioassay. PLoS One 8:e57404
62. Wang TT, Yang LB, Zhang BC et al (2010) Extracellular biosynthesis and transformation of selenium nanoparticles and application in $H_2O_2$ biosensor. Colloids Surf B Biointerfaces 8:94–102
63. Lenz M, van Aelst AC, Smit M et al (2009) Biological production of selenium nanoparticles from waste waters. Adv Materials Res 71-73:721–724
64. Pickett TM, Yanguo MA, Sonstegard J et al (2013) Selenium removal using chemical oxidation and biological reduction. US 0270181:A1
65. Jain R, Jordan N, Schild D et al (2015) Adsorption of zinc by biogenic elemental selenium nanoparticles. Chemical Engineering J 260:855–863
66. Ameri A, Shakibaie M, Ameri A et al (2016) Photocatalytic decolorization of bromothymol blue using biogenic selenium nanoparticles synthesized by terrestrial actinomycete *Streptomyces griseobrunneus* strain FSHH12. Desalin Water Treat 57:21552–21563
67. Kawagishi H, Finkel T (2014) Unraveling the truth about antioxidants: ROS and disease: finding the right balance between bedside and bench. Nat Med 20:711–713
68. Vitale G, Salvioli S, Franceschi C (2013) Oxidative stress and the aging endocrine system. Nat Rev Endocrinol 9:228–240
69. Landucci F, Mancinelli P, De Gaudio AR et al (2014) Selenium supplementation in critically ill patients: a systematic review and meta-analysis. J Crit Care 29:150–156
70. Chaudhary S, Umar A, Mehta SK (2016) Selenium nanomaterials: an overview of recent developments in synthesis, properties and potential applications. Prog Mater Sci 83:270–329

71. Wang H, Zhang J, Yu H (2007) Elemental selenium at nano size possesses lower toxicity without compromising the fundamental effect on selenoenzymes: comparison with selenomethionine in mice. Free Radic Biol Med 42:1524–1533
72. Gao X, Zhang J, Zhang L (2002) Hollow sphere selenium nanoparticles: their in-vitro anti hydroxyl radical effect. Adv Mater 14:290–293
73. Chen F, Zhang XH, Hu XD et al (2017) The effects of combined selenium nanoparticles and radiation therapy on breast cancer cells in *vitro*. Artif Cells Nanomed Biotechnol 46:937–948
74. Olmsted SS, Padgett JL, Yudin AI et al (2001) Diffusion of macromolecules and virus-like particles in human cervical mucus. Biophys J 81:1930–1937
75. Sahay G, Alakhova DY, Kabanov AV (2010) Endocytosis of nanomedicines. J Control Release 145:182–195
76. Jiang X, Rocker C, Hafner M et al (2010) Endo and exocytosis of zwitterionic quantum dot nanoparticles by liver Hela cells. ACS Nano 4:6787–6797

# 12

# Biogenic Synthesis, Characterization, Toxicity Assessment, Antiparasitic and Antibacterial Activities of Silver Nanoparticles from *Lippia multiflora*

Rotimi Larayetan, Abdulrazaq Yahaya, Gideon Ayeni, and Bridget Moronkola

**Abstract**

This research evaluates the antimalarial and antimicrobial potential of silver nanoparticles (AgNPs) biosynthesized from the aqueous extract of *Lippia multiflora* (*L. multiflora*). The biophysical characteristic of the synthesized nanoparticle (NPs) was examined by X-ray diffraction (XRD), scanning electron microscopy (SEM), energy dispersive X-ray (EDX), transmission electron microscopy (TEM), and Fourier transform infrared (FTIR). The FTIR spectra obtained signifies that the phenolic constituents present in *L. multiflora* leaf extract could be responsible for the biosynthesis and stabilization of the AgNPs. The peak at about 480 $cm^{-1}$ assigned to the Ag-O band confirms the successful synthesis of AgNPs, while the XRD and TEM described the morphology and the crystalline nature of the AgNPs with an average size of 32 nm. However, the SEM and EDX revealed an irregular cuboidal shape of the materials, and the composition of the AgNPs was silver, carbon, and oxygen only. The malaria bioassay carried out on *L. multiflora* NPs reveals that the AgNPs demonstrate promising activity with an IC50 of 0.39 μg/mL against chloroquine-sensitive (3D7) strain of *Plasmodium falciparum* (*P. falciparum*) and reveals no significant growth inhibition of human cervical adenocarcinoma cells (HeLa). The antimicrobial screening reveals a strong inhibitory action of the

R. Larayetan (✉) · A. Yahaya
Department of Pure and Applied Chemistry, University of Fort Hare, Alice, South Africa

Chemistry Department, Kogi State University, Anyigba, Kogi State, Nigeria

G. Ayeni
Department of Biochemistry, Kogi State University, Anyigba, Kogi State, Nigeria

Biochemistry Department, School of Life Sciences, University of KwaZulu-Natal, WestVille Campus, Durban, South Africa

B. Moronkola
Department of Chemistry, Lagos State University, Ojo, Lagos State, Nigeria

© Springer Nature Singapore Pte Ltd. 2020

Q. Saquib et al. (eds.), *Green Synthesis of Nanoparticles: Applications and Prospects*, https://doi.org/10.1007/978-981-15-5179-6_12

tested synthesized extract against Gram-positive and Gram-negative bacteria stains.

**Keywords**

AgNPs · Antimalaria · Cytotoxicity · *Lippia multiflora* · *Plasmodium falciparum*

## 12.1 Introduction

Parasitic infections brought about by protozoa is responsible for the major morbidity and death in sub-Saharan Africa (SSA) [1], and this can be traced to the high level of poverty, pollution, decrepit infrastructure, and inaccessibility to modern medicines bringing about dependence to unconventional medicine for the management of parasitic infections [2]. The usage of alternative or traditional medicine in Africa revolves around the use of indigenous natural drugs acquired from therapeutic plants, herbs, and other materials to treat various diseases [3].

Malaria is one of the leading causes of health complications faced by human in sub-Saharan Africa, killing about two to three million people yearly with a large number of this death casualty being children below the age of 5 [4]. Malaria is spread by female *Anopheles* mosquitoes brought about by four different protozoan parasites, namely, *Plasmodium ovale* (*P. ovale*), *Plasmodium malaria* (*P. malaria*), *Plasmodium vivax* (*P. vivax*), and *Plasmodium falciparum* (*P. falciparum*) [5]. About 80%of all malaria infection is caused by *P. falciparum* [6], and this parasite has shown resistance to generally used curative drugs like aminoquinolines and antifolate drugs [7].

Workable vaccines are not obtainable at the moment for most parasitic infections, and in spite of the several researches to curtail malaria parasites, a breakthrough remains elusive [8]. Systematic assessment of important therapeutic plants employed in traditional health care proffers some hope in the detection of new antimalarial drugs [9]. Several plants from all over Africa have been examined and reported to possess levels of antimalarial potencies against strains of laboratory malaria parasites in vitro and *murine Plasmodia* in vivo [10]. Some of these plants are *Guiera senegalensis*, *Feretia apodanthera*, *Terminalia avicennioides*, *Combretum collinum*, *Lophira lanceolata*, *Momordica charantia*, *Lippia multiflora*, *Ageratum conyzoides*, and *Diospyros monbuttensis* obtained from Sao Tome, Burkina Faso, and Nigeria, respectively. They are reported to possess superior antimalarial effect against chloroquine-resistant *P. falciparum* [10–12].

Trypanosomiasis (HAT) is another disease, causing high mortality in Africa, and there is a need to research on alternative chemotherapy against trypanosomiasis, a disease of disparaging effect in human and economic animals. In several African countries, human African trypanosomiasis (HAT) and African animal trypanosomiasis (AAT) cause a large burden on the worth of life, food security, and economy [13]. Drugs like melarsoprol, suramin, and pentamidine readily available for the treatment of these diseases are costly, not easily assessable, and highly toxic with a serious increase in parasite resistance [14, 15].

In recent time, nanotechnology has turn out to be an integrative field of research that can now be incorporated into several areas of science and technology [16]. Nanoparticles (NPs) are remarkably essential due to their small size coupled with their relatively large surface area which dictates their physical, mechanical, optical, chemical, electrical, solubility, and stability properties [17]. Several metal nanoparticles including gold, silver, and copper NPs have turn out to be sought after because of their strong biological activities like antiparasitic agents, anticancer, anti-inflammatory, and antitumor activities [18–21].

*Lippia multiflora* is a perennial aromatic plant that does not have woody stem above the ground; it belongs to the Verbenaceae family and also known as *Lippia adoensis* Hochst; the Verbenaceae family is made up of about 41 genera with roughly more than 200 species [22, 23]. It is commonly found in areas consistent with the humid agroecological zones in African and Central and South American countries that have rainfall fluctuating between 900 and 1300 mm [24] alongside the South and Central American regions [25]. This plant has white sweet-scented flowers and can reach a height of about 2.7–4.0 meters. Records have shown that it is used as a traditional remedy to treat respiratory and gastrointestinal disorders, stomach disorder, bronchial inflammation, malaria fever, conjunctivitis, enteritis, stress, hypertension, conjunctivitis, venereal diseases, coughs, and colds [2, 22, 25, 26]. The extract obtained when the leaves are boiled with palm nut is used to evacuate post-delivery placenta [27]. Furthermore, the extract is used as a condiment in the management of sleeping sickness. It is believed to possess hypotensive, fatigue alleviating, and diuretic properties [28]. The therapeutic properties exhibited by this aromatic plant have been ascribed to the phytochemical components, glycosides, and essential oils of *L. multiflora* [29, 30].

Since several published articles reported that the extract of this plant possesses strong antiplasmodial potency [25, 27, 31], we therefore embarked on the biogenic synthesis of silver nanoparticles (AgNPs) using the aqueous extract of this plant and consequently tested it on 3D7 *Plasmodium* strain, trypanosome parasites, and multidrug-resistant bacteria strain.

In addition, the toxicity of the biogenic NPs was ascertained using HeLa cell line. To the best of our knowledge, no study has reported the antiparasitic and antimicrobial potentials of *L. multiflora* AgNPs.

## 12.2 Materials and Methods

### 12.2.1 Materials

#### 12.2.1.1 Chemicals and Reagents

Silver nitrate ($AgNO_3$) (Chem Lab, South Africa), Mueller-Hinton agar (Thermo Fisher Scientific, South Africa), and dimethyl sulfoxide (DMSO) (Merck, Germany) were all employed in this study. These chemicals and reagents were used as supplied.

#### 12.2.1.2 Organisms

*Vibrio alginolyticus DSM 2171 (V. alginolyticus)*, *Escherichia coli 0157:H7 ATCC 35150* (*E. coli*), *Listeria ivanovii ATCC* (*L. ivanovii*), *Salmonella typhi ACC* (*S. typhi*), *Staphylococcal enteritis ACC* (*S. enteritis*), *Staphylococcus aureus ACC 19119* (*S. aureus*), and *Mycobacterium smegmatis ATCC 19420* (*M. smegmatis*).

#### 12.2.1.3 Plant Extract Preparation

The leaf of *L. multiflora* was harvested near Emmanuel Alayande College of Education premises, Oyo State, Nigeria (7° 52′49.72″N, 3° 54′11.91″E). It was air-dried for about 2 weeks at ambient temperature, after which it was pulverized by means of an electric grinder. Roughly, 40 g of the powdered sample was drenched in 350 mL of distilled water and subjected to agitation on an orbital shaker for 24 h. After this, the extract was filtered using Whatman No.1 filter paper, and the filtrate was then lyophilized into dry power and kept in a tightly stopped centrifuge tube at 4 °C prior to the biosynthesis of AgNPs.

#### 12.2.1.4 Silver Nanoparticle Synthesis

Crude extract solution (10 mL, 20 mg/mL) was added to a solution of silver nitrate ($AgNO_3$) (90 mL, 1 mM). The reaction vessel containing the mixture was protected from light using aluminum foil to prevent auto-reduction of the $AgNO_3$ and stirred continuously for about 6 h at room temperature. The colorless $AgNO_3$ solution later turned darkish brown with a precipitate confirming the development of the AgNPs. This precipitate was separated by centrifugation, washed thrice with deionized water, and dried in an oven at 50 °C for 24 h.

#### 12.2.1.5 Characterization of the Biogenic Silver Nanoparticles

To ascertain the efficacy of the synthesized AgNPs for application toward biological activities, the characterization of the material was carried out by means of different techniques. UV-vis absorption spectrophotometer (Perkin Elmer Universal) was used to obtain information on the absorption frequencies of the synthesized material by scanning the wavelength from 200 to 450 nm. Fourier transform infrared (FTIR) spectrophotometer (Perkin Elmer Universal ATR 100) was employed for the determination of the vibrational frequencies of *L. multiflora* AgNPs. The measurement of the vibrational spectra of the NPs was achieved via a scanning range of 4000–440 $cm^{-1}$.

Scanning electron microscopy (SEM) and electron diffraction spectrophotometer (EDS) analysis were carried out on the same instrument (JEOL JSM-6490A) by placing the AgNPs on a two-sided carbon-coated stub at a voltage of 15–20 KV and observed at different magnifications. SEM and EDS provided information on the morphology and composition of the NPs, respectively. Transmission electron micrograph (TEM) of the AgNPs was obtained by using JOEL 1210 transmission electron microscope operating at100 kV. The AgNPs were dissolved in DMSO and sonicated for 20 min after which a drop from the suspension was placed on the carbon-coated copper grid and left to dry at ambient temperature before the analysis. To confirm the

crystallinity and size of the synthesized material, X-ray diffractometer (Bruker D8 advanced X-ray diffractometer) was employed and operated at 45 KV.

## 12.2.2 Biological Activity

### 12.2.2.1 In Vitro Antimicrobial Activity

The antimicrobial activity of the biosynthesized AgNPs of *L. multiflora* was determined using three Gram-negative and four Gram-positive pathogenic microorganisms including. *E. coli 0157:H7 ATCC 35150*, *V. alginolyticus DSM 2171*, *S. typhi ACC*, *S. enteritis ACC*, *S. aureus*, *L. ivanovii ATCC 19119*, and *M. smegmatis ATCC 19420*.

The antimicrobial activity of AgNPs was carried out by using the well diffusion method of the National Committee for Clinical Laboratory Standards. Diameter wells (6 mm) were dug in the solid Mueller-Hinton agar contained in petri dishes through a sterilized cork borer.

Each bacterial culture was compared to 0.5 McFarland turbidity standard, and each test microbe (0.1 mL) was inoculated with a fresh swab on the external surface of the solid medium in different petri dishes. AgNP solutions (31.25–7.8125 μg/mL) prepared from the stock solution were introduced into the wells in the petri dishes and labeled accordingly. The inoculated petri dishes were reversed and incubated at 37 °C for a day. After the expiration of 24 h, the antibacterial activities were assessed by determining the diameter of each zone of inhibition [32, 33]. DMSO was used as the negative control.

Minimum inhibitory concentration (MIC) was carried out through agar dilution procedure. Inoculums of the test microorganisms were prepared in normal saline 9 mg/mL; it was then compared with 0.5 McFarland, 1 × 108 cfu/mL. Preparation of the working stock solution was achieved by dissolving 20 mg/mL in DMSO; the resultant mixture was then diluted with Mueller-Hinton broth (MHB) to arrive at a concentration range of 31.25–7.8125 μg/mL. Inoculations of the plates containing the solid mixture of MHB and AgNPs were accomplished by injecting the standardized inocula of the test microbes into the plates which were then incubated for a day at 37 °C. MIC values were obtained from the plates with the lowest concentration where there were no visible growths.

## 12.2.3 In Vitro Assessment of Antiplasmodial Activity

The 3D7 strain of *P. falciparum* (malaria parasites) was preserved in a medium of RPMI 1640 containing 2 mM L-glutamine and 25 mM HEPES (Lonza). 60 μg/mL gentamycin, 2–4% hematocrit human red blood cells, 20 mM glucose, 0.65 mM hypoxanthine, and 5% AlbuMAX II were all added to the medium.

The antimalarial potency of the AgNPs of *L. multiflora* was assessed by evaluating the malaria parasite viability through the parasite lactate dehydrogenase (*pLDH*) technique reported by Makler et al. [34]. A stock solution of 20 mg/mL of

the AgNPs was prepared in dimethyl sulfoxide (DMSO); an aliquot of 50 μg/mL from the stock solution previously prepared was added to the parasite cultures in a 96-well plate; the mixture above was incubated at 37 °C in a $CO_2$ incubator for 2 days. After expiration of incubation period, 25 μL of the culture was removed from all the wells and added with roughly 125 μL of a mixture of nitrotetrazolium blue chloride (NBT)/phenazine ethosulfate (PES) and Malstat solutions in a new 96-well plate. A purple color usually indicates that parasite lactate dehydrogenase (*pLDH*) is present. Absorbance at 620 nm of the mixture in the new 96-well plates was documented so as to obtain the quantity of *pLDH* in each well plate. Dose-response assay which was employed to determine IC50 was carried out after the AgNPs brought about reduction in the parasite viability to less than 20%. The positive control used was chloroquine (20 μM).

### 12.2.4 In Vitro Antitrypanosomal Assay

To assess the in vitro antitrypanosomal activities of the biosynthesized AgNPs against *T. brucei*, 95 mL of the trypanosome suspension was poured into a 96-well plate, and 5.0 mL of the AgNPs (50 μg/mL) obtained from the stock solution of AgNPs in DMSO at 20 mg/mL was added. After the expiration of 48-h incubation period, the number of parasites that were able to withstand vulnerability to the AgNPs was ascertained by adding a resazurin-based reagent; this reagent contains resazurin component reduced by living cells to resorufin. Average reading of all untreated control wells was used to determine percentage parasite viability, while IC50 value was acquired by plotting % viability against log (AgNPs solution) and carrying out nonlinear regression using GraphPad Prism (v. 5.02) software [35].

### 12.2.5 Cytotoxicity Assay

Cytotoxicity is mainly regarded as the potential of a compound or extracts to bring about cell death; a promising antimalarial or antitrypanosomal compound or extract must be devoid of toxicity to host cells. Human cervical adenocarcinoma cells (HeLa) were used to determine the cytotoxicity of the biosynthesized AgNPs by employing the method of Keusch et al. [36]. A working stock solution of the AgNPs 20 mg/mL was prepared in DMSO; this was diluted with culture medium to 50 μg/mL, Emetine was employed as the positive control. The mixture of the AgNPs and culture medium was incubated in duplicate along with $1 \times 10^4$ HeLa cells per well distributed in a 96-well plate for 48 h at 37 °C in a 5% $CO_2$ incubator. Cells that stayed active after subjection to the drug were resolved by mixing resazurin-based reagent to the mixture of AgNPs and the HeLa cells; the living cells capable of changing resazurin into resorufin were quantified in a fluorescence multi-well plate reader. The % cell viability was obtained from the resorufin fluorescence in compound treated well compared to untreated control.

## 12.3 Results

### 12.3.1 Synthesis and Characterization of AgNPs

After the synthesis of the AgNPs, its characterization was carried out to determine the success of the biogenic AgNPs. Microscopic results including TEM, SEM, and EDS (Fig. 12.1) were obtained in order to evaluate the size, shape, morphology, and composition of the synthesized material. TEM measurement indicates that the AgNPs have an average size of 32 nm, with roughly triangular shape (Fig. 12.1a). The SEM measurement confirms that the AgNPs biosynthesized from the *L. multiflora* plant were well dispersed with the absence of agglomeration (Fig. 12.1c); the morphology of the material using SEM shows that the material has an irregular cuboidal shape. The EDS analysis confirms the successful synthesis of AgNPs from the plant of study as a result of the intense signal in the silver region; the weight percentage (%) of the silver in the NPs produced was 80.37% while that of oxygen was 12.63% and carbon 7% (Fig. 12.1b); the presence of carbon and oxygen as revealed by EDS spectra in the biogenic AgNPs might be as a result of phytocompounds present in the NPs formed.

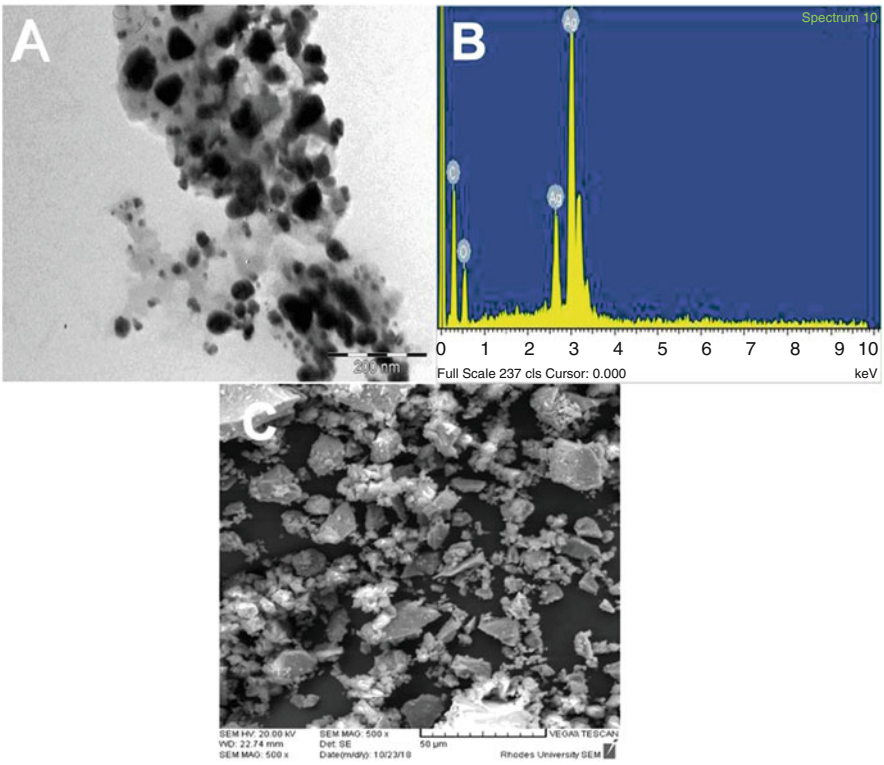


**Fig. 12.1** TEM micrographs (A), EDS (B), and SEM image (C) of LM-AgNPs

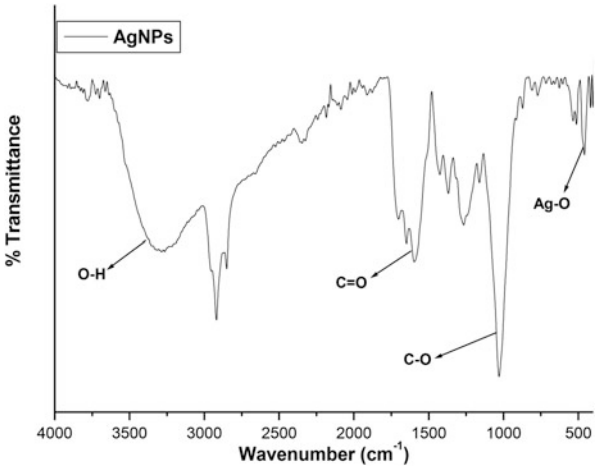


**Fig. 12.2** FTIR spectra of LM-AgNPs

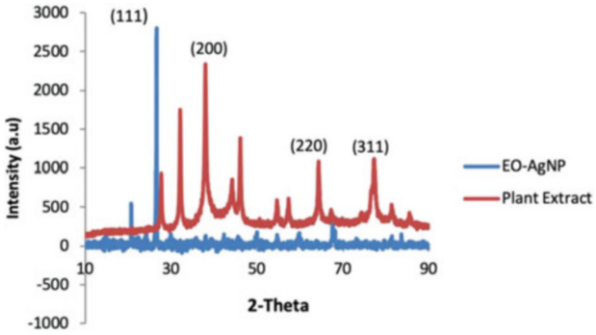


**Fig. 12.3** XRD images of LM-AgNPs and its plant extract

To confirm the vibrational frequency of the synthesized material, FTIR of the AgNPs was carried out (Fig. 12.2). The peak at about 480 $cm^{-1}$ assigned to the Ag-O band confirms the successful synthesis of AgNPs. Also, vibrational peaks around 1100, 1720, and 3800 $cm^{-1}$ assigned to C-O, C=O, and O-H stretches, respectively, indicate the functional group of the different phytochemicals present in the plant part which are responsible for the reduction of $AgNO_3$ (Fig. 12.2). These vibrational bands show that the AgNPs were obtained through the green synthetic route.

XRD examination showed four peaks at 111, 200, 220, and 311 ascribed to metal oxide nanoparticles indicating the successful synthesis of AgNPs with the highest peak at 38°. Employing the diffraction peak of 111 into the Scherrer equation, the crystallite size of the AgNPs was observed to be 30 nm similar to the size obtained from the TEM measurement of this material (Fig. 12.3).

The biogenic reduction of the $Ag^+$ in solution was observed via UV-vis spectrophotometer. UV-vis was carried out at a wavelength range of 200–450 nm; peaks noticed at 349 nm established the dawdling reaction rate (Fig. 12.4).

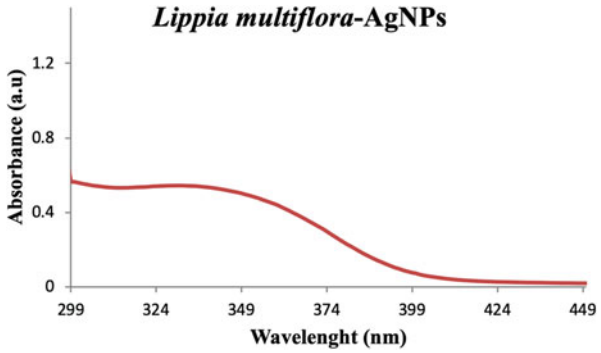


**Fig. 12.4** Absorption spectra of *Lippia multiflora* AgNPs

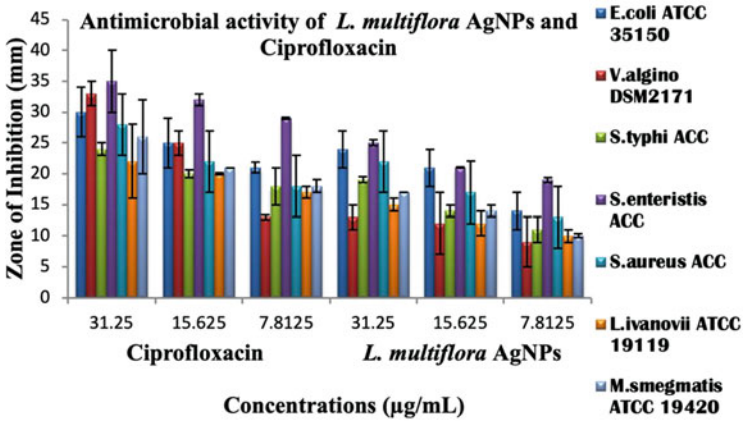


**Fig. 12.5** Antimicrobial activities of ciprofloxacin and *L. multiflora*

### 12.3.2 In Vitro Biological Assessment

Confirmation of the antibacterial activity of the biogenic *L. multiflora* AgNPs was established through the agar well diffusion method and microdilution procedure against three multidrug-resistant reference strains (*V. alginolyticus DSM 217*, *E. coli* 0157:H7 ATCC 35150, and *L. ivanovii ATCC 19119*) alongside three other multidrug-resistant bacteria (*S. typhi ACC*, *S. enteritis ACC*, *S. aureus ACC*). Measurement of zone of inhibition indicated that the *L. multiflora* AgNPs was most effective against *S. enteritis ACC* (25.0 ± 0.5 mm) and *E. coli* 0157:H7 ATCC 35150 (24.0 ± 0.5 mm) at a concentration of 31.25 as obtained from their zone of inhibition, whereas the smallest inhibitory activity was recorded for *L. ivanovii ATCC 19119* and *M. smegmatis ATCC 19420* (15.0 ± 1.0 & 17.0 ± 0.0 mm) (Fig. 12.5). Different concentrations of the AgNPs and the positive

**Table 12.1** Minimum inhibitory concentration (μg $mL^{-1}$) of LM-AgNPs and the standard drug.

| Microorganism | LM-AgNPs | Ciprofloxacin (positive control) | DMSO (negative control) |
|---|---|---|---|
| Gram-negative bacteria strains | | | |
| *Escherichia coli 0157:H7 ATCC 35150* | 31.25 | 15.625 | 0.6 mL VG |
| *Vibrio alginolyticus DSM 2171* | 15.625 | 7.8125 | 0.6 mL VG |
| *Salmonella typhi ACC* | 15.625 | 7.8125 | 0.6 mL VG |
| Gram-positive bacteria strains | | | |
| *Staphylococcal enteritis ACC* | 15.625 | 7.8125 | 0.6 mL VG |
| *Staphylococcus aureus ACC* | 15.625 | 7.8125 | 0.6 mL VG |
| *Listeria ivanovii ATCC 19119* | 15.625 | 7.8125 | 0.6 mL VG |
| *Mycobacterium smegmatis ATCC 19420* | 15.625 | 7.8125 | 0.6 mL VG |

*ACC* AEMREG culture collection, *ATCC* American-type collection center, *VG* visible growth

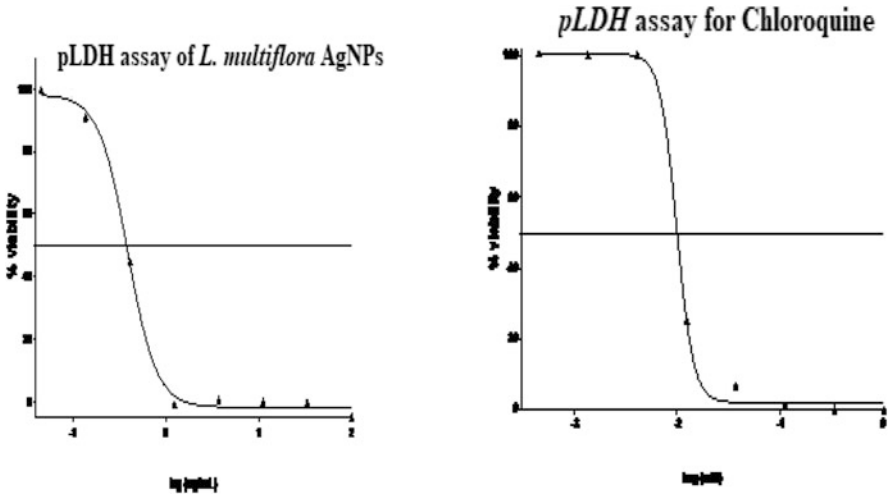


**Fig. 12.6** Dose-response curve (pLDH assay) for *L. multiflora* AgNPs and chloroquine

control ciprofloxacin ranging from 31.25–7.8125 μg/mL were used in order to ascertain their MICs. The activities of the AgNPs and ciprofloxacin were confirmed on all the tested microorganisms (Table 12.1).

The *L. multiflora* AgNPs were examined for its efficacy on trypanosome parasite using *T. brucei* assay; the percentage (%) viability of the synthesized AgNPs was 88.03%; this couldn't bring about a significant reduction to about 20%. The % viability of the biosynthesized *L. multiflora* AgNPs against *Plasmodium falciparum* 3D7 strain was 0.00 ± 1.45%), it brought about an excellent reduction of *pLDH* to less than 20%, the IC50 was then generated from the dose-response curve, and it gave an exceptional activity of 0.39 μg/mL (Fig. 12.6); similarly, the % viability of the cytotoxicity on HeLa cell line was 92.29%.

## 12.4 Discussion

One of the most commonly used methods for the biogenic synthesis of AgNPs is through the chemical reduction of $AgNO_3$ as reported by Lalitha et al. and Hyllested et al. [37, 38]. Detection of the functional groups present in the *L. multiflora* AgNPs was done using FTIR as shown in Fig. 12.2; distinct peaks such as 480, 1100, 1720, and 3800 $cm^{-1}$ were seen in the absorbance spectra recorded under the range of 4000–400 $cm^{-1}$, and they were assigned to Ag-O, C-O, C=O, and O-H stretches, respectively; such prominent peaks were documented in our previous studies [35]. Sasidharan et al. [39] had posited that FTIR is a veritable tool used in the characterization and recognition of compounds or functional groups; stretching frequency detected at 480 $cm^{-1}$ as shown in Fig. 12.2 credited to Ag-O band further substantiated the successful biosynthesis of AgNPs. The capping and reduction of $Ag^+$ in the formation of AgNPs in this study could be ascribed to the different phytochemicals in the plants extract [35]. EDS analysis carried out by measuring the energy involved and intensity allotment of X-ray signals produced via a fixed electron beam on the sample usually reveals the quantitative and qualitative elements involved in the production of the NPs. Profile from the elemental analysis of the biosynthesized *L. multiflora* AgNPs revealed the weight percentage (%) of the silver (Ag) to be 80.37% while that of oxygen was 12.63% and carbon 7% confirming that AgNPs were successfully synthesized (Fig. 12.1); the presence of carbon and oxygen as revealed by EDS spectra in the biogenic AgNPs might be as a result of phytocompounds present in the AgNPs formed; in addition, the EDS also revealed that the AgNPs are bonded to the secondary metabolites in the plant extract due to other signals observed in the range of 0–0.5 keV indicating the characteristic absorption of oxygen and carbon which clearly disclosed the presence of phytochemicals left behind in the moieties of *L. multiflora* extract used as a stabilizing agent on the surface of *L. multiflora* AgNPs [40]. Normally, nanocrystals obtained from $AgNO_3$ display a characteristic absorption peak around 3 keV [41]. TEM is a useful instrument employed to provide comprehensive information as related to the fine structures observed in NPs, with magnification factor in the range of $10^2$–$10^6$; with this magnification very fine structures can be observed [42]; TEM was used to describe the size of the bio-reduced AgNPs; measurement of the *L. multiflora* AgNPs revealed an average size of 32 nm, while the TEM imaging established the triangular nature with regular particle size distribution devoid of aggregations (Fig. 12.1); SEM on the other hand presents images on the shapes and morphology of the face topography of the extract [43]. Agglomeration brought about by high surface tension and high surface energy may be responsible for the larger size of some NPs, while the small particle-sized NPs possess a larger surface area, thereby enhancing the AgNP activity. UV absorption spectrum of the biogenic AgNPs of *L. multiflora* displayed an intense absorption peak centered at 349 nm indicating the bioreduction of the $AgNO_3$ solution to AgNPs after the addition of the aqueous extract of the plant; this absorption band of 349 nm typical of AgNPs obtained from this study is similar to the absorption peak obtained by Dong et al. [44].

The highest inhibitory activity of *Staphylococcal enteritis* (25.0 ± 0.5 mm) was similar to our previous work on gold nanoparticle from the seed of *C. citrinus* [45]. The antimicrobial activity of the AgNPs biosynthesized from *L. multiflora* was established to compete well with the positive control ciprofloxacin. The MIC values of the biogenic AgNPs for all the bacteria strains range from 15.625 to 31.25 μg/mL; the AgNPs had the lowest MIC value of 31.25 μg/mL for *Escherichia coli 0157:H7 ATCC 35150*, while the rest of the bacteria strains had the same MIC values of 15.625 μg/mL. The same observation was recorded for ciprofloxacin (positive control) which had the lowest MIC value of 15.625 μg/mL for *Escherichia coli 0157:H7 ATCC* 35150 and same MIC values of 7.8125 μg/mL for other bacteria strains (Table 12.1). The inhibitory activity with efficient MIC values of AgNPs of *L. multiflora* against bacteria strains may be due to the large surface area and small particle size which are capable of enhancing membrane permeability and subsequently cell damage [46]. The antimicrobial potencies of *L. multiflora* AgNPs revealed a profound antibacterial action against both Gram-negative and Gram-positive bacteria strains confirming that plants and silver in their nanoform have definite constituents with an antimicrobial effect that may be employed as antibacterial agents in the formation of a novel therapeutic drug used to combat ordinary bacteria pathogens.

The biosynthesized *L. multiflora* AgNPs was assessed in vitro for their antiplasmodial potency against *P. falciparum* chloroquine-sensitive 3D7 strain using parasite lactate dehydrogenase, the trypanosomal species accountable for nagana *T. brucei* and for cytotoxicity with HeLa cell line. Standard drug (chloroquine) was use as a positive control for *P. falciparum;* emetine was employed as the positive control for HeLa cells, while pentamidine was utilized for *T. brucei*. The AgNPs showed no evidence of cytotoxicity since the percentage viability was 92.29%; this was unable to significantly decrease the viability of HeLa cells to below 50%. Research was carried out on 50 people through a span of 25 years; it was discovered that there were no side effects or any toxicity in the consumption of *L. multiflora* tea [27], signifying that the crude extracts of *L. multiflora* can consequently be standardized as phytomedicine. The results obtained for antimalarial and antitrypanosomal activities are put forward in juxtaposition with cytotoxicity results to be sure that the reduction in viability is not brought about by general cytotoxicity.

The IC50 value obtained for the *L. multiflora* AgNPs was 0.39 μg/mL of inhibitory concentration against 3D7 *P. falciparum* strain; this shows a very good activity than *Lippia javanica* root (16.7 μg/mL) and the leaf, flower, and seeds of *Callistemon citrinus* (3.14, 2.99, and 5.34 μg/mL) reported in our previous study [35, 45]. Extracts with very promising antimalarial activity usually exhibit IC50 of 10 μg/mL [47, 48]. Likewise, *L. multiflora* AgNPs reduced the viability of trypanosome (*T. brucei*) at a concentration of 50 μg/mL to 88.03% making it to be inactive against *T. brucei*; similar result from our previous study also revealed that the flower and seed of *Callistemon citrinus* AgNPs were not able to reduce the percentage parasite viability to about 20% and were considered ineffective [35, 45]. Extracts which reduce parasite viability significant to about 20% in the single concentration assay are put forward for dose-response assay to determine their 50% inhibitory concentration [35].

## 12.5 Conclusion

Great success was achieved in the biosynthesis and characterization of *L. multiflora* AgNPs through the eco-friendly pathway. The obtained AgNPs were tested for their antiparasitic and antimicrobial properties; the antibacterial examination of the AgNPs revealed that they were active against the tested bacteria stains, while the antimalarial assay gave an excellent activity against *P. falciparum* chloroquine-sensitive 3D7 strain. The nontoxicity of the biogenic AgNPs against HeLa cells confirms that it can be employed in the development of nanomedicines against bacterial infection and *P. falciparum* parasites. Our future research will focus on the in vivo study of *L. multiflora* AgNPs and their mechanism of action.

**Acknowledgments** We are grateful to the Centre for Chemico- and Biomedicinal Research at Rhodes University for allowing us to carry out the antimalarial and antitrypanosomal tests of our biosynthesized AgNPs using South African Medical Research Council (MRC) funds from National Treasury under its Economic Competitiveness and Support Package. AEMREG, University of Fort Hare, South Africa, is also appreciated for the bacteria strains given to us.

**Author's Contributions** LR, AY, GA, and MB carried out the research work, and all wrote different sections of the manuscript; LR, AY, and GA helped in the characterization of the nanoparticles. All authors reviewed and approved the draft manuscript.

**Conflict of Interest** The authors affirm no conflict of interest.

## References

1. Fakae BB (1990) The epidemiology of helminthosis in small ruminants under the traditional husbandry system in eastern Nigeria. Vet Res Commun 14(5):381–391
2. Ndjonka D, Rapado L, Silber A, Liebau E, Wrenger C (2013) Natural products as a source for treating neglected parasitic diseases. Int J Mol Sci 14(2):3395–3439
3. Kasilo OM, Trapsida JM, Mwikisa Ngenda C, Lusamba-Dikassa PS, régional pour l'Afrique, B. and World Health Organization (2010) An overview of the traditional medicine situation in the African region. African Health Monitor, pp 7–15
4. WHO (2014). World malaria report 2014. Geneva, Switzerland: World Health Organization. pp. 32–42. ISBN 978-92-4156483-0
5. Cox FE (2002) History of human parasitology. Clin Microbiol Rev 15(4):595–612
6. Carter JA, Ross AJ, Neville BG, Obiero E, Katana K, Mung'ala-Odera V, Lees JA, Newton CR (2005) Developmental impairments following severe falciparum malaria in children. Tropical Med Int Health 10(1):3–10
7. Bloland PB (2001) Drug resistance in malaria. A background document for the WHO Global Strategy for Containment of Antimicrobial Resistance
8. Matuschewski K (2006) Vaccine development against malaria. Curr Opin Immunol 18 (4):449–457
9. Okunji CO, Acton N, Ellis WY, Iwu MM (2000) December. Identification of new antimalarial pharmacophores from west and central African plants. In Proceedings of the International Conference on Traditional Medicine for HIV/AIDS and Malaria. 5th-7th December
10. Ancolio C, Azas N, Mahiou V, Ollivier E, Di Giorgio C, Keita A, Timon-David P, Balansard G (2002) Antimalarial activity of extracts and alkaloids isolated from six plants used in traditional medicine in Mali and Sao Tome. Phytotherapy Res 16(7):646–649

11. Olasehinde GI, Ojurongbe O, Adeyeba AO, Fagade OE, Valecha N, Ayanda IO, Ajayi AA, Egwari LO (2014) In vitro studies on the sensitivity pattern of *Plasmodium falciparum* to antimalarial drugs and local herbal extracts. Malaria J 13(1):63
12. Sanon S, Gansane A, Ouattara LP, Traore A, Ouedraogo IN, Tiono A, Taramelli D, Basilico N, Sirima SB (2013) In vitro antiplasmodial and cytotoxic properties of some medicinal plants from western Burkina Faso. Afr J Laborat Med 2(1)
13. Simarro PP, Franco J, Diarra A, Postigo JR, Jannin J (2012) Update on field use of the available drugs for the chemotherapy of human African trypanosomiasis. Parasitology 139(7):842–846
14. Welburn SC, Maudlin I, Simarro PP (2009) Controlling sleeping sickness–a review. Parasitology 136(14):1943–1949
15. Brun R, Schumacher R, Schmid C, Kunz C, Burri C (2001) The phenomenon of treatment failures in human African trypanosomiasis. Tropical Med Int Health 6(11):906–914
16. Dai J, Mumper RJ (2010) Plant phenolics: extraction, analysis and their antioxidant and anticancer properties. Molecules 15(10):7313–7352
17. AbdelHamid AA, Al-Ghobashy MA, Fawzy M, Mohamed MB, Abdel-Mottaleb MM (2013) Phytosynthesis of au, Ag, and au–Ag bimetallic nanoparticles using aqueous extract of sago pondweed (*Potamogeton pectinatus* L.). ACS Sustain Chem Eng 1(12):1520–1529
18. Khan I, Khan M, Umar MN, Oh DH (2015) Nanobiotechnology and its applications in drug delivery system: a review. IET Nanobiotechnol 9(6):396–400
19. Shanthi S, Jayaseelan BD, Velusamy P, Vijayakumar S, Chih CT, Vaseeharan B (2016) Biosynthesis of silver nanoparticles using a probiotic Bacillus licheniformis Dahb1 and their antibiofilm activity and toxicity effects in Ceriodaphnia cornuta. Microb Pathog 93:70–77
20. Bindhu MR, Umadevi M (2014) Silver and gold nanoparticles for sensor and antibacterial applications. Spectrochim Acta A Mol Biomol Spectrosc 128:37–45
21. Rai M, Kon K, Ingle A, Duran N, Galdiero S, Galdiero M (2014) Broad-spectrum bioactivities of silver nanoparticles: the emerging trends and future prospects. Appl Microbiol Biotechnol 98 (5):1951–1961
22. Jigam AA, Akanya HO, Ogbadoyi EO, Dauda BE, Evans EC (2009) In vivo antiplasmodial, analgesic and anti-inflammatory activities of the leaf extract of Lippia multiflora mold. J Med Plants Res 3(3):148–154
23. Owolabi MS, Ogundajo A, Lajide L, Oladimeji MO, Setzer WN, Palazzo MC (2009) Chemical composition and antibacterial activity of the essential oil of Lippia multiflora Moldenke from Nigeria. Records Nat Prod 3(4)
24. Djengue HW, Dansi A, Adjatin A, Dossou-Aminon I, Dansi M, Sanni A (2017) Ethnobotanical investigation of Lippia multiflora Moldenke, a local aromatic leafy vegetable under domestication in Benin. Int J Curr Res Biosci Plant Biol 4(5):44–51
25. Pascual ME, Slowing K, Carretero E, Mata DS, Villar A (2001) Lippia: traditional uses, chemistry and pharmacology: a review. J Ethnopharmacol 76(3):201–214
26. Oladimeji FA, Orafidiya LO, Okeke IN (2004) Physical properties and antimicrobial activities of leaf essential oil of Lippia multiflora Moldenke. Int J Aromather 14(4):162–168
27. Acquaye D, Smith M, Letchamo W, Simon J (2001) Lippia tea Centre for new use agriculture and natural products. Rutgers University, New Brunswick, NJ
28. Kanko C, Koukoua G, N'Guessan YT, Fournier J, Pradère JP, Toupet L (2004) Contribution à l'étude phytochimique de Lippia multiflora (Verbenaceae). C R Chim 7(10–11):1029–1032
29. Terblanché FC, Kornelius G (1996) Essential oil constituents of the genus Lippia (Verbenaceae)—a literature review. J Essent Oil Res 8(5):471–485
30. Taoubis K, Fauvel MT, Gleye J, Moulis C, Fouraste I (1997) Phenylpropanoid glycosides from Lantana camara and Lippia multiflora. Planta Med 63(02):192–193
31. Abena AA, Ngondzo-Kombeti GR, Bioka D (1998) Psychopharmacologic properties of Lippia multiflora. L'Encephale 24(5):449–454
32. Larayetan RA, Okoh OO, Sadimenko A, Okoh AI (2017) Terpene constituents of the aerial parts, phenolic content, antibacterial potential, free radical scavenging and antioxidant activity

of *Callistemon citrinus* (Curtis) Skeels (Myrtaceae) from eastern Cape Province of South Africa. BMC Complement Altern Med 17(1):292
33. Larayetan R, Ololade ZA, Ogunmola O, Ladokun A (2019) Phytochemical constituent, antioxidant, cytotoxicity, antimicrobial, antitrypanosomal and antimalarial potentials of the crude extracts of Callistemon citrinus. Evid Complement Altern Med
34. Makler MT, Ries JM, Williams JA, Bancroft JE, Piper RC, Gibbins BL, Hinrichs DJ (1993) Parasite lactate dehydrogenase as an assay for Plasmodium falciparum drug sensitivity. Am J Trop Med Hygiene 48(6):739–741
35. Larayetan R, Ojemaye MO, Okoh OO, Okoh AI (2019) Silver nanoparticles mediated by Callistemon citrinus extracts and their antimalaria, antitrypanosoma and antibacterial efficacy. J Mol Liq 1(273):615–625
36. Keusch GT, Jacewicz M, Hirschman SZ (1972) Quantitative microassay in cell culture for enterotoxin of Shigella dysenteriae 1. J Infect Dis 125(5):539–541
37. Lalitha A, Subbaiya R, Ponmurugan P (2013) Green synthesis of silver nanoparticles from leaf extract Azhadirachta indica and to study its anti-bacterial and antioxidant property. Int J Curr Microbiol App Sci 2(6):228–235
38. Hyllested JÆ, Palanco ME, Hagen N, Mogensen KB, Kneipp K (2015) Green preparation and spectroscopic characterization of plasmonic silver nanoparticles using fruits as reducing agents. Beilstein J Nanotechnol 6(1):293–299
39. Sasidharan S, Chen Y, Saravanan D, Sundram KM, Latha LY (2011) Extraction, isolation and characterization of bioactive compounds from plants' extracts. Afr J Tradit Complement Altern Med 8(1)
40. Elemike E, Fayemi O, Ekennia A, Onwudiwe D, Ebenso E (2017) Silver nanoparticles mediated by Costus afer leaf extract: synthesis, antibacterial, antioxidant and electrochemical properties. Molecules 22(5):701
41. Magudapathy P, Gangopadhyay P, Panigrahi BK, Nair KGM, Dhara S (2001) Electrical transport studies of Ag nanoclusters embedded in glass matrix. Phys B Condens Matter 299 (1–2):142–146
42. Dudkiewicz A, Tiede K, Loeschner K, Jensen LHS, Jensen E, Wierzbicki R, Boxall AB, Molhave K (2011) Characterization of nanomaterials in food by electron microscopy. TrAC Trends Anal Chem 30(1):28–43
43. Egerton RF (2005) Physical principles of electron microscopy. Springer, New York
44. Dong JX, Gao ZF, Zhang Y, Li BL, Zhang W, Lei JL, Li NB, Luo HQ (2016) The pH-switchable agglomeration and dispersion behavior of fluorescent Ag nanoclusters and its applications in urea and glucose biosensing. NPG Asia Mater 8(12):e335
45. Rotimi L, Ojemaye MO, Okoh OO, Sadimenko A, Okoh AI (2019) Synthesis, characterization, antimalarial, antitrypanocidal and antimicrobial properties of gold nanoparticle. Green Chem Lett Rev 12(1):61–68
46. Kasthuri J, Kathiravan K, Rajendiran N (2009) Phyllanthin-assisted biosynthesis of silver and gold nanoparticles: a novel biological approach. J Nanopart Res 11(5):1075–1085
47. Krettli AU (2009) Antimalarial drug discovery: screening of Brazilian medicinal plants and purified compounds. Expert Opin Drug Discovery 4(2):95–108
48. Soh PN, Benoit-Vical F (2007) Are west African plants a source of future antimalarial drugs? J Ethnopharmacol 114(2):130–140

# Green Synthesis of MgO Nanoparticles Using *Sesbania bispinosa* and Its In Vitro Effect on Chlorophyll Content in Long Bean Plant

13

V. Tamil Elakkiya, K. Rajaram, R. V. Meenakshi, K. Ravi Shankar, and P. Sureshkumar

**Abstract**

This work focuses on the green synthesis of metal oxide nanoparticles by *Sesbania bispinosa* leaves. The main reason for choosing this green method is its eco-friendly and nontoxic characteristics. Green synthesis of metal oxide nanoparticles is a promising alternative to traditional chemical methods. In this study, *Sesbania bispinosa* leaf extract was used as a reducing agent in the synthesis of MgO nanoparticles. The synthesized NPs were characterized by different analytical techniques such as UV-visible spectroscopy, Fourier transform infrared (FTIR) spectroscopy, X-ray diffraction (XRD), and scanning electron microscopy (SEM). UV-visible peaks at 265 nm confirm the formation of MgONPs. FTIR study shows that alkyl groups are responsible for the reduction of NPs, and the reduction peaks at 524 nm confirm the presence of MgONPs. Surface morphological characteristics were studied by performing SEM analysis which shows that the particles are spherical in shape and 80–90 nm in size, and XRD analysis confirms that the particles were crystalline in nature. The synthesized MgONPs were treated with plant samples in different concentrations, and their growth parameters along with the chlorophyll content were estimated. The chlorophyll content was found to be increased in samples containing media treated with MgO nanoparticles at 5 mg/ml concentration. Since the chlorophyll acts as a key component for the plant metabolic activity, this study shows that MgONPs have greater impact on growth of plants and can be used as effective plant growth regulators.

V. Tamil Elakkiya · R. V. Meenakshi · K. Ravi Shankar · P. Sureshkumar (✉)
Department of Biotechnology, Bharathidasan Institute of Technology, Anna University, Tiruchirappalli, Tamil Nadu, India

K. Rajaram
Department of Biochemistry and Biotechnology, CSIR - Central Leather Research Institute, Chennai, Tamil Nadu, India

© Springer Nature Singapore Pte Ltd. 2020

Q. Saquib et al. (eds.), *Green Synthesis of Nanoparticles: Applications and Prospects*, https://doi.org/10.1007/978-981-15-5179-6_13

**Keywords**

Green synthesis · Magnesium oxide nanoparticles · *Sesbania bispinosa* leaves · Plan tissue culture · Characterization

## 13.1 Introduction

Nanotechnology refers to the projected ability to construct items from the bottom-up approach using techniques and tools being developed today to make complete and high-performance products. Recent applications of nanomaterial include a range of biomedical applications such as tissue engineering, drug delivery, and biosensors. Free nanoparticles are formed either through the breaking down of larger particles or by controlled assembly processes. The biosynthesis of nanoparticles is expected to be in the range of 1–100 nm, with high surface to volume ratios, which is stable, cost-effective, and environmentally friendly and acts as an alternative to chemical and physical methods [1]. Especially plant extract-mediated green synthesis is advantageous as their rich source of secondary metabolites is used as a reducing agent for the biological synthesis [2].

It is believed that the secondary metabolites such as flavonoids, phenols, and other proteins can reduce the metal used in the nanoparticle synthesis and act as a protective capping agent**.** In this aspect, *Sesbania bispinosa* was chosen to synthesize magnesium oxide nanoparticle. *Sesbania bispinosa* is a leguminous plant that is widespread in Central America and South Asian countries such as India, Vietnam, China, and Sri Lanka [3]. It is rich in bioactive compounds such as alkaloids, carbohydrates, phytosterol, and polyphenols that are responsible for several activities such as antidiabetic and antimicrobial activities. [4] It is reported that the ethyl acetate leaf extract of *Sesbania bispinosa* possesses anti-inflammatory activity, and [5] it is reported that the ethanolic leaf extract of *Sesbania bispinosa* exhibits antibacterial activity against *E. coli* at 250 μg/ml concentration. Additively, they could inhibit the fungal growths of *Fusarium oxysporum* and *Curvularia lunata* at 100 μg/ml and 500 μg/ml of the extract.

Though Ag, Au, and Zn nanoparticles are used most commonly in biosynthesis, we tried using magnesium oxide nanoparticles (MgONPs) that were synthesized by the solgel method [6, 7]. Many other methods such as hydrothermal method and microemulsion method have also been used to prepare MgO nanoparticles. Among several inorganic metal oxides, magnesium oxide (MgO) nanoparticle is a potent antibacterial agent which is nontoxic and relatively easy to obtain [8]. A similar green synthesis of nano-sized magnesium oxide was carried out using the plant leaf extracts of *Aloe vera* in an eco-friendly manner [9]**.** Synthesized nanoparticles were characterized, and its applications such as antibacterial and photocatalytic activities were observed. On comparison with the magnesium oxide nanoparticles synthesized by chemical method, the crystallite size was found to be 50 nm for chemically synthesized and 8 nm for biogenetically produced nanoparticles. Therefore, green technique is more preferred and cost-effective for the synthesis [10]. It was also

observed that magnesium oxide nanoparticles synthesized using *Aloe vera* act as an excellent sorbent from the photocatalytic studies. Chlorophyll (Chl) remains to be an important photosynthetic pigment in plant which is vital in determining photosynthesis capacity and plant growth [11]. So by combining the literature inputs, we have aimed to synthesize magnesium oxide (MgO) nanoparticles from the leaf extract of *Sesbania bispinosa*; the synthesized nanoparticle was characterized and tested for the plant growth regulator activity, especially the chlorophyll content using plant tissue culture technique.

## 13.1.1 Methodology

### 13.1.1.1 Procurement *of Sesbania bispinosa* Leaves

*Sesbania bispinosa leaves* were collected from Bharathidasan University, Trichy.

### 13.1.1.2 Solvent Extraction of *Sesbania bispinosa* Leaves

Leaves of *Sesbania bispinosa* were washed for several times, dried, and powdered. 3 g of the *Sesbania bispinosa* leaf powder was dissolved in 20 ml of ethanol in a 250 ml conical flask. The sample was boiled at the respective boiling plants for 15 min and centrifuged at 5000 rpm, and the supernatant was collected separately.

#### Reduction

Ethanolic extract of *Sesbania bispinosa* leaves was added dropwise into 0.1 M of $MgSO_4.7H_2O$ solution, and the mixture was stirred for 1 h until the precipitate of magnesium hydroxide was obtained. The complex formed after adequate time of stirring was collected by centrifugation at 7000 rpm for 20 min. The complex was calcinated at 500 °C for 3 h.

#### Biosynthesis and Purification of Nanoparticles

*Sesbania bispinosa* leaves extract was used as a reducing agent for the synthesis of magnesium oxide nanoparticles. Synthesis of MgONPs was carried out at optimized conditions with some modified protocol [12, 13]. 10 ml of extract was mixed with 50 ml of 0.1 M solution prepared in double distilled water for the synthesis of magnesium oxide nanoparticles at 50–60 °C. The reaction mixture was stirred for half an hour. Then the sample was centrifuged at 7000 rpm for 20mins. The supernatant was discarded, and the pellet was washed for three times using distilled water and finally resuspended in 1 ml of double distilled water. The concentrated sample of nanoparticles was characterized and used for further experiments.

## 13.1.2 Plant Tissue Culture Techniques

Long bean seed was cultured in MgONP-added MS medium under sterilized condition with 16-hr light and 8-h dark condition. The steps involved in the growth of plant tissue culture are given below.

## 13.1.3 Collection of Plant Material

Long bean seed was collected from Gandhi market, Trichy.

### 13.1.3.1 Media Preparation

Murashige and Skoog (MS) medium was used for all the experiments. Modification to the medium was done by adding growth regulators and other organic additives.

#### Preparation of Stocks

MS medium was commonly used for all the experiment. Stock solutions were prepared as given below in double distilled water stored at 4 °C.

#### Macronutrients

Ammonium nitrate ($NH_4NO_3$), 1650 mg/l; calcium chloride ($CaCl_2 \cdot 2H_2O$), 440 mg/l; magnesium sulfate ($MgSO_4 \cdot 7H_2O$), 370 mg/l; monopotassium phosphate ($KH_2PO_4$), 170 mg/l; potassium nitrate ($KNO_3$), 1900 mg/l

#### Micronutrients

Boric acid ($H_3BO_3$), 6.54 mg/l; cobalt chloride ($CoCl_2 \cdot 6H_2O$), 0.025 mg/l; ferrous sulfate ($FeSO_4 \cdot 7H_2O$), 27.8 mg/l; manganese (II) sulfate ($MnSO_4 \cdot 4H_2O$), 22.3 mg/l; potassium iodide (KI), 0.83 mg/l; sodium molybdate ($Na_2MoO_4 \cdot 2H_2O$), 0.25 mg/l; zinc sulfate ($ZnSO_4 \cdot 7H_2O$), 8.6 mg/l; copper sulfate ($CuSO_4 \cdot 5H_2O$), 0.025 mg/l

#### Vitamins and Other Essential Sources

Nicotinic acid, 0.5 mg/l; pyridoxine HCl, 0.5 mg/l; thiamine HCI, 0.1 mg/l; glycine, 2 mg/l. Other sources of plant growth include myo-inositol, 100 mg/l; lactalbumin hydrolysate (Edamin), 1 g; indole acetic acid, 1–30 mg/l; kinetin, 0.04–10 mg/l.

#### Preparation of Growth Regulator Stock

Stock solution of NAA was prepared by dissolving it in few drops of 1 N NaOH and then made up to the required concentration with double distilled water.

Stock solution of 2,4-D, IAA, was prepared by dissolving small volume of ethyl alcohol, and the volume was made up to the required concentration with double distilled water.

## 13.1.4 Preparation and Sterilization of Media

The stock solution was mixed in required proportion along with growth regulators and sucrose. The volume was made up by adding double distilled water. The pH of the medium was adjusted to 5.6, and the volume was finally adjusted with required amount of agar and streptomycin. Agar in the medium was completely melted by gentle heating up to 90 °C, and 20 ml of media was poured into pre-sterilized glass

culture tubes and plugged with nonabsorbent cotton wrapped in cheese cloth. The media was autoclaved at 121 °C at 15 lbs. per square inch pressure for 20 min and then allowed to cool to room temperature and stored in culture until further use [14].

### 13.1.5 Surface Sterilization of Seed

The long bean seed was first washed with distilled water. After that the seed was washed with 70% ethanol for 30 s. The final surface sterilization was done with 0.1% $HgCl_2$ for 12 minutes and then washed with distilled water for 3–4 times in the laminar airflow cabinet.

### 13.1.6 Inoculation

Long bean seeds were inoculated in test tubes containing the media with or without MgO nanoparticles (1–10 mg/L) and compared with the control.

### 13.1.7 Measurement of Plant Growth Parameters

Once the plants achieve proper growth, they were acclimatized in the green house. Later, the plants were removed and the plant root and shoot length were measured.

### 13.1.8 Sample Preparation for Chlorophyll Estimation

0.1 g fresh leaves of long bean plants were taken. Leaves were finely cut and ground with 7 ml of 80 v % acetone. It was then centrifuged at 5000 rpm for 5mins. The supernatant was collected, and the procedure was repeated till the residue becomes colorless. The absorbance of the solution was read at 645 nm and 663 nm against the acetone blank [10]. The absorbances of the samples are given in Table 13.1.

**Table 13.1** Plant growth in the presence of NPs at 5 mg/l concentration

| Plant parts | With nanoparticles (cm) | Without nanoparticles (cm) |
|---|---|---|
| Shoot | 18.5 | 13 |
| Leaf | 5 | 5 |
| Root | 5.5 | 7 |
| Total length | 24 | 20 |

## 13.2 Results

### 13.2.1 Characterization of MgONPs

#### 13.2.1.1 UV-vis Analysis

The optical property of MgONPs was determined by UV-Vis spectrophotometer (PerkinElmer, Lambda 35, Germany). After the addition of $MgSO_4 \cdot 7H_2O$ to the extract, the spectra were taken between 200 nm and 800 nm.

The synthesis of the MgONPs in aqueous solution was monitored by recording the absorption spectra at a wavelength range of 250–800 nm as shown in Fig. 13.1. In the UV-Vis spectrum, a single, strong, and broad surface plasmon resonance (SPR) peak was observed at 265 nm confirming its presence. Vergheese and Vishal [15] obtained a peak at 267 nm to confirm the absorption spectra of MgONPs synthesized using *Trigonella foenum-graecum* as similar to our study.

#### 13.2.1.2 FTIR Analysis

The chemical composition of the synthesized magnesium oxide nanoparticles was studied using FTIR spectrometer (PerkinElmer LS-55 Luminescence spectrometer). The solutions were characterized in the range 4000–500 $cm^{-1}$ using KBr pellet method.

FTIR measurements were carried out in order to identify the presence of various functional groups in biomolecules responsible for the bioreduction of Mg + and capping of magnesium oxide nanoparticles. The observed intense bands were compared with standard values to identify the functional groups. FTIR spectrum shows absorption bands at 3665, 2946, 1649, and 524, indicating the presence of capping agent with the nanoparticles. The strong sharp absorption at 1649 $cm^{-1}$ implies the presence of an aromatic ring and in plane bending of C-H and C-C bonds of the alkyl groups and aromatic ring. The absorption at 2946 $cm^{-1}$ is due to C-N stretching in amines. The band at 524 $cm^{-1}$ confirmed the metal oxide linkage,

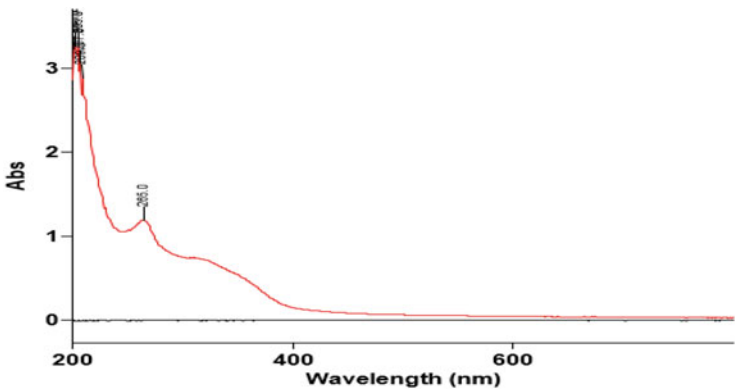


**Fig. 13.1** UV-visible spectra

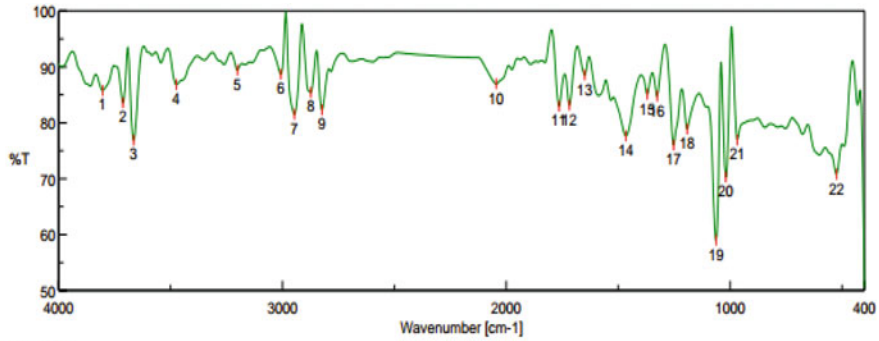


[Comments]
Sample name DDLL
Comment
User
Division
Company ANNA UNIVERSITY, TRICHY

[ Result of Peak Picking ]

| No. | Position | Intensity | No. | Position | Intensity | No. | Position | Intensity |
|---|---|---|---|---|---|---|---|---|
| 1 | 3803.9 | 85.7528 | 2 | 3712.3 | 83.5709 | 3 | 3665.05 | 76.8676 |
| 4 | 3474.13 | 86.8063 | 5 | 3201.26 | 89.405 | 6 | 3007.44 | 88.6742 |
| 7 | 2946.7 | 81.5298 | 8 | 2873.42 | 85.3889 | 9 | 2823.28 | 82.29 |
| 10 | 2045.14 | 86.9452 | 11 | 1764.55 | 82.9539 | 12 | 1718.26 | 83.1412 |
| 13 | 1649.8 | 88.5355 | 14 | 1465.63 | 77.6467 | 15 | 1370.18 | 85.0376 |
| 16 | 1325.82 | 84.7243 | 17 | 1252.54 | 75.9918 | 18 | 1191.79 | 78.8736 |
| 19 | 1062.59 | 58.9914 | 20 | 1019.19 | 70.2597 | 21 | 968.09 | 76.877 |
| 22 | 524.543 | 70.7629 | | | | | | |

**Fig. 13.2** FTIR analysis of magnesium oxide nanoparticles

Mg-O stretching vibrations as shown in Fig. 13.2. The broad and intense band at 3665 $cm^{-1}$ indicates the presence of stretching vibrations of O–H groups in water.

### 13.2.1.3 XRD Analysis

X-ray diffraction (XRD) analysis of drop-coated films of magnesium oxide nanoparticles in sample was prepared for the determination of the formation of MgO nanoparticle by an X'Pert Pro X-ray diffractometer (X'Pert High Score Plus program) operated at a voltage of 40 kV and a current of 30 mA with Cu Kα radiation.

It can be calculated using Debye-Scherrer's equation, $D = \frac{K\lambda}{\beta \cos\theta}$, where "D" is the mean diameter of the nanoparticles, "λ" is the wavelength of X-ray radiation source, and "β" is the angular FWHM of XRD peak at diffraction angle "θ."

XRD analysis was carried out for the synthesized MgONPs, and the diffraction peaks are obtained; 42.71, 62.17, and 78.06 assigned to the (101), (103), and (202) planes of a faced center cubic lattice of magnesium oxide were obtained (Fig. 13.3). The intensity of peaks reflects the high degree of crystallinity of the MgO nanoparticles. However, the diffraction peaks are broad which indicate that small crystallite size obtained was matched with database of the Joint Committee on Powder Diffraction Standards (JCPDS) file No. 74–1225. The XRD analysis of MgO nano-flowers synthesized using aqueous rosemary extract showed sharp

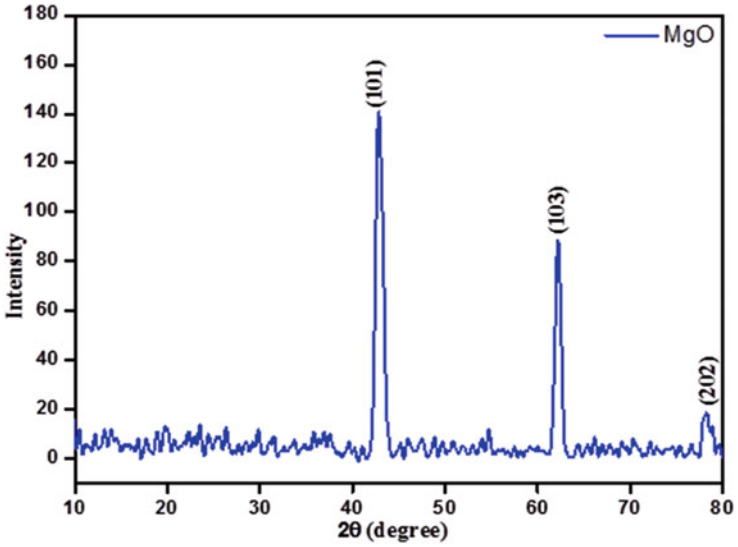


**Fig. 13.3** XRD analysis

diffraction peaks at 38.048 (100), 41.095 (101), 78.628 (202), and 62.342 (102) quite relevant as our data [16].

#### 13.2.1.4 SEM Observation of MgO Nanoparticles

The plant extract biomass after reaction spontaneously precipitates at the bottom of the tubes. After the precipitation, the suspension above the precipitate was sampled for SEM observation. SEM samples of the aqueous suspension of magnesium oxide nanoparticles were fabricated by dropping the suspension into clean electric stubs and allowing water to completely evaporate. SEM observations were carried out on a ZEISS EVO 40 EP electron microscope.

The SEM analysis confirmed that the synthesized MgO nanoparticles are in the nano-size. They were spherical in shape and the diameter of the particle was in the range of 80–90 nm (Fig. 13.4).

### 13.2.2 Effect of MgONPs on Plant Growth

After 7 days of growth, the shoot and root lengths were long enough to measure using a ruler**.** It was found that shoot length increased in the presence of nanoparticle at the concentration and no change in the number of leaves was observed. After increasing the nanoparticle concentration, shoot and root death was observed as it may be toxic to the plants. So the 5 mg/l concentration was found to be optimal for the plant's growth (Table 13.1). The seed germination results were recorded based upon their growth response as shown in Fig. 13.5 (a, b).

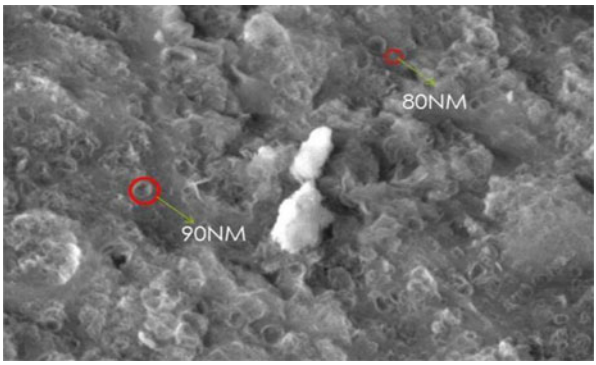


**Fig. 13.4** SEM analysis of MgONPs confirming the spherical shape and nano-size of the synthesized particle


**Fig. 13.5** (**a**, **b**) shows the synthesized nanoparticles used as nutritional source instead of Mg to grow long bean seed. The results were recorded based on their growth response

### 13.2.3 Effect of MgO Nanoparticle on Chlorophyll Content in *Sesbania bispinosa*

Effect of MgONPs on chlorophyll content (absorbance of chlorophyll A and B, total chlorophyll) in *Sesbania bispinosa* is shown in Table 13.2.

Magnesium, sulfur, and calcium are a few macronutrients required for plant growth [17]. Chlorophyll *a* has approximate absorbance maxima of 430 nm and 662 nm, while chlorophyll *b* has approximate maxima of 453 nm and 642 nm. The

**Table 13.2** Absorbance for chlorophyll estimation

| Samples | OD @ 645 nm | OD @ 663 nm |
|---|---|---|
| Sample 1 (cultured with MgONPs) | 0.674 | 1.503 |
| Sample 2 (cultured W/O MgONPs) | 0.782 | 1.968 |

**Table 13.3** The chlorophyll content of MS media with and without nanoparticles

| Samples | Chlorophyll µg/ml | Chlorophyll(a) µg/ml | Chlorophyll(b) µg/ml |
|---|---|---|---|
| MS media without nanoparticles | 25.66 | 17.27 | 8.40 |
| MS media with nanoparticles | 31.57 | 22.89 | 8.697 |

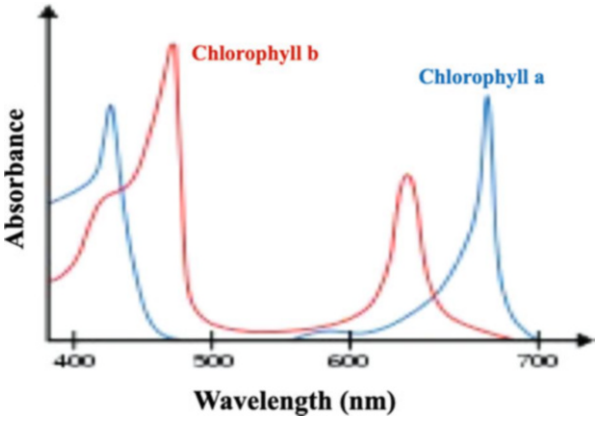


**Fig. 13.6** Chlorophyll content measurement

absorption peaks of chlorophyll *a* are at 465 nm and 665 nm. Chlorophyll *a* fluoresces at 673 nm (maximum) and 726 nm. The peak molar absorption coeffi cient of chlorophyll *a* exceeds $10^5$ $M^{-1}$ $cm^{-1}$, which is among the highest for small-molecule organic compounds. In 90% acetone-water, the peak absorption wavelengths of chlorophyll *a* are 430 nm and 664 nm; peaks for chlorophyll *b* are 460 nm and 647 nm; peaks for chlorophyll *c1* are 442 nm and 630 nm; peaks for chlorophyll *c2* are 444 nm and 630 nm; peaks for chlorophyll *d* are 401 nm, 455 nm, and 696 nm.

The concentrations of chlorophyll a, chlorophyll b and total chlorophyll in the leaves from the plant using nanoparticles in MS media were interpreted as shown in Table 13.3. The total chlorophyll concentration was found to be 31.57µg/ml. The concentration of chlorophyll a and chlorophyll b was found to be 22.8 and 8.697 µg/ml which was higher than in the control that were supplemented with normal MS media (chlorophyll a -25.66 µg/ml, chlorophyllb- 17.27 µg/ml and total chlorophyll content-8.40 µg/ml) which shows that MgO NPs can be used as an effective plant growth regulator (Fig. 13.6).

## 13.3 Discussion

Magnesium acts as micronutrients, and nearly one-fifth of the available Mg is bound in chloroplasts in the chlorophyll molecules which participate in photosynthesis [18]. A similar report to our findings was observed while using silver nanoparticle (60 ppm) concentration that increased the shoot and root lengths, leaf surface area, chlorophyll contents, carbohydrate, and protein contents in another plant belonging to the Fabaceae family, *Phaseolus vulgaris*, and also in *Zea mays* [19].

The chlorophyll content a and b absorbs are involved in photosynthesis reaction by absorbing sunlight at different wavelengths (red-orange light and blue-purple light, respectively) that is crucial for a plant's growth and survival [20]. Mg deficiency can have a serious effect on plants such as chlorophyll degradation and mature leaves senescence which has to be overcome to obtain healthy plants to completely utilize their medicinal properties [21].

Magnesium nanoparticles can be used as an alternative to the direct supply of magnesium that has to be supplemented in the lesser quantity. Subjecting to the environmental factors such as cold temperature, soil condition, and climate influencing the chlorophyll content, the magnesium NP-treated plants were cultured using aseptic plant tissue culture technique. This study encourages to further study the mechanism of MgONPs in increasing the chlorophyll content which is under progress.

## 13.4 Conclusion

Magnesium oxide nanoparticles were successfully synthesized by biological method using *Sesbania bispinosa*, and characterized through different techniques. UV-Vis peaks at 265nm initially confirms the synthesis of MgONPs, the FTIR analysis revealed that alkyl groups are responsible for the reduction and stabilization of MgONPs. The surface morphology was studied using SEM shows that the particle were spherical in nature around 80–90nm, and the XRD analysis confirms the crystalline nature of nanoparticles. The synthesized NPs (5 mg/l) was used as a macronutrient instead of Mg in the plant tissue culture media revealing their role in improving plant growth and chlorophyll content when compared with control. This shows that MgO NPs can be used as an effective plant growth regulator

## References

1. Pirtarighat S, Ghannadnia M (2019) Green synthesis of silver nanoparticles using the plant extract of Salvia spinosa grown in vitro and their antibacterial activity assessment. S J Nanostruct Chem 9(1)
2. Salam HA, Sivaraj R, Venckatesh R (2014) Green synthesis and characterization of zinc oxide nanoparticles from *Ocimum basilicum* L. var. purpurascens Benth.-Lamiaceae leaf extract. Mater Lett 131:16–18

3. Orwa C, Mutua A, Kindt R, Jamnadass A, Anthony S (2010) Agroforestree Database: a tree reference and selection guide version 4.0. World Agroforestry Centre, Kenya
4. Mythili T, Ravindhran R (2012) Phytochemical screening and antimicrobial activity of *Sesbania sesban* (l.) Merr. Asian J Pharm Clin Res 5(4):179–182
5. Boddawar G, Shashikant C, Dhawale C, Shaikh SS (2016) Assessment of anti-inflammatory potential of *Sesbania bispinosa* Linn. Leaf extracts and fractions by acute and chronic models. AJOL 52(3):289–293
6. Mirzaei H, Davoodnia A (2012) Microwave assisted sol-gel synthesis of MgO nanoparticles and their catalytic activity in the synthesis of Hantzsch. Chinese J Catal 33(9–10):1502–1507
7. Wahab R, Ansari SG, Dar MA, Kim YS, Shin HS (2007) Synthesis of magnesium oxide nanoparticles by sol-gel process. Mater Sci Forum:983–986
8. Cai L, Chen J, Liu Z, Wang H, Yang H, Ding W (2018) Magnesium oxide nanoparticles: effective agricultural antibacterial agent against Ralstonia solanacearum. Front. Microbiol 25(9)
9. Anantharaman A, Sathyabhama S, George M (2016) Green synthesis of magnesium oxide nanoparticles using *Aloe Vera* and its applications. ISJRD 4(9)
10. Chandran SP, Chaudhary M, Pasricha R, Ahmad A, Sastry M (2006) Synthesis of gold Nanotriangles and silver nanoparticles using Aloe vera plant extract. Biotechnol Prog 22 (2):577–583
11. Li Y, He N, Hou J, Xu L, Liu C, Zhang J, Wang Q, Zhang X, Wu X (2018) Factors influencing leaf chlorophyll content in natural forests at the biome scale. Front Ecol Evol 6
12. Rajaram K, Aiswarya DC, Sureshkumar P (2015) Green synthesis of silver nanoparticle using *Tephrosia tinctoria* and its antidiabetic activity. Mater Lett 138(1):251–254
13. Sasidharan J, Meenakshi RV, SureshKumar P (2018) Green synthesis, characterization and evaluation of *In-vitro* Antioxidant & Anti-diabetic Activity of nanoparticles from a Polyherbal formulation- Mehani. J Environ Nanotechnol 7(3):51–59
14. Huang LC, Murashige T (1977) Plant tissue culture media: Major constituents, their preparation and some applications. Tca Manual- Tissue Culture Association 3(1): 539–548
15. Vergheese M, Vishal SK (2018) Green synthesis of magnesium oxide nanoparticles using *Trigonella foenum-graecum* leaf extract and its antibacterial activity. J Pharmacogn Phytochem 7(3): 1193–1200
16. Abdallah Y, Ogunyemi SO, Abdelazez A, Zhang M, Hong X, Ibrahim E, Hossain A, Fouad H, Li B, Chen J (2019) The green synthesis of MgO Nano-flowers using *Rosmarinus officinalis* L. (rosemary) and the antibacterial activities against *Xanthomonas oryzae* pv", Biomed Res Int 2019, 1
17. Rajalakshmi K, Banu N (2015) Extraction and estimation of chlorophyll from medicinal plants. Int J Sci Res 4(11):209–212
18. Croft H, Chen JM, Zhang Y, Simic A (2013) Modelling leaf chlorophyll content in broadleaf and needle leaf canopies from ground, CASI, Landsat TM 5 and MERIS reflectance data. Remote Sens Environ vol 133:128–140
19. Salama HMH (2012) Effects of silver nanoparticles in some crop plants, Common bean (*Phaseolus vulgaris L.)* and corn (*Zea mays* L.). IRJOB 3(10): 190–197
20. Kume A (2017) Importance of the green color, absorption gradient, and spectral absorption of chloroplasts for the radiative energy balance of leaves. J Plant Res 130(3):501–514
21. Uchida R (2000) Essential nutrients for plant growth: nutrient functions and deficiency symptoms. University of Hawaii at Manoa, College of Tropical Agriculture and Human Resources

# Application of Green Nanosilica in Civil Engineering

14

Izabella Sant'Ana Storch, Lilian Rodrigues Rosa Souza, Leonardo Pereira Franchi, and Tiago Alves Jorge de Souza

**Abstract**

The insertion of additives in cementitious mortar and concrete can have a great impact on the properties of these compounds, such as the improvement of the mechanical, physical, and durability characteristics. In this context, several nanoparticles (NPs) have been used, with special emphasis on the use of nanosilica. Recent studies have shown that the addition of nanosilica to cement has pozzolanic effects and is associated with the filling of the cementitious matrix, reducing its pores. In this context the use of nanosilica has been especially recurrent in the manufacture of high-performance concrete (HPC) and ultrahigh-performance concrete (UHPC). However, the conventional synthetic methods employed for the production of nanosilica end up generating compounds and particles that are harmful to the environment. Therefore, the use of green nanosilica synthesis methods appears as an option to avoid the increasing use of

I. Sant'Ana Storch
Department of Structures and Civil Construction, Federal University of São Carlos – UFSCar, São Carlos, SP, Brazil

Department of Civil Engineering, Adventist University of São Paulo – UNASP, Engenheiro Coelho, SP, Brazil

L. R. R. Souza
Department of Chemistry, FFCLRP-USP, University of São Paulo – USP, Ribeirão Preto, SP, Brazil

L. P. Franchi
Department of Genetics, FMRP-USP, São Paulo University – USP, Ribeirão Preto, SP, Brazil

T. A. J. de Souza (✉)
Department of Civil Engineering, Adventist University of São Paulo – UNASP, Engenheiro Coelho, SP, Brazil

Department of Genetics, FMRP-USP, São Paulo University – USP, Ribeirão Preto, SP, Brazil
e-mail: tiagoajs@usp.br

© Springer Nature Singapore Pte Ltd. 2020

Q. Saquib et al. (eds.), *Green Synthesis of Nanoparticles: Applications and Prospects*, https://doi.org/10.1007/978-981-15-5179-6_14

these particles in civil construction which negatively impacts the environment. In this way, the present chapter discusses the various advantages of using nanosilica in civil construction, the possible environmental impacts related to the nonconscious and indiscriminate use of these particles, and the different green synthesis methods of these particles as an option to optimize the production of environmentally friendly building materials.

**Keywords**

Green nanoparticles · Nanosilica · Green nanosilica · Civil construction

## 14.1 Introduction

Silica is an element abundantly found on Earth's surface and has been widely used in its amorphous or crystallized nanoform in various industry branches due to its chemical and physical peculiarities [1–3]. Although it has the same formula, amorphous silica has a distinct structural arrangement from crystallized silica [4, 5]. Recently, due to the ease of synthesis, robust mechanical properties, and relatively inert chemical composition of silica nanoparticles (SiNPs), their employment has increased considerably in civil construction.

In this chapter, special emphasis will be given to the application of SiNPs in civil construction, addressing the advantages and disadvantages associated with their use, especially in the manufacture of concrete. The preliminary results of our research group have corroborated several other analyses already carried out, which point to the advantage deriving from the use of nanosilica in the manufacture of concrete. However, the large-scale application of SiNPs in the manufacture of concrete and other building materials can result in the release of these particles into the environment, which can alter the ecosystem's balance and harm human health.

The occupational exposure to crystalline nanosilica, for example, is associated with silicosis, pulmonary tuberculosis, emphysema, and lung cancer, and recent studies have shown that amorphous silica has similar crystalline toxicity [6]. Therefore, it is essential to carry out studies that measure the possible damages that these nanoparticles represent to ecosystems and human health, with special emphasis on the nature of the changes caused by these particles at the cellular level and in ways to mitigate the toxicity of these particles.

In this context, many studies that employ SiNPs in civil construction have described the improvements resulting from the use of these particles without characterizing their physicochemical properties (e.g., form, charge, composition, and crystallinity) making difficult to measure the real risk represented by them. As a possible solution to this problem, the present chapter proposes the use of SiNP green synthesis methods to produce ecologically friendly particles, which properly characterized would contribute to the improvement of the properties of the materials used in civil construction, such as concrete, without negatively impacting human health and the environment.

## 14.2 Silica Nanoparticles (SiNPs) in Civil Construction Materials

Nanotechnology applied to civil engineering is relatively new; its use has been studied in recent years with the main objective of improving the microscopy of concrete and mortars; the most widely used nanoparticle is nanosilica (Table 14.1). The microstructure of the concrete and mortar consists of three phases: the cement paste, the aggregate, and the interfacial transition zone (ITZ) between the cement paste and the aggregate. Any material to be implemented in the concrete or mortars will ultimately affect its microstructure. However, the alterations in the microstructure due to the application of some different material are difficult to determine, since it is highly complex and heterogeneous. The ITZ is mainly composed by the accumulation of cement particles on the surface and differs from the cement paste by its morphology and has a smaller amount of clinker and a greater number of microdefects. Moreover, it has less resistance than the aggregate and then cement paste [7].

Nanosilica promotes C-S-H nucleation favoring the hydration of the cement, making the ITZ denser and more homogeneous by disconnecting microdefects, refining the microstructure, and thereby increasing the resistance gain of the mixture in early ages. Another impact of nanosilica refers to its action as micro-fill material in the reduction of porosity of the microstructure, also known as physical packaging; however, this effect is less prominent than its highly reported pozzolanic activity [8–37].

Liu et al. [37] found that when using nanosilica in cement-based mixtures, the width of the ITZ is decreased; the lower the w/c ratio, the more intensified is this effect. This fact relates to the permeability of concrete; the smaller the width of the ITZ, the lower the permeability of the concrete or mortar, therefore, less susceptible to deterioration by the transport of deleterious agents. In concrete subjected to high temperatures, the NS produces a positive effect up to 200 ° C. However, above this temperature, its benefits are not significant. The additional formation of gel caused by nanosilica improves the microstructure of the cement matrix avoiding the propagation of cracks after exposure to high temperatures [19].

Several researchers have evaluated the efficacy of nanosilica and microsilica concomitantly. They conclude in general that applying the materials together results in greater gains than those observed in mixtures with one or the other; they also affirm that it could be a viable path for the problem of the high costs presented by the use of nanosilica or great losses in the fluidity [9, 15, 18, 21, 22, 28, 30].

Because of the observed benefits in the microstructure of the cement-based mixtures, there is a pronounced increase in the compressive strength due to the use of the nanosilica, as well as in the tensile strength; the increase in flexural strength is lower than that in the compressive strength. The modulus of elasticity, on the other hand, presents the lowest gain [8–37]. In addition to the mechanical characteristics, the durability of cement-based mixtures with addition of nanosilica is increased [9–14, 17–21, 24, 25, 27, 30–35, 37].

In relation to the limitations of the use of nanosilica, it can be stated that in general there is a reduction in the fluidity of the concrete or mortar in its fresh state [8–37];

**Table 14.1** Application of nanosilica in building materials

| Dimension | Application | Main results | Authors |
|---|---|---|---|
| 5–40 nm | Increase mechanical properties and durability of high-performance concrete (HPC) | The best percentage of nanosilica addition was 2%; with this percentage there was a gain of 23% in the compressive strength and 34% lower water absorption | Chitra et al. [14] |
| 25 nm | Increase bond behavior of steel and polypropylene fibers in high-volume fly ash | The best percentage of nanosilica addition was 2%. Nanosilica increased bond resistance considerably, especially after 28 days | Shaikh and Sarker [16] |
| 20 nm | Promote progress in mechanical properties, hydration, and pore structure | 3% of nanosilica was ideal. The compressive strength increased 33% at the age of 3 days. At the age of 28 days there was an increase of 19%. There was a 5% reduction in porosity. The pore structure was optimized | Wang et al. [17] |
| 15–40 nm | Promote better resistance to concrete in sulfuric acid medium | Combination of microsilica and nanosilica was more effective than when they are used separately. The best percentage of nanosilica addition was 1% together with 7% microsilica. At 28 days there was a reduction of 5% compressive strength. At 60 days there was a reduction of 4% of mass | Hendi et al. [18] |
| 14.6 and 35.4 nm | Increase mechanical and durability properties of mortar with sugar cane bagasse ash (SCBA) | The use of nanosilica and SCBA reduced the porosity and improved compression resistance. With 6% of NS, the compressive strength increased by 31%. And by incorporating 15% of SCBA with 6% NS, the compressive strength increased by 23% | Joshaghani and Moeini [20] |
| 5–20 nm | Enrich the durability of mortar with the combined effect of nanosilica (NS) and microsilica (MS) | The best combination of 1% NS and 10% MS. the positive effect on the durability of NS and MS combined was greater, comparing the effect of the sum of the two separately | Li et al. [21] |

(continued)

**Table 14.1** (continued)

| Dimension | Application | Main results | Authors |
|---|---|---|---|
| 5–20 nm | Enrich the strength of mortar with the combined effect of nanosilica (NS) and microsilica (MS) | Substantial increases in the strength and microstructure of the mortar are obtained by using NS and MS together, better results than when used separately. There was improvement of up to 55% strength at 28 days with 2% NS and 10% MS | Li et al. [22] |
| 14 nm | Enrich the interactive behaviors Of carbon nanotubes (CNT) and the cement matrix | The nanosilica improves bond between the CNT and the cement matrix; there were increases of up to 66% in bond between the phases | Li et al. [23] |
| 4 nm | Improve the interfacial transition zone (ITZ) in concrete | The use of nanosilica accelerates the process of hydration and is the main factor in the improvement of ITZ. There was a 15% increase in compressive strength in the cement paste and 23% in the concrete | Xu et al. [24] |
| 10–25 nm | The application of nanosilica in roller compacted concrete containing fly ash, and crumb rubber was evaluated as part of the fine aggregate | The best percentage of NS addition was 1.22%, increased the compressive strength, flexural strength, and abrasion resistance of HVFA RCC pavement. NS mitigated some of the negative effects of replacing the natural | Adamu et al. [25] |
| 5–20 nm | It studied the mechanical and durability characteristics of concrete containing coarse recycled aggregates and nanosilica | There was an increase of 21% in compressive strength and 16% in flexural strength and 6% in modulus of elasticity and a reduction of 84% in permeability in concrete with recycled aggregate and 2% of nanosilica compared to concrete with recycled aggregate without nanosilica | Erdem et al. [27] |
| 5–20 nm | Use nanosilica and microsilica together promoting synergy and improving concrete characteristics | For the compressive strength a synergistic effect occurred when NS and MS were added together. For the modulus of elasticity, the effect is not the same | Li et al. [28] |

(continued)

**Table 14.1** (continued)

| Dimension | Application | Main results | Authors |
|---|---|---|---|
| 30 nm | Improvement of early-age properties for glass-cement (GP) mortar | Improved early stiffening and pore refinement effects, significantly improve the interface between particles. With 2% of nanosilica (NS), there was a gain of 55% of compressive strength compared to GP mortar without NS | Lu and Poon [29] |
| 15 nm | Improve the mechanical and durability characteristics of the high-performance self-compacting concrete (HPSCC) | The addition of 2.5% nanosilica and 2.5% microsilica generated a 24% increase in compressive strength and a 21% reduction in porosity at 28 days. There was less mass loss, less susceptibility to carbonation, and lower capillary absorption | Massana et al. [30] |
| 12 nm | Improve mechanical and durability properties of alkali-activated slag coating mortar | In the use of nanosilica, a percentual 2% increased 14% the compressive strength. With 2% of nanosilica, there was 31% of decrease in chloride diffusion | Ramezanianpour and Moeini [31] |
| 20 nm | Improve the microstructure and impermeability Of concrete with different aggregate gradations | The nanosilica decreased the connectivity between the micropores in the ITZ and healed microcracks, leading to higher density and lower permeability of the concrete | Xiao et al. [32] |
| 8–20 nm | Increase mechanical properties and durability of hybrid fiber-reinforced self-compacting concrete | In the use of nanosilica, a percentual 0.4% increased 7.9% in compressive strength and 8.6% in the tensile strength | Mahapatra and Barai [34] |
| 20 nm | Improve the microstructures, mechanical properties, and durability performances Of ultralightweight cement composites (ULCC) | There was a gain of 35% in the compressive strength resulting from the increased packing density and improved microstructure | Du [35] |
| 20 nm | Improve the microstructure of ITZ and reducing The permeability of concrete | The densification of the ITZ upon addition of nanosilica is more significant as the relation of water/cement reduces. There was a reduction in the porosity of the concrete | Liu et al. [37] |

the nanosilica has a high-specific surface area, which demands a greater amount of water for dispersion, in concretes or mortars with low w/c ratio; this point can be critical, mainly because it demands a high amount of additional superplasticizer [11, 14, 22, 28, 30, 33, 36].

In the case of structures subjected to high temperatures, the use of low thermal conductivity aggregates exhibits thermal fragmentation; this effect is more pronounced when combined with nanosilica [19]. The high cost of nanosilica, and also the expenses related to the additional use of superplasticizer, is another limitation pointed out by the authors. When it comes to the use of nanosilica powder, another limiting factor is the dispersion capacity of the particles in the cement-based mixtures [22].

Additional possible limitation would be the great variety of mean particle size that is found in the market, causing lack of consensus on the optimum percentage of the particles in the mixture of concretes or mortars. This variation also generates divergence in the quantification of how much the nanosilica can improve a mixture in terms of mechanical characteristics and in relation to the durability [15].

## 14.3 The Effects of Nanosilica on Human Health

Several studies have pointed to the damage caused by SiNPs in human health [38–40]. SiNPs may compromise key elements of the immune system being primarily related to oxidative stress, autophagy, and pro-inflammatory responses. Upon entering the body, NPs can be absorbed by various cells of the immune system, such as antigen-presenting cells, lymphocytes, and mast cells [1].

Modifications in these cells function may occur after interaction with these nanoparticles by compromising immune-specific signaling pathways [39, 40]. Duan and colleagues, for example, have demonstrated that SiNPs can disperse to various organs from the circulatory system causing various types of damage and specifically affect the TLR5 signaling pathway, resulting in hyperlipemia and hepatic steatosis [38].

Moreover, as previously mentioned, it is essential to characterize the size of nanoparticles because there is a relationship between nanoparticle size and their toxicity. In this context, Zhou and colleagues [41] employed SiNPs of 10, 25, 50, and 100 nm in order to establish a relationship between the size and toxicity of these particles in human umbilical vein endothelial cells. Although there were differences in toxicity between the SiNPs of different sizes, it was observed that in the concentrations of 1, 5, and 25 μg/mL all four sizes of nanosilica increased the levels of reactive oxygen species (EROS), micronuclei frequencies, and DNA damage [41].

A recent study has shown that SiNPs may also be toxic to nervous system cells. In this study, Kamikubo and co-workers [42] demonstrated that SiNPs of 10–1500 nm can cause oxidative stress, swelling, fragmentation of neurons, and cell death in nerve cells (neurons and glial cells). However, they verified that several variables can influence the toxicity of these particles: surface charge, particle size, and

temperature at the time of exposure. Furthermore, the experiments presented in this study demonstrated that pretreatment of cells with antioxidants and the use of properly coated SiNPs diminished the damage caused to nerve cells [42].

## 14.4 Green Synthesis Methods of Nanosilica

Some methodologies of nanoparticle synthesis employ toxic reagents or can generate toxic waste. Nowadays the interest for the greener and more sustainable chemical process is getting more attention in the society and in the scientific community, and to develop environment-friendly methods, the green chemistry appears as a solution [32]. In order to guide the design of new chemical processes, the 12 principles of green chemistry were established (Table 14.2), and they are applied to all aspects of the chemical process from the raw material to the final product [33].

The conventional methods for nanosilica synthesis, based on the solgel process, are carried out under high temperatures, in extremely high or low pH, and employ highly toxic chemicals [43]. In view of these issues and in order to follow the green chemistry principles, some synthesis of SiNPs can be used such as biomimetic synthesis, extraction from agricultural waste, extraction from coal, and extraction from plants (Fig. 14.1).

**Table 14.2** The 12 principles of green chemistry [34]

| Principle | Description |
|---|---|
| 1. Prevention | It is better to prevent waste than to treat it |
| 2. Atom economy | The incorporation of all materials used in the processes should be necessary |
| 3. Less hazardous | Methodologies should use and generate substances that pose little or no toxicity to human health and to the environment |
| 4. Designing safer chemicals | Chemical products should be designed to preserve efficacy while reducing toxicity |
| 5. Safer solvents and auxiliaries | The use of solvents and auxiliaries should be avoided when possible, or, if it's not possible, they should be innocuous |
| 6. Design for efficient energy | If possible, the process should be conducted at ambient pressure and temperature |
| 7. Use of renewable feedstocks | Feedstock or raw material should be renewable |
| 8. Reduce derivatives | Unnecessary, derivatization should be avoided because it requires the addition of reagents and waste generation |
| 9. Catalysis | The use of catalytic reagents is better than stoichiometric reagents |
| 10. Design for degradation | At the end of the process, the chemicals should be broken down into innocuous degradation products |
| 11. Real-time analysis for pollution prevention | Development of analytical methodologies to monitor and control the formation of hazardous substances |
| 12. Inherently safer chemistry for accident prevention | Minimization of potential chemical accidents like explosions, fire, and releases |

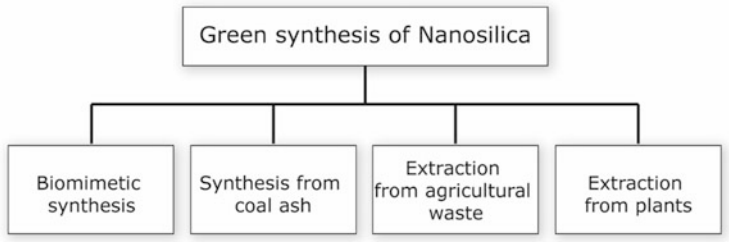


**Fig. 14.1** Methods employed for the green synthesis of nanosilica

### 14.4.1 Biomimetic Synthesis

Some organisms such as sponges and diatoms can produce silica structures with multiple morphologies in water under ambient conditions in an efficient way, which is called biomimetic synthesis [44, 45]. The biomimetic synthesis is composed of three components: (a) the organic matrix, (b) interactive proteins, and (c) a system for transporting ions to the mineral phase. The organic matrix is one of the fundamental processes involved in the regulation of mineral deposition in biological system because it controls the nucleation and growth of the inorganic structure. In this process, acid biopolymers interact with ions to initiate the nucleation and growth of the inorganic phase, and it grows following the matrix, assuming an orientation specified by the matrix architecture [46, 47].

Different biomimetic approaches have been developed using room temperature, neutral pH, and aqueous medium and also involving biomimetic molecules as templates for silica polycondensation such as polypeptides, silaffin, silicatein, and polyamines [43, 44]. The biomimetic synthesis using tetraethyl orthosilicate (TEOS) as silica source and polyallylamine hydrochloride (PAH) which acts as an accelerator of the condensation of TEOS in aqueous solution was investigated by Kang and colleagues [43]. Furthermore, the nucleation of SiNPs can be controlled by the concentration of PAH, and the SiNPs synthesized ranged from 10 to 50 nm and also showed spherical-shaped NPs [43].

Recently, Hu et al. [44] synthesized organo-SiNPs with sizes in the range of 50–500 nm using common salts with anions $NO_2^-$, F-, $HPO_4^{2-}$, $CH3COO^-$, and $SO_3^{2-}$ and surfactants. They reported that using NaF as catalytic salt, the reaction is completed after 15 min and although this salt is hydrolyzed, due to the low concentration added into the reactional medium (ranging from 2.5 to 160 mM), the pH stays neutral. The NaF catalytic characteristic has been attributed to fluoride nucleophilic property; however, the salt only has an effect when a surfactant is present which produces stable colloidal solutions [44].

Nanosilica can be polymerized in the presence of chitosan. Chang et al. synthesized nanosilica in ambient conditions, and they observed that chitosan did not significantly change the size of the individual nanoparticles, but it facilitated aggregation of the composite nanoparticles and provided aggregates measuring from 1 to 32 nm [48]. Polyethylenimine (PEI) is a polymer that can be used in nanosilica

biomimetic synthesis, which provides the advantage of being stable at room temperature and inexpensive. According to Neville and co-workers, the biomimetic synthesis of nanosilica using tetramethyl orthosilicate (TMOS) and PEI at room temperature and pH 7 produced nanosilica with a maximum size of 275 nm [49].

### 14.4.2 Synthesis from Coal Ash

The recycling of waste of coal industry is very important since its production reached 578 million tons in 2014. In view of this high amount of waste generation, recycling this waste in order to extract nanosilica is an environment-friendly process [50]. In general, this methodology employs NaOH for an alkali fusion in order to form soluble sodium silicate during the fusion process (Eq. 14.1) [51, 52].

$$SiO_2(s) + 2NaOH(aq) \rightarrow Na_2SiOH_3(aq) + H2O(l) \quad (14.1)$$

Misran et al. [53] synthesized mesoporous nanosilica with a high surface area of 732 $m^2g^{-1}$ and average pore diameter of 2.5 nm. In this method, the coal fly ash was pretreated using a ratio of 1.2 NaOH/fly ash and used a fusion temperature of 577 °C followed by hydrothermal treatment at 100 °C for 5 days [53]. Dhokte et al. [51] also synthesized mesoporous nanosilica by an alkali fusion at 570 °C using the same ratio of 1.2 NaOH/fly ash [53].

Yan and co-workers [50] synthesized ordered mesoporous nanosilica from coal fly ash by calcining the coal fly ash for 2 h at 800 °C (in order to remove organic components) and used NaOH for desilication reaction. They obtained nanosilica with high purity (99.35%), high surface area (1157 $m^2g^{-1}$), large pore volume (0.95 $cm^3g^{-1}$), and a highly ordered hexagonal mesostructure (2.88 nm) [50].

Manchanda and colleagues [54] investigated a solgel synthesis of nanosilica by autoclaving a coal fly ash with NaOH for 120-min duration at 100 °C with the further addition of HCl for precipitation of silica in the solution. This method produced spherical globular nanosilica particles with a size ranging from 10 to 40 nm [54].

### 14.4.3 Extraction from Agricultural Waste

The conventional method of production of silica requires a high temperature (up to 1300 °C), which is not a green methodology and also increase the costs [55]. Considering this fact, the utilization of a different kind of waste can provide a green process using not only lower temperatures but also reusing these materials. The rice husk is an agricultural product with high silica content and which is burnt. Mor and co-workers [55] extracted nanosilica ranging from 10 to 15 nm using 600 °C as the highest temperature for the first treatment followed by the addition of NaOH and a sequence of heating using 100, 80, and 50 °C [55].

Another agricultural waste, the *Sorghum vulgare* seed heads (SVSH), was investigated for nanosilica synthesis. Balamurugan et al. [56] calcined the SVSH

at 700 °C and used acid and alkali routes for synthesis, and they observed that acid routes formed crystalline nanosilica and alkali route produces silica with amorphous in nature [56]. Chen et al. [57] extracted nanosilica from wheat straw by two routes: (a) acid (nitric-sulfuric acid) and (b) combustion (500 °C for 8 h). After both methods, calcination was accomplished and produced nanosilica in a range of 75–320 nm [57].

Rice straw and maize stalk were also employed for nanosilica synthesis. Amutha et al. [58] calcined the waste at 650 °C and added NaOH followed by heating at 100 °C for 3 h and after added HCl followed by heating. The nanosilica particles synthesized were spherical, and the agglomerates measured 100 nm [59]. Recently, nanosilica was synthesized by Sankar et al. using rice brown husk via sonochemical synthesis. After the calcination of rice brown husk, the material was washed with HCl, and it was sonicated in an ultrasonic water producing nanosilica with a size ranging from 5 to 40 nm depending on the sonication time (the particle sizes increase with the increase of sonication time) [59].

### 14.4.4 Extraction from Plants

Extraction of nanosilica from plants is another green procedure since the plants are renewable, and this procedure employs lower temperatures compared to the conventional methods. Assefi et al. [60] used pine cones and pine needles to synthesize nanosilica. This plant was employed due to the 1.37 wt% content of silica. Using a thermal treatment of 600 °C during 3 h and the addition of sulfuric acid, nanosilica with the average size of 37 nm was obtained [60].

*Equisetum arvense* was employed for nanosilica synthesis by Sapei et al. [61] due to its high accumulation of silicon ("biogenetic silica"). Nanosilica particles with large surface area 400 $m^2\ g^{-1}$ and with the average size of 6–7 nm were synthesized using HCl and calcination at 500 °C [61]. This same plant (*Equisetum arvense*) was employed for nanosilica synthesis by Carneiro and co-workers [62]. Nanosilica particles measuring 8 nm and with a high-specific surface area of 330 $m^2\ g^{-1}$ were synthesized by acid washing (HCl) and calcination at 500 °C. The low temperature (compared with conventional methods) and the low acid concentration (2% of HCl) make this procedure environment-friendly [62].

## 14.5 Green Nanosilica Applied in Concrete Production

The cement industry is one of the most energy consuming and has a high rate of $CO_2$ emission, about 5% of the $CO_2$ global emission. In view of this fact, the incorporation of different materials in cement production can reduce greenhouse gas emission [63]. Recently, the use of nanosilica in concrete has become interesting due to their unique properties in the potential pozzolanic reaction with cement hydration products. Furthermore, the compressive strength of the concrete increases

with the addition of nanosilica, and also the resistance to water and chloride ions is improved [64].

The nanosilica obtained by green process can be added into cement after the calcination. Sinyoung and co-workers [65] calcined the rice husk at 650 °C for 1 h and added an alkali solution in order to extract nanosilica with size ranging from 20 to 50 nm which was suitable due to its reactivity for low-temperature production of belite cement especially with calcium nitrate [66]. Nanosilica from rice husk was added into cement mixture by Zareei et al. [66] in a proportion ranging from 0 to 25%. This material was calcined at 550–700 °C for 1 h and transformed the silica of the ash into amorphous silica and in a proportion of 25% in concrete; it showed the lowest ratios of water absorption besides leading to 78% reduction in chloride permeation [66].

Vishwakarma and co-workers added nanosilica from rice husk ash ranging from 40 to 60 nm in a cement mixture [67]. The rice husk ash was calcined at 600–800 °C and mixture in the cement in cement/rice husk ash ratio of 293/9 kg, and this mixture showed lower porosity and permeability. Furthermore, the presence of nanosilica increased the strength due to the polymerized layered structure and rough surface texture which increases the bonding between aggregates and cement [67]. Green nanosilica synthesized from olivine showed to be effective when applied to concrete according to Lazaro et al.'s study [60]. The addition of 5% of this green nanosilica improved the compressive strength to 20% of the concrete and also reduced the $CO_2$ emissions in concrete production by 3% [60].

## 14.6 Future Perspectives

Nowadays, due to the environmental concerns, procedures that are less polluting and reduce the energy input are gaining notoriety in the most diverse industry sectors. In view of this fact, the addition of nanosilica in concrete can decrease the emission of greenhouse gases, reuse some kind of wastes, and also improve the resistance of the concrete. Waste material such as rice husk has high silica content, and when this material is calcined and treated with alkali solution, it provides nanosilica in an environment-friendly process.

When nanosilica is added into the concrete, it forms a polymerized layered structure between the aggregates and the concrete, which increases the strength of the concrete and mortars [67]. Furthermore, the addition of nanosilica decreases the permeability of chloride ions, which induces the corrosion, and thus improves the durability of the concrete [68]. Besides these benefits, the use of green nanosilica, synthesized using agricultural waste, coal fly ash, and biomimetic synthesis, provides an environment-friendly process decreasing the release of greenhouse gases and also enhances the resistance of the concrete.

## References


1. Chen L, Liu J, Zhang Y, Zhang G, Kang Y, Chen A, Feng X, Shao L (2018) The toxicity of silica nanoparticles to the immune system. Nanomedicine 13(15):1939–1962
2. Johnston CJ, Driscoll KE, Finkelstein JN et al. (2000). Pulmonary chemokine and mutagenic responses in rats after subchronic inhalation of amorphous and crystalline silica. Toxicol Sci 56 (2): 405–413
3. Kumar MNV, Sameti R, Mohapatra SS et al (2004) Cationic silica nanoparticles as gene carriers: synthesis, characterization and transfection efficiency in vitro and in vivo. J Nanosci Nanotechnol 4(7):876–881
4. Arts JH, Muijser E, Duistermaat H, Junker E, Kuper K, C. F. (2007) Five-day inhalation toxicity study of three types of synthetic amorphous silicas in Wistar rats and post-exposure evaluations for up to 3 months. Food Chem Toxicol 45(10):1856–1867
5. Merget R, Bauer T, Küpper H et al (2001) Health hazards due to the inhalation of amorphous silica. Arch Toxicol 75(11–12):625–634
6. Leung CCY, Chen ITS, W. (2012) Silicosis. Lancet 379(9830):2008–2018
7. Mehta P, Monteiro K, Concrete PJM (2006) Microstructure, properties, and materials. McGraw-Hill Publishing, London
8. Amin M, Abu El-hassan K (2015) Effect of using different types of nano materials on mechanical properties of high strength concrete. Constr Build Mater 80:116–124
9. Hou P, Qian J, Cheng X, Shah SP (2015) Effects of the pozzolanic reactivity of nano$SiO_2$ on cement-based materials. Constr Build Mater 55:250–258
10. Mobini M, Khaloo H, Hosseini A, Esrafili P, A. (2015) Mechanical properties of fiber-reinforced high-performance concrete incorporating pyrogenic nano-silica with different surface areas. Constr Build Mater 101:130–140
11. Rong Z, Sun W, Xiao H, Jiang G (2015) Effects of nano-SiO2 particles on the mechanical and microstructural properties of ultra-high performance cementitious composites. Cem Concr Compos 56:25–31
12. Zahedi M, Ramezanianpour AA, Ramezanianpour AM (2015) Evaluation of the mechanical properties and durability of cement mortars containing nano-silica and rice husk ash under chloride ion penetration. Constr Build Mater 78:354–361
13. Zhu J, Feng C, Yin H, Zhang Z, Shah SP (2015) Effects of colloidal nanoBoehmite and nanoSiO2 on fly ash cement hydration. Constr Build Mater 101:246–251
14. Chithra S, SRR SK, Chinnaraju K (2016) The effect of colloidal nano-silica on workability, mechanical and durability properties of high performance concrete with copper slag as partial fine aggregate. Constr Build Mater 113:794–804
15. Gesoglu M, Güneyisi E, Asaad DS, Muhyaddin GF (2016) Properties of low binder ultra-high performance cementitious composites: comparison of nano-silica and microsilica. Constr Build Mater 102:706–713
16. Shaikh FUA, Shafaei Y, Sarker PK (2016) Effect of nano and micro-silica on bond behaviour of steel and polypropylene fibres in high volume fly ash mortar. Constr Build Mater 115:690–698
17. Wang L, Zheng D, Zhang S, Cui H, Li D (2016) Effect of Nano-SiO2 on the hydration and microstructure of Portland cement. Nano 241:1–15
18. Hendi A, Rahmani H, Mostofinejad D, Tavakolinia A, Khosravi M (2017) Simultaneous effects of microsilica and nano-silica on self-consolidating concrete in a sulfuric acid medium. Constr Build Mater 152:192–205
19. Horszczaruk E, Sikora P, Cendrowski K, Mijowska E (2017) The effect of elevated temperature on the properties of cement mortars containing nano-silica and heavyweight aggregates. Constr Build Mater 137:420–431
20. Joshaghani A, Moeini MA (2017) Evaluating the effects of sugar cane bagasse ash (SCBA) and nano-silica on the mechanical and durability properties of mortar. Constr Build Mater 152:818–831

21. Li L, Zhu G, Huang J, Kwam ZH, Li AKH, L. J. (2017a) Combined effects of micro-silica and nano-silica on durability of mortar. Constr Build Mater 157:337–347
22. Li LG, Huang ZH, AKH K, Chen HY (2017b) Synergistic effects of micro-silica and nano-silica on strength and microstructure of mortar. Constr Build Mater 140:229–238
23. Li W, Ji W, Isfahani F, Wang T, Li Y, Liu G, Xing Y, F. (2017c) Nano-silica sol-gel and carbon nanotube coupling effect on the performance of cement-based materials. Nano 185:1–15
24. Xu J, Wang B, Zuo J (2017) Modification effects of nano-silica on the interfacial transition zone in concrete: A multiscale approach. Cem Concr Compos 81:1–10
25. Adamu M, Mohammed BS, Liew MS (2018) Mechanical properties and performance of high volume fly ash roller compacted concrete containing crumb rubber and nano-silica. Constr Build Mater 171:521–538
26. Bu Y, Hou X, Wang C, Du J (2018) Effect of colloidal nano-silica on early-age compressive strength of oil well cement stone at low temperature. Constr Build Mater 171:690–696
27. Erdem S, Hanbay S, Guler Z (2018) Micromechanical damage analysis and engineering performance of concrete with colloidal nano-silica and demolished concrete aggregates. Constr Build Mater 171:634–642
28. Li L, Zheng G, Zhu JY, Kwan J, A. K. H. (2018) Combined usage of micro-silica and nano-silica in concrete: SP demand, cementing efficiencies and synergistic effect. Constr Build Mater 168:622–632
29. Lu J, Poon CS (2018) Improvement of early-age properties for glass-cement mortar by adding nano-silica. Cem Concr Compos 89:18–30
30. Massana J, Reyes E, Bernal J, León N, Sánches-Espinosa E (2018) Influence of nano- and micro-silica additions on the durability of a high-performance self-compacting concrete. Constr Build Mater 165:93–103
31. Ramezanianpour AA, Moeini MA (2018) Mechanical and durability properties of alkali activated slag coating mortars containing nano-silica and silica fume. Constr Build Mater 163:611–621
32. Xiao H, Liu R, Zhang F, Liu M, Li H (2018) Role of nano-SiO2 in improving the microstructure and impermeability of concrete with different aggregate gradations. Constr Build Mater 188:537–545
33. Baloch H, Usman M, Rizwan SA, Hanif A (2019) Properties enhancement of super absorbent polymer (SAP) incorporated self-compacting cement pastes modified by nano-silica (NS) addition. Constr Build Mater 203:18–26
34. Mahapatra CK, Barai SV (2019) Temperature impact on residual properties of self-compacting based hybrid fiber reinforced concrete with fly ash and colloidal nano-silica. Constr Build Mater 198:120–132
35. Du H (2019) Properties of ultra-lightweight cement composites with nano-silica. Constr Build Mater 199:696–704
36. Lavergne F, Belhadi R, Carriat J, Ben Fraj A (2019) Effect of nano-silica particles on the hydration, the rheology and the strength development of a blended cement paste. Cem Concr Compos 95:42–55
37. Liu R, Xiao H, Liu J, Guo S, Pei Y (2019) Improving the microstructure of ITZ and reducing the permeability of concrete with various water/cement ratios using nano-silica. J Mater Sci 54:444–456
38. Duan J, Liang S, Feng L, Yu Y, Sun Z (2018) Silica nanoparticles trigger hepatic lipid-metabolism disorder in vivo and in vitro. Int J Nanomedicine 13:7303–7318
39. Nel A, Xia T, Mädler L, Li N (2006) Toxic potential of materials at the nanolevel. Science 311 (5761):622–627
40. Yang H, Liu C, Yang D, Zhang H, Xi Z (2009) Comparative study of cytotoxicity, oxidative stress and genotoxicity induced by four typical nanomaterials: the role of particle size, shape and composition. J Appl Toxicol 29(1):69–78

41. Zhou F, Liao F, Chen L, Liu Y, Wang W, Feng S (2019) The size-dependent genotoxicity and oxidative stress of silica nanoparticles on endothelial cells. Environ Sci Pollut Res Int 26 (2):1911–1920
42. Kamikubo Y, Yamana T, Hashimoto Y, Sakurai T (2019) Induction of oxidative stress and cell death in neural cells by silica nanoparticles. ACS Chem Neurosci 10(1):304–312
43. Kang K, Oh H, Kim D et al (2017) Synthesis of silica nanoparticles using biomimetic mineralization with polyallylamine hydrochloride. J Colloid Interface Sci 507:145–153. https://doi.org/10.1016/j.jcis.2017.07.115
44. Hu T, Chou H, Lin C (2019) Facile green synthesis of organosilica nanoparticles by a generic " salt route ". J Colloid Interface Sci 539:634–645. https://doi.org/10.1016/j.jcis.2018.12.080
45. Chai S, Zhang J, Yang T et al (2010) Thermoresponsive microgel decorated with silica nanoparticles in shell: biomimetic synthesis and drug release application. Colloids Surfaces A Physicochem Eng Asp 356:32–39. https://doi.org/10.1016/j.colsurfa.2009.12.026
46. Naik RR, Stringer SJ, Agarwal G, Stone MO (2002) Biomimetic synthesis and patterning of silver nanoparticles. Nat Mater 1:169–172. https://doi.org/10.1038/nmat758
47. Heuer AH, Fink DJ, Laraia VJ et al (1992) Innovative materials processing strategies: a biomimetic approach. Science 255:1098–1105
48. Chang J-S, Kong Z-L, Hwang D-F, Chang KLB (2006) Chitosan-catalyzed aggregation during the biomimetic synthesis of silica nanoparticles. Chem Mater 18:702–707
49. Neville F, Broderick MJF, Gibson T, Millner PA (2011) Fabrication and activity of silicate nanoparticles and Nanosilicate-entrapped enzymes using Polyethyleneimine as a biomimetic polymer. Langmuir 27:279–285. https://doi.org/10.1021/la1033492
50. Yan F, Jiang J, Tian S et al (2016) A green and facile synthesis of ordered mesoporous Nanosilica using coal Fly ash. ACS Sustain Chem Eng 4:4654–4661. https://doi.org/10.1021/acssuschemeng.6b00793
51. Dhokte AO, Khillare SL, Lande MK, Arbad BR (2011) Synthesis, characterization of mesoporous silica materials from waste coal fly ash for the classical Mannich reaction. J Ind Eng Chem 17:742–746. https://doi.org/10.1016/j.jiec.2011.05.033
52. Yan F, Jiang J, Li K et al (2017) Green synthesis of Nanosilica from coal Fly ash and its stabilizing effect on CaO sorbents for $CO_2$ capture. Environ Sci Technol 51:7606–7615. https://doi.org/10.1021/acs.est.7b00320
53. Misran H, Singh R, Begum S, Ambar M (2007) Processing of mesoporous silica materials (MCM-41) from coal fly ash. J Mater Process Technol 186:8–13. https://doi.org/10.1016/j.jmatprotec.2006.10.032
54. Manchanda CK, Khaiwal R, Mor S (2017) Application of sol – gel technique for preparation of nanosilica from coal powered thermal power plant fl y ash. J Sol-Gel Sci Technol 83:1–7. https://doi.org/10.1007/s10971-017-4440-x
55. Mor S, Manchanda CK, Kansal SK et al (2017) Nanosilica extraction from processed agricultural residue using green technology. J Clean Prod 143:1284–1290. https://doi.org/10.1016/j.jclepro.2016.11.142
56. Balamurugan M, Saravanan S (2012) Producing nanosilica from *Sorghum vulgare* seed heads. Powder Technol 224:345–350. https://doi.org/10.1016/j.powtec.2012.03.017
57. Chen H, Wang F, Zhang C et al (2010) Preparation of nano-silica materials : the concept from wheat straw. J Non-Cryst Solids 356:2781–2785. https://doi.org/10.1016/j.jnoncrysol.2010.09.051
58. Amutha K, Sivakumar G (2013) Analytical analysis of synthesized biosilica from bioresidues. Spectrochim Acta Part A Mol Biomol Spectrosc 112:219–222. https://doi.org/10.1016/j.saa.2013.04.038
59. Sankar S, Kaur N, Lee S, Kim DY (2018) Rapid sonochemical synthesis of spherical silica nanoparticles derived from brown rice husk. Ceram Int 44:8720–8724
60. Assefi M, Davar F, Hadadzadeh H (2015) Green synthesis of nanosilica by thermal decomposition of pine cones and pine needles. Adv Powder Technol 26:1583–1589. https://doi.org/10.1016/j.apt.2015.09.004

61. Sapei L, Nöske R, Strauch P, Paris O (2008) Isolation of mesoporous biogenic silica from the perennial plant Equisetum hyemale. Chem Mater 20:2020–2025
62. Carneiro ME, Magalhães WLE, De Muñiz GIB et al (2015) Preparation and characterization of Nano silica from *Equisetum arvense*. Bioprocess Biotech 5:1–7. https://doi.org/10.4172/2155-9821.1000205
63. Said AM, Zeidan MS, Bassuoni MT, Tian Y (2012) Properties of concrete incorporating nano-silica. Constr Build Mater 36:838–844. https://doi.org/10.1016/j.conbuildmat.2012.06.044
64. Du H, Du S, Liu X (2014) Durability performances of concrete with nano-silica. Constr Build Mater 73:705–712. https://doi.org/10.1016/j.conbuildmat.2014.10.014
65. Sinyoung S, Kunchariyakun K, Asavapisit S, Mackenzie KJD (2017) Synthesis of belite cement from nano-silica extracted from two rice husk ashes. J Environ Manag 190:53–60. https://doi.org/10.1016/j.jenvman.2016.12.016
66. Zareei SA, Ameri F, Dorostkar F, Ahmadi M (2017) Case studies in construction materials Rice husk ash as a partial replacement of cement in high strength concrete containing micro silica : evaluating durability and mechanical properties. Case Stud Constr Mater 7:73–81. https://doi.org/10.1016/j.cscm.2017.05.001
67. Vishwakarma V, Ramachandran D, Anbarasan N, Rabel AM (2016) ScienceDirect studies of rice husk ash nanoparticles on the mechanical and microstructural properties of the concrete. Mater Today Proc 3:1999–2007. https://doi.org/10.1016/j.matpr.2016.04.102
68. Shaikh FUA, Supit SWM (2015) Chloride induced corrosion durability of high volume fly ash concretes containing nano particles. Constr Build Mater 99:208–225. https://doi.org/10.1016/j.conbuildmat.2015.09.030